Tai Hyun Park
Editor

Bioelectronic Nose

Integration of Biotechnology and Nanotechnology

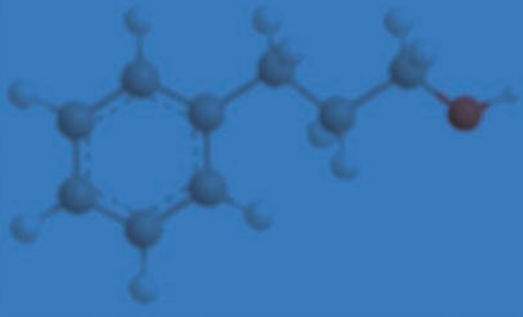

Springer

Bioelectronic Nose

Tai Hyun Park
Editor

Bioelectronic Nose

Integration of Biotechnology and Nanotechnology

Springer

Editor
Tai Hyun Park
School of Chemical and Biological
Engineering, Seoul National University
Seoul
Korea, Republic of (South Korea)

ISBN 978-94-017-8612-6 ISBN 978-94-017-8613-3 (eBook)
DOI 10.1007/978-94-017-8613-3
Springer Dordrecht Heidelberg New York London

Library of Congress Control Number: 2014937462

Printed on acid-free paper

Springer is part of Springer Science+Business Media (www.springer.com)

Preface

We have five senses: vision, hearing, touch, smell, and taste. Although some other senses including balance, pain, itch, and temperature senses have been reported, the five senses remain major classical senses. Among these five senses, three of them: vision, hearing, and touch, recognize physical stimuli, and the other two senses recognize chemical stimuli. The science and technology concerned with vision and hearing have been advanced enormously, while the understanding of the chemical senses, especially the sense of smell, has been very limited.

The stimulus energy for the sense of vision and hearing is light and sound, respectively. The camera, video camera, and recorder create recorded signals which can be even delivered to remote places. Using this technology we can watch the Olympic game on TV at home. The sense of touch has been also integrated with information technology in the form of the tablet PC.

On the contrary, there is no such a device which can capture smell or taste. The sense of smell is even more complicate and mysterious than the sense of taste. Electronic noses have been intended to mimic the signal processing of the sense of smell; however, elemental receptor materials of the conventional electronic noses are totally different from human olfactory receptors. If we consider that the sense of smell is a chemical sense, the same receptor materials as those in the human nose should be employed to accurately realize the human sense of smell.

In the last two decades, much has been learned about the smell sensing mechanism in biological systems. With knowledge about the biological olfactory system and the techniques for the expression of biological receptor proteins, we are able to utilize biological materials and systems to mimic the biological olfactory system. In addition to the advances in biological and biotechnological area, nanotechnology has progressed to a great degree. The “bioelectronic nose”, the device which has a similar function to the human smell sensing system, can be realized by combining the olfactory cells or receptors with nanotechnology.

The bioelectronic nose is a good example of the integration of biotechnology and nanotechnology. This book combines contributions from basic biological sciences of the olfactory system, biotechnology for the production of olfactory biological elements, and nanotechnology for the development of various sensing devices. The purpose of this book is to provide the reader with a concept, basic sciences, fundamental technologies, applications, and perspectives of the bioelectronics nose.

The editor is very grateful to all the contributing authors, who are leading experts in their research areas. Especially valuable suggestions from Hiroaki Matsunami and Edith Pajot-Augy are much appreciated. Proofreading assistance for the consistent format of this book was kindly provided by Hyun Seok Song, Jong Hyun Lim, and Hwi Jin Ko. The editor thanks Peter Butler and Sophie Lim at Springer for their advice and assistance in the publication process.

School of Chemical and Biological Engineering Tai Hyun Park
Advanced Institutes of Convergence Technology
Seoul National University
Seoul 151-742
Republic of Korea

Contents

Contributors

Jisub Bae Department of Brain Science, Graduate School, Daegu Gyeongbuk Institute of Science and Technology, Daegu, Republic of Korea

Christine Baly INRA, UR1197 NeuroBiologie de l'Olfaction, Jouy-en-Josas, France

Karolina Corin Center for Bits and Atoms, Massachusetts Institute of Technology, Cambridge, MA, USA

Aurélie Dewaele INRA, UR1197 NeuroBiologie de l'Olfaction, Jouy-en-Josas, France

Peter Yi Dong Department of Molecular Genetics and Microbiology, Duke University Medical Center, Durham, NC, USA

Department of Neuroscience, University of Pennsylvania Perelman School of Medicine, Philadelphia, PA, USA

Jean-François Gibrat INRA, UR1077 Mathématique Informatique et Génome, Jouy-en-Josas, France

Naihua Natalie Gong Department of Molecular Genetics and Microbiology, Duke University Medical Center, Durham, NC, USA

Seunghun Hong Department of Biophysics and Chemical Biology, Seoul National University, Seoul, Republic of Korea

Jyongsik Jang School of Chemical and Biological Engineering, Seoul National University, Seoul, Republic of Korea

Hye Jun Jin Department of Physics and Astronomy, and Institute of Applied Physics, Seoul National University, Seoul, Republic of Korea

Daesan Kim Department of Biophysics and Chemical Biology, Seoul National University, Seoul, Republic of Korea

Samhwan Kim Department of Brain Science, Graduate School, Daegu Gyeongbuk Institute of Science and Technology, Daegu, Republic of Korea

Hwi Jin Ko Bio-MAX Institute, Seoul National University, Seoul, Republic of Korea

Oh Seok Kwon School of Chemical and Biological Engineering, Seoul National University, Seoul, Republic of Korea

Hyungwoo Lee Department of Physics and Astronomy, and Institute of Applied Physics, Seoul National University, Seoul, Republic of Korea

Luke P. Lee Departments of Bioengineering, Electrical Engineering and Computer Science, Biophysics Program, Berkeley Sensor & Actuator Center, University of California, Berkeley, CA, USA

Sang Hun Lee Departments of Bioengineering, Berkeley Sensor & Actuator Center, University of California, Berkeley, CA, USA

Jong Hyun Lim School of Chemical and Biological Engineering, Seoul National University, Seoul, Republic of Korea

Hiroaki Matsunami Department of Molecular Genetics and Microbiology, Duke University Medical Center, Durham, NC, USA

Department of Neurobiology, Duke University Medical Center, Durham, NC, USA

Duke Institute for Brain Sciences, Duke University Medical Center, Durham, NC, USA

Department of Neurobiology, Duke Institute for Brain Sciences, Duke University Medical Center, Durham, NC, USA

Cheil Moon Department of Brain Science, Graduate School, Daegu Gyeongbuk Institute of Science and Technology, Daegu, Republic of Korea

Eun Hae Oh Interdisciplinary Program for Bioengineering, Seoul National University, Seoul, Republic of Korea

Edith Pajot-Augy INRA, UR1197 NeuroBiologie de l'Olfaction, Jouy-en-Josas, France

Juhun Park Department of Physics and Astronomy, and Institute of Applied Physics, Seoul National University, Seoul, Republic of Korea

Seung-min Park Departments of Bioengineering, Berkeley Sensor & Actuator Center, University of California, Berkeley, CA, USA

Tai Hyun Park School of Chemical and Biological Engineering, Seoul National University, Seoul, Republic of Korea

Interdisciplinary Program for Bioengineering, Seoul National University, Seoul, Republic of Korea

Bio-MAX Institute, Seoul National University, Seoul, Republic of Korea

Krishna C. Persaud School of Chemical Engineering and Analytical Science, The University of Manchester, Manchester, UK

Marie-Annick Persuy INRA, UR1197 NeuroBiologie de l'Olfaction, Jouy-en-Josas, France

Gabriele V. Ronnett Department of Neuroscience, Biological Chemistry, and Neurology, School of Medicine, Johns Hopkins University, Baltimore, MD, USA

Guenhaël Sanz INRA, UR1197 NeuroBiologie de l'Olfaction, Jouy-en-Josas, France

Ruchira Sharma Department of Molecular Genetics and Microbiology, Duke University Medical Center, Durham, NC, USA

Shashank Shekhar Department of Physics and Astronomy, and Institute of Applied Physics, Seoul National University, Seoul, Republic of Korea

Hyun Seok Song School of Chemical and Biological Engineering, Seoul National University, Seoul, Republic of Korea

Harvard-MIT Division of Health Sciences and Technology, Massachusetts Institute of Technology, Cambridge, MA, USA

Xubo Su Department of Pathophysiology, Shanghai Jiaotong University School of Medicine, Shanghai, P. R. China

Elena Tuccori School of Chemical Engineering and Analytical Science, The University of Manchester, Manchester, UK

Xiaoqiang Wang Center for Bits and Atoms, Massachusetts Institute of Technology, Cambridge, MA, USA

Shuguang Zhang Center for Bits and Atoms, Massachusetts Institute of Technology, Cambridge, MA, USA

Hanyi Zhuang Department of Pathophysiology, Shanghai Jiaotong University School of Medicine, Shanghai, P. R. China

Institute of Health Sciences, Shanghai Jiaotong University School of Medicine/ Shanghai Institutes for Biological Sciences of Chinese Academy of Sciences, Shanghai, P. R. China

Chapter 1
Concept of Bioelectronic Nose

Jong Hyun Lim and Tai Hyun Park

Abstract Sense of smell is an important sense to recognize environmental conditions and dangerous situations. Following the identification of the olfactory mechanism in the early 1990s, extensive studies to develop electronic devices that mimic the function of animal noses have been conducted. Most devices have been composed of an array of several sensors that react to chemical compounds. The odor is characterized by analyzing the response patterns generated by the sensor array. However, such devices have limitations in terms of sensitivity and selectivity. Hence, a novel concept for sensor devices functionalized with odor-recognizing biomolecules was suggested. Sensors which use biomolecules as a primary sensing material are commonly called bioelectronic noses. A bioelectronic nose generally consists of primary and secondary transducers. The primary transducer is a biological recognition element such as olfactory receptors and odorant-binding proteins. The secondary transducer is a highly sensitive optical or electrical sensor platform that converts biological events into measurable signals. In this chapter, the basic concept and principles of bioelectronic noses are described. In addition, specific characteristics of bioelectronic noses and the current issues are presented.

1.1 History of Artificial Smelling Methods

1.1.1 Trained Animal

Sense of smell is the most mysterious sense among five senses, and its biological mechanism was revealed relatively later than with other senses. This sense has been instinctually used for the perception of dangerous situations or subtle changes in the environment. For instance, fire can easily be recognized through the smell of smoke, and the spoilage of food can be determined by their putrid odors. However, humans have insensitive noses. Non-human vertebrates such as dogs and mice have more types and numbers of olfactory sensory neurons (OSNs) in their noses [1–3].

T. H. Park (✉) · J. H. Lim
School of Chemical and Biological Engineering, Seoul National University,
Seoul 151-744, Republic of Korea
e-mail: thpark@snu.ac.kr

T. H. Park (ed.), *Bioelectronic Nose,* DOI 10.1007/978-94-017-8613-3_1,

This makes them more sensitively smell something out than human beings. In airports, the scene of trained dogs sniffing for explosives and drugs is quite natural.

Many animal trainers and scientists have attempted to train animals for the various purposes. Dogs have been trained to detect illegal narcotics and explosives, and their reliability has been examined by many scientists [4, 5]. Trained dogs are able to find narcotics and explosives with very high accuracy [6, 7]. Therefore, they are commonly used in various places such as customs. More recently, dogs have been trained for the diagnosis of diseases. Various types of intractable diseases such as lung, bladder, and breast cancers require early diagnosis. These diseases cause tiny changes in body or urine odors. Although people cannot perceive such small changes, dogs can [8–10]. Mice and rats are also good odor detectors [11–14]. They can recognize compounds which are regarded as odorless, such as carbon dioxide [15]. For these advantages, animals are still trained as alternatives to the human nose.

Even though animals can smell with high sensitivity and reliability, they have significant limitations as odor detectors. For instance, training and maintenance require high costs. Also, various external parameters such as illness and disorders can affect their smelling abilities. Most of all, after finishing their smelling work, they require rest for a long time before working again, because their ability is easily and rapidly lost. This olfactory adaptation is a severe problem with the exploitation of animal noses [16, 17].

1.1.2 Electronic Nose

1.1.2.1 Principle of Electronic Nose

Electronic noses were first suggested in 1982 [18]. A novel smelling device was constructed using semiconductor-based transducers, and it was demonstrated that the sensor was able to reproducibly discriminate various odors. Following this achievement, many studies have been performed to find new and more advanced materials for smelling devices [19–23].

Important studies supporting the scientific background of electronic noses have been reported. In the early 1990s, Buck and Axel revealed the olfactory mechanism [24, 25]. In the nasal cavity, there are numerous OSNs, which are the primary odor-sensing cells. Each OSN expresses a single type of olfactory receptor (OR) on its surface membrane. ORs have an excellent selectivity capable of precisely discriminating ligand molecules among a mixture of analogous compounds [26]. Once a certain odorants bind with specific ORs, a signal cascade is activated and olfactory signals are generated [27]. The generated signals are transmitted to the brain, and a person becomes aware of the characteristics of odors using the combination of activated OSNs [28].

The odor-discriminating mechanism of the natural olfactory system is very similar to that of electronic noses. Electronic noses are commonly composed of an array of several sensors. Each sensor produces specific responses by reacting to chemical

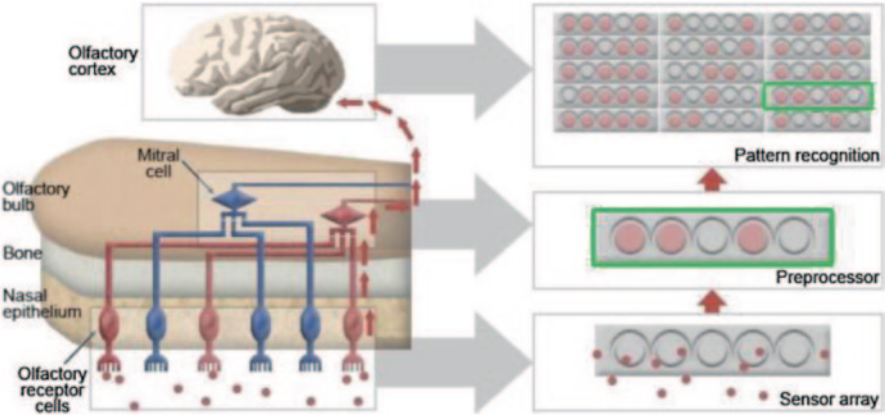

Fig. 1.1 Artificial nose devices mimic the human olfactory system. The electronic and bioelectronic nose systems simulate each stage of the human olfactory system, resulting in the recognition of volatile molecules by pattern analysis. (Reprinted from Ref. [30] with permission from Elsevier)

compounds. Thus, an electronic nose can generate 'odor fingerprints,' which are unique patterns of odorants [29].Odorants can be identified by analyzing the response pattern. This similarity is depicted in Fig. 1.1. The stimulation of odorants generates specific response patterns from olfactory cells in the natural olfactory system or sensor arrays in the electronic nose [30]. The generated patterns are analyzed as a specific characteristic of odors in the brain or electric devices. Both human and electronic noses recognize odors through this process.

1.1.2.2 Characteristics of Electronic Nose

Many compounds have been used as a sensor material for the development of electronic noses. Metal oxide (MOx)-based sensors have mostly been developed [31–35]. The surface of MOx is modified with diverse chemical compounds. An array of MOx allows the sensor to generate specific response patterns. Conducting polymers or field-effect transistors have also been applied to electronic nose systems [36–39]. Such devices have been utilized in many fields requiring the detection of toxic molecules such as amines, alcohols, and sulfur compounds. Also, surface acoustic wave transducers with an array of polymer layers have been extensively used for the development of electronic noses [40–43].

However, electronic noses have critical limitations for application in practical fields. First, the sensitivity is insufficient. It was reported that people can detect odorants at concentrations lower than the ppt level, whereas the sensitivity of electronic noses has mainly been in the ppm or ppb range. Electronic noses could not specifically distinguish one odorant within a mixture of odorants. Moreover, electronic noses cannot fundamentally mimic the human biological olfaction due to the absence of odorant-recognizing biomolecules.

1.1.3 Bioelectronic Nose

In the late 1990s, a novel and more advanced concept of sensor devices was suggested [44]. The challenge was to use ORs as a sensing material in order to mimic a human or animal olfactory system. This new device is called a 'bioelectronic nose'. The bioelectronic nose is based on OR proteins or cells expressing ORs on their surface membrane. ORs are odorant-recognition elements, and are combined with sensor devices that convert biological signals into electrical or optical signals.

Since ORs provide odorant-discriminating ability, the bioelectronic nose can closely mimic a human or animal olfactory system. The concept of odorant analysis using a bioelectronic nose fundamentally differs from the odor-discriminating strategy of electronic noses based exclusively on pattern recognition using sensor arrays. When the ORs are utilized as a primary sensing material, the sensors can precisely distinguish a target molecule among a mixture of various compounds. In addition, sensors based on ORs are more sensitive than electronic noses. The limit of detection reaches the femto-molar range in liquid conditions and the ppt range in gaseous conditions, which is similar to that of a human nose [45, 46]. By virtue of these excellent characteristics, the bioelectronic nose is now receiving great attention from diverse fields such as disease diagnosis, food safety assessment, and environmental monitoring.

1.2 Concept of Bioelectronic Nose

1.2.1 Biological Recognition Element

A bioelectronic nose consists of two main parts: an odorant-recognition element and a signal transducer, as shown in Fig. 1.2 [47]. For the odorant-recognition, cells expressing ORs in their surface membrane, OR proteins, and nanovesicles have generally been used. In the human nose, approximately 390 different types of functional ORs exist [48]. However, humans can discriminate thousands of types of odors. This asymmetry originates from the excellent odorant-recognition ability of ORs, which are capable of distinguishing between their specific ligands and partial ligands, as well as irrelevant molecules [27, 28]. A single odorant activates various types of ORs, and one OR is activated by several odorants. Thus, numerous combinations of activated ORs can be generated. These combinations are recognized as a unique property of an odor in the brain [49].

A bioelectronic nose utilizes this odor-discriminating ability of ORs. Thus, they can detect specific odors with great selectivity. For instance, the odor from decomposed seafood can be easily distinguished among other odors from various spoiled foods when a bioelectronic nose is functionalized with receptors that can selectively detect the odor of spoiled seafood [50]. However, problems still remain to be overcome. ORs have a seven-transmembrane structure with a high hydrophobicity in

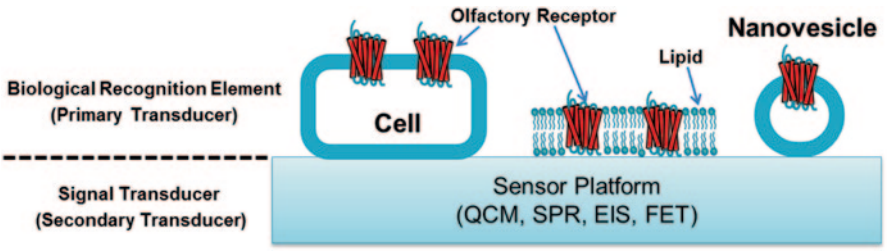

Fig. 1.2 Composition of a bioelectronic nose. The bioelectronic noses consist of a biological recognition element and a signal transducer. Cells expressing ORs, OR proteins, or nanovesicles are generally used as a biological recognition element. Various sensor platforms are used for the conversion of biological signals into measurable signals. The abbreviations used are: *QCM* quartz crystal microbalance, *SPR* surface plasmon resonance, *EIS* electrochemical impedance spectroscopy, *FET* field-effect transistor

the transmembrane region, which makes the expression of ORs in a heterologous system very difficult [51]. Several attempts have been made to achieve functional expression in various heterologous systems. Among various systems, human embryonic kidney (HEK)-293 cells are broadly used because they allow for a relatively high expression level [52–54]. The identification of membrane-targeting tags and accessary proteins assisting the membrane expression, such as rho-tag and receptor-transporting protein 1S (RTP1S), facilitated the high-level expression of ORs in mammalian cells [55–57]. Insect cells, such as SF9 cells, have also been used for the functional expression of ORs [58, 59]. *Saccharomyces cerevisiae* and *Escherichia coli* are also good OR expression systems [60, 61]. These systems allow for mass production and efficient purification processes. Thus, they are effectively being used to produce OR proteins for bioelectronic noses. Detailed information about the mechanism of olfaction and the production of ORs is described in Chaps 2 through 9.

1.2.1.1 Receptor-Based Bioelectronic Nose

The type of the bioelectronic nose can be classified on the basis of the biological recognition elements. The bioelectronic noses can be functionalized with OR proteins. The receptor proteins can be obtained from all types of expression systems, such as mammalian cells, *Saccharomyces cerevisiae*, and *E. coli.* Then, the proteins are combined with diverse types of secondary transducers, such as quartz-crystal microbalances (QCMs) [62–66], surface plasmon resonances (SPR) [67–69], and field-effect transistors (FETs) [45, 46, 70–72]. The binding event between ORs and odorants induces a mass change in ORs. This change is converted into measurable signals through QCMs. The binding can also be monitored using SPR-based devices by measuring the change in optical properties that occurs on a metal surface coated with ORs. The sensing mechanism of an FET-based sensor is based on the change in charge of the ORs. When OR binds with odorants, its conformation

changes. By the conformational change of the OR, the net charge of the OR protein subsequently changes [45, 73]. The change in charge acts as a gate potential to FET devices, and the odorants are detected.

Receptor-based bioelectronic noses have many advantages as a practical sensor, although additional studies on protein quality control are still required due to the complex structure of ORs. Most of all, they have excellent selectivity of ORs, because the whole protein is used. Therefore, the sensor can precisely discriminate its ligand from other analogous compounds [45]. In addition, the mass production of ORs is possible, and storage is relatively easy [61]. Furthermore, OR proteins expressed in *E. coli* were reported to still be active in dry conditions, which allowed for a biosensor that detects gaseous odorants to be developed [46].

1.2.1.2 Cell-Based Bioelectronic Nose

Bioelectronic noses based on cells which express ORs on their surface are classified as cell-based bioelectronic noses. The cells can generate cellular signals. The binding event between ORs and odorants triggers the olfactory signaling cascade, and positive ions flow into the cells from the outside [52, 74]. The electrical potential of the cells consequently changes. The potential change can be measured by various sensing methods, such as fluorescent dyes, SPRs, and planar microelectrodes [74–78].

One of the most important characteristics of cell-based bioelectronic noses is that the cells containing ORs produce the olfactory signals, which may be identical to the signals generated by OSNs. Because the isolation and *in vitro* culture of OSNs are very difficult, the practical use of OSNs is realistically impossible. Therefore, as an alternative to OSNs, OR-containing cells have been effectively utilized. The function of each OR has not yet been fully identified, and has to be elucidated to understand the mystery of the sense of smell. Cell-based bioelectronic noses can be effectively used for the identification of the unrevealed function of ORs.

1.2.1.3 Nanovesicle-Based Bioelectronic Nose

The concept of using nanovesicles lies between those of cells and protein. Nanovesicles can generate cellular signals similar to those produced by cells. They are produced from the cell surface by treatment with a chemical compound that destabilizes the cellular membrane [79]. When nanovesicles are isolated from cells, all membrane proteins and cytosolic components for the signal transduction are still contained in the nanovesicles. Therefore, the nanovesicle can have cell-like properties. In addition, nanovesicles have advantages as a protein-like material in terms of long-time storage and mass production.

The nanovesicle is especially suitable to be combined with nano-materials by virtue of its small size. Therefore, nanovesicles have been effectively used for the functionalization of FETs. The nanovesicle-based bioelectronic nose was first

developed in 2012 [80]. Jin et al. demonstrated that the odorants can be selectively and sensitively detected through the olfactory signaling pathway in nanovesicles. Nanovesicle-based sensors have been applied in diverse fields, such as in the assessment of food quality and the diagnosis of diseases [81, 82].

1.2.2 Signal Transducer

The biological signals generated from ORs are mainly divided into three types: conformational changes in olfactory receptors, dissociation of the α-subunit of G proteins from activated ORs, and ion influx caused by the signal transduction in cells. These biological signals should be converted into signals that can be measured. Devices for this role are called signal transducers or secondary transducers [47].

1.2.2.1 Quartz Crystal Microbalance

Quartz crystal microbalances (QCMs) have been used for the development of receptor-based bioelectronic noses [62–66]. The functionalized surface of quartz crystals is coated with olfactory receptors. The whole mass of OR increases by the binding between ORs and odorants. QCM can specifically detect this change. The adsorption of specific molecules onto the surface of quartz crystals coated with ORs results in the reduction of the resonance frequency of the quartz crystal. Odorants can be detected using this principle.

Research on QCM-based bioelectronic noses using ORs isolated from bullfrogs was reported in 1999 [66]. The specific recognition of odorants could be monitored in real-time using the QCM device. It was demonstrated that the ORs overexpressed in *E. coli* and in mammalian cells could also be utilized for the functionalization of QCM chips [62, 65]. These studies represent that the piezoelectric method can be used for the development of highly sensitive and selective bioelectronic noses. However, QCM devices have an issue that must be overcome. The oscillation frequency of quartz crystals can be easily affected by various external factors, such as electromagnetic fields and pressure. Hence, non-specific noise signals are frequently generated [83, 84].

1.2.2.2 Surface Plasmon Resonance

Surface plasmon resonance (SPR) has been broadly used to measure the association and dissociation of analytes on a surface. The SPR is an optical phenomenon that occurs when p-polarized light hits a prism covered with a metal surface [85]. At a specific incident angle, the intensity of the reflected light is reduced due to resonance energy transfer. This resonance angle is affected by the adsorption of specific molecules onto the metal surface. When the surface of SPR is coated with ORs, the binding of odorants to ORs influences the resonance angle.

In olfactory signaling, the activated ORs induce the dissociation of the α-subunit of G proteins. In order to utilize this event, ORs and $G\alpha_{olf}$ proteins were immobilized onto the chip of SPRs and can be used to analyze the association and dissociation of ligands [68, 69]. The activation of ORs could be monitored by measuring the release of Gα subunits. SPRs have also been utilized for the development of cell-based bioelectronic noses [75, 78]. The cells were cultured on SPR chips. Then, the inflow of ions into the cells was measured. The influx of calcium ions that occurs by the olfactory signaling affects the resonance angle of the SPR chip, and the odorants could be detected. Detailed information about the SPR-based bioelectronic noses is described in Chap. 11.

1.2.2.3 Electrochemical Impedance Spectroscopy

Electrochemical impedance spectroscopy (EIS) is an effective technique to characterize electrodes functionalized with biomolecules. EIS technique commonly requires counter, reference, and working electrodes. For bioelectronic noses, the surface of the working electrode was immobilized with ORs. The binding of odorants to ORs was measured by recoding the experimental impedance spectrum. Using this principle, EIS-based bioelectronic noses have been successfully developed [86, 87].

1.2.2.4 Planar Microelectrode

Planar microelectrodes have also been used to develop cell-based bioelectronic noses [77]. The cells expressing olfactory receptors are cultured in a chip patterned with planar microelectrodes. After treatment with specific odorants, positive ions flow into the cells. The influx of ions is subsequently transduced into electrical signals through planar electrodes. In addition, the signals could be amplified by electrical stimulation [76]. These results demonstrated the possibility of developing cell-based bioelectronic noses using planar microelectrodes.

1.2.2.5 Field-Effect Transistor

Nanomaterial-based field-effect transistors (FETs) have been used for the development of bioelectronic noses. FET sensors react to the event of changes in charge that occur near the sensing channels and generate highly sensitive responses. In order to improve selectivity, FETs are generally functionalized with diverse types of biomaterials such as OR proteins [45, 46, 70–72], nanovesicles [80, 81], and OR-derived peptides [50]. The binding event between OR and odorant induces changes in charge of the ORs. This change is subsequently converted into highly sensitive electrical signals through nanomaterials [45]. Nanomaterials with semiconducting properties have often been utilized to fabricate the sensing channels of FETs, such as single-walled carbon nanotubes (CNTs), conducting polymer nanotubes

(CPNTs), and graphene. Such sensors were able to detect target odorants in the femto-molar range.

Carbon Nanotubes and Graphene Carbon-based nanomaterials such as CNTs and graphene have been used for bioelectronic noses. CNTs and graphene-based FETs have excellent properties in terms of sensitivity. The limit of detection of graphene-based bioelectronic noses has reached 40 aM [72]. They can be fabricated through a self-assembly process, which means that large-scale production is possible [88]. In 2009, Kim et al. first reported a CNT-based bioelectronic nose [45]. They demonstrated the sensitivity and selectivity of the CNT-based sensor. Following this research, many studies to improve the activity of the sensor and for application to various fields are now being conducted [50, 71, 80, 81, 89, 90]. Detailed information about the CNTs and graphene-based bioelectronic noses is described in Chapter 12.

Conducting Polymer Conducting polymers are also very effective sensing elements. In 2009, polypyrrole nanotubes were first used for the development of a bioelectronic nose [70]. Polypyrrole nanotubes were able to convert the conformational change of ORs into highly sensitive electrical signals. There are many advantages in using conducting polymers as a secondary transducer. The immobilization of biomaterials becomes easier because functional groups such as carboxyl or amine group can be easily incorporated during the polymerization process. Moreover, the conformation of conducting polymers can be effectively modified to enhance the conducting properties of materials. For instance, conducting polymer nanoparticles, rather than nanotubes, have also been utilized to fabricate biosensors [91]. Lastly, conducting polymer is very stable against non-specific influences, which means conducting polymer-based sensors are suitable for practical applications requiring the detection of analytes from real samples [92]. Detailed information about the polymer-based bioelectronic noses is described in Chapter 13.

1.3 Characteristics of Bioelectronic Nose

1.3.1 Sensitivity

The sensitivity toward a specific ligand is one of the most important characteristics of sensors. Artificial olfactory sensors need to be just as sensitive as the human nose. Otherwise, direct sniffing may be more advantageous in terms of sensitivity than using complex equipment. Because the smelling ability of a person is quite excellent, it is a challenge to achieve better sensitivity.

In bioelectronic noses, olfactory receptors assist the accumulation of odorants very close to the secondary transducers and produce primary biological signals. Thus, odorants can be more sensitively detected compared to the sensors without ORs. The sensitivity of bioelectronic noses is dependent on the type of secondary

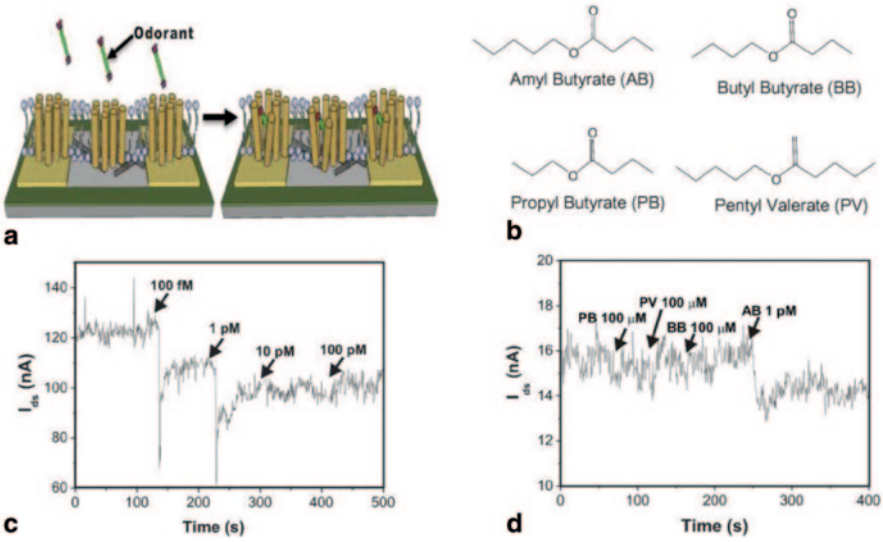

Fig. 1.3 (**a**) Plausible mechanism of odorant binding on a single-walled carbon nanotube field-effect transistor (swCNT-FET) olfactory sensor. (**b**) Structures of odorant molecules. Human olfactory receptor, hOR2AG1 is known to be activated by amyl butyrate (AB). Note that the molecules have the same active groups with a slight difference in their alkyl chain length. (**c**) A real-time conductance measurement obtained from the hOR2AG1-functionalized swCNT-FET sensor after the introduction of AB at various concentrations. Arrows indicate the points of AB injections. (**d**) The selectivity of hOR2AG1-functionalized swCNT-FET sensors. Arrows indicate the points of adding each odorant. (Reprinted from Ref. [45] with permission from John Wiley & Sons Inc.)

transducers. Nanomaterial-based secondary transducers generally show extremely high sensitivity. Kim et al. first reported on an ultrasensitive bioelectronic nose with a detection limit in the femtomolar range by functionalizing CNT-FETs with human ORs (Fig. 1.3) [45]. The binding of odorants to ORs induces the conformational change of ORs, and this conformational change results in changes in the electrical charge. This consequently affects the current of FET sensors (Fig. 1.3a). The sensor could selectively detect 100 fM of its specific odorants (Figs. 1.3c and d). When conducting polymer nanotubes were used as a secondary transducer, the sensitivity was even more improved [70]. The sensitivity of a nanovesicle-based sensor is also very high, because the nanovesicles effectively induce the accumulation of charged ions close to the sensing channel. The sensitivity of nanovesicle-based bioelectronic noses reached 1 fM [80, 81].

Recently, 40 aM detection was possible using human ORs and graphene-based FET platforms [72]. Graphene was treated with oxygen and ammonia plasma to control the bandgap of graphene. Then, OR was conjugated with oxygen plasma-treated (OR-OG) and ammonia plasma-treated (OR-NG) graphenes. Once the conformation of OR changes to an active form, the charge of OR also changes (Fig. 1.4a). The odorants were detected by measuring the change in charge using a graphene-FET. The sensor was able to detect 0.04 fM of amyl butyrate (AB), a specific ligand of the OR used (Fig. 1.4b).

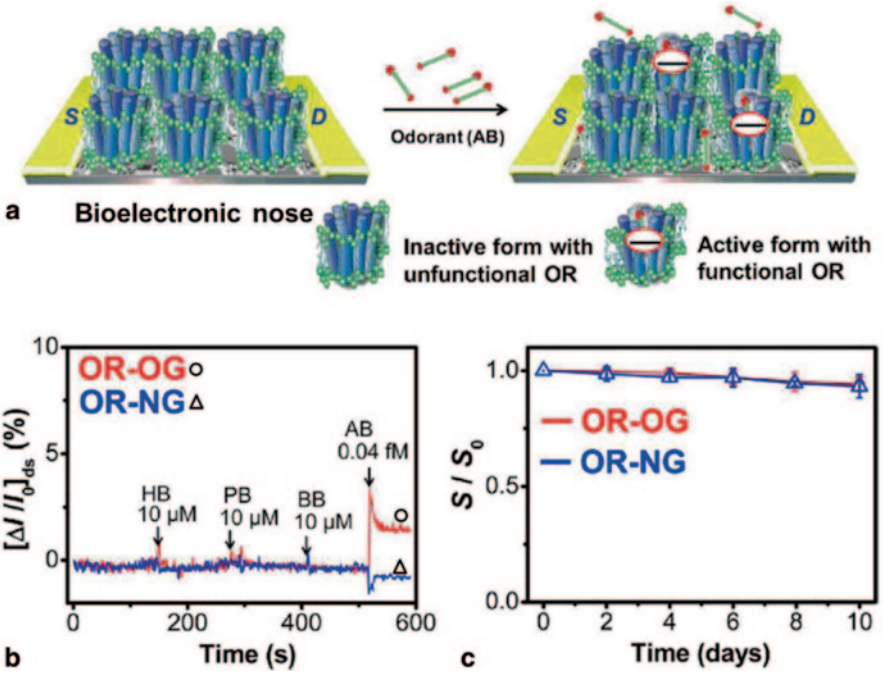

Fig. 1.4 (**a**) Plausible binding mechanism of bioelectronic nose through active and inactive olfactory receptor (OR) forms. (**b**) Selective responses of oxygen plasma-treated graphene with OR (OR-OG) and ammonia plasma-treated graphene with OR (OR-NG) upon addition of nontargets (hexyl butyrate, HB; propyl butylate, PB; butyl butyrate, BB) and target (amyl butylate, AB) odorant. This indicates that OR-OG has the atomic-resolution detection of odorant molecules. (**c**) Storage test of the OR-OG and OR-NG. (Reprinted from Ref. [72] with permission from Copyright (2012) American Chemical Society)

In the case of gas-sensing bioelectronic noses, the most sensitive sensor was reported by Lee et al. in 2012. The sensor was fabricated with human ORs and CPNT-FETs, and was able to detect 0.02 parts-per-trillion (ppt) of gaseous odorants [46]. This sensitivity was comparable to that of a human expert.

1.3.2 Selectivity

The advantage of biosensors is commonly regarded to be selectivity, the ability to specifically detect target molecules. Bioelectronic noses are able to selectively detect their ligand molecules among a mixture of other compounds. The selectivity is derived from the characteristics of ORs. Compared to other biomolecules, ORs have a higher capability to discriminate small chemicals. They can even distinguish the difference of one carbon atom [45]. The selectivity of a bioelectronic nose is presented in Fig. 1.3d. The sensor precisely recognizes amyl butyrate, a specific

ligand of the OR used, from other analogous compounds such as butyl butyrate, propyl butyrate, and pentyl valerate. The only difference between amyl butyrate and the analogous molecules is their alkyl chain length. The selectivity of cell-based or nanovesicle-based bioelectronic noses is also excellent because they generate responses through the original olfactory signaling pathway, as well as utilize the membrane-integrated intact OR proteins [80].

Due to the excellent selectivity of bioelectronic noses, they can be utilized for interesting purposes such as the determination of food quality. In 2012, it was demonstrated that the bioelectronic nose was able to determine the freshness of foods by selectively detecting the specific odorants generated from the decomposition of fatty acids [81]. Sankaran et al. reported that the unique odor from meats contaminated by *salmonella* could be detected using QCMs and peptide receptors derived from an odorant-binding protein (OBP) [64]. In addition, the odor from spoiled seafood was distinguished among odors from other spoiled foods by using peptide receptors derived from a canine olfactory receptor, as shown in Fig. 1.5 [50]. Numerous compounds are contained in real food samples. However, the bioelectronic nose selectively recognizes target odorants. For the determination of seafood quality, the sensor requires to selectively detect trimethylamine, an indicator of seafood decomposition [93]. Although the seafood sample had not been pretreated, the sensor reproducibly and repeatedly detected the trimethylamine contained in spoiled oyster samples (Fig. 1.5a). Also, the degree of spoilage of the three spoiled seafood samples was quantitatively determined (Figs. 1.5b and c). Furthermore, the sensor was able to distinguish spoiled seafood from other types of spoiled food samples and fresh seafood samples (Fig. 1.5d). This selectivity is a specific characteristic of the bioelectronic nose, which was functionalized with a highly selective OR.

1.3.3 Human-like Behavior

Since the bioelectronic nose utilizes the original ORs, it shows human-like behaviors. Lee et al. functionalized CPNT-based FETs with human ORs, and demonstrated that the sensor was able to recognize odorants with human nose-like characteristics [46]. First, they compared sensor responses generated by the OR-based bioelectronic nose to the normalized cell responses generated by the cellular signal transduction (Fig. 1.6a). The recognition pattern by the sensor against several odorants is very similar to that by the cellular signals. Because the signals generated from the cells represent the natural odor response of the human nose, it was verified that the sensor was able to recognize the odorants with human nose-like characteristics. The antagonism of ORs was also demonstrated. ORs can modulate more complex reactions such as antagonism [94]. The binding between OR proteins and agonists, a specific ligand, is interrupted by antagonists. The methylcinnamaldehyde (MCA) and hydrocinnamaldehyde (HCA) are the antagonists of the OR that were used [95]. The response intensities measured by the bioelectronic nose decreased with an increase in concentrations of MCA and HCA (Fig. 1.6b). This result clearly represents

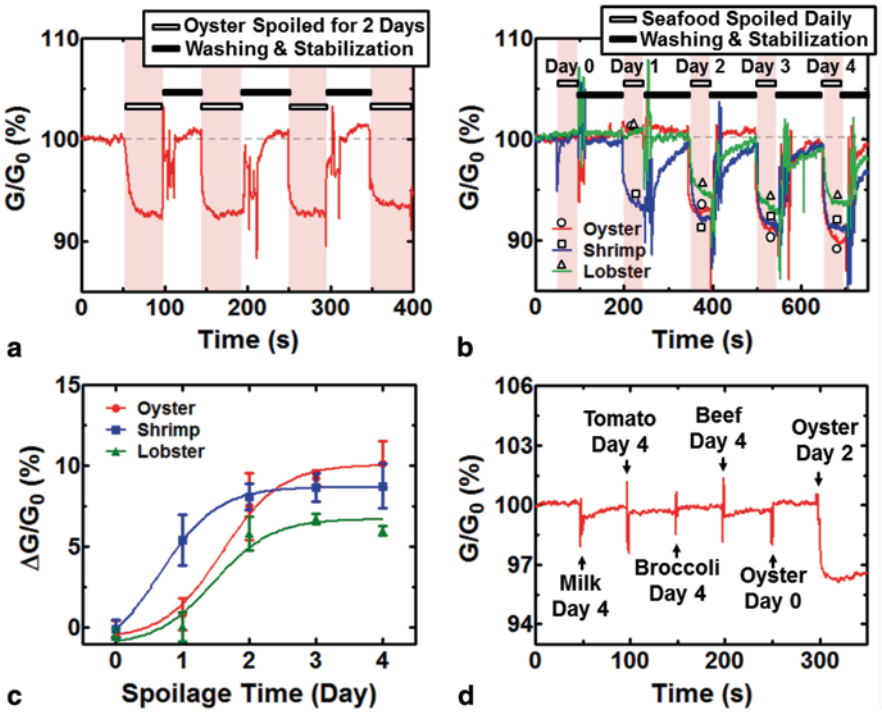

Fig. 1.5 Detection of trimethylamine (TMA) from spoiled seafood using peptide receptor-based bioelectronic noses. (**a**) A real-time measurement data exhibiting the conductance change generated by repeated treatments with a spoiled oyster sample, which was produced by storing the oyster sample at 25 °C for 2 days. Consistent and prompt responses were generated by the four treatments. The *gray dotted line* represents the initial base line. (**b**) Real-time measurements of conductance changes generated by treatments with oyster (*red line*), shrimp (*blue line*), and lobster (*green line*) samples spoiled for different periods of time. Significant decreases in the conductance were observed for the 2 day-spoiled oyster, 1 day-spoiled shrimp, and 2 day-spoiled lobster and the responses increased with an increase in the spoilage time. (**c**) Response patterns versus the degree of spoilage of the three spoiled seafood samples (oyster, shrimp, and lobster). The generated responses tended to increase with the degree of spoilage. (**d**) Real-time recognition and distinction of spoiled oyster from other types of spoiled foods (milk, tomato, broccoli, and beef) and fresh oyster. The sample solutions of milk, tomato, broccoli, and beef spoiled for 4 days and the fresh oyster had no significant effect on the conductance. However, the injection of the oyster sample that had been spoiled for 2 days caused a sharp decrease in conductance. For interpretation of the references to color in this figure legend, the reader is referred to the web version of this article. (Reprinted from Ref. [50] with permission from Elsevier)

that the antagonism can occur in the bioelectronic nose, and that the function of the OR remained entirely in the sensor system.

Human-like bioelectronic tongues have also been developed using human taste receptor [90, 92]. The structure of bitter taste receptors is very similar to that of ORs. Thus, a bioelectronic tongue can be fabricated through the same process as that of the bioelectronic nose. The bitter taste receptor was produced from *E. coli*,

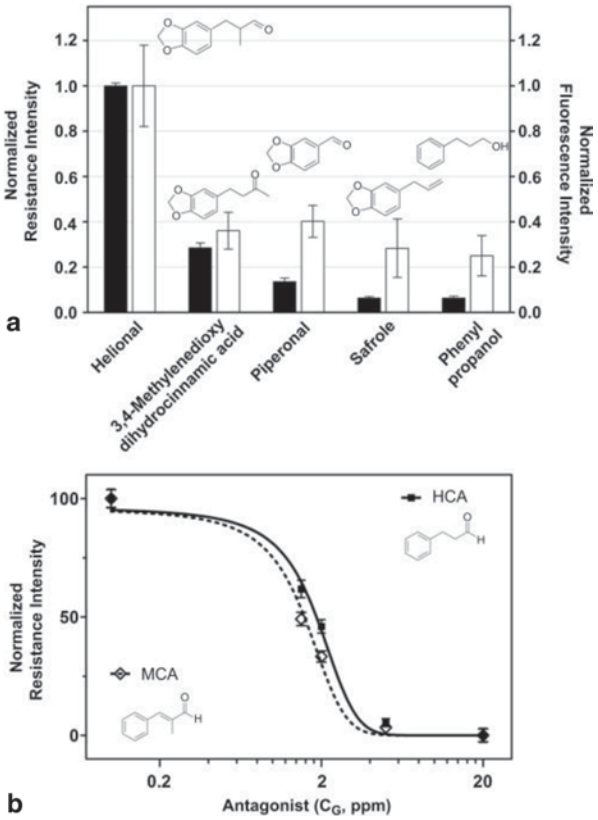

Fig. 1.6 Biological characterization of bioelectronics nose. (**a**) Relative specificity of bioelectronic nose. Magnitudes of different odorants normalized to the helional response measured by two different assays. Y-axis represents responses as a percentage of the response to helional. Helional is known to specifically bind to hOR3A1, the OR that was used for this experiment. Black-filled bar and white-filled bar represent the normalized response of the bioelectronic nose and the normalized value of the cellular signal transduction response, respectively. For the cellular signal transduction response, intracellular calcium was measured in the HEK-293 cells expressing hOR3A1 through a fluorescence cellular assay. Note that other odorant molecules used in this experiment have a similar structure with only subtle differences. (**b**) Inhibition of odorant-induced bioelectronic nose responses by antagonists, methylcinnamaldehyde (MCA) and hydrocinnamaldehyde (HCA). Each point represents the mean ± SEM of five to six experiments. Helional (2 ppm) was mixed with each antagonist at the appropriate concentrations in the liquid phase, and the odorant cocktail was then evaporated in the bubbler through N_2 gas purging. (Reprinted from Ref. [46] with permission from Elsevier)

and used for the functionalization of nanomaterial-based FETs. When human bitter taste receptor was used as a primary sensing element, the sensor also showed human tongue-like behaviors. The sensor was able to not only selectively discriminate bitter substances, but also quantitatively measure the bitterness of vegetables [92]. Human sweet taste receptor has a more complex structure than olfactory or bitter taste

receptors. The sweet taste receptor exists in a heterodimer form consisting of two different receptor molecules [96]. Thus, a nanovesicle-based approach, rather than a receptor-based sensor, is necessary for the development of a sweet taste biosensor. Like a human tongue, it generated more sensitive responses to artificial sweeteners such as aspartame and saccharin than natural sugars (unpublished results). These human-like behaviors are unique characteristics that electronic devices can never have if biological receptors are not utilized.

1.3.4 Stability

The stability of sensors is the most serious bottleneck in the practical application of biosensors. Proteins are functional only if they maintain their own three-dimensional structures. OR protein is a transmembrane protein that requires a lipid membrane for proper structure and function [53]. Thus, ORs easily lose their functions by many external factors, such as heat and physical forces, which can affect the structure of OR proteins.

Interesting results on the stability of OR-based bioelectronic noses have been reported. Song et al. reported a method for the expression and purification of whole OR proteins using an *E. coli* expression system [61]. It was regarded that OR proteins are difficult to be overexpressed and purified in *E. coil* due to its strong hydrophobicity and complicated structure. However, full-length of OR could be overexpressed by the assistance of fusion protein tag and the selection of an appropriate expression vector. ORs produced in *E. coli* were able to be stored in a freezer without any loss in their activities for more than 1 year [70]. This means that the storage lifetime of the OR-based bioelectronic noses may be more than 1 year under proper storage conditions, because sensor platforms, a secondary transducer, generally have a much better stability than biomolecules. In addition, the whole OR protein-based sensor kept in practical conditions also showed a good stability. Although the sensor was stored at 25 °C for 10 weeks, the sensitivity of the sensor maintained more than 60 % [46]. Also, the sensor fabricated with OR and graphene-FET showed excellent stability (Fig. 1.4c) [72].

In order to achieve better stability, peptide fragments derived from OR proteins or OBPs have been used instead of whole proteins for the functionalization of secondary transducers [50, 64]. Small peptides commonly do not require a tertiary structure and lipid membrane. Thus, the stability and repeatability of the biosensor can be improved.

1.4 Current Trends in Bioelectronic Noses

Bioelectronic noses cannot yet be extensively used in all areas where a person can smell. This is because the functions of all ORs have not yet been fully revealed. Three hundred and ninety types of human ORs react to different odorants. Moreover,

numerous odorants can affect ORs. Thus, incalculable combinations between ORs and odorants exist, and the relationship should be investigated further [97]. Following the further investigation of the specific function of ORs, the application area of bioelectronic noses will continue to grow.

Another current issue is the detection of gaseous odorants. In actual olfaction, the binding event between ORs and odorants occurs in the nasal mucus, an aqueous solution [27]. Although most odorants are hydrophobic and well-vaporized, odorants can dissolve well in mucus due to OBPs naturally existing in mucus [98, 99]. Thus, studies on OBPs are currently being conducted. Also, if ORs are active in dry conditions, the problem can be easily solved. Since most proteins are functional in aqueous solutions, it is challenging to make active ORs in dry conditions using nanodiscs or amphipols [100].

The most interesting thing in bioelectronic noses is that OR-based sensors can mimic the olfactory system. Types of odors have not yet been fundamentally and scientifically classified. Thus, there is no other choice but to recognize specific odors based on personal experience. However, bioelectronic noses will offer a way to classify odors. Each odor has a unique response pattern with activated ORs [28, 97]. A sensor functionalized with a multi-array of all types of ORs can represent whole response patterns *in vitro*. This means that bioelectronic noses can classify the types of odor without the help of the human nose. Thus, multi-array sensor platforms are being developed to fundamentally understand the characteristics of odors.

Other G protein-coupled receptors (GPCRs) such as taste receptors and hormone receptors can be utilized for the development of biosensor systems through the same strategy as that of the bioelectronic noses [89–92]. Most GPCRs, regardless of their GPCR classes, can be produced in mammalian cells or *E. coli,* similar to the expression of ORs. The hybridization between receptors and secondary transducers has facilitated the development of highly sensitive and selective biosensor systems. A bioelectronic tongue fabricated with human bitter taste receptors and FETs was able to selectively detect bitter compounds at concentrations as low as 1 fM [90, 92]. Moreover, target tastants were efficiently detected in a mixture and a real food sample [92]. Human parathyroid hormone receptors (hPTHRs) were also expressed in *E. coli* and used for the functionalization of conducting polymer nanoparticle-based FETs [91]. hPTHR is a class B GPCR, while OR is a class A GPCR [101]. Even though class B GPCRs have larger size and more complicated structure compared to class A GPCRs, functional hPTHRs were successfully overexpressed in *E. coli*. The biosensor based on hPTHRs sensitively and selectively detected hPTHs, as shown in Fig. 1.7. In this case, the secondary sensing material was conducting polymer nanoparticles, and the particle size had been modulated to improve the sensitivity. The small nanoparticles (20-nm diameter) detected hPTH more sensitively than the larger nanoparticles (60 or 100-nm diameter) (Figs. 1.7a and b). Moreover, the sensor had excellent selectivity capable of discriminating hPTH among other hormones, such as GLP-1, glucagon, and secretin (Figs. 1.7c and d). All these results indicate that the devices functionalized with GPCRs will allow us to develop not only bioelectronic noses and tongues, but also other biosensors for disease diagnosis.

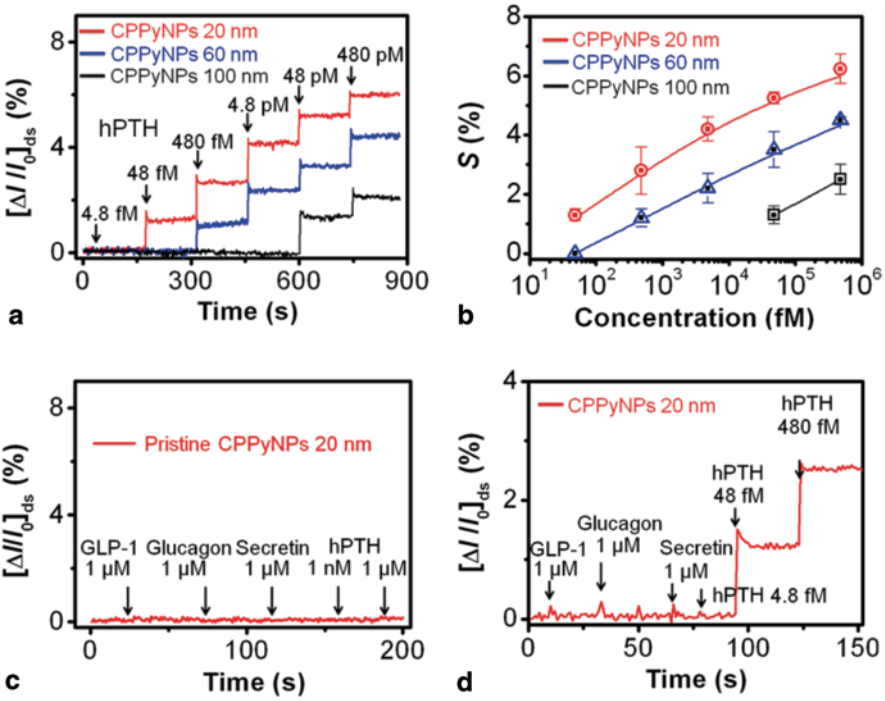

Fig. 1.7 (**a**) Real-time responses with normalized current changes ($\Delta I/I_0 = (I - I_0)/I_0$, where I_0 is the initial current and I is the instantaneous current) and (**b**) calibration curves of human parathyroid hormone receptors and conducting polypyrrol nanoparticle (hPTHR-CPPyNP)-based hormone sensors toward various human parathyroid hormone (hPTH) concentrations (S indicates the normalized current change). (**c**) Real-time responses of the pristine CPPyNP (20 nm) sensor without hPTHR measured at V_{SD} = 10 mV. Normalized I_{SD} changes upon addition of target (hPTH) and nontarget (GLP-1, glucagon, and secretin) analytes. (**d**) Selective responses of the hormone sensor using hPTHR-CPPyNP 20 nm toward nontarget (GLP-1, glucagon, and secretin) and target analytes. (Reprinted from Ref. [91] with permission from Copyright (2012) American Chemical Society)

Detailed information about bioelectronic noses is described in this book. There are not only basic explanations of concepts ranging from the mechanism of olfaction to the principles of sensor platforms, but also various applications that were recently attempted. Readers can find information about the latest technical progress on the development of bioelectronic noses and current issues on practical applications.

Acknowledgments This work was supported by the National Research Foundation of Korea (NRF) grant funded by the Ministry of Science, ICT & Future Planning (No. 2013003890).

References

1. Zhang X, Firestein S (2002) The olfactory receptor gene superfamily of the mouse. Nat Neurosci 5(2):124–133
2. Godfrey PA, Malnic B, Buck LB (2004) The mouse olfactory receptor gene family. Proc Natl Acad Sci U S A 101(7):2156–2161
3. Quignon P, Giraud M, Rimbault M, Lavigne P, Tacher S, Morin E, Retout E, Valin A-S, Lindblad-Toh K, Nicolas J, Galibert F (2005) The dog and rat olfactory receptor repertoires. Genome Biol 6(10):R83
4. Ashton EH, Eayrs JT, Moulton DG (1957) Olfactory acuity in the dog. Nature 179(4569):1069–1070
5. Moulton DG, Ashton EH, Eayrs JT (1960) Studies in olfactory acuity. 4. Relative detectability of n-aliphatic acids by the dog. Anim Behav 8(3–4):117–128
6. Furton KG, Myers LJ (2001) The scientific foundation and efficacy of the use of canines as chemical detectors for explosives. Talanta 54(3):487–500
7. Gazit I, Lavner Y, Bloch G, Azulai O, Goldblatt A, Terkel J (2003) A simple system for the remote detection and analysis of sniffing in explosives detection dogs. Behav Res Methods Instrum Comput 35(1):82–89
8. Cornu J-N, Cancel-Tassin G, Ondet V, Girardet C, Cussenot O (2011) Olfactory detection of prostate cancer by dogs sniffing urine: a step forward in early diagnosis. Eur Urol 59(2):197–201
9. Ehmann R, Boedeker E, Friedrich U, Sagert J, Dippon J, Friedel G, Walles T (2012) Canine scent detection in the diagnosis of lung cancer: revisiting a puzzling phenomenon. Eur Respir J 39(3):669–676
10. McCulloch M, Jezierski T, Broffman M, Hubbard A, Turner K, Janecki T (2006) Diagnostic accuracy of canine scent detection in early- and late-stage lung and breast cancers. Integr Cancer Ther 5(1):30–39
11. Bodyak N, Slotnick B (1999) Performance of mice in an automated olfactometer: odor detection, discrimination and odor memory. Chem Senses 24(6):637–645
12. Clarke S, Trowill JA (1971) Sniffing and motivated behavior in the rat. Physiol Behav 6(1):49–52
13. Uchida N, Mainen ZF (2003) Speed and accuracy of olfactory discrimination in the rat. Nat Neurosci 6(11):1224–1229
14. Youngentob SL, Mozell MM, Sheehe PR, Hornung DE (1987) A quantitative analysis of sniffing strategies in rats performing odor detection tasks. Physiol Behav 41(1):59–69
15. Hu J, Zhong C, Ding C, Chi Q, Walz A, Mombaerts P, Matsunami H, Luo M (2007) Detection of near-atmospheric concentrations of CO2 by an olfactory subsystem in the mouse. Science 317(5840):953–957
16. Dalton P (2000) Psychophysical and behavioral characteristics of olfactory adaptation. Chem Senses 25(4):487–492
17. O'Mahony M (1986) Sensory adaptation. J Sens Stud 1(3–4):237–258
18. Persaud K, Dodd G (1982) Analysis of discrimination mechanisms in the mammalian olfactory system using a model nose. Nature 299(5881):352–355
19. Freund MS, Lewis NS (1995) A chemically diverse conducting polymer-based "electronic nose". Proc Natl Acad Sci U S A 92(7):2652–2656
20. Gardner JW, Shurmer HV, Tan TT (1992) Application of an electronic nose to the discrimination of coffees. Sensor Actuat B-Chem 6(1–3):71–75
21. Pearce TC, Gardner JW, Friel S, Bartlett PN, Blair N (1993) Electronic nose for monitoring the flavour of beers. Analyst 118(4):371–377
22. Gardner JW, Hines EL, Wilkinson M (1990) Application of artificial neural networks to an electronic olfactory system. Meas Sci Technol 1(5):446
23. Shurmer H, Fard A, Barker J, Bartlett P, Dodd G, Hayat U (1987) Development of an electronic nose. Phys Technol 18(4):170

24. Buck LB, Axel R (1991) A novel multigene family may encode odorant receptors: a molecular basis for odor recognition. Cell 65(1):175–187
25. Ressler KJ, Sullivan SL, Buck LB (1993) A zonal organization of odorant receptor gene expression in the olfactory epithelium. Cell 73(3):597–609
26. Ressler KJ, Sullivan SL, Buck LB (1994) Information coding in the olfactory system: Evidence for a stereotyped and highly organized epitope map in the olfactory bulb. Cell 79(7):1245–1255
27. Firestein S (2001) How the olfactory system makes sense of scents. Nature 413(6852):211–218
28. Malnic B, Hirono J, Sato T, Buck LB (1999) Combinatorial receptor codes for odors. Cell 96(5):713–723
29. Branca A, Simonian P, Ferrante M, Novas E, Negri RMn (2003) Electronic nose based discrimination of a perfumery compound in a fragrance. Sens Actuat B-Chem 92(1–2):222–227
30. Oh EH, Song HS, Park TH (2011) Recent advances in electronic and bioelectronic noses and their biomedical applications. Enzyme Microb Technol 48(6–7):427–437
31. Capone S, Siciliano P, Quaranta F, Rella R, Epifani M, Vasanelli L (2000) Analysis of vapours and foods by means of an electronic nose based on a sol–gel metal oxide sensors array. Sens Actuators B-Chem 69(3):230–235
32. Cerrato Oliveros MC, Pérez Pavón JL, García Pinto C, Fernández Laespada ME, Moreno Cordero B, Forina M (2002) Electronic nose based on metal oxide semiconductor sensors as a fast alternative for the detection of adulteration of virgin olive oils. Anal Chim Acta 459(2):219–228
33. Dutta R, Hines EL, Gardner JW, Kashwan KR, Bhuyan M (2003) Tea quality prediction using a tin oxide-based electronic nose: an artificial intelligence approach. Sens Actuat B-Chem 94(2):228–237
34. El Barbri N, Amari A, Vinaixa M, Bouchikhi B, Correig X, Llobet E (2007) Building of a metal oxide gas sensor-based electronic nose to assess the freshness of sardines under cold storage. Sens Actuat B-Chem 128(1):235–244
35. González Martín Y, Cerrato Oliveros MC, Pérez Pavón JL, García Pinto C, Moreno Cordero B (2001) Electronic nose based on metal oxide semiconductor sensors and pattern recognition techniques: characterisation of vegetable oils. Anal Chimica Acta 449(1–2):69–80
36. Crone B, Dodabalapur A, Gelperin A, Torsi L, Katz HE, Lovinger AJ, Bao Z (2001) Electronic sensing of vapors with organic transistors. Appl Phys Lett 78(15):2229–2231
37. Doleman BJ, Lewis NS (2001) Comparison of odor detection thresholds and odor discriminablities of a conducting polymer composite electronic nose versus mammalian olfaction. Sens Actuat B-Chem 72(1):41–50
38. Hatfield JV, Neaves P, Hicks PJ, Persaud K, Travers P (1994) Towards an integrated electronic nose using conducting polymer sensors. Sens Actuat B-Chem 18(1–3):221–228
39. Torsi L, Dodabalapur A, Sabbatini L, Zambonin PG (2000) Multi-parameter gas sensors based on organic thin-film-transistors. Sens Actuat B-Chem 67(3):312–316
40. Hao HC, Tang KT, Ku PH, Chao JS, Li CH, Yang CM, Yao DJ (2010) Development of a portable electronic nose based on chemical surface acoustic wave array with multiplexed oscillator and readout electronics. Sens Actuat B-Chem 146(2):545–553
41. Gan HL, Man YBC, Tan CP, NorAini I, Nazimah SAH (2005) Characterisation of vegetable oils by surface acoustic wave sensing electronic nose. Food Chem 89(4):507–518
42. García M, Fernández MJ, Fontecha JL, Lozano J, Santos JP, Aleixandre M, Sayago I, Gutiérrez J, Horrillo MC (2006) Differentiation of red wines using an electronic nose based on surface acoustic wave devices. Talanta 68(4):1162–1165
43. Li C, Heinemann P, Sherry R (2007) Neural network and Bayesian network fusion models to fuse electronic nose and surface acoustic wave sensor data for apple defect detection. Sens Actuat B-Chem 125(1):301–310
44. Göpel W (1998) Chemical imaging: I. Concepts and visions for electronic and bioelectronic noses. Sens Actuat B-Chem 52(1–2):125–142
45. Kim TH, Lee SH, Lee J, Song HS, Oh EH, Park TH, Hong S (2009) Single-carbon-atomic-resolution detection of odorant molecules using a human olfactory receptor-based bioelectronic nose. Adv Mater 21(1):91–94

46. Lee SH, Kwon OS, Song HS, Park SJ, Sung JH, Jang J, Park TH (2012) Mimicking the human smell sensing mechanism with an artificial nose platform. Biomaterials 33(6):1722–1729
47. Lee SH, Park TH (2010) Recent advances in the development of bioelectronic nose. Biotechnol Bioprocess Eng 15(1):22–29
48. Malnic B, Godfrey PA, Buck LB (2004) The human olfactory receptor gene family. Proc Natl Acad Sci U S A 101(8):2584–2589
49. Buck LB (2004) Olfactory receptors and odor coding in mammals. Nutr Rev 62:S184–S188
50. Lim JH, Park J, Ahn JH, Jin HJ, Hong S, Park TH (2013) A peptide receptor-based bioelectronic nose for the real-time determination of seafood quality. Biosens Bioelectron 39(1):244–249
51. Kiefer H, Krieger J, Olszewski JD, von Heijne G, Prestwich GD, Breer H (1996) Expression of an olfactory receptor in Escherichia coli: purification, reconstitution, and ligand binding. Biochemistry 35(50):16077–16084
52. Ko HJ, Park TH (2006) Dual signal transduction mediated by a single type of olfactory receptor expressed in a heterologous system. Biol Chem, 387(1):59–68
53. Krautwurst D, Yau K-W, Reed RR (1998) Identification of ligands for olfactory receptors by functional expression of a receptor library. Cell 95(7):917–926
54. Zhao H, Ivic L, Otaki JM, Hashimoto M, Mikoshiba K, Firestein S (1998) Functional expression of a mammalian odorant receptor. Science 279(5348):237–242
55. Wu L, Pan Y, Chen G-Q, Matsunami H, Zhuang H (2012) Receptor-transporting Protein 1 short (RTP1S) mediates translocation and activation of odorant receptors by acting through multiple steps. J Biol Chem 287(26):22287–22294
56. Zhuang H, Matsunami H (2007) Synergism of accessory factors in functional expression of mammalian odorant receptors. J Biol Chem 282(20):15284–15293
57. Zhuang H, Matsunami H (2008) Evaluating cell-surface expression and measuring activation of mammalian odorant receptors in heterologous cells. Nat Protoc 3(9):1402–1413
58. Kiely A, Authier A, Kralicek AV, Warr CG, Newcomb RD (2007) Functional analysis of a Drosophila melanogaster olfactory receptor expressed in Sf9 cells. J Neurosci Methods 159(2):189–194
59. Matarazzo V, Clot-Faybesse O, Marcet B, Guiraudie-Capraz G, Atanasova B, Devauchelle G, Cerutti M, Etiévant P, Ronin C (2005) Functional characterization of two human olfactory receptors expressed in the baculovirus Sf9 insect cell system. Chem Sens 30(3):195–207
60. Minic J, Persuy MA, Godel E, Aioun J, Connerton I, Salesse R, Pajot-Augy E (2005) Functional expression of olfactory receptors in yeast and development of a bioassay for odorant screening. FEBS J 272(2):524–537
61. Song HS, Lee SH, Oh EH, Park TH (2009) Expression, solubilization and purification of a human olfactory receptor from Escherichia coli. Curr Microbiol 59(3):309–314
62. Ko HJ, Park TH (2005) Piezoelectric olfactory biosensor: ligand specificity and dose-dependence of an olfactory receptor expressed in a heterologous cell system. Biosens Bioelectron 20(7):1327–1332
63. Sankaran S, Panigrahi S, Mallik S (2011) Olfactory receptor based piezoelectric biosensors for detection of alcohols related to food safety applications. Sens Actuat B-Chem 155(1):8–18
64. Sankaran S, Panigrahi S, Mallik S (2011) Odorant binding protein based biomimetic sensors for detection of alcohols associated with Salmonella contamination in packaged beef. Biosens Bioelectron 26(7):3103–3109
65. Sung JH, Ko HJ, Park TH (2006) Piezoelectric biosensor using olfactory receptor protein expressed in Escherichia coli. Biosens Bioelectron 21(10):1981–1986
66. Wu T-Z (1999) A piezoelectric biosensor as an olfactory receptor for odour detection: electronic nose. Biosens Bioelectron 14(1):9–18
67. Benilova I, Chegel V, Ushenin Y, Vidic J, Soldatkin A, Martelet C, Pajot E, Jaffrezic-Renault N (2008) Stimulation of human olfactory receptor 17–40 with odorants probed by surface plasmon resonance. Eur Biophys J 37(6):807–814
68. Vidic J, Pla-Roca M, Grosclaude J, Persuy M-A, Monnerie R, Caballero D, Errachid A, Hou Y, Jaffrezic-Renault N, Salesse R, Pajot-Augy E, Samitier J (2007) Gold surface

functionalization and patterning for specific immobilization of olfactory receptors carried by nanosomes. Anal Chem 79(9):3280–3290
69. Vidic JM, Grosclaude J, Persuy M-A, Aioun J, Salesse R, Pajot-Augy E (2006) Quantitative assessment of olfactory receptors activity in immobilized nanosomes: a novel concept for bioelectronic nose. Lab Chip 6(8):1026–1032
70. Yoon H, Lee SH, Kwon OS, Song HS, Oh EH, Park TH, Jang J (2009) Polypyrrole nanotubes conjugated with human olfactory receptors: high-performance transducers for FET-type bioelectronic noses. Angew Chem Int Ed Engl 48(15):2755–2758
71. Lee SH, Jin HJ, Song HS, Hong S, Park TH (2012) Bioelectronic nose with high sensitivity and selectivity using chemically functionalized carbon nanotube combined with human olfactory receptor. J Biotechnol 157(4):467–472
72. Park SJ, Kwon OS, Lee SH, Song HS, Park TH, Jang J (2012) Ultrasensitive flexible graphene based field-effect transistor (FET)-type bioelectronic nose. Nano Lett 12(10):5082–5090
73. Katada S, Hirokawa T, Oka Y, Suwa M, Touhara K (2005) Structural basis for a broad but selective ligand spectrum of a mouse olfactory receptor: mapping the odorant-binding site. J Neurosci 25(7):1806–1815
74. Wetzel CH, Oles M, Wellerdieck C, Kuczkowiak M, Gisselmann G, Hatt H (1999) Specificity and sensitivity of a human olfactory receptor functionally expressed in human embryonic kidney 293 cells and Xenopus laevis oocytes. J Neurosci 19(17):7426–7433
75. Lee JY, Ko HJ, Lee SH, Park TH (2006) Cell-based measurement of odorant molecules using surface plasmon resonance. Enzyme Microb Technol 39(3):375–380
76. Lee SH, Jeong SH, Jun SB, Kim SJ, Park TH (2009) Enhancement of cellular olfactory signal by electrical stimulation. Electrophoresis 30(18):3283–3288
77. Lee SH, Jun SB, Ko HJ, Kim SJ, Park TH (2009) Cell-based olfactory biosensor using microfabricated planar electrode. Biosens Bioelectron 24(8):2659–2664
78. Lee SH, Ko HJ, Park TH (2009) Real-time monitoring of odorant-induced cellular reactions using surface plasmon resonance. Biosens Bioelectron 25(1):55–60
79. Pick H, Schmid EL, Tairi A-P, Ilegems E, Hovius R, Vogel H (2005) Investigating cellular signaling reactions in single attoliter vesicles. J Am Chem Soc 127(9):2908–2912
80. Jin HJ, Lee SH, Kim TH, Park J, Song HS, Park TH, Hong S (2012) Nanovesicle-based bioelectronic nose platform mimicking human olfactory signal transduction. Biosens Bioelectron 35(1):335–341
81. Park J, Lim JH, Jin HJ, Namgung S, Lee SH, Park TH, Hong S (2012) A bioelectronic sensor based on canine olfactory nanovesicle-carbon nanotube hybrid structures for the fast assessment of food quality. Analyst 137(14):3249–3254
82. Lim JH, Park J, Oh EH, Ko HJ, Hong S, Park TH (2014) Nanovesicle-based bioelectronic nose for the diagnosis of lung cancer from human blood. Adv Healthc Mater 3(3):360–366
83. Auge J, Hauptmann P, Hartmann J, Rösler S, Lucklum R (1995) New design for QCM sensors in liquids. Sens Actuat B-Chem 24(1–3):43–48
84. Resa P, Castro P, Rodríguez-López J, Elvira L (2012) Broadband spike excitation method for in-liquid QCM sensors. Sens Actuat B-Chem 166–167(0):275–280
85. Shen S, Liu T, Guo J (1998) Optical phase-shift detection of surface plasmon resonance. Appl Optics 37(10):1747–1751
86. Benilova IV, Minic Vidic J, Pajot-Augy E, Soldatkin AP, Martelet C, Jaffrezic-Renault N (2008) Electrochemical study of human olfactory receptor OR 17–40 stimulation by odorants in solution. Mater Sci Eng C 28(5–6):633–639
87. Hou Y, Jaffrezic-Renault N, Martelet C, Zhang A, Minic-Vidic J, Gorojankina T, Persuy M-A, Pajot-Augy E, Salesse R, Akimov V, Reggiani L, Pennetta C, Alfinito E, Ruiz O, Gomila G, Samitier J, Errachid A (2007) A novel detection strategy for odorant molecules based on controlled bioengineering of rat olfactory receptor I7. Biosens Bioelectron 22(7):1550–1555
88. Rao SG, Huang L, Setyawan W, Hong S (2003) Nanotube electronics: Large-scale assembly of carbon nanotubes. Nature 425(6953):36–37

89. Kim B, Song HS, Jin HJ, Park EJ, Lee SH, Lee BY, Park TH, Hong S (2013) Highly selective and sensitive detection of neurotransmitters using receptor-modified single-walled carbon nanotube sensors. Nanotechnology 24(28):285501
90. Kim TH, Song HS, Jin HJ, Lee SH, Namgung S, Kim U-k, Park TH, Hong S (2011) "Bioelectronic super-taster" device based on taste receptor-carbon nanotube hybrid structures. Lab Chip 11(13):2262–2267
91. Kwon OS, Ahn SR, Park SJ, Song HS, Lee SH, Lee JS, Hong J-Y, Lee JS, You SA, Yoon H, Park TH, Jang J (2012) Ultrasensitive and selective recognition of peptide hormone using close-packed arrays of hPTHR-conjugated polymer nanoparticles. ACS Nano 6(6):5549–5558
92. Song HS, Kwon OS, Lee SH, Park SJ, Kim U-K, Jang J, Park TH (2012) Human taste receptor-functionalized field effect transistor as a human-like nanobioelectronic tongue. Nano Lett 13(1):172–178
93. Egashira M, Shimizu Y, Takao Y (1990) Trimethylamine sensor based on semiconductive metal oxides for detection of fish freshness. Sens Actuat B-Chem 1(1–6):108–112
94. Oka Y, Omura M, Kataoka H, Touhara K (2004) Olfactory receptor antagonism between odorants. EMBO J 23(1):120–126
95. Jacquier V, Pick H, Vogel H (2006) Characterization of an extended receptive ligand repertoire of the human olfactory receptor OR17-40 comprising structurally related compounds. J Neurochem 97(2):537–544
96. Nelson G, Hoon MA, Chandrashekar J, Zhang Y, Ryba NJP, Zuker CS (2001) Mammalian sweet taste receptors. Cell 106(3):381–390
97. Saito H, Chi Q, Zhuang H, Matsunami H, Mainland JD (2009) Odor coding by a mammalian receptor repertoire. Sci Signal 2(60):ra9
98. Briand L, Eloit C, Nespoulous C, Bézirard V, Huet J-C, Henry C, Blon F, Trotier D, Pernollet J-C (2002) Evidence of an odorant-binding protein in the human olfactory mucus: location, structural characterization, and odorant-binding properties. Biochemistry 41(23):7241–7252
99. Pelosi P (1994) Odorant-binding proteins. Crit Rev Biochem Mol Biol 29(3):199–228
100. Goldsmith BR, Mitala JJ, Josue J, Castro A, Lerner MB, Bayburt TH, Khamis SM, Jones RA, Brand JG, Sligar SG, Luetje CW, Gelperin A, Rhodes PA, Discher BM, Johnson ATC (2011) Biomimetic chemical sensors using nanoelectronic readout of olfactory receptor proteins. ACS Nano 5(7):5408–5416
101. Hoare SRJ (2005) Mechanisms of peptide and nonpeptide ligand binding to Class B G-protein-coupled receptors. Drug Discov Today 10(6):417–427

Chapter 2
Mechanisms of Olfaction

Ruchira Sharma and Hiroaki Matsunami

Abstract Molecular mechanisms of olfaction have been intensively studied in the last quarter century. Receptors by which olfactory stimuli are detected are vastly different between different animal species and even between different olfactory organs of the same species. This chapter includes a description of the anatomy of the mammalian olfactory system and an overview of the receptors. The signaling mechanism and expression pattern of these receptors is discussed along with how the brain decodes olfactory information gathered from the environment and then translates these signals into behaviors. This chapter also contains brief comparison of the fish, insect and nematode olfactory receptors.

2.1 Importance of Olfaction

A sense of smell is crucial for the survival of any species, and in our own experience, we detect dangers like fire or spoilt food with our noses. The hedonistic pleasure derived from eating and drinking is also heavily reliant on the sense of smell. Olfaction is an important tool used in so many facets of animal life and is often the deciding factor between surviving an encounter with a predator, passing on genes to offspring and finding a source of food. Although Santiago Cajal described the peripheral olfactory system in 1891, very little was uncovered about the mechanisms of odor detection and differentiation in the next 100 years, and the olfactory system continues to elude our understanding. The method by which sensory inputs are converted to behavioral output is still a mystery.

R. Sharma (✉) · H. Matsunami
Department of Molecular Genetics and Microbiology, Duke University Medical Center, Durham, NC 27710, USA
e-mail: ruchira.sharma@duke.edu

H. Matsunami
Department of Neurobiology, Duke University Medical Center, Durham, NC 27710, USA

Duke Institute for Brain Sciences, Duke University Medical Center, Durham, NC 27710, USA

T. H. Park (ed.), *Bioelectronic Nose,* DOI 10.1007/978-94-017-8613-3_2,

Phylogenetically, chemosensation such as olfaction and gustation are one of the oldest senses and are important for the simplest to the most complex organisms. Our taste system only allows us to detect and distinguish a limited number of taste modalities: sweet, sour, salty, bitter and umami. In contrast, our sense of smell can detect and distinguish among tens of thousands of volatiles, such as flavors offered to our palate from food. The important role of olfaction in our eating experience was most notably demonstrated in a study where a majority of participants who ate either a piece of apple or boiled potato while wearing a blindfold and a nose plug failed to make the correct identification when asked what they had eaten [2].

Certain odorants released by predators evoke innate avoidance behaviors in animals that have never encountered that predator before. One example of such a phenomenon is trimethylthiazoline (TMT), a chemical found in the feces of the red fox (*Vulpes vulpes*), which causes laboratory bred mice, who have never experienced an external environment, to freeze and display other anxious behaviors [3]. Mating and maternal behavior are both heavily reliant on olfaction as manipulating the olfactory system has been shown to change social behaviors in both vertebrates and invertebrates [4–9]. In fruit flies, the male-specific transcription factor *fruitless* is required for the appropriate functioning of the components of the olfactory system, and in its absence male flies have been shown to court other male flies or to abolish all courtship behaviors. Female rats whose olfactory bulbs are surgically removed have been shown to lose their normal nursing behaviors as well as other maternal behaviors like retrieving pups that have been taken out of their nest, and male rats lose their aggression to non-conspecific male intruders [10–12].

In humans, olfactory dysfunction has been linked to a number of neurodegenerative diseases, primary amongst which are idiopathic Parkinson's disease and Alzheimer's [13, 14]. Our sense of smell is also linked to our limbic system. Hence, there is a strong, but as of yet elusive link between memory, emotion and certain smells that invoke them. Further study of this sensory modality is of vital importance for us to better understand many aspects of our own nature and behavior.

2.2 The Vertebrate Olfactory System

The peripheral olfactory system is comprised of the main olfactory epithelium and the accessory olfactory system, which contains the vomeronasal organ (VNO), the Grueneberg ganglion and the septal organ of Masera in rodents (Fig. 2.1). The main olfactory epithelium's primary function is the detection of volatile odorants in the air [15] whereas the VNO detects semiochemicals such as pheromones [16–18]. The Grueneberg ganglion is implicated in the detection of stress signals from conspecifics [19–21] and the septal organ contains neurons expressing a subset of odorant receptors (ORs) that are also expressed in the ventral domain of the olfactory epithelium [22, 23].

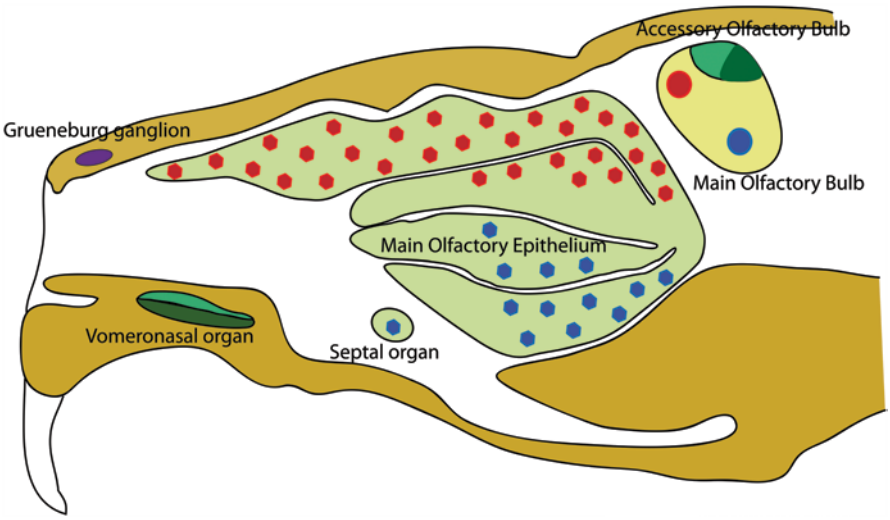

Fig. 2.1 Sagittal view of a mouse head. The anterio-dorsal tip contains the *Grueneberg ganglion*. The VNO is located on the ventral side and is divided into 2 halves, each expressing a unique receptor repertoire, which project to the accessory olfactory bulb located at the distal end of the olfactory bulb. The dorsal receptors in the olfactory epithelium are depicted in *red* and the ventral receptors in *blue*. The areas they project to on the olfactory bulb are labeled with the same *colors*. The septal organ is shown at the ventral base of the nasal septum

2.3 Main Olfactory Epithelium

2.3.1 Anatomy

Neurons responsible for the detection of odors from the environment are found in the olfactory epithelium (OE) located in the dorso-caudal nasal vault along the upper portion of the nasal septum, cribriform plate and the medial wall of the superior turbinate from where they project their dendrites into the nasal passage. These olfactory sensory neurons (OSNs) lie in a pseudostratified columnar epithelium along with supporting cells (sustentacular cells), microvillar cells and basal cells [24]. The epithelium lies on top of a highly vascular lamina propia, which contains the Bowman's gland. Basal cells are stem cells responsible for the replacement of the OSNs and the Bowman's gland is responsible for secreting the serous component of the mucous layer covering the OE [25]. OSNs form a dendritic knob at the junction between the tissue and the nasal passage from which 5 to 20 cilia emerge; these cilia are bathed in the mucus in which odor molecules dissolve and then come in contact with the OR [26]. These cilia lack dynein and therefore do not exhibit any motility. Their main advantage is to increase the surface area of the neuron so as to increase the probability of a molecule encountering its receptor [27]. Mature OSNs are identified by the expression of olfactory marker protein (OMP) [28, 29] and are bipolar cells that project their un-myelinated axons through the cribriform

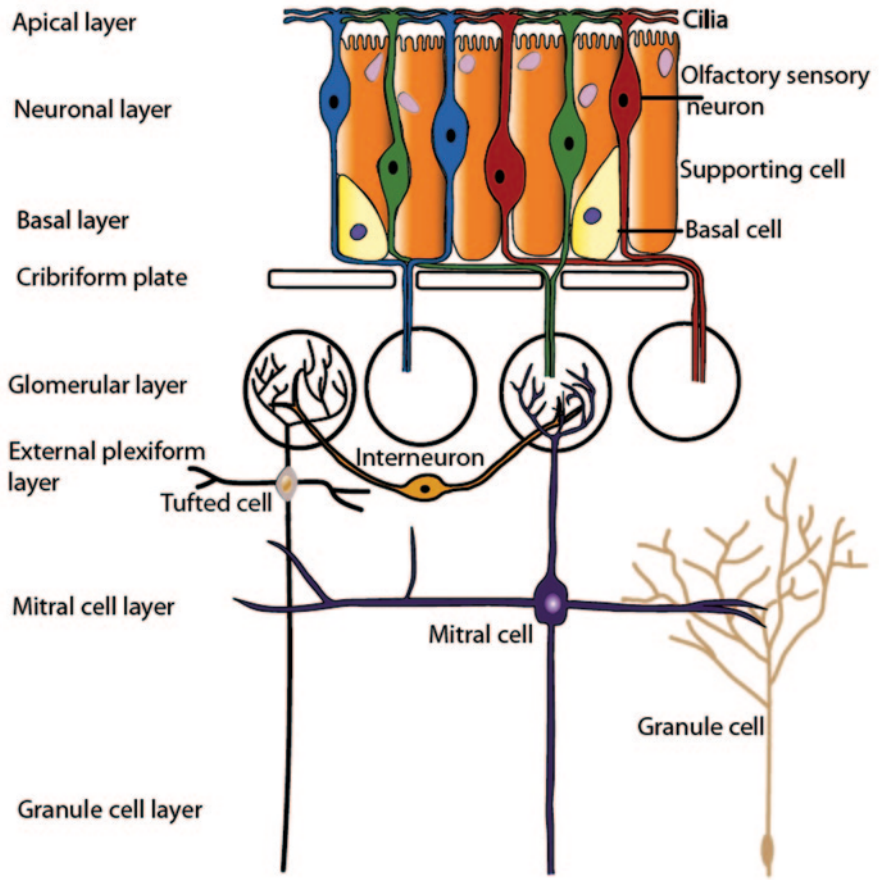

Fig. 2.2 A representation of the cellular organization of the olfactory system. OSNs expressing the same receptors (represented here in the same *color*) project to the same glomeruli, which are innervated by afferent mitral and tufted cells. Interneurons connect neighboring glomeruli and coordinate their response. Supporting cells flank the OSNs while the underlying basal cell layer contains the stem cells from which OSNs are regularly replaced

plate to the olfactory bulb (OB) where they converge with axons from other neurons expressing the same OR to form a single anatomical unit called the glomerulus [30]. (Fig. 2.2) Glomeruli are spheroid structures composed of a cellular shell composed of periglomerular cells surrounding a core of neuropil [31].

2.4 Odorant Receptors

ORs are members of the seven transmembrane domain super family of G protein coupled receptors (GPCR). The number of ORs in different species is highly variable. Most mammals have a very large number of ORs (humans ~400 and mice

~1,000 ORs) while others such as dolphins may only have a handful of ORs, which likely reflects the relative importance of olfaction in a given species [15, 32–34]. Though the ORs contain several conserved motifs, some of which may be important for G-protein coupling, there are many variable sequences in transmembrane and extracellular domains of the protein that come together in the tertiary structure to form a ligand-binding site. The high degree of variability is thought to be important for activation by a structurally diverse set of volatile odor molecules [35].

2.4.1 Receptor Signaling and Termination

The binding of a cognate ligand to its OR releases a specialized stimulatory G protein α subunit called $G_{\alpha olf}$ into the membrane from the βγ subunits [36]. $G_{\alpha olf}$ activates adenylate cyclase III (ACIII), and causes the conversion of ATP into cAMP [37, 38]. This was demonstrated by a rapid increase in cAMP levels when cilia from OSNs were exposed to odorants [39, 40]. A surge in cAMP levels in the neurons leads to the activation of calcium permeable, tetrameric cyclic nucleotide gated (CNG) [41] channels and an influx of Na^+ and Ca^{2+} [42], which in turn leads to an efflux of chloride resulting in the depolarization of the membrane [43]. (Fig. 2.3) Once an action potential has been generated, the cell extrudes Ca^{2+} by Na^+/Ca^{2+} exchangers in order to return to its resting membrane potential [44, 45]. The major subunit of the Ca^{2+} channel was identified as CNGA2 [46] and the Cl^- channel as Ano2/Tmem16b [47–49]. The deletion of CNGA2 causes mice to become anosmic [50] but the deletion of ANO2 does not seem to abolish the sense of smell, although electrophysiological and cell culture experiments show that the OSNs maintain a high baseline of Cl^- concentration and the opening of these channels leads to a low noise, nonlinear amplification of the signal [51–53]. An increase in inositol-1,4,5-trisphosphate (IP3) and cGMP levels is also commensurate with depolarization in some cases [54], although these are produced on a different time scale [46, 55] and may have more to do with desensitization [56].

2.4.2 Desensitization and Adaptation

Constant exposure to a stimulus makes OSNs lose their responsiveness in a process called desensitization or adaptation, which can take place via various negative feedback pathways. CNG channels, ACIII and cAMP hydrolysis by phosphodiesterase are mediated by calcium through a calcium binding protein calmodulin [57–59]. (Fig. 2.3) ORs themselves may be phosphorylated or internalized to desensitize the cell. [60–62]. GRK3 and β arrestin 2 mediate the uncoupling of the OR from its G protein. [62–64]. Incubating OSNs with antibodies to β arrestin 2 and GRK3 leads to elevation of cAMP response in the presence of an odorant [60] and β arrestin 2 has also been shown to be responsible for receptor internalization [61].

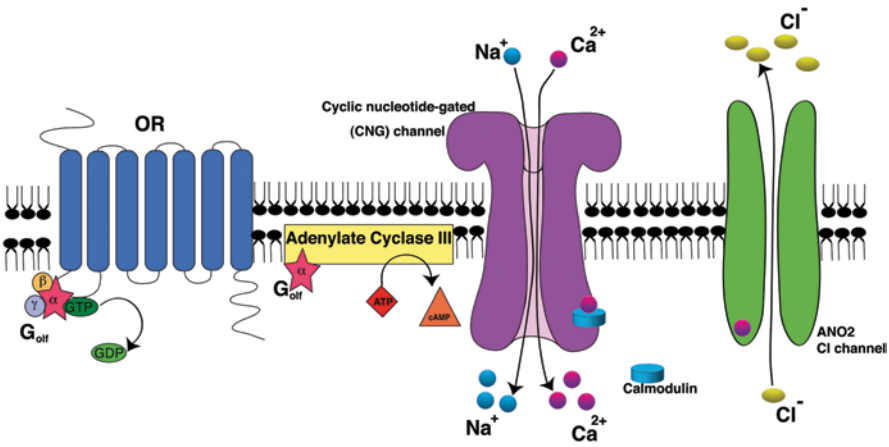

Fig. 2.3 The Olfactory signaling cascade. When activated, the *OR* catalyzes the release of the G_{olf} subunit, which in turn activates ACIII, leading to an increase in the cAMP levels that activate CNGA2, the calcium channel responsible for the depolarization, and the chloride channel Tmem16b that opens after the surge of $Ca2^{+}$ into the cell

2.4.3 Receptor Surface Expression

The vast majority of ORs are still "orphan" receptors, i.e. the ligands that activate those ORs remain unknown. One of the most straightforward ways to study OR-odor interaction would be to first express the OR in cell culture and screen a number of odorous ligands to see which ligands activate the receptor, and then to study common motifs in ORs activated by the same ligand. The main obstacle in this type of study is that ORs in cell culture accumulate in the ER and are not transported to the cell surface [65, 66]. In 2004, studies showed that co-expression of ORs with a family of proteins called RTP (Receptor Transporting Protein) increased the efficiency of the trafficking of receptors to the cell surface [67]. Based on these findings, a heterologous cell assay system was developed for large scale screening with ligands in order to identify active ligands for many ORs [68]. It is now routine to study a single OR and find out which ligands activate it. However, whether the current system allows functional expression of all ORs is unclear.

2.4.4 Receptor Gene Regulation

A single OSN expresses a single allele of one OR [32, 69, 70]. Experiments have shown that OSNs do not express the endogenous OR if a transgene carrying an OR has been forcibly expressed. Additionally, in the case of multiple integrations of the same transgene in tandem, only one of these transgenes is expressed, suggesting

that there are cellular mechanisms limiting expression to only one OR per OSN [71]. The mechanisms used by cells to make this choice remain largely unknown but studies indicate that the epigenetic modification of OR genes as well as the unfolded protein response pathway (UPR) [195] inactivate all but one OR in a given OSN [72–80].

2.4.5 Receptor Expression Zones and Projection of OSN Axons

Examination of OR mRNAs in the OE showed topographically distinct expression patterns that could be broadly divided into two zones along the dorso—ventral axis [70, 81, 82]. Within a zone, it seems that OR expression is largely stochastic, although in the ventral zone there are further subdivisions into several overlapping zones [83]. OR genes are divided into class I and class II receptors based on their phylogeny with class I being expressed in the dorsal zone [84, 85]. Microdissection followed by microarray experiments showed about 300 class II receptors expressed in the dorsal epithelium while the remaining are expressed in the ventral zone [83]. Axons from OSNs expressing the same receptors converge and project to a few glomeruli in the OB. Axon targeting is primarily controlled by gradients of molecules divided into 2 major classes. Class I molecules include Neuropilin-1 and Plexin-A1, which establish the anterior-posterior axis, while class II molecules like Kirrel2 and Kirrel3 aid in activity-dependent refined sorting. More recently the deletion of BIG −2, which is only expressed in a subset of OSNs, lead to the erroneous innervation of glomeruli by those axons [86]. ORs play a pivotal role in axon targeting because the expression of some axon targeting molecules depends on the cAMP levels, which are in turn modulated by a functioning OR [87–91]. (Fig. 2.3) In the case of a non-functioning OR, the cAMP levels are low and the axon is often unable to converge and find its position; such OSNs undergo apoptosis [91, 92]. Compromised cilia in the OE lead to aberrant axon targeting in the OB, suggesting proper OSN activation is also important in this process [93]. Studies have shown that the OR itself does not have a unique role in axon targeting as replacing an OR with a functional G protein-like β adrenergic receptor leads to an ectopic but seemingly functional glomerulus [90].

The organization of the glomeruli follows the logic of the epithelium where all the dorsal receptors project to the dorsal portion of the OB, while the class II ventral receptors project to the ventral portion of the bulb. The glomeruli in the OB are connected to one another by the dendro-dendritic connections of local inhibitory interneurons found in the glomerular layer [94–96]. It seems that these neurons are capable of silencing neighboring glomeruli responding with lower intensity to the same odor in order to reduce redundancy [97]. Mitral and tufted cells are long distance projection neurons that sample information from glomeruli with their dendrites and project their axons in the olfactory tract to the primary olfactory cortex in the brain [98]. (Fig. 2.2) The primary olfactory cortex is defined by the accessory

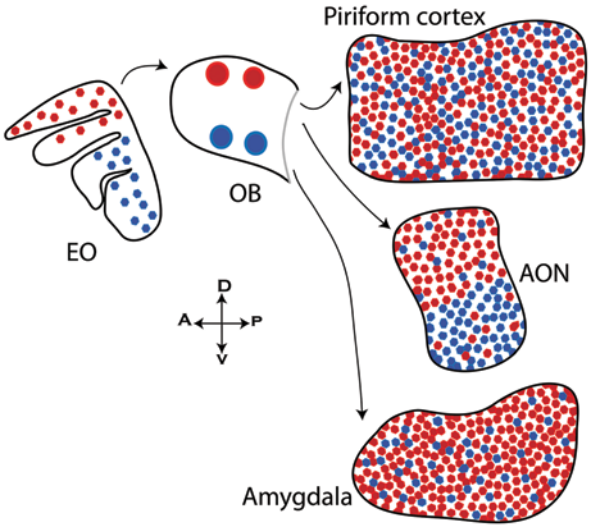

Fig. 2.4 OSNs expressing dorsal receptors project to the dorsal portion of the *OB*, and the same logic applies to the ventral receptors. The projections from the *OB* to the accessory olfactory nucleus (*AON*) also have the same pattern with the dorsal glomeruli projecting to the dorsal regions in the *AON*. On the other hand, the projections to the piriform seem to be organized randomly, and the projections to the *amygdala* are heavily biased towards the dorsal glomeruli

olfactory nucleus, piriform cortex, lateral enterorhinal cortex, olfactory tubercle and the amygdala [99]. Projections from the primary cortex are diffused over the brain and project to a large number of regions like the limbic system and the neocortex [27]. The dorso-ventral projection pattern is conserved in the anterior olfactory nucleus, but for the amygdala, projections are mostly traced back to the dorsal portion of the bulb, and no discernable pattern can be traced from the projections to the piriform cortex [100]. (Fig. 2.4)

2.5 Odor Coding

Precise odor detection and discrimination has its basis in deciphering a combinatorial code of activated ORs. A given OR may be activated by a number of molecules and one odorant is capable of activating a number of ORs, enabling the olfactory system to detect and discriminate among tens of thousands of odorants [101]. (Fig. 2.5) The range of unique odorants able to elicit a response from the OR defines how broadly or narrowly it is tuned. There are ORs that are excited by a wide range of molecules and ORs that respond to only very specific cues. One example of a narrowly tuned OR is the human OR7D4, which is activated very selectively by androstenone and androstadienone. The receptor has common variants that differ the function and alter the perception of these volatile steroids, showing an essential role of a single OR in odor perception [102–104]. The first step towards the identification of an odorant is the specific set of ORs it can activate to cause the OSN to depolarize, and hence the pattern of glomeruli it excites. It has been found that the glomeruli excited by a single odorant are consistent

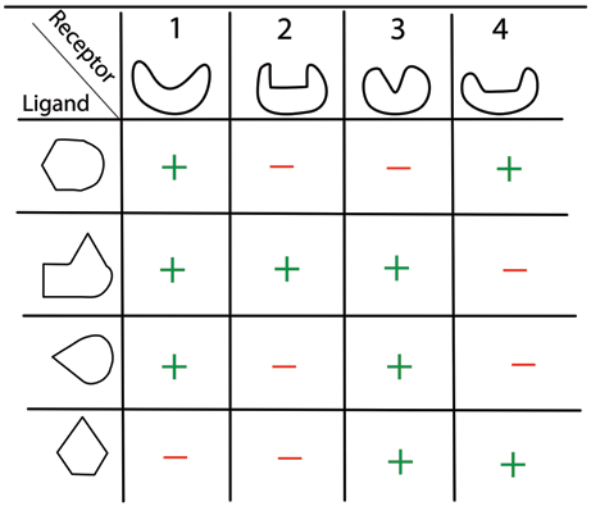

Fig. 2.5 Combinatorial code for odor recognition. One odorant can activate many receptors (indicated by the *green* +) and a single receptor can get activated by a number of odorants. The second receptor is narrowly tuned, responding to only 1 odorant whereas one and three are broadly tuned, responding to many odorants

across different individuals and that the higher centers of the brain are capable of identifying odors based on these patterns of activation [105]. The olfactory system may also utilize temporally coded odor information because when different odorants stimulate the same OSN, the OSN depolarizes at different frequencies [106]. The OB could also be generating complex temporal patterns encoding information about odors [107, 108].

2.6 Minority Receptors

ORs are the predominant receptors found in the olfactory epithelium but they are not the only sensory receptors expressed in the OE. A small number of OSNs express trace amine-associated receptors (TAARs) of which there are 15 members in mice [109–111]. These receptors, which detect volatile amines found in urine, are implicated in playing a role in stress response, gender recognition and predator avoidance [109, 112–114]. 0.1 % of OSNs in the OE express guanyl cyclase D (GC-D) and do not have the signaling elements associated with OR signal transduction [115–117]. They instead express a cGMP-gated Ca^{2+} channel CNGA3 [115] and project to very specific glomeruli known as the necklace glomeruli [116]. These neurons all express carbonic anhydrase II and show a concentration dependent Ca^{2+} response to CO_2, indicating that they might be responsible for its detection. They also respond to certain natriuretic peptide hormones and seem to be responsible for the detection of carbon disulphide, which is a signal associated with food related social learning [6, 118, 119].

2.7 Odorant Binding Proteins (OBPs)

OBPs are extracellular proteins localized to chemosensory systems of most terrestrial species. Non-neuronal support cells secrete a small number of vertebrate odorant binding protein (vOBP) into the mucus [120]. vOBP are members of the lipocalin family of molecules, like the retinol binding proteins, and bind to odorants. For example, a vOBP binds to an odorant pyrazine with dissociation constants in the micromolar range [121]. Insect binding proteins (iOBP) are a family unrelated to vOBPs in sequence and x-ray crystallography reveals that there are no structural analogs between the two. vOBPs are active as dimers whereas iOBPs are active as monomers [122].

Lush is a iOBP mutation in Drosophila that causes their repulsion to high concentrations of alcohol [123]. Studies have shown that in addition to alcohol, lush also binds to the insect pheromone 11-cis-vaccenyl acetate (VA), and that non-functional mutants do not display aggregation behavior usually displayed in response to its release [124]. Other OBPs have still not been assigned well defined roles.

2.8 Vomeronasal Organ (VNO)

The VNO in mammals, a tube-like organ also called Jacobson's organ after the scientist who first described it in 1811, is found separated from the main OE in a bony cartilaginous cavity opening into the anterior portion of the nasal cavity [125]. It is split by the nasal septum, forming two crescent-shaped lumens lined by a pseudostratified epithelium consisting of supporting cells, neurons and basal cells that act like stem cells for regeneration, similar to the organization of the OE [126]. The VNO neurons do not possess cilia, but rather have apical microvilli [27] and project their axons to the accessory olfactory bulb (AOB) [127], which may be sexually dimorphic with males having a slightly larger bulb than females [128]. The VNO contains neurons expressing receptors belonging to a 7 transmembrane domain GPCR family, unrelated to the ORs. They are divided into 2 subgroups: V1R and V2R [16, 129–132], each expressed in a distinct region of the VNO. V1Rs are expressed in the apical region of the VNO, linked to $G_{\alpha i2}$ [133], have short amino terminals and have great sequence diversity in their transmembrane domains [134] consistent with the idea that the transmembrane domains are important for responding to structurally diverse ligands. The V2Rs are linked to $G_{\alpha 0}$, have long amino terminal chains and are located in the basal region of the VNO. The amino terminal domains of V2Rs are diverse, suggesting that these domains may be responsible for binding to ligands. TRPC2 channels, a diacylglycerol activated transient receptor potential Ca^{2+} ion channel, mediates the signaling cascade in VNO neurons. These channels are found exclusively in the VNO [135, 136]. $TRPC2^{-/-}$ mice were shown to be deficient in pheromone sensing using neurophysiology and behavior.

Unlike OSNs, VNO neurons expressing the same receptors project to more than one glomerulus, and each glomerulus in the AOB may receive input from multiple types of VNO neurons [137]. In addition, afferent AOB mitral cells also contact more than one glomerulus with their dendrites, increasing the complexity [138]. The AOB mitral cells send the information to different brain areas from the areas that receive information from the OB. The hypothalamus plays an important role in exerting effects starting from VNO activation.

The VNO is essential in mediating innate behaviors and physiological changes triggered by external chemical cues like the synchronization of the estrous cycle amongst females housed together [139], pregnancy block caused by the exposure of mated female mice to a strange male [140], enhancement of sexual receptivity in females [141], early onset of puberty in females in response to exposure to males [142], nursing behavior of lactating dams [8], male aggressive behaviors [17] and attraction to the odors of the opposite sex [7], all of which are either completely lost or partially affected in the mice lacking TRPC2 [5, 136, 143]. More recently, a third family of receptors has been discovered in the VNO called formyl peptide receptor-like proteins (FPRs) [144], which are expressed in a set of neurons that do not express other known VNO receptors. Since some FPR members are found in immune cells, the VNO may provide sensitivity to molecules associated with disease and inflammation [145]. In humans, though a VNO can be clearly detected in the embryonic stages [146], the organ in adults does not contain any cells with properties of sensory neurons [147]. TRPC2 is pseudogenized in humans, supporting the idea that the human VNO is vestigial. It is interesting to note that a few V1Rs seem to be intact in humans, though the vast majority of the VNO receptors are pseudogenized [16, 129, 148–151].

2.9 Olfactory System in Aquatic Vertebrates

Fish carry out chemosensation via olfaction, gustation and general chemosensation mediated by solitary chemosensory cells. Unlike terrestrial animals, the fish olfactory system detects water-soluble chemicals. They detect four main classes of odorants: amino acids, gonadal steroids, bile acids and prostaglandins [152]. Fish have a single olfactory organ called an olfactory rosette, which contains 3 types of OSNs: ciliated, microvillous and crypt cells, and projects a tightly fasciculated olfactory nerve to the OB (Fig. 2.6) [153]. These 3 types of neurons differ from each other based on morphology (number of cilia, length of dendrite), position (depth in the OE) and their receptor expression profile. The type of receptors expressed by crypt cells remains unknown, but the ciliated cells express ORs and the microvillous cells express V2R-like receptors [154–156]. mRNA for V1R-like receptors has been found in the OE [157]. Each class of these receptors is believed to use the same or similar signaling pathways as their mammalian orthologs. The fish receptor repertoire is smaller than that of mammals, but their receptors are more diverse in sequence [158, 159] and the repertoire size itself varies significantly amongst

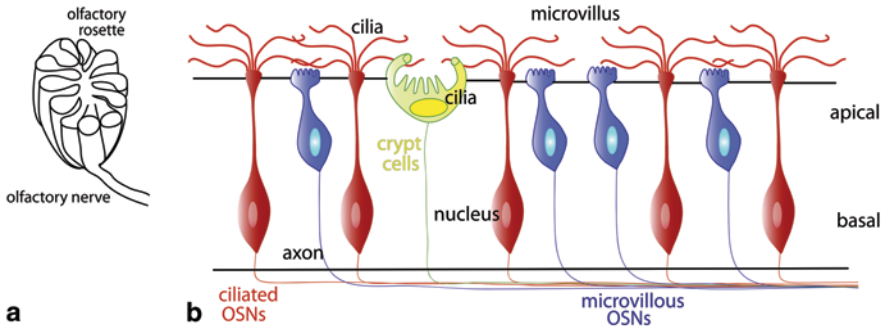

Fig. 2.6 (**a**) A depiction of a single olfactory rosette, (**b**) the 3 types of OSNs found in the fish OE. Ciliated neurons tend to be positioned more basally than *microvillous OSNs* and crypt cells depicted in *yellow*, are usually at the most apical tip of the tissue

species; for example, pufferfish have fewer than 50 ORs compared to the 102 intact and 35 pseudogenized OR genes found in zebrafish [160, 161]. Fish OE have also been shown to express TAARs that act as candidate receptors for polyamines [111, 162, 163], and have a much larger repertoire than mammals in some cases like zebrafish with 109 TAAR genes [111]. Again, different species of fish have large variations in the number of TAAR genes their genomes contain.

A single OSN in zebrafish may either express one OR or multiple ORs as in the case of the zOR103 family of receptors, which express either 2 or 3 receptors in some ciliated neurons [164]. Ciliated neurons in the zebrafish project to the dorsal and medial regions in the OB while the microvillous neurons project to the lateral regions [164, 165]. In contrast, catfish ciliated neurons project to the medial and ventral regions and the microvillous OSNs project to the dorsal OB [166, 167]. Ciliated and microvillous OSNs project to mutually exclusive glomeruli in the zebrafish, where no glomeruli were observed to be innervated by both types of OSNs [164, 165].

2.10 The Insect Olfactory System

Most insects have two major olfactory organs on their heads, the antenna and the maxillary palp (Fig. 2.7a). These organs are covered in sensory hairs called sensilla, which contain up to four sensory neurons, olfactory receptor neurons (ORNs), bathed in the sensory lymph. There are small openings on the surface of these sensilla that allow odorants to dissolve in the lymph and come in contact with the ORN dendrites (Fig. 2.7b). These ORNs project a single axon to a single spatially invariant glomerulus, which is also innervated by other ORNs expressing the same OR, and synapses with second order projection neurons in the antennal lobe in a manner analogous to the mammalian olfactory system [168]. There are a total of 43 glomeruli in the antennal lobe in Drosophila, and output neurons project ipsilaterally

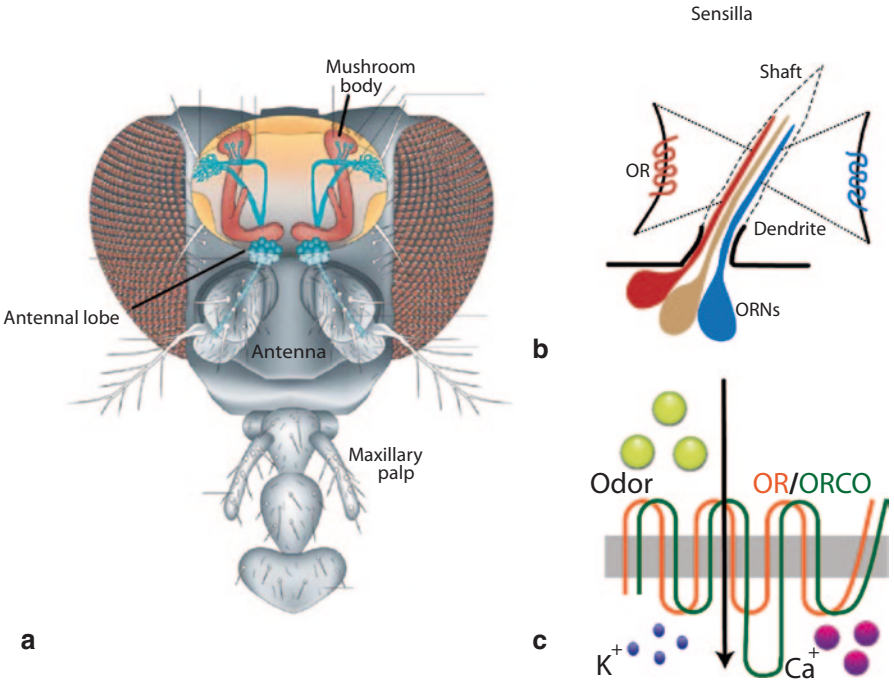

Fig. 2.7 **a** The head of *Drosophila melanogaster* showing the olfactory organs and the antennal lobe along with higher centers like the mushroom body (modified from [1]). **b** A single sensory sensilla with its porous shaft containing 3 ORNs each expressing a unique *OR* along with OR83b. **c** The insect *OR* is in itself an ion channel capable of conducting Ca^{2+} and K^{+} into the cell when activated by an odorant

to Kenyon cells of the mushroom bodies and the lateral horn of the proto cerebrum in the central brain [169]. There are some sexually dimorphic neural circuits which may be involved in the courtship and mating behavior [170].

Insect OR gene families have been identified for Drosophila (62 ORs) [171, 172], Anopheles (79 ORs) [173], Aedes (131 ORs) [174], Apis (157 ORs) [175] and many more. These highly divergent OR genes are not homologous to vertebrate GPCR ORs and they display a novel topology where their N terminus is intracellular and C terminus is extracellular [176, 177]. An inside-out single channel recording of cell membrane excised from an insect OR expressing mammalian cell cultures gave rise to evidence that the insect OR itself is an ion channel [178, 179] that is gated by its cognate ligands (Fig. 2.7c). The metabotropic signaling pathway that contributes to activation of ORNs remains a controversial field with many players seemingly playing odor specific roles. RNAi knockdown of $G_{\alpha q}$ in the Drosophila antenna results in the flies becoming insensitive to high concentrations of isoamyl acetate which normally repels flies [180]. Flies with mutations in norp A phospholipase C have defective maxillary palps [181].

Insects undergo metamorphosis and their larval repertoire of ORs is different from that of adults. Some ORs expressed exclusively in the adult may be responsible for the detection of pheromones responsible for mating. ORNs express up to three different ORs along with odorant receptor co-receptor, ORCO, also known as Or83b. Unlike other insect ORs, ORCO is conserved across diverse species [173–175] and co-expressed with the other ORs [182]. This receptor does not seem to participate directly in odor binding, but instead it forms a heteromer responsible for the transport and transduction of the receptors [182, 183].

Much progress has been made in deorphanizing Drosophila ORs with the use of an "empty neuron" strategy where Or22a/b is deleted, giving rise to a Δhalo mutant fly which has an "empty" ab3A neuron. Using a UAS/Gal4 expression system, the ectopic expression of any OR expression can be driven in ab3A neurons that can then be electrophysiologically tested to study its response to various odorants [184–186]. These studies also showed that insects also detect odors using a combinatorial code of activated glomeruli, just like mammals.

A family related to the ionotropic glutamate receptors (IRs) that mediate neuronal communication at synapses has also been shown in insect ORNs. These ORNs respond to a number of distinct odors without expressing canonical ORs. IRs are extremely divergent with an overall sequence identity of 10–70% and up to 3 IRs are expressed in an individual ORN [187].

2.11 Nematode Olfactory System

Nematodes such as C. elegans carry out chemosensation with chemosensory neurons that extrude their sensilla into the environment via openings made by glial cells called the socket and sheath cells [188]. There are 32 such neurons arranged in bilaterally symmetric pairs along the amphid, phasmid and the inner labia. C elegans can detect volatile molecules (mostly byproducts of bacterial metabolism) in the nanomolar range and exhibit long-range chemotaxic behavior towards them [189]. Amphid sensory neurons AWC and AWA detect attractants, and their bilateral symmetry aids the detection of gradients [190]. As in vertebrates, chemosensation is mediated by 7 transmembrane domain GPCRs that make up 7% of the genome (more than 500 functional chemosensory receptors) [4, 191–193] and are concentrated on chromosome V, but unlike higher animals, worms do not have the same anatomical structures such as glomeruli to process olfactory information. Their olfactory receptors are evolutionarily divergent from both mammalian and insect ORs, and each neuron expresses a number of olfactory receptors as worms have only 32 neurons [194]. The activation of a single neuron is sufficient for directing behavioral output to environmental cues. Ectopic expression of the olfactory receptor ODR-10 in AWB neurons, which detects repellents, makes the transgenic worms avoid the normally attractive odorant diacetyl, an active ligand for ODR-10 [9, 192] which suggests that this behavior is encoded in the neural circuit (Fig. 2.8).

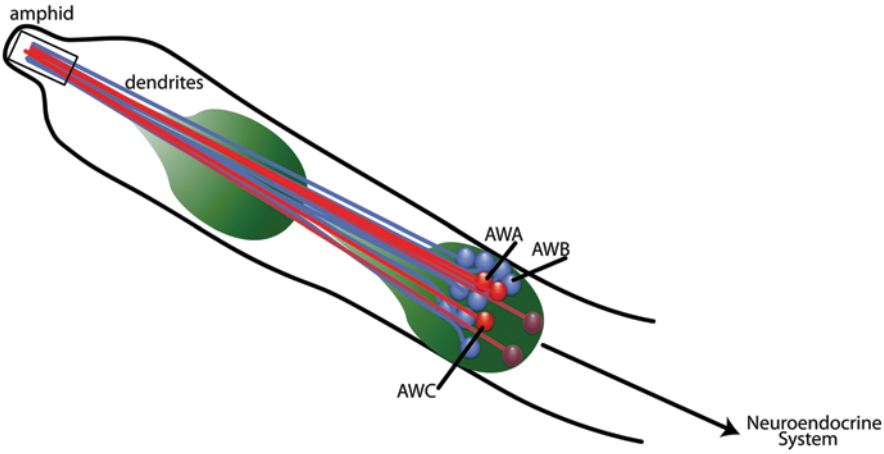

Fig. 2.8 The head of *C. elegans* depicting the sensory neurons found in the *amphid*. The pharynx is shown in *green* and a number of sensory neurons project their dendrites though the opening

2.12 Future Directions in the Field

Matching ORs with active odor ligands is fundamental to understanding how olfaction works. Given the vast number of odor chemicals and ORs, new technologies enabling comprehensive characterization of an OR repertoire that is activated by a given odorant should tremendously benefit the field. The elucidation of this question could lead to many advances not only in understanding the basic logic of odor detection, but also in the food and flavor industry. Identifying receptors for key flavors will enable pharmaceutical screening for new flavor chemicals, which could lead to engineering unpalatable food to improve flavor and revolutionize the way we eat.

Understanding of the olfactory system could also address certain national security concerns. There is great scope for innovation of new detection technologies for security threats like explosives or illegal substances like drugs. Though trained dogs are currently used because of their superior ability in olfaction, olfaction-based biosensors could one day be used in place of dogs.

OR gene choice is another black box that is being approached with new and innovative methods. OR gene choice serves as a unique and excellent model to understand how epigenetic modifications contribute to gene expression.

The ultimate goal of understanding the olfactory system is to understand how we detect and subsequently recognize an odorant, followed by perception and a behavioral output in the appropriate context. Olfactory information processing in the brain has just begun to be understood. Recent studies have demonstrated that the loss of a single receptor can lead to a change in odor perception or innate aversive behaviors, demonstrating that a single receptor can have a huge impact in odor perception and odor-mediated behavior. But how do we reconcile the decisive role of single ORs

with the idea of combinatorial odor coding? Are some ORs more important than others? How often does a mutation of a single receptor cause dramatic changes in perception? Large strides need to be made in understanding how our nervous system processes odor information.

Acknowledgments We thank Helena You and Naihua Natalie Gong for editing. NIH supports the work of the Matsunami lab.

References

1. Keene AC, Waddell S (2007) *Drosophila* olfactory memory: single genes to complex neural circuits. Nat Rev Neurosci 8(5):341–354
2. Herz R (2007) The scent of desire: discovering our enigmatic sense of smell. HarperCollins
3. Kobayakawa K et al (2007) Innate versus learned odour processing in the mouse olfactory bulb. Nature 450(7169):503–508
4. Bargmann CI, Hartwieg E, Horvitz HR (1993) Odorant-selective genes and neurons mediate olfaction in *C. elegans*. Cell 74(3):515–527
5. Leypold BG et al (2002) Altered sexual and social behaviors in trp2 mutant mice. Proc Natl Acad Sci 99(9):6376–6381
6. Munger SD et al (2010) An olfactory subsystem that detects carbon disulfide and mediates food-related social learning. Curr Biol 20(16):1438–1444
7. Romero PR, Beltramino CA, Carrer HF (1990) Participation of the olfactory system in the control of approach behavior of the female rat to the male. Physiol Behav 47(4):685–690
8. Saito TR et al (1990) Nursing behavior in lactating rats-the role of the vomeronasal organ, Jikken dobutsu. Exp Anim 39(1):109–111
9. Troemel ER, Kimmel BE, Bargmann CI (1997) Reprogramming chemotaxis responses: sensory neurons define olfactory preferences in *C. elegans*. Cell 91(2):161–169
10. Bernstein H, Moyer K (1970) Aggressive behavior in the rat: effects of isolation, and olfactory bulb lesions. Brain Res 20(1):75–84
11. Fleming AS, Rosenblatt JS (1974) Olfactory regulation of maternal behavior in rats: I. Effects of olfactory bulb removal in experienced and inexperienced lactating and cycling females. J Comp Physiol Psychol 86(2):221
12. Heimer L, Larsson K (1967) Mating behavior of male rats after olfactory bulb lesions. Physiol Behav 2(2):207–209
13. Ansari K, Johnson A (1975) Olfactory function in patients with Parkinson's disease. J Chronic Dis 28(9):493–497
14. Mesholam RI et al (1998) Olfaction in neurodegenerative disease: a meta-analysis of olfactory functioning in Alzheimer's and Parkinson's diseases. Arch Neurol 55(1):84
15. Buck L, Axel R (1991) A novel multigene family may encode odorant receptors: a molecular basis for odor recognition. Cell 65(1):175–187
16. Dulac C, Axel R (1995) A novel family of genes encoding putative pheromone receptors in mammals. Cell 83(2):195–206
17. Bean NJ (1982) Modulation of agonistic behavior by the dual olfactory system in male mice. Physiol Behav 29(3):433–437
18. Papes F, Logan DW, Stowers L (2010) The vomeronasal organ mediates interspecies defensive behaviors through detection of protein pheromone homologs. Cell 141(4):692–703
19. Fleischer J et al (2006) A novel population of neuronal cells expressing the olfactory marker protein (OMP) in the anterior/dorsal region of the nasal cavity. Histochem Cell Biol 125(4):337–349

20. Fleischer J et al (2006) Olfactory receptors and signalling elements in the Grueneberg ganglion. J Neurochem 98(2):543–554
21. Brechbühl J, Klaey M, Broillet M-C (2008) Grueneberg ganglion cells mediate alarm pheromone detection in mice. Science 321(5892):1092–1095
22. Tian H, Ma M (2004) Molecular organization of the olfactory septal organ. J Neurosci 24(38):8383–8390
23. Storan MJ, Key B (2006) Septal organ of Grüneberg is part of the olfactory system. J Comp Neurol 494(5):834–844
24. Buck LB (1996) Information coding in the vertebrate olfactory system. Annu Rev Neurosci 19(1):517–544
25. Shipley M, Ennis M, Puche A (2003) The olfactory system. In: Conn PM (ed) Neuroscience in medicine. Humana Press, p 579–593
26. Lancet D (1986) Vertebrate olfactory reception. Annu Rev Neurosci 9(1):329–355
27. Doty RL (2001) Olfaction. Annu Rev Psychol 52(1):423–452
28. Laissue P et al (1999) Three-dimensional reconstruction of the antennal lobe in *Drosophila melanogaster*. J Comp Neurol 405(4):543–552
29. Margolis FL (1972) A brain protein unique to the olfactory bulb. Proc Natl Acad Sci 69(5):1221–1224
30. Mombaerts P et al (1996) Visualizing an olfactory sensory map. Cell 87(4):675–686
31. Mombaerts P (2006) Axonal wiring in the mouse olfactory system. Annu Rev Cell Dev Biol 22(1):713–737
32. Ressler KJ, Sullivan SL, Buck LB (1994) A molecular dissection of spatial patterning in the olfactory system. Curr Opin Neurobiol 4(4):588–596
33. Lancet D, Ben-Arie N (1993) Olfactory receptors. Curr Biol 3(10):668
34. Ben-Arie N et al (1994) Olfactory receptor gene cluster on human chromosome 17: possible duplication of an ancestral receptor repertoire. Hum Mol Genet 3(2):229–235
35. Kobilka B (1992) Adrenergic receptors as models for G protein-coupled receptors. Annu Rev Neurosci 15(1):87–114
36. Belluscio L et al (1998) Mice deficient in Golf are anosmic. Neuron 20(1):69–81
37. Wong ST et al (2000) Disruption of the type III adenylyl cyclase gene leads to peripheral and behavioral anosmia in transgenic mice. Neuron 27(3):487–497
38. Imai T, Sakano H (2008) Odorant receptor-mediated signaling in the mouse. Curr Opin Neurobiol 18(3):251–260
39. Pace U et al (1985) Odorant-sensitive adenylate cyclase may mediate olfactory reception. Nature 316(6025):255–258
40. Sklar P, Anholt R, Snyder S (1986) The odorant-sensitive adenylate cyclase of olfactory receptor cells. Differential stimulation by distinct classes of odorants. J Biol Chem 261(33):15538–15543
41. Brunet LJ, Gold GH, Ngai J (1996) General anosmia caused by a targeted disruption of the mouse olfactory cyclic nucleotide gated cation channel. Neuron 17(4):681–693
42. Firestein S, Werblin F (1989) Odor-induced membrane currents in vertebrate-olfactory receptor neurons. Science 244(4900):79–82
43. Reisert J et al (2005) Mechanism of the excitatory Cl^- response in mouse olfactory receptor neurons. Neuron 45(4):553–561
44. Noé J et al (1997) Sodium/calcium exchanger in rat olfactory neurons. Neurochem Int 30(6):523–531
45. Stephan AB et al (2011) The Na+/Ca2+exchanger NCKX4 governs termination and adaptation of the mammalian olfactory response. Nat Neurosci 15(1):131–137
46. Nakamura T, Gold GH (1987) A cyclic nucleotide-gated conductance in olfactory receptor cilia. Nature 325(6103):442–444
47. Rasche S et al (2010) Tmem16b is specifically expressed in the cilia of olfactory sensory neurons. Chem Senses 35(3):239–245
48. Kleene S, Gesteland R (1991) Calcium-activated chloride conductance in frog olfactory cilia. J Neurosci 11(11):3624–3629

49. Kleene SJ (1993) Origin of the chloride current in olfactory transduction. Neuron 11(1):123–132
50. Brunet LJ, Gold GH, Ngai J (1996) General anosmia caused by a targeted disruption of the mouse olfactory cyclic nucleotide-gated cation channel. Neuron 17(4):681–693
51. Kurahashi T, Yau K-W (1993) Co-existence of cationic and chloride components in odorant-induced current of vertebrate olfactory receptor cells. Nature 363(6424):71–74
52. Lowe G, Gold GH (1993) Nonlinear amplification by calcium-dependent chloride channels in olfactory receptor cells. Nature 366(6452):283–286
53. Reuter D et al (1998) A depolarizing chloride current contributes to chemoelectrical transduction in olfactory sensory neurons in situ. J Neurosci 18(17):6623–6630
54. Breer H, Boekhoff I (1991) Odorants of the same odor class activate different second messenger pathways. Chem Senses 16(1):19–29
55. Ronnett G et al (1993) Odorants differentially enhance phosphoinositide turnover and adenylyl cyclase in olfactory receptor neuronal cultures. J Neurosci 13(4):1751–1758
56. Ronnett GV, Moon C (2002) G proteins and olfactory signal transduction. Annu Rev Physiol 64(1):189–222
57. Munger SD et al (2001) Central role of the CNGA4 channel subunit in Ca2+-calmodulin-dependent odor adaptation. Science 294(5549):2172–2175
58. Yan C et al (1995) Molecular cloning and characterization of a calmodulin-dependent phosphodiesterase enriched in olfactory sensory neurons. Proc Natl Acad Sci 92(21):9677–9681
59. Wayman GA, Impey S, Storm DR (1995) Ca2+inhibition of type III adenylyl cyclase in vivo. J Biol Chem 270(37):21480–21486
60. Dawson T et al (1993) Beta-adrenergic receptor kinase-2 and beta-arrestin-2 as mediators of odorant-induced desensitization. Science 259(5096):825–829
61. Mashukova A et al (2006) β-arrestin2-mediated internalization of mammalian odorant receptors. J Neurosci 26(39):9902–9912
62. Ferguson SS (2001) Evolving concepts in G protein-coupled receptor endocytosis: the role in receptor desensitization and signaling. Pharmacol Rev 53(1):1–24
63. Willets JM, Challiss R, Nahorski SR (2003) Non-visual GRKs: are we seeing the whole picture? Trends Pharmacol Sci 24(12):626–633
64. Pitcher JA, Freedman NJ, Lefkowitz RJ (1998) G protein-coupled receptor kinases. Annu Rev Biochem 67(1):653–692
65. Gimelbrant AA et al (1999) Truncation releases olfactory receptors from the endoplasmic reticulum of heterologous cells. J Neurochem 72(6):2301–2311
66. McClintock TS et al (1997) Functional expression of olfactory-adrenergic receptor chimeras and intracellular retention of heterologously expressed olfactory receptors. Mol Brain Res 48(2):270–278
67. Saito H et al (2004) RTP family members induce functional expression of mammalian odorant receptors. Cell 119(5):679–691
68. Zhuang H, Matsunami H (2008) Evaluating cell-surface expression and measuring activation of mammalian odorant receptors in heterologous cells. Nat Protocols 3(9):1402–1413
69. Chess A et al (1994) Allelic inactivation regulates olfactory receptor gene expression. Cell 78(5):823–834
70. Vassar R et al (1994) Topographic organization of sensory projections to the olfactory bulb. Cell 79(6):981–991
71. Serizawa S et al (2000) Mutually exclusive expression of odorant receptor transgenes. Nat Neurosci 3(7):687–693
72. Clowney EJ et al (2012) Nuclear aggregation of olfactory receptor genes governs their monogenic expression. Cell 151(4):724–737
73. Clowney EJ et al (2011) High-throughput mapping of the promoters of the mouse olfactory receptor genes reveals a new type of mammalian promoter and provides insight into olfactory receptor gene regulation. Genome Res 21(8):1249–1259
74. Lewcock JW, Reed RR (2004) A feedback mechanism regulates monoallelic odorant receptor expression. Proc Natl Acad Sci U S A 101(4):1069–1074

75. Lomvardas S et al (2006) Interchromosomal interactions and olfactory receptor choice. Cell 126(2):403–413
76. Lyons DB et al (2013) An epigenetic trap stabilizes singular olfactory receptor expression. Cell 154(2):325–336
77. Magklara A et al (2011) An epigenetic signature for monoallelic olfactory receptor expression. Cell 145(4):555–570
78. Michaloski JS, Galante PA, Malnic B (2006) Identification of potential regulatory motifs in odorant receptor genes by analysis of promoter sequences. Genome Res 16(9):1091–1098
79. Nguyen MQ et al (2007) Prominent roles for odorant receptor coding sequences in allelic exclusion. Cell 131(5):1009–1017
80. Shykind BM et al (2004) Gene switching and the stability of odorant receptor gene choice. Cell 117(6):801–815
81. Vassar R, Ngai J, Axel R (1993) Spatial segregation of odorant receptor expression in the mammalian olfactory epithelium. Cell 74(2):309–318
82. Yoshihara Y et al (1997) OCAM: a new member of the neural cell adhesion molecule family related to zone-to-zone projection of olfactory and vomeronasal axons. J Neurosci 17(15):5830–5842
83. Miyamichi K et al (2005) Continuous and overlapping expression domains of odorant receptor genes in the olfactory epithelium determine the dorsal/ventral positioning of glomeruli in the olfactory bulb. J Neurosci 25(14):3586–3592
84. Zhang X, Firestein S (2002) The olfactory receptor gene superfamily of the mouse. Nat Neurosci 5(2):124–133
85. Zhang X et al (2004) High-throughput microarray detection of olfactory receptor gene expression in the mouse. Proc Natl Acad Sci U S A 101(39):14168–14173
86. Kaneko-Goto T et al (2008) BIG-2 mediates olfactory axon convergence to target glomeruli. Neuron 57(6):834–846
87. Bozza T et al (2002) Odorant receptor expression defines functional units in the mouse olfactory system. J Neurosci 22(8):3033–3043
88. Imai T, Suzuki M, Sakano H (2006) Odorant receptor-derived cAMP signals direct axonal targeting. Science 314(5799):657–661
89. Serizawa S et al (2006) A neuronal identity code for the odorant receptor-specific and activity-dependent axon sorting. Cell 127(5):1057–1069
90. Feinstein P et al (2004) Axon guidance of mouse olfactory sensory neurons by odorant receptors and the β2 adrenergic receptor. Cell 117(6):833–846
91. Feinstein P, Mombaerts P (2004) A contextual model for axonal sorting into glomeruli in the mouse olfactory system. Cell 117(6):817–831
92. Yu CR et al (2004) Spontaneous neural activity is required for the establishment and maintenance of the olfactory sensory map. Neuron 42(4):553–566
93. Tadenev ALD et al (2011) Loss of Bardet-Biedl syndrome protein-8 (BBS8) perturbs olfactory function, protein localization, and axon targeting. Proc Natl Acad Sci 108(25):10320–10325
94. Kosaka K et al (1998) How simple is the organization of the olfactory glomerulus?: the heterogeneity of so-called periglomerular cells. Neurosci Res 30(2):101–110
95. Pinching AJ, Powell TPS (1971) The neuropil of the glomeruli of the olfactory bulb. J Cell Sci 9(2):347–377
96. Adam Y, Mizrahi A (2010) Circuit formation and maintenance-perspectives from the mammalian olfactory bulb. Curr Opin Neurobiol 20(1):134–140
97. Murthy VN (2011) Olfactory maps in the brain. Annu Rev Neurosci 34(1):233–258
98. Hayar A et al (2004) External tufted cells: a major excitatory element that coordinates glomerular activity. J Neurosci 24(30):6676–6685
99. Stockhorst U, Pietrowsky R (2004) Olfactory perception, communication, and the nose-to-brain pathway. Physiol Behav 83(1):3–11
100. Miyamichi K et al (2011) Cortical representations of olfactory input by trans-synaptic tracing. Nature 472(7342):191–196

101. Malnic B et al (1999) Combinatorial receptor codes for odors. Cell 96(5):713–723
102. Saito H et al (2009) Odor coding by a mammalian receptor repertoire. Sci Signal 2(60):ra9
103. Sicard G, Holley A (1984) Receptor cell responses to odorants: similarities and differences among odorants. Brain Res 292(2):283–296
104. Keller A et al (2007) Genetic variation in a human odorant receptor alters odour perception. Nature 449(7161):468–472
105. Belluscio L, Katz LC (2001) Symmetry, stereotypy, and topography of odorant representations in mouse olfactory bulbs. J Neurosci 21(6):2113–2122
106. Laurent G, Davidowitz H (1994) Encoding of olfactory information with oscillating neural assemblies. Science 265(5180):1872–1875
107. Laurent G et al (2001) Odor encoding as an active, dynamical process: experiments, computation, and theory. Annu Rev Neurosci 24(1):263–297
108. Spors H, Grinvald A (2002) Spatio-temporal dynamics of odor representations in the mammalian olfactory bulb. Neuron 34(2):301–315
109. Liberles SD, Buck LB (2006) A second class of chemosensory receptors in the olfactory epithelium. Nature 442(7103):645–650
110. Fleischer J, Schwarzenbacher K, Breer H (2007) Expression of trace amine-associated receptors in the Grueneberg ganglion. Chem Senses 32(6):623–631
111. Hashiguchi Y, Nishida M (2007) Evolution of trace amine-associated receptor (TAAR) gene family in vertebrates: lineage-specific expansions and degradations of a second class of vertebrate chemosensory receptors expressed in the olfactory epithelium. Mol Biol Evol 24(9):p 2099–2107
112. Dewan A et al (2013) Non-redundant coding of aversive odours in the main olfactory pathway. Nature 497(7450):486–489
113. Ferrero DM et al (2011) Detection and avoidance of a carnivore odor by prey. Proc Natl Acad Sci 108(27):11235–11240
114. Zhang J et al (2013) Ultrasensitive detection of amines by a trace amine-associated receptor. J Neurosci 33(7):3228–3239
115. Meyer MR et al (2000) A cGMP-signaling pathway in a subset of olfactory sensory neurons. Proc Natl Acad Sci 97(19):10595–10600
116. Juilfs DM et al (1997) A subset of olfactory neurons that selectively express cGMP-stimulated phosphodiesterase (PDE2) and guanylyl cyclase-D define a unique olfactory signal transduction pathway. Proc Natl Acad Sci 94(7):3388–3395
117. Fülle H-J et al (1995) A receptor guanylyl cyclase expressed specifically in olfactory sensory neurons. Proc Natl Acad Sci 92(8):3571–3575
118. Hu J et al (2007) Detection of near-atmospheric concentrations of CO2 by an olfactory subsystem in the mouse. Science 317(5840):953–957
119. Leinders-Zufall T et al (2007) Contribution of the receptor guanylyl cyclase GC-D to chemosensory function in the olfactory epithelium. Proc Natl Acad Sci 104(36):14507–14512
120. Pelosi P (1996) Perireceptor events in olfaction. J Neurobiol 30(1):3–19
121. Flower D (1996) The lipocalin protein family: structure and function. Biochem J 318:1–14
122. Pelosi P (1994) Odorant-binding proteins. Crit Rev Biochem Mol Biol 29(3):199–228
123. Kim M-S, Repp A, Smith DP (1998) LUSH odorant-binding protein mediates chemosensory responses to alcohols in *Drosophila melanogaster*. Genetics 150(2):711–721
124. Lin W et al (2004) Odors detected by mice deficient in cyclic nucleotide-gated channel subunit A2 stimulate the main olfactory system. J Neurosci 24(14):3703–3710
125. Jacobson L (1811) Description anatomique d'un organe observe dans les mammiferes. Ann Mus Hist Natl (Paris) 18:412–424
126. Keverne EB (1999) The vomeronasal organ. Science 286(5440):716–720
127. Rodriguez I, Feinstein P, Mombaerts P (1999) Variable patterns of axonal projections of sensory neurons in the mouse vomeronasal system. Cell 97(2):199–208
128. Segovia S, Guillamón A (1993) Sexual dimorphism in the vomeronasal pathway and sex differences in reproductive behaviors. Brain Res Rev 18(1):51–74

129. Herrada G, Dulac C (1997) A novel family of putative pheromone receptors in mammals with a topographically organized and sexually dimorphic distribution. Cell 90(4):763–773
130. Martini S et al (2001) Co-expression of putative pheromone receptors in the sensory neurons of the vomeronasal organ. J Neurosci 21(3):843–848
131. Matsunami H, Buck LB (1997) A multigene family encoding a diverse array of putative pheromone receptors in mammals. Cell 90(4):775–784
132. Ryba NJP, Tirindelli R (1997) A new multigene family of putative pheromone receptors. Neuron 19(2):371–379
133. Jia C, Halpern M (1996) Subclasses of vomeronasal receptor neurons: differential expression of G proteins ($G_{i\alpha 2}$ and $G_{o\alpha}$) and segregated projections to the accessory olfactory bulb. Brain Res 719(1):117–128
134. Tirindelli R, Mucignat-Caretta C, Ryba NJ (1998) Molecular aspects of pheromonal communication via the vomeronasal organ of mammals. Elsevier
135. Hofmann T et al (2000) Cloning, expression and subcellular localization of two novel splice variants of mouse transient receptor potential channel 2. Biochem J 351:115–122
136. Liman ER, Corey DP, Dulac C (1999) TRP2: A candidate transduction channel for mammalian pheromone sensory signaling. Proc Natl Acad Sci 96(10):5791–5796
137. Scalia F, Winans SS (1975) The differential projections of the olfactory bulb and accessory olfactory bulb in mammals. J Comp Neurol 161(1):31–55
138. Halpern M (1987) The organization and function of the vomeronasal system. Annu Rev Neurosci 10(1):325–362
139. Johns MA et al (1978) Urine-induced reflex ovulation in anovulatory rats may be a vomeronasal effect. Nature 272(5652):446–448
140. Bellringer J, Pratt HP, Keverne E (1980) Involvement of the vomeronasal organ and prolactin in pheromonal induction of delayed implantation in mice. J Reprod Fertil 59(1):223–228
141. Rajendren G, Dudley C, Moss R (1990) Role of the vomeronasal organ in the male-induced enhancement of sexual receptivity in female rats. Neuroendocrinology 52(4):368–372
142. Lomas D, Keverne E (1982) Role of the vomeronasal organ and prolactin in the acceleration of puberty in female mice. J Reprod Fertil 66(1):101–107
143. Stowers L et al (2002) Loss of sex discrimination and male-male aggression in mice deficient for TRP2. Science 295(5559):1493–1500
144. Liberles SD et al (2009) Formyl peptide receptors are candidate chemosensory receptors in the vomeronasal organ. Proc Natl Acad Sci 106(24):9842–9847
145. Riviere S et al (2009) Formyl peptide receptor-like proteins are a novel family of vomeronasal chemosensors. Nature 459(7246):574–577
146. Boehm N, Gasser B (1993) Sensory receptor-like cells in the human foetal vomeronasal organ. NeuroReport 4(7):867–870
147. Takami SL, Getchell TV (1993) Vomeronasal epithelial cells in the adult human express neuron-specific substances. NeuroReport 4:375–378
148. Zhu X et al (1996) *Trp*, a novel mammalian gene family essential for agonist-activated capacitative Ca^{2+} entry. Cell 85(5):661–671
149. Rodriguez I et al (2000) A putative pheromone receptor gene expressed in human olfactory mucosa. Nat Genet 26(1):18–19
150. Vannier B et al (1999) Mouse trp2, the homologue of the human trpc2 pseudogene, encodes mTrp2, a store depletion-activated capacitative Ca2+entry channel. Proc Natl Acad Sci 96(5):2060–2064
151. Giorgi D et al (2000) Characterization of nonfunctional V1R-like pheromone receptor sequences in human. Genome Res 10(12):1979–1985
152. Hara T (1994) The diversity of chemical stimulation in fish olfaction and gustation. Rev Fish Biol Fisheries 4(1):1–35
153. Yoshihara Y (2009) Molecular genetic dissection of the zebrafish olfactory system, in chemosensory systems in mammals, fishes, and insects. Springer. p 1–19

154. Cao Y, Oh BC, Stryer L (1998) Cloning and localization of two multigene receptor families in goldfish olfactory epithelium. Proc Natl Acad Sci 95(20):11987–11992
155. Hansen A, Anderson KT, Finger TE (2004) Differential distribution of olfactory receptor neurons in goldfish: structural and molecular correlates. J Comp Neurol 477(4):347–359
156. Speca DJ et al (1999) Functional identification of a goldfish odorant receptor. Neuron 23(3):487–498
157. Pfister P, Rodriguez I (2005) Olfactory expression of a single and highly variable V1r pheromone receptor-like gene in fish species. Proc Natl Acad Sci U S A 102(15):5489–5494
158. Ngai J et al (1993) Coding of olfactory information: topography of odorant receptor expression in the catfish olfactory epithelium. Cell 72(5):667–680
159. Weth F, Nadler W, Korsching S (1996) Nested expression domains for odorant receptors in zebrafish olfactory epithelium. Proc Natl Acad Sci 93(23):13321–13326
160. Alioto T, Ngai J (2005) The odorant receptor repertoire of teleost fish. BMC Genomics 6(1):173
161. Niimura Y, Nei M (2005) Evolutionary dynamics of olfactory receptor genes in fishes and tetrapods. Proc Natl Acad Sci 102(17):6039–6044
162. Michel W et al (2003) Evidence of a novel transduction pathway mediating detection of polyamines by the zebrafish olfactory system. J Exp Biol 206(10):1697–1706
163. Rolen SH et al (2003) Polyamines as olfactory stimuli in the goldfish *Carassius auratus*. J Exp Biol 206(10):1683–1696
164. Sato Y, Miyasaka N, Yoshihara Y (2007) Hierarchical regulation of odorant receptor gene choice and subsequent axonal projection of olfactory sensory neurons in zebrafish. J Neurosci 27(7):1606–1615
165. Sato Y, Miyasaka N, Yoshihara Y (2005) Mutually exclusive glomerular innervation by two distinct types of olfactory sensory neurons revealed in transgenic zebrafish. J Neurosci 25(20):4889–4897
166. Hansen A et al (2003) Correlation between olfactory receptor cell type and function in the channel catfish. J Neurosci 23(28):9328–9339
167. Morita Y, Finger TE (1998) Differential projections of ciliated and microvillous olfactory receptor cells in the catfish, *Ictalurus punctatus*. J Comp Neurol 398(4):539–550
168. Sato K, Touhara K (2009) Insect olfaction: receptors, signal transduction, and behavior, in chemosensory systems in mammals, fishes, and insects. Springer, p 203–220
169. Stocker R et al (1990) Neuronal architecture of the antennal lobe in *Drosophila melanogaster*. Cell Tissue Res 262(1):9–34
170. Datta SR et al (2008) The *Drosophila* pheromone cVA activates a sexually dimorphic neural circuit. Nature 452(7186):473–477
171. Clyne PJ et al (1999) A novel family of divergent seven-transmembrane proteins: candidate odorant receptors in *Drosophila*. Neuron 22(2):327–338
172. Gao Q, Chess A (1999) Identification of candidate *Drosophila* olfactory receptors from genomic DNA sequence. Genomics 60(1):31–39
173. Hill CA et al (2002) G protein-coupled receptors in anopheles gambiae. Science 298(5591):176–178
174. Bohbot J et al (2007) Molecular characterization of the Aedes aegypti odorant receptor gene family. Insect Mol Biol 16(5):525–537
175. Robertson HM, Wanner KW (2006) The chemoreceptor superfamily in the honey bee, *Apis mellifera*: expansion of the odorant, but not gustatory, receptor family. Genome Res 16(11):1395–1403
176. Benton R et al (2006) Atypical membrane topology and heteromeric function of *Drosophila* odorant receptors in vivo. PLoS Biol 4(2):e20
177. Lundin C et al (2007) Membrane topology of the *Drosophila* OR83b odorant receptor. Febs Letters 581(29):5601–5604
178. Sato K et al (2008) Insect olfactory receptors are heteromeric ligand-gated ion channels. Nature 452(7190):1002–1006

179. Wicher D et al (2008) *Drosophila* odorant receptors are both ligand-gated and cyclic-nucleotide-activated cation channels. Nature 452(7190):1007–1011
180. Kalidas S, Smith DP (2002) Novel genomic cDNA hybrids produce effective RNA interference in adult *Drosophila*. Neuron 33(2):177–184
181. Riesgo-Escovar J, Raha D, Carlson JR (1995) Requirement for a phospholipase C in odor response: overlap between olfaction and vision in *Drosophila*. Proc Natl Acad Sci 92(7):2864–2868
182. Vosshall LB et al (1999) A spatial map of olfactory receptor expression in the *Drosophila* antenna. Cell 96(5):725–736
183. Larsson MC et al (2004) *Or83b* encodes a broadly expressed odorant receptor essential for *Drosophila* olfaction. Neuron 43(5):703–714
184. Dobritsa AA et al (2003) Integrating the molecular and cellular basis of odor coding in the *Drosophila* antenna. Neuron 37(5):827–841
185. Hallem EA, Carlson JR (2006) Coding of odors by a receptor repertoire. Cell 125(1):143–160
186. Hallem EA, Ho MG, Carlson JR (2004) The molecular basis of odor coding in the *Drosophila* antenna. Cell 117(7):965–979
187. Benton R et al (2009) Variant ionotropic glutamate receptors as chemosensory receptors in *Drosophila*. Cell 136(1):149–162
188. White JG et al (1986) The structure of the nervous system of the nematode *Caenorhabditis elegans*. Philos Trans R Soc Lond B Biol Sci 314(1165):1–340
189. Chen N et al (2005) Identification of a nematode chemosensory gene family. Proc Natl Acad Sci U S A 102(1):146–151
190. Bargmann CI (2006) Comparative chemosensation from receptors to ecology. Nature 444(7117):295–301
191. Troemel ER et al (1995) Divergent seven transmembrane receptors are candidate chemosensory receptors in *C. elegans*. Cell 83(2):207–218
192. Sengupta P, Chou JH, Bargmann CI (1996) *odr*-10 encodes a seven transmembrane domain olfactory receptor required for responses to the odorant diacetyl. Cell 84(6):899–909
193. Robertson HM (2001) Updating the str and srj (stl) families of chemoreceptors in Caenorhabditis nematodes reveals frequent gene movement within and between chromosomes. Chem Senses 26(2):151–159
194. McCarroll SA, Li H, Bargmann CI (2005) Identification of transcriptional regulatory elements in chemosensory receptor genes by probabilistic segmentation. Curr Biol 15(4):347–352
195. Dalton RP, Lyons DB, Lomvardas S (2013) Co-opting the unfolded protein response to elicit olfactory receptor feedback. Cell 155(2):321–332

Chapter 3
Olfactory Receptor Proteins

Guenhaël Sanz, Jean-François Gibrat and Edith Pajot-Augy

Abstract Bioelectronic noses can utilize olfactory receptors (ORs) as recognition elements. This chapter describes biochemical characteristics of these OR proteins. ORs being G protein-coupled receptors (GPCRs) are integral membrane proteins composed of seven transmembrane spanning helices. In mammals, there exist as many as 1,000 OR genes accounting for about 3 % of the genome. Unfortunately, no three-dimensional (3D) structure of OR is available and one must infer OR properties from those of better characterized GPCRs. The chapter offers a brief overview of the characteristics of known 3D structures of complexes of GPCRs with various types of ligands (agonists, inverse agonists, antagonists, etc.) and, in one case, also with a G protein. Based on these structural data, it then reviews hypotheses and experiments regarding the GPCR transduction mechanism. The chapter then describes how the set of known 3D structures (17 different GPCRs to date) can be used to model OR 3D structures that will be subsequently used as platform for ligand virtual screening. The following section examines the different mechanisms that regulate OR activity. Lastly, we focus on the use of OR proteins in bioelectronic noses.

3.1 Olfactory Receptors: Genes and Protein Expression

Olfactory receptor (OR) genes represent more than 3 % of the mammalian genome and are the largest gene superfamily. For instance, the number of OR genes exceeds 1,700 in rat and is around 860 in humans [1]. Nevertheless, during evolution, some OR genes became nonfunctional pseudogenes. The proportion of OR pseudogenes differs between species, being ≈ 20 % in mouse and dog [2, 3] and ≈ 60 % in humans

G. Sanz (✉) · E. Pajot-Augy
INRA, UR1197 NeuroBiologie de l'Olfaction,
78350, Jouy-en-Josas, France
e-mail: guenhael.sanz@jouy.inra.fr

E. Pajot-Augy
e-mail: edith.pajot@jouy.inra.fr

J.-F. Gibrat
INRA, UR1077 Mathématique Informatique et Génome, 78350, Jouy-en-Josas, France
e-mail: jean-francois.gibrat@jouy.inra.fr

T. H. Park (ed.), *Bioelectronic Nose,* DOI 10.1007/978-94-017-8613-3_3,

[1, 4, 5]. Mammalian OR genes are organized in clusters and distributed on most of the chromosomes, while being more abundant on chromosomes 11 and 1 in humans. OR pseudogenes are interspersed with full-length OR genes. OR genes are characterized by a single coding exon of about 1 kb and encode membrane receptors belonging to the seven-transmembrane domain Gprotein coupled receptors (GPCR) superfamily. ORs genes seem to carry no signal peptide sequence. According to the GRAFS classification [6], GPCRs are divided into five families, and ORs belong to the class R family, which corresponds to the "Rhodopsin-like" receptors. Moreover, mammalian OR genes are divided into two classes. Class I gathers OR genes closely related to fish OR genes and are clustered on chromosome 11 in humans [4] and class II contains ORs found in vertebrate species. The pseudogene fraction among the human class I ORs (52%) is lower than that observed for human class II ORs (77%) [4], supporting the idea that class I ORs are not evolutionary relics and still have functional significance.

Expression of OR genes was first discovered in the olfactory epithelium by the Nobel laureates Buck and Axel [7]. There, OR are expressed by the olfactory sensory neurons (OSNs) and each OSN expresses a single allele of a single OR gene. OR role in the olfactory epithelium is to detect and to discriminate odorant molecules according to a combinatorial code in which an OR can detect various odorant molecules and an odorant can activate various ORs (see Chap. 2 and 4). Thus, an odorant activates a specific group of ORs, and different groups of ORs are activated by different odorants. Moreover, there may be some overlapping of the groups of ORs stimulated by two different odorants. Furthermore, it has been reported that odorants activating the same OR share 3D structural similarities (odotopes) and similar odor qualities, suggesting that an odotope could be associated to a perceived odor quality via a specific group of activated ORs [8].

Besides their well-known role in olfaction, ORs appear to be expressed in tissues other than the olfactory epithelium and to exhibit additional functions. For instance, some ORs are involved in sperm chemotaxis and migration [9, 10], in enterochromaffin cell serotonin secretion [11, 12], in muscle cell migration and adhesion [13] and in renin secretion in the kidney [14, 15]. There is also evidence that some ORs are overexpressed in tumor cells where they could constitute tumor markers and be involved in tumor progression [16–18]. Recently, ORs were reported to participate in early cytokinesis by exerting a regulatory role on actin cystoskeleton, and particularly in cancer cell lines [19].

The regulation of OR gene expression seems to be different in OSNs and in other cells, since it was reported that sperm cells and enterochromaffin cells co-express various ORs contrary to OSNs [20, 21]. It should be of great interest to explore more extensively the regulation of OR expression in cells other than OSNs, and particularly their up-regulation in tumor cells.

While ORs display various functions depending on their expression site, the signal transduction cascade was mainly described in OSNs, where ORs are known to activate the $G_{\alpha olf}$ protein subunit and then the adenylate cyclase III, leading to an increase of cAMP and intracellular calcium through the opening of cyclic nucleotide gated channels. This kind of signaling could be comparable in some other cells

where both ORs and $G_{\alpha olf}$ subunit are expressed [14, 22]. However, alternative signaling pathways also exist, for instance in OSNs where some odorants can induce PI3 kinase activation through Gβγ subunits [23, 24], or in enterochromaffin cells where PLC, IP3 receptors and L-type calcium channels are involved downstream of OR activation [11]. Thus the existence of different signal transduction cascades can be exploited for the design of OR based biosensors (see Sect. 6).

3.2 G-protein Coupled and Olfactory Receptors Sequences and Three-Dimensional Structures

ORs belong to the G-protein coupled receptor (GPCR) superfamily characterized by the conservation of seven helical segments (7-TMHs) spanning the plasmic membrane. According to the GRAFS classification of Fredriksson and coll., ORs belong to the δ-subclass of the R (rhodopsin-like) class where they form a monophyletic cluster [6]. Most ORs have been identified through analyses of sequenced genomes [25] thus very little is known about their biochemical properties beyond their amino-acid sequences. In particular, most ORs are so-called "orphans", i.e., their ligands are unknown. Knowledge about OR characteristics and mechanism of action must be inferred from those of the limited set of GPCRs that have been experimentally characterized. The study of GPCR molecular mechanisms has long been plagued by the lack of structural data. The first high resolution X-ray structure, that of rhodopsin, dates back to 2000 [26]. Seven more years of intensive developments were needed to obtain a second 3D structure (for the human β2 adrenergic receptor, [27]). Since then, the field has steadily progressed and in August 2013, 17 3D structures of different GPCRs are available (Table 3.1), all belonging to the R class, nine to the α–subclass (Bovine and Squid rhodopsin, Human β2 adrenergic, Turkey β1 adrenergic, Human A_{2A} adenosine, Human dopamine D3, Human histamine H1, Human sphingosine 1-phosphate, Human M2 muscarinic acetylcholine, Rat M3 muscarinic acetylcholine), five to the γ–subclass (Human chemokine CXCR1, Human chemokine CXCR4, Mouse μ–opioid, Human κ–opioid, Mouse δ–opioid, Human nociception/orphanin FQ), one to the β–subclass (Rat neurotensin) and one to the δ–subclass (Human protease activated receptor 1). Except for the structure of the Human chemokine CXCR1 receptor obtained by solid-state NMR [28], all other 3D structures have been solved by X-ray crystallography and feature complexes of the receptors with different types of ligands (agonists, partial agonists, biased agonists, inverse agonists, antagonists, selective antagonists, irreversible antagonists, see Fig. 3.1 for definitions of these terms). In the structures of receptor-antagonist/inverse agonist complexes the receptors adopt an inactive conformation. In 2012, the structures of a number of receptor-agonist complexes (see Table 3.1) have been solved, stabilized by the introduction of a camelid antibody fragment (nanobody) [29]. The structure of the complex of the β2 adrenergic receptor with the Gs α-subunit was also released in 2011 [30]. In these structures, the receptor adopts an active conformation (see next section).

Table 3.1 Experimental structures of complexes of GPCRs with different types of ligand

Receptor	Class/[a] subclass	Year	PDB code	Resolution (Å)	Ligand	Type[b]	Conformational state	Reference
Bovine rhodopsin	R/α	2000	1F88	2.8	11-cis retinal	Inverse agonist	Inactive	Palczewski et al. [26]
		2004	1U19	2.2	11-cis retinal	Inverse agonist	Inactive	Okada et al. [78]
		2011	3PQR	2.8	All-trans retinal	Agonist	*Activated*[c]	Choe et al. [35]
Squid rhodopsin	R/α	2008	2Z73	2.5	11-cis retinal	Inverse agonist	Inactive	Murakami and Kouyama [79]
Human β2 adrenergic	R/α	2007	2RH1	2.4	Carazolol	Inverse agonist	Inactive	Rasmussen et al. [27]
		2008	3D4S	2.8	Timolol	Inverse agonist	Inactive	Hanson et al. [80]
		2010	3NY8	2.8	ICl118551	Inverse agonist	Inactive	Wacker et al. [81]
		2010	3NYA	3.2	Alprenolol	Antagonist	Inactive	Wacker et al. [81]
		2011	3P0G	3.5	BI-167107	Agonist	*Activated*[d]	Rasmussen et al. [29]
		2011	3PDS	3.5	FAUC50	Irreversible agonist	Intermediate	Rosenbaum et al. [82]
		2011	3SN6	3.2	BI-167107	Agonist	*Activated*[e]	Rasmussen et al. [30]
Turkey β1 adrenergic	R/α	2008	2VT4	2.7	Cyanopindolol	Antagonist	Inactive	Warne et al. [83]
		2011	2Y00	2.5	Dobutamine	Partial agonist	Inactive	Warne et al. [84]
		2011	2Y04	3.0	Salbutamol	Partial agonist	Inactive	Warne et al. [84]
		2011	2Y02	2.6	Carmoterol	Agonist	Inactive	Warne et al. [84]
		2011	2Y03	2.8	Isoprenaline	Agonist	Inactive	Warne et al. [84]
		2011	2YCW	3.0	Carazolol	Inverse agonist	Inactive	Moukhametzianov et al. [85]
		2012	4AMI	3.2	Bucindolol	Biased agonist	Inactive	Warne et al. [76]
		2012	4AMJ	2.3	Carvedilol	Biased agonist	Inactive	Warne et al. [76]
Human A2A adenosine	R/α	2008	3EML	2.6	ZM241385	Inverse agonist	Inactive	Jaakola et al. [86]
		2011	3QAK	2.7	UK-432097	Agonist	Intermediate	Xu et al. [87]
		2011	2YDO	3.0	Adenosine	Agonist	Intermediate	Lebon et al. [88]
		2011	2YDV	2.6	NECA	Agonist	Intermediate	Lebon et al. [88]
		2011	3REY	3.3	XAC	Antagonist	Inactive	Dore et al. [89]
		2011	3RFM	3.6	Caffeine	Antagonist	Inactive	Dore et al. [89]

Table 3.1 (continued)

Receptor	Class/[a] subclass	Year	PDB code	Resolution (Å)	Ligand	Type[b]	Conformational state	Reference
Human chemokine CXCR4	R/γ	2010	3ODU	2.5	IT1t	Antagonist	Inactive	Wu et al. [90]
		2010	2OE0	2.9	CVX15	Antagonist	Inactive	Wu et al. [90]
Human dopamine D3	R/α	2010	3PBL	2.9	Eticlopride	Antagonist	Inactive	Chien et al. [91]
Human histamine H1	R/α	2011	3RZE	3.1	Doxepin	Inverse agonist	Inactive	Shimamura et al. [92]
Human sphingosine 1-phosphate	R/α	2012	3V2Y	2.8	ML056	Antagonist	Inactive	Hanson et al. [93]
Human M2 muscarinic acetylcholine	R/α	2012	3UON	3.0	QNB	Antagonist	Inactive	Haga et al. [94]
Rat M3 muscarinic acetylcholine	R/α	2012	4DAJ	3.4	Tiotropium	Inverse agonist	Inactive	Kruse et al. [95]
Mouse μ-opioid	R/γ	2012	4DKL	2.8	β-FNA	Irreversible antagonist	Inactive	Manglik et al. [96]
Human κ-opioid	R/γ	2012	4DJH	2.9	JDTic	Selective antagonist	Inactive	Wu et al. [77]
Mouse δ-opioid	R/γ	2012	4EJ4	3.4	Naltrindole	Selective antagonist	Inactive	Granier et al. [97]
Human nociceptin/ orphanin FQ	R/γ	2012	4EA3	3.0	C-24	Antagonist	Inactive	Thompson et al. [98]
Rat neurotensin	R/β	2012	4GRV	2.8	Neurotensin	Agonist	Intermediate	White et al. [99]
Human protease activated receptor 1	R/δ	2012	3VW7	2.2	Vorapaxar	Antagonist	Inactive	Zhang C. et al. [100]
Human chemokine CXCR1	R/γ	2012	2LNL	NMR	–	–	inactive	Park et al. [28]

[a]GRAFS classification [6]
[b]see Fig. 3.1
Ternary complex with: [c]11 amino acid C terminal fragment of Gt α-subunit, [d]camelid nanobody, [e]Gs protein

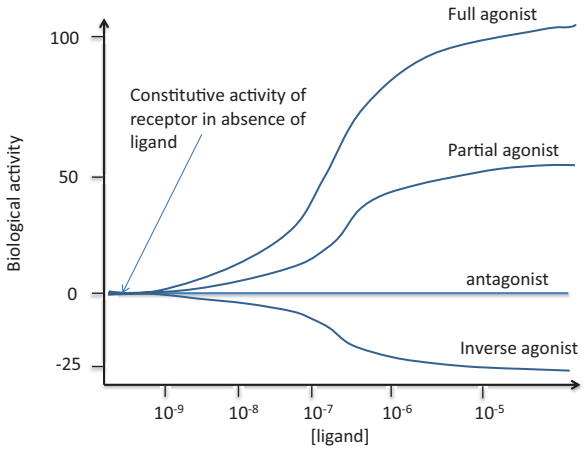

Fig. 3.1 Pharmaceutical definitions of different ligand types: full agonists are ligands that have the same biological activity as the endogenous ligand (100 % efficacy), partial agonists show intermediate efficacy. Some receptors exhibit a constitutive (basal) activity even in absence of their ligand. Inverse agonists are ligands that decrease this basal activity (negative efficacy). Biased agonists are ligands that stimulate G-protein independent signaling pathways (e.g., the arrestin pathway) while acting as either inverse or partial agonists of G-protein signaling pathways [76]. Antagonists do not modify the receptor basal activity but prevent agonists from binding and activating the receptor. Irreversible antagonists/agonists, as their name suggests, bind irreversibly to the receptor (usually by being covalently tethered to it). Subtype-selective agonists/antagonists are ligands that are able to discriminate between different receptor subtypes. For instance, JDTiC (see Table 3.1) is an antagonist with a high affinity and subtype selectivity for the human κ–opioid receptor but not for the δand μ-opioid receptors [77]

This panel of 3D structures of class R GPCRs is sufficiently large to allow us to reasonably identify features and properties common to receptors of this class and extrapolate these findings to receptors for which no 3D structure is available yet, in particular, ORs.

GPCR 3D structure consists of an extracellular N-terminus of various length in class R receptors, from a short peptide for ORs to a large extra-cellular folded domain for glycoprotein receptors, a bundle of seven transmembrane helices that are connected by three extracellular loops (ECLs) and three intracellular loops (ICLs) and a cytoplasmic C-terminus that often contains an eighth α-helix that lies against the cytoplasmic face of the membrane. The 3D structure can be roughly divided into two modules, one containing the binding pocket and devoted to ligand recognition, and one dedicated to signal transduction by binding to the Gα protein [31]. As a rule, residues of the outermost part show a tendency to be less conserved than those of the innermost part. This is in particular true for ORs since their binding pocket contains so-called “hypervariable” residues needed to accommodate the large spectrum of possible odorant molecules [32]. This is reflected by the larger structural diversity of the first module with an average root-mean-square deviation (RMSD) of 2.7 Å compared to the second module with an average RMSD of 1.5 Å [31].

The 7-TMH domain (7TMD) is the most structurally conserved region of GPCRs although its sequence conservation is only moderate, with sequence identities for 7TMDs ranging from about 70% for receptors of the same subfamily (e.g., the opioid receptor subfamily, the adrenergic receptor subfamily), to a mere 17% (well within the homology twilight zone) between the protease activated receptor 1 (PDB code 3vw7) and the sphingosine 1-phosphate receptor (PDB code 2v2y), see Table 3.2. In spite of this relatively low sequence identity between families, a number of highly conserved residues and motifs are found in the transmembrane helices. The most conserved residue in each TMH forms the basis of the Ballesteros-Weinstein numbering system [33] in which this residue gets the number 50, residues to the N-terminus of this residue get numbers smaller than 50 and residues to its C-terminus get numbers greater than 50. Each residue within the 7TMD is thus identified by two numbers: the TMH number and a number indicating its relative position with respect to the most conserved one in this TMH. For instance, 7.49 represents the residue preceding the most conserved one (a Proline) in the TMH7 sequence. Ballesteros-Weinstein 50 (N50) residues are highlighted in yellow in Fig. 3.2. Functionally important sequence motifs for GPCRs are also found in the TMHs (shown in bold in Fig. 3.2), for instance the D[E]RY motif at the end of TMH3 that is part of a "ionic lock", the FxxCWxP motif in TMH6 and NPxxY motif at the end of TMH7 that are suspected to be involved in the activation mechanisms (see next section). The presence of these conserved residues facilitates the alignment of GPCR sequences. However, N50 residues for TMH5 and TMH6 are not conserved in olfactory receptor sequences. In particular, obtaining an accurate alignment for OR TMH6 is challenging since the CWxP motif is not preserved in most OR sequences.

Loops are more diverse in terms of length, sequence similarity and 3D conformation. There exist two types of structures, those in which the binding pocket is occluded by the N-terminus and the ECLs (e.g., rhodopsin and sphingosine 1-phosphate receptors) and those in which the binding pocket is accessible from the extracellular side. ECL2 exhibits a more pronounced structural diversity than ECL1 and ECL3 that are short loops, respectively 5–6 and 7–8 residue long. In most GPCRs, ECL2 that connects TMH4 to TMH5 is tethered to TMH3 by a disulfide bridge between $Cys^{3.25}$ at the extracellular tip of TMH3 and a highly conserved Cys in the loop. This generates two "pseudo-loops": ECL2a and ECL2b. In a number of structures, ECL2b acts as a lid on top of the binding pocket and its residues interact with the ligand. The conformation of the 6-residue long ICL1 is conserved in all known structures. The 9–12 residue long ICL2 that has been shown to interact with the N-terminus of the Gα subunit [30] is very flexible and adopts diverse conformations in the known structures. ICL3 has a highly variable length, ranging from 5 residues in CXCR4 up to tens of residues in some other receptors. Presumably, ICL3 is responsible of the receptor affinity for different G proteins.

The ligand binding pocket is located in the first one-third of the helical bundle from the extracellular side. GPCRs bind very different ligands (proteins, peptides, lipids, nucleotides, small organic molecules, ions) that exhibit diverse shapes, sizes and chemical properties and penetrate to different depths in the pocket. Venkatakrishnan and coll. have analyzed the positions in the binding pocket at which

Table 3.2 RMSD and percentage of sequence identity of transmembrane domains of GPCRs with known 3D structures

	2lnlA	4grvA	3vw7A	3uonA	4ea3A	4ej4A	4djhA	4dajA	3v2yA	3rzeA	1u19A	2rh1A	2vt4A	3emlA	4dklA	3oduA	3pblA
2lnlA	–	30.1	32.7	26.0	39.3	36.2	33.7	23.0	22.4	22.4	23.0	28.1	32.1	26.5	36.2	43.4	29.1
4grvA	6.43	–	21.9	24.5	31.1	28.1	32.1	24.5	23.0	21.4	23.0	20.9	24.0	22.4	25.5	27.6	27.6
3vw7A	6.21	2.50	–	25.5	30.6	29.6	28.6	23.0	16.8	24.0	17.9	23.5	23.0	21.4	28.6	28.1	24.0
3uonA	5.92	2.92	3.30	–	27.6	28.1	30.6	70.4	27.6	35.7	23.0	30.6	30.1	26.0	29.6	24.0	31.1
4ea3A	5.58	2.61	2.44	2.16	–	63.3	62.2	25.5	21.9	26.5	22.4	28.1	29.1	26.0	62.8	34.2	30.6
4ej4A	5.89	2.54	2.37	2.24	0.98	–	72.4	27.6	21.4	30.1	24.0	30.1	29.1	29.1	73.5	29.6	30.6
4djhA	5.95	2.53	2.72	2.37	1.41	1.45	–	28.1	21.9	31.1	21.9	30.6	31.1	29.1	71.9	30.6	27.6
4dajA	5.84	2.70	3.13	1.32	2.33	2.42	2.43	–	26.5	38.3	19.9	36.7	34.2	29.6	28.6	25.5	30.6
3v2yA	5.63	3.09	3.16	2.27	2.50	2.66	2.79	2.29	–	25.0	21.4	27.0	28.6	29.6	20.4	21.9	26.5
3rzeA	5.71	2.31	2.61	1.65	1.85	1.87	1.98	1.59	2.25	–	20.4	35.7	35.7	33.2	29.6	24.5	34.2
1u19A	5.76	2.77	2.52	2.37	2.04	2.16	2.55	2.46	2.60	2.03	–	22.4	21.4	23.0	25.5	22.4	27.6
2rh1A	6.07	2.41	2.83	1.38	2.09	2.13	2.16	1.53	2.14	1.48	2.04	–	69.4	34.2	29.6	25.5	37.8
2vt4A	6.54	2.54	3.32	2.81	2.75	2.83	2.40	2.64	3.23	2.12	2.91	2.30	–	35.7	28.1	25.0	40.8
3emlA	5.79	2.51	3.10	2.23	2.23	2.39	2.59	2.32	1.98	2.13	2.44	2.08	2.86	–	28.1	22.4	31.6
4dklA	5.57	2.82	2.70	2.32	0.89	1.09	1.46	2.50	2.62	1.99	2.18	2.31	2.95	2.43	–	33.2	31.1
3oduA	5.65	3.05	2.91	2.77	1.89	1.91	2.40	2.88	2.88	2.33	2.47	2.78	3.35	2.75	1.76	–	27.0
3pblA	5.70	2.12	2.62	1.66	1.66	1.78	1.91	1.93	1.98	1.40	1.77	1.31	1.63	1.56	1.81	2.12	–

Lower triangular matrix: TMH RMSD (Å), Upper triangular matrix: TMH % of sequence identity

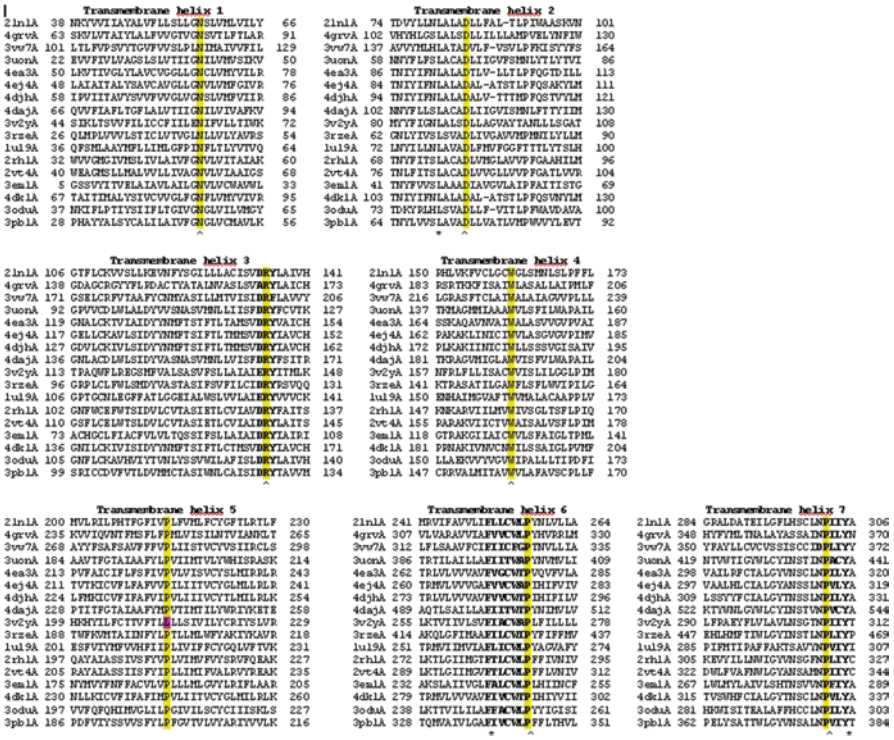

Fig. 3.2 Multiple sequence alignment of the 7 transmembrane helices for the 17 GPCRs whose 3D structure has been experimentally solved

the amino acid residue contacts the ligand in all known GPCR 3D structures [34]. They found that residues at positions 3.32, 3.33, 3.36, 6.48, 6.51 and 7.39 (Ballesteros-Weinstein nomenclature), irrespective of their type, always establish contacts with the ligand. Among these consensus positions, two pairs of positions (3.36–6.46 and 6.51–7.39) are also present in the network of conserved TMH contacts that maintain the helical bundle scaffold. They dubbed the latter positions the "ligand-binding cradle".

3.3 Signal Transduction Mechanisms

To date, only three structures of GPCR in an activated conformational state are available: rhodopsin in a complex with the C-terminus peptide of the α–subunit of the transducin G protein [35, 36], β2 adrenergic receptor in a ternary complex with an agonist and a camelid antibody fragment (nanobody) that mimics G protein behavior [29] and the same agonist-receptor system in complex with the whole heterotrimeric Gs protein [30]. A number of other structures in which the receptor

is bound to an agonist show intermediate conformational states (e.g., A_{2A} adenosine and neurotensin receptors, see Table 3.1). Indeed, except for rhodopsin in which the covalently bound agonist (all-trans retinal) alone appears sufficient to stabilize the active state conformation, experimental evidence has shown that the G protein is required to fully stabilize the active state conformation of other GPCRs [37]. These three structures shed light on the molecular changes occurring during receptor activation.

Upon binding of the agonist, small conformational changes in the ligand-binding extracellular side are amplified in the cytoplasmic side leading, more conspicuously, to a large structural rearrangement of TMH6 (14 Å outward movement) and a smaller outward movement and 7-residue cytoplasmic helix extension of TMH5 (see Fig. 3.3) [30]. According to Venkatakrishnan and coll. [34] the sequence of events is the following: (i) agonist binding causes a small local structural change in the $Pro^{5.50}$ that induces a distortion of TMH5, (ii) there is a relocation of TMH3 and TMH7 (in the β2 adrenergic and A_{2A} adenosine receptors the agonist ligand pulls the extracellular tips of TMH3, TMH5 and TMH7 inward, resulting in a moderate contraction of the binding pocket – notice that for rhodopsin this is the contrary, the volume of the binding pocket increases upon retinal isomerization [38]), (iii) there is a rotation/translation of TMH5 and TMH6. Venkatakrishnan and coll. identified a cluster of conserved hydrophobic/aromatic residues mostly at the TMH5-TMH6 interface (positions 3.40, 5.51, 6.44, 6.48). Rearrangements of residues of this interface lead to the rotation of TMH6 near the conserved $Phe^{6.44}$. Combined with the strong kink of TMH6 at position 6.50 (which is a Pro in most GPCRs), this rotation produces the observed large TMH6 movement. This region of TMH6 corresponds to the sequence motif FxxCWxP (5.44–5.50). As mentioned above, neither $Pro^{5.50}$ nor the CWxP motif (6.47–6.50) is conserved in most OR sequences, therefore one may wonder whether the activation mechanism is similar in these receptors. In the rhodopsin complex there is also a change in the water mediated hydrogen bond network near the NPxxY motif of TMH7 [36].

In the rhodopsin and β2 adrenergic complexes, the receptor interacts with the G protein α–subunit through an interface made of residues belonging to ICL2, TMH3, TMH5 and TMH6.

As mentioned above, for GPCRs other than rhodopsin, the binding of the agonist is not sufficient to stabilize the activated state. A number of biophysical experiments suggest that there exist several activated conformational states, and that different ligands are able to shift the equilibrium between these states. Nygaard and coll., using NMR techniques complemented with molecular dynamics simulations, have studied the existence of conformational states not observed in crystal structures [37]. They propose the model shown in Fig. 3.4 to explain the GPCR activation mechanisms. There are three types of conformational states: inactive, intermediate and activated. Each state consists of several microstates in which the receptor adopts slightly different conformations. The probability of finding the system in a

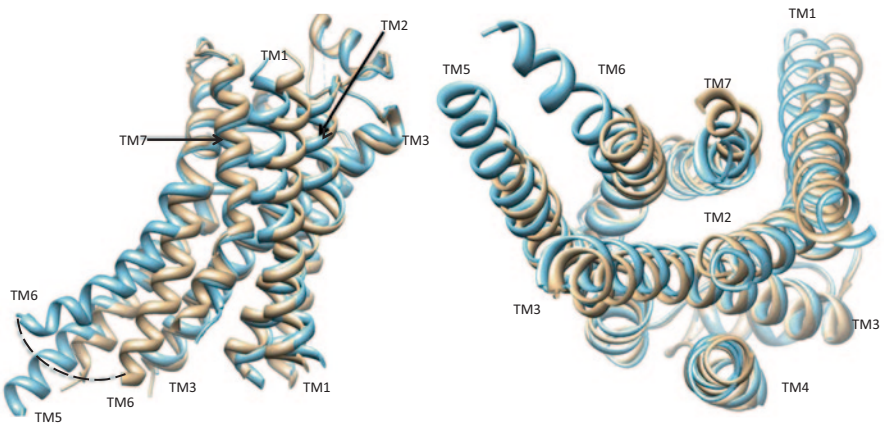

Fig. 3.3 Left panel: lateral view of the β2 adrenergic receptor (*light blue* is the activated conformation and *light brown* is the inactive conformation). The bottom of the panel corresponds to the cytoplasmic region. Right panel: view of the cytoplasmic region of the receptor. Cytoplasmic loops have been removed for clarity. TMH6 displays a 14 Å outward movement in the activated state. TMH5 shows a smaller outward movement and a 7-residue extension of the helix

given state depends on the free energy of this state. Free energy barriers control the kinetics of the transition between states. Without ligand, the inactive state has the lowest free energy (the lower the free energy, the more stable the conformational state and therefore the more populated the state at a given temperature). When an agonist binds to the receptor, the intermediate state becomes the one with the lowest free energy (this does not modify the free energy of the inactive and activated states). Energy barriers between the inactive and the intermediate states and also between the intermediate and the activated states are reduced. The drop of the latter barrier height allows the system to occasionally explore the activated state even though, in absence of the G protein, it will not remain for a long time in this state. The G protein locks the system in place by markedly decreasing the free energy of the activated state which becomes the lowest free energy state.

The analysis of complexes of β2 adrenergic receptor with different types of ligands (inverse agonist, neutral antagonist, partial and full agonists and the β-arrestin biased agonists' carvedilol and isoetharine) by ^{19}F NMR reveals that the cytoplasmic ends of TMH6 and TMH7 adopt two different conformational states. One is characteristic of the coupling of the receptor with the G protein and occurs when the receptor binds "regular" agonists. The second takes place when the receptor binds β-arrestin biased agonists and involves more specifically the cytosolic tip of TMH7 [39]. Therefore, there exist several activated states that allow the receptor to couple to different effectors leading to functional selectivity or biased signaling. Different ligands are able to switch the equilibrium toward one state or the other, selecting different signaling pathways [40].

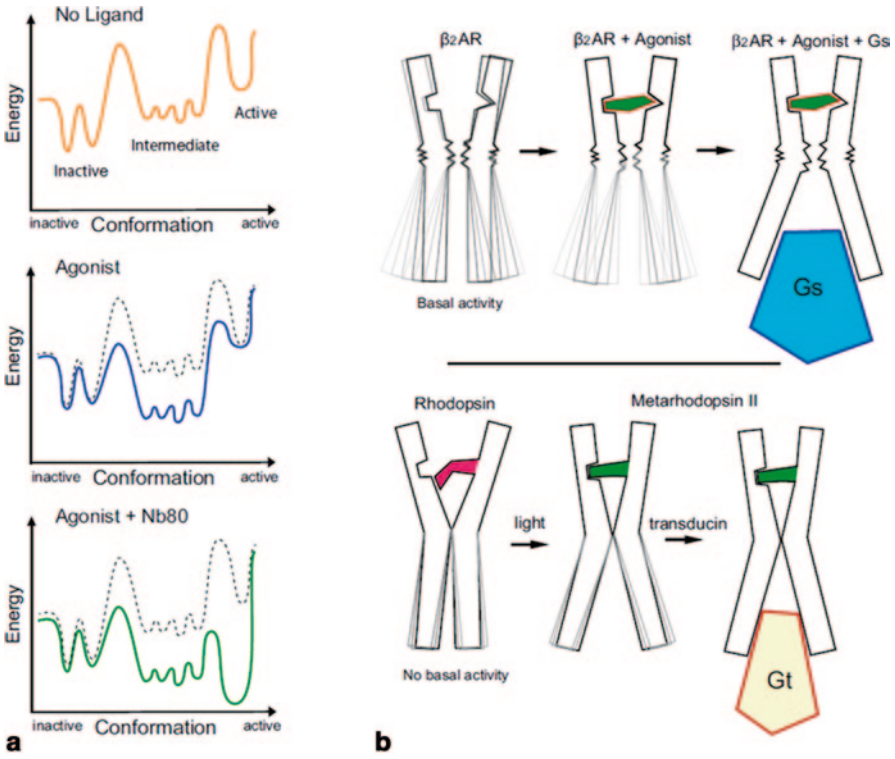

Fig. 3.4 **a** Schematic representation of the GPCR free energy hypersurface (see text). **b** Different stabilization of the GPCR 3D structure by agonists for the β2 adrenergic receptor and the rhodopsin receptor. This figure has been reprinted from [37], with permission

3.4 Olfactory Receptors Molecular Modeling and Virtual Screening

According to Kontoyianni and Liu, only 46 of the about 800 GPCRs found in the human genome have been assayed with small molecules [41]. Indeed, a vast majority of GPCRs has not been experimentally characterized, in particular ORs whose genes have been, mostly, discovered *in silico* by analyses of sequenced genomes [42], although Buck and Axel [7] had previously uncovered the existence of a novel multigene family encoding odorant receptors. Most ORs are thus orphan, meaning that their ligands remain unknown. Therefore, one way of obtaining clues about these odorant ligands is to use the knowledge acquired from 3D GPCRs structure solved employing rational computer-aided techniques such as molecular modeling and virtual screening [43]. Molecular modeling is based on the properties of homologous proteins; hence this technique is also known as "homology modeling". Two proteins are homologous if they descend from a common ancestor and, as such, they often have conserved similar sequences, 3D structures and functions.

The homology modeling procedure for a query protein consists of four steps: (i) identification of at least one homologous protein for which the 3D structure is available (the template), (ii) alignment of the query sequence to the template sequence, (iii) construction of the model from the template structure, guided by the sequence alignment and (iv) assessment and refinement of the model [44]. Different software exist that allow the use of the known 3D structure of a protein to build a model of the 3D structure of a homologous protein, e.g., MODELER [45] to name but one. The accuracy of the resulting model strongly depends on the second step that is, in turn, conditioned by the evolutionary distance between the homologous proteins [46]. This evolutionary distance can be approximately estimated by the percentage of sequence identity (%seqID) between the query and template sequences. Structure similarity decreases in a non-linear fashion with decreasing %seqIDs. Homologous proteins with %seqIDs above 50% have very similar 3D structures whereas only the "core" of the homologous proteins, i.e., a set of structural features (usually secondary structure elements), is conserved in all members of the protein family, below a %seqID of 25%. In this so-called "twilight zone", homologous protein sequences harbor many insertions/deletions that make their alignment unreliable with adverse consequences on the model accuracy; molecular modeling techniques cannot recover from an alignment error, resulting in a model that is irremediably wrong. For instance, a shift of two residues in the alignment of amino acids belonging to TMHs will locate those that ought to be in the lumen of the binding pocket and thus potentially in a position to interact with the ligand, in the opposite side of the helix, facing the membrane lipids.

An additional challenge arises, due to the modeling of loops, which are the most variable regions of proteins. Some loops are important for the function of GPCRs, for instance ECL2 is known to interact with ligands. For homologous proteins close to the twilight zone, their structural conformations are usually not conserved, as it is illustrated by the known 3D structures of GPCRs. Therefore, one cannot use homology modeling techniques for loops and must resort to knowledge-based or *de novo* modeling. In the first approach, one screens protein structural databases for loops having the same length as the loop to be modeled and a suitable distance between their N and C-terminus to allow for an easy connection of both ends of the modeled loop on the model backbone. This works well for loops up to 8 residues; on average 1.35 Å RMSD for 8-residues loops [47]. In the second approach, the model is described by a detailed physical energy function and the conformational space of the loop to be modeled is sampled, as exhaustively as possible, with algorithms such as Monte Carlo or Molecular Dynamics simulations. These techniques allow modelers to reproduce the conformation of loops up to 12 residues with an RMSD of 2 Å, on average. Accurately modeling longer loops remains a difficult task [48]. This is clearly a problem for ECL2 that can be up to 30-residue long in some GPCRs; this is unfortunately the case for ORs.

Once a model is obtained, it can be used as a platform for computer-aided ligand discovery. This is done by virtual screening techniques, which is commonly used by pharmaceutical companies worldwide to screen millions of chemical compounds *in silico*, in order to rank and select a limited number of compounds for further experimental tests.

There are two common approaches used for virtual screening: ligand-based and structure-based techniques. The former can be employed even though no 3D structure of the receptor is available but requires the knowledge of a set of ligands of a given type (agonists, antagonists, inverse agonists). The underlying concept is that compounds with similar "pharmacophoric" features will display similar biological responses (this corresponds to methodologies called quantitative structure-activity relationship (QSAR) and 3D-QSAR [49]). This approach cannot be used for most ORs because their ligands are unknown, however see Sanz et al. 2008 [8] for an example of use of 3D-QSAR for odorants: ligands of a human OR.

The second approach, structure-based virtual screening, seeks to model the binding of the ligands (also referred to as docking) to the experimentally solved GPCR 3D structure (or a homology model, if the latter is not available, as for ORs). Unlike the previous approach, it has the great advantage of enabling the user to grasp the molecular basis of the ligand receptor interaction and, thus, rationalizes how different compounds might activate (or inhibit) the receptor biological activity. However, ligand docking requires a "scoring" function to correctly rank the binding poses [50], that should ideally reach a global minimum (or maximum) value for the observed conformation of the ligand in the receptor. Physically, this function is the ligand free energy of binding to the receptor (as described in the previous section). Three categories of functions are used to perform ligand docking. One can use physics-based functions in order to compute the free energy of ligand binding *in silico*, incorporating many terms such as: van der Waals, electrostatic, hydrogen bond, solvation, etc. This amounts to estimating, directly or indirectly, the entropy of the system which is always a difficult endeavor. In addition, physics-based functions are quite sensitive to small inaccuracies in the 3D structure of the receptor. They thus require the receptor conformation to be flexible. The second category corresponds to empirical functions that seek to obtain a coarse estimate of the binding free energy. This pseudo free energy is represented by the sum of a weighted set of features of interest (accessible surface, hydrogen bond, etc.) that are fitted to experimental data. Finally, the last category consists of knowledge-based functions whose parameters are obtained by computing distances between relevant ligand and receptor sites (e.g., chemical functions) in known complexes. The last two categories of functions are better able to put up with a rigid conformation of the receptor and are thus much faster to use for screening millions of compounds against a receptor.

As mentioned above, scoring functions are sensitive to inaccuracies in the receptor 3D structure. Of course, this problem is amplified when a model, instead of the real structure, is used. Beuming and Sherman have recently assessed the accuracy of ligand docking on homology models [46]. For this purpose, they built models of the 3D structure of the known ligand-receptor complexes (Table 3.1) using the 3D structure of receptors in other complexes. Not surprisingly, they observed a clear correlation between the rate of docking success and the sequence similarity of the target and template proteins. They proposed guidelines about what sort of docking accuracy users can expect under different sequence similarity regimes.

In any cases, to better the odds of success, it is absolutely essential to consider all the available pieces of experimental information regarding the system [43]. The search for ligands binding to a given receptor must consist in going back and forth between *in silico* analyses and experiments. In the latter, site-directed mutagenesis of residues predicted by the computer model to have a potential influence on the ligand binding are performed. The real effects of these mutations on the receptor biological activity is monitored through functional assays, e.g., calcium imaging, electrophysiology or surface plasmon resonance [51]. Sometimes, complementary alterations of the receptor and the ligands can even be considered [52]. If required, the results of the experiments are injected back in the docking simulation to correct for erroneous features. The whole process is iterated until, hopefully, ligands with the desired properties are discovered.

Since we now have structures of receptors both in the inactive and activated states, it has been proposed that agonists should preferentially be docked in the activated state of the receptor, given that the G protein enhances their binding affinity through an allosteric mechanism [53]. Conversely, antagonists and inverse agonists ought to be docked in the inactive state of the receptor.

Since 1994, a number of OR homology modeling and odorant virtual screening simulations have been carried out in an effort to decipher the largely uncharted "odor space" of these receptors (see Table 4 in [54]).

No doubt that, with the present bloom of new X-ray and NMR GPCR structures, exploration of OR structures will very rapidly expand. To help in this undertaking, we recently developed an automatic pipeline called GPCRautomodel that allows users to perform homology modeling and ligand docking of ORs [55]. We update the web site (http://genome.jouy.inra.fr/GPCRautomodel) to incorporate all the recently published GPCR 3D structures.

3.5 Olfactory Receptor Activity Regulation: Homodimerization, Binding Cooperativity and Allostery

Clues relative to the functional response of ORs expressed in heterologous systems, displaying a bell-shaped dose-response curve when stimulated with increasing concentrations of odorants [56, 57], in apparent contradiction with the sigmoid curves observed in natural tissues for the OR/ligand interaction [58, 59], resulted in a model of OR activation involving allosteric modulation of OR activity by odorant binding proteins (OBPs) [60] and binding cooperativity within an OR homodimer [61] (Fig. 3.5).

Indeed, it was demonstrated that OBPs can bind ORs [62] and they restore OR activity at high odorant doses [60], probably by exerting an allosteric control of OR activity within an OR dimer. ORs were shown to exist as constitutive homodimers by bioluminescence resonance energy transfer (BRET) and to display different con-

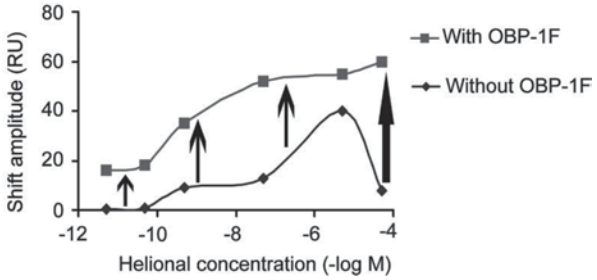

Fig. 3.5 Effect of OBP-1F on helional detection by OR17-40 assayed by Surface Plasmon Resonance (redrawn from [60]). Each curve is plotted as the difference in response to helional relative to controls obtained by replacing the odorant with water. The SPR shift amplitude is shown as a function of the helional concentration, without or with OBP-1F. The OBP restores OR activity at high odorant dose, from a bell-shaped to a sigmoid curve

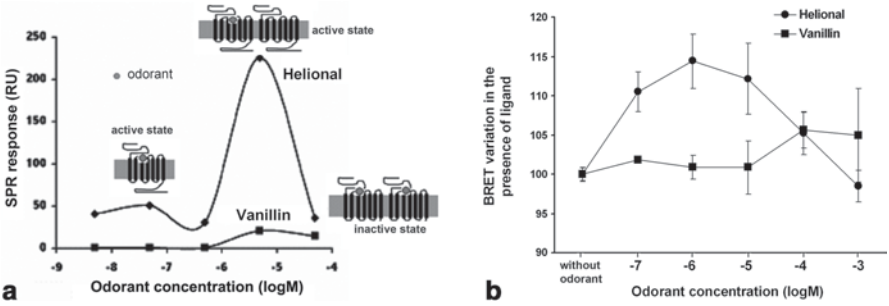

Fig. 3.6 **a** Surface Plasmon Resonance (SPR) response (RU: relative units) obtained from the stimulation of the OR17-40 receptor with helional (agonist) or vanillin (negative control odorant) at different concentrations. A schematic representation of the proposed molecular mechanism for odorant interaction with the OR is shown. At low and moderate odorant doses, the receptor binds only one odorant molecule and is active, while at high odorant dose it binds two odorant molecules and is in an inactive state (redrawn from [61]). **b** Bioluminescence Resonance Energy Transfer (BRET) level variation upon OR17-40 stimulation with various helional or vanillin concentrations. BRET levels are expressed relative to that measured in the absence of odorant. OR17-40 receptor dimers conformational changes induced upon stimulation with various odorant doses elicit an evolution in the BRET level that correlates with the different levels of activity shown in panel A

formational changes upon stimulation with various odorant doses, corresponding to different levels of activity [61] (Fig. 3.6): (i) low and moderate odorant doses (below the micromolar) induce an increase of the initial BRET level, showing a conformational change of the OR dimers which are activated at these odorant doses, (ii) whereas higher odorant doses induce a lesser increase or no increase at all of the initial BRET level, indicating another conformation of the OR dimers, which corresponds to a decreased activity. It was thus assumed that at low and moderate odorant doses, only one odorant molecule could bind to the OR dimer on one protomer, this binding inducing a conformational change of the second protomer and a

reduced affinity for the odorant. At high ligand doses, and in absence of OBPs, the OR dimer could then bind two odorant molecules, one on each protomer, and this would inactivate the receptors. Yet, in presence of OBPs and at high odorant doses, OBPs binding to the OR dimer at an allosteric site would prevent the binding of a second odorant molecule and would thus preserve OR activity. Such "multi-state" models have already been reported for other GPCRs [63], in which the activity depends on the occupation rate of the various sites on the dimers.

This negative modulation of OR activity by odorants themselves is essential to take into account when searching to identify OR odorant ligands or to detect odorants using biosensors carrying ORs.

3.6 Use of Olfactory Receptor Protein in Bioelectronic Noses

The animal olfactory system, with its ability to identify and discriminate thousands of odorant compounds with very low thresholds (10^{-11}–10^{-17} M for some odorants in humans or in dogs, [64, 65]), is worth mimicking to engineer bioelectronic noses. Using ORs as basic sensing elements instead of chemical sensors in electronic noses allows researchers to benefit from the naturally optimized molecular recognition of odorants to develop these new devices. ORs first have to be expressed in heterologous systems, which is not yet an easy task (see the next chapters for the various expression systems considered). Then, several procedures can be used depending on the method considered for measuring their functional response, in order to improve the technical performances of the devices.

ORs can be purified in the presence of surfactants, or prepared as membrane fractions, micelles, nanodisks, nanoliposomes or nanovesicles, then specifically grafted on functionalized surfaces, including gold electrodes or carbon or polymer nanotubes. Their functional response can then be monitored by physical or biophysical measurements, at submillimetric to micrometric scales. Detection limits and odorants discrimination can in some cases reach the femtomolar (fM), an intrinsic property of the ORs themselves.

Olfactory receptors carrying a His tag can be produced in a baculovirus/insect cells system [66] or in *Escherichia coli* [67], and affinity-purified using nickel-magnetic beads. The response of these ORs prepared either as digitonin micelles, or as soluble nanodiscs, and deposited on nickel-nitrilotriacetic acid (Ni-NTA) carbon nanotubes (CNTs) can be followed by a change of conductivity measured by the CNT transistor [66]. Alternately, purified ORs are deposited on conducting polymers nanotubes (CPNTs) [68], or on single-wall functionalized carbon nanotubes [67]. With CPNTs deposited on interdigitated microelectrodes, the resulting resistance varies linearly between the detection limit of 0,02 ppt and 2 ppm.

Starting from HEK293 cells, nanovesicles with a diameter of 100–200 nm carrying ORs can be prepared using cytochalasin [69, 70], and directly attached to carbon nanotubes (swCNT). In this case, exposition of the nanovesicles to the

odorant ligand of the receptor activates the signaling cascade, resulting in an increase of the intracellular calcium concentration inside the nanovesicles, thus producing a field effect on the transistor carrying the swCNT, which induces a change in its conductance. Depending on the OR-ligand couple, a specific detection of the odorant present can be achieved, with sensitivity down to the femtomolar.

Human breast cancer MCF-7 cells can also be used for expression of an OR, their membrane fraction containing the receptor extracted, and integrated with a surface acoustic wave (SAW)-based biosensor, resulting in a highly sensitive device (10^{-13} M) [71].

ORs are also prepared from *Saccharomyces cerevisiae*, and Surface Plasmon Resonance is performed on *nanoliposomes* prepared from their membrane fraction for quantitative evaluation of OR response to odorant stimulation. ORs retain full activity and discrimination power in immobilized nanosomes, thus allowing their use in the fabrication of the nanobiosensors. Nanosomes are specifically immobilized on nanoelectrodes of compatible size, using mixed Self Assembled Monolayers and an antibody specifically targeting the ORs. Electrochemical Impedancemetric Spectroscopy is used to detect OR conformational changes induced by odorant binding, at concentrations as low as 10^{-10} M [72].

Other biosensors are designed based on BRET2 between a bioluminescent donor (RLuc) and a fluorescent acceptor (GFP), the sequences of which are inserted in that of an OR (C-terminus for RLuc, 3rd intracellular loop for GFP), then expressed at the plasmic membrane of *S. cerevisiae*. Measurements are then performed on yeast membranes, and show a decrease of the BRET2 signal in the presence of the OR odorant ligand, witnessing a conformational change of the receptor upon ligand binding, inducing a re-orientation or a separation of donor and acceptor. The dose-dependence indicates an EC50 in the femtomolar range for specific diacetyl detection by ODR10 [73].

Other biophysical approaches, with bioluminescence measurements in yeasts, or BRET on yeast membrane fractions, are also promising techniques (see Chap. 8: [74, 75]).

References

1. Gilad Y, Man O, Glusman G (2005) A comparison of the human and chimpanzee olfactory receptor gene repertoires. Genome Res 15:224–230
2. Young JM, Trask BJ (2002) The sense of smell: genomics of vertebrate odorant receptors. Hum Mol Genet 11:1153–1160
3. Quignon P, Kirkness E, Cadieu E, Touleimat N, Guyon R et al (2003) Comparison of the canine and human olfactory receptor gene repertoires. Genome Biol 4:R80.81–80.89
4. Glusman G, Yanai I, Rubin I, Lancet D (2001) The complete human olfactory subgenome. Genome Res 11:685–902
5. Zozulya S, Echeverri F, Nguyen T (2001) The human olfactory receptor repertoire. Genome Biol 2:0018.0011–0018.0012
6. Fredriksson R, Lagerström MC, Lundin LG, Schiöth HB (2003) The G-protein-coupled receptors in the human genome form five main families. Phylogenetic analysis, paralogon groups, and fingerprints. Mol Pharmacol 63:1256–1272

7. Buck L, Axel R (1991) A novel multigene family may encode odorant receptors: a molecular basis for odor recognition. Cell 65:175–187
8. Sanz G, Thomas-Danguin T, Hamdani EH, Le Poupon C, Briand L et al (2008) Relationships Between Molecular Structure and Perceived Odor Quality of Ligands for a Human Olfactory Receptor. Chem Senses 33(7):639–653
9. Spehr M, Gisselmann G, Poplawski A, Riffell JA, Wetzel C et al (2003) Identification of a testicular odorant receptor mediating human sperm chemotaxis. Science 299:2054–2058
10. Spehr M, Schwane K, Heilmann S, Gisselmann G, Hummel T et al (2004) Dual capacity of a human olfactory receptor. Curr Biol 14:R832–R833
11. Braun T, Voland P, Kunz L, Prinz C, Gratzl M (2007) Enterochromaffin cells of the human gut: sensors for spices and odorants. Gastroenterology 132:1890–1901
12. Kidd M, Modlin IM, Gustafsson BI, Drozdov I, Hauso O et al (2008) Luminal regulation of normal and neoplastic human EC cell serotonin release is mediated by bile salts, amines, tastants, and olfactants. Am J Physiol Gastrointest Liver Physiol 295:G260–272
13. Griffin CA, Kafadar KA, Pavlath GK (2009) MOR23 promotes muscle regeneration and regulates cell adhesion and migration. Dev Cell 17:649–661
14. Pluznick JL, Zou DJ, Zhang X, Yan Q, Rodriguez-Gil DJ et al (2009) Functional expression of the olfactory signaling system in the kidney. Proc Natl Acad Sci U S A 106:2059–2064
15. Pluznick JL, Protzko RJ, Gevorgyan H, Peterlin Z, Sipos A et al (2013) Olfactory receptor responding to gut microbiota-derived signals plays a role in renin secretion and blood pressure regulation. Proc Natl Acad Sci U S A 110:4410–4415
16. Weng J, Wang J, Cai Y, Stafford LJ, Mitchell D et al (2005) Increased expression of prostate-specific G-protein-coupled receptor in human prostate intraepithelial neoplasia and prostate cancers. Int J Cancer 113:811–818
17. Leja J, Essaghir A, Essand M, Wester K, Oberg K et al (2009) Novel markers for enterochromaffin cells and gastrointestinal neuroendocrine carcinomas. Mod Pathol 22:261–272
18. Muranen TA, Greco D, Fagerholm R, Kilpivaara O, Kampjarvi K et al (2011) Breast tumors from CHEK2 1100delC-mutation carriers: genomic landscape and clinical implications. Breast Cancer Res 13: R90
19. Zhang X, Bedigian AV, Wang W, Eggert US (2012) G protein-coupled receptors participate in cytokinesis. Cytoskeleton (Hoboken) 69:810–818
20. Fukuda N, Touhara K (2006) Developmental expression patterns of testicular olfactory receptor genes during mouse spermatogenesis. Genes Cells 11:71–81
21. Sanz G, Leray I, Dewaele A, Sobilo J, Lerondel S et al (2014) Promotion of cancer cell invasiveness and metastasis emergence caused by olfactory receptor stimulation. PLOS ONE 9(1):e85110
22. Regnauld K, Nguyen QD, Vakaet L, Bruyneel E, Launay JM et al (2002) G-protein alpha(olf) subunit promotes cellular invasion, survival, and neuroendocrine differentiation in digestive and urogenital epithelial cells. Oncogene 21:4020–4031
23. Ukhanov K, Brunert D, Corey EA, Ache BW (2011) Phosphoinositide 3-kinase-dependent antagonism in Mammalian olfactory receptor neurons. J Neurosci 31:273–280
24. Ukhanov K, Corey EA, Ache BW (2013) Phosphoinositide 3-kinase dependent inhibition as a broad basis for opponent coding in Mammalian olfactory receptor neurons. PLoS One 8:e61553
25. Fredriksson R, Schioth HB (2005) The repertoire of G-protein-coupled receptors in fully sequenced genomes. Mol Pharmacol 67:1414–1425
26. Palczewski K, Kumasaka T, Hori T, Behnke CA, Motoshima H et al (2000) Crystal structure of rhodopsin: a G protein-coupled receptor. Science 289:739–745
27. Rasmussen SG, Choi HJ, Rosenbaum DM, Kobilka TS, Thian FS et al (2007) Crystal structure of the human beta2 adrenergic G-protein-coupled receptor. Nature 450:383–387
28. Park SH, Das BB, Casagrande F, Tian Y, Nothnagel HJ et al (2012) Structure of the chemokine receptor CXCR1 in phospholipid bilayers. Nature 491:779–783
29. Rasmussen SG, Choi HJ, Fung JJ, Pardon E, Casarosa P et al (2011) Structure of a nanobody-stabilized active state of the beta(2) adrenoceptor. Nature 469:175–180

30. Rasmussen SG, DeVree BT, Zou Y, Kruse AC, Chung KY et al (2011) Crystal structure of the beta2 adrenergic receptor-Gs protein complex. Nature 477:549–555
31. Katritch V, Cherezov V, Stevens RC (2012) Diversity and modularity of G protein-coupled receptor structures. Trends Pharmacol Sci 33:17–27
32. Pilpel Y, Lancet D (1999) The variable and conserved interfaces of modeled olfactory receptor proteins. Protein Sci 8:969–977
33. Ballesteros JA, Weinstein H (1995) Integrated methods and computational probing of structure-function relations in G protein-coupled receptors. Methods Neurosci 25:366–428
34. Venkatakrishnan AJ, Deupi X, Lebon G, Tate CG, Schertler GF et al (2013) Molecular signatures of G-protein-coupled receptors. Nature 494:185–194
35. Choe HW, Kim YJ, Park JH, Morizumi T, Pai EF et al (2011) Crystal structure of metarhodopsin II. Nature 471:651–655
36. Standfuss J, Edwards PC, D'Antona A, Fransen M, Xie G et al (2011) The structural basis of agonist-induced activation in constitutively active rhodopsin. Nature 471:656–660
37. Nygaard R, Zou Y, Dror RO, Mildorf TJ, Arlow DH et al (2013) The dynamic process of beta(2)-adrenergic receptor activation. Cell 152:532–542
38. Deupi X, Standfuss J (2011) Structural insights into agonist-induced activation of G-protein-coupled receptors. Curr Opin Struct Biol 21:541–551
39. Liu JJ, Horst R, Katritch V, Stevens RC, Wuthrich K (2012) Biased signaling pathways in beta2-adrenergic receptor characterized by 19F-NMR. Science 335:1106–1110
40. Kenakin T (2011) Functional selectivity and biased receptor signaling. J Pharmacol Exp Ther 336:296–302
41. Kontoyianni M, Liu Z (2012) Structure-based design in the GPCR target space. Curr Med Chem 19:544–556
42. Nordstrom KJ, Sallman Almen M, Edstam MM, Fredriksson R, Schioth HB (2011) Independent HHsearch, Needleman–Wunsch-based, and motif analyses reveal the overall hierarchy for most of the G protein-coupled receptor families. Mol Biol Evol 28:2471–2480
43. Costanzi S (2013) Modeling G protein-coupled receptors and their interactions with ligands. Curr Opin Struct Biol 23:185–190
44. Xiang Z (2006) Advances in homology protein structure modeling. Curr Protein Pept Sci 7:217–227
45. Sali A, Blundell TL (1993) Comparative protein modelling by satisfaction of spatial restraints. J Mol Biol 234:779–815
46. Beuming T, Sherman W (2012) Current assessment of docking into GPCR crystal structures and homology models: successes, challenges, and guidelines. J Chem Inf Model 52:3263–3277
47. Michalsky E, Goede A, Preissner R (2003) Loops In Proteins (LIP)—a comprehensive loop database for homology modelling. Protein Eng 16:979–985
48. Congreve M, Langmead CJ, Mason JS, Marshall FH (2011) Progress in structure based drug design for G protein-coupled receptors. J Med Chem 54:4283–4311
49. Kubinyi H (1997) QSAR and 3D QSAR in drug design. Drug Discov Today 2:457–467
50. Kufareva I, Rueda M, Katritch V, Stevens RC, Abagyan R (2011) Status of GPCR modeling and docking as reflected by community-wide GPCR Dock 2010 assessment. Structure 19:1108–1126
51. Zhukov A, Andrews SP, Errey JC, Robertson N, Tehan B et al (2011) Biophysical mapping of the adenosine A2A receptor. J Med Chem 54:4312–4323
52. Jacobson KA, Gao ZG, Liang BT (2007) Neoceptors: reengineering GPCRs to recognize tailored ligands. Trends Pharmacol Sci 28:111–116
53. Shoichet BK, Kobilka BK (2012) Structure-based drug screening for G-protein-coupled receptors. Trends Pharmacol Sci 33:268–272
54. Launay G, Sanz G, Pajot E, Gibrat JF (2012) Modeling of mammalian olfactory receptors and docking of odorants. Biophys Rev 4:255–269
55. Launay G, Teletchea S, Wade F, Pajot-Augy E, Gibrat JF et al (2012) Automatic modeling of mammalian olfactory receptors and docking of odorants. Protein Eng Des Sel 25:377–386

56. Minic J, Persuy MA, Godel E, Aioun J, Connerton I et al (2005) Functional expression of olfactory receptors in yeast and development of a bioassay for odorant screening. FEBS J 272:524–537
57. Minic Vidic J, Grosclaude J, Persuy MA, Aioun J, Salesse R et al (2006) Quantitative assessment of olfactory receptors activity in immobilized nanosomes: a novel concept for bioelectronic nose. Lab Chip 6:1026–1032
58. Duchamp-Viret P, Duchamp A, Sicard G (1990) Olfactory discrimination over a wide concentration range. Comparison of receptor cell and bulb neuron abilities. Brain Res 517:256–262
59. Grosmaitre X, Vassalli A, Mombaerts P, Shepherd GM, Ma M (2006) Odorant responses of olfactory sensory neurons expressing the odorant receptor MOR23: a patch clamp analysis in gene-targeted mice. Proc Natl Acad Sci U S A 103:170–1975
60. Vidic J, Grosclaude J, Monnerie R, Persuy MA, Badonnel K et al (2008) On a chip demonstration of a functional role for Odorant Binding Protein in the preservation of olfactory receptor activity at high odorant concentration. Lab Chip 8:678–688
61. Wade F, Espagne A, Persuy MA, Vidic J, Monnerie R et al (2011) Relationship between homo-oligomerization of a mammalian olfactory receptor and its activation state demonstrated by bioluminescence resonance energy transfer. J Biol Chem 286:15252–15259
62. Matarazzo V, Zsürger N, Guillemot JC, Clot-Faybesse O, Botto JM et al (2002) Porcine odorant-binding protein selectively binds to a human olfactory receptor. Chem Senses 27:691–701
63. Franco R, Casado V, Mallol J, Ferrada C, Ferré S et al (2006) The two-state dimer receptor model: a general model for receptor dimers. Mol Pharmacol 69:1905–1912
64. Wetzel C, Oles M, Wellerdieck C, Kuczkowiak M, Gisselmann G et al (1999) Specificity and sensitivity of a human olfactory receptor functionally expressed in human embryonic kidney 293 cells and Xenopus Laevis oocytes. J Neurosci 19:7426–7433
65. Dulac C (2000) The physiology of taste, vintage 2000. Cell 100:607–610
66. Goldsmith BR, Mitala JJ, Josue J, Castro A, Lerner MB et al (2011) Biomimetic Chemical Sensors Using Nanoelectronic Readout of Olfactory Receptor Proteins. ACS Nano 5:5408–5416
67. Lee SH, Jin HJ, Song HS, Hong S, Park TH (2012) Bioelectronic nose with high sensitivity and selectivity using chemically functionalized carbon nanotube combined with human olfactory receptor. J Biotechnol 157:467–472
68. Lee SH, Kwon OS, Song HS, Park SJ, Sung JH et al (2012) Mimicking the human smell sensing mechanism with an artificial nose platform. Biomaterials 33:1722–1729
69. Jin HJ, Lee SH, Kim TH, Park J, Song HS et al (2012) Nanovesicle-based bioelectronic nose platform mimicking human olfactory signal transduction. Biosens Bioelectron 35:335–341
70. Park J, Lim JH, Jin HJ, Namgung S, Lee SH et al (2012) A bioelectronic sensor based on canine olfactory nanovesicle-carbon nanotube hybrid structures for the fast assessment of food quality. Analyst 137:3249–3254
71. Wu C, Du L, Wang D, Wang L, Zhao L et al (2011) A novel surface acoustic wave-based biosensor for highly sensitive functional assays of olfactory receptors. Biochem Biophys Res Commun 407:18–22
72. Benilova IV, Minic Vidic J, Pajot-Augy E, Soldatkin AP, Martelet C et al (2008) Electrochemical study of human olfactory receptor OR 17–40 stimulation by odorants in solution. Mater Sci Eng C 28:633–639
73. Dacres H, Wang J, Leitch V, Horne I, Anderson AR et al (2011) Greatly enhanced detection of a volatile ligand at femtomolar levels using bioluminescence resonance energy transfer (BRET). Biosens Bioelectr 29:119–124
74. Fukutani Y, Nakamura T, Yorozu M, Ishii J, Kondo A et al (2012) The N-terminal replacement of an olfactory receptor for the development of a Yeast-based biomimetic odor sensor. Biotechnol Bioeng 109:205–212
75. Radhika V, Proikas-Cezanne T, Jayaraman M, Onesime D, Ha JH et al (2007) Chemical sensing of DNT by engineered olfactory yeast strain. Nat Chem Biol 3:325–330
76. Warne T, Edwards PC, Leslie AG, Tate CG (2012) Crystal structures of a stabilized beta1-adrenoceptor bound to the biased agonists bucindolol and carvedilol. Structure 20:841–849

77. Wu H, Wacker D, Mileni M, Katritch V, Han GW et al (2012) Structure of the human kappa-opioid receptor in complex with JDTic. Nature 485:327–332
78. Okada T, Sugihara M, Bondar AN, Elstner M, Entel P et al (2004) The retinal conformation and its environment in rhodopsin in light of a new 2.2 A crystal structure. J Mol Biol 342:571–583
79. Murakami M, Kouyama T (2008) Crystal structure of squid rhodopsin. Nature 453:363–367
80. Hanson MA, Cherezov V, Griffith MT, Roth CB, Jaakola VP et al (2008) A specific cholesterol binding site is established by the 2.8 A structure of the human beta2-adrenergic receptor. Structure 16:897–905
81. Wacker D, Fenalti G, Brown MA, Katritch V, Abagyan R et al (2010) Conserved binding mode of human beta2 adrenergic receptor inverse agonists and antagonist revealed by X-ray crystallography. J Am Chem Soc 132:11443–11445
82. Rosenbaum DM, Zhang C, Lyons JA, Holl R, Aragao D et al (2011) Structure and function of an irreversible agonist-beta(2) adrenoceptor complex. Nature 469:236–240
83. Warne T, Serrano-Vega MJ, Baker JG, Moukhametzianov R, Edwards PC et al (2008) Structure of a beta1-adrenergic G-protein-coupled receptor. Nature 454:486–491
84. Warne T, Moukhametzianov R, Baker JG, Nehme R, Edwards PC et al (2011) The structural basis for agonist and partial agonist action on a beta(1)-adrenergic receptor. Nature 469:241–244
85. Moukhametzianov R, Warne T, Edwards PC, Serrano-Vega MJ, Leslie AG et al (2011) Two distinct conformations of helix 6 observed in antagonist-bound structures of a beta1-adrenergic receptor. Proc Natl Acad Sci U S A 108:8228–8232
86. Jaakola VP, Griffith MT, Hanson MA, Cherezov V, Chien EY et al (2008) The 2.6 angstrom crystal structure of a human A2A adenosine receptor bound to an antagonist. Science 322:1211–1217
87. Xu F, Wu H, Katritch V, Han GW, Jacobson KA et al (2011) Structure of an agonist-bound human A2A adenosine receptor. Science 332:322–327
88. Lebon G, Warne T, Edwards PC, Bennett K, Langmead CJ et al (2011) Agonist-bound adenosine A2A receptor structures reveal common features of GPCR activation. Nature 474:521–525
89. Dore AS, Robertson N, Errey JC, Ng I, Hollenstein K et al (2011) Structure of the adenosine A(2A) receptor in complex with ZM241385 and the xanthines XAC and caffeine. Structure 19:1283–1293
90. Wu B, Chien EY, Mol CD, Fenalti G, Liu W et al (2010) Structures of the CXCR4 chemokine GPCR with small-molecule and cyclic peptide antagonists. Science 330:1066–1071
91. Chien EY, Liu W, Zhao Q, Katritch V, Han GW et al (2010) Structure of the human dopamine D3 receptor in complex with a D2/D3 selective antagonist. Science 330:1091–1095
92. Shimamura T, Shiroishi M, Weyand S, Tsujimoto H, Winter G et al (2011) Structure of the human histamine H1 receptor complex with doxepin. Nature 475:65–70
93. Hanson MA, Roth CB, Jo E, Griffith MT, Scott FL et al (2012) Crystal structure of a lipid G protein-coupled receptor. Science 335:851–855
94. Haga K, Kruse AC, Asada H, Yurugi-Kobayashi T, Shiroishi M et al (2012) Structure of the human M2 muscarinic acetylcholine receptor bound to an antagonist. Nature 482:547–551
95. Kruse AC, Hu J, Pan AC, Arlow DH, Rosenbaum DM et al (2012) Structure and dynamics of the M3 muscarinic acetylcholine receptor. Nature 482:552–556
96. Manglik A, Kruse AC, Kobilka TS, Thian FS, Mathiesen JM et al (2012) Crystal structure of the micro-opioid receptor bound to a morphinan antagonist. Nature 485:321–326
97. Granier S, Manglik A, Kruse AC, Kobilka TS, Thian FS et al (2012) Structure of the delta-opioid receptor bound to naltrindole. Nature 485:400–404
98. Thompson AA, Liu W, Chun E, Katritch V, Wu H et al (2012) Structure of the nociceptin/orphanin FQ receptor in complex with a peptide mimetic. Nature 485:395–399
99. White JF, Noinaj N, Shibata Y, Love J, Kloss B et al (2012) Structure of the agonist-bound neurotensin receptor. Nature 490:508–513
100. Zhang C, Srinivasan Y, Arlow DH, Fung JJ, Palmer D et al (2012) High-resolution crystal structure of human protease-activated receptor 1. Nature 492:387–392

Chapter 4
Odorant-Receptor Interaction

Xubo Su, Hiroaki Matsunami and Hanyi Zhuang

Abstract Odorant-receptor interactions constitute a key step in the olfactory detection of chemical compounds. Various studies support the combinatorial coding of olfaction, in which each odorant activates an array of odorant receptors and each odorant receptor is capable of recognizing multiple odorants, while large-scale studies involving numerous odorants and odorant receptors help to resolve the tuning specificities of receptor repertoires. In the meantime, the proteinaceous content of the nasal mucus, including odorant binding proteins and different types of xenobiotic-metabolizing enzymes, also contributes to odorant receptor activation by transporting, concentrating, converting, and/or ultimately removing odorants from nasal mucosa. In addition, the presence of metal ions, notably copper ions, is known to be important for the activation of odorant receptors for certain types of metal-coordinating odorants. Finally, prediction algorithms based on odorant properties and receptor structures are becoming increasingly feasible for investigating detailed mechanisms involved in odorant-receptor interactions.

4.1 Introduction

The binding of an odorant to an odorant receptor (OR) is one of the crucial steps from odorant inhalation to the eventual odor perception. Odorants are small, volatile molecules of variable sizes, charges, and functional groups. The presence of tens of thousands of odorant molecules in nature mandates that mammals be capable

H. Zhuang (✉) · X. Su
Department of Pathophysiology, Shanghai Jiaotong
University School of Medicine, Shanghai, P. R. China
e-mail: hanyizhuang@sjtu.edu.cn

H. Zhuang
Institute of Health Sciences, Shanghai Jiaotong University School of Medicine/Shanghai
Institutes for Biological Sciences of Chinese Academy of Sciences, Shanghai, P. R. China

H. Matsunami
Department of Molecular Genetics and Microbiology,
Duke University Medical Center, Durham, NC, USA

Department of Neurobiology, Duke University Medical Center, Durham, NC, USA

T. H. Park (ed.), *Bioelectronic Nose,* DOI 10.1007/978-94-017-8613-3_4,

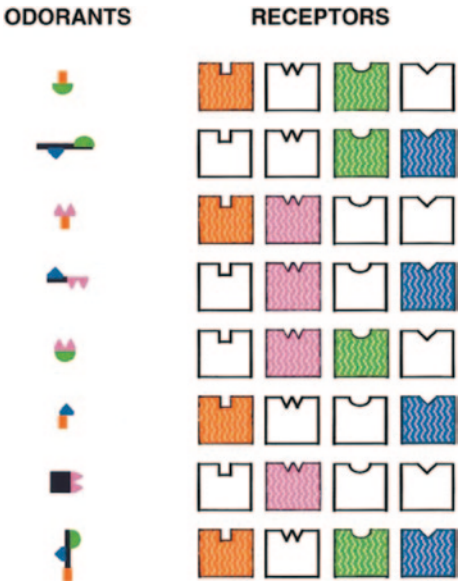

Fig. 4.1 A schematic showing the concept of combinatorial coding of olfaction. Different odorants have varied structural features that allow them to be recognized by a different combination of ORs while each OR can bind to one or more odorants. (Adapted with permission from [5]. Copyright 1999, *Cell*)

of perceiving and discriminating a large number of odorants of diverse structures with a large, yet limited number of OR genes. It is known that the human OR repertoire is composed of more than 300 intact OR genes and around 1,000 of these are found in the mouse [1–3]. Since the number of perceived odors exceeds the number of ORs by far, it has been proposed that the mammalian olfactory system uses a combinatorial receptor coding scheme to encode odor identity and discriminate odors [4, 5]. In this scheme, each OR uses its unique binding pocket(s) to accommodate odorants based on their structural features, allowing each OR to recognize multiple odorants, while a particular odorant may contain a number of structural features so that one odorant can be recognized by more than one OR (Fig. 4.1).

4.2 Combinatorial Coding of Olfaction

Since the initial cloning of the OR genes in 1991, scientists have developed effective methodologies aimed at analyzing the exact mode of odor coding by the OR repertoire through functional characterization of the ORs. A few pioneering studies explored two important aspects of the combinatorial coding theory. First, a given odorant may activate a certain set of ORs, resulting in its distinctive odor. Malnic et al. [5] used functional cloning from single olfactory sensory neurons (OSN) responding to given odorants. This method allowed for the identification of receptors for cognate ligands by coupling calcium imaging of OSNs and single-cell RT-PCR. Upon analyzing a small group of structurally-related aliphatic odorants, the authors demonstrated for the first time that different odorants, and sometimes different con-

centrations of the same odorant, may be encoded by unique combinations of ORs, resulting in different glomeruli activation patterns in the olfactory bulb (OB) and ultimately leading to different perceived odor identities. In a later study, the effectiveness of this homologous system was complemented by the expression of the cloned receptor in a heterologous system, in which an N-terminal rhodopsin tag was used to promote the cell-surface expression of ORs [6]. It was found that two structurally-related receptors were activated by overlapping sets of odorants, reinforcing the idea of combinatorial coding at the odorant level, and that activation of a combination of ORs comprises the perception of an odorant.

A second aspect of the combinatorial coding scheme is that a given receptor may respond to a group of odorants, thereby defining an OR's molecular receptive range. Using a similar calcium imaging system on isolated OSNs, Araneda et al. [7] found that the rat OR I7 was highly specific for an aldehyde group but also tolerated the structural features of other cognate odorant molecules. Here, the use of a sizeable odorant library helped to characterize the tuning of an OR. In a later study by the same group, they found that different OSNs/ORs exhibited different tuning specificities and also that octanal may activate at least tens of different OSNs [8]. The mouse OR, OREG, the human OR, OR1D2, and others were among the first ORs characterized to exhibit broad and yet selective molecular receptive ranges [9–13].

4.3 Odorant Receptor Tuning

Given the vast number of ORs and odorants, the execution of combinatorial coding and the extent of diverse OR tuning could be much more complicated. While minute differences in the chemical features of a ligand may affect the ORs it can activate, different receptors may exhibit different breadth of tuning, some acting as "generalist" receptors and others "specialists". In order to thoroughly investigate these dynamic features of the olfactory system, large-scale analyses involving a lot more receptors and odorants were necessary for investigating the identity-encoding of odorants. For example, using a HEK293T-based heterologous OR expression system, in which OR trafficking is greatly enhanced by the receptor-transporting protein (RTPs) family members and OR activation is coupled to a cAMP-based luciferase assay readout [14–16], Saito et al. [17] performed high-throughput screening of 93 odorants against 464 ORs and identified agonists for 52 mouse and 10 human ORs, representing a total of 340 odorant-receptor interactions. Consistent with findings from previous studies using OSNs, the 62 ORs included both broadly-tuned and narrowly-tuned ORs. Among the 52 mouse ORs, 11 were tuned to a single odorant while two were tuned to more than 20 odorants. For the 10 human ORs, two of them were tuned to a single odorant and two broadly-tuned ORs responded to 37 and 20 odorants, respectively (Fig. 4.2).

In another study using isolated OSNs, Nara et al. [18] performed an analysis of the responses to a large group of 125 diverse odorants by 3,000 OSNs and were able to define several important features of the mouse olfactory system. While both Saito

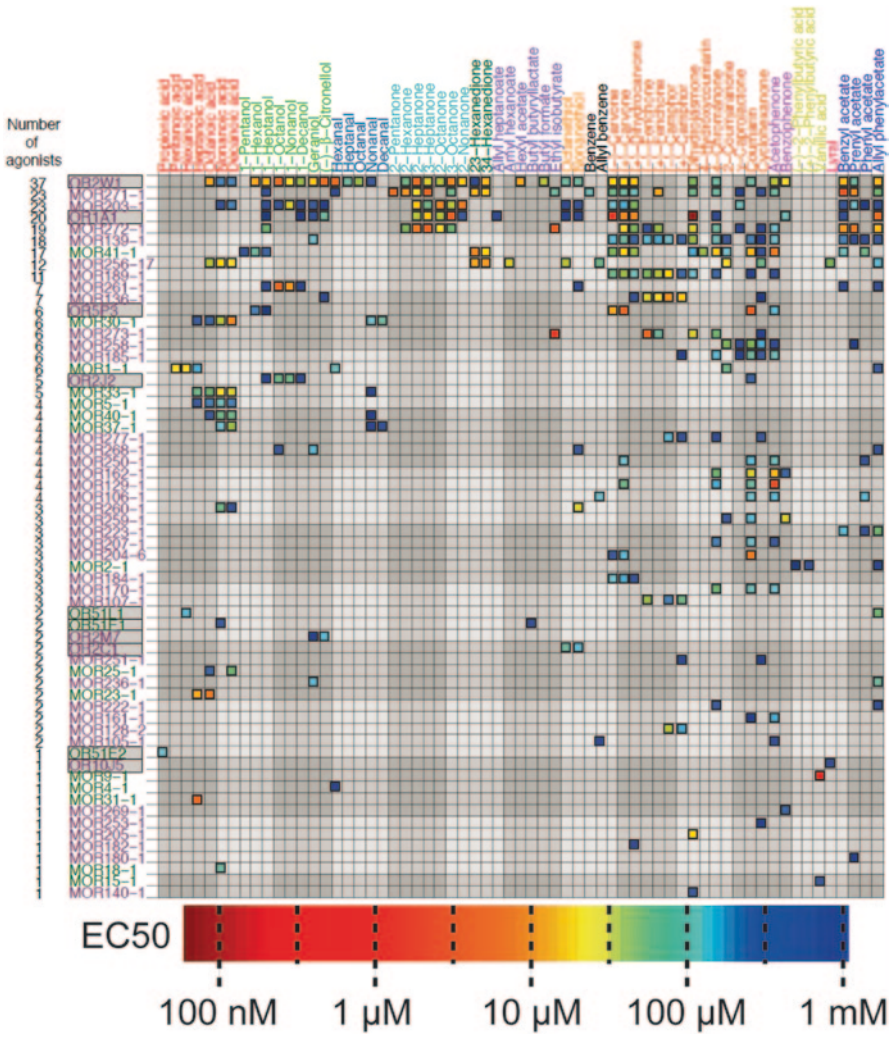

Fig. 4.2 A matrix with 340 odorant-receptor pairs, involving a total of 62 human and mouse ORs and 63 odorants. Odorants on the *x*-axis are ordered and color-coded by functional groups and ORs on the *y*-axis by number of agonists. The heat map color scale represents EC_{50} values of the different odorant-receptor interactions. Class I ORs are shown in *green* and class II ORs in *purple*. Human ORs are shown on a *gray* background. (Modified with permission from [17]. Copyright 2009, *Science Signaling*)

et al. and Nara et al. found broadly- and narrowly-tuned ORs, they found that a larger proportion of mouse OSNs were narrowly tuned with only a very small proportion being broadly tuned. Of the 97 OSNs that responded to only one odorant mixture, 43 responded to only one odorant. There is one case in which one OSN corresponding to Olfr42 was activated by 12 single odorants. While the apparent differences in olfactory response profiles between the two studies may indicate that odor tuning of

heterologously-expressed ORs and OSNs expressing the corresponding ORs are not exactly the same, the discrepancy can also be explained by other reasons including the difference in the size of the odorant library, odor concentrations, and perhaps a biased expression of certain ORs in mouse OSNs.

4.4 Role of Mucus in Odorant Recognition

The functional studies done in heterologous system or isolated OSNs represent efficient and replicable means of identifying odorant-receptor interactions; however, there are concerns that the functional profiles generated in these systems may not precisely reflect *in vivo* odorant perception. Alternatively, *in vivo* methodologies based upon glomeruli activity in the OB may circumvent the uncertainties and help to establish a combinatorial code that more accurately reflects sensory activities under physiological conditions. By combining calcium imaging, retrograde dye labeling, and single cell RT-PCR, Oka et al. successfully isolated the most sensitive ORs for eugenol, methyl isoeugenol, and isovaleric acid using glomeruli activation pattern in dorsal OB [19]. Notably, in some cases, OR sensitivity and ligand specificity obtained from olfactory bulbar activation patterns are found to be different from that in isolated OSNs or cell-based heterologous expression systems [19]. One possibility is that events prior to receptor-ligand interaction may influence which and how ORs are activated. Indeed, when nasal mucus was eliminated from the nasal cavity, the specificity of glomeruli *in vivo* became more repeatable and more similar to OR activity *in vitro* [19]. It is known that ORs are expressed on the cilia on the dendritic end of OSNs and the cilia on this epithelial surface are immersed in nasal mucus, so odorants from external environment must cross the mucosal perireceptor space to interact with ORs [20]. Proteomic analyses revealed that the nasal mucus contains odorant-binding proteins and various metabolic enzymes [21, 22]. The nasal mucus may, therefore, play an important role in odorant recognition by influencing the ways ORs interact with odorants.

Odorant-binding proteins Odorant-binding proteins (OBPs) were first discovered in the nasal olfactory mucosa of bovines as a soluble protein capable of binding the odorant 2-isobutyl-3-methoxypyrazine [23]. OBPs belong to the lipocalin family, which are extracellular transport proteins for small hydrophobic molecules in aqueous solutions [24]. OBPs are present at high levels in nasal mucus (100 μM–1 mM) [25] and can reversibly bind odorants with dissociation constants in the micromolar range and thus effectively solubilizing volatile odorants, facilitating their diffusion through the mucus barrier towards ORs [26]. Though it has been speculated that OBPs may be responsible for carrying and concentrating odorants for subsequent presentation to ORs, their exact role in olfaction remains to be explored. Some studies have demonstrated that OBPs have a broad binding spectrum toward hydrophobic molecules [27–29] since there are numerous hydrophobic molecules but only limited numbers of OBP genes found in mammals (four each in human [30] and mouse [31]). Moreover, it is unclear whether OBPs could act as co-activators

for ORs. While it was shown that a porcine OBP exhibited high-affinity binding to the human OR17-210 [32], there is no evidence showing the release of odorants from OBPs. Furthermore, to maintain the function of the olfactory epithelium, it is not only necessary to dispense the hydrophobic compounds, but also to eliminate these signaling molecules. A research group showed that the OBP-odorant complexes undergo a rapid internalization in the sustentacular cells containing different enzymes to inactivate the odorants [33], pointing to a possible role of OBPs in the clearance of odorants.

Enzymes in nasal mucus Xenobiotic-metabolizing enzymes found at high levels in the nasal mucosa are thought to play a role in protecting the olfactory epithelium, the lungs, and the brain against toxicity from foreign substances inhaled [34–36]. The clearance of xenobiotics involves biotransformation processes mediated by enzymes, such as cytochrome P450 monooxygenases, aldehyde dehydrogenases, aldehyde oxidases, aldehyde reductases, carbonic anhydrases, carboxyl esterases, and various transferases and transporters [37–42], and is carried out in distinct phases. Expectedly, volatile odorants undergo similar biotransformations as other xenobiotics when they cross the nasal mucus. Prior evidence from insects showed that enzymes such as carboxyl esterases or aldehyde oxidases can metabolize odorant molecules and pheromones [43–47]. In mammals, several mouse and human cytochrome P450s were shown to be responsible for the metabolism of the odorant coumarin and at least 6 coumarin metabolites were identified by GC-MS [48]. Nagashima and Touhara showed for the first time, at both pharmacological and behavioral levels, that odorants with functional groups such as aldehydes and esters are targets of metabolic enzymes secreted into the mouse nasal mucus, resulting in their oxidative and hydrolytic conversions to the corresponding acids and alcohols, respectively [49]. Notably, the ultimate perception is of a mixture of the original odorant and its metabolic derivatives, rather than of a single species of odorant molecule [49]. Similarly, a recent study also showed that quinoline and coumarin were both oxidized by cytochrome P450 whereas isoamyl acetate was hydrolyzed by carboxyl esterases in rat olfactory mucosa [50]. Furthermore, Lazard et al. found that odorants are substrates of the olfactory UDP glucuronosyl transferase, which alters odorants' chemical properties in a later phase of xenobiotic clearance and may be responsible for terminating odorant signals [51]. Therefore, in addition to investigating OR pharmacology, growing evidence points to the importance of examining the role of the proteinaceous content of the nasal mucus in determining the exact manner ORs are activated, that is, through effective transportation, concentration, and clearance of odorants.

Metal ions and olfaction The role of metal ions in G protein-coupled receptors activation has long been speculated. For example, certain divalent cations could modulate ligand-binding of some opioid receptor subtypes [52], increase the affinity of a ligand to CXCR4 chemokine receptor [53], and bind and activate the melanocortin MC1 and MC4 receptors [54]. As early as in the 1960s, scientists have proposed that transition metals, such as copper and zinc, may mediate taste or odor perception of metal-coordinating molecules [55–57]. In 2003, Wang et al.

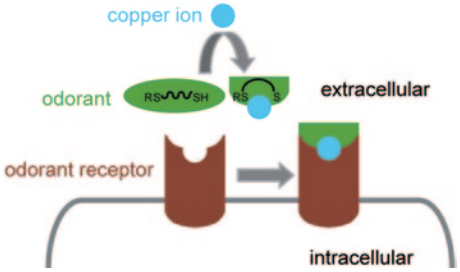

Fig. 4.3 A model for copper ion involvement in odorant-receptor interaction. For copper-coordinating odorants, such as the one shown with a thiol and a thioether group, the copper ion binds to the ligand, resulting in a conformation change in the ligand, followed by binding of the copper ion-ligand complex to the OR. (Adapted with permission from [59]. Copyright 2012, *PNAS*)

[58] revisited the subject and proposed that ORs may function as metalloproteins. They found that the synthetic pentapeptide HACKE, corresponding to a conserved sequence in the extracellular loop of human ORs, has high affinity for copper and zinc ions and therefore may form the basis for sensitive detection of certain odorant molecules with intense smells, including thiols, amines, and carboxylic acids [58].

A recent study from our group showed that copper ion plays a key role in the activation of MOR244–3 [59]. Using the HEK293T cell-based OR expression system, we found that copper ion specifically enhanced the mouse OR's response to a strong-smelling semiochemical, named (methylthio)methanethiol [60], and structurally-related sulfur-containing compounds, as well as a few unrelated metal-coordinating compounds. The results were replicated using electrophysiological recordings on mouse septal organ neurons, where MOR244-3 is abundantly expressed [61]. Given the above observations, it is probable that under *in vivo* conditions, copper may be present in the mucus to exert its function. Indeed, it was found that the total copper concentration of mouse nasal mucus is around 40 μM, similar to that used in the *in vitro* study [59]. Based on these findings, we proposed a model for OR activation involving copper ion as a cofactor with the copper ion binding to the ligand for subsequent binding of the metal-odorant complex to the OR (Fig. 4.3). In contrast, in a separate study, Viswaprakash et al. [62] demonstrated that Zn^{2+} ion *decreased* the odorant response in rat olfactory epithelium while a small amount of zinc nanoparticles *strongly increased* the odorant response in a dose-dependent manner. Further work needs to be carried out to explain the differential effects between the neutral (nanoparticle) and ionic forms of zinc. Though both studies mentioned above showed that metal ions could modulate the activation of ORs, important aspects of the metal involvement remain unresolved, including OR active site identity, the binding mode of metal ions (and neutral metal atoms) alongside metal-coordinating ligands, unifying structural features defining metal-requiring ORs and ligands, if any, and finally, an assessment of the prevalence of the metal ion requirement in the mammalian OR repertoire. Answers to these questions should facilitate the elucidation of the exact role of metal ions in OR activation.

4.5 Predicting Odorant-Receptor Interactions

Odorant-based predictions Given the enormous numbers of odorous compounds and the expansiveness of the mammalian OR repertoires, to be able to infer odorant-receptor interactions based on known ones represent a crucial step in identifying additional odorant-receptor pairs and for elucidating the mechanism of activation of ORs. Previously, the number of carbon atoms and the presence of functional groups have often been considered as determining factors associated with olfactory responses; however, later studies found that there is no simple correlation among an odorant's properties, the ORs it activates, and its perceived odor [63, 64]. Various studies have since attempted to use physicochemical properties of odorants in a quantitative way to predict receptor activation [65–67]. As odorants are chemical molecules that can vary in myriad ways in multidimensional space, are there certain properties that are more important than others in predicting olfactory responses? A meta analysis based on nine olfactory response datasets measured in different organisms and using different techniques revealed an optimized set of 32 physicochemical descriptors, or mathematical values that describe a molecule, among a complete set of 1,664 descriptors, that explained 48% of the variance in neural responses [65]. Using a more uniform data set containing only human and mouse OR responses measured in a heterologous OR expression system, Saito et al. found a smaller set of 18 of the 1,664 descriptors that could explain at least 62% of the variance [17]. It is thus evident from both studies that a relatively small set of physicochemical properties can be used to provide the link between chemical structures and receptor activation.

Receptor-based predictions Identifying odorant binding sites is another way to interrogate odorant-receptor interaction on the molecular level. Multiple alignments of the whole human and mouse OR repertoires revealed both conserved and variable regions in the seven-transmembrane receptor family [68, 69]. Like other GPCRs, ORs contain consensus sequences and motifs that are important for signaling via G-proteins and structural integrity. Variable amino acid residues, on the other hand, are found mostly in the transmembrane domains and contribute to ORs' selectivity in the binding to a plethora of odorant molecules. Different systematic approaches were taken to identify amino acids involved in odorant recognition in the OR repertoire. For example, Man et al. [70] used the reasoning that amino acid involved in binding must be more conserved in mouse-human orthologous pairs than paralogous pairs, and based on this assumption, they identified 22 amino acid positions that may line the OR binding pocket. Saito et al. [17] utilized the functional profile of 52 mouse ORs and 10 human ORs and found a different set of 16 amino acid sites with descriptors of volume, polarity, and composition that could explain approximately 50% of the variance in their data set.

In the recent decades, with the availability of high-resolution and sometimes agonist-bound crystal structures of other GPCR family members, OR homology modeling became an increasingly feasible option in investigating odorant binding

mechanisms for specific receptors of interest and predicting their binding specificities. The rodent I7 receptor is one of the well-studied receptors in computational studies. Using the 7.5 Å structure of bacteriorhodopsin as a template for homology modeling, Singer were able to characterize two residues, K164 and D204, that interacted with octanal and other hydrophobic residues that came into van der Waals interaction with the hydrocarbon moiety of octanal [71]. Using paralleled mouse and rat I7 homology structures, another group identified Cys117 and Ser208 as additional residues that line the binding pocket [72]. Ten years from the original Singer study, Kurland et al. refined the rat I7 homology model using the 2.2 Å structure of bovine rhodopsin [73]. They were able to confirm the hydrophobic interactions and the strong hydrogen bonding with K164, consistent with the models in the other two studies. They also suggested a new role of D204 as a counter-ion stabilizing the interaction at K164. In summary, while all three studies found good agreement between computational results and experimental data available at the time of the study, better resolution of the template and dynamic modeling strategies allowed for more microscopic examination of the molecular events at the active site and more precise identification of molecular criteria for receptor activation. The case of I7 proves that homology modeling and docking simulations may help to resolve structure-function relations by coupling ligands to their corresponding receptors.

4.6 Conclusion

Odorant-receptor interaction is only one step amidst a series of events from inhalation through the nose to odor processing in the brain. Understanding the combinatorial code, integrating pre-receptor events, and modeling ORs with binding requirements for specific odorants could all be valuable for resolving the complexity of receptor-ligand interactions and bridging the gap among events from initial contact with odorant to odor detection. Recent advances in the field summarized in this chapter represent significant progress in making sense of, and predicting, OR structure and function. However, the olfactory percept could still be more complicated than a question of "which receptors are activated and to what extent". For example, phenomena such as OR antagonism are just an example of confounding factors that could add layers of complexity to odorant-receptor relationship. Future studies systematically addressing different relevant aspects may unveil a molecular level understanding of odorant binding to ORs, which might ultimately be useful for the development of biosensors to be used in cosmetic and food industries and in countering bioterrorism and chemical warfare agents.

Acknowledgments We are indebted to Dr. Tai Hyun Park for the invitation to contribute to the book. Our work described here is supported by grants from National Institutes of Health (to H.M.), Chinese National Natural Science Foundation, the National Basic Research Program of China's 973 Program, Shanghai Municipal Education Commission, Shanghai Education Development Foundation, the Science and Technology Commission of Shanghai (all to H.Z.), and Shanghai Jiaotong University School of Medicine (to X.S.).

References

1. Malnic B, Godfrey PA, Buck LB (2004) The human olfactory receptor gene family. Proc Natl Acad Sci U S A 101(8):2584–2589
2. Godfrey PA, Malnic B, Buck LB (2004) The mouse olfactory receptor gene family. Proc Natl Acad Sci U S A 10(7):2156–2161
3. Niimura Y, Nei M (2005) Evolutionary changes of the number of olfactory receptor genes in the human and mouse lineages. Gene 346:23–28
4. Polak EH (1973) Multiple profile-multiple receptor site model for vertebrate olfaction. J Theor Biol 40:469–484
5. Malnic B, Hirono J, Sato T, Buck LB (1999) Combinatorial receptor codes for odors. Cell 96:713–723
6. Kajiya K, Inaki K, Tanaka M, Haga T, Kataoka H, Touhara K (2001) Molecular bases of odor discrimination: Reconstitution of olfactory receptors that recognize overlapping sets of odorants. J Neurosci 21(16):6018–6025
7. Araneda RC, Kini AD, Firestein S (2000) The molecular receptive range of an odorant receptor. Nat Neurosci 3(12):1248–1255
8. Araneda RC, Peterlin Z, Zhang X, Chesler A, Firestein S (2004) A pharmacological profile of the aldehyde receptor repertoire in rat olfactory epithelium. J Physiol 555(Pt 3):743–756
9. Katada S, Hirokawa T, Oka Y, Suwa M, Touhara K (2005) Structural basis for a broad but selective ligand spectrum of a mouse olfactory receptor: mapping the odorant-binding site. J Neurosci 25(7):1806–1815
10. Spehr M, Gisselmann G, Poplawski A, Riffell JA, Wetzel CH, Zimmer RK, Hatt H (2003) Identification of a testicular odorant receptor mediating human sperm chemotaxis. Science 299(5615):2054–2058
11. Gaillard I, Rouquier S, Pin JP, Mollard P, Richard S, Barnabe C, Demaille J, Giorgi D (2002) A single olfactory receptor specifically binds a set of odorant molecules. Eur J Neurosci 15(3):409–418
12. Wetzel CH, Oles M, Wellerdieck C, Kuczkowiak M, Gisselmann G, Hatt H (1999) Specificity and sensitivity of a human olfactory receptor functionally expressed in human embryonic kidney 293 cells and *Xenopus Laevis* oocytes. J Neurosci 19(17):7426–7433
13. Bozza T, Feinstein P, Zheng C, Mombaerts P (2002) Odorant receptor expression defines functional units in the mouse olfactory system. J Neurosci 22(8):3033–3043
14. Saito H, Kubota M, Roberts RW, Chi Q, Matsunami H (2004) RTP family members induce functional expression of mammalian odorant receptors. Cell 119(5):679–691
15. Zhuang H, Matsunami H (2007) Synergism of accessory factors in functional expression of mammalian odorant receptors. J Biol Chem 282(20):15284–15293
16. Zhuang H, Matsunami H (2008) Evaluating cell-surface expression and measuring activation of mammalian odorant receptors in heterologous cells. Nat Protoc 3(9):1402–1413
17. Saito H, Chi Q, Zhuang H, Matsunami H, Mainland JD (2009) Odor coding by a mammalian receptor repertoire. Sci Signal 2(60):ra9.
18. Nara K, Saraiva LR, Ye X, Buck LB (2011) A large-scale analysis of odor coding in the olfactory epithelium. J Neurosci 31(25):9179–9191
19. Oka Y, Katada S, Omura M, Suwa M, Yoshihara Y, Touhara K (2006) Odorant receptor map in the mouse olfactory bulb: in vivo sensitivity and specificity of receptor-defined glomeruli. Neuron 52(5):857–869
20. Getchell TV, Margolis FL, Getchell ML (1984) Perireceptor and receptor events in vertebrate olfaction. Prog Neurobiol 23(4):317–345
21. Debat H, Eloit C, Blon F, Sarazin B, Henry C, Huet JC, Trotier D, Pernollet JC (2007) Identification of human olfactory cleft mucus proteins using proteomic analysis. J Proteome Res 6(5):1985–1996
22. Mayer U, Kuller A, Daiber PC, Neudorf I, Warnken U, Schnolzer M, Frings S, Mohrlen F (2009) The proteome of rat olfactory sensory cilia. Proteomics 9(2):322–334

23. Pelosi P, Baldaccini NE, Pisanelli AM (1982) Identification of a specific olfactory receptor for 2-isobutyl-3-methoxypyrazine. Biochem J 201(1):245–248
24. Flower DR, North AC, Sansom CE (2000) The lipocalin protein family: structural and sequence overview. Biochim Biophys Acta 1482(1-2):9–24
25. Steinbrecht RA (1998) Odorant-binding proteins: expression and function. Ann N Y Acad Sci 855:323–332
26. Briand L, Nespoulous C, Perez V, Remy JJ, Huet JC, Pernollet JC (2000) Ligand-binding properties and structural characterization of a novel rat odorant-binding protein variant. European J Biochem 267(10):3079–3089
27. Pevsner J, Hou V, Snowman AM, Snyder SH (1990) Odorant-binding protein. Characterization of ligand binding. J Biol Chem 265(11):6118–6125
28. Herent MF, Collin S, Pelosi P (1995) Affinities of nutty and green-smelling pyrazines and thiazoles to odorant-binding proteins, in relation with their lipophilicity. Chem Senses 20(6):601–608
29. Tcatchoff L, Nespoulous C, Pernollet JC, Briand L (2006) A single lysyl residue defines the binding specificity of a human odorant-binding protein for aldehydes. FEBS Lett 580(8): 2102–2108
30. Lacazette E, Gachon AM, Pitiot G (2000) A novel human odorant-binding protein gene family resulting from genomic duplicons at 9q34: differential expression in the oral and genital spheres. Hum Mol Genet 9(2):289–301
31. Pes D, Pelosi P (1995) Odorant-binding proteins of the mouse. Comp Biochem Physiol B Biochem Mol Biol 112(3):471–479
32. Matarazzo V, Zsurger N, Guillemot JC, Clot-Faybesse O, Botto JM, Dal Farra C, Crowe M, Demaille J, Vincent JP, Mazella J, Ronin C (2002) Porcine odorant-binding protein selectively binds to a human olfactory receptor. Chem Senses 27(8):691–701
33. Strotmann J, Breer H (2011) Internalization of odorant-binding proteins into the mouse olfactory epithelium. Histochem Cell Biol 136(3):357–369
34. Mori I, Nishiyama Y, Yokochi T, Kimura Y (2005) Olfactory transmission of neurotropic viruses. J Neurovirol 11(2):129–137
35. Minn A, Leclerc S, Heydel JM, Minn AL, Denizcot C, Cattarelli M, Netter P, Gradinaru D (2002) Drug transport into the mammalian brain: the nasal pathway and its specific metabolic barrier. J Drug Target 10(4):285–296
36. Dahl AR, Briner TJ (1980) Biological fate of a representative lipophilic metal compound (ferrocene) deposited by inhalation in the respiratory tract of rats. Toxicol App Pharmacol 56(2):232–239
37. Iyanagi T (2007) Molecular mechanism of phase I and phase II drug-metabolizing enzymes: implications for detoxification. Int Rev Cytol 260:35–112
38. Ayrton A, Morgan P (2001) Role of transport proteins in drug absorption, distribution and excretion. Xenobiotica 31(8–9):469–497
39. Bogdanffy MS, Randall HW, Morgan KT (1987) Biochemical quantitation and histochemical localization of carboxylesterase in the nasal passages of the Fischer-344 rat and B6C3F1 mouse. Toxicol Appl Pharmacol 88(2):183–194
40. Kurosaki M, Terao M, Barzago MM, Bastone A, Bernardinello D, Salmona M, Garattini E (2004) The aldehyde oxidase gene cluster in mice and rats. Aldehyde oxidase homologue 3, a novel member of the molybdo-flavoenzyme family with selective expression in the olfactory mucosa. J Biol Chem 279(48):50482–50498
41. Thornton-Manning JR, Nikula KJ, Hotchkiss JA, Avila KJ, Rohrbacher KD, Ding X, Dahl AR (1997) Nasal cytochrome P450 2A: identification, regional localization, and metabolic activity toward hexamethylphosphoramide, a known nasal carcinogen. Toxicol Appl Pharmacol 142(1):22–30
42. Kimoto M, Iwai S, Maeda T, Yura Y, Fernley RT, Ogawa Y (2004) Carbonic anhydrase VI in the mouse nasal gland. J Histochem Cytochem 52(8):1057–1062
43. Durand N, Carot-Sans G, Chertemps T, Bozzolan F, Party V, Renou M, Debernard S, Rosell G, Maibeche-Coisne M (2010) Characterization of an antennal carboxylesterase from the pest moth Spodoptera littoralis degrading a host plant odorant. PLoS One 5(11):e15026

44. Ishida Y, Leal WS (2005) Rapid inactivation of a moth pheromone. Proc Natl Acad Sci U S A 102(39):14075–14079
45. Rybczynski R, Reagan J, Lerner MR (1989) A pheromone-degrading aldehyde oxidase in the antennae of the moth Manduca sexta. J Neurosci 9(4):1341–1353
46. Ishida Y, Leal WS (2008) Chiral discrimination of the Japanese beetle sex pheromone and a behavioral antagonist by a pheromone-degrading enzyme. Proc Natl Acad Sci U S A 105(26):9076–9080
47. Maibeche-Coisne M, Nikonov AA, Ishida Y, Jacquin-Joly E, Leal WS (2004) Pheromone anosmia in a scarab beetle induced by in vivo inhibition of a pheromone-degrading enzyme. Proc Natl Acad Sci U S A 101(31):11459–11464
48. Zhuo X, Gu J, Zhang QY, Spink DC, Kaminsky LS, Ding X (1999) Biotransformation of coumarin by rodent and human cytochromes P-450: metabolic basis of tissue-selective toxicity in olfactory mucosa of rats and mice. J Pharmacol Exp Ther 288(2):463–471
49. Nagashima A, Touhara K (2010) Enzymatic conversion of odorants in nasal mucus affects olfactory glomerular activation patterns and odor perception. J Neurosci 30(48):16391–16398
50. Thiebaud N, Veloso DSilvaS, Jakob I, Sicard G, Chevalier J, Menetrier F, Berdeaux O, Artur Y, Heydel JM, Le Bon AM (2013) Odorant metabolism catalyzed by olfactory mucosal enzymes influences peripheral olfactory responses in rats. PLoS One 8(3):e59547
51. Lazard D, Zupko K, Poria Y, Nef P, Lazarovits J, Horn S, Khen M, Lancet D (1991) Odorant signal termination by olfactory UDP glucuronosyl transferase. Nature 349(6312):790–793
52. Kinouchi K, Standifer KM, Pasternak GW (1990) Modulation of mu 1, mu 2, and delta opioid binding by divalent cations. Biochem Pharmacol 40(2):382–384
53. Gerlach LO, Jakobsen JS, Jensen KP, Rosenkilde MR, Skerlj RT, Ryde U, Bridger GJ, Schwartz TW (2003) Metal ion enhanced binding of AMD3100 to Asp262 in the CXCR4 receptor. Biochemistry 42(3):710–717
54. Holst B, Elling CE, Schwartz TW (2002) Metal ion-mediated agonism and agonist enhancement in melanocortin MC1 and MC4 receptors. J Biol Chem 277(49):47662–47670
55. Crabtree RH (1978) Copper(I)—possible olfactory binding-site. J Inorg Nucl Chem 40(7):1453
56. Henkin RI, Bradley DF (1969) Regulation of taste acuity by thiols and metal ions. Proc Natl Acad Sci U S A 62(1):30–37
57. Day JC (1978) New nitrogen bases with severe steric hindrance due to flanking tert-butyl groups—cis-2,6-di-tert-butylpiperidine—possible steric blocking of olfaction. J Org Chem 43(19):3646–3649
58. Wang J, Luthey-Schulten ZA, Suslick KS (2003) Is the olfactory receptor a metalloprotein? Proc Natl Acad Sci U S A 100(6):3035–3039
59. Duan X, Block E, Li Z, Connelly T, Zhang J, Huang Z, Su X, Pan Y, Wu L, Chi Q, Thomas S, Zhang S, Ma M, Matsunami H, Chen GQ, Zhuang H (2012) Crucial role of copper in detection of metal-coordinating odorants. Proc Natl Acad Sci U S A 109(9):3492–3497
60. Lin DY, Zhang SZ, Block E, Katz LC (2005) Encoding social signals in the mouse main olfactory bulb. Nature 434(7032):470–477
61. Tian H, Ma M (2008) Differential development of odorant receptor expression patterns in the olfactory epithelium: a quantitative analysis in the mouse septal organ. Dev Neurobiol 68(4):476–486
62. Viswaprakash N, Dennis JC, Globa L, Pustovyy O, Josephson EM, Kanju P, Morrison EE, Vodyanoy VJ (2009) Enhancement of odorant-induced responses in olfactory receptor neurons by zinc nanoparticles. Chem Senses 34(7):547–557
63. Triller A, Boulden EA, Churchill A, Hatt H, Englund J, Spehr M, Sell CS (2008) Odorant-receptor interactions and odor percept: a chemical perspective. Chem Biodivers 5(6):862–886
64. Khan RM, Luk CH, Flinker A, Aggarwal A, Lapid H, Haddad R, Sobel N (2007) Predicting odor pleasantness from odorant structure: pleasantness as a reflection of the physical world. J Neurosci 27(37):10015–10023
65. Haddad R, Khan R, Takahashi YK, Mori K, Harel D, Sobel N (2008) A metric for odorant comparison. Nat Methods 5(5):425–429

66. Schmuker M, de Bruyne M, Hahnel M, Schneider G (2007) Predicting olfactory receptor neuron responses from odorant structure. Chem Cent J 1:11
67. Liu X, Su X, Wang F, Huang Z, Wang Q, Li Z, Zhang R, Wu L, Pan Y, Chen Y, Zhuang H, Chen G, Shi T, Zhang J (2011) ODORactor: a web server for deciphering olfactory coding. Bioinformatics 27(16):2302–2303
68. Zozulya S, Echeverri F, Nguyen T (2001) The human olfactory receptor repertoire. Genome Biol 2(6):RESEARCH0018
69. Zhang X, Firestein S (2002) The olfactory receptor gene superfamily of the mouse. Nat Neurosci 5(2):124–133
70. Man O, Gilad Y, Lancet D (2004) Prediction of the odorant binding site of olfactory receptor proteins by human-mouse comparisons. Protein Sci 13(1):240–254
71. Singer MS (2000) Analysis of the molecular basis for octanal interactions in the expressed rat 17 olfactory receptor. Chem Senses 25(2):155–165
72. Hall SE, Floriano WB, Vaidehi N, Goddard WA 3rd (2004) Predicted 3-D structures for mouse I7 and rat I7 olfactory receptors and comparison of predicted odor recognition profiles with experiment. Chem Senses 29(7):595–616
73. Kurland MD, Newcomer MB, Peterlin Z, Ryan K, Firestein S, Batista VS (2010) Discrimination of saturated aldehydes by the rat I7 olfactory receptor. Biochemistry 49(30):6302–6304

Chapter 5
Cell-Based System for Identification of Olfactory Receptors

Peter Yi Dong, Naihua Natalie Gong and Hiroaki Matsunami

Abstract The discovery and characterization of odorant receptors (ORs) beginning in the early 1990s have opened up the ability to study olfaction from a molecular perspective. Hundreds of OR genes that differ between organisms exist, and each gene codes for a G protein coupled receptor (GPCR) that can be activated by a large variety of odorants. Thus, the process of deorphaning, or identifying the cognate ligand(s) for each receptor, is critical for understanding how smells are perceived. This chapter reviews the usage of heterologous systems and associated accessory proteins for expressing ORs in vitro, notably the luciferase assay system for high-throughput OR screening. This in vitro method of characterizing ORs is also compared to ex vivo preparations, with a discussion of advantages and drawbacks of each supported by experimental evidence.

5.1 Introduction

The modern age of olfaction research began in 1991 with the discovery of a family of genes encoding odorant receptors (ORs), which are localized in the cilia of olfactory sensory neurons (OSNs) found in the olfactory epithelium [1]. These OSNs adhere to the "one gene-one neuron" paradigm in that only one type of OR is expressed in each OSN [2–4]. Mammals have up to 1,500 OR genes, and within this class, mice have about 1,200 OR-encoding genes while humans have about 400 [5–8]. ORs are G protein coupled receptors that consist of seven hydrophobic transmembrane domains. They feature both conserved amino acid sequences that serve as consensus regions that provide receptor family identity as well as unique residues which impart each type of receptor

H. Matsunami (✉) · P. Y. Dong · N. N. Gong
Department of Molecular Genetics and Microbiology,
Duke University Medical Center, Durham, NC, USA
e-mail: hiroaki.matsunami@duke.edu

P. Y. Dong
Department of Neuroscience, University of Pennsylvania
Perelman School of Medicine, Philadelphia, PA, USA

H. Matsunami
Department of Neurobiology, Duke Institute for Brain Sciences,
Duke University Medical Center, Durham, NC, USA

T. H. Park (ed.), *Bioelectronic Nose,* DOI 10.1007/978-94-017-8613-3_5,

with unique binding affinities for a distinct set of odorous ligands. When a ligand binds to a binding pocket consisting of combinations of these variable residues, the alpha subunit of G_{olf} (a G protein specific to the olfactory pathway) dissociates and activates adenylyl cyclase III (ACIII), which converts adenosine triphosphate (ATP) into cyclic adenosine monophosphate (cAMP). This second messenger then binds to and opens cyclic nucleotide-gated sodium and calcium ion channels that depolarize the cell. Axons of OSNs expressing the same OR coalesce into bundles called glomeruli in the olfactory bulb, where they synapse with mitral and tufted cells that transmit information to higher-order brain regions for perceptual processing. Receptors and molecules are thought to interact with each other in a combinatorial fashion, as perception of a single odorant may involve the activation of several different receptors while a single receptor may contribute the perception of a wide range of odorants [9]. Some receptors, such as the mouse SR1, bind to a wide spectrum of these chemical ligands, while others, like the human OR7D4, are narrowly tuned [10–14].

In order to fully elucidate this immensely complex pattern of odorant detection, each receptor must be deorphanized, or paired with its cognate ligands. This process of deorphaning receptors is one of the most fundamental pursuits in olfactory research and requires an assay that is robust and efficient, with the capability to screen hundreds of receptors against thousands of odors. One of the most effective ways to perform such extensive assays is to utilize cells cultured in multi-well plates that would facilitate high-throughput deorphaning. However, the introduction of ORs in what are termed "heterologous" cells, or non-OSN cells that normally do not express such proteins, means that there are potential roadblocks and differences in OR function when accounting for the cell type that is used. Heterologous expression of ORs alone has traditionally been difficult due to problems with receptor trafficking to the cell surface, while the separate environments that heterologous cells and endogenous OSNs exist in brings into question whether ligands found to activate an OR in a heterologous system will elicit the same result in an OR expressed in an OSN. Thus, one of the debates in OR deorphaning lies in the advantages and disadvantages of using in vivo (or OSN-based) versus in vitro (or non OSN-based) methods of receptor isolation. Here we review different methods developed for deorphaning ORs.

5.2 OSN-Based Methods for Identifying Odorant Receptor Function

Adenovirus-Mediated Ectopic OR Expression in the OSN Methods that involve the use of OSNs are best at reproducing the unique conditions found within the mammalian nose as an odor reaches its receptor(s). In the natural world, odorants are delivered through the air in a mucous-filled environment, which may contain enzymes that facilitate pre-receptor odorant modifications [15]. The first OR to be functionally expressed was the rat I7 receptor by way of an engineered adenoviral bicistronic expression vector that drives an expression unit for I7 along with a green fluorescent protein (GFP) marker inserted through

an internal ribosomal entry site (IRES). Through subsequent electroolfactogram recordings, it was discovered that rat I7 preferentially responds to octanal and related chemicals [2, 4, 6]. While this method led to the first deorphaned OR, the inefficiency of generating and infecting such adenoviral constructs to OSNs in the olfactory epithelium makes it troublesome to perform high-throughput assays linking receptor with ligand.

Genetic Marker Knock-In Mice Other notable in vivo deorphaning methods include utilizing gene knock-in techniques through the generation of a construct consisting of a marker gene such as tau-GFP inserted downstream of the endogenous OR gene by way of IRES [16, 17]. Through this method, OSNs that express a particular OR can be easily viewed through fluorescence imaging and then subjected to calcium imaging or patch-clamp recordings to analyze their response to various odorants. This process of characterizing ORs began with the mouse M71 receptor, which was found to be responsive to acetophenone and benzaldehyde, with steep dose-response relationships between odorant concentration and calcium response [9, 11, 13, 18]. Calcium imaging was also used for later studies such as those examining mOR-EG, which responds to chemicals such as eugenol and vanillin [19]. The first patch-clamp analysis of knock-in mice involved the examination of MOR23 OSNs, which showed a responsiveness to lyral that was spread over a very broad dynamic range spanning as many as three log units of lyral concentration [6, 20]. Further patch-clamp experiments revealed the dose-response profiles of other ORs such as SR1 and I7 [11, 21, 22]. However, this method is limited in terms of efficiency, since one needs to generate gene knock-in mice for each OR of interest. Thus, in order to more efficiently decode the complex levels of interactions between receptor and ligand, higher-throughout in vitro methods were devised to better assay the large number of ORs and even greater number of chemicals that bind to these receptors.

Calcium Imaging of OSNs Followed by Single-Cell RT-PCR Single neuron dissociation methods have also been applied to OR deorphaning. Calcium imaging has proven to be particularly useful in measuring OR response to specific ligands. In OSNs, cation influx through cyclic nucleotide-gated calcium channels results in transient increases in intracellular calcium levels upon OR activation. The varying degrees of these calcium fluctuations can be detected using fluorescent calcium indicators like fura-2. Because of the “one-neuron one-receptor” rule in OSNs, follow-up single-cell RT-PCR of the dissociated OSNs indicates the specific OR involved in OSN responses to the odorants screened [7]. Calcium imaging of dissociated OSNs with subsequent single-cell RT-PCR demonstrates the diversity in the responsiveness of ORs to various ligands. For instance, the multiple receptors identified for odorants with similar structure, such as aliphatic compounds, were shown to include ORs that are both highly related and divergent [12]. Broadly tuned receptors that respond to a variety of odorants have also been elucidated. For example, out of thirteen distinct odorant mixtures, Olfr42 responded to ten [12]. In addition, changes in odorant concentration have been shown to change OR response to a particular ligand [9].

5.3 Functional Expression of Odorant Receptors in Heterologous Cells

ORs are notoriously difficult to functionally express in heterologous cells when expressed alone. OR proteins are usually retained in the endoplasmic reticulum and subsequently ubiquitinated and targeted by the proteasome for degradation [17, 23], preventing their localization to the surface of cell membranes where they can be assayed. However, additions to the OR itself as well as the usage of other proteins within the heterologous system can enhance OR expression and response in a combinatorial fashion.

N-Terminal Modifications Various groups have found that N-terminal tag additions to the OR sequence facilitates the expression of some ORs at the membrane surface. One particular tag, which consists of the 20 N-terminal amino acids of rhodopsin (Rho-tag), can be fused to the full-length cDNA of an OR and expressed in HEK-293 (human embryonic kidney) cells. This at least allows a small proportion of the ORs to be localized at the plasma membrane [5, 11, 18–20, 22]. Other groups have also used signal peptides to increase expression of ORs. Recently, it was found that another peptide—a cleavable leucine-rich signal peptide sequence called the Lucy tag—can induce the expression of ORs to the cell surface with even greater success when combined with the Rho-tag than with the Rho-tag alone [24]. However, these N-terminus modifications on their own are insufficient for promoting the expression of many ORs at the membrane surface. Certain accessory proteins, discussed below, have been shown to promote OR surface expression to a greater degree when used in conjunction with N-terminus tags.

Receptor Transporting Proteins (RTPs) and Other Accessory Proteins for Enhancing Functional OR Expression Gprotein coupled receptors such as ORs often require the aid of accessory proteins or chaperones for correct targeting to the cell surface [23, 25]. Receptor transporting proteins (RTPs) were found as chaperones which further aid in the localization of ORs to the cellular membrane [26]. These proteins were first found through conducting a search of genes encoding membrane-associated proteins in the OSNs. Subsequent co-transfection of RTPs with an OR into HEK293T cells enhanced the cell surface expression of ORs. RTPs offered the best results when co-transfected with ORs while receptor expression-enhancing proteins (REEPs), another class of accessory proteins, offered a lesser level of expression. Later experiments showed that a truncated version of RTP1, called RTP1S, displayed greater efficacy in trafficking ORs to the plasma membrane surface [27, 28]. In addition, a putative guanine nucleotide exchange factor for $G_{\alpha olf}$ called Ric-8B was shown to promote the expression of ORs in heterologous systems [27]. More recently, the muscarinic receptor M3 has also been demonstrated as an additional accessory protein that facilitates the response of ORs [29]. The practice of combining N-terminal tags with accessory proteins in expressing ORs in vitro represents an increasingly robust method that allows functional expression of most if not all the ORs.

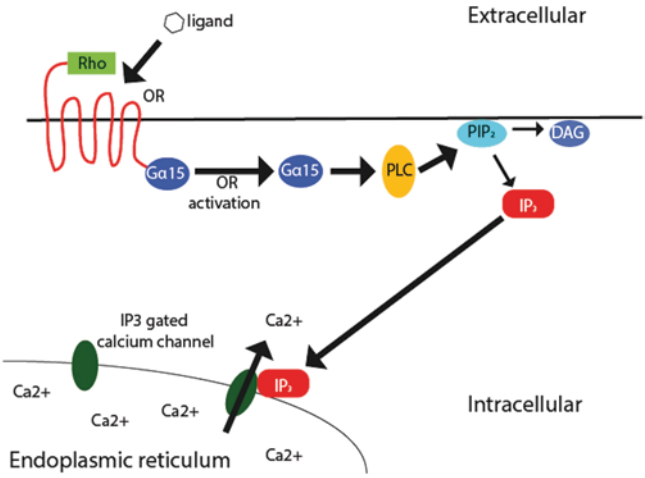

Fig. 5.1 $G_{\alpha 15}$ –mediated calcium imaging. When an odorant binds and activates the OR, $G_{\alpha 15}$ dissociates from the OR and activates phospholipase C (*PLC*), which hydrolyses the membrane phospholipid PIP2 to form inositol triphosphate (*IP3*) and diacylglycerol (*DAG*). IP3 binds to gated calcium channels on the endoplasmic reticulum, resulting in an increase in calcium in the cytosol

5.4 Heterologous Cell Types

HEK293 and Other Mammalian Cell Lines A high-throughput method for screening ORs would involve the expression of ORs in a heterologous expression system so as to eliminate the need to generate transgenic mouse lines with the receptor of interest labeled with a marker for gene expression. However, as previously stated, this method of expression was complicated by the difficulty of expressing ORs at the surface of the plasma membrane, as they would be broken down in the endoplasmic reticulum, preventing functional expression at the cell membrane.

The first successful attempt at expressing ORs within a heterologous system utilized HEK-293 cells [5, 30]. A method was developed in which N-terminus rhodopsin tags were attached to OR coding regions, thus facilitating the translocation of proteins to the plasma membrane in HEK cells. HEK cells were transfected with a construct containing an N-terminus rhodopsin tag attached to an altered coding region of the rat M4 OR in which transmembrane domains $^{(TM)}$ II-VII (regions implicated in OR ligand-binding) were first replaced with that of the beta-2 adrenergic receptor, and then the rat I7 OR (the cognate ligands of which had been elucidated through adenovirus-mediated in vivo expression; see Sect. 5.2). When cells transfected with the beta-2 adrenergic receptor chimera along with $G_{\alpha 15}$ were stimulated with isoproterenol, an adrenergic agonist, a transient increase in intracellular Ca2+ levels was observed through the inositol triphosphate (IP_3) receptor-mediated pathway (Fig. 5.1), an effect that was repeated when the cells transfected with the I7 chimera were stimulated with octanal. This confirmed that the rhodopsin tag facilitated cell surface expression

of ORs in a heterologous system. A library of chimeric ORs was then generated in which TM II-VII of the rat I7 OR were systematically replaced by that of the beta-2 adrenergic receptor. These chimeric constructs were transfected into the system with $G_{\alpha 15}$ and then exposed to odorants, and their intracellular calcium levels were determined through calcium imaging. The heterologous system was able to determine the selectivity of certain receptors to citronellal and carvone while the usage of chimeras led to the determination of single amino acid residues responsible for conferring that selectivity. With the door to functionally expressing ORs in heterologous systems opened, further studies began to use other receptors such as human ORs.

The introduction of the cAMP assay opened the door to further developments in OR deorphanization through heterologous cells such as HEK-293 cells. cAMP assays allowed for more ORs to be measured and required far less preparation than calcium imaging or patch-clamp analysis. The level of OR response to a particular ligand is correlated to the level of cAMP generated by adenylyl cyclase, so by assaying the level of cAMP, the responsiveness of an OR to a chemical can be elucidated. Initial studies involved the use of an enzyme immunoassay to detect cAMP levels [31], although this was soon superseded by the luciferase reporter gene assay. The luciferase reporter gene assay allows for the amplification of cAMP signal through the usage of a cAMP-response element (CRE) promoter that drives a firefly luciferase reporter gene. As cAMP levels increase with the binding of a ligand to the receptor, protein kinase A is activated and phosphorylates cAMP response element-binding protein (CREB), a transcription factor, and luciferase gene transcription is induced through CREB-mediated gene expression. The CRE-driven luciferase gene, along with an OR expression construct containing an N-terminus modification (such as a rhodopsin tag) and accessory RTPs, is transfected into HEK cells. The cells are then stimulated with odorants before being measured for luminescence [30–32], which indicates the level of OR activation in response to an odorant (Fig. 5.2).

Xenopus Oocyte Expression Along with HEK cells, ORs can also be functionally expressed in *Xenopus laevis* oocytes. Xenopus oocytes are used frequently to express a wide variety of receptors and channels, and their large size (~1 mm) makes them convenient for electrophysiological analysis as well. First usage of this method began with the purpose of expressing fish ORs—notably, a goldfish OR that belongs to the V2R vomeronasal receptor class gene family [33]. Xenopus oocytes allow for detecting the activation of multiple signaling pathways by coexpression of G-protein-gated inwardly rectifying potassium channels (GIRKs) and $G_{\alpha olf}$, along with ORs [33, 34]. Activation of the OR results in activation of $G_{\alpha olf}$, which in turn leads to GIRK gating and thus detectable OR agonist-dependent currents in the oocytes. Soon afterwards, Drosophila and human ORs were also expressed in Xenopus oocytes [35, 36]. Functional responses for mouse ORs were also obtained in Xenopus oocytes, initially with MOR42–3 acting through the $G_{\alpha olf}$/cystic fibrosis transmembrane conductance (CFTR) signal transduction pathway [37] (Fig. 5.3), and then with mOR-EG [31]. This system was then used for other detailed analyses of MOR42–3, such as mutagenic studies in which the amino acids responsible for conferring the specificity of the OR were elucidated [38]. Recently, the usage of Xenopus oocytes has also facilitated the deorphanization of an OR using natural ligands [39].

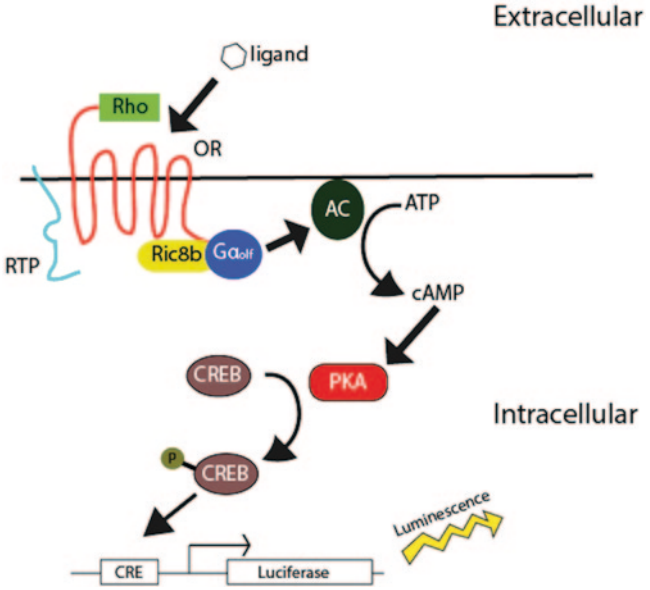

Fig. 5.2 Cre-luciferase system for measuring OR activation takes advantage of OR cAMP signaling. The OR is expressed at the surface of heterologous cells with the aid of a Rho-tag and RTPs. Activation of the OR leads to dissociation of Gαolf, activation of adenylyl cyclase III (*AC*) and cAMP production. cAMP activates protein kinase A (*PKA*), which phosphorylates CREB, driving expression of the luciferase gene

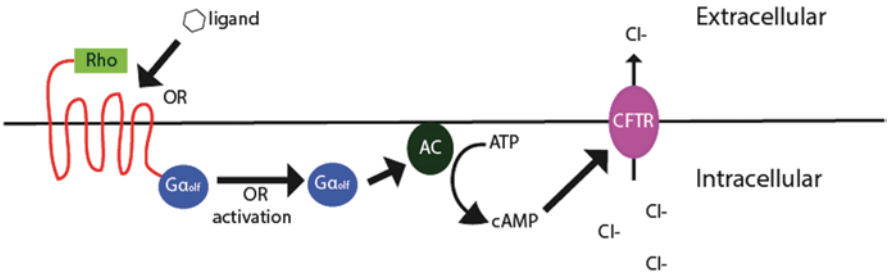

Fig. 5.3 The Xenopus oocyte expression cystem involving the CFTR channel, a cAMP-sensitive chloride ion channel. Upon OR activation, cAMP binds to and opens the CFTR channel, allowing chloride ions to flow out of the cell. OR activation is measured as the resultant current

Other Cells In addition to the cell systems mentioned above, the expression of ORs has also been established in the baculovirus-Sf9 insect cell system, which allows GPCR and other foreign DNA to be expressed with high efficiency [40]. The first OR to be expressed in Sf9 cells was the rat OR5, and receptor activity was subsequently assayed via odorant-induced generation of cAMP or inositiol triphosphate ($InsP_3$) [41]. However, the usage of Sf9 cells for expressing ORs has been

relatively rare since, with most studies limited to the assaying of *Drosophila* ORs such as Or22a and Or43b [42, 43]. ORs have also been successfully introduced into *E. coli* bacteria when overexpressed as a fusion protein, where they were able to display interactions with odorants [44]. The HeLa-Cx43 cell line has also been used to express ORs, most notably to show that odorants can function as agonists or antagonists for various ORs based on the type of G-protein used [45].

5.5 Do in Vitro Systems Replicate in Vivo OR Responses?

Despite the growing ability of in vitro heterologous systems to parallel odorant-induced receptor activity in vivo, there still exist doubts concerning the ability of in vitro systems to truly replicate unique conditions encountered within the live olfactory system. Odors are delivered though solution in heterologous systems whereas they travel through the air during normal mammalian olfaction. Thus, nasal airflow rate can alter the apparent sensitivity of certain odorants assayed through glomerular response. For example, glomerular response in the olfactory bulb can differ in response to passive breathing versus sniffing [46]. In addition, the presence of pre-receptor events in vivo involving enzymes present in the nasal mucus can affect olfactory perception. Odorants with functional groups such as aldehydes and esters are converted into corresponding acids and alcohols when contact is made with metabolic enzymes secreted in the mouse mucus. When an enzyme inhibitor was used in parallel with exposure to the relevant odorants, glomerular activation patterns and olfactory discrimination test results differed in those mice compared to mice with the enzymes intact [15]. Studies have also shown differences in ligand responsiveness when comparing ORs measured through calcium imaging or patch-clamp versus ORs expressed in the heterologous system, although these studies have also shown the effectiveness of expressing ORs in vitro as well. The receptor mOR-EG, which responds to eugenol, shows similar patterns of activation both in vivo and in vitro when calcium imaging is applied [19]. In addition, heterologous cells expressing the receptor SR1, which responds to a broad panel of odorants, do not all respond consistently to the same panel—instead, each SR1 cell responds to different odorants at a wide variety of concentrations, although this diversity of responses is also mirrored in vivo with patch clamp analysis [11].

The human OR OR7D4, when expressed in heterologous cells, has been shown to mirror odor perception in humans in terms of responding to the steroids androstenone and androstadienone. In humans, the OR7D4 gene exists as one of two variants that differ by two amino acid substitutions (the most common variant “RT”, and “WM”, which contains R88W and T133M amino acid substitutions), and it was found that the RT variant responds to the steroids at a much higher level than the WM variant in vitro. Likewise, human test subjects with both copies of the RT variant found the steroids to be more intense and “sickening” then those with just one copy of RT or two copies of WM [14].

Thus, to test for the efficacy, reliability and accuracy of our heterologous system versus live-cell recordings of olfactory sensory neurons, we selected previous studies

which examined ORs expressed in their native OSNs [18–20, 22]. Based on those studies, we focused on four ORs found in mouse (M71, mOR-EG, I7, and MOR23). Previously, the cognate ligands of mouse I7 and MOR23 OSNs were analyzed using patch clamp, and M71 and mOR-EG OSNs using calcium imaging. We tested each OR against odorants that had been previously cited as either agonists for or evoked no response from each OR, and unless otherwise stated, we chose two odorants from each category for each OR. We then compared the dose response curves obtained in vitro to the published data in order to determine the selectivity and sensitivity of the aforementioned luciferase assay. Expression of ORs in the heterologous system and luciferase assay were performed as described above. We then compared their dose response curves with the previously published graphs which utilized normalized electrophysiological and calcium response data. From the dose response curves, we found that our heterologous system-derived data was similar to the data obtained from OSN recordings in terms of both selectivity and sensitivity in the cases of mouse I7, mOR-EG and M71. The chemical for which each OR responded to best at each concentration (from the two agonists) within the heterologous system mirrored that of the live-cell data. Mouse I7 receptors had greater affinity for heptanal that octanal, M71 receptors had greater affinity for acetophenone than benzaldehyde and mOR-EG receptors had greater affinity for vanillin that eugenol in both experimental conditions that were compared. In addition, the relative shapes of the dose response curves were similar.

To evaluate sensitivity, we compared the EC50 values of both odorants for each receptor. For three of the four ORs examined for which we had an available published EC50 value to compare, our in vitro EC50 value was greater (all except for mOR-EG), indicating that OSNs expressing the same receptor are more sensitive than heterologous cells. However, in terms of ranking the EC50 values of the two odorants for each receptor, we found that the odorant with the higher EC50 for each receptor studied using olfactory sensory neurons was the same when using the heterologous system. Mouse I7 had a greater EC50 for octanal than heptanal, M71 had a greater EC50 for benzaldehyde than acetophenone and mOR-EG had a greater EC50 for eugenol than vanillin in both experimental paradigms.(Fig. 5.4). These data indicate that ligand selectivity is consistent in vivo and in vitro.

Such direct relationships were not as easily drawn between in vitro and OSN data when observing MOR23. In the OSNs, MOR23 responds to lyral in a highly dynamic range, as threshold and saturation in individually tested cells cover three log units of lyral concentration. In addition, there were great differences in the response kinetics and sensitivity between cells. While we were not able to obtain luciferase response values for individual cells, our normalized luciferase response for MOR23 lied within the range of single-cell responses measured using OSNs.

5.6 Concluding Remarks

In this chapter, we reviewed various methods for evaluating OR ligand selectivity and sensitivity. OSN-based methods for OR deorphanization most effectively reproduce endogenous conditions and thus provide the most accurate pairing of

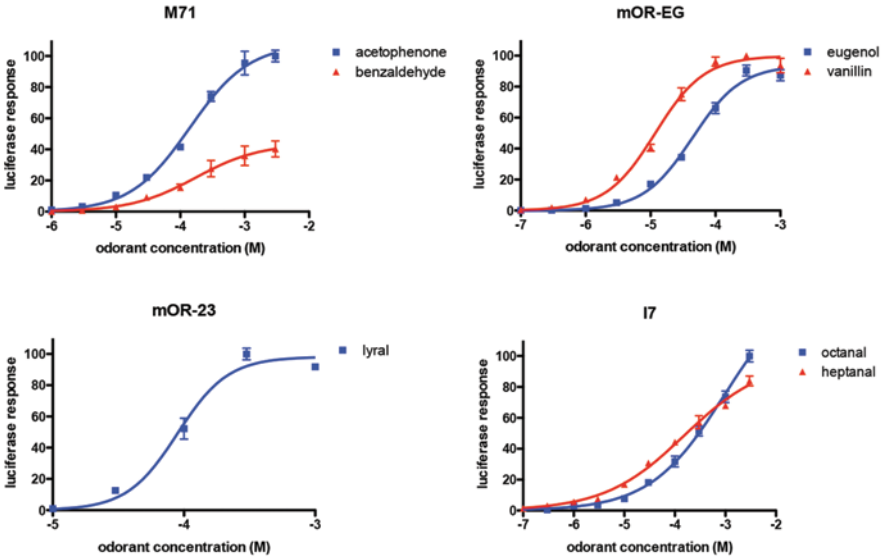

Fig. 5.4 Dose-response curves for M71, mOR-EG, mOR-23, and mouse I7 obtained through heterologous receptor expression (n=3)

ORs to their cognate ligands in vivo, but are limited in their efficiency. In vitro methods involving expressing ORs in heterologous systems have been developed for the high-throughput evaluation of OR selectivity. OR receptor trafficking to the cell surface, initially found to be difficult due to OR retention and degradation in the endoplasmic reticulum, has been found to be facilitated through modifications to the OR protein itself as well as various accessory proteins. Although in vitro methods are advantageous in that they eliminate the need to generate transgenic mouse lines that express the ORs of interest, the question remains whether or not in vitro OR response to ligands accurately parallels that of ORs in vivo.

Our experiment, as well as other studies, have shown ORs tested in in vitro heterologous system can mimic the behavior of ORs expressed in the OSNs. We compared in vitro dose responses of the ORs to other studies that measured normalized electrical or calcium response by ORs located on olfactory sensory neurons. Tested ORs showed similar selectivity when in vitro and OSN data were compared. While mI7, mOR-EG and M71 ORs transfected into HEK cells showed similar sensitivity to activating odorants, in vitro ORs were not able to perfectly predict the behavior of all tested ORs and as such, the heterologous system may not be able to fully characterize the odor response profiles of all ORs. There exist possible explanations for this inability to mirror in vivo conditions such as enzymatic conversion of odor chemicals in the mucus as described earlier. However, our results do not preclude the usefulness of in vitro assays utilizing the heterologous system in high-throughput analyses of receptor-ligand interactions. One can use the heterologous system to screen a receptor against a library of odorants to deorphanize

ORs, or, alternatively, screen a particular chemical against a library of receptors to find the OR responsible for detecting a particular ligand. When the data produced by in vitro heterologous system can predict the perception of odors, as in the case of human OR7D4 variants and their in vitro responses to androstanone and androstadienone, they will be a strong indication that the in vitro responses mimic OR activation in vivo.

References

1. Buck L, Axel R (1991) A novel multigene family may encode odorant receptors: a molecular basis for odor recognition. Cell 65:175–187
2. Zhao H, Ivic L, Otaki JM et al (1998) Functional expression of a mammalian odorant receptor. Science 279:237–242
3. DeMaria S, Ngai J (2010) The cell biology of smell. J Cell Biol 191:443–452. doi: 10.1083/jcb.201008163
4. Araneda RC, Kini AD, Firestein S (2000) The molecular receptive range of an odorant receptor. Nat Neurosci 3:1248–1255. doi:10.1038/81774
5. Krautwurst D, Yau KW, Reed RR (1998) Identification of ligands for olfactory receptors by functional expression of a receptor library. Cell 95:917–926
6. Feinstein P, Mombaerts P (2004) A contextual model for axonal sorting into glomeruli in the mouse olfactory system. Cell 117:817–831. doi:10.1016/j.cell.2004.05.011
7. Touhara K, Sengoku S, Inaki K, et al (1999) Functional identification and reconstitution of an odorant receptor in single olfactory neurons. Proc Natl Acad Sci U S A 96:4040–4045
8. Nei M, Niimura Y, Nozawa M (2008) The evolution of animal chemosensory receptor gene repertoires: roles of chance and necessity. Nat Rev Genet 9:951–963. doi:10.1038/nrg2480
9. Malnic B, Hirono J, Sato T, Buck LB (1999) Combinatorial receptor codes for odors. Cell 96:713–723
10. Firestein S (2001) How the olfactory system makes sense of scents. Nature 413:211–218. doi:10.1038/35093026
11. Grosmaitre X, Fuss SH, Lee AC et al (2009) SR1, a mouse odorant receptor with an unusually broad response profile. J Neurosci 29:14545–14552. doi:10.1523/JNEUROSCI.2752-09.2009
12. Nara K, Saraiva LR, Ye X, Buck LB (2011) A large-scale analysis of odor coding in the olfactory epithelium. J Neurosci 31:9179–9191. doi:10.1523/JNEUROSCI.1282-11.2011
13. Saito H, Chi Q, Zhuang H et al. (2009) Odor coding by a Mammalian receptor repertoire. Sci Signal 2:ra9. doi:10.1126/scisignal.2000016
14. Keller A, Zhuang H, Chi Q et al (2007) Genetic variation in a human odorant receptor alters odour perception. Nature 449:468–472. doi:10.1038/nature06162
15. Nagashima A, Touhara K (2010) Enzymatic conversion of odorants in nasal mucus affects olfactory glomerular activation patterns and odor perception. J Neurosci 30:16391–16398. doi:10.1523/JNEUROSCI.2527-10.2010
16. Sakano H (2010) Neural map formation in the mouse olfactory system. Neuron 67:530–542. doi:10.1016/j.neuron.2010.07.003
17. Mombaerts P, Wang F, Dulac C et al (1996) Visualizing an olfactory sensory map. Cell 87:675–686
18. Bozza T, Feinstein P, Zheng C, Mombaerts P (2002) Odorant receptor expression defines functional units in the mouse olfactory system. J Neurosci 22:3033–3043
19. Oka Y, Katada S, Omura M et al (2006) Odorant receptor map in the mouse olfactory bulb: in vivo sensitivity and specificity of receptor-defined glomeruli. Neuron 52:857–869. doi:10.1016/j.neuron.2006.10.019

20. Grosmaitre X, Vassalli A, Mombaerts P et al (2006) Odorant responses of olfactory sensory neurons expressing the odorant receptor MOR23: a patch clamp analysis in gene-targeted mice. Proc Natl Acad Sci U S A 103:1970–1975. doi:10.1073/pnas.0508491103
21. Ressler KJ, Sullivan SL, Buck LB (1994) Information coding in the olfactory system: evidence for a stereotyped and highly organized epitope map in the olfactory bulb. Cell 79:1245–1255
22. Tan J, Savigner A, Ma M, Luo M (2010) Odor information processing by the olfactory bulb analyzed in gene-targeted mice. Neuron 65:912–926. doi:10.1016/j.neuron.2010.02.011
23. Lu M, Echeverri F, Moyer BD (2003) Endoplasmic reticulum retention, degradation, and aggregation of olfactory G-protein coupled receptors. Traffic 4:416–433
24. Shepard BD, Natarajan N, Protzko RJ et al (2013) A cleavable N-terminal signal peptide promotes widespread olfactory receptor surface expression in HEK293T cells. PLoS ONE 8:e68758. doi:10.1371/journal.pone.0068758
25. Brady AE, Limbird LE (2002) G protein-coupled receptor interacting proteins: emerging roles in localization and signal transduction. Cell Signal 14:297–309
26. Saito H, Kubota M, Roberts RW et al (2004) RTP family members induce functional expression of mammalian odorant receptors. Cell 119:679–691. doi:10.1016/j.cell.2004.11.021
27. Dannecker Von LEC, Mercadante AF, Malnic B (2006) Ric-8B promotes functional expression of odorant receptors. Proc Natl Acad Sci U S A 103:9310–9314. doi:10.1073/pnas.0600697103
28. Zhuang H, Matsunami H (2007) Synergism of accessory factors in functional expression of mammalian odorant receptors. J Biol Chem 282:15284–15293. doi:10.1074/jbc.M700386200
29. Li YR, Matsunami H (2011) Activation state of the M3 muscarinic acetylcholine receptor modulates mammalian odorant receptor signaling. Sci Signal 4:ra1. doi:10.1126/scisignal.2001230
30. Zhuang H, Matsunami H (2008) Evaluating cell-surface expression and measuring activation of mammalian odorant receptors in heterologous cells. Nat Protoc 3:1402–1413. doi:10.1038/nprot.2008.120
31. Katada S, Nakagawa T, Kataoka H, Touhara K (2003) Odorant response assays for a heterologously expressed olfactory receptor. Biochem Biophys Res Commun 305:964–969
32. Ronnett GV, Moon C (2002) G proteins and olfactory signal transduction. Annu Rev Physiol 64:189–222. doi:10.1146/annurev.physiol.64.082701.102219
33. Speca DJ, Lin DM, Sorensen PW et al (1999) Functional identification of a goldfish odorant receptor. Neuron 23:487–498
34. Touhara K (2007) Deorphanizing vertebrate olfactory receptors: recent advances in odorant-response assays. Neurochem Int 51:132–139. doi:10.1016/j.neuint.2007.05.020
35. Wetzel CH, Oles M, Wellerdieck C et al (1999) Specificity and sensitivity of a human olfactory receptor functionally expressed in human embryonic kidney 293 cells and Xenopus Laevis oocytes. J Neurosci 19:7426–7433
36. Wetzel CH, Behrendt HJ, Gisselmann G et al (2001) Functional expression and characterization of a Drosophila odorant receptor in a heterologous cell system. Proc Natl Acad Sci U S A 98:9377–9380. doi:10.1073/pnas.151103998
37. Abaffy T, Matsunami H, Luetje CW (2006) Functional analysis of a mammalian odorant receptor subfamily. J Neurochem 97:1506–1518. doi:10.1111/j.1471-4159.2006.03859.x
38. Abaffy T, Malhotra A, Luetje CW (2007) The molecular basis for ligand specificity in a mouse olfactory receptor: a network of functionally important residues. J Biol Chem 282:1216–1224. doi:10.1074/jbc.M609355200
39. Yoshikawa K, Nakagawa H, Mori N et al (2013) An unsaturated aliphatic alcohol as a natural ligand for a mouse odorant receptor. Nat Chem Biol 9:160–162. doi:10.1038/nchembio.1164
40. George ST, Arbabian MA, Ruoho AE et al (1989) High-efficiency expression of mammalian beta-adrenergic receptors in baculovirus-infected insect cells. Biochem Biophys Res Commun 163:1265–1269
41. Raming K, Krieger J, Strotmann J et al (1993) Cloning and expression of odorant receptors. Nature 361:353–356. doi:10.1038/361353a0

42. Kiely A, Authier A, Kralicek AV et al (2007) Functional analysis of a Drosophila melanogaster olfactory receptor expressed in Sf9 cells. J Neurosci Methods 159:189–194. doi:10.1016/j.jneumeth.2006.07.005
43. Smart R, Kiely A, Beale M et al (2008) Drosophila odorant receptors are novel seven transmembrane domain proteins that can signal independently of heterotrimeric G proteins. Insect Biochem Mol Biol 38:770–780. doi:10.1016/j.ibmb.2008.05.002
44. Kiefer H, Krieger J, Olszewski JD et al (1996) Expression of an olfactory receptor in Escherichia coli: purification, reconstitution, and ligand binding. Biochemistry 35:16077–16084. doi:10.1021/bi9612069
45. Shirokova E, Schmiedeberg K, Bedner P et al (2005) Identification of specific ligands for orphan olfactory receptors. G protein-dependent agonism and antagonism of odorants. J Biol Chem 280:11807–11815. doi:10.1074/jbc.M411508200
46. Oka Y, Takai Y, Touhara K (2009) Nasal airflow rate affects the sensitivity and pattern of glomerular odorant responses in the mouse olfactory bulb. J Neurosci 29:12070–12078. doi:10.1523/JNEUROSCI.1415-09.2009

Chapter 6
Neurobiology and Cultivation of Olfactory Receptor Neurons on a Chip

Cheil Moon, Samhwan Kim, Jisub Bae and Gabriele V. Ronnett

Abstract The continued study of the olfactory system is essential, as elucidation of its molecular, cellular, and systems neurobiology will undoubtedly reveal a complex interplay that transduces odorant molecule-induced action potentials into odor information processes in the brain such as the mediation of emotion, memory and behavior. Additionally, interest in the olfactory system and its potential applications in the industrial and engineering fields continue to increase. In this chapter, we describe various aspects of olfactory cells ranging from their cellular structures and functions to the development of olfactory cell cultivation methods and the application of cultivated olfactory cells and bio-engineered cells to various types of bioelectronic devices. These applications may ultimately facilitate the development of biomimetic artificial noses.

6.1 Introduction

The mammalian olfactory system has excellent ability to detect and discriminate thousands of odors with high sensitivity and precision [1, 2]. Over the last decade, huge interests have been focused on the olfactory system and considerable researches have been made to understand the mechanisms from odorants detection in the olfactory receptor neurons to (ORNs) information processing in the olfactory bulb (OB). These achievements have inspired researches on the development of artificial noses using ORNs as a sensor with growing public needs. In this chapter, we will describe the olfactory system in aspect of neurobiology, cultivation methods, and its application to the development of artificial noses.

C. Moon (✉) · S. Kim · J. Bae
Department of Brain Science, Graduate School, Daegu Gyeongbuk Institute of Science and Technology, Daegu 711–873, Republic of Korea
e-mail: cmoon@dgist.ac.kr

G. V. Ronnett
Department of Neuroscience, Biological Chemistry, and Neurology, School of Medicine, Johns Hopkins University, Baltimore, MD 21205, USA
e-mail: gronnett@jhmi.edu

T. H. Park (ed.), *Bioelectronic Nose,* DOI 10.1007/978-94-017-8613-3_6,

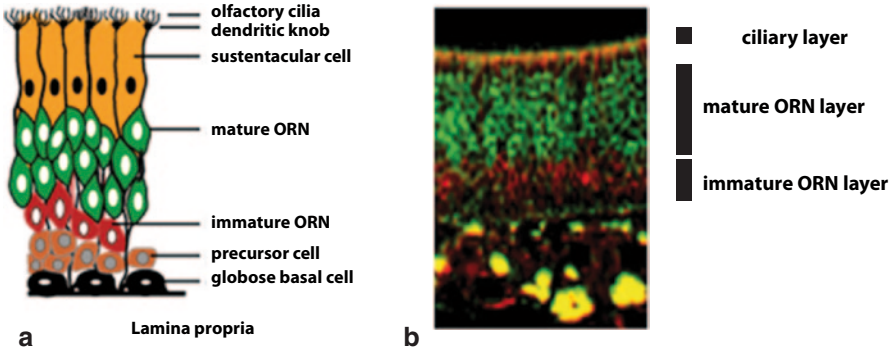

Fig. 6.1 Olfactory Epithelium. **a** OE consists of three principal cell types; globose basal cell, ORN and sustentacular cell. Apical dendritic extension of ORN forms dendritic knob. Dendritic knob contains non-motile cilia where ORs are highly expressed and detect odorants. **b** OE section labeled by two cell type markers, GAP43 and OMP. GAP43 is expressed in immature neurons, and OMP is expressed exclusively in terminally differentiated ORNs. ORNs migrate apically to the top of the epithelium. Thus people can recognize age of neurons by position

6.2 Cellular Structures of Olfactory Cells

The peripheral olfactory system is structurally well adapted to detect environmental chemicals. For example, the localization of ORNs in the olfactory epithelium (OE) facilitates their direct contact with inhaled odorous chemicals (Fig. 6.1). When considering the OE, it is important to be mindful of the three OE cell types: ORNs, sustentacular (or supporting) cells (SCs), and basal cells (BCs) [3, 4].

6.2.1 ORNs

ORNs are bipolar neurons, extending apical dendrites to the surface of the epithelium and sending unmyelinated axons projecting to glomeruli on mitral and tufted neurons in the olfactory bulb OB of the brain. The apical dendrites of ORNs form dendritic knobs upon which non-motile cilia are located and it is here that the initial events of olfactory signal transduction occur [5–7]. Results of electrophysiological studies have indicated that odorant sensitivity and the odorant-induced current are uniformly distributed along the cilia, suggesting that all the components of the immediate responses to odorants are localized to the cilia [7]. Furthermore, results of immunoelectron microscopic studies have confirmed the ciliary localization of many of these olfactory signaling molecules [8, 9]. ORNs account for 75–80 % of the cells in the OE (Fig. 6.2) [10]. They are functionally homogeneous in that they all detect odorants. As they mature, ORNs migrate apically to the surface of the OE, which allows for determination of neuronal age by position [11]. Replacement ORNs are supplied by the differentiation of globose basal cells (GBCs) [12–14]. These unique characteristics of neurogenesis allow for cultivation of ORNs *in vitro* [15–17].

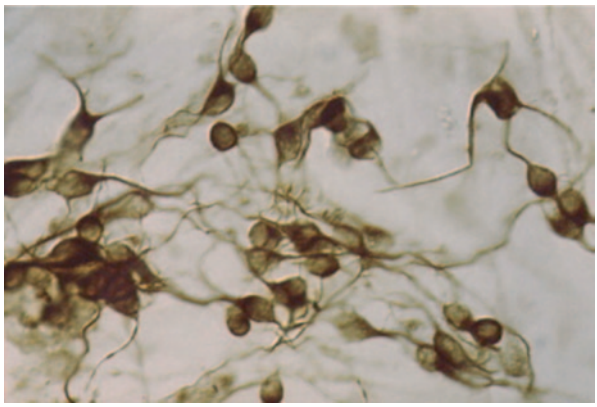

Fig. 6.2 ORNs cultivated *in vitro*. ORNs are stained with TuJ1 (neuronal specific tubulin). Cell bodies and processes of ORNs are well preserved

6.2.2 Olfactory Precursor Cells

BCs are located directly above the lamina propria and also underlie the ORNs. Functionally, BCs are known to serve as precursors for replacement ORNs throughout adulthood [4, 14, 18]. There are two general classes of BCs; horizontal cells (HCs) and GBCs. HCs are flat and express cytokeratin [18, 19], whereas GBCs have a round shape [20, 21]. ORNs survive for several months and therefore have a shorter survival time than many other types of neurons. This shortened survival time may be attributable to the toxic or infectious nature of the agents that ORNs are directly exposed via the environment. Thus, the differentiation of GBCs to new ORNs is crucial for maintenance of the sense of smell. As previously mentioned, adult neurogenesis of ORNs is a unique characteristic that facilitates the cultivation of ORNs *in vitro* on biosensor devices and culture dishes.

6.2.3 SCs

SCs stretch from the surface of the OE to the basal lamina, where they maintain foot processes [6, 22]. SCs are electrically isolated from ORNs, secretory components into the mucus, and contain detoxifying enzymes [23]. Recent studies suggest that SCs may produce growth factors critical to the ORN development [24]. For example, neuropeptide Y functions as a neuroproliferative factor for olfactory neuronal precursors both *in vivo* and *in vitro* [24]. This is only the first of many potential growth factors that SCs contribute to ORN homeostasis. Therefore, understanding the roles of SCs in the process of ORN development may be important for the stable cultivation of ORNs on sensor chips.

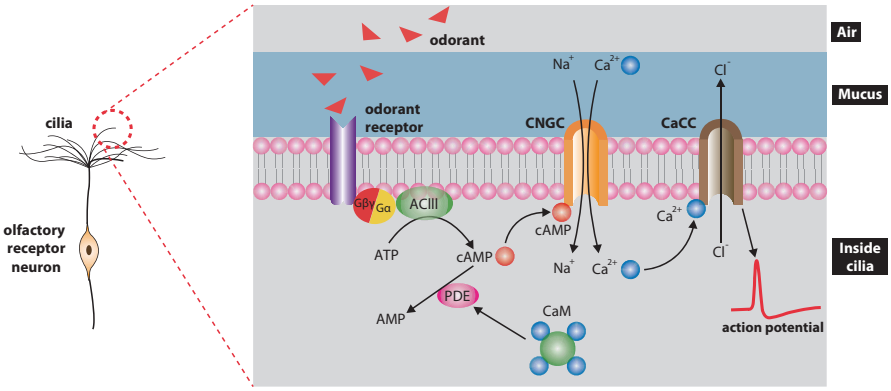

Fig. 6.3 Olfactory signal transduction in the mammalian ORN. See text for details

6.2.4 Olfactory Signal Transduction in the Olfactory Cilia

ORNs transduce chemical signals in the environment into the electrical signals (Fig. 6.3) [25]. The first step of olfactory signal transduction begins with binding of the odorant molecule to the specific receptor, referred to as an olfactory receptor (OR) in the sensory cilia. The binding of odorants activates G-protein(Golf) which is a member of the stimulatory G protein family expressed specifically in the olfactory system. Then, Golf stimulates adenylate cyclases (ACs), which produce cyclic adenosine triphosphate (cAMP). The ACs involved in this process are type 3 (ACIII) and specifically expressed in the olfactory system. The cAMP produced by ACIII opens cyclic nucleotide-gated channel (CNGC), allowing for influx of sodium and calcium ions. Incoming calcium ions open calcium activated chloride channel, and action potential occurs by releasing intracellular chloride ions. The entire signal transduction process happens within 500 msec. Some amount of calcium ions are bound to the calmodulin (CaM) and activate the calcium/CaM-dependent enzyme phosphodiesterase (PDE), which hydrolize cAMP into AMP.

6.2.5 Neuronal Differentiation of Olfactory Precursor Cells

Regeneration of the OE is a process of neuronal stem cell differentiation (Fig. 6.4). During stem cell differentiation, cells pass through sequential phases of maturation (for review see references [26, 27]). Progression is controlled primarily through the sequential and/or combinatorial exposure of the cells to growth factors [28–33]. Neuronal differentiation is recapitulated in the OE, as it undergoes replacement of its resident ORNs throughout life [34–37]. The OE contains a developmentally dynamic neuronal population comprised of GBCs, neuronal precursors, and immature and mature ORNs [38]. SCs provide many growth factors that regulate the dynamics of the neuronal population [39–41]. As stem cells may be manipulated to replace damaged neurons, identification

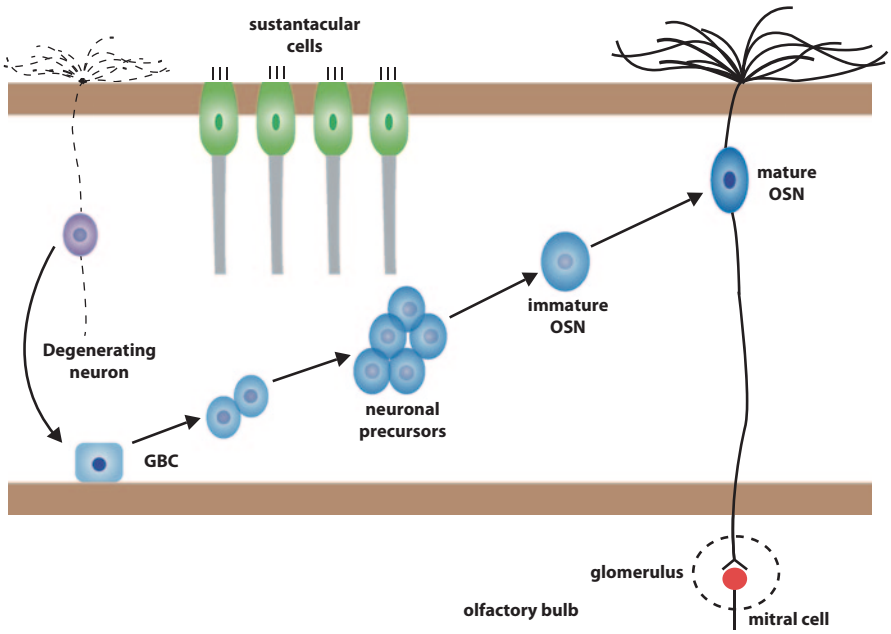

Fig. 6.4 Regeneration of ORNs. When ORNs are degenerating, GBCs respond to signals from dying ORNs. GBCs are differentiated into ORN precursors. ORN precursors are then differentiated to ORNs. As ORNs get mature, dendritic processes and axonal projection occur to form olfactory cilia and synapse in the OB

and understanding of the growth factors regulating ORN development will be critical for *in vitro* cultivation of ORNs on chips. Precise application of growth factors may improve the quality of ORN cultivation, which in turn may provide healthy ORNs that allow for proper functioning of bio-sensor chips. To date, neurotrophins, neuropeptides and neurocytokines are known to influence ORN development [24, 42, 43].

6.2.6 Olfactory Cells as Biosensors

Following the elucidation of olfactory signal transduction mechanisms in the ORNs, many studies have attempted to develop artificial olfactory systems by cultivating ORNs in order to make artificial noses with high specificity and sensitivity. Electronic noses are typically composed of two parts, one is a sensing part detecting chemicals in the environment, and the other is a transducing part converting the chemical signals to the electrical signals. So-called 'electric nose (e-nose)' use non-biological components as the sensing part, and bioelectric nose uses biological components to detect odorants. Conventionally developed electric noses have disadvantages such as huge volume of device, low sensitivity, and limited number of detectable chemicals. Whereas, bioelectric noses are regarded as more miniaturized, sensitive, and selective chemical sensors due to use of the mammalian ORNs.

6.3 Current Knowledge Regarding *in vitro* ORN Cultivating Methods

As mentioned, the initial attempt of the ORN cultivation was conducted in 1984 by Noble et al. [44]. Before this attempt, cell suspension techniques had been widely used for dissociation of intact ORNs. Although these techniques did not provide sufficient quality ORNs for olfactory-specific experiments, they did contribute to the development of advanced ORN cultivating methods. In 1991, Ronnett et al. introduced a primary ORN cultivation method that provided almost pure ORNs [45]. However, ORNs cultured using this method rarely survived beyond culture day 7, prompting researchers to attempt the engineering of ORN cell lines.

6.3.1 Development of ORN Cultivation Methods

Before ORN primary culture was introduced, several attempts to collect pure populations of ORNs had been made. Initial efforts pioneered by Kowen et al. in 1966 involved dispersing olfactory cells using mechanical, chemical, and enzymatic treatments to make cell suspensions [46]. Hirsch and Margolis attempted to use similar methods with some modification, primarily the dissociation of cells by centrifugation with a bovine serum albumin gradient [47]. These pioneering attempts were critical, as they represented some of the earliest steps in the progression to biological artificial electric nose development. However, the ORN yield achieved using these techniques was too low to advance biomimetic artificial nose development. Another method employed to dissociate OE cells used N-ethylmaleimide. Unfortunately, this method also deactivated the electrical excitability of cells and therefore could not be used to contribute to future studies.

Initial ORN cultivation methods used only isolated OE *in vitro*. In 1984, Noble et al. employed purified astrocytes to support OE neurons [44]. Gonzales et al. also succeeded in cultivating OE cells in 1985 [48]. The results of these studies allowed not only for measurable growth of olfactory neurons *in vitro*, but also for more advanced study of the mechanisms of olfactory signal transduction. However, these ORN cultivation methods were suboptimal, as cultivation of isolated OE cells without ORN purification provided ORN yields unsuitable for biochemical experiments. Additionally, cultivated cells were associated with poor survival times. Furthermore, the heterogeneous cell populations derived using these methods impaired the ability to study olfactory signal transduction with precision.

Ronnett et al. established a cultivation method which yielded a nearly pure population of ORNs in 1991 [45]. This method consisted of mechanical disruption, enzymatic dissociation, and a series of filtrations, followed by incubation in medium conducive to neuronal survival. Thus, this technique overcame shortcomings of other methodologies regarding purity and yield of ORNs in culture. Most importantly, the development of this primary ORN culture, which could respond to odorous chemicals and evoke electronic signals, allowed for further research regarding olfactory signal transduction at the cellular and molecular levels.

Despite the aforementioned advantages of the method established by Ronnett et al., some limitations remained. For example, ORNs rarely survived beyond culture day 7. Several attempts have been made to overcome this important limitation. One such approach involved the development of immortalized ORNs and to date, several stable cell lines have been developed. In one example, cell lines capable of detecting odor and expressing olfactory-specific proteins have been successfully isolated from adult humans and human fetus neuroblasts. Additionally, cells have been immortalized via expression of the Simian virus 40 (SV40) large tumor antigen (T-ag) [49]. SV40 T-ag promotes expression of an oncogene within the olfactory neuronal lineage. Similarly, cells have been successfully immortalized using the oncogene n-myc [50]. Both cell lines express olfactory-specific proteins which are usually expressed in ORNs. However, cell lines developed by Largent's group have not shown reliable endogenous functional responses. Furthermore, cell lines developed by Macdonald's group have never been used for functional studies, so it is totally unknown if this cell line is suitable for biosensors. Ronnett's group introduced other immortalized cell lines using the H-2K^{b}-tsA58 transgenic mouse [51]. ORN cell lines developed by Ronnett's group express olfactory-specific proteins, respond to odorants, and evoke electrical signals. Thus, this cell line may be the most promising material for the development of biological artificial noses to date.

6.4 Use of Cultivated ORN for Biosensors

The driving concept behind cell-based biosensors is the use of live cells to sense chemicals. Thus, cell-based biosensors can be characterized by cells used for detection. Several in characteristics of cells for development of cell-based biosensors need to be considered: how to maintain the organic components, how to attach cells to sensor devices with minimal interruption of biological functions, how to extend the lifespan of cells on sensors, and how to convert cellular activities into signals for sensors. Such characteristics are dependent on the particular cells which have been utilized.

Living cells that express ORs can detect millions of distinct odorous chemicals and evoke electronic signals upon binding with chemical molecules. Therefore, these characteristics make OR (or ORN)-based biosensors superior to other types of chemical sensors. In ORN-based biosensors, ORNs are not only detectors, but also serve as target samples for monitoring of cellular signals. These devices can measure electronic signals from cells without invasive procedures. Moreover, the procedures are much simpler and cheaper than previously reported methods [52].

An electrochemical dynamic system characterizes the activity of living cells, including their function, growth and development. Activity can be measured by monitoring reduction-oxidation (redox) reactions and changes of ionic compositions and concentrations which are accompanied by the transfer of electrons and the generation of electrical charges. Thus, we can monitor the information of cellular status through measurement of extracellular signals acquired by sensing the

changes of electrochemical activities. Monitoring of cellular activity within cell-based biosensors is often accomplished through detection of electrochemical parameters. Active progress in the development of biosensors combined with ORNs has been made due to the highly feasible nature of this model for live monitoring of electrochemical changes. Moreover, this high level of progress is also attributable increasing demands from fragrance-related businesses and anti-terror businesses, such as explosive detection.

In the last three decades, there has been eruptive progress in microfabrication technology and micro-electromechanical systems due to the tremendous advances made by microconductor industries. This has provided a solid foundation for improvement in biosensors themselves, as well as sensor technologies such as MEA, FET, LAPS, surface plasmon resonance (SPR), etc.

6.4.1 Planar Electrode and MEA

MEA, originally developed in 1972 [53], provides many advantages as compared to the conventional patch clamp method. It uses a basic type of electrochemical sensor to measure the extracellular signals of neuronal networks or organotypic/slice cultured tissue. One of the advantages of MEA-based biosensors is the easy fabrication process using conventional techniques as array type devices to cover multi-site detections. In addition, MEA represents a more powerful tool as compared to the patch clamp method due to its non-invasive measurements of extracellular electrical activities. Moreover, integration of amplifier electronic circuits on the electrode substrate enables more stable and reliable measurements under various conditions.

Cell-based biosensors can be used for the detection of various odorous chemicals and for screening ligands that bind to a single OR. Detection of extracellular potentials upon octanal stimulation of HEK 293 cells was reported by S. H. Lee et al. [54]. The experiments used a planar electrode to measure the extracellular electrical signal induced by odorant stimulation in a heterologous OR-expressing cell-based system. HEK 293 cells are bioengineered to express gustatory CNG channels as well as OR I7, which can intensify the membrane potential upon binding of the odorant octanal (Fig. 6.5).

MEA-ORN-based biosensor can monitor neuronal signals from neuronal networks as shown in Fig. 6.6. As MEA can measure various sites of neurons in the network, this system can be used for statistical analysis of neuronal signals and for generating odor-response maps [55].

Direct measurement of extracellular electric signals in dissociated and cultivated ORNs using the indium-tin oxide (ITO) planar electrode as a sensing material has been reported (Fig. 6.7) [52]. Novel findings of this study are direct cultivation of ORNs on the device and detection of the membrane action potential without coupling to the layer using biocompatible ITO. This approach enables convenient measurements and analyses of signals from cells.

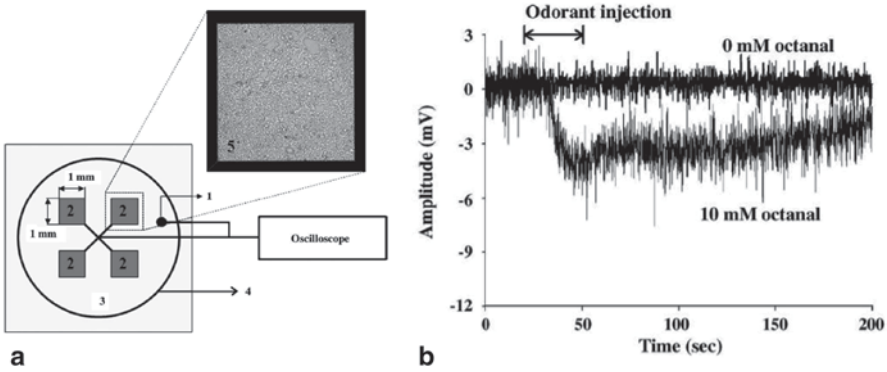

Fig. 6.5 **a** Schematic illustration of the planar electrode culture system. **b** Field potential profile of HEK-293 cells expressing I7 in the Ca^{2+} standard solution. (Reprinted from Ref. Lee et al. with permission from ELSEVIER)

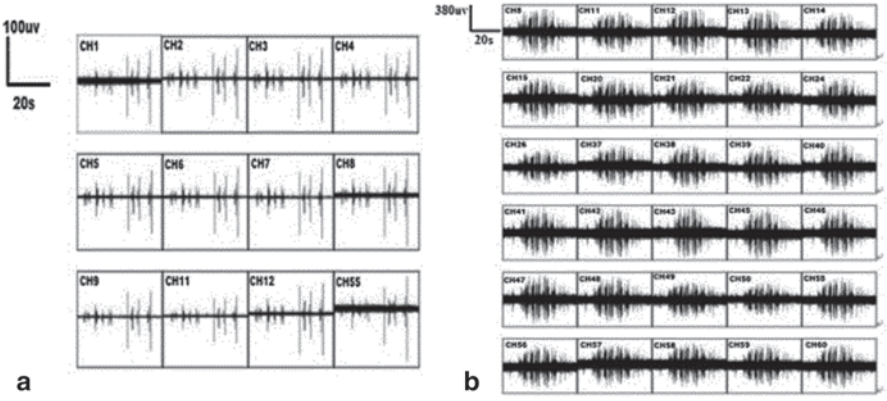

Fig. 6.6 Responses of ORNs from multiple recording sites of planar MEA. **a** Firing spikes map from the responses of ORNs that excited by odor (LIM). **b** Firing spikes map from responses of ORNs that excited by odor (ISO). (Reprinted from Ref. Ling et al. with permission from ELSEVIER)

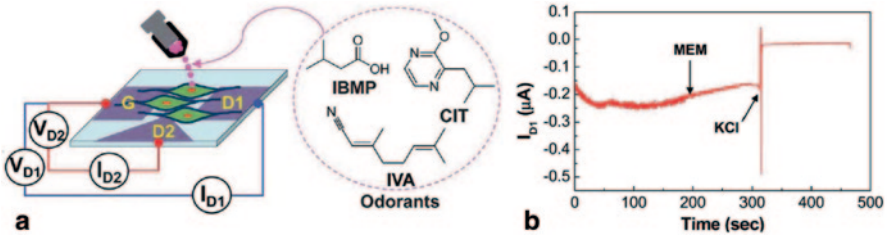

Fig. 6.7 **a** Illustration of odorant-stimulated experiment from rat OSNs on the planar triode (ITO) substrates. **b** D1 current signal from the planar triode olfactory devices by stimulating with MEM and KCl solutions. (Reprinted from Ref. Kim et al. with permission from RSC)

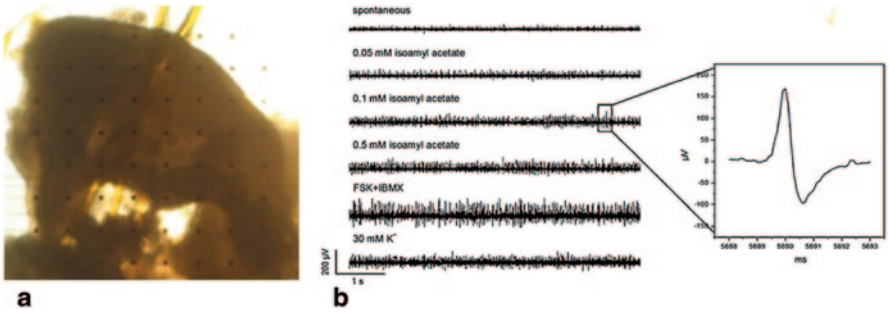

Fig. 6.8 **a** Slice of the olfactory epithelium on top of the MEA. **b** Typical extracellular potential traces of one electrode during spontaneous firing and stimulation with different concentration of isoamyl acetate (0.05, 0.1 and 0.5 mM), FSK + IBMX and 30 mM K^+. (Reprinted from Ref. Micholt et al. with permission from ELSEVIER)

A research team from the University of Leuven has developed an MEA which employs intact OE and OB tissue slices [56]. The experiments coupled the OE connected to an intact OB to an 8 × 8 MEA for spatial odor detection (Fig. 6.8). Sagittal slices of olfactory tissue were analyzed for their electrical responses to odorants and stimulants. This device was able to discriminate isoamyl acetate and L-carvone by measuring spike frequencies and patterns. Introduction of intact OE and OB tissue slices combined with MEA may provide a potentially powerful tool for odorant identification and quantification.

6.4.2 LAPS

The primary function of LAPS is detection of surface potentials from a device combined with a cell culture chamber that illuminates a small spot on the device surface with a focused, pulsed light-pointer. LAPS provides many advantages, such as convenience, simplicity, low cost, and fast addressable measurement. For example, the fabrication process of LAPS is easier due to its simple structure and absence of the need for an enclosure process. Moreover, the flat surface provides convenience for incorporation into the micro-volume cell culture chamber [57, 58].

Several reports have described the use of LAPS as an olfactory cell-semiconductor hybrid system for monitoring extracellular potentials from cells cultivated on the surface of the LAPS chip. Wang et al. have fabricated a LAPS-based device using olfactory and taste cells and have measured signals upon stimulation with glutamate to olfactory cell-based LAPS [59]. Additionally, signals were also detected successfully upon tastant stimulation, e.g. glucose, HCl, NaCl, quinine and monosodium mimicking sweetness, sourness, saltiness, bitterness, and umami, respectively. Thus, this device has to some extent mimicked the bioelectronic nose and tongue, which can detect both odors and tastants.

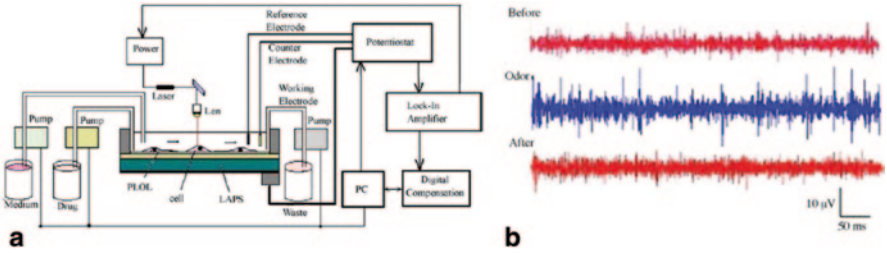

Fig. 6.9 **a** Schematic drawing of the LAPS system. **b** Odor-treated extracellular potential of the olfactory receptor cells before, during and after odor (acetic acid, CH_3COOH) treatment. (Reprinted from Ref. Wang et al. with permission from ELSEVIER)

Chunsheng et al. have demonstrated that the LAPS-OSNs hybrid biosensor has the potential to use ORN-based sensors in cellular signal monitoring (Fig. 6.9; [60]). Either MAL12330A or LY294002, which induce inhibitory effects in ORNs and enhance olfactory signals of ORNs, respectively, were found (Fig. 6.9). Although this device displays some room for improvement in sensitivity, ORN-based biosensors still seem to represent promising tools for monitoring cellular signals and olfactory transduction mechanisms.

6.4.3 FET

One of the advantages of FETs is easy access to the detection sites of neuronal networks due to the composition of multi recording sites. Additionally, FETs allow the device to monitor various parameters of cells, such as extracellular action potentials, cellular ionic communications, and communication velocity of cellular signals in a long-term, non-invasive manner. In addition, these devices provide several potential advantages, such as their small size and light weight, fast response time, high reliability, compatibility with other advanced microfabrication technologies, and the feasibility of on-chip integration of transducer arrays and signal processing schemes. The combination of living cells and silicon chips might allow for not only the creation of functional hybrid systems with new unique functional and practical potentials, but also may be applied to fundamental research on the elucidation of cellular physiological processes [61, 62].

To date, ORN-conjugated FETs have not been reported, however M. J. Schöning et al. have presented a biosensor using a FET combined with insect antenna, the odorant detector for insects (Fig. 6.10; [63]). Two different types of devices have been developed, a whole-beetle-BioFET and an isolated-antenna-BioFET. Both devices have demonstrated high sensitivity and selectivity for a plant odorant, Z-3-hexen-1-ol.

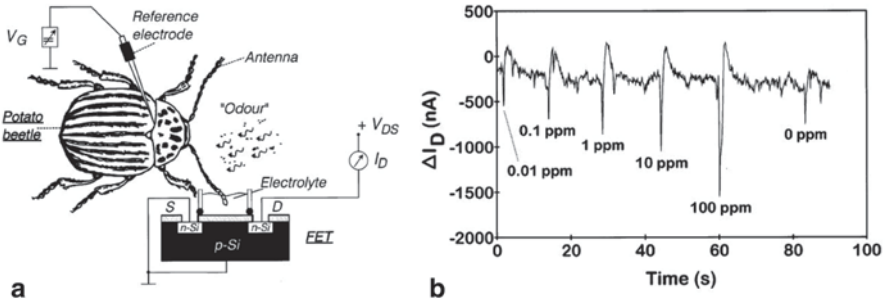

Fig. 6.10 **a** Schematic of the sensor equipment consisting of the intact chemoreceptor and the FET device. **b** Typical sensor response: Variation of I_D of the whole-beetle-BioFET by changing the Z-3-hexen-1-ol gas concentration. (Reprinted from Ref. Schöning et al. with permission from ELSEVIER)

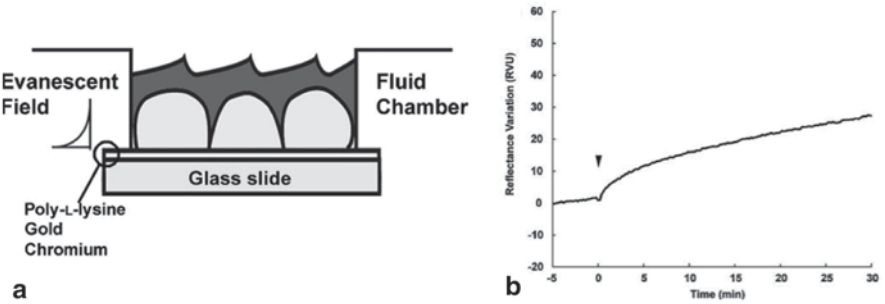

Fig. 6.11 **a** The evanescent field created by the surface plasmon resonance only allow monitoring of events occurring at the basal level of the cell. **b** Typical reflectance measured over a 30 min period following the injection of 5 mg/ml LPS on a bare gold substrate. (Reprinted from Ref. Chabot et al. with permission from ELSEVIER)

6.4.4 SPR

SPR has been applied practically for the real-time detection of molecular interactions occurring at the cellular membrane without a labeling process [64]. It employs an optical measurement system which detects changes of the refractive index of the fading wave very close to the surface of the device. Discrimination of fine changes of the refractive index at the surface of a thin metal film with high sensitivity is the key principle of the technique. SPR-based sensors allow researchers to measure communications between biomolecules, morphological changes, and enzymatic reactions [64, 65].

Chabot et al. have fabricated a SPR-based device and have monitored changes in activity and morphology of living cells (Fig. 6.11; [64]). Using various agents known to regulate cellular activity and morphology, three types of stimulations were specifically evaluated: an endotoxin (lipopolysaccharides), a chemical toxin

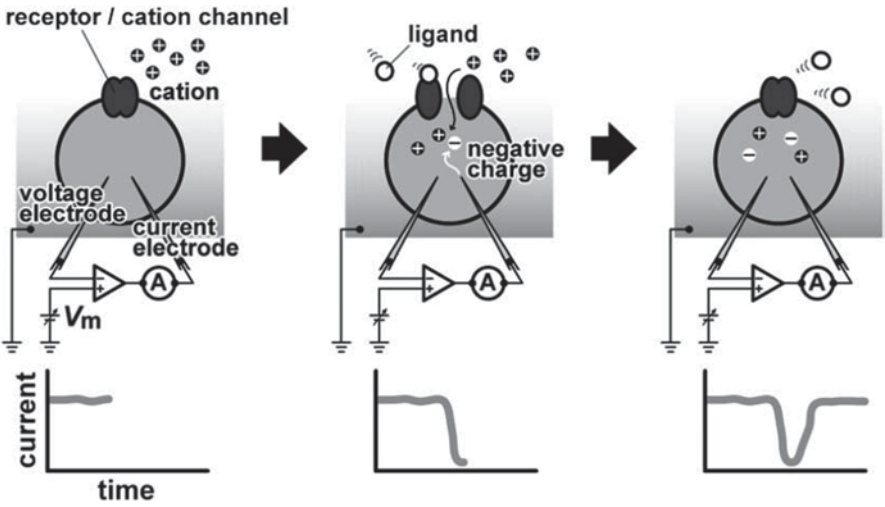

Fig. 6.12 Principle of measuring electronic signal in OR-bioengineered cell

(sodium azide) and a physiological agonist (thrombin). The feasibility of this sensing method was verified through detection of the refractive index. Additionally, this method was found to have the capability to be applied to various cellular dynamics involving morphological changes by specific agents.

Due to its reliability, SPR may have excellent potential for use in olfaction-inspired biosensors. Instead of using ORNs, this technology may be applied using isolated, specific OR proteins.

6.4.5 Characteristics of ORN-Based Biosensors

ORN-based biosensors have a few limitations as sensor devices. First, it is difficult to acquire high quality cultures of ORNs. Second, it is difficult to take advantage of this technology due to the lack of a complete understanding of ORN signal transduction mechanisms. One strategy to overcome these limitations involves the bioengineering of non-ORN-based biosensors. Although non-ORN-based biosensors may not be as amenable to the study of olfactory transduction as compared to ORN-based sensors, they may display advantages in sensitivity and selectivity. These devices, in general, are made by introduction of ORs into heterogeneous cells, therefore allowing researchers to select specific ORs for better sensitivity and selectivity. Studies from Nobuo et al. and Sindhuja et al. are typical examples [66–68]. Nobuo et al. have made insect ORs expressed in oocytes (Fig. 6.12) and have measured currents from cells expressing heterogeneous populations of ORs. Although this device can not react to diverse functional groups of chemicals, it has displayed high sensitivity and selectivity to specific functional groups such as –OH, –CHO and –C(═O)–.

Moreover, Sindhuja et al. conducted similar experiments focused on selectivity and sensitivity. Both of these studies involved food safety applications; one used an OR-based biosensor with specialized selectivity to alcohols and the other attempted to increase sensitivity by an odorant binding protein [67, 68].

6.5 Conclusion

We here have overviewed neurobiology and cultivation of ORNs for the use of cell-based sensors. Moreover, we have also discussed bioengineered cells heterogeneously expressing ORs for uses of biosensor chips [5–9, 15–17, 44, 45, 48, 54].

The development of cell-based sensors has been advanced due to progress in the areas of general cultivation techniques, genetic engineering, and micro and nano fabrications. Simultaneously, the demand for cell-based sensors has increased dramatically due to a proliferation of industrial applications. ORNs can discriminate millions of distinct chemicals, and therefore represent prime candidates for the detector portion of cell-based sensors. The common features of ORN-based sensor devices are discrimination of chemicals by specific ORs and measurement of electrical activities from ORNs upon odorant stimulation. The differential advantage of such devices is the promise of non-invasive and long-term measurements with fast responses and high sensitivity. Although OR-based biosensors have demonstrated high sensitivity and selectivity, ORN-based biosensors require improvement predicated on further elucidation of the neurobiology of olfactory signal transduction.

Acknowledgments This research was supported by the Converging Research Center Program through the Ministry of Science, ICT and Future Planning, Korea (2013K000363).

References

1. Lancet D (1986) Vertebrate olfactory reception. Annu Rev Neurosci 9:329–355. doi:10.1146/annurev.ne.09.030186.001553
2. Snyder SH, Sklar PB, Pevsner J (1988) Molecular mechanisms of olfaction. J Biol Chem 263(28):13971–13974
3. Graziadei GA, Graziadei PP (1979) Neurogenesis and neuron regeneration in the olfactory system of mammals. II. Degeneration and reconstitution of the olfactory sensory neurons after axotomy. J Neurocytol 8(2):197–213
4. Moulton DG, Beidler LM (1967) Structure and function in the peripheral olfactory system. Physiol Rev 47:1–52
5. Labarca P, Bacigalupo J (1988) Ion channels from chemosensory olfactory neurons. J Bioenerg Biomembr 20:551–569
6. Getchell TV (1986) Functional properties of vertebrate olfactory receptor neurons. Physiol Rev 66:772–818
7. Lowe G, Gold GH (1993) Contribution of the ciliary cyclic nucleotide-gated conductance to olfactory transduction in the salamander. J Physiol 462:175–196

8. Menco BP, Cunningham AM, Qasba P, Levy N, Reed RR (1997) Putative odour receptors localize in cilia of olfactory receptor cells in rat and mouse: a freeze-substitution ultrastructural study. J Neurocytol 26(10):691–706
9. Menco BP, Bruch RC, Dau B, Danho W (1992) Ultrastructural localization of olfactory transduction components: the G protein subunit Golf alpha and type III adenylyl cyclase. Neuron 8(3):441–453
10. Farbman AI (1992) Structure of olfactory mucous membrane. In: Barlow PW, Bray D, Green PB, Slack JMW (eds) Cell biology of olfaction, vol 6. Cambridge University Press, Cambridge, pp 24–74
11. Roskams AJ, Cai X, Ronnett GV (1998) Expression of neuron-specific beta-III tubulin during olfactory neurogenesis in the embryonic and adult rat. Neuroscience 83(1):191–200
12. Graziadei PP (1973) Cell dynamics in the olfactory mucosa. Tissue Cell 5(1):113–131
13. Graziadei PP (1971) Topological relations between olfactory neurons. Z Zellforsch Mikrosk Anat 118(4):449–466
14. Caggiano M, Kauer JS, Hunter DD (1994) Globose basal cells are neuronal progenitors in the olfactory epithelium: a lineage analysis using a replication-incompetent retrovirus. Neuron 13:339–352
15. Carr VM, Farbman AI (1993) The dynamics of cell death in the olfactory epithelium. Exp Neurol 124:308–314
16. Constanzo RM, Morrison EE (1989) Three-dimensional scanning electron microscopic study of the normal hamster olfactory epithelium. J Neurocytol 18:381–391
17. Hirsch JD, Margolis FL (1980) Influence of unilateral bulbectomy on opiate and other binding sites in the contralateral bulb. Brain Res 199:39–47
18. Graziadei PP, Graziadei GA (1979) Neurogenesis and neuron regeneration in the olfactory system of mammals. I. Morphological aspects of differentiation and structural organization of the olfactory sensory neurons. J Neurocytol 8(1):1–18
19. Calof AL, Chikaraishi DM (1989) Analysis of neurogenesis in a mammalian neuroepithelium: proliferation and differentiation of an olfactory neuron precursor in vitro. Neuron 3:115–127
20. Goldstein BJ, Schwob JE (1996) Analysis of the globose basal cell compartment in rat olfactory epithelium using GBC-1, a new monoclonal antibody against globose basal cells. J Neurosci 16(12):4005–4016
21. Huard JM, Youngentob SL, Goldstein BJ, Luskin MB, Schwob JE (1998) Adult olfactory epithelium contains multipotent progenitors that give rise to neurons and non-neural cells. J Comp Neurol 400(4):469–486
22. Getchell TV, Margolis FL, Getchell ML (1985) Perireceptor and receptor events in vertebrate olfaction. Prog Neurobiol 23:317–345
23. Okano TM (1974) Secreation and electrogenesis of the supporting cell in the olfactory epithelium. J Physiol (London) 242:353–370
24. Hansel DE, Eipper BA, Ronnett GV (2001) Neuropeptide Y functions as a neuroproliferative factor. Nature 410(6831):940–944
25. Buck L, Axel R (1991) A novel multigene family may encode odorant receptors: a molecular basis for odor recognition. Cell 65(1):175–187
26. Taupin P, Gage F (2002) Adult neurogenesis and neural stem cells of the central nervous system in mammals. J Neurosci Res 69:745–749
27. Vaccarino FM, Ganat Y, Zhang Y, Zheng W (2001) Stem cells in neurodevelopment and plasticity. Neuropsychopharmacology 25(6):805–815
28. Pincus DW, Keyoung HM, Harrison-Restelli C, Goodman RR, Fraser RA, Edgar M, Sakakibara S, Okano H, Nedergaard M, Goldman SA (1998) Fibroblast growth factor-2/brain-derived neurotrophic factor- associated maturation of new neurons generated from adult human subependymal cells. Ann Neurol 43(5):576–585
29. Carpenter MK, Cui X, Hu ZY, Jackson J, Sherman S, Seiger A, Wahlberg LU (1999) In vitro expansion of a multipotent population of human neural progenitor cells. Exp Neurol 158(2):265–278

30. Maric D, Maric I, Chang YH, Barker JL (2003) Prospective cell sorting of embryonic rat neural stem cells and neuronal and glial progenitors reveals selective effects of basic fibroblast growth factor and epidermal growth factor on self-renewal and differentiation. J Neurosci 23(1):240–251
31. Riaz SS, Theofilopoulos S, Jauniaux E, Stern GM, Bradford HF (2004) The differentiation potential of human foetal neuronal progenitor cells in vitro. Brain Res Dev Brain Res 153(1):39–51
32. Li X-J, Du Z-W, Zarnowska ED, Pankratz M, Hansen LO, Pearce RA, Zhang S-C (2005) Specification of motoneurons from human embryonic stem cells. Nature Biotechnology Advance online publication
33. Bally-Cuif L, Hammerschmidt M (2003) Induction and patterning of neuronal development, and its connection to cell cycle control. Curr Opin Neurobiol 13:16–25
34. Altman J, Das GD (1965) Autoradiographic and histological evidence of postnatal hippocampal neurogenesis in rats. J Comp Neurology 124(3):319–335
35. Graziadei PPC, Monti-Graziadei GA (1978) Continuous nerve cell renewal in the olfactory system. In: Jacobson M (ed) Handbook of sensory physiology, vol IX. Springer-Verlag, Berlin, pp 55–82
36. Altman J (1969) Autoradiographic and histological studies of postnatal neurogenesis. IV. Cell proliferation and migration in the anterior forebrain, with special reference to persisting neurogenesis in the olfactory bulb. J Comp Neurol 137(4):433–457
37. Luskin MB (1993) Restricted proliferation and migration of postnatally generated neurons derived from the forebrain ventricular zone. Neuron 11:173–189
38. Calof AL, Bonnin A, Crocker C, Kawauchi R, Murray RC, Shou J, Wu H-H (2002) Progenitor cells of the olfactory receptor neuron lineage. Micro Res Tech 58:176–188
39. Hansel DE, May V, Eipper BA, Ronnett GV (2001) PACAP peptides and a-amidation in olfactory neurogenesis and neuronal survival in vitro. J Neurosci 21(13):4625–4636
40. Simpson PJ, Miller I, Moon C, Hanlon AL, Liebl DJ, Ronnett GV (2002) Atrial natriuretic peptide type C induces a cell-cycle switch from proliferation to differentiation in brain-derived neurotrophic factor- or nerve growth factor-primed olfactory receptor neurons. J Neurosci 22(13):5536–5551
41. Simpson PJ, Wang E, Moon C, Matarazzo V, Cohen D, Leibl DJ, Ronnett GV (2003) Neurotrophin-3 signaling maintains maturational homeostasis between neuronal populations in the olfactory system. Mol Cell Neurosci 24:858–874
42. Uranagase A, Katsunuma S, Doi K, Nibu K (2012) BDNF expression in olfactory bulb and epithelium during regeneration of olfactory epithelium. Neurosci Lett 516(1):45–49. doi:10.1016/j.neulet.2012.03.051
43. Moon C, Liu BQ, Kim SY, Kim EJ, Park YJ, Yoo JY, Han HS, Bae YC, Ronnett GV (2009) Leukemia inhibitory factor promotes olfactory sensory neuronal survival via phosphoinositide 3-kinase pathway activation and Bcl-2. J Neurosci Res 87(5):1098–1106. doi:10.1002/jnr.21919
44. Noble M, Mallaburn PS, Klein N (1984) The growth of olfactory neurons in short-term cultures of rat olfactory epithelium. Neurosci Lett 45(2):193–198
45. Ronnett GV, Hester LD, Snyder SH (1991) Primary culture of neonatal rat olfactory neurons. J Neurosci 11(5):1243–1255
46. Ash KO, Bransford JE, Koch RB (1966) Studies on dispersion of rabbit olfactory cells. J Cell Biol 29(3):554–561
47. Hirsch JD, Margolis FL (1979) Cell suspensions from rat olfactory neuroepithelium: biochemical and histochemical characterization. Brain Res 161(2):277–291
48. Gonzales F, Farbman AI, Gesteland RC (1985) Cell and explant culture of olfactory chemoreceptor cells. J Neurosci Meth 14(2):77–90
49. Largent BL, Sosnowski RG, Reed RR (1993) Directed expression of an oncogene to the olfactory neuronal lineage in transgenic mice. J Neurosci 13(1):300–312
50. MacDonald KP, Mackay-Sim A, Bushell GR, Bartlett PF (1996) Olfactory neuronal cell lines generated by retroviral insertion of the n-myc oncogene display different developmental phenotypes. J Neurosci Res 45(3):237–247. doi:10.1002/(SICI)1097-4547(19960801)45:3 & lt;237::AID-JNR5 & gt;3.0.CO;2-E

51. Barber RD, Jaworsky DE, Yau KW, Ronnett GV (2000) Isolation and in vitro differentiation of conditionally immortalized murine olfactory receptor neurons. J Neurosci 20(10):3695–3704
52. Kim H, Kim SY, Nam S, Ronnett GV, Han HS, Moon C, Kim Y (2012) Direct measurement of extracellular electrical signals from mammalian olfactory sensory neurons in planar triode devices. Analyst 137(9):2047–2053. doi:10.1039/c2an16205a
53. Thomas CA Jr, Springer PA, Loeb GE, Berwald-Netter Y, Okun LM (1972) A miniature microelectrode array to monitor the bioelectric activity of cultured cells. Exp Cell Res 74(1):61–66
54. Lee SH, Jun SB, Ko HJ, Kim SJ, Park TH (2009) Cell-based olfactory biosensor using microfabricated planar electrode. Biosens Bioelectron 24(8):2659–2664. doi:10.1016/j.bios.2009.01.035
55. Ling SC, Gao TY, Liu J, Li YQ, Zhou J, Li J, Zhou CC, Tu CL, Han F, Ye XS (2010) The fabrication of an olfactory receptor neuron chip based on planar multi-electrode array and its odor-response analysis. Biosens Bioelectron 26(3):1124–1128. doi: 10.1016/j.bios.2010.08.071
56. Micholt E, Jans D, Callewaert G, Bartic C, Lammertyn J, Nicolai B (2013) Extracellular recordings from rat olfactory epithelium slices using micro electrode arrays. Sens Actuators B-Chem 184:40–47. doi:10.1016/j.snb.2013.03.134
57. Liu QJ, Cai H, Xu Y, Li Y, Li R, Wang P (2006) Olfactory cell-based biosensor: a first step towards a neurochip of bioelectronic nose. Biosens Bioelectron 22(2):318–322. doi: 10.1016/j.bios.2006.01.016
58. Liu QJ, Ye WW, Hu N, Cai H, Yu H, Wang P (2010) Olfactory receptor cells respond to odors in a tissue and semiconductor hybrid neuron chip. Biosens Bioelectron 26(4):1672–1678. doi:10.1016/j.bios.2010.09.019
59. Wang P, Liu QJ, Xu Y, Cai H, Li Y (2007) Olfactory and taste cell sensor and its applications in biomedicine. Sens Actuators A-Phys 139(1–2):131–138. doi:10.1016/j.sna.2007.05.018
60. Wu CS, Chen PH, Yu H, Liu QJ, Zong XL, Cai H, Wang P (2009) A novel biomimetic olfactory-based biosensor for single olfactory sensory neuron monitoring. Biosens Bioelectron 24(5):1498–1502. doi:10.1016/j.bios.2008.07.065
61. Schoning MJ, Poghossian A (2002) Recent advances in biologically sensitive field-effect transistors (BioFETs). Analyst 127(9):1137–1151. doi:10.1039/B204444 g
62. Schoning MJ, Poghossian A (2006) Bio FEDs (Field-Effect devices): state-of-the-art and new directions. Electroanalalysis 18 (19–20):1893–1900. doi:10.1002/elan.200603609
63. Schoning MJ, Schutz S, Schroth P, Weissbecker B, Steffen A, Kordos P, Hummel HE, Luth H (1998) A BioFET on the basis of intact insect antennae. Sens Actuators B-Chem 47(1–3):235–238. doi:10.1016/S0925-4005(98)00029-X
64. Chabot V, Cuerrier CM, Escher E, Aimez V, Grandbois M, Charette PG (2009) Biosensing based on surface plasmon resonance and living cells. Biosens Bioelectron 24(6):1667–1673. doi:10.1016/j.bios.2008.08.025
65. Yotter RA, Lee LA, Wilson DM (2004) Sensor technologies for monitoring metabolic activity in single cells - part I: optical, methods. IEEE Sens J 4(4):395–411. doi:10.1109/Jsen.2004.830952
66. Misawa N, Mitsuno H, Kanzaki R, Takeuchi S (2010) Highly sensitive and selective odorant sensor using living cells expressing insect olfactory receptors. Proc Natl Acad Sci U S A 107(35):15340–15344. doi:10.1073/pnas.1004334107
67. Sankaran S, Panigrahi S, Mallik S (2011) Odorant binding protein based biomimetic sensors for detection of alcohols associated with Salmonella contamination in packaged beef. Biosens Bioelectron 26(7):3103–3109. doi:10.1016/j.bios.2010.07.122
68. Sankaran S, Panigrahi S, Mallik S (2011) Olfactory receptor based piezoelectric biosensors for detection of alcohols related to food safety applications. Sens Actuators B-Chem 155(1):8–18. doi:10.1016/j.snb.2010.08.003

Chapter 7
Production of Olfactory Receptors Using Commercial *E. coli* Cell-free Systems

Karolina Corin, Xiaoqiang Wang and Shuguang Zhang

Abstract The first bottleneck in olfactory receptor (OR) structural and functional studies is to produce sufficient quantities of soluble, functional, and stable receptors. Other production systems have been used and summarized in other chapters of this book. We here show that commercial cell-free *in vitro* translation systems can be used to produce milligrams of soluble and functional olfactory receptors within several hours directly from plasmid DNA with select optimal detergents. These olfactory receptors can be purified using immunoaffinity 1D4 monoclonal antibody rhodopsin-tag and gel filtration, and can be analyzed using gel electrophoresis and with other standard techniques. The olfactory receptors and other scent-related receptors produced by the cell-free method fold properly and are able to bind their odorants.

7.1 Production of Olfactory Receptors is Required for Study and New Technology

The molecular basis of olfaction is poorly understood, primarily due to the extreme difficulty of producing sufficient quantities of soluble and functional olfactory receptors (ORs). Olfactory receptors belong to the G protein-coupled receptor family, which is characterized by seven transmembrane helical segments arranged in a barrel-like conformation. These transmembrane regions, which include the receptor-binding pocket, can cause problems with protein expression, and make it difficult to functionally stabilize the receptors outside of their native membrane environment. Receptor production in eukaryotic or bacterial cells frequently encounters problems such as low yields, cell toxicity, protein degradation, protein inhomogeneity and aggregation in internal compartments or inclusion bodies [1–5]. Cell-free *in vitro* translation is an alternative and enabling method allowing for rapid, cost-effective, high-yield protein expression [6–11]. The produced olfactory receptor proteins can

S. Zhang (✉) · K. Corin · X. Wang
Center for Bits and Atoms, Massachusetts Institute of Technology, 77 Massachusetts Avenue E15-401, Cambridge, MA 02139-4307, USA
e-mail: Shuguang@MIT.EDU

T. H. Park (ed.), *Bioelectronic Nose,* DOI 10.1007/978-94-017-8613-3_7,

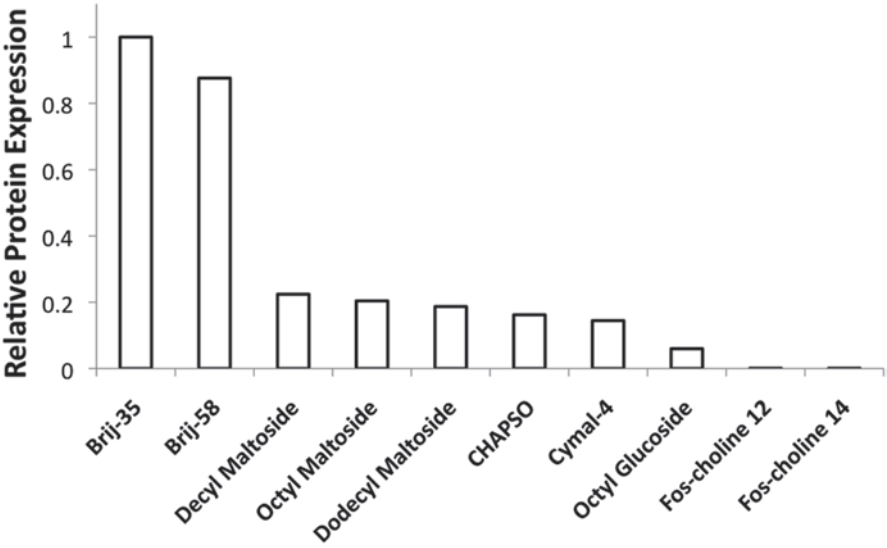

Fig. 7.1 Detergent screen for cell-free GPCR production. Detergent screen showing the relative expression of hOR17-210 in 10 different detergents. The Brij35 and Brij58 detergents yielded 4–5 times more protein than the next best detergent that was tested [8]

be purified using the affinity column chromatography of a monoclonal antibody 1D4 to very high purify [12–17], followed by a conventional gel filtration chromatography.

7.2 Cell-Free Olfactory Receptor Protein Production

Cell-free expression is an established technology for producing soluble proteins. This can be adapted for membrane proteins by including an appropriate detergent in the reaction mixture [7–11] (Fig. 7.1). Indeed, using the optimal detergent, it is possible to use cell-free systems to rapidly produce milligram quantities of receptors within several hours directly from plasmid DNA. Immunoaffinity chromatography and gel filtration chromatography can then be used to purify the expressed protein for structural and function studies (Fig. 7.2) [12–17].

Our study demonstrates that cell-free membrane protein production is a useful technology for expressing milligrams of olfactory receptors and other GPCRs (Table 7.1). The receptors could be purified to ~90% purity using immunoaffinity chromatography alone. CD measurements on a subset of purified olfactory receptors and other GPCRs showed that they had the predicted secondary structures, which suggests that they were properly folded (Fig. 7.3). Microscale thermophoresis indicated that the cell-free produced olfactory receptors and other GPCRs were functional by showing that the purified receptors could bind their

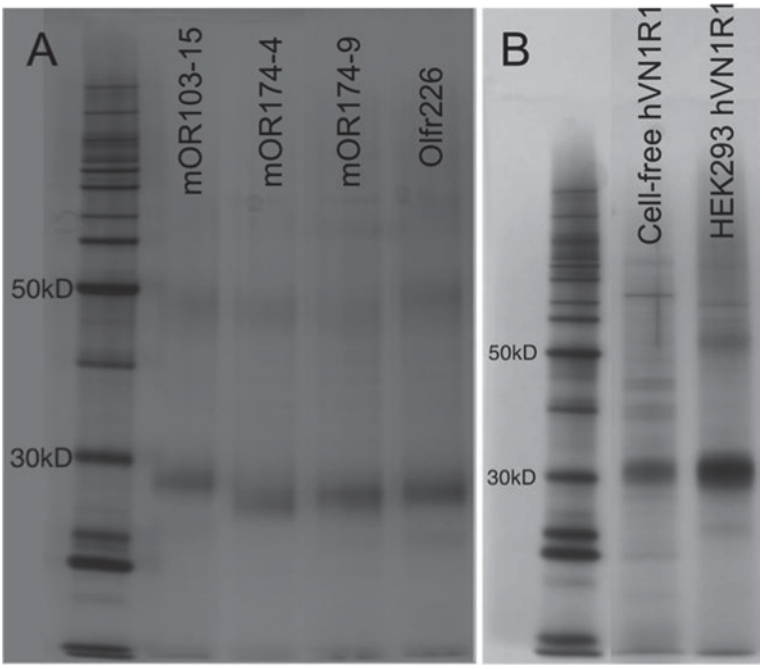

Fig. 7.2 Silver stains of purified olfactory receptors. **a**) Four cell-free expressed olfactory receptors. **b**) Comparison between cell-free and HEK293 expressed scent-related hVN1R1. Most olfactory receptors could be purified to >90% purity, and all showed two *bands* characteristic of a monomer and a dimer. The cell-free and HEK293 expressed receptors run at the same size, and have similar purities

reported small-molecule ligands (Fig. 7.4). Comparison of HEK293 and cell-free expressed protein (Figs. 7.2, 7.3 and 7.4) suggests that cell-free systems are a practical alternative to cell-based platforms for producing olfactory receptors and other GPCRs.

Although cell-free production is a mature technology for soluble proteins, very few membrane proteins have been produced, largely due to the lack of suitable detergents, requiring laborious detergent screens. We found that Brij-35 seemed to consistently be the optimal detergent for olfactory receptors and scent-related GPCRs. Brij-35 may not be optimal for all membrane proteins or GPCRs; the Brij family of detergents may function best with cell-free olfactory receptors and scent-related GPCRs and perhaps other membrane protein expressions. While the best detergent for protein production may not be the best detergent for downstream applications, we have shown that a single detergent exchange with FC14 is possible without compromising olfactory receptor's and other GPCR's structure and function. Since FC14 has been used to obtain protein structures, it should be possible to couple cell-free expression with crystal screens or NMR structural studies.

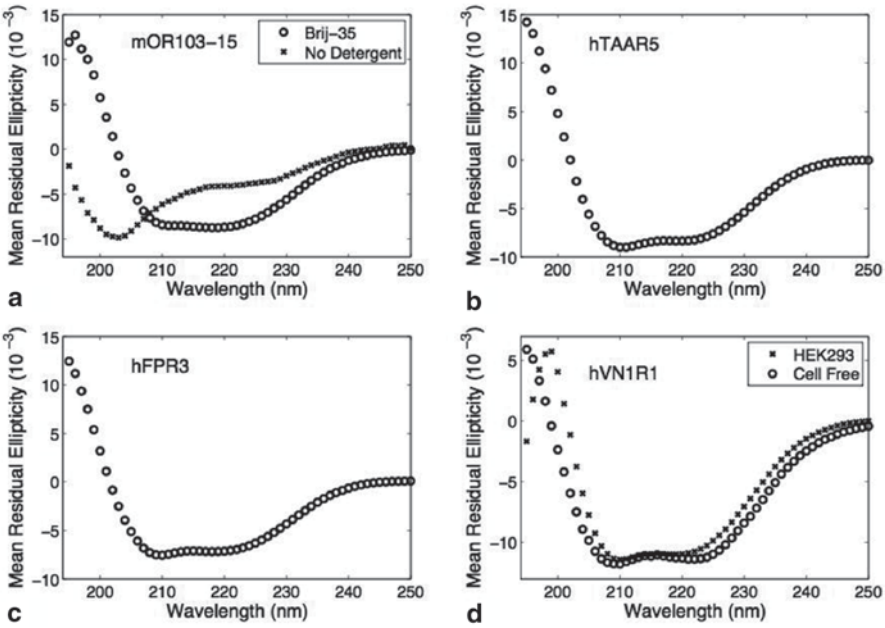

Fig. 7.3 Circular dichroism spectra of 5 purified scent-related GPCRs**. a**) Cell-free expressed mouse olfactory receptor mOR103-15 made with Brij-35 or no detergent, **b**) Cell-free expressed hTAAR5, **c**) Cell-free expressed hFPR3, and **d)** Cell-free and HEK293 expressed hVN1R1. All purified GPCRs have characteristic alpha-helical spectra, except mOR103-15 made without detergent. Since GPCRs have 7-transmembrane helices, and an overall α-helix content of ~50%, the CD spectra suggest that these receptors are properly folded. The near overlap of the spectra for cell-free and HEK293 expressed hVN1R1 suggests that both receptors are properly folded, and further indicates that cell-free produced scent-related receptors are comparable to those expressed in mammalian cells

In order to accelerate membrane protein structure and function studies, it is absolutely vital to develop simple, straightforward methods of producing sufficient quantities of membrane proteins. Commercial cell-free kits offer an attractive alternative to cell-based systems. Milligrams of protein can be produced within hours directly from plasmid DNA. The produced proteins can be purified quickly using conventional methods, and are amenable to detergent exchange for downstream applications. Using commercially available kits, the necessary reagents are easily and widely available, and results are reproducible. Although the 13 olfactory receptors and other scent-related GPCRs represent a small fraction of all receptors, it is the largest number presented in a single study with the same cell-free production method. Our ability to produce significant quantities of olfactory receptors and other GPCRs using commercial cell-free systems demonstrates the usefulness of this technology in the field. Indeed, the critical production bottleneck in membrane protein studies may potentially be overcome. Structure and function studies of olfactory receptors and other GPCRs may be stimulated and accelerated in the coming years.

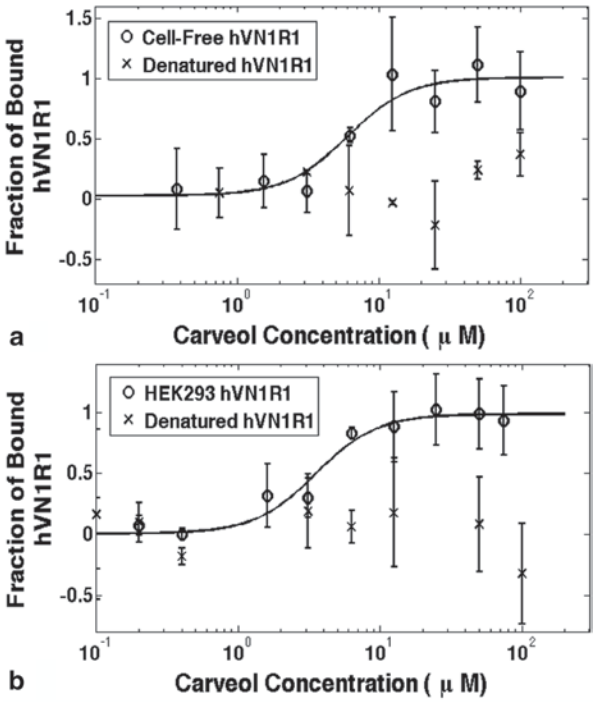

Fig. 7.4 Microscale thermophoresis measurements of purified GPCRs. **a**) Cell-free expressed hVN1R1 with and without heat-denaturation. **b**) HEK293 expressed hVN1R1 with and without heat-denaturation. The non-denatured receptors show typical sigmoidal binding curves, with plateaus at low and high concentrations. Cell-free expressed hVN1R1 has an EC_{50} of 6±2 μM, and HEK293 expressed hVN1R1 has an EC_{50} of 3.5±0.7 μM. The heat-denatured controls had flat responses or random amplitudes throughout the ligand titration range. These results show that hVN1R1 is binding carveol. Furthermore, the similar EC_{50} values and binding curves in **a**) and **b**) demonstrate that cell-free produced receptors function as well as HEK293 expressed receptors. The curves were normalized to the fraction of bound receptor. Each data point represents the mean of 3 independent experiments; error *bars* show the standard deviation. The binding curves were fit to the Hill equation. The binding results shown are representative of the data from other binding measurements

7.2.1 Reagents for Cell-Free Expression in Test Tubes

1. *E. coli* lysate (RiNA GmbH, http://rina-gmbh.eu/, Qiagen and Life Technologies). The lysate should be stored at −80 °C, thawed on ice, and used within 4 h of defrosting. It can be re-frozen and thawed once for optimal results. Repeated freezes and thaws of the lysate may not produce reproducible results. Small aliquots should be made from larger volumes of lysate for future uses.
2. Reaction buffer. The buffer should be stored at −80 °C, thawed on ice, and used within 4 h of defrosting. It can be re-frozen and thawed once for optimal results.

Table 7.1 Solubility and maximum yields of GPCRs produced using cell-free *in vitro* translation in the presence of Brij-35

GPCR	% solubility	Yield (mg)[a]	GPCR %	Solubility	Yield (mg)[a]
Olfr226	86±8	3.7	hOR17-209	88±4	2.5
mOR33-1	85±2	5.9	hOR17-210	91±2	4.5
mOR103-15	90±4	4.5	hFPR3	83±5	5.5
mOR106-13	86±13	2.4[b]	hTAAR5	90±1	4.5
mOR174-4	89±2	2	hVN1R1	88±0.1	0.4
mOR174-9	86±3	6	hVN1R5	85±2	1[b]
mOR175-1	81±8	2.5			

[a] Milligrams of receptor that could be produced in a 10 ml cell-free reaction. These yields were calculated from smaller batches of protein purified using immunoaffinity chromatography. Experiments showed that up to 1 mg/ml of protein could be produced, but that up to half could be lost during the purification process. The yields were determined by spectrophotometer readings

[b] These yields were calculated by comparing the intensities of the receptor samples against a sample with a known concentration

Aliquots can be made for larger volumes of buffer. The specific buffer varies with each kit, but contains all essential amino acids, RNA polymerases, ribosomes, elongation factors, etc.

3. Sterile, DNase-free and RNase-free water
4. Non-ionic Detergent Brij-35 [2% (10X) or 10% (50X) concentration]
5. Olfactory receptor gene ligated into the pIVex2.3d plasmid vector (Life Technologies)

7.2.2 Cell-Free Protein Production

1. Thaw the *E. coli* lysate, reaction buffer, and DNA on ice.
2. Add 175 µl of the *E. coli* lysate to a sterile, DNAse-free, RNAse-free Eppendorf tube Add the plasmid to the lysate so that the final DNA concentration is 1 µg/100 µl.
3. Add DNAase-free and RNAse-free water so that the final volume of the cell-free reaction will be 500 µl.
4. Add Brij-35 to a final concentration of 0.2% w/v.
5. Add 200 µl of the reaction buffer, and mix thoroughly with a pipette.
6. Briefly (~5 s) spin down the Eppendorf tube.
7. Place the cell-free reaction in an Eppendorf rack in a shaking incubator at 33 °C and 250 rpm for 1 h.
8. After the reaction is complete, spin it down in a microcentrifuge for 5 min at 10,000 rpm.
9. Carefully transfer the supernatant to a fresh tube without disturbing the pellet. The supernatant contains solubilized receptor.
10. The synthesized receptors can be purified or run on an SDS-PAGE gel immediately, or stored at −20 °C for longer periods of time.

7.3 Olfactory Receptor Purification

After production of olfactory receptors, they need to be purified from the cell-free system for subsequent studies and uses. We adopted an affinity purification system using a rhodopsin tag that was developed by Khorana and colleagues [18]. This monoclonal antibody-coupled bead has very high specificity and binding capacity. In most cases, a single step can purify olfactory receptor and other rho-tag proteins to near homogeneity [9–17]. Before affinity purification, the special antibody-coupled beads need to be prepared. It is described below.

7.3.1 Monoclonal Antibody Rho1D4 Bead Coupling

1. Rho1D4 monoclonal antibody (Cell Essentials, http://www.cell-essentials.com/) at 2–8 mg/ml (Cell Essentials, hybridoma 1B4-1) in coupling buffer (0.25 M $NaHCO_3$, 0.5 M NaCl, pH 8.3, in milliQ water). If the antibody is not in the correct coupling buffer upon arrival, it must first be first dialyzed into the coupling buffer above. Otherwise, it will not couple very well and with low yield.
2. CNBr-activated Sepharose 4B (GE Healthcare)
3. Coupling buffer: 0.25 M $NaHCO_3$, 0.5 M NaCl, pH 8.3, in milliQ water
4. HCl buffer: 1 mM HCl in milliQ water
5. Ethanolamine buffer: 1 M ethanolamine, pH 8.0 in milliQ water
6. Acetate buffer: 0.1 M NaOAc, 0.5 M NaCl, pH 4.0 in milliQ water
7. Sodium azide buffer: 0.05 % NaN_3 in PBS, pH 7.2

7.3.2 Method for Rho1D4 Monoclonal Antibody-Sepharose Bead Coupling

1. Suspend the sepharose beads in HCl buffer. The hydrated beads will swell: 1 g of bead powder will yield approximately 3.5 ml of bead slurry.
2. Wash the beads for 15 min with the HCl buffer in a sintered glass funnel and vacuum flask. The beads should be resuspended in the buffer as they fall out of solution. After ~1 min, a vacuum should be applied until the liquid is removed. Do not over dry the beads. Approximately 200 ml of HCl buffer should be used per gram of bead powder. Several aliquots may be necessary.
3. Add the washed beads to the antibody in coupling buffer. Add 20 ml of bead slurry to 130–200 mg of antibody. The ratio should be 5–10 mg of antibody per ml of bead slurry.
4. Rotate the slurry/antibody solution at 4 °C until the antibody is bound to the beads. The antibody concentration in the supernatant can be monitored by measuring its absorbance at 280 nm. When the concentration is below 5 % of the

original concentration, the binding reaction is complete. This procedure takes 4 h to overnight.
5. Remove the supernatant after the binding reaction is complete by spinning down the beads for 5 min at 2,000 rpm.
6. Remove excess antibody by washing the beads with 5 slurry volumes of coupling buffer.
7. Block remaining active groups with the ethanolamine buffer. Add a volume equal to the original supernatant volume, and rotate overnight at 4 °C or 2 h at room temperature.
8. Remove excess uncoupled antibody by washing the beads 4 times alternating between coupling buffer and acetate buffer. Use a sintered glass filter, and a wash volume at least 5 times the original slurry volume.
9. Suspend the beads in 1 slurry volume of sodium azide buffer, and store them at 4 °C.

7.3.3 Affinity Olfactory Receptor Purification Using Rho-Tag Monoclonal Antibody

1. Rho1D4 monoclonal antibody-coupled sepharose beads
2. DPBS (Life Technologies, 14190-250)
3. DNase1 (Life Technologies**,** 18047-019)
4. RNaseA (Life Technologies, 12091-039)
5. Sterile filtered water (0.22 μm) with a resistivity of at least 18 MΩ-cm.
6. Wash buffer: 0.2 % fos-choline-14 (FC14) (Anatrace/Affymatrix). This is made from a 10 % FC14 stock solution in DPBS.
7. Elution buffer: 800 μM elution peptide Ac-TETSQVAPA-NH_2 (with an acetylated N-terminus and amidated C-terminus) dissolved in wash buffer.
8. High pH buffer: 0.1 M Tris-HCl, 0.5 M NaCl, pH 8.5.
9. Low pH buffer: 0.1 M sodium acetate, 0.5 M NaCl, pH 4.5.

7.3.4 Olfactory Receptor Purification Using 1D4 Rho-Tag Monoclonal Antibody

1. Pipette the necessary amount of antibody-coupled beads into a fresh tube. Mix the beads first by gently shaking them to ensure that they are homogeneously suspended. The binding capacity of fresh beads is ~0.7 mg/ml, and the capacity of regenerated beads is ~0.35 mg/ml.
2. Wash the beads with DPBS to remove excess sodium azide. Spin the beads down at 1,400 rpm for 1 min, and then let them sit for a minute to allow them to completely settle to the bottom of the tube. Using a pipette, slowly remove the supernatant without disturbing the bead pellet. Add one bead volume of DPBS

to re-suspend the pellet. Repeat this process three times. After the last repetition, do not add more DPBS.

3. Add the supernatant from the cell-free reaction to the washed beads.
4. Add 1 µl of DNAse and 1 µl of RNAse for each ml of cell-free reaction volume.
5. Rotate the supernatant with the beads overnight at 4 °C to capture the synthesized protein.
6. After the overnight rotation, spin the beads at 1,400 rpm for 1 min, and let them sit for 1 min to allow the bead pellet to settle. Remove the supernatant and transfer it to a tube labeled FT (Flow Thru). Save a small sample of the FT for analysis, and freeze the remainder at −80 °C in case the beads did not capture all of the synthesized receptors. Add one bead volume of wash buffer to the beads, and rotate at 4 °C for 10 min.
7. Wash the OR-bound beads to remove any impurities. For each wash, spin the tube at 1,400 rpm for 1 min, and allow it to sit for 1 min. Carefully remove the supernatant without disturbing the bead pellet, and transfer it to a fresh tube (labeled Wash 1, Wash 2, etc). Add 1 bead volume of wash buffer, and rotate at 4 °C for 10 min. Repeat this process until the absorbance at 280 nm of the removed supernatant is less than 0.01 mg/ml. Typically, 13–20 washes are required. The washes can be run overnight at 4 °C if necessary.
8. Elute the synthesized ORs from the beads. Add one bead volume of elution buffer to the beads, and rotate at room temperature for 1 h. Spin the beads at 1,400 rpm, and let them sit for 1 min. Carefully remove the supernatant without disturbing the bead pellet, and transfer it to a fresh, clean tube (labeled Elution 1, Elution 2, etc). Repeat this process until the absorbance of the removed supernatant at 280 nm is less than 0.01 mg/ml. The supernatant contains the synthesized receptors. Typically, 5–7 elutions are required. Any of the elutions can be run overnight at 4 °C if necessary.
9. The washes and elutions can be stored at 4 °C until they are ready for use.
10. The elutions can be pooled and concentrated in centrifugal units with 50 kDa molecular weight cut-off filters. If residual elution peptide must be removed (i.e. for circular dichroism), then the protein must be washed on the centrifugal units with excess wash buffer. 10 ml of wash buffer is usually sufficient to remove elution peptide from a concentrated protein sample with a total volume of 300 µl. If the receptors will be run on a size exclusion column, they must be concentrated to a volume that will fit in the loading loop. The receptors should be concentrated immediately prior to being loaded on the column to minimize aggregation and precipitation.
11. Used beads can be regenerated for re-use by washing them with 2–3 column volumes of alternating high pH (0.1 M Tris-HCl, 0.5 M NaCl, pH 8.5) and low pH (0.1 M sodium acetate, 0.5 M NaCl, pH 4.5) buffers. This cycle should be repeated 3 times followed by re-equilibration in binding buffer.

7.4 Gel Filtration for Further Purification

In order to separate the monomers from dimers, trimmers and multimers, it is important to further purify the olfactory receptors using conventional gel filtration method. This is to fractionate dimers, trimers and multimers for subsequent studies.

7.4.1 Materials and Reagents Required for Gel Filtration

1. Amicon Ultra Centrifugal Filter Units with Ultracel membranes (Millipore, 50 kDa MWCO membranes)
2. Sterile 96-well plates with V-shaped bottoms, ~500 µl/well capacity
3. Wash buffer: 0.2% FC14 in DPBS, sterile filtered through 0.22 µm filters

7.4.2 Gel Filtration Chromatography

1. Equilibrate the gel filtration column with at least 1–2 column volumes of wash buffer. We use a HiLoad 16/60 Superdex 200 column (GE Healthcare) on an ÄKTA Purifier FPLC system (GE Healthcare).
2. Load the freshly concentrated OR sample into the system.
3. Run the system at 0.3 ml/min, and monitor the UV absorbance at 215 nm and 280 nm. The monomeric form of our receptors typically exits the column at 60–65 ml. We collect the first 40 ml in a clean bottle. The remainder is collected in four 96-well V-bottom plates with 100 µl in each well.
4. Pool the appropriate eluted protein fractions together.
5. Concentrate the pooled fractions to the desired volume or concentration, and store them at 4 °C until they are ready for further analysis. Samples can be kept at −80 °C for long-term storage and should only be thawed once as repeated freeze-thaw cycles can induce protein aggregation.

7.5 Notes

1. Brij-35 has been the optimal detergent in our experiments. However, other groups have found other detergents to be optimal for their GPCRs, especially other polyoxyethylenes related to Brij-35 [7]. A preliminary detergent screen in which the cell-free reaction volumes are scaled down to a total volume of 25–50 µl may be necessary.
2. The olfactory receptor genes have a 5' NcoI site and a 3' XhoI site for ligation. They also have a C-terminal bovine rho1D4 epitope tag (TETSQVAPA) for puri-

fication followed by a double stop codon, and have potential glycosylation sites removed. The codons were optimized for *E. coli* expression.
3. The volumes listed here are for a total reaction volume of 500 µl. The volumes can be scaled up (to 5 ml) and down (50 µl) as necessary.
4. These are the optimal temperature, time, and rotation speed for the receptors we tested. We did not notice significant differences in olfactory receptor yield with longer incubation times (up to 6 h), rotation speeds up to 300 rpm, and at temperatures between 30 and 37 °C. However, the optimal conditions may vary with different receptors. In particular, lower temperatures can increase the yield of soluble receptor, while higher temperatures can increase the total receptor yield.

Acknowledgements We gratefully acknowledge the initial supported by a generous grant from ROHM, Kyoto, Japan, later in part by DARPA-HR0011-09-C-0012 and Yang Trust Fund.

References

1. Grisshammer R, Duckworth R, Henderson R (1993) Expression of a rat neurotensin receptor in *Escherichia coli*. Biochem J 295:571–576
2. Hampe W et al (2000) Engineering of a proteolytically stable human β2-adrenergic receptor/maltose-binding protein fusion and production of the chimeric protein in *Escherichia coli* and baculovirus infected insect cells. J Biotechnol 77:219–234
3. Sarramegna V, Talmont F, Demange P, Milon A (2003) Heterologous expression of G-protein-coupled receptors: comparison of expression systems from the standpoint of large-scale production and purification. Cell Mol Life Sci 60:1529–1546
4. McCusker EC, Bane SE, O'Malley MA, Robinson AS (2007) Heterologous GPCR expression: a bottleneck to obtaining crystal structures. Biotechnol Prog 23:540–547
5. Tate CG, Grisshammer R (1996) Heterologous expression of G-protein-coupled receptors. Trends Biotechnol 14:426–430
6. Ishihara G et al (2005) Expression of G protein coupled receptors in a cell-free translational system using detergents and thioredoxin-fusion vectors. Protein Expr Purif 41:27–37
7. Klammt C et al (2007) Cell-free production of G protein-coupled receptors for functional and structural studies. J Struct Biol 158:482–493
8. Kaiser L et al (2008) Efficient cell-free production of olfactory receptors: detergent optimization, structure, and ligand binding analyses. Proc Natl Acad Sci 105:15726–15731
9. Corin K et al (2011) A robust and rapid method of producing soluble, stable, and functional G-protein coupled receptors. PLoS ONE 6:e23036
10. Corin K et al (2011) Designer lipid-like peptides: a class of detergents for studying functional olfactory receptors using commercial cell-free systems. PLoS ONE 6:e25067
11. Wang X et al (2011) Peptide surfactants for cell-free production of functional G protein-coupled receptors. Proc Natl Acad Sci U S A 108:9049–9054
12. Takayama H et al (2008) High-level expression, single-step immunoaffinity purification and characterization of human tetraspanin membrane protein CD81. PLoS ONE 3:e2314
13. Cook BL et al (2008) Study of a synthetic human olfactory receptor 17-4: expression and purification from an inducible mammalian cell line. PLoS ONE 3:e2920
14. Cook BL et al (2009) Large-scale production and study of a synthetic GPCR: human olfactory receptor 17-4. Proc Natl Acad Sci U S A 106:11925–11930
15. Wang X et al (2011) Study of two G-protein coupled receptor variants of human trace amine-associated receptor 5. Sci Rep 1:e102

16. Corin et al (2011) Biochemical study of a bioengineered functional G-protein coupled receptor human vomeronasal type 1 receptor 1. Sci Rep 1:e172
17. Corin et al (2012) Insertion of T4-lysozyme (T4L) can be a useful tool for studying olfactory-related GPCRs. Mol Biosyst 8:1750–1759
18. Reeves PJ, Thurmond RL, Khorana HG (1996) Structure and function in rhodopsin: high-level expression of a synthetic bovine opsin gene and its mutants in stable mammalian cell lines. Proc Natl Acad Sci 93:11487–11492

Chapter 8
Production of Olfactory Receptors and Nanosomes Using Yeast System for Bioelectronic Nose

Marie-Annick Persuy, Guenhaël Sanz, Aurélie Dewaele, Christine Baly and Edith Pajot-Augy

Abstract Olfactory receptors (ORs) constitute the largest multigenic G protein-coupled receptor family, and are involved in the recognition of thousands of odorant molecules. However, if most of these ORs are identified on the basis of their DNA sequences, they are still unmatched to their natural ligands, and their deorphanization remains a challenging bottleneck. To identify odorant-olfactory receptor pairs, various techniques have been developed to clone and produce ORs in cells, to allow the screening of their response to odorants. During the last decade, various ORs were successfully expressed in *S. cerevisiae*, and many improvements achieved. This chapter reviews the latest developments of yeast-based technologies to produce ORs and test their functional response.

8.1 Introduction

Olfaction in mammals is mediated by a repertoire of several hundreds to more than a thousand olfactory receptors (ORs), which are G protein coupled receptors (GPCRs). Like other GPCRs of the class R family [1], ORs are predicted to have a alpha-helical structure with 7 transmembrane domains (named TM I to TM VII), a short extracellular N-terminal part outside the plasma membrane and a C-terminal region inside the cytoplasm. The knowledge of many complete mammalian genomes

M.-A. Persuy (✉) · G. Sanz · A. Dewaele · C. Baly · E. Pajot-Augy
INRA, UR1197 NeuroBiologie de l'Olfaction, 78350
Jouy-en-Josas, France
e-mail: marie-annick.persuy@jouy.inra.fr

G. Sanz
e-mail: guenhael.sanz@jouy.inra.fr

A. Dewaele
e-mail: aurelie.dewaele@jouy.inra.fr

C. Baly
e-mail: christine.baly@jouy.inra.fr

E. Pajot-Augy
e-mail: edith.pajot@jouy.inra.fr

T. H. Park (ed.), *Bioelectronic Nose,* DOI 10.1007/978-94-017-8613-3_8,

and the fact that ORs coding sequence extends on a single exon, gives the possibility to clone easily any of the OR cDNA sequences from genomic DNA and to insert them in expression vectors to produce these ORs in various heterologous expression systems, such as bacteria, mammalian or insect cells, *Xenopus laevis* oocytes or yeast cells (see other chapters).

However, a major hindrance to functional expression of ORs in heterologous systems has been the tendency of ORs to remain sequestered in the endoplasmic reticulum of the cells, probably due to inefficient folding. This process results in the formation of aggregates and in the degradation of ORs within the trafficking pathways, thus resulting in low levels of expression at the plasma membrane [2, 3]. The failure of ORs to translocate efficiently to the plasma membrane was also associated with the absence of adequate accessory proteins and chaperones in non-native cells, or with the absence of glycosylation at the N-terminus of the OR [4]. However, ORs do not even traffic well to the plasma membrane when overexpressed in a cell line derived from olfactory epithelium (ODORA cells) that exhibits some olfactory sensory neuron characteristics [5–7]. Yet, lentivirus-driven expression of heterologous ORs in cultured olfactory sensory neurons was successful [8].

Yeast constitutes an attractive system to study mammalian GPCRs, since it carries very few endogenous GPCRs (Ste2/Ste3: pheromone receptors, Gpr1: glucose receptor), contrary to mammalian cells. As an eukaryotic system, it allows the glycosylation of expressed proteins. Moreover, yeast cells could provide a means for detailed investigation of receptor pharmacology through the use of sensitive reporter systems taking advantage of the functional homologies between yeast pheromone and mammalian GPCR signalling pathways. *Saccharomyces cerevisiae* was first used to functionally express many different GPCRs [9–15] before being optimized as a host system for expressing ORs and for efficient coupling to a signalling pathway able to produce a measurable response to odorant stimulation [16–19].

8.2 ORs cDNA Sequences Cloning Strategies

Since an OR can recognize a few or multiple odorant molecules with different affinities and each odorant can be detected by a specific combination of ORs and because of the important number of expressed ORs, most of them are still orphan receptors. Firstly, guided strategies using ORs with identified odorant ligands were used, so as to test yeast strains, plasmid constructs, to monitor OR expression and response upon stimulation by the odorant, and to check odorant specificities [16–18].

Secondly, non-targeted strategies were used to identify ORs specific of odorants of interest, so as to identify new odorant-receptor couples. For this purpose, Radhika et al. cloned a library of cDNA inserts encoding the ligand-binding domains of rat ORs, derived from rat olfactory epithelium, into a yeast expression vector [18]. After several screenings of the transformed yeasts with an odorant of interest, isolation of the plasmids from the responding yeast cells and sequencing of the cDNA inserts, they succeeded in identifying a new rat OR specific to this odorant.

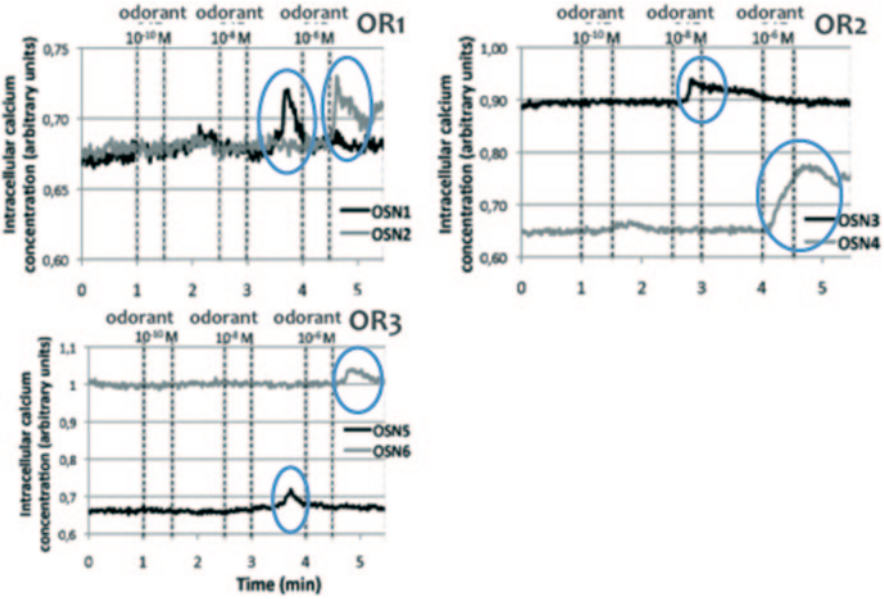

Fig. 8.1 Calcium imaging on dissociated cells stimulated by a flow of diluted target odorant in normal saline buffer at the indicated concentration during the periods in-between the *dashed* vertical lines. *OSNs* 1–6 respond to various odorant concentrations by transitory intracellular calcium pulses. *OSNs* 1 and 2, *OSNs* 3 and 4, *OSNs* 5 and 6 were shown to host *OR1*, *OR2*, and *OR3*, respectively

Our lab followed yet another strategy, requiring several preliminary steps to increase the chances of success [20]. Since the expression of most ORs is spatially restricted in the olfactory mucosa, we first explored which of the 4 main turbinates best responds to the target odorant by performing ElectroOlfactoGram (EOG) recordings on rat olfactory mucosa [21]. Different doses of the target odorant were applied in a vapor phase to potentially stimulate and locate different responding neurons. The olfactory tissue from the best responding turbinates was dissected and prepared to plate freshly dissociated cells as described [22]. We then combined calcium imaging analysis of cells stimulated using the target odorant and single-cell reverse transcription of collected cells, as previously described [23, 24]. Figure 8.1 shows the calcium response profile of representative responding cells stimulated with increasing odorant concentrations. The whole cell content of individual responsive neurons was collected and used for mRNA retrotranscription. Controls corresponding to nonresponsive cells or culture medium were also prepared in parallel. The sequence of the OR expressed in each neuron was amplified by nested-PCR using 2 pairs of rat degenerate primers designed to match the highest proportion of olfactory receptors sequences. This design is not trivial because of the large number of OR genes in a given species and of their highly variable sequences, which prevents a total covering of the OR sequences, even using degenerate primers positioned over highly conserved sequences. Indeed, identities range

from 38 to 90%, with a hypervariability of amino acids lining the odorant binding pocket (TMIII to VII and extracellular loop 2) [25–30], related to the diversity of the odorants that ORs can bind. Final PCR products were sequenced so as to identify the ORs expressed in the responsive neurons. Although this multi-step approach is risky, this protocol allowed us to identify several ORs for a given target odorant. Finding several receptors responding to one odorant is not surprising because the number of ORs specific for a given odorant is still unknown [31] and can vary greatly depending on the odorant. However, since single cell approach often gives false positive results, it is necessary to check the functional response of the identified ORs by expressing them in heterologous expression systems, such as *S. cerevisiae.*

8.3 Yeast Plasmid Constructs and Yeast Strains

The yeast *S. cerevisiae* growth characteristics and genetics have been well known for years, making it a suitable host for OR expression.

8.3.1 Plasmids Constructs

The pJH2 plasmid used for the first time for a successful expression of a GPCR in yeast [9] also allowed expression of 2 different ORs in *S. cerevisiae*, under the control of the galactose-inducible GAL1 promoter combined to the GAL4 synthesis under the control of the GAL10 inducible promoter [16, 17]. Indeed, overexpression of the GAL4 protein has been shown to increase the expression of the OR cDNA under the control of the GAL1 promoter [32]. Insertion of the OR cDNA in pJH2 was obtained by homologous recombination. However, this plasmid was not useable to create cassette plasmids.

Following these pioneers' works, new expression vectors (pESC vectors) were developed by Stratagene to express heterologous proteins in yeast cells. From these vectors, three different types of shuttle plasmids were developed.

Because the N-terminal region of GPCRs often plays an important role in expression or membrane trafficking of the protein and the C-terminal region interacts with the G protein, Radhika et al. constructed an expression cassette vector which contains an insert encoding the N-terminal part (amino acids 1 to 61) and the C-terminal part (amino acids 295 to 327) of the rat ORI7, separated by multiple cloning sites in which the ligand-binding pocket of any OR can be inserted in frame [18].

Fukutani et al. also used two different N terminal parts of the I7 cDNA sequences to construct chimeric ORs, and cloned them into a pESC vector [19]. These chimeric ORs (32 or 58 amino acids from the ORI7) were translated with the c-myc tag of the vector at their N-terminus.

Alternately, pESC vectors were modified as described in Wade et al. to allow the expression of ORs tagged at their N terminus with either the c-myc or the human

influenza hemagglutinin (HA) tag [33]. Basically, pESC vectors are designed for expression of genes under the control of *GAL1* or *GAL10* promoters. The plasmids were modified by cloning the coding sequence of OR under the control of the GAL1 promoter, and the GAL 4 sequence under the control of the Gal10 promoter to achieve the over-induction of OR synthesis as with pJH2-OR vectors (see above).

8.3.2 Yeast Strains

Two different strategies, both based on growth of transformed yeasts on selective media, were adopted by different labs to establish prototypic *S. cerevisiae* yeast strains.

The first strategy was to develop strains in which several modifications of the mating signal transduction pathway allow agonist-induced growth on selective medium (a-b) or expression of a reporter gene (c). (a): in the LY790 strain (*MATa/MATα ura3-52 lys2-801 ade2-101 trp1Δ63 his3Δ200 leu2-Δ1 ste2::LEU2 sst2ΔADE2 gpa1Δfar1Δ*), genes encoding Ste2 (endogenous GPCR) and Gpa1 (endogenous Gα subunit) were respectively replaced by the ORI7 cDNA and the chimeric Gpa1-Gαi2 or Gpa1-Golf cDNA. Activation of the OR by odorant stimulation induces the G protein dissociation and triggers the mating signal transduction pathway. One of the genes activated by this pathway is the FUS1 gene. Its replacement by the HIS reporter gene provides the His3 enzyme necessary for histidine biosynthesis, thus enabling growth in a selective medium without histidine. The SST2 gene, which encodes the negative regulator of Gpa1 subunit, is also deleted to increase OR response to its odorant agonist [16]. (b): in the MC20 strain (*MATa gpa1::lacZ[LEU2] ade2-1 his3-11,15 leu2-3,112 trp1-1,ura3-1, can1-100,sst2Δ*), the SST2 gene is also deleted and the GPA1 gene is inactivated by disruption. Odorant stimulation of the OR activates the mating signal transduction pathway, then inducing the expression of the hygromycin phosphotransferase (Hph) gene under the FUS1 promoter, thus allowing growth in presence of hygromycin. In this strain, the STE2 gene is still present and the stimulation of the mating signal transduction pathway by the α-factor provides a positive control of growth [16]. (c): The *S. cerevisiae* BY4741 strain (*MATa his3*Δ1 *leu*Δ0 met15Δ0 ura3Δ0) [34] was also modified by disruption of the STE2 and SST2 genes [35]. An OR was functionally expressed on the yeast membrane instead of the endogenous Ste2 receptor. Replacement of the FUS1 gene by the luciferase gene enabled Fukutani et al. to detect a luminescent signal after OR activation [19]. In a derived strain, the endogenous Gα protein Gpa1 was also replaced by the OR-specific Gα, Gαolf.

The second strategy was to create a *S. cerevisiae* strain in which the sequences of the whole mammalian olfactory transduction pathway are introduced to couple OR functional response with this heterologous transduction pathway [18]. In olfactory neurons, signalling by OR specifically involves the Gαolf subunit, and the subunits Gβ2 and Gγ5 are preferentially expressed [36, 37]. In the present strategy, the YPH501 (*MATa/MATα ura3-52 lys2-801 ade2-101 trp1Δ63 his3Δ200 leu2-Δ1*)

yeast cells were transformed using rat cDNAs encoding Gαolf, ACIII, Gβ2 and Gγ5. To engineer a cAMP-responsive reporter gene-activation system in these yeast transformants, the cDNAs encoding the human cAMP response element binding protein (CREB) and the CRE-driven green fluorescent protein (GFP) were then introduced to generate the WIF-1α strain. This WIF-1α strain, transformed by a library of pESC-OR, was suitable for screening odorants of interest [18].

8.4 Strategies Used for OR Expression Optimization

Monitoring OR expression requires classical biochemical approaches such as Western Blotting using whole cell lysates [18, 19] or total membrane fractions [17], or immunocytochemistry to check the localization of the OR on the plasma membrane of the recombinant yeasts. Due to the lack of specific antibodies directed against each OR, the primary antibodies used for these techniques often recognize a tag localized at the NH2-terminus of the OR, mostly c-myc or HA. These specific antibodies can be used for the relative quantification of the expression level of the ORs.

Improving the OR expression level in yeast cells relies on optimization of galactose induction conditions (in temperature and duration). It may also depend on the expression plasmid, and on the recombinant OR construct.

8.4.1 Improvement of Galactose Induction Conditions

Yeast colonies are grown in medium containing glucose, usually at 30 °C, until exponential growth is reached (1–2 OD). All the yeast expression plasmids used allow the induction of OR expression in medium supplemented with galactose (see plasmid constructs). The induction is started after cells washing and dilution to an OD 600 of 0.5 in medium supplemented with galactose. For their experiments, some authors used classical conditions of induction at 30 °C and during a relatively short time (14 or 18 h respectively) [18, 19]. Several improvements of culture conditions were then considered, in order to optimize ORs expression yields.

8.4.1.1 Optimization of Induction Temperature

Hansen et al. had previously reported the crucial influence of induction time and temperature for heterologous expression of a rat GPCR (VPAC1) under the control of a galactose-inducible promoter in *S. cerevisiae* [38]. The highest specific ligand binding to the expressed receptor had been obtained after a galactose induction performed at 15 °C, reaching a plateau after 60 h induction, whereas an induction temperature of 30 °C resulted in the lowest amount of surface binding. In Pajot-Augy et

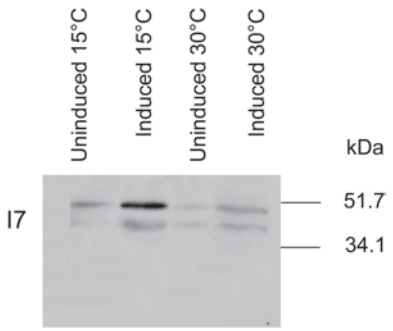

Fig. 8.2 Effect of galactose induction and temperature on the functional expression of the ORI7 in yeast. Strains were grown in minimal media with 2% glucose (uninduced) or in minimal media with 2% galactose (induced) at 15 or 30 °C. A Western blot analysis of the ORI7 expression levels was performed on yeast membrane fraction (20 µg of protein per lane). The band near 52 kDa is attributed to the receptor dimer. (Adapted from Fig. 4 in [17], with permission)

al., induction was thus performed at 15–19 °C for 60 h, before testing the functional response or ORs by growth in selective (histidine-deprived) medium, or at 20 °C for 48 h prior to testing the functional response or ORs by hygromycin-resistance growth (see below; [16]). Galactose induction at temperatures higher than 20 °C prevented the detection of a functional expression of the OR in terms of differential growth of the yeast strain in response to odorant stimulation. Temperature thus seems to play a major role in optimizing OR expression under galactose induction in these yeast strains.

Minic et al. monitored the effects of temperature on OR expression upon galactose induction by western blotting (Fig. 8.2) [17]. They observed that the ORI7 expression level was increased in membrane fractions from yeasts induced by galactose, at 15 °C rather than 30 °C. This effect can be ascribed in part to the low temperature positively affecting the yield of properly folded proteins along the trafficking pathways, and the insertion of the transmembrane domains in the plasma membrane [39]. An exceptionally high recombinant production of a membrane protein, human aquaporin-1 (8.5% of total membrane protein content), was obtained in *S. cerevisiae* at 15 °C, a temperature which was mentioned as crucial for the correct protein folding [40]. It was also reported that a temperature downshift to 10–18 °C leads to an induction of specific cold shock proteins, some of them able to serve as molecular chaperones [41]. Interestingly, among these yeast cold shock proteins, YOP1 is the homologous of mouse REEP1, one of the transmembrane proteins (RTP1, RTP2 and REEP1) known to increase the functional expression of several ORs in mammalian cells (HEK293) [42]. Chaperone proteins, as members of the Hsp70 family, are also endogenously expressed in mouse mature olfactory neurons and play an important role in ORs expression [43]. Moreover, at 15 °C the yeast membrane composition changes to increase sterols concentration [44], allowing a better cryo-protection for cells. It was also reported that sterols play a decisive role

in GPCRs function in yeast, as demonstrated for the μ-opioid receptor [45], and that they can favor their insertion in the membrane [46]. Thus, several mechanisms induced by mild low temperature may simultaneously act to increase considerably ORs functional surface expression. A higher level of expression of GPCRs and ORs in the plasma membrane of insect cells in comparison with mammalian cells could also be partially explained by their relatively lower temperature of growth (27 versus 37 °C) [47–49].

8.4.1.2 Optimization of Induction Duration

The heterologous OR expression in yeast can be further characterized, especially in terms of kinetics of expression and ORs subcellular localization. Since it is expected that ORs are fully functional at the plasma membrane level, conditions for an improvement of ORs trafficking to the plasma membrane were investigated, especially by increasing expression induction time at 15 °C. For long induction times, refeeding yeast cells has already been described to improve protein synthesis, folding and trafficking [50]. Therefore, fresh induction medium was added and OD600 adjusted at 1 after 60 h of induction.

OR expression was monitored during up to 120 h of induction by preparing crude membranes. Internal and plasma membranes were separated using subcellular fractionation on sucrose density gradients, and analyzed by immunoblotting, using antibodies targeting the yeast plasma membrane marker Pma1 (anti-Pma1, Abcam) and the yeast endoplasmic reticulum membrane marker Dpm1p (anti-Dpm1p, Molecular Probes).

As shown in Fig. 8.3, the human OR17-40 receptor was mainly present in inner membranes, whatever the induction time until 72 h. After 72 h of induction, a detectable level of hOR1740 was observed at the plasma membrane, with a maximal expression at this level starting from 96 h of induction. Thus, even if global levels of production of heterologous receptors are high starting from 72 h of induction, the efficient trafficking of ORs to the plasma membrane requires induction times longer than 72 h, and may be further improved up to 108 h of induction. These results were confirmed with other ORs from various species (data not shown), showing that increasing the induction time improves OR trafficking to the yeast plasma membrane.

8.4.2 Expression Plasmids and Recombinant OR Constructs

The types of multicopy plasmids allowing the functional overexpression of OR in *S. cerevisiae* is limited: plasmids pJH2-I7 based on pJH2, described by Price et al 1995 [9], with a divergent GAL1/10 promoter and GAL4 gene, and pESC vectors from Stratagene, used by several teams [18, 19, 33]. The level of hOR17-40 or ORI7 expression from pJH2 constructs seems to be lower than from pESC constructs.

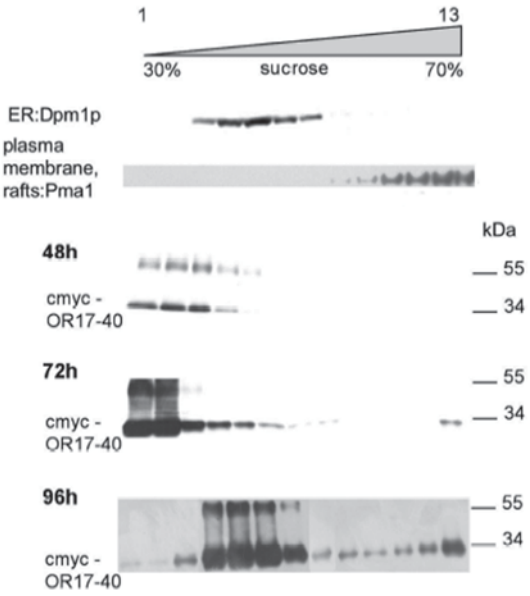

Fig. 8.3 Analysis of sucrose density gradient membrane subfractions by immunoblotting. A sucrose density gradient was realized using crude membranes of *S. cerevisiae* heterologously expressing the hOR17-40 receptor (after 48 h-72 h-96 h of induction in galactose medium at 15 °C). Antibodies used: anti-Dpm1p (yeast endoplasmic reticulum (ER) marker), anti-Pma1 (yeast plasma membrane and raft marker), anti-cmyc (cmyc epitope tagging the hOR17-40 receptor)

For developing a yeast-based odor sensing system, Fukutani et al. investigated how the design of the N-terminus of a chimeric receptor can affect the expression level of the resulting OR [19]. Their results suggested that the replacement of the N-terminus of one receptor by the corresponding region of another one could modify the expression level of the OR. However, no systematic study has been carried out to monitor the precise impact of the N-terminus region or the addition of various tags on the expression level of ORs in yeast. But it seems that the coding sequence of the OR itself could influence its expression level.

8.5 Functional Tests

8.5.1 Growth in Selective Medium

Two different strategies were reported which offer a positive screening to monitor the functional response of ORI7 to different odorants [16]. The OR and Gα protein were introduced into the yeast cells such that they hijack the pheromone response pathway usually resulting in cell cycle arrest. The first strategy utilizes ligand-induced expression of a FUS1-HIS3 reporter gene, providing the His3 enzyme necessary for histidine biosynthesis, permitting growth on a selective medium lacking this amino-acid. The second strategy is to induce ligand-dependent expression of a FUS1-Hph reporter gene, conferring resistance to hygromycin. Validation of the systems was performed using rat ORI7 response to a range of aldehyde odor-

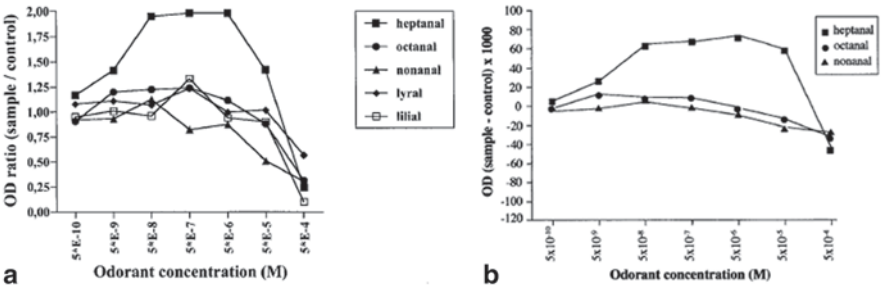

Fig. 8.4 Functional bioassays of yeast strain growth on selective medium, after OR expression by induction at mild cold temperature: (**a**) Differential yeast strain (I7/GPA1-Gαi2) growth plotted as the ratio of optical density of yeast strain incubated for 3 days at 30 °C with odorants relative to that of yeast control, as a function of odorant concentration. For each sample, the control was prepared by replacing the initial amount of odorant by water. Optical density measurements were averaged on duplicate samples. (**b**) Ratio between optical densities of the yeast suspensions tested in liquid culture containing 200 μg/mL hygromycin, in the presence and absence of odorant containing the same quantities of solvent, from samples prepared in triplicate. Experimental error on the ratios is 0.2. (Adapted from Figs. 4 and 6 in [16], with permission)

ants previously characterized as functional ligands. Of these, only heptanal produced a positive growth response in the concentration range 5×10^{-8} to 5×10^{-6} M. Figure 8.4 shows the results of both growth assays plotted in presence or absence of odorant. These experiments were the first demonstration that *S. cerevisiae* could be engineered to screen the functional expression of ORs. Heptanal was perceived as the preferential odorant for ORI7 in yeast with a threshold concentration around 10^{-8} M. However, the yeast growth in selective or hygromycin-medium required 2–3 days at 30–33 °C, which is not most appropriate when using odorants, and were not very sensitive, even though reproducible. Therefore, other functional tests needed to be developed.

8.5.2 Radioligand Binding and Scatchard Plots

To assess the ligand binding ability of expressed ORs or chimeric receptors, and quantify the number of receptors expressed in yeast cells, binding studies can be carried out on yeast spheroplasts using a radio-ligand. Spheroplasts are prepared by treating cells with lyticase and centrifugation on a sucrose-Ficoll gradient. Spheroplasts are incubated with varying concentrations of odorant radio-ligand, at 25–30 °C for 15 min. Nonspecific binding is determined with 100-fold molar excess of unlabeled ligand. Similar binding analysis is carried out with the parental cells not expressing ORI7. The bound radiolabel is quantified by scintillation counting. Specific binding is calculated by subtracting the specific binding of control cells from that obtained with ORI7-expressing cells. The slope and intercept of a Scatchard plot are obtained by regression analysis, and the x intercept is used to calculate the number of receptors expressed per yeast cell. For instance, a representative Scatchard plot analysis of 14C-octanal binding onto the expressed chimeric ORI7

indicates the presence of 90 receptors per cell with a Ka value of 0.1×10^4 M^{-1} [18]. This is in agreement with the 10–100 μM threshold levels seen for this ligand and the view that ORs are generally low-affinity receptors [51, 52].

8.5.3 Fluorescence

Radhika et al. monitored the GFP response of WIF-1α-ORI7 cells to characterize the functionality of this prototypic yeast strain [18]. This strain was engineered with the mammalian olfactory signalling pathway so that the functional response of OR to the specific odorant stimulation induces fluorescence emission after synthesis of the reporter protein GFP. Indeed, the cells were exposed to a range of octanal concentrations, known to be one of the preferential ligands of the ORI7 receptor, and GFP expression was measured in a microplate reader at intervals of 1 h, revealing a ligand dose-dependent increase in GFP expression. The maximal levels of fluorescence of the cells were reached by 3 h. Moreover, the GFP response of the cells is well correlated with the known different affinity of ORI7 for closely related aliphatic aldehydes (heptanal or hexanal), indicating that GFP is a useful reporter to study the OR response in WIF-1α-OR strains. This strategy was then used by these authors to identify an OR capable of detecting 2,4-dinitrotoluene (DNT). The WIF-1α-OR transformants, obtained by the cloning of a library of OR cDNAs and transformation of the yeast cells, were exposed to 50 μM DNT and scored for emitted fluorescence. Several DNT-positive clones were identified, which were enriched by serial dilution, and their response to DNT 25 μM monitored by fluorescence microscopy. The recovery of the plasmids from positive cells allowed to sequence the insert in the expression vector. This strategy involving the GFP reporter allowed the authors to identify a new rat olfactory receptor, exhibiting an extensive sequence homology with two different mouse olfactory receptors (Olfr2 and mOR226-1) that can detect DNT. This system thus appears as reliable, easy to handle, and useful to identify OR ligands.

8.5.4 Luminescence

To address the functional integrity of the olfactory receptors expressed in yeast cells, two labs have developed a luciferase reporter bioassay by modifying the yeast pheromonal signal transduction pathway (see yeast strain constructs). The firefly luciferase gene is used as luminescence reporter gene due to its high sensitivity.

Fukutani et al. tested the sensing abilities of 3 chimeric ORs for DNT [19]. They investigated the role of the N-terminal region of ORs on their functional expression (see plasmid constructs). After induction of the ORs expression in galactose medium, the cells were incubated in media containing the ligand. At 1 mM DNT, the 2 chimeric ORs obtained by replacing the N-terminal region of OR226 by the N-terminal region of ORI7 exhibited a measurable functional response. The chimeric OR for which the replacement was up to the first intracellular loop of ORI7

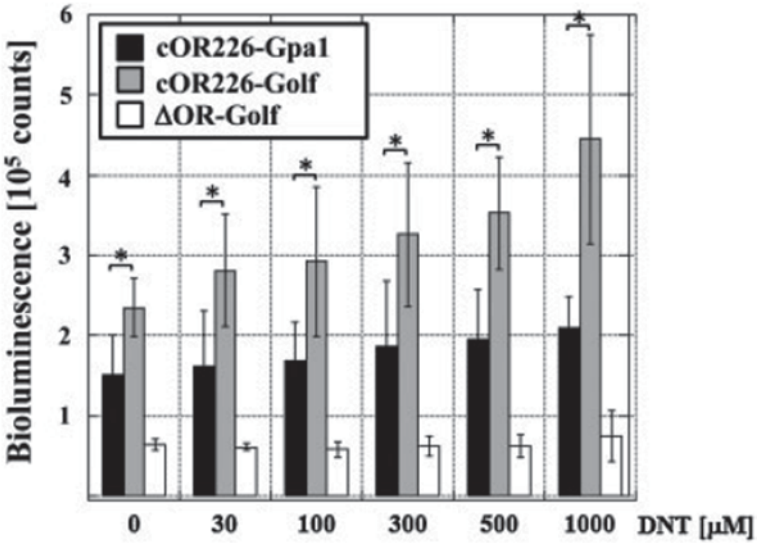

Fig. 8.5 DNT sensing using the luc reporter gene assay in yeast cells co-expressing the $cI7_{N58}$OR226 chimeric receptor with Golf. FL150-$cI7_{N58}$OR226-Golf (cOR226-Golf), FL50-$cI7_{N58}$OR226 (cOR226-Gpa1), and FL150-ΔOR-Golf (ΔOR-Golf) yeast transformants were tested for their ability to sense the odorant DNT. Bioluminescence was measured in the yeast strains stimulated by addition of DNT in the culture medium. The data shown represent the mean ± SEM of three separate experiments. Statistical significance was assessed by the t-test (*$P<0.05$). (Adapted from Fig. 1 in [18], with permission)

exhibited the highest enhancement of bioluminescence relative to the other constructs, suggesting that this N-terminal part of ORI7 was more suitable for the functional expression of the chimeric OR. Furthermore, the substitution of Gpa1 with Gαolf enabled a better coupling between the chimeric OR and the G-protein, increasing the sensitivity of the reporter gene in a dose-dependent assay (Fig. 8.5).

The luciferase bioluminescence assay was also used to optimize the yeast induction temperature for ORs expression, and to compare the coupling efficiency of OR to the cognate Gαolf protein relative to the promiscuous Gα15 commonly used for pharmacological studies of recombinant ORs [17]. A higher sensitivity was observed with Gαolf. The specificity of ORs response relative to various ligands was also analyzed, and dose-response curves show OR activation even by very low concentrations of ligands (Fig. 8.6) [17, 53].

8.6 Conclusion

Among the various heterologous cell systems that can be used to functionally express ORs, *S. cerevisiae* seems an ideal candidate for screening large-scale libraries, allowing the development of several sensitive, rapid and reproducible tests. The

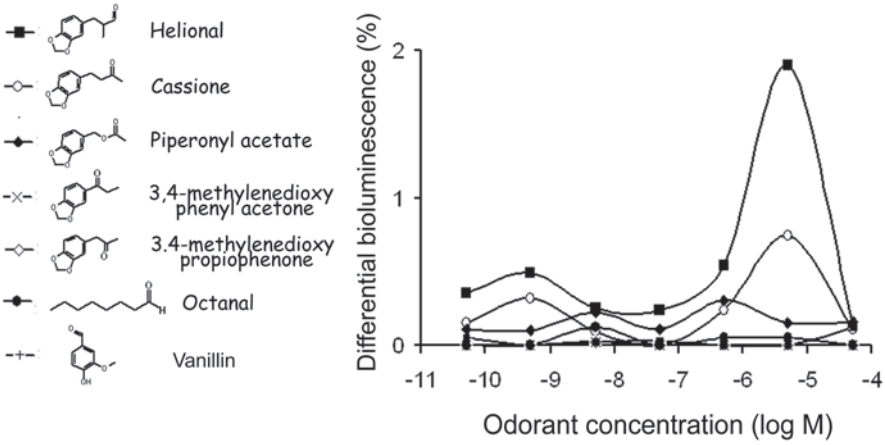

Fig. 8.6 Differential bioluminescence dose-response upon odorant stimulation of yeast-expressed olfactory receptors. Measurements were performed on yeast transformed to co-express hOR17-40, Golf and the luciferase reporter. This strain was induced with 2% galactose at 15 °C. Dose-response curves are plotted as a difference of bioluminescence response to odorants relative to controls obtained by replacing odorants with water. (Adapted from Fig. 3 in [53] with permission from the Royal Society of Chemistry)

expression level reached for ORs is noteworthy, since it could easily be monitored by direct Western Blotting from cell lysates without prior purification or immunoprecipitation, even if this level may vary from receptor to receptor and depends on the construct. Moreover, it is a relatively cheap and easy to use system. However, some aspects still require extensive studies. The first question is related to the specificity of ORs expressed in heterologous systems. Indeed, Touhara et al. pointed out the potential influence of a different cellular environment in an heterologous system relative to the native one to modulate OR specificity [54]. The preferential ligand of an OR might thus depend on the heterologous system used, an hypothesis that has not been systematically tested. The second question is about the OR sensitivity to odorants in heterologous systems, and the odorant concentration used to monitor the functional response of the ORs expressed. These two points are quite interconnected. For instance, ORI7 preferential ligand is reported to be octanal by Zhao et al. [55] after adenovirus-mediated expression in olfactory epithelium, but heptanal in both COS cells and *S. cerevisiae* [16, 17]. However, Zhao's experiments on adenovirus-infected olfactory epithelium were conducted with varying carbon chain length aldehydes using a single odorant concentration of 10^{-3} M [55]. At this concentration, they reported that octanal exhibited the largest response. On the contrary, Levasseur et al. used concentrations down to 10^{-13} M, and demonstrated that COS-I7 cells exhibit response to heptanal in a low concentration range (10^{-14} to 10^{-12} M), to nonanal in an intermediate concentration range (10^{-13} to 10^{-10} M), and to octanal for higher odorant concentrations over a broader range (10^{-12} to 10^{-7} M), thus defining heptanal as the preferential odorant ligand for rat ORI7, inducing a response at the lowest concentration [5]. Concentrations down to 10^{-11} or 10^{-17} M

have indeed been reported as physiological detection limits for some odorants in humans or in dogs [56, 57]. In the yeast system, heptanal was also found to induce the highest response among linear aldehydes [16, 17], but within a higher odorant concentration range (around 5×10^{-8} to 5×10^{-6} M).

Another example is provided by OR17-40 expression in ODORA cells [5], where the maximum functional response was obtained with 10^{-11} M of helional, while it was reported at 10^{-5} M [56] or 5×10^{-5} M [58] in HEK293 cells, at 10^{-7} M in *Xenopus laevis* oocytes [56], and at 5×10^{-6} M in yeast [17, 53] relative to series of other odorants.

Thus, it seems, from the limited number of ORs extensively studied, that the ranking of odorants specifically stimulating an OR remains identical whatever the heterologous system, be it defined as inducing a response at the lowest odorant concentration, or otherwise inducing the highest response at a given concentration.

References

1. Fredriksson R, Lagerstrom MC, Lundin LG, Schioth HB (2003) The G-protein-coupled receptors in the human genome form five main families. Phylogenetic analysis, paralogon groups, and fingerprints. Mol Pharmacol 63:1256–1272
2. Lu M, Echeverri F, Moyer BD (2003) Endoplasmic reticulum retention, degradation, and aggregation of olfactory G-protein coupled receptors. Traffic 4:416–433
3. McClintock TS, Sammeta N (2003) Trafficking prerogatives of olfactory receptors. Neuroreport 14:1547–1552
4. Katada S, Tanaka M, Touhara K (2004) Structural determinants for membrane trafficking and G protein selectivity of a mouse olfactory receptor. J Neurochem 90:1453–1463
5. Levasseur G, Persuy MA, Grebert D, Remy JJ, Salesse R et al (2003) Ligand-specific dose-response of heterologously expressed olfactory receptors. Eur J Biochem 270:2905–2912
6. Murrell JR, Hunter DD (1999) An olfactory sensory neuron line, odora, properly targets olfactory proteins and responds to odorants. J Neurosci 19:8260–8270
7. Gimelbrant AA, Haley SL, McClintock TS (2001) Olfactory receptor trafficking involves conserved regulatory steps. J Biol Chem 276:7285–7290
8. Chen H, Dadsetan S, Fomina AF, Gong Q (2008) Expressing exogenous functional odorant receptors in cultured olfactory sensory neurons. Neural Dev 3:22
9. Price LA, Kajkowski EM, Hadcock JR, Ozenberger BA, Pausch MH (1995) Functional coupling of a mammalian somatostatin receptor to the yeast pheromone response pathway. Mol Cell Biol 15:6188–6195
10. King K, Dohlman HG, Thorner J, Caron MG, Lefkowitz RJ (1990) Control of yeast mating signal transduction by a mammalian beta 2-adrenergic receptor and Gs alpha subunit. Science 250:121–123
11. Miret JJ, Rakhilina L, Silverman L, Oehlen B (2002) Functional expression of heteromeric calcitonin gene-related peptide and adrenomedullin receptors in yeast. J Biol Chem 277:6881–6887
12. Sander P, Grunewald S, Bach M, Haase W, Reilander H et al (1994) Heterologous expression of the human D2S dopamine receptor in protease-deficient Saccharomyces cerevisiae strains. Eur J Biochem 226:697–705
13. David NE, Gee M, Andersen B, Naider F, Thorner J et al (1997) Expression and purification of the Saccharomyces cerevisiae alpha-factor receptor (Ste2p), a 7-transmembrane-segment G protein-coupled receptor. J Biol Chem 272:15553–15561

14. Erickson JR, Wu JJ, Goddard JG, Tigyi G, Kawanishi K et al (1998) Edg-2/Vzg-1 couples to the yeast pheromone response pathway selectively in response to lysophosphatidic acid. J Biol Chem 273:1506–1510
15. Erlenbach I, Kostenis E, Schmidt C, Hamdan FF, Pausch MH et al (2001) Functional expression of M(1), M(3) and M(5) muscarinic acetylcholine receptors in yeast. J Neurochem 77:1327–1337
16. Pajot-Augy E, Crowe M, Levasseur G, Salesse R, Connerton I (2003) Engineered yeasts as reporter systems for odorant detection. J Recept Signal Transduct Res 23:155–171
17. Minic J, Persuy MA, Godel E, Aioun J, Connerton I et al (2005) Functional expression of olfactory receptors in yeast and development of a bioassay for odorant screening. FEBS J 272:524–537
18. Radhika V, Proikas-Cezanne T, Jayaraman M, Onesime D, Ha JH et al (2007) Chemical sensing of DNT by engineered olfactory yeast strain. Nat Chem Biol 3:325–330
19. Fukutani Y, Nakamura T, Yorozu M, Ishii J, Kondo A et al (2012) The N-terminal replacement of an olfactory receptor for the development of a yeast-based biomimetic odor sensor. Biotechnol Bioeng 109:205–212
20. Pajot-Augy E, Badonnel K, Dewaele A, Daligault J, Persuy M-A, Meunier N, Congar P, Baly C, Salesse R, Launay G, Téletchéa S, Wade SF, Gibrat J-F, Sanz G, Zine N, Errachid A, Jaffrezic-Renault N (2012) Bioelectronic odor detection. In: Abstracts of the XVI international symposium on olfaction and taste, XXII meeting of ECRO, Stockholm, Sweden, 23–27 June 2012
21. Lacroix MC, Badonnel K, Meunier N, Tan F, Schlegel-Le Poupon C et al (2008) Expression of insulin system in the olfactory epithelium: first approaches to its role and regulation. J Neuroendocrinol 20:1176–1190
22. Brunert D, Kurtenbach S, Isik S, Benecke H, Gisselmann G et al (2009) Odorant-dependent generation of nitric oxide in Mammalian olfactory sensory neurons. PLoS One 4:e5499
23. Malnic B, Hirono J, Sato T, Buck LB (1999) Combinatorial receptor codes for odors. Cell 96:713–723
24. Touhara K, Sengoku S, Inaki K, Tsuboi A, Hirono J et al (1999) Functional identification and reconstitution of an odorant receptor in single olfactory neurons. Proc Natl Acad Sci U S A 96:4040–4045
25. Abaffy T, Malhotra A, Luetje CW (2007) The molecular basis for ligand specificity in a mouse olfactory receptor: a network of functionally important residues. J Biol Chem 282:1216–1224
26. Hall SE, Floriano WB, Vaidehi N, Goddard WA 3rd (2004) Predicted 3-D structures for mouse I7 and rat I7 olfactory receptors and comparison of predicted odor recognition profiles with experiment. Chem Senses 29:595–616
27. Katada S, Hirokawa T, Oka Y, Suwa M, Touhara K (2005) Structural basis for a broad but selective ligand spectrum of a mouse olfactory receptor: mapping the odorant-binding site. J Neurosci 25:1806–1815
28. Man O, Gilad Y, Lancet D (2004) Prediction of the odorant binding site of olfactory receptor proteins by human-mouse comparisons. Protein Sci 13:240–254
29. Schmiedeberg K, Shirokova E, Weber HP, Schilling B, Meyerhof W et al (2007) Structural determinants of odorant recognition by the human olfactory receptors OR1A1 and OR1A2. J Struct Biol 159:400–412
30. Stary A, Suwattanasophon C, Wolschann P, Buchbauer G (2007) Differences in (-)citronellal binding to various odorant receptors. Biochem Biophys Res Commun 361:941–945
31. Saito H, Chi Q, Zhuang H, Matsunami H, Mainland JD (2009) Odor coding by a Mammalian receptor repertoire. Sci Signal 2:ra9
32. Schultz LD, Hofmann KJ, Mylin LM, Montgomery DL, Ellis RW et al (1987) Regulated overproduction of the GAL4 gene product greatly increases expression from galactose-inducible promoters on multi-copy expression vectors in yeast. Gene 61:123–133

33. Wade F, Espagne A, Persuy MA, Vidic J, Monnerie R et al (2011) Relationship between homo-oligomerization of a mammalian olfactory receptor and its activation state demonstrated by bioluminescence resonance energy transfer. J Biol Chem 286:15252–15259
34. Brachmann CB, Davies A, Cost GJ, Caputo E, Li J et al (1998) Designer deletion strains derived from Saccharomyces cerevisiae S288C: a useful set of strains and plasmids for PCR-mediated gene disruption and other applications. Yeast 14:115–132
35. Iguchi Y, Ishii J, Nakayama H, Ishikura A, Izawa K et al (2010) Control of signalling properties of human somatostatin receptor subtype-5 by additional signal sequences on its amino-terminus in yeast. J Biochem 147:875–884
36. Liang JJ, Cockett M, Khawaja XZ (1998) Immunohistochemical localization of G protein beta1, beta2, beta3, beta4, beta5, and gamma3 subunits in the adult rat brain. J Neurochem 71:345–355
37. Asano T, Shinohara H, Morishita R, Ueda H, Kawamura N et al (2001) Selective localization of G protein gamma5 subunit in the subventricular zone of the lateral ventricle and rostral migratory stream of the adult rat brain. J Neurochem 79:1129–1135
38. Hansen MK, Tams JW, Fahrenkrug J, Pedersen PA (1999) Functional expression of rat VPAC1 receptor in Saccharomyces cerevisiae. Receptors Channels 6:271–281
39. Arora D, Khanna N (1996) Method for increasing the yield of properly folded recombinant human gamma interferon from inclusion bodies. J Biotechnol 52:127–133
40. Bomholt J, Helix-Nielsen C, Scharff-Poulsen P, Pedersen PA (2013) Recombinant production of human Aquaporin-1 to an exceptional high membrane density in Saccharomyces cerevisiae. PLoS One 8:e56431
41. Kandror O, Bretschneider N, Kreydin E, Cavalieri D, Goldberg AL (2004) Yeast adapt to near-freezing temperatures by STRE/Msn2,4-dependent induction of trehalose synthesis and certain molecular chaperones. Mol Cell 13:771–781
42. Saito H, Kubota M, Roberts RW, Chi Q, Matsunami H (2004) RTP family members induce functional expression of mammalian odorant receptors. Cell 119:679–691
43. Neuhaus EM, Mashukova A, Zhang W, Barbour J, Hatt H (2006) A specific heat shock protein enhances the expression of mammalian olfactory receptor proteins. Chem Senses 31:445–452
44. Gasch AP, Spellman PT, Kao CM, Carmel-Harel O, Eisen MB et al (2000) Genomic expression programs in the response of yeast cells to environmental changes. Mol Biol Cell 11:4241–4257
45. Lagane B, Gaibelet G, Meilhoc E, Masson JM, Cezanne L et al (2000) Role of sterols in modulating the human mu-opioid receptor function in Saccharomyces cerevisiae. J Biol Chem 275:33197–33200
46. Meijberg W, Booth PJ (2002) The activation energy for insertion of transmembrane alpha-helices is dependent on membrane composition. J Mol Biol 319:839–853
47. Raming K, Krieger J, Strotmann J, Boekhoff I, Kubick S et al (1993) Cloning and expression of odorant receptors. Nature 361:353–356
48. Matarazzo V, Clot-Faybesse O, Marcet B, Guiraudie-Capraz G, Atanasova B et al (2005) Functional characterization of two human olfactory receptors expressed in the baculovirus Sf9 insect cell system. Chem Senses 30:195–207
49. Goldsmith BR, Mitala JJ, Josue J, Castro A, Lerner MB et al (2011) Biomimetic chemical sensors using nanoelectronic readout of olfactory receptor proteins. ACS Nano 5:5408–5416
50. Huang D, Gore PR, Shusta EV (2008) Increasing yeast secretion of heterologous proteins by regulating expression rates and post-secretory loss. Biotechnol Bioeng 101:1264–1275
51. Araneda RC, Peterlin Z, Zhang X, Chesler A, Firestein S (2004) A pharmacological profile of the aldehyde receptor repertoire in rat olfactory epithelium. J Physiol 555:743–756
52. Firestein S (2001) How the olfactory system makes sense of scents. Nature 413:211–218
53. Vidic JM, Grosclaude J, Persuy MA, Aioun J, Salesse R et al (2006) Quantitative assessment of olfactory receptors activity in immobilized nanosomes: a novel concept for bioelectronic nose. Lab Chip 6:1026–1032

54. Touhara K (2007) Deorphanizing vertebrate olfactory receptors: recent advances in odorant-response assays. Neurochem Int 51:132–139
55. Zhao H, Ivic L, Otaki JM, Hashimoto M, Mikoshiba K et al (1998) Functional expression of a mammalian odorant receptor. Science 279:237–242
56. Wetzel CH, Oles M, Wellerdieck C, Kuczkowiak M, Gisselmann G et al (1999) Specificity and sensitivity of a human olfactory receptor functionally expressed in human embryonic kidney 293 cells and Xenopus Laevis oocytes. J Neurosci 19:7426–7433
57. Dulac C (2000) The physiology of taste, vintage 2000. Cell 100:607–610
58. Hatt H, Lang K, Gisselmann G (2001) Functional expression and characterization of odorant receptors using the Semliki Forest virus system. Biol Chem 382:1207–1214

Chapter 9
Production of Olfactory Receptors and Nanovesicles Using Heterologous Cell Systems for Bioelectronic Nose

Hyun Seok Song and Tai Hyun Park

Abstract Olfactory receptors, belonging to a family of G protein-coupled receptors (GPCRs), which are involved in various important physiological processes, are integral membrane proteins composed of seven transmembrane helices. It is difficult to produce GPCRs including olfactory receptors (ORs) using heterologous cell systems, because of their strong hydrophobicity, and complicated structure. The production of ORs should be a critical process for the development of an olfactory receptor-based bioelectronic nose. Significant efforts have been made for the production of ORs for the utilization as recognition elements of bioelectronic noses, and also for other applications. In addition, the construction method of mammalian cell-derived nanovesicles containing ORs has been demonstrated and applied for an bioelectronic nose, due to their unique properties, and suitable size for integration with a nanosensor platform. In this chapter, advances in the production of ORs and nanovesicles using various heterologous cell systems for the development of a bioelectronic nose are described.

9.1 Production of Olfactory Receptors Using Heterologous Cell Systems

Olfactory receptors (ORs) belonging to the GPCR family recognize a number of odorous compounds with high selectivity, and trigger the signal transduction in olfactory neurons [1, 2]. These receptors are composed of 7 transmembrane spanning domains, and have strong hydrophobicity and complicated structures. Chemical determination and odorous coding can be accomplished by different types of receptors, expressed in olfactory neurons [3, 4]. Because of their specificity for odorous

T. H. Park (✉) · H. S. Song
School of Chemical and Biological Engineering, Seoul National University,
Seoul 151-744, Republic of Korea
e-mail: thpark@snu.ac.kr

H. S. Song
Harvard-MIT Division of Health Sciences and Technology,
Massachusetts Institute of Technology, Cambridge, MA 02139, USA

T. H. Park (ed.), *Bioelectronic Nose,* DOI 10.1007/978-94-017-8613-3_9,

compounds and biomimetic properties, ORs have been utilized for the development of a high-performance bioelectronic nose [5–13]. Most GPCRs including ORs are poorly expressed in nature, and thus the heterologous expression of receptors is the critical process for the development of a protein-based bioelectronic nose [14, 15].

There are about 390 functional OR genes that have been identified in the human genome, and the family of the OR gene are distributed on almost every chromosome [9, 16–18]. The cloning of all functional OR genes has been completed, and each gene has been subclassified, according to their sequence conservation [18, 19]. Since the OR genes have an intronless coding region, of around 1 kb length, it is easy to amplify these genes by PCR, using human genomic DNA library as a template [1, 17]. The current information of ORs is mainly based on genes and mRNA studies, and computational prediction of structure, thus the understanding of actual properties of ORs is still limited [20–22]. In the case of other GPCRs, the high-resolution structures of only several GPCRs, including rhodopsin and human adrenergic receptors, which were determined by X-ray crystallography, are currently available [23–26]; however, the knowledge of the actual structure of GPCRs is also limited. To investigate the three-dimensional structure of GPCR with atomic resolution, large amounts of purified receptor protein with high purities are required [27]. However, it is very difficult to produce these receptors from heterologous cell systems, and thus it is essential to develop efficient production strategies for various processes. The production of ORs for the development of a bioelectronic nose requires several steps, including expression, solubilization, purification and reconstitution [19].

Previous studies have reported that the heterologous expression of ORs appears to be difficult, especially from bacterial cell [15, 28–31]. The expression of GPCRs in their cell membrane is very complicated, and quite unpredictable. The folding and membrane insertion mechanism when expressing has not been well understood. It has been assumed that eukaryotic GPCRs are difficult to be expressed in prokaryotic cell membranes with proper orientation, because of their different charge distribution and inserting mechanism [29, 30, 32]. Therefore, when those receptors are overexpressed in bacterial cells, they tend to be expressed as insoluble inclusion bodies [31]. The misfolded and aggregated forms of receptors derived from inclusion bodies have to be properly refolded to obtain their own function [29, 33]. For refolding GPCRs, the reconstitution in a lipid environment is required after the expression, solubilization and purification.

The mammalian expression system has been widely used for functional assay of GPCRs [34]. However, the information of the selectivity of ORs to specific ligands is still limited, since it is also difficult to express ORs in the mammalian cell system [35]. Although little is known about the reason for this difficulty, some reports suggested that ORs are easily retained in the epidermal reticular (ER), and degraded in the proteosome [36, 37]. Natively, olfactory neurons have particular machinery for proper targeting and the expression of ORs in the cell surface, but this machinery has not yet been identified [36, 38]. For the proper expression of ORs in heterologous mammalian cells, foreign signal peptides or accessory proteins are mostly required, for correct targeting to the cell membrane [39–41].

Although there are various difficulties in the production of olfactory receptors, including expression, solubilization, purification and reconstitution, it should be a critical step for the development of an olfactory receptor-based bioelectronic nose. Advances in the production of the olfactory receptor and nanovesicle containing olfactory receptor using bacteria and animal cell system will be discussed in this chapter.

9.2 Production of Olfactory Receptors Using Bacterial Cells

The production of GPCRs including olfactory receptors using bacterial cell as a host cell system appears to be difficult, due to many reasons, such as their different charge distribution, strong hydrophobicity and complicated structure [14]. The cells are easily lysed, when membrane proteins including GPCRs are expressed in bacterial cells [29]. In addition, they cannot contain large amounts of foreign membrane protein in their membrane. Therefore, the expression of GPCRs in bacterial cells normally tends to be as inclusion bodies [31, 42]. A few examples for successful purification and reconstitution of olfactory receptors from inclusion bodies have been reported [29, 42].

Even with these difficulties in using bacterial cells for the production of GPCRs, researchers have attempted to use bacterial cells, in most cases using *Escherichia coli* (*E. coli*), with some reasons, including low cost, homogeneity of the recombinant proteins, and short generation time [15, 43, 44]. The milligram quantities of membrane proteins, which are the suitable amount for the study of high-resolution structures and the utilization for the development of biosensors, can only be obtained by the production from bacterial cells as inclusion bodies [28, 31, 44]. The production of olfactory receptors has become easier, through optimization of the production process [6, 10, 13, 28, 29, 45]. For the development of a protein-based bioelectronic nose, the production of olfactory receptors from bacterial cells should be a critical process.

9.2.1 Large-Scale Production of GPCRs from Bacterial Cells

The bacterial cell allows an efficient host cell system for the production of recombinant protein, with low cost and easy process [43]. The bacterial expression system can be easily optimized for scaling up [15, 27]. Even with difficulties of the production of GPCRs using the bacterial cell system, it has become easier through advances in the expression and purification, and the development of large-scale production process [15, 27].

The utilization of GPCRs obtained from *E. coli* has several disadvantages. The bacterial cells including *E. coli* cannot offer the native G-proteins and other machin-

eries required for the receptor mediated signaling transduction, or the production of a fully functionalized receptor [27, 46–48]. In addition, the post-translational modifications cannot occur during the expression in *E. coli* [27]. For example, glycosylation is required for the ligand binding or G-protein coupling for some GPCRs, including rhodopsin, somatostatin and β2 adrenergic receptors [49–51]. These disadvantages should be considered, before using *E. coli* as a host cell for the production of GPCRs.

The membrane environment of the host cell is very important for the functional expression of GPCRs with intact forms. However, the membrane composition of *E. coli* is very different from the eukaryotic cell membrane, and this can interrupt the insertion and location of recombinant receptors in membranes [15]. In addition, the production of functional membrane proteins can be slowed down by the reduction condition of the bacterial cytoplasm, which inhibits formation of disulfide bridges for the correct folding of membrane proteins [15]. In some cases, the fusion partner proteins, originating from periplasmic membrane protein in *E. coli*, such as the maltose binding protein (MBP), were applied for the successful insertion of GPCRs in the periplasmic oxidative environment. The utilization of MBP for the successful expression in membranes has been applied for human adenosine A_{2A} receptor, M_1 and M_2 muscarinic acetylcholine receptor, human $5HT_{1a}$ receptor, human β_2a receptor and human cannabinoid CB_2 receptor [52–56]. In these cases, the expressions were improved, using the bacterial expression vector containing weak promoter element, culturing at low temperature or inducing with low concentration of IPTG, to reduce the toxicity to cell membranes. Furthermore, similar strategies were also applied using the outer membrane protein, LamB, and the periplasmic protein, alkaline phosphatase for the production of GPCRs [57–59].

The extraction from cell membranes should be the best way to produce the functional GPCRs. However, in many cases, the recombinant GPCRs have been overexpressed in *E. coli* as inclusion bodies [14, 15, 28, 29, 43]. Since the bacterial cells cannot contain large amounts of foreign recombinant protein in their membranes, the formation of an inclusion body allows high productivity [43, 60]. Moreover, the overexpression as an aggregated form of inclusion bodies can be protected from degradation by cytosolic and periplasmic proteases [61]. However, the aggregated form of GPCRs was usually inactive, and functional reconstitution with membrane environment after purification is required [60]. The purification process using chromatographic methods after the solubilization is quite fastidious to optimize [14, 29, 60]. In many cases, GPCRs overexpressed as inclusion bodies have extremely low solubility, and are difficult to be solubilized by detergents and chaotropic agents [14, 28, 29]. These aggregated forms of GPCRs can only be solubilized by strong anionic detergents. However, the treatment of these strong detergents easily denatures the proteins, and disrupts the functionalization of recombinant receptors [14, 29, 31]. In addition, the activity of affinity chromatography, which is widely used for the purification of recombinant proteins, is normally decreased by detergents [28, 29]. After purification, the reconstitution should be carried out with lipid membrane environment, to obtain functional receptors [14, 43]. The biological lipid membrane originating from cells has a complex environment, and desirable and

reproducible reconstitution cannot be guaranteed [27]. Therefore, the reconstitution of recombinant GPCRs is normally carried out with artificial lipid membranes [27]. Various artificial membrane compositions should be tested for reconstitution with membrane-mimetic environments [14]. The purification and reconstitution of recombinant membrane protein is often a matter of trial and error, using detergents.

Since there is no well-established strategy for the systematic and efficient production of GPCRs from inclusion bodies, there are not many examples reported. For the successful expression of GPCRs in *E. coli* at high-level, optimization of several factors is needed, including the promoter and origin in the bacterial expression vector, fusion partner, strain of *E. coli*, culture condition and induction condition [62]. These conditions should be different for each GPCR, and the optimization process can be time consuming and labor intensive [63]. The systematic evaluation of expression methodologies for obtaining a large amount of inclusion bodies of GPCRs in *E. coli* has been carried out on 100 mammalian GPCRs, by exploring various different expression vectors and *E. coli* strains [42]. The Gateway bacterial expression vectors and the C43 *E. coli* strain allowed a large amount of insoluble GPCRs. It is also demonstrated by other reports that the Gateway vector and the C43 strain offer high-level expression of GPCRs as inclusion bodies [28, 31, 62–64]. The production process was scaled up using large-scale fermentation, and several 100 mg of GPCRs per liter were produced [42, 65].

9.2.2 Production of Olfactory Receptors from Bacterial Cells

With advances in the production of GPCRs, the production of olfactory receptors from bacterial cells has become easier, and allowed efficient recognition elements for bioelectronic noses, with human-like performances.

The first example for successful production of an olfactory receptor from bacterial cell is the production of olfactory receptor (OR) 5 [29]. The OR5 was produced from *E. coli* as a gluathione-S-transferase (GST) fusion protein, in the form of inclusion body. A mutant form of OR5, which contained some positive charge in the loop connecting transmembrane domain 1 and 2, was constructed, to block the insertion into cell membranes. It is known that the loops with some positive charge make it difficult to translocate to the periplasmic side in bacterial cells [66, 67]. The toxicity along with the translocation in membranes was reduced, and the mutant form of OR5 was successfully expressed as the inclusion body. The overexpressed OR5 was solubilized with strong anionic detergent. It failed to use a GST affinity column for the purification of the receptor, which was probably because the GST domain was denatured and misfolded, under the condition of strong anionic detergent. However, a Ni-NTA agarose column allowed successful purification of hexahistidine tagged olfactory receptor. After the purification, the detergent condition was replaced with digitonin, which is a well-known detergent for the stabilization of GPCR [68], and reconstituted in lipid vesicles composed of artificial lipids. This study suggested that the difficulties in expression of OR might be because of the toxicity, during the insertion of receptors into the bacterial membranes. Fur-

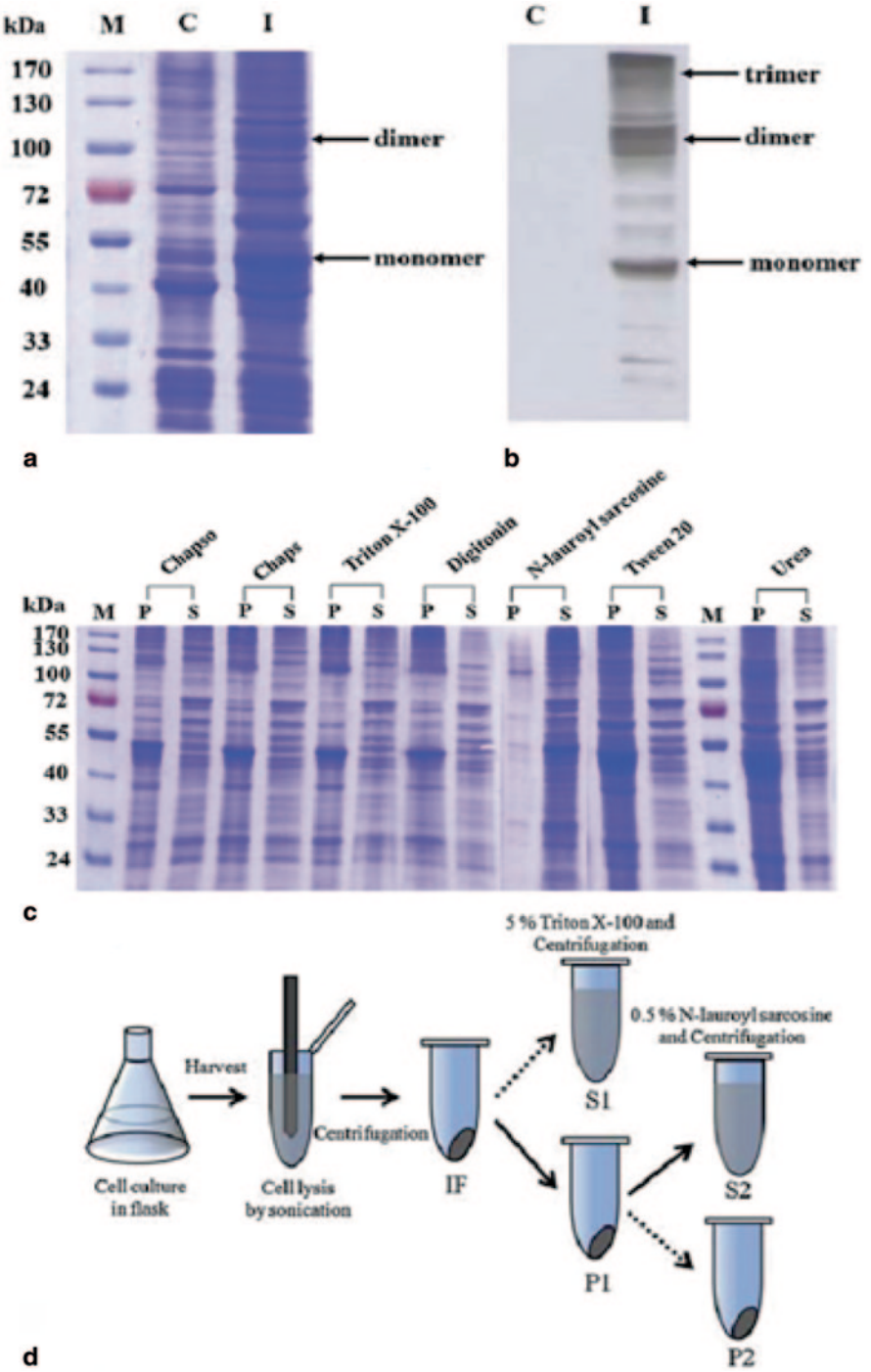

Fig. 9.1 **a** SDS-PAGE and **b** Western blotting of the expression of olfactory receptor. Lane M Protein size marker, Lane C Non-induced cells (control), Lane I Induced cells, **c** Solubilization of olfactory receptors using various detergents and a chaotropic agent, and **d** Schematic diagram of the column-free purification protocol using detergents. (Reprinted from Ref. [28] with permission from Elsevier.)

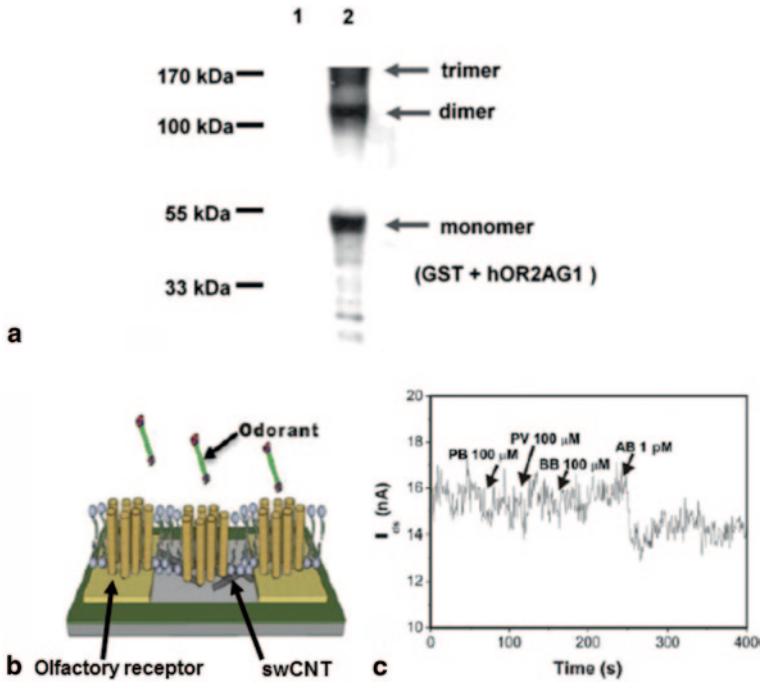

Fig. 9.2 **a** Western blot analysis of the hOR2AG1 expression. Lane 1, cytosol fraction, lane 2, insoluble fraction. **b** Schematic diagram of the OR-immobilized swCNT-FET. **c** The selectivity of hOR2AG1-functionalized swCNT-FET sensors. *Arrows* indicate the points of adding each odorant. *PB* propyl butyrate, *PV* pentyl valerate, *BB* butyl butyrate, *AB* amyl butyrate. (Reprinted from Ref. [6] with permission from Wiley.)

thermore, the OR in aggregated and misfolded state can be reconstituted with an efficient function through solubilization, detergent exchange and embedding with lipid environments [29].

The full-length of human olfactory receptor (hOR) 2AG1 was expressed in *E. coli* as an inclusion body, and purified by sequential treatment, using different detergents [28]. In this work, a suitable expression vector was screened, and it was found that the Gateway vector allowed high-level expression of OR in *E. coli* as the inclusion body (Figs. 9.1a, b). The aggregated form of expressed OR was difficult to be solubilized by various detergents and chaotropic agents, but the strong anionic detergent efficiently solubilized the receptor (Fig. 9.1c). The OR was first treated with weak detergent to remove impurity proteins, and the remaining insoluble fraction was then further treated with strong anionic detergent, to solubilize the OR protein (Fig. 9.1d). This work offered a simple method for the production of purified OR, with milligram quantities.

Along with advances in nanotechnology, nanomaterial-based sensor platforms that have high sensitivity are available [69, 70]. The unique chemical and electrical properties of nanomaterials have allowed high performance sensing devices [69–72]. Therefore, the integration of OR and nanomaterial-based sensor platform

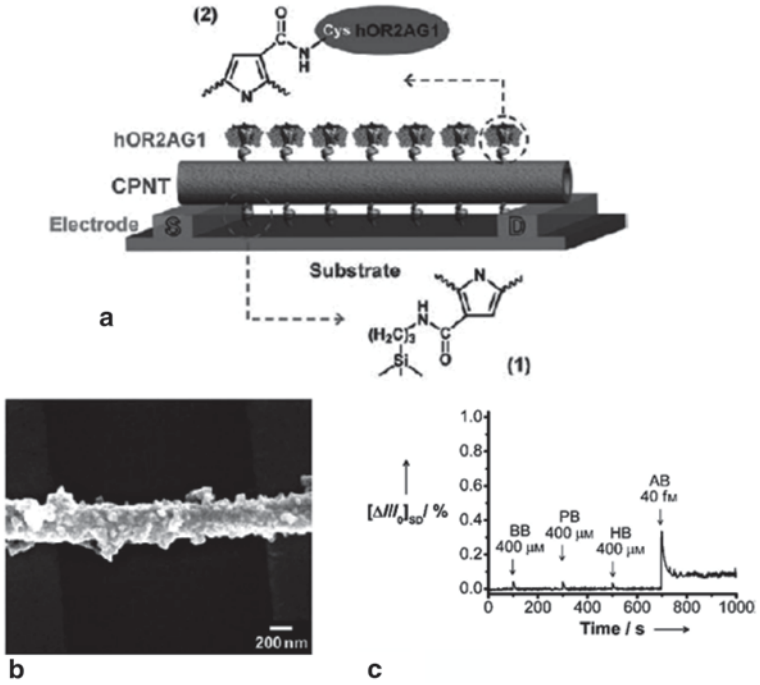

Fig. 9.3 **a** Schematic illustration. Only one nanotube is shown for clarity; covalent attachments (*1*) and (*2*) were used to bind CPNTs on the electrode substrate and to immobilize hORs to the nanotube, respectively. **b** Typical FE-SEM image of a hOR2AG1-conjugated CPNT. **c** The selectivity of hOR2AG1-functionalized swCNT-FET sensors. *Arrows* indicate the points of adding each odorant. *BB* butyl butyrate, *PB* propyl butyrate, *HB* hexyl butyrate, *AB* amyl butyrate. (Reprinted from Ref. [13] with permission from Wiley.)

opened up opportunities for the development of a bioelectronic nose showing high selectivity and sensitivity, with human-like performance [9, 72, 73]. For the development of a protein-based bioelectronic nose using a nanomaterial-based sensor platform, hOR2AG1 has been widely used as a model OR, because its biological function and specific odorant, amyl butyrate, are well known [74–76]. The ORs were successfully applied to the development of a protein-based bioelectronic nose, by integration with nanomaterial-based FET sensor platforms, including swCNT [6, 7], conducting polymer nanotube (CPNT) [13, 45], and graphene sensors [10]. The hOR2AG1 was produced using the method described above (Fig. 9.2a), and immobilized on swCNT-FET sensor by drying under vacuum condition (Fig. 9.2b) [6]. The hOR2AG1-immobilized swCNT-FET detected a specific odorant, amyl butyrate, with high selectivity and sensitivity (Fig. 9.2c). This work can be the first example for the development of a bioelectronic nose by the integration of nanomaterial-based sensor and the OR produced from bacterial cells. More details about the swCNT-based bioelectronic nose are described in Chap. 13. After this work, the hOR2AG1 was also utilized as the recognition element for the CPNT-FET-based bioelectronic nose [13]. The receptors were immobilized on carboxylated

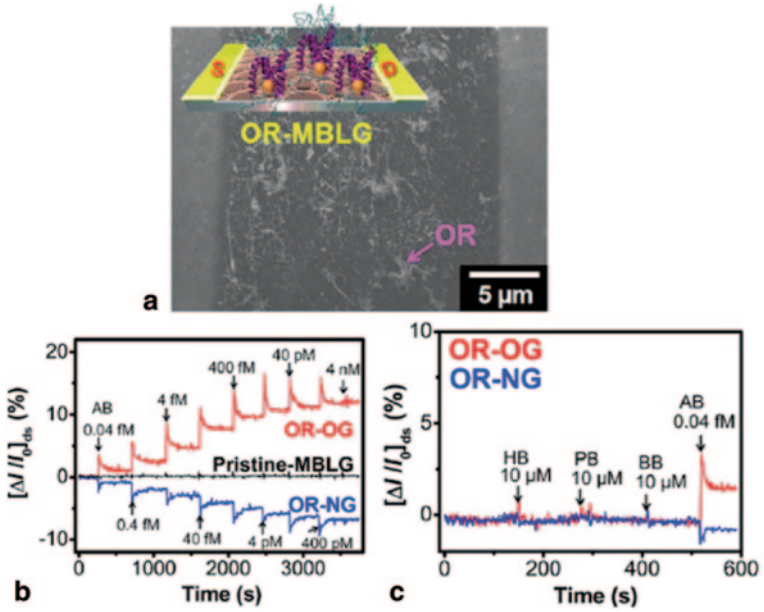

Fig. 9.4 **a** Typical FE-SEM images of the modified bilayer graphene (*BMLG*) surface after immobilization of the OR. **b** Real-time response of graphene FET based on OR-conjugated p type of oxygen plasma-treated graphene (*OG*) and n-type of ammonia plasma-treated graphene (*NG*) upon the stimulation of various concentration of amyl butyrate. **c** Selective responses of graphene-based bioelectronic nose *OG* and *NG* upon addition of non-targets (*HB* hexyl butyrate, *PB* propyl butyrate, *BB* butyl butyrate) and target (*AB* amyl butyrate) odorants (Reprinted from Ref. [10] with permission from Copyright (2012) American Chemical Society.)

CPNTs more elaborately by covalent bonding, and this immobilization strategy offered excellent electrical properties, and quantitative control of the receptor immobilization (Figs. 9.3a, b). The bioelectronic nose showed specific odorant detection with high sensitivity at the femtomolar detection limit, and with high selectivity (Fig. 9.3c). More details about the CPNT-based bioelectronic nose are described in Chap. 14. The graphene-based sensor was also used for the development of a bioelectronic nose by the immobilization of hOR2AG1 [10]. The OR was immobilized on graphene surface by surface modification (Fig. 9.4a). The hOR2AG1-immobilized graphene-based bioelectronic tongue detected the target odorant with high selectivity and ultrasensitivity, at the detection limit of the concentration down to attomolar level (Figs. 9.4b, c). The unique physical properties of graphene, such as extremely high carrier mobility and capacity, an ambipolar field-effect, and a highly tunable conductance, allow the development of high-performance electrochemical sensors [77, 78]. The method for the production of ORs using *E. coli* with the Gateway vector system, and purification using detergents, was also applied, to produce other ORs and GPCRs. Using these GPCRs as recognition elements, high-performance receptor-based biosensors have been developed, by the integration with highly sensitive secondary transducers [6, 7, 10, 13, 28, 45, 79–81].

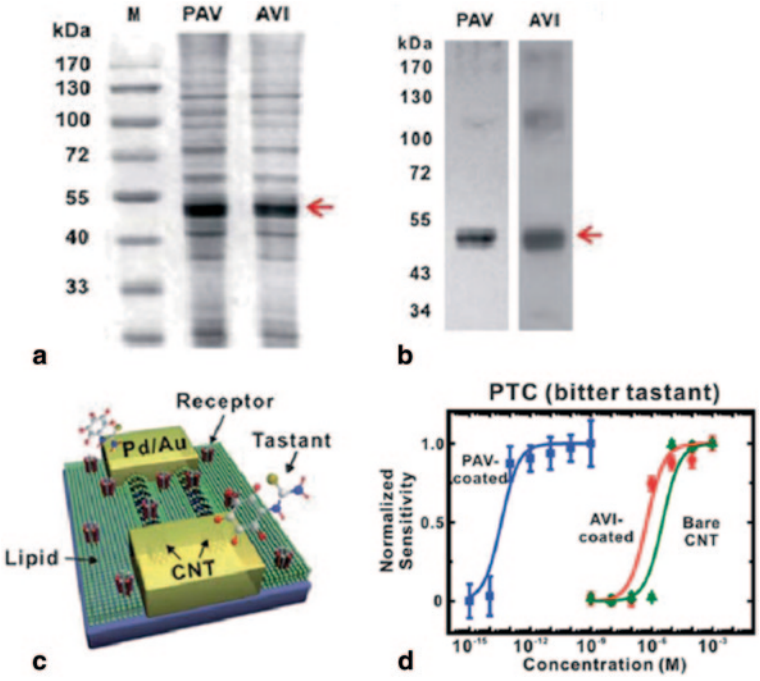

Fig. 9.5 **a** SDS-PAGE of the hTAS2R38, human taste receptor protein, expressed in *E. coli*. *PAV* and *AVI* represent the receptor protein types of tasters and non-tasters, respectively. **b** Western blot analysis of the hTAS2R38 expressed in *E. coli*. The *dark bands* marked by the *arrow* indicate the expression of human taste receptor protein. **c** Schematic diagram showing the structure of human taste receptor functionalized swCNT. **d** Response of PAV-functionalized, AVI-functionalized and bare CNT-FETs to PTC. (Reprinted from Ref. [79] with permission from Royal Society of Chemistry.)

9.2.3 Production of Taste Receptors and Other Receptors from Bacterial Cells

These approaches developed for the bioelectronic nose were applied to the development of bioelectronic tongues utilizing taste receptors, and opened up opportunities for the development of various biosensors using GPCRs as recognition elements. Advances in the production of GPCR using bacterial cells offered efficient recognition for the development of high-performance biosensors, including bioelectronic tongues, neurotransmitter sensor, and peptide hormone sensor. The human bitter taste receptors, hTAS2R38s, were successfully produced from inclusion bodies in *E. coli*, and utilized as recognition elements for the development of a bioelectronic tongue with the integration of a nanomaterial-based sensor platform including single-walled carbon nanotube (swCNT) [79], and conducting polymer nanotube (CPNT) [81] field effect transistor (FET). It is known that sequence variants in the hTAS2R38 gene correlate with different bitterness recognition for tasting bitter compound phenylthiocarbamide (PTC) and propylthiouracil (PROP), and this

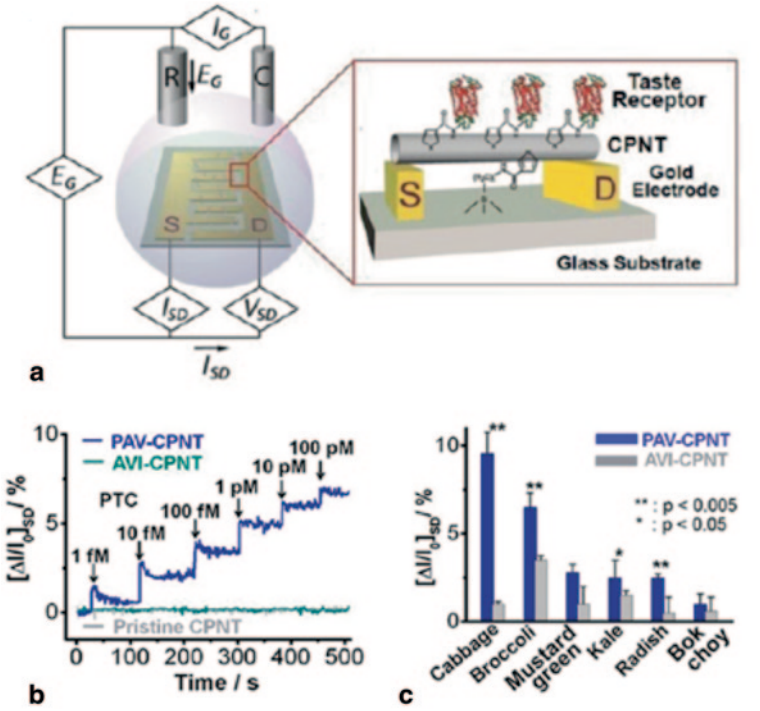

Fig. 9.6 **a** Schematic diagram showing a liquid-ion gate FET using hTAS2R38-functionalized CPNT and one nanotube shown for clarity on interdigitated gold microelectrodes. **b** Real-time responses of FETs using *PAV* and *AVI* type hTAS2R38-functionalized CPNT and pristine CPNT stimulated with PTC. **c** Responses of *PAV* and *AVI* type hTAS2R38-functionalized CPNTs to various cruciferous vegetables. Differences in responses from *PAV* and *AVI-CPNT* to cabbage, broccoli, kale, and radish were highly significant (**$p < 0.005$, *$p < 0.05$ by Student's t-test). (Reprinted from Ref. [81] with permission from Copyright (2013) American Chemical Society.)

different bitter taste perception is important in genetic and anthropological studies [82, 83]. Each taster (PAV) and non-taster (AVI) type of hTAS2R38s was produced from *E. coli* (Figs. 9.5a, b), and used as recognition elements for bioelectronic tongues [79, 81]. The hTAS2R38 was functionalized with swCNT-FET (Fig. 9.5c) and offered high selectivity and sensitivity for the target tastant detection, with human-like performances. The different types of hTAS2R38s-functionalized swCNT-FET showed different bitter taste perception (Fig. 9.5d) [79]. The hTAS2R38s were also functionalized on CPNT-FET, and showed high selectivity and sensitivity to target bitter tastants (Figs. 9.6a, b). The hTAS2R38-based bioelectronic tongue using CPNT-FET exhibited different bitter-taste perception to PTC, PROP, and even to anti-thyroid toxin in vegetables, which corresponded to the haplotype of hTAS2R38 (Figs. 9.6b, c) [81]. These bioelectronic tongues can be utilized as a substitute for cell-based assays, and study of the mechanisms of human taste. Recently, human muscarinic acetylcholine receptor (mAChR) was produced from *E. coli,* and utilized as a recognition element for the detection of the neurotransmitter,

acetylcholine, by integration with swCNT-FET. The mAChR-based neurotransmitter sensor showed high selectivity and sensitivity to acetylcholine [84]. In addition, the class B GPCR, human parathyroid hormone receptor (hPTHR), was also successfully expressed as an inclusion body in *E. coli,* and purified [80]. The produced hPTHR was applied to the development of a hormone sensor, by integration with the conducting polymer nanoparticle field effect transistor, and offered high selectivity and sensitivity for peptide hormone detection, with human-like performance. In these works, the Gateway vector system also allowed high-level expression of GPCR in *E. coli*.

9.3 Production of Olfactory Receptors Using Animal Cells

9.3.1 Production of Olfactory Receptors Using Mammalian Cells

The mammalian cells present a suitable environment, including a lipid membrane composition closed to native tissues, for the production of fully functional ORs [15, 27, 39, 85, 86]. In addition, these cell systems offer native machineries, including G-protein and ion channels, for OR-mediated signal transduction [87–89]. Thus, the mammalian cell system can be the most appropriate for functional study of ORs, and also for the development of a cell-based bioelectronic nose, using whole cell expressing ORs in cell membranes [88, 90–93]. About 20 ORs have been identified for their specific odorants, using the screening assay with mammalian cell systems [88, 89, 95–101]. Although there are many advantages, it has been difficult to utilize the mammalian cell system for the production of ORs for the development of a cell-based bioelectronic nose and for functional study, because of difficulties in the expression of ORs [15, 27, 88]. The mammalian cell system cannot produce the recombinant proteins in large amount, compared with the bacterial cell system [15, 27, 88]. Furthermore, ORs are easily degraded in the proteosome, when expressed in mammalian cells [36, 37, 101].

Since ORs do not possess the import sequence, fusion tags and accessory proteins are required for the enhancement of expression of ORs in cell membranes [9, 88, 102]. HEK-293 cells offer a high-level expression of rhodopsin, with efficient translocation to the plasma membrane [103]. By taking this advantage, the first 20 amino acids of bovine rhodopsin, a rho-tag, was found, that facilitates translocation of synthesized ORs to the plasma membrane [88]. This approach has been widely used as a model system for the study of ligand specificity and function of ORs [88, 100, 104, 105]. In addition, there are also some examples of the use of import sequences from other GPCRs, which allowed efficient membrane integration for ORs [99, 106]. The receptor transporting proteins (RTPs) were also screened as accessory proteins for targeting ORs to the cell surface [39, 107]. It was discovered

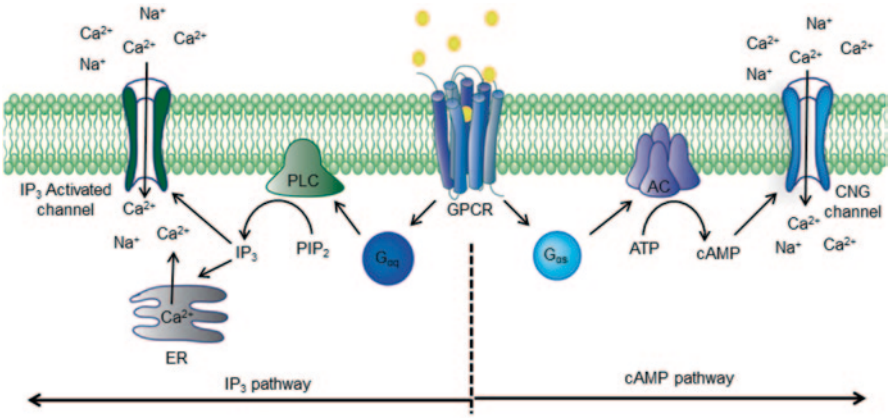

Fig. 9.7 Olfactory receptor-mediated signal transduction. The cytosolic ions are increased by cAMP or IP_3 pathway.

that RTPs promote cell surface expression of ORs, and enhance the responses to odorants in HEK-293 cells co-expressed with ORs [39]. The receptor expression enhancing protein (REEP), and heat shock protein (Hsc70t) have also been identified as accessory proteins, for the enhancement of proper expression of ORs in cell membrane [39, 74, 108]. These fusion tag and accessory proteins allowed efficient expression of ORs in the mammalian cell system, for the development of cell-based bioelectronic noses, and high-throughput screening of ORs.

Usually, expression levels of GPCRs including ORs are very low, even with fusing tags and accessory proteins, but there are some cases for the production of GPCRs by scaled-up suspension culture of stable cell lines [109, 110]. Due to the toxicity of the high-level expression of GPCRs to cells, it is difficult to obtain reliable stable cell lines for suspension culture [111–113]. Inducible mammalian cells have been constructed, and allowed high-level (some mg/L quantities) expression of GPCRs [111–113]. After screening of many GPCRs, it was found that the Semliki Forest virus vector with mammalian host cell allows high level expression of GPCRs for crystallization [114]. Even with time consuming and labor intensive process, mammalian expression systems have the possibility of being applied to the development of a receptor-based bioelectronic nose using fully functional ORs.

The mammalian expression systems, HEK-293 cells in most cases, have been applied for the development of cell-based bioelectronic noses. The HEK-293 cell system offers olfactory neuron-like OR-mediated signal transduction [90–92]. The cyclic adenosine monophosphate (cAMP) pathway is the major signal transduction pathway involving ORs [87, 115, 116]. When the specific olfactory receptor binds to the OR, it causes a conformational change in the receptor, and then G protein is dissociated to downstream intracellular signaling proteins, or target functional proteins. The enzyme, adenylyl cyclase, can be activated by the alpha subunit of G protein, and exchanges ATP with cAMP. A cyclic-nucleotide-gated (CNG) channel is finally opened, and leads to an influx of Ca^{2+} and Na^{+} (Fig. 9.7). The cytosolic ions are also increased through OR-mediated 1,4,5-triphosphate (IP_3) pathway [117, 118] (Fig. 9.7). The spe-

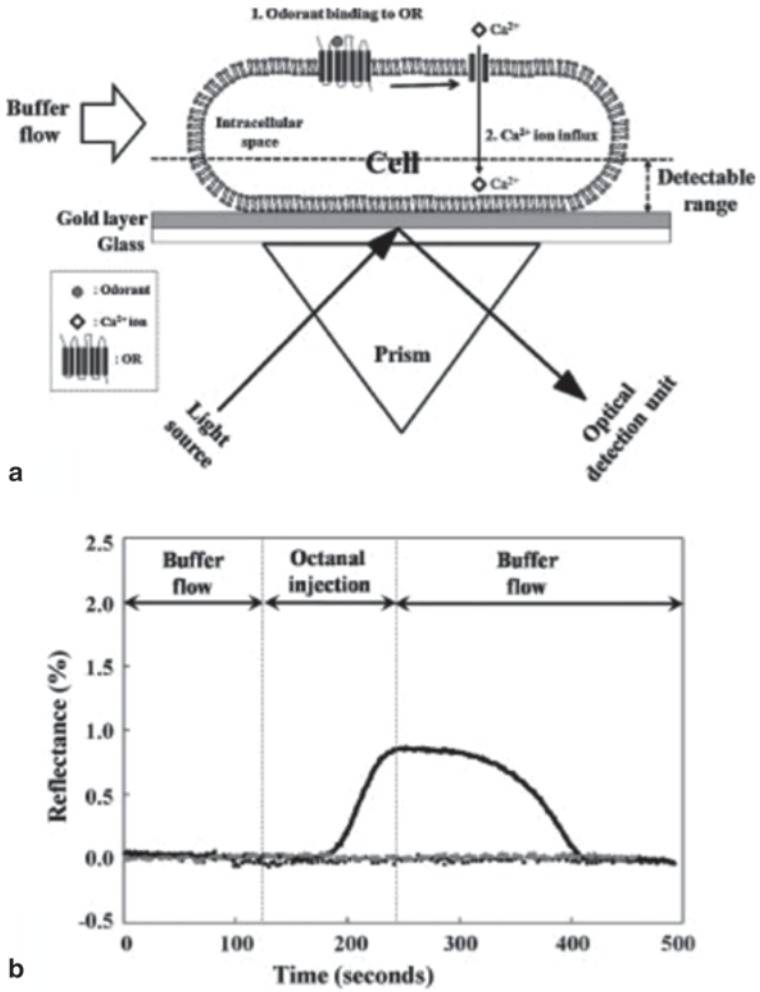

Fig. 9.8 **a** Principle of the cell-based bioelectronic nose for odorant detection using SPR. Odorant binding to OR triggers Ca^{2+} ion influx, and SPR detects the increase of intracellular components. **b** SPR response to the injection of odorant, octanal in this case, in Ca^{2+} standard solution (*black*) and in Ca^{2+}-free solution (*gray*). (Reprinted from Ref. [92] with permission from Elsevier.)

cific odorants of ORs expressed in the surface of HEK-293 cells can be detected, by measuring OR-mediated ion influx with secondary sensor platforms.

Mammalian cells expressing ORs were combined with optical or electrochemical sensor platforms, such as surface plasmon resonance (SPR), micro-electrode array (MEA) and light-addressable potentiometric (LAPS), for the development of cell-based bioelectronic noses and tongues [90–92, 119, 120]. For these sensors, mammalian cell systems expressing ORs allow cultivable artificial olfactory cells, with olfactory neuron-like signal transduction. The signal transduction triggered

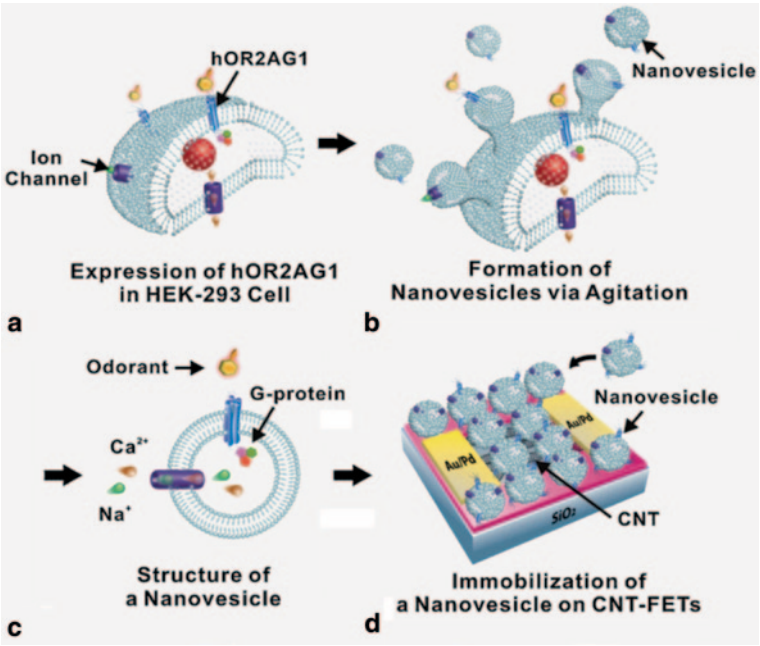

Fig. 9.9 Schematic diagram depicting the preparation of nanovesicles containing hOR2AG1, and the hybridization of the nanovesicles with a carbon nanotube-based FET transducer, to build a nanovesicle-based bioelectronic nose. (Reprinted from Ref. [121] with permission from Elsevier.)

by the specific interaction of odorants to ORs causes Ca^{2+} ion influx through the CNG channel or endogenous channel, and the specific binding can be detected by measuring the changes in intracellular components, using sensor platforms like SPR (Figs. 9.8a, b).

9.3.2 Production of Olfactory Receptor-Containing Nanovesicles Derived from Mammalian Cells

Nanomaterial-based sensor platforms offer highly sensitive electrochemical sensors, and they offer high-performance bioelectronic noses, when integrated with ORs. However, it seems to be very difficult to develop cell-based bioelectronic noses by the combination of nanomaterial-based sensors and mammalian cells expressing ORs, because of their sizes. Normally, the size of mammalian cells is about 10 μm in diameter, which is too big, when compared with nanomaterial. The OR-mediated signal transduction should highly depend on the viability of the cells, and it is difficult to maintain cells on sensor platforms with a suitable condition for the measurement of signaling. In addition, the whole cell should generate enormous noise signal from the metabolism, to the highly sensitive nanomaterial-based sensor

platform. To overcome these limitations for the development of a cell-based bioelectronic nose using a nanomaterial-based sensor platform, nanovesicles derived from mammalian cells expressing ORs in their membranes have been constructed [121, 122].

The nanovesicles derived from the mammalian cells expressing ionotropic 5-HT3 receptor, and the receptor-mediated signal transduction, were successfully monitored [123]. These nanovesicles exhibited whole cell-like cellular signaling with miniaturized sizes [123]. By taking these advantages, nanovesicles containing ORs have been constructed from mammalian cells expressing ORs, and applied to cell-based bioelectronic noses [121, 122]. After the construction of mammalian cells expressing ORs (Fig. 9.9a), the cells are treated with cytochalasin B, which allows the cytoskeletons to become unstable, then the nanovesicles are budded out (Fig. 9.9b). These nanovesicles containing ORs exhibit whole cell-like OR-mediate signal transduction (Fig. 9.9c). After the production of nanovesicles, they were immobilized on the swCNT-FET sensor platform, to build a nanovesicle-based bioelectronic nose (Fig. 9.9d). The nanovesicles derived from cells showed a sphere-like shape, with a uniform diameter of around 200 nm (Fig. 9.10a). The nanovesicles contained efficient amounts of ORs (Fig. 9.10b), and exhibited OR-mediated signal transduction, which was measured by Ca^{2+} assay, using fluorescent Fura dye (Fig. 9.10c). Then, these nanovesicles were immobilized on the swCNT-FET sensor platform. The selective binding of odorant to OR was detected by monitoring OR-mediated cellular signaling, using swCNT-FET with high sensitivity and selectivity (Fig. 9.10d). As an example, this nanovesicle-based bioelectronic nose can be used for the fast assessment of food quality [122]. Hexanal is produced by lipid oxidation during the incubation, and can be an indicator of the oxidation of food. For this purpose, nanovesicles were produced from mammalian cells expressing the canine OR, which binds to hexanal. Nanovesicles containing the OR were immobilized on swCNT-FET, and detected hexanal with high selectivity and sensitivity. This nanovesicle-based bioelectronic nose also detected hexanal in spoiled milk, without any pretreatment process.

9.3.3 Production of Olfactory Receptors Using Insect Cells

Insect cell types, such as *Spodoptera frutiperda* (Sf9 and Sf21) and *Trichoplusia ni* (Hi_5 and MG_1), can be selectively infected by the baculovirus *Autographa californica*, which has a double-stranded DNA covered by a lipid membrane. The gene of interest is inserted into the baculovirus DNA, using a homologous recombination. The baculovirus DNA has a strong polyhedrin promoter. Polyhedrin is one of the major components of the protective matrix, and is nonessential for viral propagation in cell culture. Therefore, the gene of interest can be inserted by the replacement of the Polyhedrin gene [124]. Along with the advances in cell culture technology, and transfer vectors, and the commercial availability of reagents, insect cells have been able to be cultured in suspension with scale-up in large fermenters [27]. Insect cells

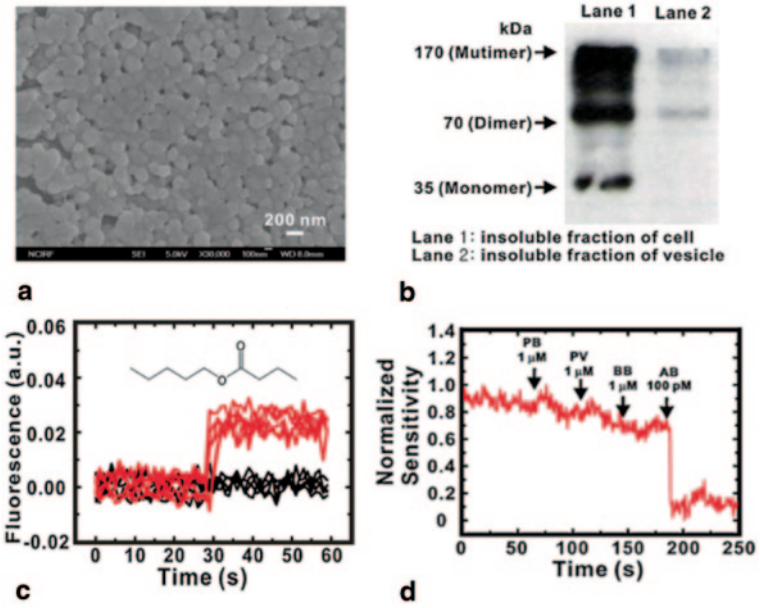

Fig. 9.10 **a** FE-SEM image of nanovesicles. **b** Western blot analysis of hOR2AG1 protein expressed in HEK-293 cells and nanovesicles. **c** Transient Ca^{2+} ion signaling assay of nanovesicles containing hOR2AG1 and Fura2-AM. **d** Graph showing conductance changes in real-time after the introduction of different odorant molecules. *PB* propyl butyrate, *PV* pentyl valerate, *BB* butyl butyrate, *AB* amyl butyrate. (Reprinted from Ref. [121] with permission from Elsevier.)

provide post-translational modifications, such as phosphorylation, fatty acid acylation, and glycosylation, and recombinant proteins exhibit similar characteristics to their native counterparts [124, 125].

Another advantage to the use of insect cell system is a correct folding of GPCRs and certain G_{α} subunits [126–128]. The insect cells have showed high efficiency for the production of GPCRs. The amounts of these receptors are 25–600 times higher than those obtained from mammalian cells, and the receptors exhibited correct function for the specific ligand binding [129–133]. In addition, it has been reported that various signal sequences from baculoviral, prokaryotic or eukaryotic origin successfully increased the amount of secreted soluble proteins [134–136].

Since ORs were first successfully cloned and expressed in Sf9 cells in 1993, some studies have been reported for the production of ORs and the functional assay, using the insect cell system [137]. Two ORs, rat OR olp4 and human OR-17-4, were expressed in the membrane of insect cells with the baculovirus infection [138]. It was found that lysophosphatidylcholine is a suitable detergent for efficient solubilization of the overexpressed ORs, and compatible for the purification. After solubilization, the ORs were purified by affinity chromatography using nickel nitrilotriacetic acid resin, and subsequently by cation-exchange chromatography, and then reconstituted in phospholipid vesicles. In another example, human OR17-209

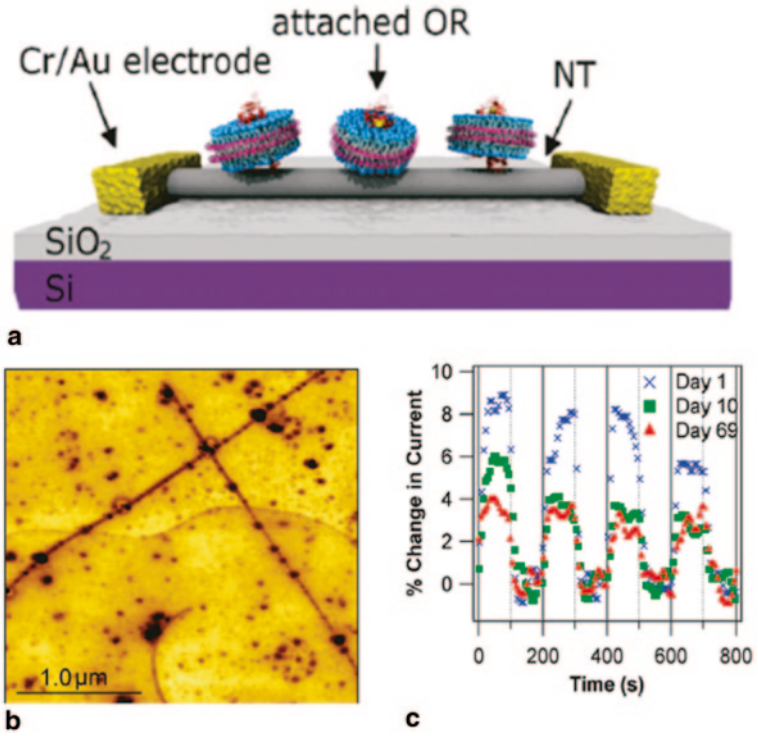

Fig. 9.11 **a** Schematic of a carbon nanotube transistor functionalized with mouse ORs in nanodiscs. **b** AFM image demonstrating preferential attachment of His-tag-labeled mouse *OR* in micelles to Ni-NTA-functionalized carbon nanotubes. **c** Real-time response of disc packaged OR-NT devices to specific odorant over 10 weeks. (Reprinted (adapted) with permission from reference [5]. Copyright (2011) American Chemical Society.)

and 17-210 were expressed in Sf9 cells colocalized with G_{α} subunits, and odorant-induced calcium response was successfully measured [139].

ORs produced from insect cells allowed efficient recognition elements for the bioelectronic nose, by integration with the CNT sensor platform [5]. Three mouse OR proteins were overexpressed in Sf9 cells, with N-terminal His-tags for purification and attachment on the CNT surface (Fig. 9.11a). The mouse ORs were solubilized with digitonin, and purified using magnetic beads treated with Ni-NTA. Purified mouse ORs were then reconstituted in detergent micells and nanodiscs that are disk-shaped protein lipid particles designed to self-assemble, with well-controlled size and composition [140, 141]. The CNT sensor devices were functionalized with carboxylated diazonium salts, and the reconstituted ORs were immobilized on CNT surface with covalent bonds (Figs. 9.11a, b). The mouse ORs-based sensors showed high performance for the detection of odorants, compared with the detergent micells, and nanodiscs allowed significant enhancement of mouse ORs stability in solution (Fig. 9.11c).

9.4 Conclusion and Perspective

ORs allow high selectivity and human nose-like performance for the bioelectronic nose. Therefore, the production of ORs or cells expressing ORs should be a critical process for the development of the bioelectronic nose. Along with advances in the production of ORs using heterologous cell systems, including bacterial, mammalian and insect cells, ORs have been applied as very efficient sensor elements for bioelectronic noses. However, the production of ORs still remains as a bottleneck. To mimic the natural human nose more closely, multiplexed sensors functionalized with various different human ORs should be developed. There are about 390 functional OR genes that have been identified in the human genome, and the suitable conditions for their production will be different from each other. For practical applications and successful commercialization, some technical issues, including the stability, functional reproducibility and mass production, will be required to be established. Therefore, more elaborate process for the production of olfactory receptors, including expression, solubilization, purification, reconstitution and immobilization of the sensor material, need to be further investigated.

Acknowledgments This work was supported by the National Research Foundation of Korea (NRF) grant funded by the Ministry of Science, ICT & Future Planning (No. 2013003890, No. 2013055375).

References

1. Buck L, Axel R (1991) A novel multigene family may encode odorant receptors: a molecular basis for odor recognition. Cell 65(1):175–187
2. Reed RR, Bakalyar HA, Cunningham AM, Levy NS (1992) The molecular basis of signal transduction in olfactory sensory neurons. Soc Gen Physiol Ser 47:53–63
3. Firestein S (2001) How the olfactory system makes sense of scents. Nature 413(6852):211–218
4. Lancet D, Chen Z, Ciobotariu A, Eckstein F, Khen M, Heldman J, Ophir D, Shafir I, Pace U (1987) Toward a comprehensive molecular analysis of olfactory transduction. Ann N Y Acad Sci 510(1):27–32
5. Goldsmith BR, Mitala Jr JJ, Josue J, Castro A, Lerner MB, Bayburt TH, Khamis SM, Jones RA, Brand JG, Sligar SG (2011) Biomimetic chemical sensors using nanoelectronic readout of olfactory receptor proteins. ACS Nano 5(7):5408–5416
6. Kim TH, Lee SH, Lee J, Song HS, Oh EH, Park TH, Hong S (2009) Single-carbon-atomic-resolution detection of odorant molecules using a human olfactory receptor-based bioelectronic nose. Adv Mater 21(1):91–94
7. Lee SH, Jin HJ, Song HS, Hong S, Park TH (2012) Bioelectronic nose with high sensitivity and selectivity using chemically functionalized carbon nanotube combined with human olfactory receptor. J Biotech 157(4):467–472
8. Lee SH, Kwon OS, Song HS, Park SJ, Sung JH, Jang J, Park TH (2012) Mimicking the human smell sensing mechanism with an artificial nose platform. Biomaterials 33:1722–1729
9. Lee SH, Park TH (2010) Recent advances in the development of bioelectronic nose. Biotechnol Bioproc Eng 15(1):22–29
10. Park SJ, Kwon OS, Lee SH, Song HS, Park TH, Jang J (2012) Ultrasensitive flexible graphene based FET-type bioelectronic nose. Nano Lett 12:5082–5090

11. Vidic J, Pla-Roca M, Grosclaude J, Persuy M-A, Monnerie R, Caballero D, Errachid A, Hou Y, Jaffrezic-Renault N, Salesse R (2007) Gold surface functionalization and patterning for specific immobilization of olfactory receptors carried by nanosomes. Anal Chem 79(9):3280–3290
12. Vidic JM, Grosclaude J, Persuy M-A, Aioun J, Salesse R, Pajot-Augy E (2006) Quantitative assessment of olfactory receptors activity in immobilized nanosomes: a novel concept for bioelectronic nose. Lab Chip 6(8):1026–1032
13. Yoon H, Lee SH, Kwon OS, Song HS, Oh EH, Park TH, Jang J (2009) Polypyrrole nanotubes conjugated with human olfactory receptors: high-performance transducers for FET-type bioelectronic noses. Angew Chem Int Edit 48(15):2755–2758
14. Sarramegna V, Muller I, Milon A, Talmont F (2006) Recombinant G protein-coupled receptors from expression to renaturation: a challenge towards structure. Cell Mol Life Sci 63(10):1149–1164
15. Sarramegna V, Talmont F, Demange P, Milon A (2003) Heterologous expression of G-protein-coupled receptors: comparison of expression systems from the standpoint of large-scale production and purification. Cell Mol Life Sci 60(8):1529–1546
16. Rouquier S, Taviaux S, Trask BJ, Brand-Arpon V, van den Engh G, Demaille J, Giorgi D (1998) Distribution of olfactory receptor genes in the human genome. Nat Gen 18(3):243–250
17. Malnic B, Godfrey PA, Buck LB (2004) The human olfactory receptor gene family. Proc Nat Acad Sci 101(8):2584–2589
18. Glusman G, Yanai I, Rubin I, Lancet D (2001) The complete human olfactory subgenome. Genome Res 11(5):685–702
19. Zozulya S, Echeverri F, Nguyen T (2001) The human olfactory receptor repertoire. Gen Biol 2(6):research0018
20. Gat U, Nekrasova E, Lancet D, Natochin M (2005) Olfactory receptor proteins. Eur J Biochem 225(3):1157–1168
21. Hall SE, Floriano WB, Vaidehi N, Goddard WA (2004) Predicted 3-D structures for mouse I7 and rat I7 olfactory receptors and comparison of predicted odor recognition profiles with experiment. Chem Sens 29(7):595–616
22. Katada S, Hirokawa T, Oka Y, Suwa M, Touhara K (2005) Structural basis for a broad but selective ligand spectrum of a mouse olfactory receptor: mapping the odorant-binding site. J Neurosci 25(7):1806–1815
23. Palczewski K, Kumasaka T, Hori T, Behnke CA, Motoshima H, Fox BA, Trong IL, Teller DC, Okada T, Stenkamp RE (2000) Crystal structure of rhodopsin: a G protein-coupled receptor. Science 289(5480):739–745
24. Cherezov V, Rosenbaum DM, Hanson MA, Rasmussen SG, Thian FS, Kobilka TS, Choi H-J, Kuhn P, Weis WI, Kobilka BK (2007) High-resolution crystal structure of an engineered human 2-adrenergic G protein coupled receptor. Science 318(5854):1258–1265
25. Rasmussen SG, Choi H-J, Rosenbaum DM, Kobilka TS, Thian FS, Edwards PC, Burghammer M, Ratnala VR, Sanishvili R, Fischetti RF (2007) Crystal structure of the human beta2 adrenergic G-protein-coupled receptor. Nature 450(7168):383–387
26. Warne T, Serrano-Vega MJ, Baker JG, Moukhametzianov R, Edwards PC, Henderson R, Leslie AG, Tate CG, Schertler GF (2008) Structure of a beta 1-adrenergic G-protein-coupled receptor. Nature 454(7203):486–491
27. McCusker EC, Bane SE, O'Malley MA, Robinson AS (2008) Heterologous GPCR expression: a bottleneck to obtaining crystal structures. Biotech Prog 23(3):540–547
28. Song HS, Lee SH, Oh EH, Park TH (2009) Expression, solubilization and purification of a human olfactory receptor from *Escherichia coli*. Curr Microbiol 59(3):309–314
29. Kiefer H, Krieger J, Olszewski JD, von Heijne G, Prestwich GD, Breer H (1996) Expression of an olfactory receptor in Escherichia coli: purification, reconstitution, and ligand binding. BioChemistry 35(50):16077–16084
30. Grisshammer R, Tateu CG (1995) Overexpression of integral membrane proteins for structural studies. Q Rev Biophys 28(03):315–422

31. Bane SE, Velasquez JE, Robinson AS (2007) Expression and purification of milligram levels of inactive G-protein coupled receptors in *E. coli*. Protein Expr Purif 52(2):348–355
32. Grisshammer R, White JF, Trinh LB, Shiloach J (2005) Large-scale expression and purification of a G-protein-coupled receptor for structure determination–an overview. J Struct Funct Genom 6(2):159–163
33. Carrio M, Villaverde A (2002) Construction and deconstruction of bacterial inclusion bodies. J Biotechnol 96(1):3–12
34. Thomsen W, Frazer J, Unett D (2005) Functional assays for screening GPCR targets. Curr Opin Biotechnol 16(6):655–665
35. Mombaerts P (2004) Genes and ligands for odorant, vomeronasal and taste receptors. Nat Rev Neurosci 5(4):263–278
36. McClintock TS, Sammeta N (2003) Trafficking prerogatives of olfactory receptors. Neuroreport 14(12):1547–1552
37. Lu M, Echeverri F, Moyer BD (2003) Endoplasmic reticulum retention, degradation, and aggregation of olfactory G- protein coupled receptors. Traffic 4(6):416–433
38. Gimelbrant AA, Haley SL, McClintock TS (2001) Olfactory receptor trafficking involves conserved regulatory steps. J Biol Chem 276(10):7285–7290
39. Saito H, Kubota M, Roberts RW, Chi Q, Matsunami H (2004) RTP family members induce functional expression of mammalian odorant receptors. Cell 119(5):679–691
40. Hatt H, Gisselmann G, Wetzel C (1999) Cloning, functional expression and characterization of a human olfactory receptor. Cell Mol Biol 45(3):285
41. Brady AE, Limbird LE (2002) G protein-coupled receptor interacting proteins: emerging roles in localization and signal transduction. Cell Signal 14(4):297–309
42. Michalke K, Gravière M, Huyghe C, Vincentelli R, Wagner R, Pattus F, Schroeder K, Oschmann J, Rudolph R, Cambillau C (2009) Mammalian G-protein-coupled receptor expression in *Escherichia coli*: I. High-throughput large-scale production as inclusion bodies. Anal Biochem 386(2):147–155
43. Grisshammer R, Tate C (1995) Overexpression of integral membrane proteins for structural studies. Q Rev Biophys 28(3):315–422
44. Bouvier M, Ménard L, Dennis M, Marullo S (1998) Expression and recovery of functional G-protein-coupled receptors using baculovirus expression systems. Curr Opin Biotechnol 9(5):523–527
45. Lee SH, Kwon OS, Song HS, Park SJ, Sung JH, Jang J, Park TH (2012) Mimicking the human smell sensing mechanism with an artificial nose platform. Biomaterials 33(6):1722–1729
46. Davis D, Liu X, Segaloff DL (1995) Identification of the sites of N-linked glycosylation on the follicle-stimulating hormone (FSH) receptor and assessment of their role in FSH receptor function. Mol Endocrinol 9(2):159–170
47. Dong C, Filipeanu CM, Duvernay MT, Wu G (2007) Regulation of G protein-coupled receptor export trafficking. Biochim Biophys Acta 1768(4):853–870
48. Jayadev S, Smith RD, Jagadeesh G, Baukal AJ, Hunyady L, Catt KJ (1999) N-linked glycosylation is required for optimal AT1a angiotensin receptor expression in COS-7 cells. Endocrinology 140(5):2010–2017
49. Kaushal S, Ridge KD, Khorana HG (1994) Structure and function in rhodopsin: the role of asparagine-linked glycosylation. Proc Nat Acad Sci 91(9):4024–4028
50. Rands E, Candelore M, Cheung A, Hill WS, Strader C, Dixon R (1990) Mutational analysis of beta-adrenergic receptor glycosylation. J Biol Chem 265(18):10759–10764
51. Rens-Domiano S, Reisine T (1991) Structural analysis and functional role of the carbohydrate component of somatostatin receptors. J Biol Chem 266(30):20094–20102
52. Bertin B, Freissmuth M, Breyer R, Schütz W, Strosberg A, Marullo S (1992) Functional expression of the human serotonin 5-HT1A receptor in Escherichia coli. Ligand binding properties and interaction with recombinant G protein alpha-subunits. J Biol Chem 267(12):8200–8206

53. Furukawa H, Haga T (2000) Expression of functional M2 muscarinic acetylcholine receptor in *Escherichia coli*. J Biochem 127(1):151–161
54. Hampe W, Voss R-H, Haase W, Boege F, Michel H, Reiländer H (2000) Engineering of a proteolytically stable human β_2-adrenergic receptor/maltose-binding protein fusion and production of the chimeric protein in *Escherichia coli* and baculovirus-infected insect cells. J Biotechnol 77(2):219–234
55. Weiß HM, Grisshammer R (2002) Purification and characterization of the human adenosine A_{2a} receptor functionally expressed in *Escherichia coli*. Eur J Biochem 269(1):82–92
56. Yeliseev AA, Wong KK, Soubias O, Gawrisch K (2005) Expression of human peripheral cannabinoid receptor for structural studies. Protein Sci 14(10):2638–2653
57. Freissmuth M, Selzer E, Marullo S, Schütz W, Strosberg AD (1991) Expression of two human beta-adrenergic receptors in Escherichia coli: functional interaction with two forms of the stimulatory G protein. Proc Nat Acad Sci 88(19):8548–8552
58. Hill RA, Sillence MN (1997) Improved membrane isolation in the purification of β_2-adrenoceptors from transgenic *Escherichia coli*. Protein Expr Purif 10(1):162–167
59. Lacatena RM, Cellini A, Scavizzi F, Tocchini-Valentini GP (1994) Topological analysis of the human beta 2-adrenergic receptor expressed in *Escherichia coli*. Proc Nat Acad Sci 91(22):10521–10525
60. Kiefer H, Maier K, Vogel R (1999) Refolding of G-protein-coupled receptors from inclusion bodies produced in *Escherichia coli*. Biochem Soc Trans 27(6):908–912
61. LaVallie ER, McCoy JM (1995) Gene fusion expression systems in *Escherichia coli*. Curr Opin Biotechnol 6(5):501–506
62. Lundstrom K, Wagner R, Reinhart C, Desmyter A, Cherouati N, Magnin T, Zeder-Lutz G, Courtot M, Prual C, André N (2006) Structural genomics on membrane proteins: comparison of more than 100 GPCRs in 3 expression systems. J Struct Funct Gen 7(2):77–91
63. Bernaudat F, Frelet-Barrand A, Pochon N, Dementin S, Hivin P, Boutigny S, Rioux J-B, Salvi D, Seigneurin-Berny D, Richaud P (2011) Heterologous expression of membrane proteins: choosing the appropriate host. PLoS One 6(12):e29191
64. Miroux B, Walker JE (1996) Over-production of proteins in Escherichia coli: mutant hosts that allow synthesis of some membrane proteins and globular proteins at high levels. J Mol Biol 260(3):289–298
65. Michalke K, Huyghe C, Lichière J, Gravière M-E, Siponen M, Sciara G, Lepaul I, Wagner R, Magg C, Rudolph R (2010) Mammalian G protein-coupled receptor expression in *Escherichia coli*: II. Refolding and biophysical characterization of mouse cannabinoid receptor 1 and human parathyroid hormone receptor 1. Anal Biochem 401(1):74–80
66. Nilsson I, von Heijne G (1990) Fine-tuning the topology of a polytopic membrane protein: role of positively and negatively charged amino acids. Cell 62(6):1135–1141
67. Gafvelin G, von Heijne G (1994) Topological "frustration" in multispanning *E. coli* inner membrane proteins. Cell 77(3):401–412
68. Hulme E (1992) Receptor biochemistry: a practical approach. IRL Press, Oxford
69. Wang J (2005) Nanomaterial-based electrochemical biosensors. Analyst 130(4):421–426
70. Jianrong C, Yuqing M, Nongyue H, Xiaohua W, Sijiao L (2004) Nanotechnology and biosensors. Biotechnol Adv 22(7):505–518
71. Jacobs CB, Peairs MJ, Venton BJ (2010) Review: carbon nanotube based electrochemical sensors for biomolecules. Anal Chim Acta 662(2):105–127
72. Song HS, Park TH (2011) Integration of biomolecules and nanomaterials: towards highly selective and sensitive biosensors. Biotechnol J 6(11):1310–1316
73. Oh EH, Song HS, Park TH (2011) Recent advances in electronic and bioelectronic noses and their biomedical applications. Enzyme Microb Technol 48(6):427–437
74. Neuhaus EM, Mashukova A, Zhang W, Barbour J, Hatt H (2006) A specific heat shock protein enhances the expression of mammalian olfactory receptor proteins. Chem Senses 31(5):445–452

75. Gelis L, Wolf S, Hatt H, Neuhaus EM, Gerwert K (2012) Prediction of a ligand-binding niche within a human olfactory receptor by combining site-directed mutagenesis with dynamic homology modeling. Angew Chem Int Ed Engl 51(5):1274–1278
76. Mashukova A, Spehr M, Hatt H, Neuhaus EM (2006) β-arrestin2-mediated internalization of mammalian odorant receptors. J Neurosci 26(39):9902–9912
77. Kwon OS, Lee SH, Park SJ, An JH, Song HS, Kim T, Oh JH, Bae J, Yoon H, Park TH (2013) Large- scale graphene micropattern nano- biohybrids: high- performance transducers for FET- type flexible fluidic HIV immunoassays. Adv Mater 25(30):4177–4185
78. Park SJ, Kwon OS, Lee SH, Song HS, Park TH, Jang J (2012) Ultrasensitive flexible graphene based field-effect transistor (FET)-type bioelectronic nose. Nano Lett 12(10):5082–5090
79. Kim TH, Song HS, Jin HJ, Lee SH, Namgung S, Kim U-k, Park TH, Hong S (2011) "Bio-electronic super-taster" device based on taste receptor-carbon nanotube hybrid structures. Lab Chip 11(13):2262–2267
80. Kwon OS, Ahn SR, Park SJ, Song HS, Lee SH, Lee JS, Hong J-Y, Lee JS, You SA, Yoon H, Park TH, Jang J (2012) Ultrasensitive and selective recognition of peptide hormone using close-packed arrays of hPTHR-conjugated polymer nanoparticles. ACS Nano 6(6):5549–5558
81. Song HS, Kwon OS, Lee SH, Park SJ, Kim U-K, Jang J, Park TH (2013) Human taste receptor-functionalized field effect transistor as a human-like nanobioelectronic tongue. Nano Lett 13(1):172–178
82. Kim U-k, Jorgenson E, Coon H, Leppert M, Risch N, Drayna D (2003) Positional cloning of the human quantitative trait locus underlying taste sensitivity to phenylthiocarbamide. Science 299(5610):1221–1225
83. Bufe B, Breslin PA, Kuhn C, Reed DR, Tharp CD, Slack JP, Kim U-K, Drayna D, Meyerhof W (2005) The molecular basis of individual differences in phenylthiocarbamide and propylthiouracil bitterness perception. Curr Biol 15(4):322–327
84. Kim B, Song HS, Jin HJ, Park EJ, Lee SH, Lee BY, Park TH, Hong S (2013) Highly selective and sensitive detection of neurotransmitters using receptor-modified single-walled carbon nanotube sensors. Nanotechnology 24(28):285501
85. Schwartz TW (1994) Locating ligand-binding sites in 7TM receptors by protein engineering. Curr Opin Biotechnol 5(4):434–444
86. Rosenbaum DM, Rasmussen SG, Kobilka BK (2009) The structure and function of G-protein-coupled receptors. Nature 459(7245):356–363
87. Firestein S (2001) How the olfactory system makes sense of scents. Nature 413(6852):211–218
88. Krautwurst D, Yau K-W, Reed RR (1998) Identification of ligands for olfactory receptors by functional expression of a receptor library. Cell 95(7):917–926
89. Malnic B, Hirono J, Sato T, Buck LB (1999) Combinatorial receptor codes for odors. Cell 96(5):713–723
90. Lee SH, Jun SB, Ko HJ, Kim SJ, Park TH (2009) Cell-based olfactory biosensor using microfabricated planar electrode. Biosens Bioelectron 24(8):2659–2664
91. Lee JY, Ko HJ, Lee SH, Park TH (2006) Cell-based measurement of odorant molecules using surface plasmon resonance. Enzyme Microb Technol 39(3):375–380
92. Lee SH, Ko HJ, Park TH (2009) Real-time monitoring of odorant-induced cellular reactions using surface plasmon resonance. Biosens Bioelectron 25(1):55–60
93. Saito H, Chi Q, Zhuang H, Matsunami H, Mainland JD (2009) Odor coding by a mammalian receptor repertoire. Sci Signal 2(60):ra9
94. Zhao H, Ivic L, Otaki JM, Hashimoto M, Mikoshiba K, Firestein S (1998) Functional expression of a mammalian odorant receptor. Science 279(5348):237–242
95. Hatt H, Gisselmann G, Wetzel C (1999) Cloning, functional expression and characterization of a human olfactory receptor. Cell Mol Biol 45(3):285–291
96. Touhara K, Sengoku S, Inaki K, Tsuboi A, Hirono J, Sato T, Sakano H, Haga T (1999) Functional identification and reconstitution of an odorant receptor in single olfactory neurons. Proc Nat Acad Sci 96(7):4040–4045

97. Bozza T, Feinstein P, Zheng C, Mombaerts P (2002) Odorant receptor expression defines functional units in the mouse olfactory system. J Neurosci 22(8):3033–3043
98. Gaillard I, Rouquier S, Pin JP, Mollard P, Richard S, Barnabe C, Demaille J, Giorgi D (2002) A single olfactory receptor specifically binds a set of odorant molecules. Eur J Neurosci 15(3):409–418
99. Spehr M, Gisselmann G, Poplawski A, Riffell JA, Wetzel CH, Zimmer RK, Hatt H (2003) Identification of a testicular odorant receptor mediating human sperm chemotaxis. Science 299(5615):2054–2058
100. Kajiya K, Inaki K, Tanaka M, Haga T, Kataoka H, Touhara K (2001) Molecular bases of odor discrimination: reconstitution of olfactory receptors that recognize overlapping sets of odorants. J Neurosci 21(16):6018–6025
101. Lu M, Staszewski L, Echeverri F, Xu H, Moyer BD (2004) Endoplasmic reticulum degradation impedes olfactory G-protein coupled receptor functional expression. BMC Cell Biol 5(1):34
102. Brady AE, Limbird LE (2002) G protein-coupled receptor interacting proteins: emerging roles in localization and signal transduction. Cell Signal 14(4):297–309
103. Sung C-H, Schneider BG, Agarwal N, Papermaster DS, Nathans J (1991) Functional heterogeneity of mutant rhodopsins responsible for autosomal dominant retinitis pigmentosa. Proc Nat Acad Sci 88(19):8840–8844
104. Oka Y, Omura M, Kataoka H, Touhara K (2003) Olfactory receptor antagonism between odorants. EMBO J 23(1):120–126
105. Katada S, Nakagawa T, Kataoka H, Touhara K (2003) Odorant response assays for a heterologously expressed olfactory receptor. Biochem Biophys Res Commun 305(4):964–969
106. Wetzel CH, Oles M, Wellerdieck C, Kuczkowiak M, Gisselmann G, Hatt H (1999) Specificity and sensitivity of a human olfactory receptor functionally expressed in human embryonic kidney 293 cells and Xenopus Laevis Oocytes. J Neurosci 19(17):7426–7433
107. Abaffy T, Matsunami H, Luetje CW (2006) Functional analysis of a mammalian odorant receptor subfamily. J Neurochem 97(5):1506–1518
108. Cooray SN, Chan L, Webb TR, Metherell L, Clark AJ (2009) Accessory proteins are vital for the functional expression of certain G protein-coupled receptors. Mol Cell Endocrinol 300(1):17–24
109. Kohno M, Fukushima N, Yoshida A, Ueda H (2000) G_{i1} and G_{oA} differentially determine kinetic efficacies of agonists for κ-opioid receptor. FEBS Lett 473(1):101–105
110. Fredriksson R, Lagerström MC, Lundin L-G, Schiöth HB (2003) The G-protein-coupled receptors in the human genome form five main families. Phylogenetic analysis, paralogon groups, and fingerprints. Mol Pharmacol 63(6):1256–1272
111. Chelikani P, Reeves PJ, Rajbhandary UL, Khorana HG (2006) The synthesis and high-level expression of a β2- adrenergic receptor gene in a tetracycline- inducible stable mammalian cell line. Protein Sci 15(6):1433–1440
112. Reeves PJ, Callewaert N, Contreras R, Khorana HG (2002) Structure and function in rhodopsin: high-level expression of rhodopsin with restricted and homogeneous N-glycosylation by a tetracycline-inducible N-acetylglucosaminyltransferase I-negative HEK293S stable mammalian cell line. Proc Nat Acad Sci 99(21):13419–13424
113. Reeves PJ, Kim J-M, Khorana HG (2002) Structure and function in rhodopsin: a tetracycline-inducible system in stable mammalian cell lines for high-level expression of opsin mutants. Proc Nat Acad Sci 99(21):13413–13418
114. Hassaine G, Wagner R, Kempf J, Cherouati N, Hassaine N, Prual C, André N, Reinhart C, Pattus F, Lundstrom K (2006) Semliki Forest virus vectors for overexpression of 101 G protein-coupled receptors in mammalian host cells. Protein Expr Purif 45(2):343–351
115. Krieger J, Breer H (1999) Olfactory reception in invertebrates. Science 286(5440):720–723
116. Zufall F, Firestein S, Shepherd G (1994) Cyclic nucleotide-gated ion channels and sensory transduction in olfactory receptor neurons. Annu Rev Biophy Biomol Struct 23(1):577–607
117. Ache BW, Zhainazarov A (1995) Dual second-messenger pathways in olfactory transduction. Curr Opin Neurobiol 5(4):461–466

118. Ko HJ, Park TH (2006) Dual signal transduction mediated by a single type of olfactory receptor expressed in a heterologous system. Biol Chem 387(1):59–68
119. Liu Q, Cai H, Xu Y, Li Y, Li R, Wang P (2006) Olfactory cell-based biosensor: a first step towards a neurochip of bioelectronic nose. Biosens Bioelectron 22(2):318–322
120. Wang P, Xu G, Qin L, Xu Y, Li Y, Li R (2005) Cell-based biosensors and its application in biomedicine. Sens Actuators B 108(1):576–584
121. Jin HJ, Lee SH, Kim TH, Park J, Song HS, Park TH, Hong S (2012) Nanovesicle-based bioelectronic nose platform mimicking human olfactory signal transduction. Biosens Bioelectron 35(1):355–341
122. Park J, Lim JH, Jin HJ, Namgung S, Lee SH, Park TH, Hong S (2012) A bioelectronic sensor based on canine olfactory nanovesicle–carbon nanotube hybrid structures for the fast assessment of food quality. Analyst 137(14):3249–3254
123. Pick H, Schmid EL, Tairi A-P, Ilegems E, Hovius R, Vogel H (2005) Investigating cellular signaling reactions in single attoliter vesicles. J Am Chem Soc 127(9):2908–2912
124. Massotte D (2003) G protein-coupled receptor overexpression with the baculovirus–insect cell system: a tool for structural and functional studies. Biochim Biophys Acta 1610(1):77–89
125. Ailor E, Betenbaugh MJ (1999) Modifying secretion and post-translational processing in insect cells. Curr Opin Biotechnol 10(2):142–145
126. Kleymann G, Boege F, Hahn M, Hampe W, Vasudeva S, Reiländer H (1993) Human β2-adrenergic receptor produced in stably transformed insect cells is functionally coupled via endogenous GTP- binding protein to adenylyl cyclase. Eur J Biochem 213(2):797–804
127. Kühn B, Gudermann T (1999) The luteinizing hormone receptor activates phospholipase C via preferential coupling to Gi2. Biochemistry 38(38):12490–12498
128. Mulheron JG, Casanas SJ, Arthur JM, Garnovskaya MN, Gettys TW, Raymond JR (1994) Human 5-HT1A receptor expressed in insect cells activates endogenous G (o)-like G protein (s). J Biol Chem 269(17):12954–12962
129. Hiroaki Y, Arimoto I, Fujiyoshi Y, Okamoto T, Satoh M, Furuichi Y (1997) Characterization of human endothelin B receptor and mutant receptors expressed in insect cells. Eur J Biochem 248(1):139–148
130. Robeva AS, Woodard R, Luthin DR, Taylor HE, Linden J (1996) Double tagging recombinant $A_1$and A_{2A}-adenosine receptors with hexahistidine and the FLAG epitope: development of an efficient generic protein purification procedure. Biochem Pharmacol 51(4):545–555
131. Glass M, Northup JK (1999) Agonist selective regulation of G proteins by cannabinoid CB1 and CB2 receptors. Mol Pharmacol 56(6):1362–1369
132. Hartman JL, Northup JK (1996) Functional reconstitution in situ of 5-hydroxytryptamine2c (5HT2c) receptors with αq and inverse agonism of 5HT2c receptor antagonists. J Biol Chem 271(37):22591–22597
133. Parker EM, Kameyama K, Higashijima T, Ross EM (1991) Reconstitutively active G protein-coupled receptors purified from baculovirus-infected insect cells. J Biol Chem 266(1):519–527
134. Mroczkowski BS, Huvar A, Lernhardt W, Misono K, Nielson K, Scott B (1994) Secretion of thermostable DNA polymerase using a novel baculovirus vector. J Biol Chem 269(18):13522–13528
135. Murphy CI, McIntire J, Davis Dv, Hodgdon H, Seals J, Young E (1993) Enhanced expression, secretion, and large-scale purification of recombinant HIV-1 gp120 in insect cells using the baculovirus egt and p67 signal peptides. Protein Expr Purif 4(5):349–357
136. Allet B, Bernard AR, Hochmann A, Rohrbach E, Graber P, Magnenat E, Mazzei GJ, Bernasconi L (1997) A bacterial signal peptide directs efficient secretion of eukaryotic proteins in the baculovirus expression system. Protein Expr Purif 9(1):61–68
137. Raming K, Krieger J, Strotmann J, Boekhoff I, Kubick S, Baumstark C, Breer H (1993) Cloning and expression of odorant receptors. Nature 361(6410):353–356

138. Nekrasova E, Sosinskaya A, Natochin M, Lancet D, Gat U (1996) Overexpression, solubization and purification of rat and human olfactory receptors. Eur J Biochem 238(1):28–37
139. Matarazzo V, Clot-Faybesse O, Marcet B, Guiraudie-Capraz G, Atanasova B, Devauchelle G, Cerutti M, Etiévant P, Ronin C (2005) Functional characterization of two human olfactory receptors expressed in the baculovirus Sf9 insect cell system. Chem Sens 30(3):195–207
140. Bayburt TH, Grinkova YV, Sligar SG (2002) Self-assembly of discoidal phospholipid bilayer nanoparticles with membrane scaffold proteins. Nano Lett 2(8):853–856
141. Denisov I, Grinkova Y, Lazarides A, Sligar S (2004) Directed self-assembly of monodisperse phospholipid bilayer Nanodiscs with controlled size. J Am Chem Soc 126(11):3477–3487

Chapter 10
Biosensors Based on Odorant Binding Proteins

Krishna C. Persaud and Elena Tuccori

Abstract Both the sensillary lymph of insects and the nasal mucus of vertebrates contain large amounts of small soluble proteins, odorant-binding proteins that specifically and reversibly bind odors and pheromones. Proteins from different sources have affinities toward a wide range of compounds with different sizes and shapes. They can be easily expressed in heterologous systems, they show high thermal stability and it is possible to modify their binding sites by site-directed mutagenesis. We describe the development of an odor sensing biosensor array based on immobilization of odorant binding proteins on to suitable transducers. Using a quartz crystal microbalance platform as a transduction element, it is possible to detect and measure quantitatively concentrations of volatile analytes at parts per million concentrations in air.

10.1 Introduction

A biosensor can be defined as an analytical device that converts a biological interaction into a measurable electrical signal [1]. Biosensors are commonly composed of a recognition element (receptor), a signal conversion unit (transducer) and an output interface. It is possible to classify them on the basis of commonly used receptor and transducer elements as summarized in Fig. 10.1. This involves a combination of two steps: a recognition step and a transduction step. The recognition step involves a biological sensing element or receptor that can recognize biological or chemical analytes in solution or in the ambient atmosphere. The receptor may be proteins, such as antibodies or enzymes, DNA, peptide sequences or whole cells. The receptor elements are in close contact with a transducer that converts the analyte-receptor interaction into a quantitative electrical or optical signal [2].

The detection of chemical signals in the environment, which provides information on food, mates, danger, predators and pathogens, is essential for the survival of most mammals and insects. Animals have developed a highly sophisticated olfactory system, able to distinguish between thousands of diverse volatile compounds.

K. C. Persaud (✉) · E. Tuccori
School of Chemical Engineering and Analytical Science, The University of Manchester, Manchester M13 9PL, UK
e-mail: krishna.persaud@manchester.ac.uk

T. H. Park (ed.), *Bioelectronic Nose,* DOI 10.1007/978-94-017-8613-3_10,

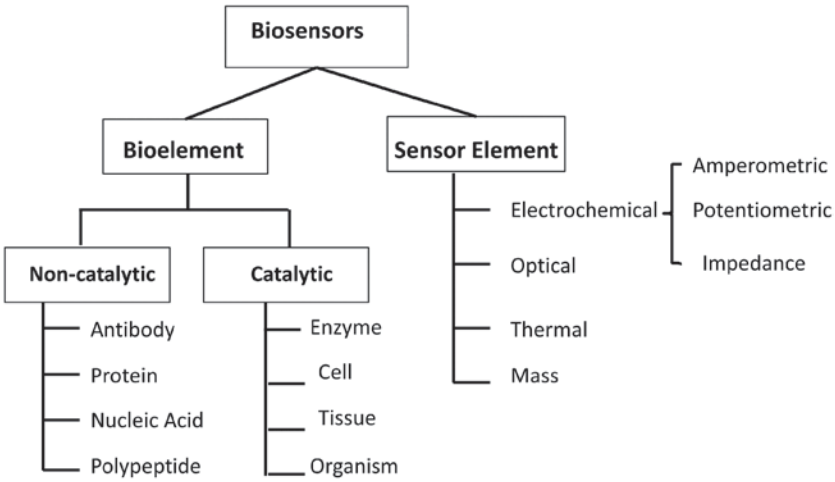

Fig. 10.1 Biosensor transduction methods

Humans, for example, can detect many thousands of different molecules [3]. There is much interest in development of olfactory biosensors that may mimic some aspects of performance of the olfactory system and these activities have been reviewed by Persaud (2012) [4] and Du (2013) [5].

Vertebrates and insects detect volatile compounds from the environment and integrate these signals with other sensory stimuli such as sight and hearing in order to obtain a complete map of the immediate environment. In vertebrates and in insects, the olfactory neurons are separated from the air by a protective layer made up of the nasal mucus and sensillary lymph, respectively. The odorants, and pheromones which are hydrophobic and volatile molecules, have to cross this hydrophilic barrier to reach the olfactory receptor neurons. Both the sensillary lymph of insects and the nasal mucus of vertebrates contain large amounts of small soluble proteins, odorant-binding proteins that specifically and reversibly bind odors and pheromones [6]. The very high concentrations of these proteins in their respective fluids, as well as their rapid turnover, suggest functions important in the perception of olfactory stimuli. They are involved in the binding of numerous hydrophobic ligands with affinity in the micromolar range. The high conformational stability of these proteins as well as the wide variety of OBPs isolated in mammals and insects make them interesting in constructing biosensors that can also function as chemical sensors for volatiles [7]. In this chapter we describe the development of an odor sensing biosensor array based on odorant binding proteins.

10.1.1 Biosensor Recognition Elements

The recognition element is the biological component of the biosensor that produces the signal. There are various types of recognition elements, ranging from whole

cells to specific molecules. Recognition elements can be divided into two general categories: non-catalytic elements and catalytic elements [8, 9].

Non-catalytic elements, such as antibodies, protein receptors, polypeptides, DNA, are often used for direct detection biosensors, in which the interaction with the target compound is monitored in real time. Antibodies are the most commonly used non-catalytic recognition elements, because they are highly specific, versatile and have high affinities towards the target molecules.

For the catalytic elements, the recognition elements can be enzymes, organelles, whole cells or organisms. They are used primarily in indirect detection biosensors, in which the interaction between the biological component and the target analyte releases a detectable second molecule.

Enzymes are the most widely used catalytic detectors, because they have high level of amplification in biorecognition processes and good selectivity. The most important enzymes from an analytical point of view are the oxidoreductases, which use oxygen or nicotinamide adenine dinucleotide (NAD) to catalyze the oxidation of substrates, or hydrolases, which catalyze the hydrolysis of compounds. For example, glucose oxidase (GOD) catalyses the oxidation of glucose to gluconic acid, which forms the basis of glucose monitoring for diabetics [1].

10.1.2 Transducers

The transducer converts the bio-recognition event into a measurable signal. Transducers can be clustered in four main classes on the basis of the method used [10]:

1. Electrochemical detection methods;
2. Optical detection methods;
3. Acoustic (mass detection) methods;
4. Thermal detection method (not described here).

Amperometric and potentiometric systems typify the most commonly used electrochemical transducers. The detection of analytes by the biological elements of biosensor often generates chemical species that can be measured by electrochemical methods. The principle of operation of amperometric biosensors is defined by a constant potential applied between a working and a reference electrode. The imposed potential promotes a redox reaction at the electrode surface, which produces a current. The magnitude of this current is proportional to the concentration of electro active species present in solution [11–13]. The simplest amperometric biosensor in common usage is the Clark oxygen electrode (Fig. 10.2). This consists of a platinum cathode at which oxygen is reduced and a silver/silver chloride reference electrode. When a potential is applied to the platinum cathode, a current proportional to the oxygen concentration is produced. In potentiometry, a glass membrane or a polymeric membrane electrode is used for measuring the membrane potential resulting from the difference in the concentrations of H^+ or other positive ions across the membrane. Amperometric or potentiometric transducers can be employed in the

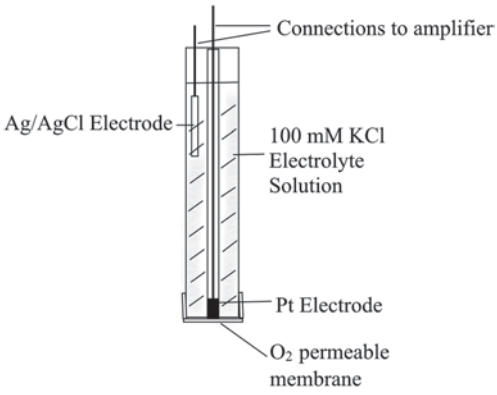

Fig. 10.2 Clark oxygen electrode. The reaction chamber is separated from the electrodes by a semipermeable membrane, which permits oxygen to diffuse from the reaction buffer into the potassium chloride solution that bathes the electrodes: a platinum cathode and a silver anode. A voltage is applied between the electrodes and the resulting current (in the μA range) is proportional to the concentration of oxygen

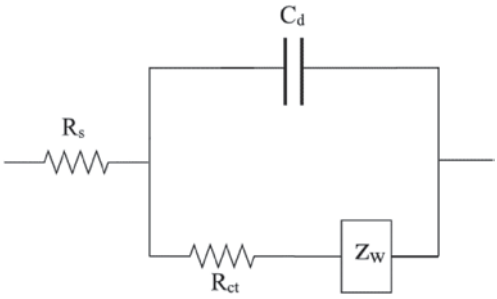

Fig. 10.3 Randles equivalent circuit. Impedance measurements are often fitted to the Randles equivalent circuit, where R_{ct} is the charge-transfer resistance, C_d is the differential capacitance, R_s is the solution-phase resistance and Z_w is the Warburg diffusion element

case of catalytic receptor elements, mainly enzymes that convert the target analyte into a detectable product.

Biosensors based on impedance, can be also classified as electrochemical transducers. Impedance measurements involve application of a small sinusoidal alternate current (AC) voltage probe and determination of the current response. Impedance measurements are often fitted to the Randles equivalent circuit shown in Fig. 10.3, where R_{ct} is the charge-transfer resistance, C_d is the differential capacitance, R_s is the solution-phase resistance and Z_w is the Warburg diffusion element [14]. The Randles circuit describes the Faradaic impedance. In this case, it is necessary to have a redox species in solution where it is possible to monitor the charge transfer resistance. Impedance sensors detect a change in one of these equivalent circuit parameters due to the direct interactions of the target analyte with the probe.

Optical sensors rely on the optical transduction of the signal and comprise ultraviolet, visible and infrared spectrophotometry in transmission or reflectance modes. The relationship between the incident light intensity and the transmitted radiation is given by the Beer–Lambert law. Optical methods have been used classically to determine analyte concentrations. Properties like absorption, refractive indices, fluorescence, phosphorescence, chemiluminescence, etc., can be used in order to

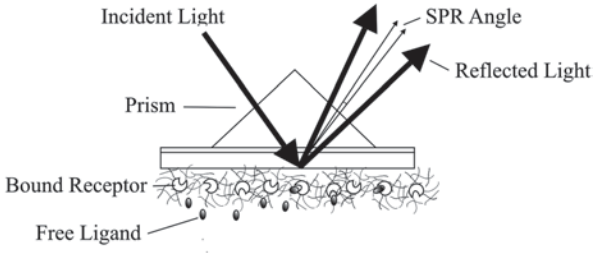

Fig. 10.4 Surface plasmon resonance sensor. SPR measures minute changes in refractive index at and near the surface of the sensing element. SPR measurement is based on the detection of the attenuated total reflection of light in a prism with one side coated with a metal. When a p-polarized incident light passes through the prism and strikes the metal at an adequate angle, it induces a resonant charge wave at the metal/dielectric interface that propagates a few microns. The total reflection is measured with a photodetector, as a function of the incident angle. For example, when an ligand binds to a recognition element (protein, antibody or other) that is immobilized on the exposed surface of the metal the measured reflectivity increases. This increase in reflectivity can then be correlated to the concentration of the ligand

monitor the biological recognition in biosensors. The devices can be miniaturized by using optical fibers, which act as light guides. The detectors are often semiconductor photodiodes. These devices are often used for remote analysis as the light signal is resistant to electrical noise. Optical fiber biosensors can be used in combination with different types of spectroscopic techniques, e.g. absorption, fluorescence, phosphorescence, surface plasmon resonance, etc [15].

Surface Plasmon Resonance (SPR) is a real-time, label-free, optical detection method for studying the interaction of soluble analytes with immobilized ligands or receptors [16–18]. SPR measures minute changes in refractive index at and near the surface of the sensing element. SPR measurement is based on the detection of the attenuated total reflection of light in a prism with one side coated with a metal (Fig. 10.4). When a p-polarized incident light passes through the prism and strikes the metal at an adequate angle, it induces a resonant charge wave at the metal/dielectric interface that propagates a few microns. The total reflection is measured with a photo detector, as a function of the incident angle. For example, when an antigen binds to an antibody that is immobilized on the exposed surface of the metal the measured reflectivity increases. This increase in reflectivity can then be correlated to the concentration of the antigen [19].

Mass transducers measure small changes in mass due to the interaction between the analyte and the biological component of the biosensor. The piezoelectric silica crystals called quartz crystal microbalances (QCM) are the most common mass transducers (Fig. 10.5) and is used to measure very small mass changes in the order of picograms [20–22]. The principle is based on the piezo-electric properties of quartz crystals. Indeed, if an electrical field is applied through quartz, the inner dipoles are re-orientated and a crystalline mechanical strain is observed. When the

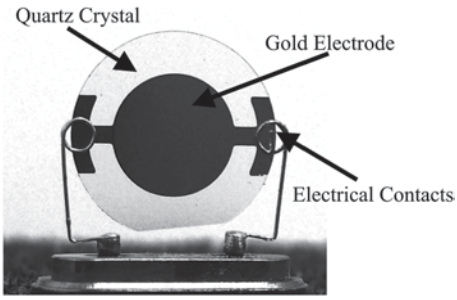

Fig. 10.5 Quartz crystal microbalance. A typical quartz crystal microbalance (QCM) used for mass measurements. If a potential difference is applied between the electrodes of the QCM, the physical orientation of the crystal lattice is distorted, resulting in a mechanical oscillation of a standing shear wave across the bulk of the quartz disk at a characteristic vibrational frequency (i.e. the crystal's natural resonant frequency). The direction of the oscillation depends on the exact geometry of the cut of the quartz crystal

crystal is included in an appropriate electronic circuit, the oscillation frequency measured is closed to the resonant frequency and the generated wave amplitude reaches a maximum value. Modification of a physical characteristic of the resonator, for example changes in global mass or thickness, lead to a variation of the resonant frequency. The frequency change is directly proportional to the mass of the crystal [23]. For biosensors, mass changes occurring when the modified transducer surface interacts with the detected species are common, and this change can be easily measured.

10.1.3 Immobilization

One key factor in the construction of a biosensor is to develop an immobilization method for binding biomolecules on the surface of the transducer. The immobilization technique should not alter the activity, structure and function of the biological component and should assure long-term stability of the active layer of the biosensor. Biological films need to be immobilized using reproducible methods, and once formed these should adapt to different environments, maintaining their stability and activity during changes in temperature, pH, ionic strength and chemical composition [19, 24–26].

The principal methods of immobilization are:

1. Physical or chemical adsorption;
2. Covalent binding;
3. Entrapment within a membrane, surfactant matrix, polymer or Microcapsule;
4. Cross-linking between molecules.

The immobilization method employed depends on many factors, but in general the method needs to be compatible with the biomolecules to be immobilized, the sensor surface or matrix and ultimately the end use of the sensor.

Adsorption of biomolecules from solution onto solid surfaces can proceed via either physical or chemical interactions. Physical adsorption involves Van der Waals forces, ionic binding or hydrophobic forces, whereas in chemical adsorption there is a sharing or transfer of electrons to form a chemical bond. The main advantage associated with direct adsorption onto solid surfaces is that is a simple method which can be performed under mild conditions. In general, however, biomolecules that are adsorbed on to a surface exhibit some degree of reversibility, and with few exceptions, the forces involved in the binding are not very strong. Moreover, irregular distributions of randomly oriented proteins are commonly observed on the surface [27, 28]. Since such protein molecules exhibit multiple-binding sites, they can bind to solid surfaces through various groups in a disorganized manner. Despite these problems, simple adsorption remains the major method used in clinical assays.

An alternative approach to attach biomolecules on sensor surfaces is via covalent binding. Biomolecules are immobilized on solid surfaces through the formation of defined linkages. Covalent binding of biomolecules to the surface is a procedure resulting in minimal loss of biomolecules activity. This method has been employed to improve uniformity, density and distribution of the bound proteins, as well as the reproducibility of the surfaces. Problems associated with instability, diffusion, aggregation or inactivation of proteins can also be overcome by using covalent immobilization. Biomolecules such as enzymes and proteins expose many functional groups on their surface that can be used for covalent immobilization on the transducer; these include amino-acid side chains (e.g. amino groups of lysine), carboxyl groups (aspartic acid and glutamic acid), sulfhydryl groups (cysteine), etc. It is important that functional groups involved in the immobilization reaction of biomolecules on the surface do not result in a loss of activity. Suitable functional groups which are available for covalent attachment are also present on some transducer materials (hydroxyl groups on silica). Metal surfaces such as gold and silver can be modified by reaction with hydroxyalkanethiols to generate hydroxyl, carboxyl or amino groups which may react with enzymes or proteins. This technique includes the Self Assembled Monolayer's (SAMs) method. SAMs are well organized two- or three-dimensional supramolecular structures formed by the adsorption of an active surfactant on a solid surface [29–31] (Fig. 10.6). The spontaneous self assembly is driven by specific interactions between the head functional groups of the "self-assembling molecules" and the surface, followed by a self-organization of a monomolecular film on the surface, which is stabilized by non-covalent interactions among the same molecules. This process is widely used to modify solid surfaces.

The class of monolayer, commonly used in biosensor applications is based on the strong adsorption of disulfides (R–S– S–R), sulfides (R–S–R) and thiols (R–SH) on a metal surface, gold, platinum, silver [32]. Gold is the substrate more commonly used for growing SAMs, since it is possible to obtain thin gold films by thermal evaporation; it is inert to the gases present in the atmosphere and is easy to clean.

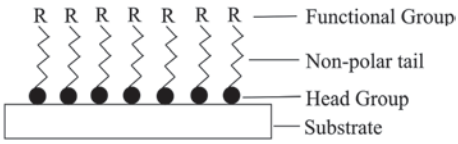

Fig. 10.6 Self assembled monolayers. The spontaneous self assembly is driven by specific interactions between the head functional groups of the "self-assembling molecules" and the surface, followed by a self-organization of a monomolecular film on the surface, which is stabilized by non-covalent interactions among the same molecules

Thiols are chemisorbed on gold through the oxidation of the S-H bond, followed by a reductive elimination of hydrogen and formation of thiolate ions, while the adsorption of disulfides is due to a simple oxidative addition of the S-S bond on the gold surface. The formation of a self assembly monolayer of alkylthiols on gold surfaces has a biphasic kinetic behavior. After an initial fast step which is led by the reaction of the sulphur group on the gold surface, a slow second phase starts the formation of a crystallized surface, where alkyl chains relax from the disordered state and organize into unit cells, thus forming a two-dimensional crystal [33].

SAMs of thiols on gold seems to be the most promising technique for making protein biosensors. Alkylthiols used in the SAMs often carrying carboxylic functional groups that may be easily activated by carbodiimide, forming stable peptide bonds with the proteins' amino groups.

The procedure of entrapping biological components in polymer gels, membranes or surfactant matrices has been used with success in the past and it is still widely employed [34]. The immobilization of an enzyme in a polymeric gel or behind a membrane is a relatively straightforward process. A number of polymers have been used for the inclusion of enzymes, cells and organelles. These include polyvinyl alcohol, polyvinyl chloride, polycarbonate, polyacrylamide and cellulose acetate. Methods used for the entrapment of biological components, however, suffer from the disadvantage of leakage of the biological species during the use, resulting in a loss of activity [35].

Cross-linking of biological components by multifunctional reagents affords good stability to the adsorbed enzymes or proteins. Glutaraldehyde, which couples with the lysine amino groups of enzymes, is by far the most common cross-linking agent in biosensor applications. Biosensors, where the enzymes were immobilized in a glutaraldehyde matrix or in combination with natural polymers as chitosan, were often used [36]. However, there are a number of disadvantages associated with this method: the reaction is difficult to control, the protein layer formed is usually gelatinous and not rigid and large amounts of biological material are required. Cross-linking can result in the formation of multilayer's of protein or enzyme resulting in low activity of the immobilized layers and large diffusion barriers to the transport of the biological species may result, leading to slow interactions [35].

10.2 Odorant Binding Proteins

Discovered almost simultaneously by Pelosi and coworkers in vertebrates [37] and by Vogt and Riddiford in insects [38], it was shown that the nasal mucus of vertebrates and the chemosensillar lymph of insect antennae contain large amounts of small soluble proteins, odorant-binding proteins, that specifically and reversibly bind odor molecules and pheromones [6, 39, 40]. The very high concentrations of these proteins in their respective fluids, as well as their rapid turnover, suggest functions that are important for the individual or for the species. They are involved in the binding of numerous hydrophobic ligands with affinity in the micromolar range. Some similar proteins such as pheromone-binding proteins (PBPs) [41], major urinary proteins (MUPs) in rodents [42–46] or salivary lipocalin (SAL) in the boar [47, 48] are clearly involved in vertebrate chemical communication, binding with high specificity sex pheromone components. On the contrary, the sub-class of odorant binding proteins (OBPs) has the ability to bind a wide range of ligands, without displaying high specificity [6, 39, 40].

When OBPs were first isolated in vertebrates, it was hypothesized that they could be responsible for recognizing olfactory stimuli acting as carriers or scavengers for the hydrophobic molecules of odorants, but their exact role in olfaction is still uncertain. It is largely agreed that OBPs function as solubilizers for odorants [49–52]. Generally, odorants are small hydrophobic molecules that are unable to easily cross the air-liquid interface of the olfactory epithelium in vertebrates or the sensillary lymph in insects. Upon binding to the hydrophilic water soluble OBPs, odorants become solubilized and can thus be transported across perireceptor space, to odorant receptors (ORs). This serves to protect the ligands against degradation by enzymes, such as UDP-glycosyltransferases and sensillary esterases [53]. Opposed to the view that OBPs function as general odorant carriers, the numerous OBPs discovered and the selectivity of each of these for odorant subclasses, in addition to interactions with specific subclasses of olfactory sensory neurons, suggest that OBPs serve a much wider function [54, 55].

It is now proposed that OBPs are involved in the peripheral processing of olfaction. This is demonstrated by the generation of LUSH mutant Drosophila flies, which fail to display normal behavioral responses to odorants. Kim et al. (1998) [56] developed mutant flies for LUSH, an OBP expressed in the third antennal segment of Drosophila, from a 3 kb genetic deletion, which included a transcription unit for LUSH, thereby preventing its expression. These LUSH mutants did not display the normal aversive behavior to high concentrations of short-chain alcohols, observed in control flies. Interestingly, the reintroduction of the LUSH transgene allowed recovery of the avoidance response. Xu et al (2005) [57, 58] further demonstrated that LUSH mutants do not exhibit social aggregation in response to the pheromone 11-cis vaccenyl acetate. Together, these findings highlight OBPs as essential for olfaction, and necessary for processing of specific odorants. It may suggest that OBPs are selectively binding to distinct odor subgroups, and thus, in combination with the selectivity of ORs, contribute to the responsiveness and sensitivity of OSNs, and ultimately, evoked behavioral responses.

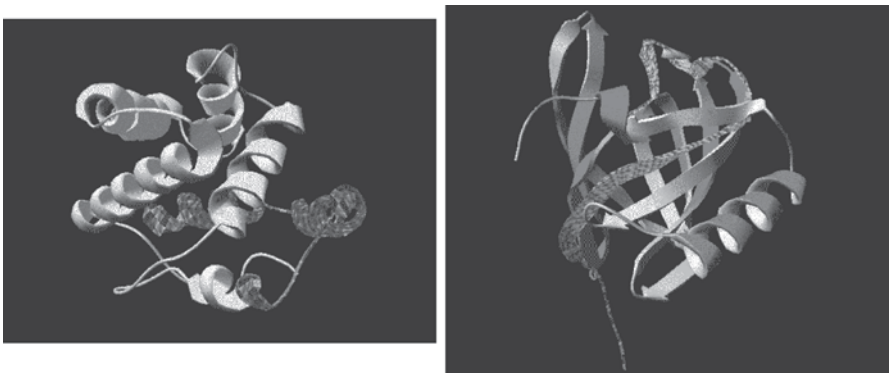

Fig. 10.7 Structure of OBPs from insects and vertebrates. The figure shows OBPs from the wasp *Polistes dominula* (left), and pig *Sus scrofa* (right)

10.2.1 Structure of Odorant Binding Proteins

The secondary structures of OBPs are widely different between vertebrates and insects. The insect's OBPs are mainly organized in α-helical domains, in contrast to the β-barrel motif found in vertebrates (Fig. 10.7).

The three dimensional structure of an insect OBP is very compact and stabilized by three interlocked disulphide bridges connecting six cysteines, which is the fingerprint of this protein family. The first OBP of insects was discovered at the beginning of the 1980's in the giant moth *Antheraea polyphemus* [38] using a tritium-labelled specific pheromone (E, Z)-6,11-hexadecadienyl acetate as a probe. A great number of proteins similar in their amino acid sequences to the OBP were later identified in many Lepidopteran species, *Lymantria dispar* [59], *Manduca sexta* [60], *Bombyx mori* [61] and many others. According to their length and the number of cysteines, insect OBPs can be grouped into: classic OBPs (having the typical six-cysteine signature), tandem OBPs (constituted by two classic OBPs linked by few amino acids), C-plus OBPs (containing more cysteines in addition to the six of the conserved motif), C-minus OBPs (presenting only four of the six conserved cysteines), and atypical OBPs (having a variable number of additional cysteines and generally a longer C-terminus) [62–67]. Beside odorant binding proteins, a second classes of polypeptides have been identified in the lymph of chemosensilla: chemosensory proteins (CSPs). OBPs are believed to be an evolved form of CSPs which are mainly present in primitive arthropods [68].

Vertebrate odorant-binding proteins were discovered almost simultaneously with insect OBPs using a ligand-binding approach. Pelosi et al. [37] detected in the nasal olfactory mucosa of bovines and other mammals soluble proteins able of binding 2-isobutyl-3-methoxypyrazine, an odorant with a low detection thresholds. Several members of this family were later purified from different mammals: pigs, rabbits [69], mice [70], porcupine [71] and humans [72]. OBPs expressed in mammals are dimers or monomers of acidic polypeptides of about 17–20 kDa, belonging to the

DSDIAVKKYL HAVPEPVLAK CLKESGLEAD KDKLLSDEST VDQGKFSCLI
ACTLKDNGALVNGELKYDVL SELLSKLLTN KEDKLQERLE KACIPEGA
NAKNDCEYIG KIMQCKLSKA KEMGL

Fig. 10.8 Amino acid sequence of OBP1 from the wasp *Polistes dominulus*

superfamily of lipocalins [6]. They are synthesized in several glands located in the respiratory region of the nasal tissue, such as the lateral nasal glands and the glands of the septum [73–75]. Vertebrate OBPs are mainly organized in a β-barrel structure, with a calyx-shaped cavity, made up of eight antiparallel β-sheets with a short segment of α-helix at the C-terminus [76, 77]. The ligand binding site is located in the core of the β-barrel, as was demonstrated by the use of a selenium-containing ligand, 2-amino-4-butyl-5-propylselenazole [78]. Figure 10.7 compares the structure of vertebrate and insect OBPs.

OBPs from different sources display specific affinities toward a wide range of compounds with different sizes and shapes. They can be easily expressed in heterologous systems, they show high thermal stability and it is possible to modify their binding sites by site-directed mutagenesis. These factors make them attractive for the design of biosensors that can be used for detection of ligands in the liquid phase or in vapor phase.

10.2.2 Construction of an OBP Biosensor

10.2.2.1 Protein Expression

Because the amino-acid sequences of many OBPs are available, it is now a fairly straightforward procedure to create plasmids containing the appropriate gene sequence coding for a particular protein using either vertebrate or invertebrate OBPs. For example, the amino acid sequence for OBP1 from the wasp *Polistes dominulus* is shown in Fig. 10.8. The nucleotide sequence of the OBPs can be easily insert inside a plasmid , such as pET (Promega). The obtained expression vector was used to transform *E. coli* BL21(D3) cells (Agilent technology). The construct included the nucleotide sequence coding for the protein, an ATG codon at the 5' end and a stop codon at the 5' end. These two extra codons were inserted in the sequence of primers in the forward and reverse direction respectively, to allow the correct expression of the protein.

Bacteria colonies were grown overnight in 10 ml Luria-Bertani/Miller broth containing 100 mg l^{-1} of ampicillin. The culture was diluted 1:100 with fresh medium and grown at 37 °C until the absorbance at 600 nm reached 0.7 AU. At this stage, 0.4 mM isopropyl thio- D-galactoside was added to the culture to induce expression. After 2 h at 37 °C, the cells were harvested by centrifugation, resuspended in 50 mM Tris-HCl pH 7.4 and lysed by sonication. The recombinant OBP was present at this stage in the supernatant and was expressed with yields of about 15 mg l^{-1}

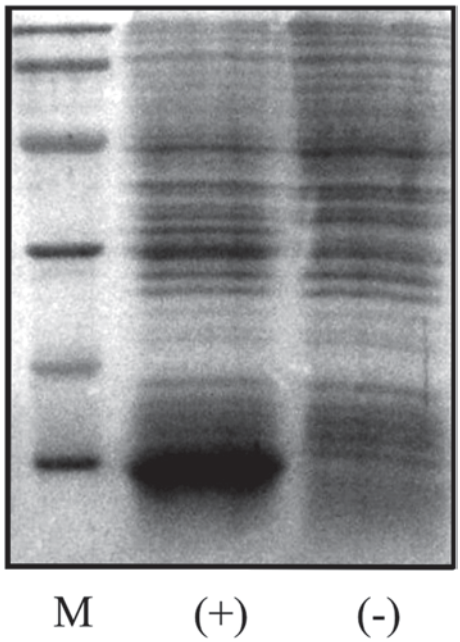

Fig. 10.9 Electrophoretic analysis in denaturing conditions (14% SDS-PAGE) of bacterial cultures expressing OBP, sampled before (−) and after (+) induction with isopropyl-beta-D-thiogalactopyranoside

of culture. The proteins were purified by two chromatographic steps on anion-exchange resin DE-52 (Whatman), using a gradient of 0.5 M NaCl in Tris buffer, followed by gel filtration on Superose-12. Fractions were analysed by SDS-PAGE and by UV spectroscopy to evaluate the amount of DNA co-eluted with the protein. At the end of the purification procedure, the proteins were more than 95% pure, as judged by SDS-PAGE, and virtually free from DNA.

The protein was expressed in good yields (around 15 mg of OBP per litre of bacterial culture) and in soluble form.

Figure 10.9 shows the electrophoretic analysis in denaturing conditions (14% SDS-PAGE) of crude bacterial cultures expressing OBP, sampled before (−) and after (+) induction with isopropyl-beta-D-thiogalactopyranoside. The expressed protein had a molecular weight of about 15 kDa.

10.2.2.2 Quartz Crystals

Piezoelectric AT- cut quartz crystals, with a resonance frequency of 20 MHz and 7.95 mm of diameter were used as the transduction elements for an OBP biosensor. The crystals were coated on both sides with a layer of gold (Au geometric surface of 4.9 mm diameter). The gold was deposited on the quartz surface with an adhesion layer of titanium.

10.2.2.3 Protein Immobilization

Proteins were immobilized on the gold surfaces of the quartz crystals using two different methodologies:

- direct covalent immobilization
- Covalent immobilization—Self assembled monolayer (SAM)

Before immobilization of proteins, the gold surface was rinsed with absolute ethanol and double distilled H_2O in case of new crystals. If quartz crystals were to be reused, they were cleaned by dipping the crystal in Piranha solution (1:3 = 30% H_2O_2: H_2SO_4) for few minutes to remove any organic residues from the surface.

10.2.2.4 Direct covalent immobilisation

For direct covalent immobilization, we modified the OBP by adding a cysteine residue at the N-terminal end of the protein—allowing a stable bond to be formed between the thiol group of cysteine and the gold surface. The immobilisation was carried out by spreading 5 µl of proteins (2.3 mg ml^{-1}) on the gold surface. The protein was added about every 2 hours for at least four times. After that, the surface was gently rinsed with sterile double distilled H_2O and was left to dry. The same procedure was applied for the gold electrode on the other side of the QCM.

10.2.2.5 Covalent Immobilization

OBPs were immobilised on the gold surface through covalent immobilization via a Self assembled monolayer (SAM). Thioctic acid (TA) ((R)-5-(1,2-dithiolan-3-yl) pentanoic acid). The sulphur atoms of the TA forms a strong bond with the gold, while the other end of the molecule is free to bind to the proteins. TA (100 mM in absolute ethanol) was dropped on the gold surface of the crystal, repeatedly every 20 min, for at least 2 hours. The same procedure was used for the gold electrode on other side of the quartz crystal. The SAM procedure was carried out in a controlled environment under nitrogen. The quartz crystal was then rinsed with an excess of absolute ethanol and was left to dry at air. In order to activate the carboxylic acid groups of the SAM, 20 µl of a solution consisting of a mixture of ethyl(dimethylaminopropyl)carbodiimide (30 mM) and N-hydroxysuccinimide (60 mM) was placed on the gold surface for 2 hours. The solution was then rinsed with distilled water and was dried at air. These procedures for the SAM activation were applied to both sides of the gold surfaces for all the quartz crystals. The immobilization of proteins on the activated SAM layer was carried out by pipetting the OBP solution onto the gold surface and leaving it for 1 hour before gently rinsing with distilled water and drying in air. The amount of protein deposited on to the gold surface corresponded to about 10 µg of OBP.

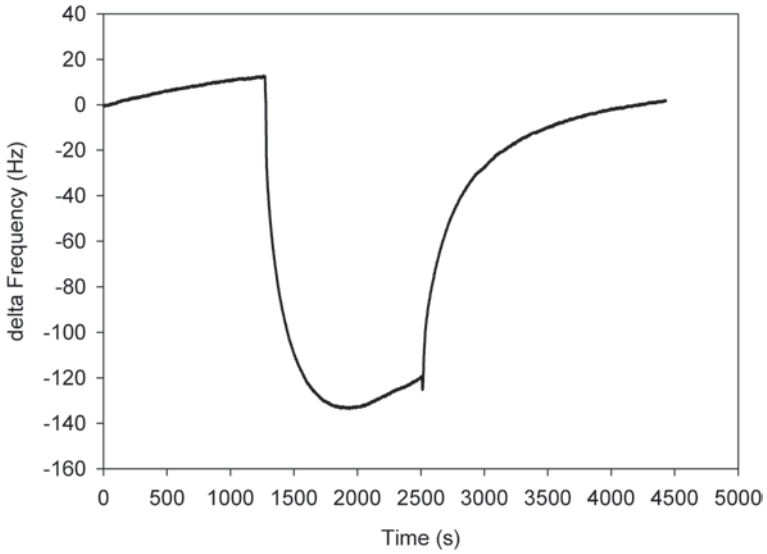

Fig. 10.10 Response of a QMB coated with *P. dominulus* OBP to a pulse 350 ppm of 2-isobutyl-3-methoxypyrazine in air

The best performance were obtained using covalent immobilization by using self assembled monolayers rather than direct covalent binding of the proteins.

10.3 Sensor Responses

Although the binding affinities of odorant binding proteins have been characterized to a range of analytes in solutions [49, 79, 80], there is little data available about how they interact with ligands in the vapour phase. Here we report our first experiments in this area.

The raw response signal from a QCM with immobilized odorant binding proteins from the *Polistes dominulus* to 350 ppm of 2-isobutyl-3-methoxypyrazine in air are shown in Fig. 10.10. The decrease of the quartz crystals basic oscillator frequency due to the changes of mass over time is recorded as the sensing signal. Sensors were stabilized under a constant flow of air before the introduction of target gas in order to obtain a reference frequency and eliminate the effect of flow dynamics. The baseline frequency was then re-established by a flow of clean air in order to remove bound analytes. The sensor showed good reversibility as well as stability over time, although the baseline frequency measured was prone to long term drift. Control experiments with gold surfaces on bare crystals indicated that responses specific to the presence of OBPs were being detected.

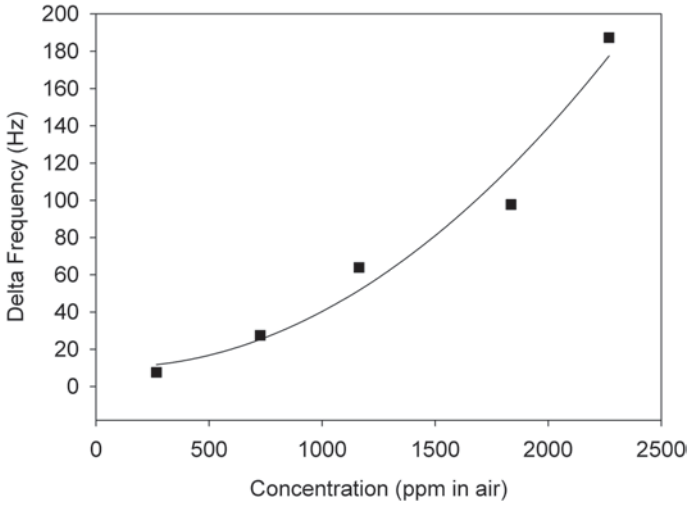

Fig. 10.11 Concentration-response curve for 2,3-dimethylpyrazine—QMB coated with pig OBPm2. A quadratic polynomial $f = y0 + ax + bx^2$ was fitted with coefficients $y0 = 10.57$, $a = -0.005$, $b = 3.45E\text{-}5$ with $R^2 = 0.97$

Intriguingly, pyrazines are a group of chemicals to which good responses are normally found from proteins over a range of species from ligand binding experiments carried out in solution [80]. In the vapour phase, for all species of proteins immobilized on quartz crystal microbalances we observed a concentration-dependence in the responses to these compounds. The change in frequency of the QMB is proportional to concentration of analyte in the vapour phase as illustrated in Fig. 10.11, which can be fitted with a quadratic polynomial. In this case the concentration-response curve of pig OBP to 2,3-dimethylpyrazine is shown, and similar response curves with different initial slopes are seen with other types of OBPs, or with other analytes for the same OBP. Mass transduction mechanisms in QMBs have been reviewed by Mecea [81] who indicates that the QMB is not only a sensitive mass sensor but it is also an actuator generating a mega gravity field on the surface of the quartz resonator. It is claimed that the very high mass sensitivity of the QCM is explained by the very high acceleration acting on the deposited film.

We have investigated the selectivity of proteins from different sources to a range of different pyrazines. This indicated that the binding sites are sensitive to the size and shapes of the ligands. There are some intriguing similarities and differences in the trends found. Both the protein from the pig and the protein from the wasp gave similar trends in terms of response—2-isobutyl-3-methoxypyrazine always giving the best response, although the protein from the wasp was less sensitive than the pig protein as shown in Fig. 10.12.

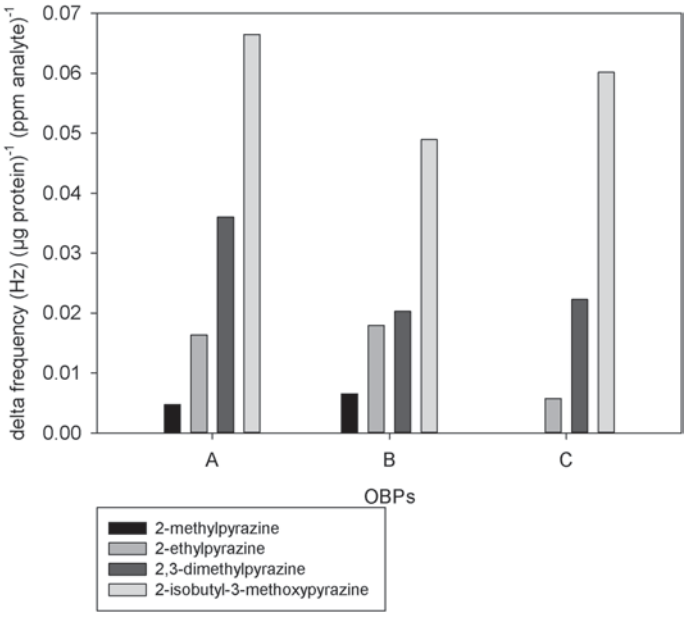

Fig. 10.12 Normalised responses of *A*—pig *Sus scrofa* OBP, *B*—wasp *P. dominula*, *C*—locust *L. migratoria* OBP immobilized on quartz microbalances to pyrazine derivatives, 2-methyl pyrazine, 2-ethyl pyrazine, 2,3-dimethylpyrazine, 2-isobutyl-3-methoxypyrazine

10.4 Conclusions

The exceptional stability of OBPs to thermal denaturation and proteolytic degradation makes these proteins interesting for incorporation into sensing devices. There is now a large body of knowledge available on the protein sequences, ligand binding specificities and affinities, as well as crystal structures for key members of the family, so it is possible to tailor proteins in the future for selected target analytes. Few papers so far describe the potentialities of OBPs as biosensors. We show here that it is possible to express different OBPs from many sources using conventional molecular genetics methods. These proteins can be immobilized and are able to capture volatile analytes from the vapour phase. Using a quartz crystal microbalance platform as a transduction element, it is possible to detect and measure quantitatively concentrations of volatile analytes at ppm concentrations in air. Further work is necessary to improve the versatility of these new sensors in matching the complexity and variety of environmental odours.

Acknowledgements Elena Tuccori was supported via a Marie Curie Early Stage Researcher grant (FLEXSMELL GA-2009-238454).

References

1. Turner AP (2013) Biosensors: sense and sensibility. Chem Soc Rev 42(8):3184–3196
2. Arora P, Sindhu A, Kaur H, Dilbaghi N, Chaudhury A (2013) An overview of transducers as platform for the rapid detection of foodborne pathogens. Appl Microbiol Biotechnol 97(5):1829–1840
3. Buck LB (2004) Olfactory receptors and odor coding in mammals. Nutr Rev 62(11):S184–S188
4. Persaud KC (2012) Biomimetic olfactory sensors. Ieee Sens J 12(11):3108–3112
5. Du L, Wu C, Liu Q, Huang L, Wang P (2013) Recent advances in olfactory receptor-based biosensors. Biosens Bioelectron 42:570–580
6. Pelosi P (2001) The role of perireceptor events in vertebrate olfaction. Cell Mol Life Sci 58(4):503–509
7. Persaud KC, Ng SM, Mucignat C, Pelosi P (2009) Odorant binding proteins and mouse urinary proteins: potential biomimetic sensing systems. Chem Senses 34(3):E36–E37
8. Lucarelli F, Tombelli S, Minunni M, Marrazza G, Mascini M (2008) Electrochemical and piezoelectric DNA biosensors for hybridisation detection. Anal Chim Acta 609(2):139–159
9. Mascini M, Tombelli S (2008) Biosensors for biomarkers in medical diagnostics. Biomarkers 13(7–8):637–657
10. De Corcuera JIR, Cavalieri RP (2003) Biosensors. Encyclopedia of agricultural, food, and biological engineering. Ed. Dennis Heldman, Pub. Marcel-Dekker, New York (ISBN 0-8247-0938-1) pp 119–123
11. Erden PE, Kilic E (2013) A review of enzymatic uric acid biosensors based on amperometric detection. Talanta 107:312–323
12. Labuda J, Oliveira Brett AM, Evtugyn G, Fojta M, Mascini M, Ozsoz M et al (2010) Electrochemical nucleic acid-based biosensors: concepts, terms, and methodology (IUPAC technical report). Pure Appl Chem 82(5):1161–1187
13. Liu Y, Du Y, Li CM (2013) Direct electrochemistry based biosensors and biofuel cells enabled with nanostructured materials. Electroanalysis 25(4):815–831
14. Daniels JS, Pourmand N (2007) Label-free impedance biosensors: opportunities and challenges. Electroanalysis 19(12):1239–1257
15. Wang XD, Wolfbeis OS (2013) Fiber-Optic chemical sensors and biosensors (2008–2012). Anal Chem 85(2):487–508
16. Manera M, Spadavecchia J, Leone A, Quaranta F, Rella R, Dell'atti D et al (2008) Surface plasmon resonance imaging technique for nucleic acid detection. Sens Actuators B-Chem 130(1):82–87
17. Scarano S, Scuffi C, Mascini M, Minunni M (2011) Surface plasmon resonance imaging-based sensing for anti-bovine immunoglobulins detection in human milk and serum. Anal Chim Acta 707(1):178–183
18. Scarano S, Mascini M, Turner AP, Minunni M (2010) Surface plasmon resonance imaging for affinity-based biosensors. Biosens Bioelectron 25(5):957–966
19. Glaser RW (2000) Surface plasmon resonance biosensors. In: Yang VCM, Ngo TT (eds) Biosensors and their applications. Kluwer Academic/Plenum Publishers, pp 195–212
20. Lec RM (2001) Piezoelectric biosensors: recent advances and applications. Proceedings of the 2001 Ieee International Frequency Control Symposium & Pda Exhibition, pp 419–429
21. Ferreira GN, da-Silva AC, Tome B (2009) Acoustic wave biosensors: physical models and biological applications of quartz crystal microbalance. Trends Biotechnol 27(12):689–697
22. Speight RE, Cooper MA (2012) A survey of the 2010 quartz crystal microbalance literature. J Mol Recognit 25(9):451–473
23. Sauerbrey G (1959) Verwendung Von Schwingquarzen Zur Wagung Dunner Schichten und Zur Mikrowagung. Zeitschrift fur Physik 155(2):206–222
24. Putzbach W, Ronkainen NJ (2013) Immobilization techniques in the fabrication of nanomaterial-based electrochemical biosensors: a review. Sensors 13(4):4811–4840
25. Senveli SU, Tigli O (2013) Biosensors in the small scale: methods and technology trends. Iet Nanobiotechnol 7(1):7–21

26. Wang R, Zhang Y, Lu D, Ge J, Liu Z, Zare RN (2013) Functional protein-organic/inorganic hybrid nanomaterials. Wiley Interdiscip Rev Nanomed Nanobiotechnol 5(4):320–328
27. Caruso F, Rinia HA, Furlong DN (1996) Gravimetric monitoring of nonionic surfactant adsorption from nonaqueous media onto quartz crystal microbalance electrodes and colloidal silica. Langmuir 12(9):2145–2152
28. Lin JN, Drake B, Lea AS, Hansma PK, Andrade JD (1990) Direct observation of immunoglobulin adsorption dynamics using the atomic force microscope. Langmuir 6(2):509–511
29. Giuseppone N (2012) Toward self-constructing materials: a systems chemistry approach. Acc Chem Res 45(12):2178–2188
30. Koepsel JT, Murphy WL (2012) Patterned self-assembled monolayers: efficient, chemically defined tools for cell biology. Chembiochem 13(12):1717–1724
31. Deshmukh PK, Ramani KP, Singh SS, Tekade AR, Chatap VK, Patil GB, et al (2013) Stimuli-sensitive layer-by-layer (LbL) self-assembly systems: targeting and biosensory applications. J Control Release 166(3):294–306
32. Ulman A (1996) Formation and structure of self-assembled monolayers. Chem Rev 96(4):1533–1554
33. Wink T, vanZuilen SJ, Bult A, vanBennekom WP (1997) Self-assembled monolayers for biosensors. Analyst 122(4):R43–R50
34. Kajiya Y, Sugai H, Iwakura C, Yoneyama H (1991) Glucose sensitivity of polypyrrole films containing immobilized glucose-oxidase and hydroquinonesulfonate ions. Anal Chem 63(1):49–54
35. Collings AF, Caruso F (1997) Biosensors: recent advances. Rep Prog Phys 60(11):1397–1445
36. Miao Y, Chia LS, Goh NK, Tan SN (2001) Amperometric glucose biosensor based on immobilization of glucose oxidase in chitosan matrix cross-linked with glutaraldehyde. Electroanalysis 13(4):347–349
37. Pelosi P, Baldaccini NE, Pisanelli AM (1982) Identification of a specific olfactory receptor for 2-isobutyl-3-methoxypyrazine. Biochem J 201(1):245–248
38. Vogt RG, Riddiford LM (1981) Pheromone binding and inactivation by moth antennae. Nature 293(5828):161–163
39. Pelosi P, Calvello M, Ban LP (2005) Diversity of odorant-binding proteins and chemosensory proteins in insects. Chem Senses 30:i291–i292
40. Pelosi P, Zhou J, Ban L, Calvello M (2006) Soluble proteins in insect chemical communication. Cell Mol Life Sci 63(14):1658–1676
41. Leal WS (2013) Odorant reception in insects: roles of receptors, binding proteins, and degrading enzymes. Annu Rev Entomol 58:373–391
42. Cavaggioni A, Mucignat-Caretta C (2000) Major urinary proteins, alpha(2u)-globulins and aphrodisin. Biochim Biophys Acta-Protein Struct Mol Enzymol 1482(1–2):218–228
43. Marchlewska-Koj A, Cavaggioni A, Mucignat-Caretta C, Olejniczak P (2000) Stimulation of estrus in female mice by male urinary proteins. J Chem Ecol 26(10):2355–2366
44. Hurst JL, Payne CE, Nevison CM, Marie AD, Humphries RE, Robertson DHL, et al (2001) Individual recognition in mice mediated by major urinary proteins. Nature 414(6864):631–634
45. Cavaggioni A, Mucignat C, Tirindelli R (1999) Pheromone signalling in the mouse: role of urinary proteins and vomeronasal organ. Arch Ital Biol 137(2–3):193–200
46. Mucignat-Caretta C, Cavaggioni A, Caretta A (2004) Male urinary chemosignals differentially affect aggressive behavior in male mice. J Chem Ecol 30(4):777–791
47. Marchese S, Pes D, Scaloni A, Carbone V, Pelosi P (1998) Lipocalins of boar salivary glands binding odours and pheromones. Eur J Biochem 252(3):563–568
48. Loebel D, Scaloni A, Paolini S, Fini C, Ferrara L, Breer H et al (2000) Cloning, post-translational modifications, heterologous expression and ligand-binding of boar salivary lipocalin. Biochem J 350:369–379
49. Pevsner J, Hou V, Snowman AM, Snyder SH (1990) Odorant-binding protein—characterization of ligand-binding. J Biol Chem 265(11):6118–6125
50. Pevsner J, Snyder SH (1990) Odorant-binding protein—odorant transport function in the vertebrate nasal epithelium. Chem Senses 15(2):217–222

51. Vogt RG (1991) Pheromone and general-odorant binding-proteins in Lepidoptera. Am Zool 31(5):A16
52. Vogt RG (1992) Multiple classes of insect OBP provide a functional and developmental model for olfactory specificity. Chem Senses 17(5):712–713
53. Wang Q, Hasan G, Pikielny CW (1999) Preferential expression of biotransformation enzymes in the olfactory organs of *Drosophila melanogaster*, the antennae. J Biol Chem 274(15):10309–10315
54. Lobel D, Marchese S, Krieger J, Pelosi P, Breer H (1998) Subtypes of odorant-binding proteins—heterologous expression and ligand binding. Eur J Biochem 254(2):318–324
55. Lobel D, Jacob M, Volkner M, Breer H (2002) Odorants of different chemical classes interact with distinct odorant binding protein subtypes. Chem Senses 27(1):39–44
56. Kim MS, Repp A, Smith DP (1998) LUSH odorant-binding protein mediates chemosensory responses to alcohols in *Drosophila melanogaster*. Genetics 150(2):711–721
57. Xu PX, Atkinson R, Jones DNM, Smith DP (2005) Drosophila OBP LUSH is required for activity of pheromone-sensitive neurons. Neuron 45(2):193–200
58. Xu PX (2005) Eppendorf 2005 winner—a *Drosophila* OBP required for pheromone signaling. Science 310(5749):798–799
59. Vogt RG, Kohne AC, Dubnau JT, Prestwich GD (1989) Expression of pheromone binding-proteins during antennal development in the gypsy-moth *Lymantria dispar*. J Neurosci 9(9):3332–3346
60. Gyorgyi TK, Robyshemkovitz AJ, Lerner MR (1988) Characterization and cDNA cloning of the pheromone-binding protein from the tobacco hornworm, *Manduca sexta*—a tissue-specific developmentally regulated protein. Proc Natl Acad Sci U S A 85(24):9851–9855
61. Krieger J, von Nickisch-Rosenegk E, Mameli M, Pelosi P, Breer H (1996) Binding proteins from the antennae of *Bombyx mori*. Insect Biochem Mol Biol 26(3):297–307
62. Hekmat-Scafe DS, Scafe CR, McKinney AJ, Tanouye MA (2002) Genome-wide analysis of the odorant-binding protein gene family in *Drosophila melanogaster*. Genome Res 12(9):1357–1369
63. Riviere S, Lartigue A, Quennedey B, Campanacci V, Farine JP, Tegoni M et al (2003) A pheromone-binding protein from the cockroach *Leucophaea maderae*: cloning, expression and pheromone binding. Biochem J 371:573–579
64. Vieira FG, Sanchez-Gracia A, Rozas J (2007) Comparative genomic analysis of the odorant-binding protein family in 12 Drosophila genomes: purifying selection and birth-and-death evolution. Genome Biol 8(11):R235
65. Xu PX, Zwiebel LJ, Smith DP (2003) Identification of a distinct family of genes encoding atypical odorant-binding proteins in the malaria vector mosquito, *Anopheles gambiae*. Insect Mol Biol 12(6):549–560
66. Zhou JJ, Zhang GA, Huang WS, Birkett MA, Field LM, Pickett JA et al (2004) Revisiting the odorant-binding protein LUSH of *Drosophila melanogaster*: evidence for odour recognition and discrimination. Febs Lett 558(1–3):23–26
67. Zhou JJ, Huang WS, Zhang GA, Pickett JA, Field LM (2004) "Plus-C" odorant-binding protein genes in two Drosophila species and the malaria mosquito *Anopheles gambiae*. Gene 327(1):117–129
68. Vieira FG, Rozas J (2011) Comparative genomics of the odorant-binding and chemosensory protein gene families across the arthropoda: origin and evolutionary history of the chemosensory system. Genome Biol Evol 3:476–490
69. Dalmonte M, Andreini I, Revoltella R, Pelosi P (1991) Purification and characterization of 2 odorant-binding proteins from nasal tissue of rabbit and pig. Comp Biochem Physiol B-Biochem Mol Biol 99(2):445–451
70. Pes D, Dalmonte M, Ganni M, Pelosi P (1992) Isolation of 2 odorant-binding proteins from mouse nasal tissue. Comp Biochem Physiol B-Biochem Mol Biol 103(4):1011–1017
71. Felicioli A, Ganni M, Garibotti M, Pelosi P (1993) Multiple types and forms of odorant-binding proteins in the old-world porcupine *Hystrix cristata*. Comp Biochem Physiol B-Biochem Mol Biol 105(3–4):775–784

72. Lacazette E, Gachon AM, Pitiot G (2000) A novel human odorant-binding protein gene family resulting from genomic duplicons at 9q34: differential expression in the oral and genital spheres. Hum Mol Genet 9(2):289–301
73. Hwang PM, Pevsner J, Sklar PB, Venable JC, Snyder SH (1988) Localization of rat odorant-binding protein to the lateral nasal gland suggests an odorant transport function. Chem Senses 13(4):699
74. Pevsner J, Snyder SH (1990) Odorant-binding protein—odorant transport function in the vertebrate nasal epithelium. Chem Senses 15(2):217–222
75. Utsumi M, Ohno K, Kawasaki Y, Tamura M, Kubo T, Tohyama M (1999) Expression of major urinary protein genes in the nasal glands associated with general olfaction. J Neurobiol 39(2):227–236
76. Flower DR (1996) The lipocalin protein family: structure and function. Biochem J 318:1–14
77. Flower DR, North ACT, Sansom CE (2000) The lipocalin protein family: structural and sequence overview. Biochim Biophys Acta-Protein Struct Mol Enzymol 1482(1–2):9–24
78. Napolitano E, Pelosi P (1992) Synthesis of thiazole and selenazole derivatives with affinity for the odorant-binding protein. Bioorg Med Chem Lett 2(12):1603–1606
79. Pelosi P, Dal MM (1990) Purification and characterization of odorant binding proteins from nasal mucosa of pig and rabbit. Chem Senses 15(5):614
80. Dalmonte M, Centini M, Anselmi C, Pelosi P (1993) Binding of selected odorants to bovine and porcine odorant-binding proteins. Chem Senses 18(6):713–721
81. Mecea VM (2005) From quartz crystal microbalance to fundamental principles of mass measurements. Anal Lett 38(5):753–767

Chapter 11
Optical Methods in Studies of Olfactory System

Sang Hun Lee, Seung-min Park and Luke P. Lee

Abstract The olfactory receptor (OR) comprises the largest multi-gene G protein-coupled receptor (GPCR) family by playing a critical role in recognizing thousands of odorant molecules. Odorant-OR pairs have been characterized using various functional assays, and have provided an understanding of molecular basis in olfaction as well as characterizing specificity between agonist and antagonist. This chapter introduces the most commonly employed, labeled or label-free optical techniques employed to identify the odorant-OR pairs on a cellular and molecular level, and reviews recent developments in odorant binding assays to ORs with optical methods such as Ca^{2+} imaging, reporter-gene technology, surface plasmon resonance (SPR) and so on. For OR and GPCR study, a set of optical technologies including—but not limited to—Raman spectroscopy, photonic crystal, and total internal reflection (TIR) are also discussed in an analytical science point of view.

11.1 Molecular and Neural Basis of Olfaction

11.1.1 Olfactory System

Landmark discovery of the gene family encoding vertebrate olfactory receptors (ORs) in rats by Buck and Axel has led to a detailed understanding of the molecular and neurological bases in the olfaction [1]. The initial steps in an olfaction take place in olfactory sensory neurons located in the olfactory epithelium inside the nasal cavity. These neurons are responsible for the detection of odorants and the generation of the neural signal that is transmitted to the brain via olfactory bulb as shown in Fig. 11.1. Based on this process, the olfactory sensory system can detect thousands of different single and mixed odorants. For many organisms, the olfac-

L. P. Lee (✉)
Departments of Bioengineering, Electrical Engineering and Computer Science, Biophysics Program, Berkeley Sensor & Actuator Center, University of California, Berkeley, CA 94720, USA
e-mail: lplee@berkeley.edu

S. H. Lee · S.-m. Park
Departments of Bioengineering, Berkeley Sensor & Actuator Center, University of California, Berkeley, CA, USA

T. H. Park (ed.), *Bioelectronic Nose,* DOI 10.1007/978-94-017-8613-3_11,

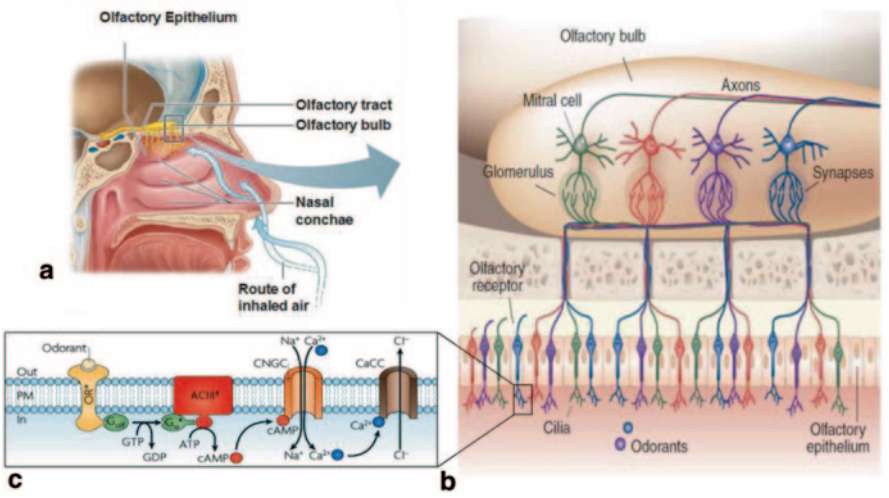

Fig. 11.1 Functional anatomy and structure of the olfactory system. **a** Localization of the olfactory apparatus in a human. **b** Structure of the olfactory epithelium showing the different cell types and the connecting from axons to glomeruli of the olfactory bulb. Bipolar olfactory sensory neurons are embedded in a small area of OE. These neurons project axons to the olfactory bulb of the brain. (Reprinted from Ref. [5] with permission from NPG). **c** Schematic diagram of olfactory signal transduction pathway. When an odorants binds to an OR protein (OR) in the olfactory cilia membrane a G protein ($G_{\alpha\ olf}$) is activated, leading to an increases in the generation of cAMP from ATP by adenylyl cyclase (ACIII). Olfactory cyclic nucleotide-gated channels (CNGC) conduct Na^+ and Ca^{2+} into the cilia. Ca^{2+} in turn opens Ca^{2+} -activated Cl^- channels (CaCC), which as intracellular Cl^- concentration is high, leads to Cl^- efflux. (Reprinted from Ref. [34] with permission from NPG)

tory sensory system can efficiently distinguish among numerous odorant molecules, specifically hydrophobic organic molecules at very low concentrations [2–5]. Unlike unique receptor-ligand interactions, the olfactory sensory system is based on combinatorial codes where a single receptor type can respond to many different odorants [6–8]. The broad tuning of olfactory cells with overlapping odorant response profiles allows for the identification and discrimination of odor signals for ORs, revealing a combinatorial receptor coding scheme in the entire system [9–11].

Numerous ligand-binding assays have been developed and used to figure out binding specificity with various ORs. These assays have generally utilized olfactory neurons or heterologous cells to express recombinant ORs and allow detection of OR-ligand pairs for the purpose of research in the olfaction mechanism. Researchers have also developed a much broader range of olfactory biosensor platforms such as surface plasmon resonance (SPR) [12–15], quartz crystal microbalance (QCM) [16–19], nanomaterial based-field effect transistor (FET)-type sensors [20–25], light-addressable potentiometric sensor (LAPS) [26–29], and microelectrode array [30–32] that utilize characterized OR-ligand interactions to validate the sensors [33].

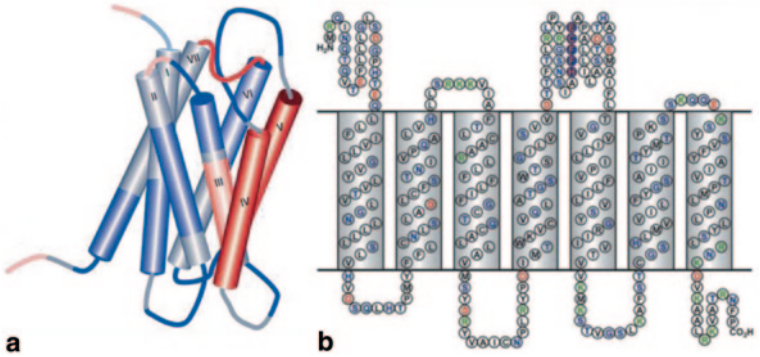

Fig. 11.2 **a** Schematic view of the proposed three-dimensional structure of the OR. The each color indicates the conserved (*blue*) and variable (*red*) regions. (Reprinted from Ref. [3] with permission from NPG). **b** Secondary structure prediction with amino acid aligned to the TM helix and loop regions. The each color represent as follows: hydrophobic residues in black, polar residue in green, positively charged in blue, and negatively charged in red metal ion-binding site in orange on blue. (Reprinted from Ref. [42] with permission from NAS)

11.1.2 Olfactory Receptor

ORs belong to the G protein-coupled receptor (GPCR) family and play a critical role in recognizing thousands of odorant molecules in the olfactory system. In the last decade, the Human Genome Project has enabled the comprehensive analysis of the OR gene family and revealed the genomic structure and distribution of OR genes from various organisms. It has been estimated that the OR family includes at least several hundred members [35, 36]. Analysis of the human genome has revealed 1,000 unique OR genes along with 350 potentially functional genes. Recent studies indicate that some 70 % of all human OR genes may be pseudogenes, compared with fewer than 5 % in rodents or lower primates [37–39]. The human OR genes, like those of other mammals, were classified as class I (fish-like) ORs, originally identified in fish, and class II (terrestrial-type) ORs [40, 41]. Within the family of ORs, there is a range of similarity, from less than 40 % to over 90 % identity in sequence. Interestingly, there is a region of hyper variability, where sequences show particularly strong divergence (Fig. 11.2).

ORs are seven-transmembrane (7TM) domain proteins, sharing many features with other G protein-coupled receptors (GPCRs), including a coding region that lacks introns, a structure that predicts seven α-helical membrane-spanning domains connected by intracellular and extracellular loops of variable lengths, and numerous conserved short sequences as shown in Fig. 11.1 [3, 42]. The odorant-binding site in OR proteins has been elucidated using a functional assay, showing that a binding pocket constructed by TM helices provides the molecular basis for agonist and antagonist specificity [10]. A multitude of up to 1,000 OR and numerous combinatorial odorant recognition properties have made it difficult to assign ligand profiles to an individual OR [43]. The question also rises whether the ligand specificity deter-

mined in heterologous cells really reflects *in vivo* responsiveness of the target OR. As such, caution must be prioritized when evaluating structure-activity relationship of ORs *in vitro* expression systems [44].

11.1.3 Olfactory Signal Transduction

Odorant stimulation elicits a signal transduction cascade mediated by OR expression on the surface of the olfactory neuronal cilia. The olfactory signal cascade is generated through two pathways: cAMP and IP_3. The cAMP cascade is dominant in transmitting odorant signals in the olfactory neurons, whereas the role of the inositol-1,4,5-triphosphate (IP_3)-mediated pathway remains unclear [45]. The initial step in the cAMP pathway is binding of odorant molecules to specific OR proteins on the cilia surface [8, 34, 46]. Ligand binding triggers a change in the OR structural conformation via the activation of a membrane-bound type III adenylyl cyclase (ACIII) in an olfactory-specific G protein subunit ($G_{\alpha olf}$). ACIII leads to the generation of cyclic adenosine monophosphate (cAMP), which directly opens a heteromeric cyclic nucleotide-gated (CNG) in the cilia membrane. The opened CNG-channel leads to an influx of Ca^{2+} and Na^{+}, and subsequent opening of the Ca^{2+}-activated Cl^{-} channel results in the depolarization of olfactory cells through cation influx as shown in Fig. 11.1 (c). The secondary mechanism in olfactory signal transduction involves the generation of IP_3 from phosphatidyl inositol 4,5-bisphosphate (PIP_2) by phospholipase C [4, 47]. For example, the specific binding of diacetyl to ODR-10 is the OR protein of the nematode *Caenorhabditis elegans* (*C. elegans*), which triggers signal transduction through the IP_3 pathway. Activated OR subsequently activates phospholipase C (PLC), which converts the phosphatidyl inositol 4,5-bisphosphate (PIP_2) into inositol 1,4,5-triphosphate (IP_3). The IP_3 opens the Ca^{2+} channel on the surface of endoplasmic reticulum (ER), which increases cytosolic Ca^{2+} ion. Ultimately, both the cAMP- and $IP_{3\_}$ pathway can be analyzed by simply measuring the influx or efflux of Ca^{2+} ions upon ligand stimulation.

11.2 Labeled Optical Methods for Odorant Binding Assay

Fluorescence or bioluminescence measurements are some of the techniques used in standard optical assays developed for monitoring cellular activation events. For the characterization of ORs, these basic optical methods include Ca^{2+} imaging, cAMP-reporter assay, fluorescent resonant energy transfer (FRET), bio-luminescence resonant energy transfer (BRET), and so on, used to measure the interaction between the OR and odorant in the cellular level that result from signal transduction. These cell-based assays, which use cells as the sensing elements, have many advantages over other techniques in molecular interaction study and can be used to derive functional information of biologically active analytes. This section provides a general overview of the most common types of optical detection technique.

11.2.1 Intracellular Ca^{2+} Imaging-based Odorant Sensing

Measuring the change in intracellular Ca^{2+} levels via olfactory signal transduction is a very useful tool for examining the function of the OR proteins expressed in olfactory neuron and heterologous cell systems [45, 48]. In this regard, Ca^{2+} imaging is a basic strategy for detecting physiological odorant responses by measuring the temporal and spatial properties of Ca^{2+} changes caused by odorant stimuli. Ca^{2+} signals in the cytosol and organelles are important for cellular signal transduction and are usually measured using a synthetic fluorescent chelator, such as Fura-2. Odorant stimulation causes Ca^{2+} entry through CNG channels in individual responsive neurons, which is then regulated by a series of signal transductions. Essentially, if an OR specifically binds with a ligand, a signal cascade induces an influx of Ca^{2+} ions. Intracellular Ca^{2+} ions then bind to Fura-2, which was previously loaded into cells. The excitation wavelength of Fura-2 changes from 380 to 340 nm when Fura-2 binds to the Ca^{2+} ions. As a result, the increase in the amount of intracellular Ca^{2+} ions can be estimated by the ratio of fluorescence emissions (excitation at 340/380 nm).

Identification and functional characterization of human OR (hOR)17-4 by the ratio-fluorometric Ca^{2+} imaging was reported by Spehr et al. [49]. This expression of hOR17-4 protein in a heterologous HEK-293 cell line allowed for the identification and structure-function analysis of cognate receptor-odorant pairs using single cell Ca^{2+} recording as shown in Fig. 11.3. An *in situ* Ca^{2+}-imaging technique was adopted to monitor odorant responses of more than several hundreds of neurons simultaneously through an intact coronal slice of the olfactory epithelium. The sensitivity and resolution of Ca^{2+}-imaging were high enough to distinguish between olfactory neurons with threshold concentrations for a particular odorant at the single cell level. Increasing odorant concentrations resulted in increases in the numbers of odorant-responsive neurons. This methodology is powerful tool to visualize spatial distributions of odorant responsive neurons at a cellular resolution, and to construct odor maps in a coronal view of the olfactory epithelium [50].

Ca^{2+} imaging technique can be used for identification of OR-odorant pair and structure-activity relationship. In a study from Wetzel and co-workers, an odorant screening strategy in heterologous cells was demonstrated using Ca^{2+} imaging [51]. A mixture of 100 different odorants (Henkel 100) elicited a transient increase in intracellular Ca^{2+}, and a specific single odorant component to human olfactory receptor (hOR) 17-40 protein was identified by subdividing the odorant mixture into progressively smaller groups. Ca^{2+} imaging was also applied for de-orphaning of the OR through high-throughput screening using fluorescence imaging plate reader (FLIPR) experiments [43]. Ca^{2+} imaging and HeLa/OR heterologous cell systems were applied to a large-scale odorant-receptor that screened and established receptor-specific odorant profiles, resulting in the de-orphaning of two ORs for the odorants from an expression library of 93 receptors. Unfortunately, the de-orphaning of OR is still complicated by its combinatorial odorant coding and lack of efficient assay tools. Although ORs are efficiently expressed in various mammalian cell lines (e.g., HEK-293, COS-7, Hana3A, *X. laevis oocyte* and CHO-K1 cells) [51–55],

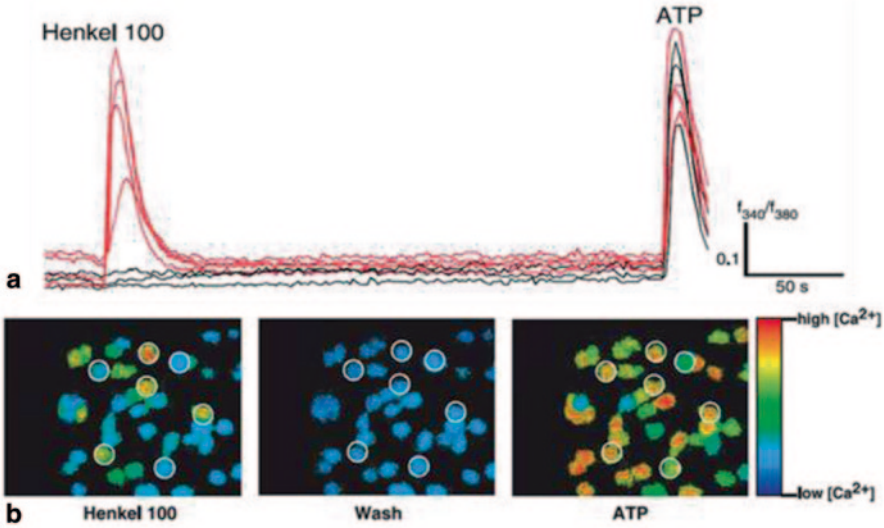

Fig. 11.3 Identification of odorant-responsive cell in Ca^{2+} imaging experiments. **a** Ca^{2+} changes in individual cells. The integrated fluorescence ratio (F340/380 nm) for various fura-2-loaded cells is shown as a function of time. **b** In a randomly selected field of view, the complex odorant mixture Henkel 100 induced transient Ca^{2+} signals in transfected HEK-293 cells (red traces). Adenosine triphosphate (ATP) served as a control of HEK cells excitability. Ca^{2+} changes in individual cells are indicated in pseudocolors. (Reprinted from Ref. [49] with permission from AAAS.)

the heterologous expression system still requires additional components that allow for expression of enough OR proteins on the cell membrane and enhancement of the signal transduction efficacy. Co-expression of Ric8B greatly facilitates signal transduction of ORs by enhancing GDP-GTP exchange activity of $G_{\alpha s}$ [56]. RTP (receptor-transporting protein) and REEP (receptor expression enhancing protein) assists and promote the cell surface expression of OR proteins by acting as a kind of chaperone [23, 55, 57].

In terms of odorant quality, individual olfactory neurons appear to have broad odorant tuning specificity that is determined based on structural features in odorant molecules such as differences in terminal groups, chain lengths, and positions of functional groups [58]. Furthermore, single responsive cells, in conjunction with a certain odorant, showed an increased in response to additional odorants with higher concentrations. Data from the Ca^{2+} imaging suggested a combinatorial receptor code model in which different odorants are recognized by overlapping sets of OR [9]. In the case of OR proteins, odorants can function both as agonists and antagonist, suggesting that the interactions between ORs and odorants is quite complicated [59]. The Touhara research group reported that the odorants can inhibit odorant responses of ORs at the receptor level by Ca^{2+} imaging in the olfactory neuron olfactory epithelium [11]. As an example, the eugenol response of mouse OR-EG was potently blocked by some structurally related odorants such as methyl isoeugenol and isosafrol. In complex mixtures of odorants, antagonism between odorants at

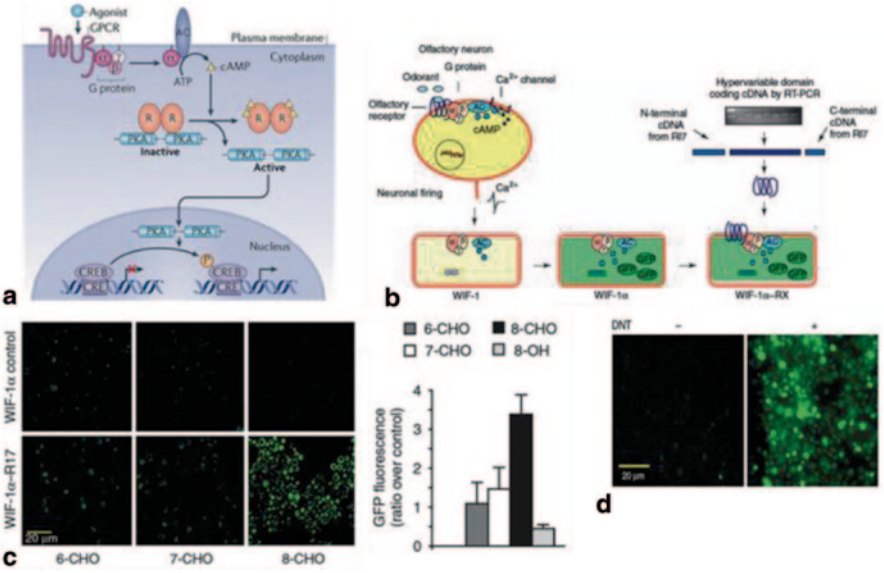

Fig. 11.4 Reporter gene technology for whole-cell olfactory biosensor using fluorescence and bioluminescence. **a** An analyte or a stimulus i.e odorant specifically activates a regulatory gene sequence via signal transduction that controls the reporter gene expression and the synthesis of the reporter protein, which is then measured by fluorescence or bioluminescence. (Reprinted from Ref. [65] with permission from NPG). **b** Yeast cells containing rat ORs were used as a 2,4-dinitrotoluene (DNT) detection. Schematic showing the construction of olfactory yeast strain WIF-1α-RX. Transfection with a plasmid containing the GFP gene formed the WIF-1α strain, in which GFP expression serves as a reporter. **c** Specificity of WIF-1α-ORI7 response. Cells were incubated with hexanal (6-CHO), heptanal (7-CHO), octanal (8-CHO) or octanol (8-OH). **d** Response of WIF-1α-Olfr226 strain to DNT. (Reprinted from Ref. [66] with permission from NPG)

the receptor level could be involved in the perceptual complexities seen in odorant mixtures. This phenomenon, known as mixture suppression, has been verified in behavioral experiments, as well as at the cellular and olfactory epithelial levels for various OR [43, 48, 60, 61].

11.2.2 Reporter Gene-based Selective Odorant Sensing

Reporter gene technology represents one of the major recent achievements in molecular biology. Reporter genes are DNA sequences that encode an easily detectable protein or enzyme such as luciferase or GFP [62–64]. The rate of fluorescence and bioluminescence output is directly proportional to the concentration of the indicator material present. The principle of reporter gene technology applied to the development of whole-cell olfactory biosensors is shown in Fig. 11.4.

The cAMP responsive binding protein is a well-characterized transcription factor regulated by cAMP [50]. The transcription factor cAMP-responsive element

binding protein (CREB) and its binding site (cAMP response element, CRE) have been suggested to play a major role in reporter gene assay. CREB belongs to the family of basic leucine zipper transcription factors and modulates gene transcription by binding to the CRE in the promoter regions of various genes. In the CRE-based odorant sensing system, odorant binding to OR stimulates adenylyl cyclase (AC) via G protein activation. Activated AC causes a rise in intracellular cAMP from ATP, which activates protein kinase A (PKA). The catalytic unit of PKA can then move into the nucleus and phosphorylate a CREB to CREB-P, allowing it to bind to a CRE in the promoter of a target gene, thus increasing transcription [63, 67]. Generally CRE/CREB-driven gene expression via ligand stimulation can be measured as luciferase activity or fluorescence protein expression. As mentioned above, cAMP is the second messenger involved in olfactory signal transduction. Thus, it would be of interest to measure cAMP since it is a molecule that transmits the signal from the membrane to the metabolic machinery of the cytosol.

Katada and co-workers reported that odorant-induced cAMP response can be observed using a CRE-regulated luciferase reporter gene assay [52]. A luciferase reporter gene assay using the zif268 promoter, known to contain CREs, was adopted to amplify the cAMP signals. An intracellular cAMP increase upon exposure to the proper agonist initiates a cascade that leads to CRE-mediated gene expression. In addition, odorant-induced cAMP increases via Gαs and AC activation can be measured directly using an enzyme-linked immunoassay [43]. Bioluminescence measurements through a luciferase reporter were applied in response to odorant stimulation [68]. Yeast functional activity, which co-expresses rat OR (rOR) I7 and G_{olf}, was evaluated by a luciferase reporter placed under an inducible promoter, triggered by the specific odorant to its related OR interaction, and having the dose-response curves, from 10^{-12} to 10^{-4} M of a specific odorant, plotted as a difference to negative controls. The luciferase reporter can be used as a useful tool for simple, rapid odorant screening of ORs to provide olfactory coding mechanisms. Fukutani and co-workers reported a bioluminescence reporter-based 2,4-dinitrotoluene (DNT)-sensing system using OR-expressing yeast [69]. A biomimetic odor-sensing system was constructed with engineered yeast expressing OR, using firefly luciferase (luc) as the reporter. In addition, Radhika et al. used *S. cerevisiae* to screen for the rat OR226 gene that possesses sensitivity for DNT, an analog of the explosive trinitrotoluene [66] (see Fig. 11.4). This screening was accomplished by constructing a chimeric OR receptor that both the N- and C-terminal regions of the endogenous protein replaced with the rORI7 receptor. This system can be expected to enable the quantification of flavors, fragrances, and/or the avoidance of harmful agents or explosive accidents.

11.2.3 Fluorescence and Bioluminescence Resonant Energy Transfer-based Odorant Sensing

Recent progress in molecular biology has made several biotechnological tools such as FRET and BRET available. These developments provide inroads to continuous

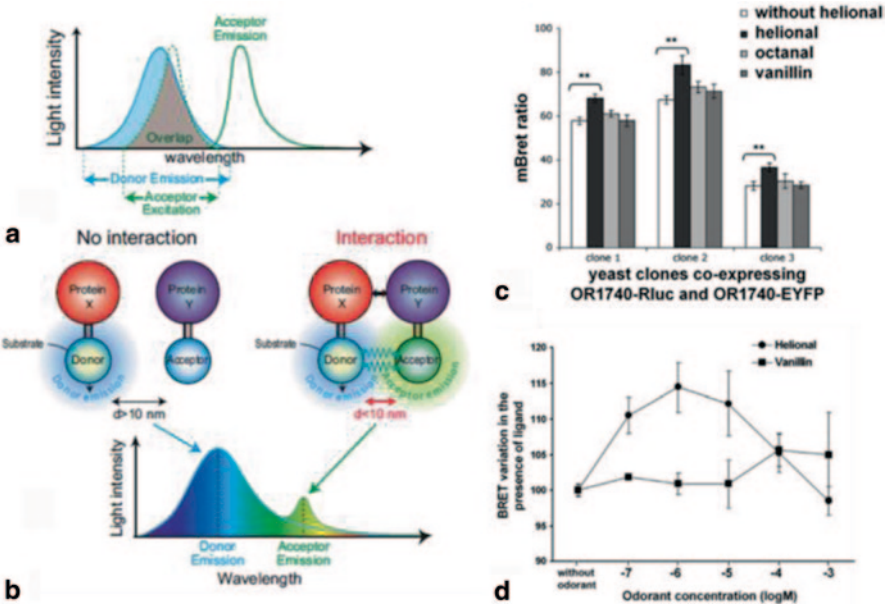

Fig. 11.5 The principle of BRET-based assay. **a** To have an energy transfer between a donor (light-producing enzyme) and an acceptor (fluorophore), the emission spectrum of the donor must overlap with the excitation spectrum of the acceptor. **b** The energy transfer can occur only when the donor and the acceptor are spatially close. BRET signal will be measured using fusion with protein of interest when the two proteins studied physically interact. (Reprinted from Ref. [70] for **a** and **b** with permission from John Wiley & Sons, Inc). **c** Odorant-induced BRET signal measurement. Crude membranes from three different clones co-expressing hOR1740-Rluc and hOR1740-EGFP were used to perform BRET assays without or with odorants (helional as a hOR1740 agonist) **d** BRET level variation upon hOR1740 stimulation with different helional concentrations. (Reprinted from Ref. [71] for **c** and **d** with permission from ASBME)

in vivo monitoring of biological events via signal cascades such as gene expression and protein-protein interaction. Such technical progresses have led to the development of sensitive and selective bio-analytical tools like recombinant whole-cell biosensors. In order to investigate protein-protein interactions, one protein is fused to the donor and the other to the acceptor. If the two fusion proteins interact and the distance between the energy donor and acceptor is less than 10 nm, a resonance energy transfer occurs and an additional light signal corresponding to the acceptor reemission can be detected (see Fig. 11.5).

Fluorescent methods which include FRET, utilize specific changes in conformation or interaction of fluorescently labeled molecules as a result of a biological process, to produce an increase or decrease in fluorescence [72]. Such interactions can be measured within, or independently of a cell. German et al. described an insect OR protein by the FRET technique [73]. Fusion proteins containing cyan fluorescent protein (CFP) or yellow fluorescent protein (YFP) were produced using the baculovirus-mediated expression. In another example, the use of FRET-

based “cameleon”, which is the genetically encoded calcium-sensitive fluorescence protein, was reported to visualize odorant-evoked intracellular calcium concentration changes [74, 75]. Cameleons for measuring the level of intracellular Ca^{2+} ions are genetically engineered proteins that can detect free Ca^{2+} and are comprised of tandem fusions of a blue or cyan mutant of the green fluorescent protein (GFP), calmodulin, calmodulin-binding M13 fragment of myosin light chain kinase. If Ca^{2+} binds to the calmodulin of these cameleons, the distance between the two GFP variants shortens and FRET follows. The light emitted from the first GFP variant (458 nm) excites the other GFP variant (480 nm), and the second variant emits a photon with an even longer wavelength (520 nm). Hence, the FRET between the GFP variants can be used to monitor the localized Ca^{2+} signals in olfactory cells upon ligand stimulation [75].

BRET studies are conducted commonly during the heterologous expression of GPCRs in mammalian cells [76]. The BRET method is based on the FRET occurring in some marine species (i.e. *Renilla reniformis*) and leading to a non-radiative energy transfer between an energy donor and an energy acceptor [70]. The homodimerization of the hOR17-40 protein and its involvement in receptor activation upon odorant ligand binding was addressed by BRET approaches [71] (see Fig. 11.4). This study demonstrated that the BRET signal increases upon odorant ligand stimulation, which supports a conformational change of the OR. Modulation of the BRET signal upon stimulation with increasing amounts of helional displays a bell-shaped curve and a two-state model (active and inactive states) of OR addressed by different ligand concentrations. Most BRET studies in GPCR rely on the detection of the consequences of GPCR activation by monitoring the conformational change of the receptor dimer [77–79]. Also, a cAMP sensor using YFP-Epac (known as a cAMP-regulated guanine nucleotide exchange factor)-Luc, a quantitative cAMP BRET-sensor assay able to monitor he modulation of cAMP levels in cells, has been developed and used to follow G protein activation by GPCRs [80] (Fig. 11.6).

11.2.4 Total Internal Reflection Based Sensor

Total internal reflection fluorescent microscopy (TIRFM) provides high signal to noise ratio by collecting signals form a thin region of a biological specimen [82]. In total internal reflection, one can expect there will be evanescent wave propagating into the second medium at the boundary according to Maxwell’s equation. Assuming harmonic oscillation of an electric field of the incident light, the transmitted electric field, denoted E_T can be obtained through the combination of Maxwell equation and Snell’s law as shown in equation, derived from the Helmholtz equation with dispersive, homogeneous, isotropic conditions.

$$\nabla^2 E + \frac{\omega^2}{c^2}\varepsilon E = 0$$

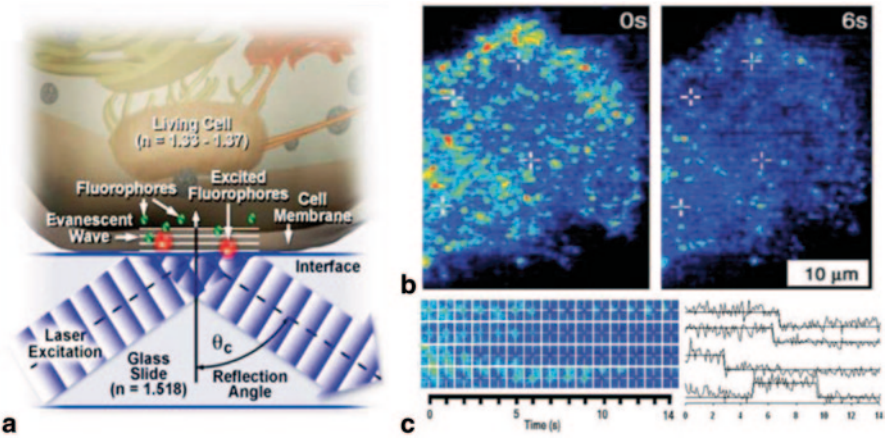

Fig. 11.6 **a** The concept of total internal reflection fluorescence (TIRF) microscopy. TRIF employs the properties of an induced evanescent wave to selectively illuminate and excite fluorophores in a restricted region adjacent to a glass-water. At a critical angle, the light is totally reflected from the glass/water interface, rather than passing through and refracting in accordance with Snell's law. The reflection generates a very thin electromagnetic field (usually less than 200 nm). Fluorophores in the membrane near the glass interface (small green spheres) are excited by the evanescent wave and subsequently emit secondary fluorescence (*red*). (Reprinted from Davidson with permission from the Florida State University). **b** Detection of single molecules of eGFP-PH123 in the lamella of a living mouse myoblast. Individual TIRF images taken 0, and 6 s after the start of recording. **c** Representative images of four different individual fluorescent spots marked by cross-hairs. Right graph shows variation in the average fluorescence of the total area. (Reprinted from Ref. [81] with permission from ASBMB)

$$E_T = E_0 e^{-\kappa z} e^{i(kx-\omega t)}$$

where

$$\kappa = \frac{\omega}{c}\sqrt{(n_1 \sin(\theta_I))^2 - n_2^2}$$

and

$$k = \frac{\omega n_1}{c}\sin(\theta_I)$$

Here θ_I stands for the incident angle of the electric field, n for refractive index of a medium, k for propagating vector, ω for oscillating frequency and c for the speed of the light. This equation displays a property of the wave propagating along x-axis and its exponential attenuation along z-axis. This attenuation in z-axis is responsible for the evanescent field, which is highly localized on the penetrated plane. Typical order of this attenuation due to the factor of κ in the equation is around 100 to 200 nm depending upon the parameters.

Because of its evanescence property, a restricted area of interest—typically less than 200 nm—will allow extremely narrow sample profiling, which enables compact and high-resolution observation of a large number of molecular events in cellular surface. Examples are direct observation of cell adhesion, binding of cells by bacterial toxin [83] and dimerization of GPCR [84] by using an Alexa Fluor594 conjugated N-formyl peptide ligand. Since TIRFM is a universal microscopic technique to observe biological processes, it is critical to combine this technology with other representative biochemical methods to envision biological processes. Combination of the two conventional biochemical technologies—FRET and TIRF provides synergistic effects on probing physiological implication of the M_2-$GABA_B$ heterodimer [85]. Also combination of TIRFM with SNAP-tag protein labeling system [86] (labeling cell-surface GPCRs with small organic fluorophore which enables the specific, covalent attachment of virtually any molecules to a target protein) was demonstrated to visualize individual GPCRs on the surface of living cells. And this allowed a time-lapse monitoring with the spatial arrangement, mobility, and supramolecular organization of GPCRs [87].

11.2.5 Fluorescent Correlation Spectroscopy Based Study on GPCR

Fluorescent Correlation Spectroscopy (FCS) is a powerful tool used to examine molecular level dynamics/kinetics through correlation analysis of fluctuation of a target fluorescent intensity in equilibrium. FCS provides very sensitive analysis on molecule kinetics by observing an extremely small number of analytes ranging from nM to pM, typically in an extremely confined volume (~1 μm^3). As a result, this powerful observation technique enables one to measure the diffusion of target analytes (mostly protein) in intact living cells. GPCRs are related with many proteins via molecular association/dissociation dynamics and an ideal molecular process to be monitored by the FCS. The one-dimensional autocorrelation is given by the equation [88]

$$G(\tau) = \frac{1}{N} \frac{1}{\sqrt{1+\tau/\tau_d}} \exp\left[\frac{\tau}{\tau_f} \frac{1}{\sqrt{1+\tau/\tau_d}} \right]$$

where N stands for the number of the analyte in the confined volume, τ_d for the diffusion of coefficient of the analyte and τ_f for an external kinetic factor.

A typical FCS set-up as shown in Fig. 11.7 is comprised of illumination laser optics with 405–633 nm wavelength lasers and a dichroic mirror through which the lasers are guided to a microscope objective [89]. The laser then is tightly focused onto the site of analytes, yielding a very confined area of analysis. Fluorescent bursts by laser excitation are recorded using a highly sensitive

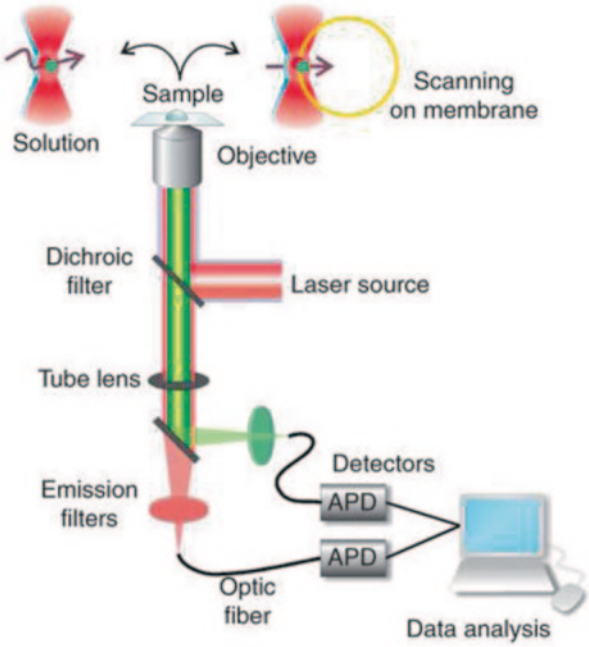

Fig. 11.7 A typical FCS set up on an inverted laser-scanning microscope. In a fixed focal volume, diffusion and binding of labeled proteins in aqueous environment can be monitored with FCS. To measure the molecular events in the membrane, scanning FCS is employed and the focal volume is scanned vertically through the membrane. (Reprinted from Ref. [89] with permission from NPG.)

semiconductor based photodetector, avalanche photodiode (APD). Information regarding molecular kinetics including can be acquired through FCS analysis including diffusion coefficient of analytes (denoted as τ_d), average concentration of analytes (denoted as N), and kinetic factor by external perturbation (denoted as τ_f) as shown in equation 1. In GPCR applications, fluorescently labeling the molecule of interest is the very first step to utilize this powerful technique. The detailed information can be found in a review paper by Jakobs et al. [90]. Also the FCS application for single-cell pharmacology is well described by Briddon et al. [91]. Other detailed methods for examining GPCRs including FCS itself, were well introduced in the book by Poyner et al. [92]. Examples of GPCR applications are numerous. First, Herrick-Davis et al. determined the diffusion coefficient and oligomeric size of GPCR by using an FCS and photon counting histogram (PCH) and concluded that dimeric 5-HT_{2C} receptors freely diffuse within the plasma membrane [93]. Gao et al. [94] utilized FCS to identify SP-bound NK1R-containing NLPs for measuring their dissociation constant (~83 nM) in aqueous solution. For general FCS applications in observing intracellular events, two review papers are very helpful to understand the practical and theoretical applications of FCS to cell biology [95, 96].

11.3 Label-free Optical Methods for ORs and GPCRs

Optical techniques have been developed using a wide range of platforms and are potentially useful for high-throughput ligand screening and functional analyses of hundreds of ORs. This section provides detailed label-free optical techniques for receptor-ligand assays.

11.3.1 Surface Plasmon Resonance (SPR) Based Odorant Sensing

SPR is a well-known and powerful technique that can measure molecular interactions on the surface of a sensor chip in real-time without any labeling. SRP detection relies on the measurement of a reflective index change at a metal surface which has been functionalized with probe molecules [97, 98]. Basically, a surface plasmon (SP) wave is an electromagnetic wave which propagates along the boundary between a dielectric and a metal interface [99–101].

An SPW is a transverse-magnetic ™ wave (magnetic vector is parallel to the plane of interface) and is characterized by the propagation constant and electromagnetic field distribution. The propagation constant of an SP wave, can be depicted as below:

$$k_{SP} = \frac{\omega}{c}\sqrt{\frac{\varepsilon_d \cdot \varepsilon_m}{\varepsilon_d + \varepsilon_m}}$$

where, ω is the angular frequency of the SP wave, c is the velocity of light in vacuum, and ε_d and ε_m are dielectric functions of the dielectric material and metal, respectively (see Fig. 11.8). The electromagnetic field of an SP wave is confined at the metal-dielectric boundary and decreases exponentially into media. The SP wave propagates in the x- and y-axis along the metal/dielectric interface, for distances of tens to hundreds of microns and decays evanescently in the z-axis. The interactions between the biomolecular layer and metal surface lead to a change in the plasmon resonance conduction such as angle and wavelength shift [102]. These interactions can be measured the reflectivity of light as a function of either angle of incidence (at constant wavelength) or wavelength (at constant angle of incidence).

The degree of the change in the propagation constant of an SPW depends on the refractive index (RI) change and its distribution regarding the profile of SPW field. Therefore, the RI change (Δn) by the binding event, produces a change in the propagation constant ($\Delta\beta$), which is directly proportional to the RI change:

$$\mathrm{Re}\{\Delta\beta\} \cong k\Delta n$$

where k denotes the free-space wave number. If the RI change is caused by a binding event occurring within a distance from the surface d, the corresponding change in the propagation constant can be expressed as follows:

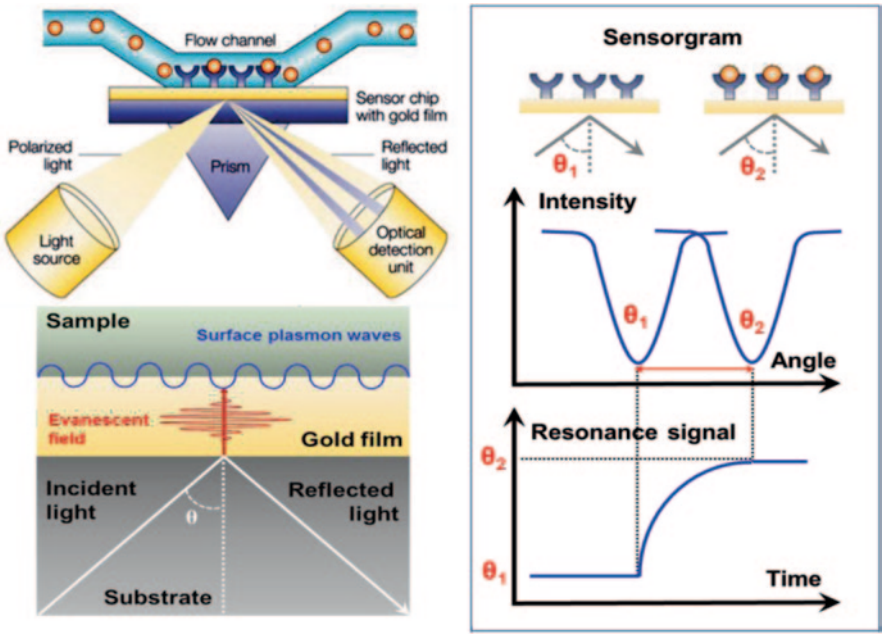

Fig. 11.8 Schematic diagrams illustration of surface plasmon resonance biosensor. (Reprinted from Ref. [98] with permission from NPG)

$$Re\{\Delta\beta\} \cong \frac{2n_s \cdot n_f \cdot k^2 d}{\sqrt{\left|Re\{\varepsilon_m\}\right|}} \Delta n = k\Delta n$$

where n_f and n_s denote the RI of the biomolecular and the background dielectric medium (sample), respectively. The propagation constant of SP wave by the binding event is proportional to the RI change and depth of the area [101]. Based on this theory, Fig. 11.8 shows the principles of the SPR sensor. An evanescent wave appears on the interface between a gold (Au) surface and a prism when light is irradiated onto the Au surface through the prism. A SP, a compression wave of electrons, on the Au surface fronting the sample solution is excited by the evanescent wave. When the wave numbers of the SP and evanescent waves are equal, the intensity of refraction is reduced because the photon energies are used to excite the SP resonance. The resonance angle, which is the incident angle when the refraction intensity is minimum, is affected by the refractive indices of the thin Au film and the attached solution. As such, the resonance angle is markedly shifted by the binding of specific ligands to an immobilized biomolecules on the Au thin film.

Recently, several studies have attempted to use SPR to investigate the interactions between ORs and odorants. SPR sensors can provide tools to understand the molecular mechanisms of odorant detection, with the direct evaluation of competitive

OR-odorant interactions or indirect detection via signal transduction by the binding OR-odorant in living cell. SPR techniques are implemented for real-time monitoring of step-by-step surface immobilization to test the functional response of an immobilized OR [103]. ORs were immobilized onto a gold surface functionalized by mixed self-assembled monolayers and biotin/neurtravidin. The study showed that the specific immobilization of capturing the OR via an antibody yields a uniform orientation of OR protein onto the surface while keeping the receptor activity preserved by a binding assay. Vidic et al. reported that the rORI7 and hOR17-40 could be functionally expressed in *S. cerevisiae* [15]. They also developed yeast-derived nanosomes with OR protein-grafted SPR technique to quantitatively evaluate OR stimulation by an odorant (see Fig. 11.9).

In another example, Benilova et al. described OR-carrying nanosomes based olfactory biosensor using SPR [104]. The hOR17-40 was heterologously co-expressed with $G_{\alpha olf}$ protein in yeast, and nanosomes were prepared and then specifically immobilized. The result showed the bell-shaped response profile with two maximum (1 nM and 1 μM) observed for the helional, which is a specific odorant. Interestingly, the molecular mechanisms by focusing on dynamic interactions between OR, odorant binding protein (OBP) and odorant was investigated using the SPR technique [14]. OBPs can bind and solubilize volatile odorants, facilitating their diffusion through the mucus barrier towards ORs. The high-affinity binding of a porcine OBP to a human OR has been demonstrated, suggesting that a specific OR-OBP association may occur in the absence of any odorant [105]. Results show that SPR-based assay enables the direct demonstration of interactions between the three components involved in the initial step of olfactory signal transduction.

The SPR technique was used for the analysis of interaction between living olfactory cells and odorants. This technique was applied to the cell-based measurement of odorant molecules [13, 102]. ODR-10, with the help of the rho-tag import sequence, the OR protein of the nematode *C. elegans*, was expressed on the surface of the HEK-293 cell and cultured in Au film. Exposure of the cells to diacetyl, an odorant molecule specific to the ODR-10, induced a SPR signal. The ODR-10 on the *C. elegans* neuron is coupled to an IP_3 pathway, which leads to the release of Ca^{2+} from the intracellular stores such as ER [106, 107]. This intracellular signaling through the binding of odorant molecules to OR can make SPR signals. In other example, Real-time monitoring of odorant-induced cellular reaction via signal transduction was demonstrated using an SPR system [12]. The key features are the intracellular signal transduction triggered by the specific binding of odorants to the ORs and the SPR response generated by the intracellular change. The SPR response to the odorant molecules was quantitative and selective. It was linearly dependent on the odorant concentration and the response signal was much lower than other odorant molecules sharing similar chemical structures and properties.

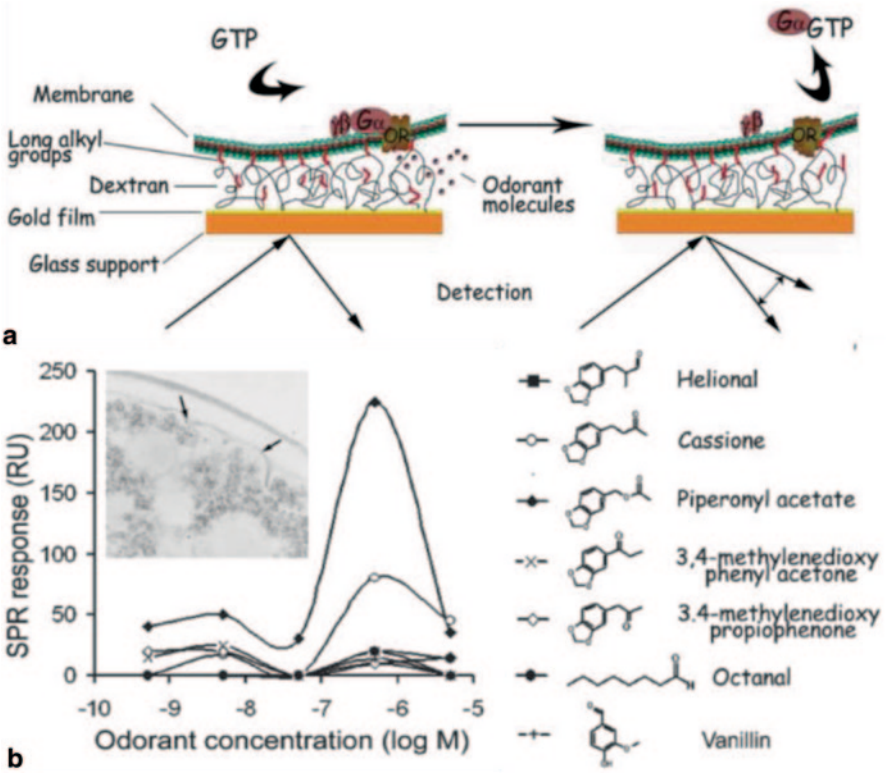

Fig. 11.9 **a** Principle of SPR sensor system using yeast nanosome for odorant detection. The scheme presents ruptured and fused nanosomes. Upon stimulation of an OR with an odorant, the G_α subunit in the presence of GTP is activated and desorption of G_α from the lipidic bilayer can be measured. **b** Detection of odorants in immobilized nanosomes containing OR protein by SPR sensor. Differential SPR responses obtained upon stimulation of the ORs in nanosomes with various odorants. Arrows indicate the expression of OR protein on the membrane of yeast cells in inset. (Reprinted from Ref. [15] with permission from RSC)

11.3.2 Raman and its Derivative Technique

Visible wavelength scattered by certain molecules differs from that of the incident beam and is conferred the shifts in wavelength depending upon the chemical structure of the molecules responsible for the scattering as shown in Fig. 11.10. These phenomena can be understood throughout the inelastic scattering and Raman spectroscopy probes the vibrational transitions in a sample through the collection and analysis of scattered photons after sample excitation by laser. A classical picture of Raman and Rayleigh scattering with a diatomic molecule can be explained by following equations. Starting with the harmonic incident light, $E = E_0\cos(\omega_i t)$ will induce dipole from the E-field as below:

$$\mu_{ind} = \alpha E = \alpha E_0 \cos(\omega_i t)$$

The molecular polarizability changes with bond length and the bond length oscillating at vibrational frequency would yield.

$$\alpha = \alpha_0 + (r - r_{eq})\frac{d\alpha}{dr}, \quad r - r_{eq} = r_{\max}\cos(\omega_{vib} t)$$

Therefore, combining all conditions together with simple Euler's formula, we obtain the basic equation for Raman.

$$\mu_{ind} = \underbrace{\alpha_0 E_0 \cos(\omega_i t)}_{\text{Rayleigh}} + \underbrace{\frac{1}{2} E_0 r_{\max} \frac{d\alpha}{dr}[\cos((\omega_i + \omega_{vib})t)}_{\text{Anti-Stokes}} + \underbrace{\cos((\omega_i - \omega_{vib})t)]}_{\text{Stokes}}$$

Due to the near instantaneous results allowing samples to be analyzed at some distance from the instrumentation [43], the potential of this technique for use as biological molecule detection has led to considerable work within this area. A review that describes advances in the capacity of portable Raman instrumentation has also highlighted some of the issues relating to producing instrumentation for field deployable apparatus [44]. Sensitivity is a key, and much of this has been addressed by using techniques such as surface enhanced Raman spectroscopy that displays significantly higher sensitivity. Since much of the equipment used is still laboratory based, future trends indicate that portable instruments are increasing in need and being developed. Use of fiber optic technology to allow remote sampling is also being investigated as an alternative avenue. To examine GPCR, the Mathies laboratory at UC Berkeley utilized resonance Raman spectroscopy to observe rhodopsin mutants with effect of substitutions in the third transmembrane helix [109], photoactivation of the GPCR rhodopsin [110] and the structure of primary isomerization [111].

In liue of a weak Raman signal from Raman spectroscopy, a complementary technique, Surface-Enhanced Raman Scattering (SERS) is used to enhance the intensity of Raman scattering spectra through the proximity of a molecule to a bumpy metal surface or, in the case of nanoparticles, between gaps in nanostructures or nanoparticles. As shown in Fig. 11.11, the embedded equation estimates the scattering signal amplification for SERS. The total amplified SERS signal, $P_{SERS}(\nu_S)$ is directly proportional to the Raman cross section σ^R_{ads}, the excitation laser intensity I_L, and the number of molecules N involved in the SERS process. In the equation, $A(\nu_L)$ and $A(\nu_S)$ stands for the local enhancement factors for the laser and for the Raman scattered field, respectively. These were demonstrated to show extreme signal amplification (up to $10^{12} \sim 10^{15}$) of biological molecules including viruses [112], beta-amyloid and so forth with their unique Raman signatures. Thanks to its unique merit in significant signal amplification and molecular signatures, the University of Ottawa research laboratory utilized functionalized silver nanoparticle for tagging β_2ARs to observe signaling domain formation under SERS microscopy [113]. A Polish research group then monitored natural ligands of the GPCRs using systematic SERS characteristics [114–118]. Silver, gold and copper surfaces were

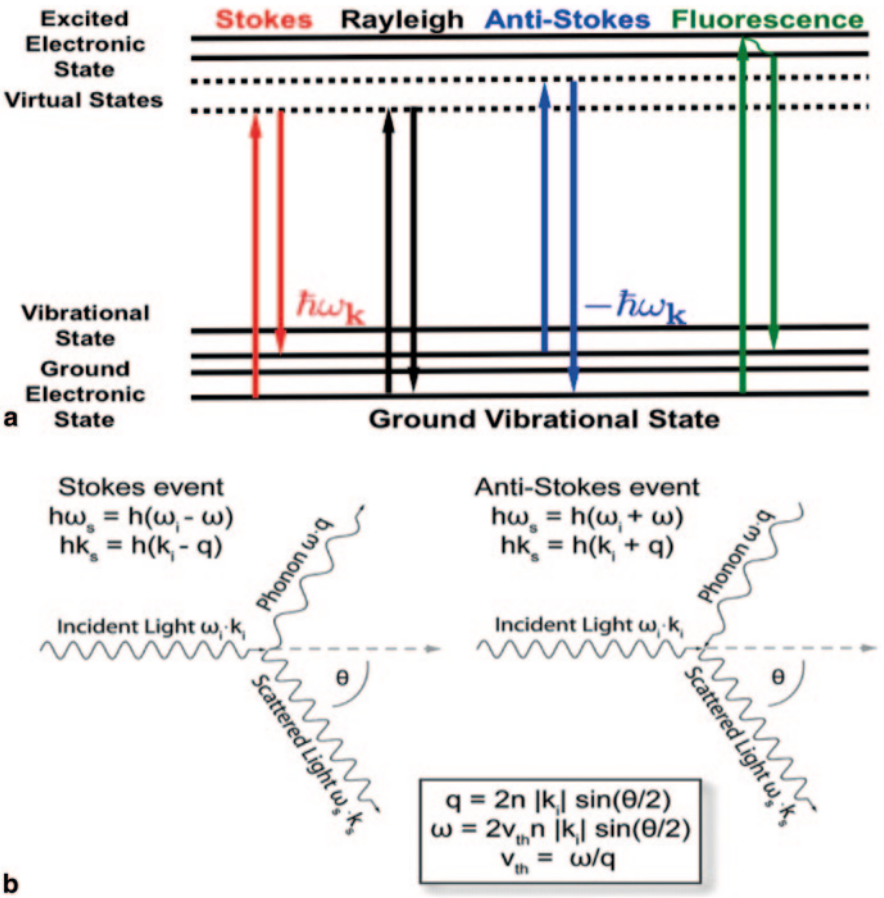

Fig. 11.10 **a** Energy diagram of Raman (Stokes and Anti-Stokes), Rayleigh (elastic scattering) and fluorescence. Raman spectra are different from fluorescence in terms of their shift wavelengths. While fluorescence is anchored at their shifted wavelength, Raman shift can take any wavelengths. **b** Inelastic processes of Stokes and Anti-Stokes. (Reprinted from Ref. [108] with permission from Schweizerbart, Science Publishers)

used for determine the absorption mechanisms of these peptides. The absorption mechanisms were then extensively studied.

11.3.3 Photonic Crystal-based Optical Sensing

Periodic nanostructures with dielectric or metallo-dielectric properties are extremely sensitive in optical modulation of nearby photons with regards to their environmental changes or perturbation. This is, labeled as a photonic crystal sensor, which garners extreme sensitivity. Periodicity of photonic crystal nanostructures defined by crystal symmetries, lattice formation and its reciprocal lattice determine

the conduction of electrons in crystalline solids. This periodicity strengthened by Bloch state, significantly enhances the detection capability by fine-tuning several parameters for the photonic crystal. According to Bloch state, the energy eigenvalues can be depicted as below:

$$\varepsilon_n(\vec{k}) = \varepsilon_n(\vec{k} + \vec{K})$$

where $\vec{K}$ stands for periodicity of the reciprocal lattice vector (Fig. 11.12).

The unique eigen-states become very effective in resonance mode. The resonance mode can be modulated when refractive indices of the surrounding environments changes or the analyte is absorbed on a sensing surface, by changing the resonance condition of the Fabry-Perot microcavity:

$$2\frac{2\pi}{\lambda} nd\cos\theta + \alpha = (2m+1)\pi \quad \text{where} \quad (m = 0,1,2,....)$$

α stands for the ***Goos–Hänchen*** phase shift between sensing surface and bulk environmen, θ for the incident angle of the beam, n for the refractive index.

Because of its extreme sensitivity, it has been used to build a general-purpose platform for label-free and fluorescent assays [121–123]. The Cunningham research laboratory develops a method to investigate alterations of cell adhesion induced on photonic crystal sensors by exposing them to drugs with selective activation of a sub-class GPCR. Schematics of commercial photonic crystal product and their mechanisms are shown in Fig. 11.11. BIND® (SRU Biosystems) employs photonic crystal structures to provide sensitive measurements of changes in binding or adherence adjacent to the BIND Biosensor surface. These biosensors incorporate a novel nanostructured optical grating which reflects a narrow range of wavelengths of illuminating light with broadband light. BIND is able to test numerous biomolecular interactions including receptor activation, cell adhesion, protein-protein binding and so forth. Specifically, they have demonstrated a GPCR subtype (G_i, G_q, G_s, $G_{12/13}$ coupled) activation based on a variety of cellular responses including calcium mobilization, β-arrestin localization or second messenger levels.

Corning Corporation have also developed an EPIC® system for a high-throughput label-free screening platform based on optical biosensor technology [120]. Numerous applications on cell-based GPCR assays can be found [124–126] and compared to other label-free detection methodologies to provide interesting side-to-side evaluation [127, 128]. Fang et al. organized a list of publications regarding a label-free optical biosensor utilizing resonant waveguide gating for whole cell GPCR assays [129, 130]. These optical waveguide structures are fabricated by technologies based on microelectromechanical systems (MEMS); therefore it can be easily integrated with microfluidics for precise analyte controls over the optical waveguide. Many types of the microfluidic and nanofluidic systems have shown its compatibility with a variety of MEMS (i.e. electrochemical pump [131], microheater [132], NEMS resonator [133] etc.). In addition, a wide range of these micro and nanofluidic system (down to few nanometer [88]) will allow the same scale analysis of analytes incorporated onto this optical waveguide or any MEMS structure for receptor-relevant analysis.

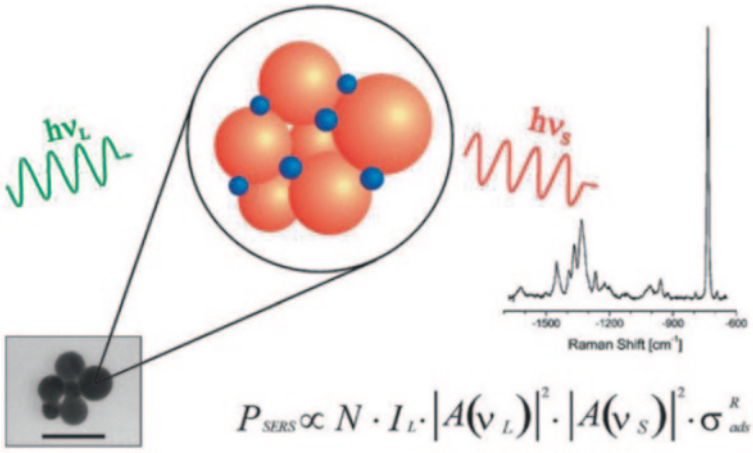

Fig. 11.11 Surface-enhanced Raman scattering (SERS) schematic is shown. Target molecules (represented by *blue dots*) are attached to metal-particles (*orange balls*). Inset shows the TEM graph of the actual particles. (Scale bar: 100 nm). The spectrum shown as an example was observed from 10^{-9} M adenine in a solution of silver slurry. (Reprinted from Ref. [119] with permission Elsevier)

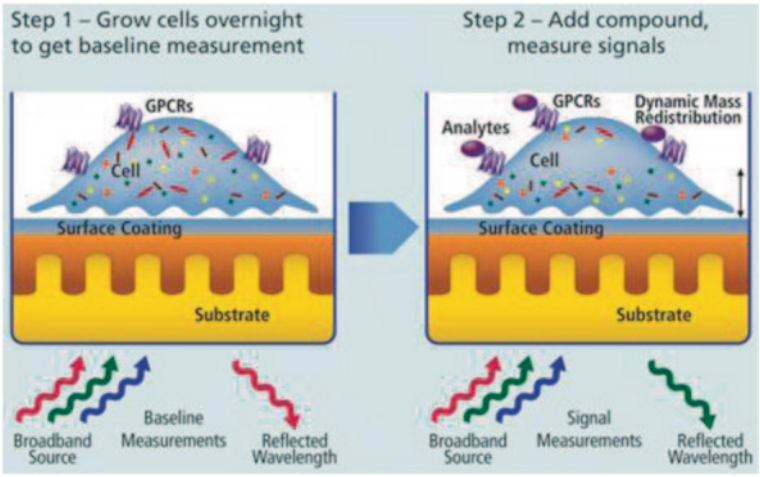

Fig. 11.12 Principle of label-free cell-based assay. A detection scheme of cellular events was demonstrated. A broadband light source will be filtered to a narrow range of wavelengths enabling sensitive and label-free detection. This reflects biological processes in Corning EPIC® systems. (Reprinted from Ref. [120] with permission GEN)

11.3.4 Fourier Transform Infrared Spectroscopy for GPCR Study

Fourier Transform Infrared Spectroscopy (FTIR) offers an analysis based on infrared spectra from absorption, emission, photoconductivity or Raman scattering from complex biological macromolecules. Mostly FTIR is to measure the absorption spectra from each wavelength. A typical setup for FTIR is shown in Fig. 11.11. As the name of this technique implies, the Fourier transformation as below is required to convert the acquired data to the actual spectra in a reciprocal space [134] where ω is the angular frequency.

$$\hat{f}(\omega) = \int_{-\infty}^{\infty} f(x) e^{-2\pi\omega x i} dx$$

The measured interferogram, I, is given by

$$I(x) = \int_{0}^{\infty} \hat{I}(\nu) \cos(2\pi x \nu) d\nu$$

This measure intererogram is converted into the computed spectrum denoted $\hat{I}$ by Fourier transformation.

$$\hat{I}(\nu) = 2\int_{0}^{\infty} I(x) \cos(2\pi x \nu) dx$$

The Michelson's interferometer is the core of the FTIR spectrometer for splitting beam into two paths so that the paths of the two beams are different resulting in interference. Assuming the distance between two paths is l, the light intensity can be described as:

$$I = \left|\vec{E}\right|^2 = \left|\vec{E}_1\right|^2 + \left|\vec{E}_2\right|^2 + 2\vec{E}_1 \cdot \vec{E}_2 \cos(\theta)$$

which can be approximated to

$$I(l) = 21 + \cos(kl)$$

This intensity can be transformed into the spectrum by Fourier transformation as below:

$$= \int_{0}^{\infty} 1 + \cos(kl) G(k) dk = \int_{0}^{\infty} G(k) dk + \int_{0}^{\infty} G(k) \frac{e^{ikx} + e^{-ikx}}{2} dk$$

$$= \frac{1}{2} I(0) + \frac{1}{2} \int_{-\infty}^{\infty} G(k) e^{ikx} dk$$

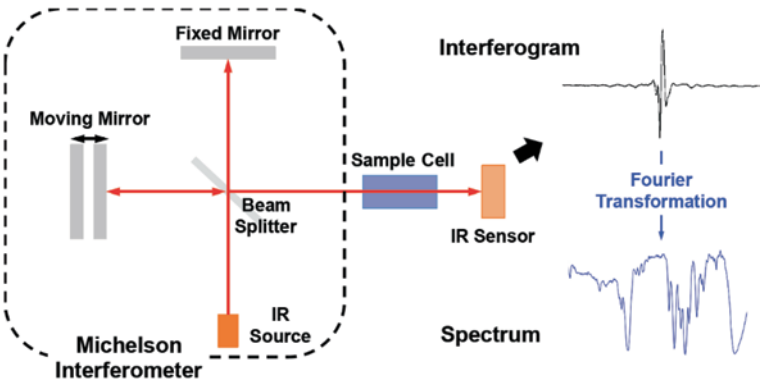

Fig. 11.13 A representative setup for FTIR microscopy. After data acquisition, the Fourier transformation converts raw data into analyzable spectra in a reciprocal domain

Thanks to this advanced technology, the accuracy of wavenumber is very sensitive with the errors within the range of ± 0.01 cm^{-1} (Fig. 11.13).

Since the working condition resides in infrared spectra, target analytes should be incorporated with IR-active tags such as azido probes [135] which has antisymmetric stretch vibration for absorption at ~2,100 cm^{-1}. Combining with molecular dynamic (MD) simulation allowed researchers to study the conformational diversity of rhodopsin in membrane environment, which yields perfect switching with high fidelity and rhodopsin/G protein transducin coupling [136]. The structural changes occurring in rhodopsin was dynamically monitored using FTIR-difference spectroscopy, while the rhodopsin underwent characteristic conformational change after photoisomerization of its 11-*cis*-retinal chromophore [137]. FTIR spectroscopy leads to the argument of an active opsin conformation presence in the crystal structure [138]. Vogel et al. demonstrated a conformation, which is similar to light-activated rhodopsin at neutral pH ranges [139], while low pH provides an environment for opsin in an inactive conformation [140]. The heterotrimeric G protein transducin plays a key role in opsin conformation in the opsin crystal resulting from co-crystallization of opsin with the key fragment from the transducin [141]. Further details regarding this argument can be found in the reference [138].

11.4 Conclusion

We have reviewed recent progress in various optical techniques focused on how optical techniques can be applied to detect specific odorant-OR interactions (see summary in Table 11.1). Our understanding of olfactory sensory systems by these optical techniques as well as other approaches has grown impressively in recent years as a result of intense efforts to characterize the mechanisms underlying olfaction. The subtle mechanisms for monitoring however are not completely elucidated, and many questions remain open. Still, recent accomplishments in optical

Table 11.1 Summary of the various optical techniques to utilize ORs and GPCRs as a biological sensing element

Transduction system	Receptor type	Analyte	Key features	Literature
Labeled optical method				
Ca^{2+} imaging	hOR17-4	Bourgeonal	Fluorescence, intracellular Ca^{2+} imaging, single cell	Spehr et al.
	Olfr43	Citronellal	Fluorescence, intracellular Ca^{2+} by FLIPR, Cell population	Shirokova et al.
Reporter gene-based system	Olfr226	2,4-dinitrotoluene	Fluorescence, CRE-mediated GFP expression	Radhika et al.
	mOR-EG	Eugenol	Bioluminescence, CRE-mediated luciferase expression	Katada et al.
FRET	rORI7, ODR-10	Octanal, Diacetyl	Calmodulin-based Ca^{2+} measurement, whole cell	Ko et al.
BRET	hOR17-40	Helional	Bioluminescence resonance energy transfer	Wade et al.
FRET-Total Internal Reflection	M_2-$GABA_B$	–	Dimer formation measurement by FRET	Boyer et al.
FCS	5-HT_{2C}	Psychoactive agent	Confined analysis, Diffusion analysis and single molecule sensitivity	Herrick-Davis et al.
Label-free optical method				
SPR	rOR I7	Octanal	Surface plasmon resonance, whole cell	Lee et al.
	hOR17-40	Helional	Surface plasmon resonance, nanosome	Vidic et al.
Raman spectroscopy	β2AR	Catecholamines	Vibration spectrum and surface enhanced resonance	Kennedy et al.
Photonic crystal-based sensor	PAR_1	Thrombin	Ligand induced dynamic mass redistribution, whole cell anaylsis	Fang et al.
	β2AR	Epinephrine		
	LPA_1	Lysophosphatidic acid		
FTIR	Rhodopsin	11-*cis*-retinal chromophore	Fourier transform infrared spectra	Jager et al.

techniques have demonstrated new and unique opportunities towards a sensitive and selective biophotonic nose as well as basic olfaction research in combinatorial code and the *in situ* topographic map in the olfactory bulb and brain.

Acknowledgements This research was supported by the Converging Research Center Program through the Ministry of Science, ICT and Future Planning, Korea (2013K000383), the National Research Foundation of Korea (NRF-2011-357-D00072), and Samsung Electronics, Inc.

References

1. Buck L, Axel R (1991) A novel multigene family may encode odorant receptors: a molecular basis for odor recognition. Cell 65:175–187
2. Keller A, Zhuang H, Chi Q et al (2007) Genetic variation in a human odorant receptor alters odour perception. Nature 449:468–472
3. Firestein S (2001) How the olfactory system makes sense of scents. Nature 413:211–218
4. Krieger J, Breer H (1999) Olfactory reception in invertebrates. Science 286:720–723
5. Bomback AS, Raff AC (2011) Olfactory function in dialysis patients: a potential key to understanding the uremic state. Kidney Int 80:803–805
6. Malnic B, Hirono J, Sato T et al (1999) Combinatorial receptor codes for odors. Cell 96:713–723
7. Touhara K, Sengoku S, Inaki K et al (1999) Functional identification and reconstitution of an odorant receptor in single olfactory neurons. Proc Natl Acad Sci USA 96:4040–4045
8. Zou D-J, Chesler A, Firestein S (2009) How the olfactory bulb got its glomeruli: a just so story? Nat Rev Neurosci 10:611–618
9. Touhara K (2002) Odor discrimination by G protein-coupled olfactory receptors. Microsc Res Tech 58:135–141
10. Katada S, Hirokawa T, Oka Y et al (2005) Structural basis for a broad but selective ligand spectrum of a mouse olfactory receptor: mapping the odorant-binding site. J Neurosci 25:1806–1815
11. Oka Y, Omura M, Kataoka H et al (2004) Olfactory receptor antagonism between odorants. EMBO J 23:120–126
12. Lee SH, Ko HJ, Park TH (2009) Real-time monitoring of odorant-induced cellular reactions using surface plasmon resonance. Biosens Bioelectron 25:55–60
13. Lee JY, Ko HJ, Lee SH et al (2006) Cell-based measurement of odorant molecules using surface plasmon resonance. Enzyme Microb Technol 39:375–380
14. Vidic J, Grosclaude J, Monnerie R et al (2008) On a chip demonstration of a functional role for odorant binding protein in the preservation of olfactory receptor activity at high odorant concentration. Lab Chip 8:678–688
15. Vidic JM, Grosclaude J, Persuy M-A et al (2006) Quantitative assessment of olfactory receptors activity in immobilized nanosomes: a novel concept for bioelectronic nose. Lab Chip 6:1026–1032
16. Ko HJ, Park TH (2005) Piezoelectric olfactory biosensor: ligand specificity and dose-dependence of an olfactory receptor expressed in a heterologous cell system. Biosens Bioelectron 20:1327–1332
17. Sung JH, Ko HJ, Park TH (2006) Piezoelectric biosensor using olfactory receptor protein expressed in *Escherichia coli*. Biosens Bioelectron 21:1981–1986
18. Sankarana S, Panigrahia S, Mallikb S (2011) Olfactory receptor based piezoelectric biosensors for detection of alcohols related to food safety applications. Sens Actuators B Chem 155:8–18
19. Sankaran S, Panigrahi S, Mallik S (2011) Odorant binding protein based biomimetic sensors for detection of alcohols associated with Salmonella contamination in packaged beef. Biosens Bioelectron 26:3103–3109

20. Lee SH, Kwon OS, Song HS et al (2012) Mimicking the human smell sensing mechanism with an artificial nose platform. Biomaterials 33:1722–1729
21. Lee SH, Jin HJ, Song HS et al (2012) Bioelectronic nose with high sensitivity and selectivity using chemically functionalized carbon nanotube combined with human olfactory receptor. J Biotechnol 157:467–472
22. Park SJ, Kwon OS, Lee SH et al (2012) Ultrasensitive flexible graphene based (FET)-type bioelectronic nose. Nano Lett 12:5082–5090
23. Lim JH, Park J, Oh EH et al (2013) Nanovesicle-based bioelectronic nose for the diagnosis of lung cancer from human blood. Adv Healthc Mater. doi:10.1002/adhm.201300174
24. Kim TH, Lee SH, Lee J et al (2009) Single-carbon-atomic-resolution detection of odorant molecules using a human olfactory receptor-based bioelectronic nose. Adv Mater 21:91–94
25. Goldsmith BR, Mitala JJ, Josue J et al (2011) Biomimetic chemical sensors using nanoelectronic readout of olfactory receptor proteins. ACS Nano 5:5408–5416
26. Liu Q, Ye W, Hu N et al (2010) Olfactory receptor cells respond to odors in a tissue and semiconductor hybrid neuron chip. Biosens Bioelectron 26:1672–1678
27. Liu Q, Cai H, Xu Y et al (2006) Olfactory cell-based biosensor: a first step towards a neurochip of bioelectronic nose. Biosens Bioelectron 22:318–322
28. Wu C, Chen P, Yu H et al (2009) A novel biomimetic olfactory-based biosensor for single olfactory sensory neuron monitoring. Biosens Bioelectron 24:1498–1502
29. Liu Q, Ye W, Yu H et al (2010) Olfactory mucosa tissue-based biosensor: a bioelectronic nose with receptor cells in intact olfactory epithelium. Sens Actuators B Chem 146:527–533
30. Lee SH, Jun SB, Ko HJ et al (2009) Cell-based olfactory biosensor using microfabricated planar electrode. Biosens Bioelectron 24:2659–2664
31. Lee SH, Jeong SH, Jun SB et al (2009) Enhancement of cellular olfactory signal by electrical stimulation. Electrophoresis 30:3283–3288
32. Liu Q, Ye W, Xiao L et al (2010) Extracellular potentials recording in intact olfactory epithelium by microelectrode array for a bioelectronic nose. Biosens Bioelectron 25:2212–2217
33. Lee SH, Park TH (2010) Recent advances in the development of bioelectronic nose. Biotechnol Bioprocess Eng 15:22–29
34. Kaupp UB (2010) Olfactory signalling in vertebrates and insects: differences and commonalities. Nat Rev Neurosci 11:188–200
35. Zhang X, Firestein S (2002) The olfactory receptor gene superfamily of the mouse. Nat Neurosci 5:124–133
36. Godfrey PA, Malnic B, Buck LB (2003) The mouse olfactory receptor gene family. Proc Natl Acad Sci U S A 101:2156–2161
37. Zozulya S, Echeverri F, Nguyen T (2001) The human olfactory receptor repertoire. Genome Biol 2:research0018.1–0018.12
38. Glusman G, Yanai I, Rubin I et al (2001) The complete human olfactory subgenome. Genome Res 11:685–702
39. Fuchs T, Glusman G, Horn-Saban S et al (2001) The human olfactory subgenome: from sequence to structure and evolution. Hum Genet 108:1–13
40. Malnic B, Godfrey PA, Buck LB (2004) The human olfactory receptor gene family. Proc Natl Acad Sci U S A 101:2584–2589
41. Glusman G, Bahar A, Sharon D et al (2000) The olfactory receptor gene superfamily: data mining, classification, and nomenclature. Mamm Genome 11:1016–1023
42. Wang J, Luthey-Schulten ZA, Suslick KS (2003) Is the olfactory receptor a metalloprotein? Proc Natl Acad Sci U S A 100:3035–3039
43. Shirokova E, Schmiedeberg K, Bedner P et al (2005) Identification of specific ligands for orphan olfactory receptors. J Biol Chem 280:11807–11815
44. Touhara K (2007) Deorphanizing vertebrate olfactory receptors: recent advances in odorant-response assays. Neurochem Int 51:132–139
45. Kajiya K, Inaki K, Tanaka M et al (2001) Molecular bases of odor discrimination: reconstitution of olfactory receptors that recognize overlapping sets of odorants. J Neurosci 21:6018–6025

46. Peterlin Z, Li Y, Sun G et al (2008) The importance of odorant conformation to the binding and activation of a representative olfactory receptor. Chem Biol 15:1317–1327
47. Ko HJ, Park TH (2006) Dual signal transduction mediated by a single type of olfactory receptor expressed in a heterologous system. Biol Chem 387:59–68
48. Jacquier V, Pick H, Vogel H (2006) Characterization of an extended receptive ligand repertoire of the human olfactory receptor OR17-40 comprising structurally related compounds. J Neurochem 97:537–544
49. Spehr M, Gisselmann G, Poplawski A et al (2003) Identification of a testicular odorant receptor mediating human sperm chemotaxis. Science 299:2054–2058
50. Omura M, Sekine H, Shimizu T et al (2003) In situ Ca^{2+} imaging of odor responses in a coronal olfactory epithelium slice. Neuroreport 14:1123–1127
51. Wetzel CH, Oles M, Wellerdieck C et al (1999) Specificity and sensitivity of a human olfactory receptor functionally expressed in human embryonic kidney 293 cells and *Xenopus laevis* oocytes. J Neurosci 19:7426–7433
52. Katada S, Nakagawa T, Kataoka H et al (2003) Odorant response assays for a heterologously expressed olfactory receptor. Biochem Biophys Res Commun 305:964–969
53. Hamana H, Shou-xin L, Breuils L et al (2010) Heterologous functional expression system for odorant receptors. J Neurosci Methods 185:213–220
54. Zhao H, Ivic L, Otaki JM et al (1998) Functional expression of a mammalian odorant receptor. Science 279:237–242
55. Saito H, Kubota M, Roberts RW et al (2004) RTP family members induce funcitonal expression of mammalian odorant receptors. Cell 119:679–691
56. Zhuang H, Matsunami H (2007) Synergism of accessory factors in functional expression of mammalian odorant receptors. J Biol Chem 282:15284–15293
57. Behrens M, Bartelt J, Reichling C et al (2006) Members of RTP and REEP gene families influence functional bitter taste receptor expression. J Biol Chem 281:20650–20659
58. Saito H, Chi Q, Zhuang H et al (2009) Odor coding by a mammalian receptor repertoire. Sci Signal 2:1–14
59. Oka Y, Nakamura A, Watanabe H et al (2004) An odorant derivative as an antagonist for an olfactory receptor. Chem Senses 29:815–822
60. Araneda RC, Kini AD, Firestein S (2000) The molecular receptive range of an odorant receptor. Nat Neurosci 3:1248–1255
61. Mori K, Sakano H (2011) How is the olfactory map formed and interpreted in the mammalian brain? Annu Rev Neurosci 34:467–499
62. Wilson T, Hastings JW (1998) Bioluminescence. Annu Rev Cell Dev Biol 14:197–230
63. Hill SJ, Baker JG, Rees S (2001) Reporter-gene systems for the study of G-protein-coupled receptors. Curr Opin Pharmacol 1:526–532
64. Roda A, Pasini P, Mirasoli M et al (2004) Biotechnological applications of bioluminescence and chemiluminescence. Trends Biotechnol 22:295–303
65. Altarejos JY, Montminy M (2011) CREB and the CRTC co-activators: sensors for hormonal and metabolic signals. Nat Rev Mol Cell Biol 12:141–151
66. Radhika V, Proikas-Cezanne T, Jayaraman M et al (2007) Chemical sensing of DNT by engineered olfactory yeast strain. Nat Chem Biol 3:325–330
67. Shan Q, Storm DR (2010) Optimization of a cAMP response element signal pathway reporter system. J Neurosci Methods 191:21–25
68. Minic J, Persuy MA, Godel E et al (2005) Functional expression of olfactory receptors in yeast and development of a bioassay for odorant screening. FEBS J 272:524–537
69. Fukutani Y, Noguchi K, Kondo A et al (2012) An improved bioluminescence-based signaling assay for odor sensing with a yeast expressing a chimeric olfactory receptor. Biotechnol Bioeng 109:3143–3151
70. Bacart J, Corbel C, Jockers R et al (2008) The BRET technology and its application to screening assays. Biotechnol J 3:311–324
71. Wade F, Espagne A, Persuy MA et al (2011) Relationship between homo-oligomerization of a mammalian olfactory receptor and its activation state demonstrated by bioluminescence resonance energy transfer. J Biol Chem 286:15252–15259

72. Miyawaki A, Llopis J, Heim R et al (1997) Fluorescent indicators for Ca^{2+} based on green fluorescent proteins and calmodulin. Nature 388:882–887
73. German PF, van der Poel S, Carraher C et al (2013) Insights into subunit interactions within the insect olfactory receptor complex using FRET. Insect Biochem Mol Biol 43:138–145
74. Fiala A, Spall T, Diegelmann S et al (2002) Genetically expressed cameleon in drosophila melanogaster is used to visualize olfactory information in projection neurons. Curr Biol 12:1877–1884
75. Ko HJ, Park TH (2007) Functional analysis of olfactory receptors expressed in a HEK-293 cell system by using cameleons. J Microbiol Biotechnol 17:928–933
76. Bouvier M, Heveker N, Jockers R et al (2007) BRET analysis of GPCR oligomerization: newer does not mean better. Nat Methods 4:3–4
77. Charest PG, Terrillon S, Bouvier M (2005) Monitoring agonist-promoted conformational changes of b-arrestin in living cells by intramolecular BRET. EMBO Rep 6:334–340
78. Jensen AA, Hansen JL, Sheikh SP et al (2002) Probing intermolecular protein–protein interactions in the calcium-sensing receptor homodimer using bioluminescence resonance energy transfer (BRET). Eur J Biochem 269:5076–5087
79. Ayoub MA, Couturier C, Lucas-Meunier E et al (2002) Monitoring of ligand-independent dimerization and ligand-induced conformational changes of melatonin receptors in living cells. J Biol Chem 277:21522–21528
80. Jiang Li, Collins, Davis R et al (2007) Use of a cAMP BRET sensor to characterize a novel regulation of cAMP by the sphingosine 1-phosphate/G13 pathway. J Biol Chem 282:10576–10584
81. Mashanov GI, Tacon D, Peckham M et al (2004) The spatial and temporal dynamics of pleckstrin homology domain binding at the plasma membrane measured by imaging single molecules in live mouse myoblasts. J Biol Chem 279:15274–15280
82. Mattheyses AL, Simon SM, Rappoport JZ (2010) Imaging with total internal reflection fluorescence microscopy for the cell biologist. J Cell Sci 123:3621–3628
83. Moran-Mirabal JM, Edel JB, Meyer GD et al (2005) Micrometer-sized supported lipid bilayer arrays for bacterial toxin binding studies through total internal reflection fluorescence microscopy. Biophys J 89:296–305
84. Kasai RS, Suzuki KG, Prossnitz ER et al (2011) Full characterization of GPCR monomer-dimer dynamic equilibrium by single molecule imaging. J Cell Biol 192:463–480
85. Boyer SB, Slesinger PA (2010) Probing novel GPCR interactions using a combination of FRET and TIRF. Commun Integr Biol 3:343–346
86. Keppler A, Gendreizig S, Gronemeyer T et al (2003) A general method for the covalent labeling of fusion proteins with small molecules in vivo. Nat Biotechnol 21:86–89
87. Calebiro D, Rieken F, Wagner J et al (2013) Single-molecule analysis of fluorescently labeled G-protein-coupled receptors reveals complexes with distinct dynamics and organization. Proc Natl Acad Sci U S A 110:743–748
88. Park SM, Huh YS, Szeto K et al (2010) Rapid prototyping of nanofluidic systems using size-reduced electrospun nanofibers for biomolecular analysis. Small 6:2420–2426
89. Garcia-Saez AJ, Ries J, Orzaez M et al (2009) Membrane promotes tBID interaction with BCL(XL). Nat Struct Mol Biol 16:1178–1185
90. Jakobs D, Sorkalla T, Haberlein H (2012) Ligands for fluorescence correlation spectroscopy on g protein-coupled receptors. Curr Med Chem 19:4722–4730
91. Briddon SJ, Hill SJ (2007) Pharmacology under the microscope: the use of fluorescence correlation spectroscopy to determine the properties of ligand-receptor complexes. Trends Pharmacol Sci 28:637–645
92. Poyner D, Wheatley M (2010) G-protein coupled receptors: methods express, ed. Series. 2010. Chichester: Wiley, xiv, 296 p
93. Herrick-Davis K, Grinde E, Lindsley T et al (2012) Oligomer size of the serotonin 5-hydroxytryptamine 2C ($5\text{-}HT_{2C}$) receptor revealed by fluorescence correlation spectroscopy with photon counting histogram analysis: evidence for homodimers without monomers or tetramers. J Biol Chem 287:23604–23614

94. Gao T, Petrlova J, He W et al (2012) Characterization of de novo synthesized GPCRs supported in nanolipoprotein discs. PLoS One 7:e44911
95. Vukojevic V, Pramanik A, Yakovleva T et al (2005) Study of molecular events in cells by fluorescence correlation spectroscopy. Cell Mol Life Sci 62:535–550
96. Schwille P (2001) Fluorescence correlation spectroscopy and its potential for intracellular applications. Cell Biochem Biophys 34:383–408
97. Myers FB, Lee LP (2008) Innovations in optical microfluidic technologies for point-of-care diagnostics. Lab Chip 8:2015–2031
98. Cooper MA (2002) Optical biosensors in drug discovery. Nat Rev Drug Discov 1:515–528
99. Barnes WL, Dereux A, Ebbesen TW (2003) Surface plasmon subwavelength optics. Nature 424:824–830
100. Huber W, Mueller F (2006) Biomolecular interaction analysis in drug discovery using surface plasmon resonance technology. Curr Pharm Des 12:3999–4021
101. Homola J (2003) Present and future of surface plasmon resonance biosensors. Anal Bioanal Chem 377:528–539
102. Fang Y, Ferrie AM, Fontaine NH et al (2006) Resonant waveguide grating biosensor for living cell sensing. Biophys J 91:1925–1940
103. Vidic J, Pla-Roca M, Grosclaude J et al (2007) Gold surface functionalization and patterning for specific immobilization of olfactory receptors carried by nanosomes. Anal Chem 79:3280–3290
104. Benilova I, Chegel VI, Ushenin YV et al (2008) Stimulation of human olfactory receptor 17-40 with odorants probed by surface plasmon resonance. Eur Biophys J 37:807–814
105. Matarazzo V, Zsürger N, Guillemot JC et al (2002) Porcine odorant-binding protein selectively binds to a human olfactory receptor. Chem Senses 27:691–701
106. Coburn CM, Bargmann CI (1996) A putative cyclic nucleotide-gated channel is required for sensory development and function in *C. elegans*. Neuron 17:695–706
107. Komatsu H, Mori I, Rhee JS et al (1996) Mutations in a cyclic nucleotide-gated channel lead to abnormal thermosensation and chemosensation in *C. elegans*. Neuron 17:707–718
108. Angel RJ, Jackson JM, Reichmann HJ et al (2009) Elasticity measurements on minerals: a review. Eur J Mineral 21:525–550
109. Lin SW, Sakmar TP, Franke RR et al (1992) Resonance Raman microprobe spectroscopy of rhodopsin mutants: effect of substitutions in the third transmembrane helix. Biochemistry 31:5105–5111
110. Yan EC, Kazmi MA, Ganim Z et al (2003) Retinal counterion switch in the photoactivation of the G protein-coupled receptor rhodopsin. Proc Natl Acad Sci U S A 100:9262–9267
111. Kukura P, McCamant DW, Yoon S et al (2005) Structural observation of the primary isomerization in vision with femtosecond-stimulated Raman. Science 310:1006–1009
112. Park SM, Huh YS, Craighead HG et al (2009) A method for nanofluidic device prototyping using elastomeric collapse. Proc Natl Acad Sci U S A 106:15549–15554
113. Kennedy DC, Tay L-L, Lyn RK et al (2009) Nanoscale aggregation of cellular β2-adrenergic receptors measured by plasmonic interactions of functionalized nanoparticles. ACS Nano 3:2329–2339
114. Kennedy DC, McKay CS, Tay LL et al (2011) Carbon-bonded silver nanoparticles: alkyne-functionalized ligands for SERS imaging of mammalian cells. Chem Commun (Camb) 47:3156–3158
115. Podstawka-Proniewicz E, Kudelski A, Kim Y et al (2011) Structure of monolayers formed from neurotensin and its single-site mutants: vibrational spectroscopic studies. J Phys Chem B 115:6709–6721
116. Podstawka E (2008) Investigation of molecular structure of bombesin and its modified analogues nonadsorbed and adsorbed on electrochemically roughened silver surface. Biopolymers 89:506–521
117. Podstawka-Proniewicz E, Kudelski A, Kim Y et al (2011) Structure and binding of specifically mutated neurotensin fragments on a silver substrate: vibrational studies. J Phys Chem B 115:7097–7108

118. Podstawka E, Niaura G (2009) Potential-dependent characterization of bombesin adsorbed states on roughened Ag, Au, and Cu electrode surfaces at physiological pH. J Phys Chem B 113:10974–10983
119. Kneipp J, Kneipp H, Wittig B et al (2010) Novel optical nanosensors for probing and imaging live cells. Nanomedicine 6:214–226
120. Cloutier T, Park J, Butler P (2011) Combining labeled and label-free tools. Genet Eng Biotechnol News 31:32–33
121. Cunningham BT (2010) Photonic crystal surfaces as a general purpose platform for label-free and fluorescent assays. JALA Charlottesv Va 15:120–135
122. Cunningham BT, Laing L (2006) Microplate-based, label-free detection of biomolecular interactions: applications in proteomics. Expert Rev Proteomics 3:271–281
123. Lin B, Qiu J, Gerstenmeier J et al (2002) A label-free optical technique for detecting small molecule interactions. Biosens Bioelectron 17:827–834
124. Antony J, Kellershohn K, Mohr-Andra M et al (2009) Dualsteric GPCR targeting: a novel route to binding and signaling pathway selectivity. FASEB J 23:442–450
125. Dodgson K, Gedge L, Murray DC et al (2009) A 100K well screen for a muscarinic receptor using the Epic label-free system-a reflection on the benefits of the label-free approach to screening seven-transmembrane receptors. J Recept Signal Transduct Res 29:163–172
126. Martins SA, Trabuco JR, Monteiro GA et al (2012) Towards the miniaturization of GPCR-based live-cell screening assays. Trends Biotechnol 30:566–574
127. Zhang R, Xie X (2012) Tools for GPCR drug discovery. Acta Pharmacol Sin 33:372–384
128. Halai R, Croker DE, Suen JY et al (2012) A comparative study of impedance versus optical label-free systems relative to labelled assays in a predominantly Gi coupled GPCR (C5aR) signalling. Biosensors 2:273–290
129. Fang Y, Ferrie AM, Tran E (2009) Resonant waveguide grating biosensor for whole-cell GPCR assays. Methods Mol Biol 552:239–252
130. Fang Y, Frutos AG, Verklereen R (2008) Label-free cell-based assays for GPCR screening. Comb Chem High Throughput Screen 11:357–369
131. Park SM, Lee KH, Craighead HG (2008) On-chip coupling of electrochemical pumps and an SU-8 tip for electrospray ionization mass spectrometry. Biomed Microdevices 10:891–897
132. Park SM, Ahn JY, Jo M et al (2009) Selection and elution of aptamers using nanoporous sol-gel arrays with integrated microheaters. Lab Chip 9:1206–1212
133. Aubin KL, Huang J, Park SM et al (2007) Microfluidic encapsulated nanoelectromechanical resonators. J Vac Sci Technol B 25:1171–1174
134. Erukhimovitch V, Huleihel M (2013) Use of fourier-transform infrared (FTIR) microscopy method for detection of phyto-fungal pathogens. In: GV (ed) Laboratory protocols in fungal biology. Ed. Vijai Kumar Gupta, Maria G. Tuohy, Springer, New York, pp 161–167
135. Ye S, Huber T, Vogel R et al (2009) FTIR analysis of GPCR activation using azido probes. Nat Chem Biol 5:397–399
136. Elgeti M, Rose AS, Bartl FJ et al (2013) Precision vs. flexibility in GPCR signaling. J Am Chem Soc 135(33):12305–12312
137. Jager S, Lewis JW, Zvyaga TA et al (1997) Chromophore structural changes in rhodopsin from nanoseconds to microseconds following pigment photolysis. Proc Natl Acad Sci U S A 94:8557–8562
138. Choe HW, Park JH, Kim YJ et al (2011) Transmembrane signaling by GPCRs: insight from rhodopsin and opsin structures. Neuropharmacology 60:52–57
139. Vogel R, Siebert F (2001) Conformations of the active and inactive states of opsin. J Biol Chem 276:38487–38493
140. Cohen GB, Oprian DD, Robinson PR (1992) Mechanism of activation and inactivation of opsin: role of Glu113 and Lys296. Biochemistry 31:12592–12601
141. Scheerer P, Park JH, Hildebrand PW et al (2008) Crystal structure of opsin in its G-protein-interacting conformation. Nature 455:497–502

Chapter 12
Carbon Nanotube-Based Sensor Platform for Bioelectronic Nose

Juhun Park, Hye Jun Jin, Hyungwoo Lee, Shashank Shekhar, Daesan Kim and Seunghun Hong

Abstract Since carbon nanotubes (CNTs) have an extremely large surface-to-volume ratio, the electrical properties of CNTs can be easily changed by the adsorption of small molecules. Due to this attribute, CNT-based sensors can detect small molecules with a high sensitivity. Recently, bioelectronic noses based on CNTs have been developed by immobilizing olfactory receptors or nanovesicles on the surface of CNTs. By taking advantages of CNT structures, these bioelectronic nose devices allowed one to detect target odorants with a high sensitivity. Furthermore, they exhibited highly selective responses to target odorants with a single-carbon-atomic resolution just like human olfactory systems. These bioelectronic nose devices based on CNTs can be utilized for various practical applications such as food screening, medical diagnostics, and the fabrication of artificial noses.

12.1 Carbon Nanotube-Based Device Fabrication

12.1.1 Carbon Nanotubes

A tube made of a single or multiple graphene layers rolled up into a hollow cylinder is called a carbon nanotube (CNT) [1]. A single-walled CNT (SWCNT) consists of a single graphene sheet with the diameter of about 1∼2 nm, while a multi-walled CNT (MWCNT) consists of several graphene sheets. Among those nanotubes, special attentions have been focused on SWCNTs, since they can have semiconducting properties which are optimal for electronic device applications. Despite the fact that all SWCNTs are based on a hexagonal honeycomb lattice, different orientations in the basic structure with respect to a nanotube axis lead to electrically different

S. Hong (✉) · D. Kim
Department of Biophysics and Chemical Biology,
Seoul National University, Seoul 151-747, Republic of Korea
e-mail: shong@phya.snu.ac.kr

J. Park · H. J. Jin · H. Lee · S. Shekhar
Department of Physics and Astronomy, and Institute of Applied
Physics, Seoul National University, Seoul 151-747, Republic of Korea

T. H. Park (ed.), *Bioelectronic Nose*, DOI 10.1007/978-94-017-8613-3_12,

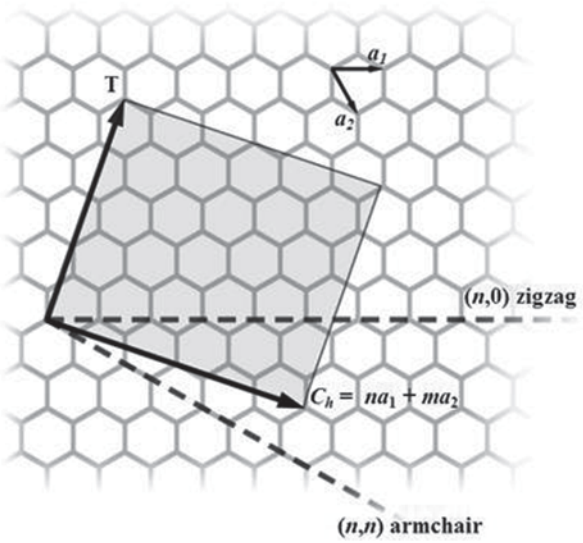

Fig. 12.1 Honeycomb lattice of carbon atoms in graphene. A graphene piece with different direction was rolled up to form a CNT

materials. Such atomic structures can be specified by a vector which corresponds to the section of the SWCNT perpendicular to the tube axis. As shown in Fig. 12.1, the translational vector $\boldsymbol{T}$ is the direction of a nanotube axis. The $\boldsymbol{C}_h$ is a chiral vector which can be specified by the pair of integers (n, m), and the $\mathbf{a}_1$ and $\mathbf{a}_2$ represent each unit vectors. Then, the chiral vector can be written like

$$C_h = n\mathbf{a}_1 + m\mathbf{a}_2 \equiv (n,m),\ (n,m \text{ are integer},\ 0 \le m \le n) \tag{12.1}$$

The chiral angle θ is defined by taking the inner product of $\boldsymbol{C}_h$ and $\mathbf{a}_1$, yielding an expression for cosθ,

$$\cos\theta = \frac{C_h \cdot a_1}{|C_h||a_1|} = \left(\frac{2n+m}{2\sqrt{n^2+m^2+nm}}\right) \tag{12.2}$$

In particular, if n equals to m in the chiral vector $\boldsymbol{C}_h$ (θ=30°), the tube is called an armchair tube. If m equals to zero (θ=0°), then we call the tube a zigzag tube. For all other configurations, the tubes are known as chiral tubes (Fig. 12.1).

The electrical properties of SWCNTs can be predicted by periodic boundary conditions from the chiral vector $\boldsymbol{C}_h$. Briefly, if $n-m$ is the integer multiple of three, then the SWCNT has metallic properties else it possesses semiconducting properties [1]. The electrical properties of the SWCNTs can also be predicted by the atomic structures of the SWCNTs. For example, the armchair SWCNTs always exhibit metallic properties, whereas zigzag and chiral SWCNTs exhibit either metallic or semiconducting properties [1].

Due to the versatile electrical properties of CNTs, they exhibit many interesting phenomena such as a single electron tunneling, a spin-polarized electron transport,

a resonant tunneling, and a field emission [2–4]. Furthermore, CNTs have been utilized to build the surprisingly wide range of applications such as nanochannels for field-effect transistors [5], a surface probe microscopy [6], a new electronic nanomaterial for quantum wires [7], nanologic circuits [8], non-volatile memories [9], display technology by field emission [10], transparent and conducting electrodes or films [11], actuators [12], light emitting diodes [13], and highly sensitive biological and chemical sensors [14, 15].

12.1.2 Surface-Programmed Assembly for Carbon Nanotube-Based Devices

Recently, various methods have been developed for the massive fabrication of CNT network-based devices [16–23]. "Surface-programmed assembly" is one of the most versatile methods. Figure 12.2a shows the schematic diagrams depicting the surface-programmed assembly processes [5].

In this method, first, the self-assembled monolayer (SAM) of organic molecules with non-polar terminal groups is patterned on solid substrates so as to create polar and non-polar regions on the surface of the substrates [5]. Here, an octadecyltrichlorosilane (OTS) SAM is utilized on silicon oxide (SiO_2) substrates. The OTS SAM patterning can be carried out by a conventional photolithography method (Fig. 12.2a). In this process, a photoresist layer is first patterned onto a SiO_2 substrate with a short baking time (< 10 min at 95 °C). Note that heating up the photoresist-patterned substrates for a long time can result in residual photoresist on the substrate surface even after a development process. Such residual photoresist can inhibit the formation of a high-quality OTS SAM on the substrates. Then, the substrates are thoroughly rinsed with anhydrous hexane to remove residual water molecules on the surface of substrates. And, then, the substrate is placed in the OTS solution (1:500 v/v in anhydrous hexane) for ~ 100 s so that OTS SAM is formed on the bare SiO_2 surface. Subsequently, the photoresist patterns on the substrates are removed by acetone. Using this process, a high-quality OTS SAM can be patterned on substrates, leaving the surface of the substrates unaltered.

CNT suspensions are prepared by putting CNTs in o-dichlorobenzene and applying a sonication for ~ 20 min. When the OTS-patterned substrates are placed in the well-dispersed SWCNT suspension, CNTs are adsorbed onto the bare SiO_2 region of the substrates. Note that the CNTs in dichlorobenzene have strong affinity to polar surfaces, while they do not adhere to non-polar surfaces. Therefore, the non-polar molecular patterns on substrates can guide the adsorption of CNTs directly onto the polar surface regions of the substrates. This selective adsorption property of CNTs allows one to precisely pattern the CNT networks onto the desired locations on solid substrates [5].

Metal electrodes can be fabricated on the CNT networks via an additional photolithography process. It should be noted that the CNT adhesion onto polar surface regions is so stable that additional photolithography processes can be performed

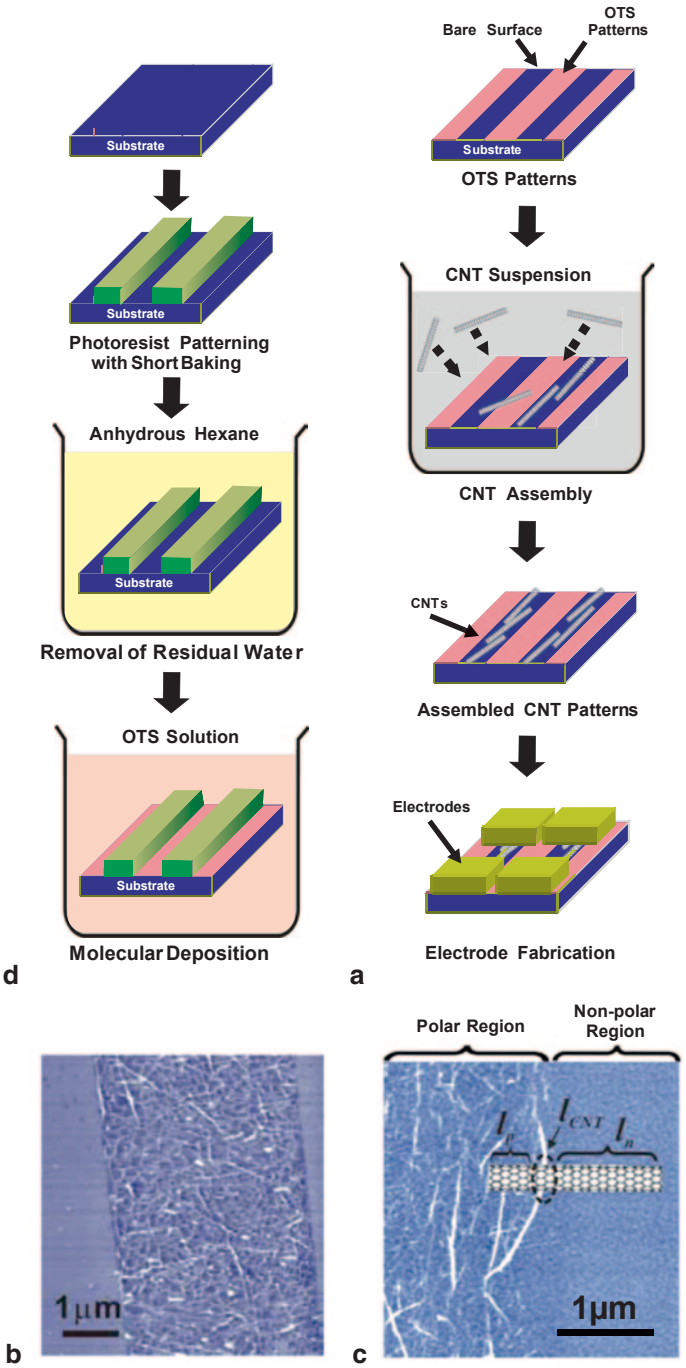

Fig. 12.2 "Surface programmed assembly" method for the massive production of CNT-based sensor transducers. **a** Schematic diagram depicting the fabrication process for CNT-based sensor transducers via the "surface-programmed assembly" method. **b** AFM topography image of patterned CNT networks on a SiO_2 substrate. The figures were adapted with permission from Lee et al. [5] **c** AFM topography image showing the sliding motion of a CNT near a pattern boundary. (The figure was adapted with permission from Im et al. [25])

directly on the CNT networks. Using the photolithography process, a photoresist layer is patterned on the CNT networks. Then, a metal film is deposited on the photoresist-patterned samples via a conventional thermal evaporation method. Lastly, the metal electrodes are fabricated by a lift-off process with acetone.

Using the above "surface-programmed assembly" method, the CNT network-based devices can be simply fabricated with any desired structures in large-scale. Therefore, this method should be a powerful strategy for the large-scale assembly of CNT-based devices which can be utilized for practical applications such as electrical sensors.

Figure 12.2b shows the atomic force microscopy (AFM) images of the selectively adsorbed CNTs in the shape of line patterns. The CNTs are confined only to the polar regions of the substrates and define the line-shaped patterns well. Here, it is worth discussing a few interesting phenomena of CNT adsorptions during the surface-programmed assembly process. One interesting phenomenon related to the CNT adsorption process is a "self-limiting" mechanism. When the substrates are placed in CNT suspensions, the CNTs are first adsorbed quickly, but the number of adsorbed CNTs reaches the saturated value soon [5, 24]. Such adsorption behavior of CNTs can be explained by Langmuir isotherm [24, 25]. Here, the density Θ of adsorbed CNTs at the time t can be written as

$$\Theta(t) = \Theta_0 \frac{C}{C + (k_d / k_a)}\left[1 - \exp(-(k_a C + k_d)t)\right] \tag{12.3}$$

where Θ_0, C, k_a, and k_d represent the maximum surface density of adsorbed CNTs, the concentration of CNT suspensions, association coefficient, and dissociation coefficient, respectively [24, 25]. In this Langmuir isotherm-like adsorption behavior, the adsorption rate is proportional to the CNT concentration and the number of vacant sites on substrates, and the desorption rate is proportional to the number of adsorbed CNTs. It means that the CNTs adsorbed on the substrate can block the additional adsorption of CNTs and the number of adsorbed CNTs can be self-limited [5]. Therefore, this "self-limiting" adsorption behavior of CNTs allows one to prepare CNT networks with a uniform spatial density.

Another important phenomenon in the surface-programmed assembly process is the alignment of adsorbed CNTs on polar surface regions. As shown in Fig. 12.2c, adsorbed CNTs near the pattern boundary can make a "sliding" motion and can be aligned along the channel direction to stay inside the polar surface regions. In this "sliding" kinetics, the final conformation of a CNT is determined from the energy minimum condition such that the length of the CNT portions lying on a non-polar surface region (l_n) and other CNTs (l_{CNT}) is minimized, and that lying on a polar surface region (l_p) is maximized [25] (Fig. 12.2c). Therefore, the CNTs adsorbed near the pattern boundaries could be aligned along the channel direction without any external forces. This alignment behavior of the CNTs can be a mean to precisely control the alignment structure of CNT networks [25].

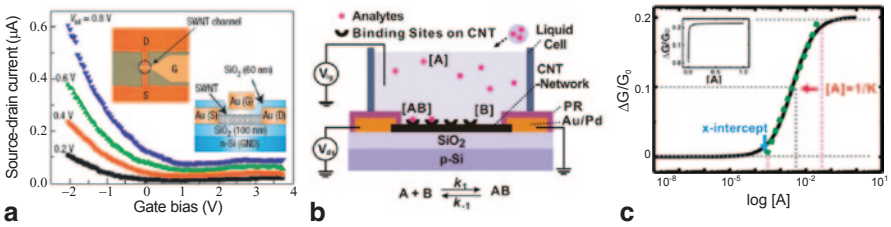

Fig. 12.3 Basic characteristics of a CNT-based transducer and the mechanism of CNT-based sensors. **a** Gating effect of a top-gate CNT-FET under different source-drain voltages. The insets show the optical image (*left*) and the cross-sectional structure (*right*) of a fabricated CNT device where S, D, and G are source, drain, and gate electrodes, respectively.(Adapted with permission from Lee et al. [5]) **b** Schematic diagram depicting the theoretical model for CNT-based sensors. The [A], [B], and [AB] represent the concentration of analytes in bulk solution, the surface density of binding sites, and the surface density of adsorbed analytes, respectively. It is assumed that analytes A adsorb to the binding sites B following the Langmuir isotherm process. Then, adsorbed analytes AB generate the sensor response, $\Delta G/G_0$. **c** Graph showing the typical response of CNT-based sensors. (Adapted with permission from Lee et al. [26])

12.2 Carbon Nanotube-Based Sensor Transducer

12.2.1 Mechanism of Carbon Nanotube Transistor-Based Transducers

In this section, various sensing mechanisms and applications of CNT-based biosensors will be discussed. Figure 12.3a shows gate voltage dependent electrical characteristics with the schematics of a typical CNT-field effect transistor (CNT-FET) [5]. A typical CNT-FET is composed of source, drain and gate electrodes as shown in the left inset, and the source and drain electrodes are connected by CNTs (the right inset in Fig. 12.3a). The gating effect of a CNT-FET on different biases (Fig. 12.3a) shows a decrease in a source-drain current as the gate voltage is swept from negative to positive, which is a typical p-type behavior.

Figure 12.3b and c illustrate the *mechanism* and the *theoretical model* of CNT-based sensors, respectively [26]. In this model, it is assumed that analytes A bind to the finite number of binding sites B on solid substrates. Then, the binding between A in the bulk solution and B follows the Langmuir isotherm model. Thus, bound analytes and free analytes in solution maintain an equilibrium state in general. It should be noted that the binding sites of CNT sensors vary depending on sensor types. For example, the binding sites of CNT-based gas sensors are usually the bare surfaces of CNTs [27, 28]. In the case of CNT-based biosensors, specific receptor molecules fixed on CNT surfaces work as binding sites [29]. In Fig. 12.3b, c, *[A]*, *[B]*, *[AB]*, and $[B]_{max}$ represent *the concentration of analytes in the bulk solution*, *the surface density of the binding sites on CNTs*, *the surface density of adsorbed analyte molecules*, and *the maximum surface density of the binding sites on CNTs*, respectively. The surface density of adsorbed analytes can be expressed by the following Langmuir isotherm equation:

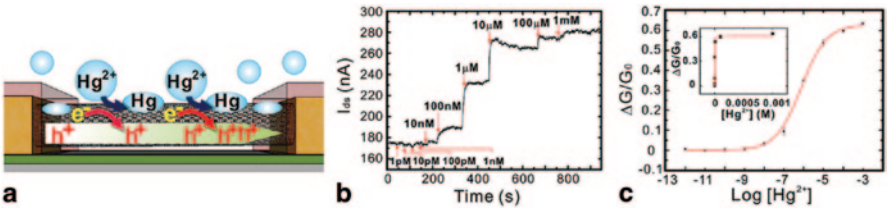

Fig. 12.4 Hg^{2+} sensor as an example of basic sensors based on bare CNTs. **a** Plausible mechanisms for a Hg^{2+} detection. **b** Real-time current measurement obtained from a CNT-FET sensor after the injection of Hg^{2+} solutions at various concentrations. **c** Conductance change of the CNT-FET sensor by the injection of Hg^{2+} solutions at various concentrations. The red line indicates the fitting curve for the estimation of equilibrium constant. (Adapted with permission from Kim et al. [30])

$$[\mathrm{AB}] = [\mathrm{B}]_{\max} \times \frac{[\mathrm{A}]}{[\mathrm{A}] + 1/\mathrm{K}} \tag{12.4}$$

with the equilibrium constant $K = k_1/k_{-1}$, where k_1 and k_{-1} are the *association* and *dissociation* constants, respectively. If we assume that the conductance changes of a CNT-based transducer (ΔG) are linearly proportional to the number of adsorbed analytes, the sensor sensitivity $|\Delta G/G_0|$ of the CNT transistor transducer can be approximated as $|\Delta G/G_0| \sim k[\mathrm{AB}]$, where k is a constant representing the response characteristics of the CNT transistor transducer. Thus, we can write the sensitivity $|\Delta G/G_0|$ of the CNT transistor transducer as,

$$|\Delta G/G_0| = k[\mathrm{B}]_{\max} \times \frac{[\mathrm{A}]}{[\mathrm{A}] + 1/K} \tag{12.5}$$

By fitting measured data using this equation, we can estimate the equilibrium constant K between A and B.

12.2.2 Examples of Basic Sensors Based on Carbon Nanotubes

The extremely large surface to volume ratio of CNTs is favorable for the adsorption of molecules. In addition, CNTs exhibit significant changes in their conductance when small molecules are adsorbed. Based on these properties, CNT-FETs have been employed to detect specific molecules. For example, Kim et al. [30] developed Hg^{2+} sensors based on the redox reaction between CNTs and Hg^{2+} ions (Fig. 12.4a). They employed the fact that the adsorption of Hg^{2+} ions on the surface of CNTs leads to the reduction of the Hg^{2+} ions and the oxidation of the CNTs. In this process, the CNTs give electrons to the Hg^{2+} ions, and then, consequential hole injections cause conductance increases in CNT junctions due to the *p-type* characteristics of CNTs. Using the CNT-based Hg^{2+} sensors, the authors found that the injection of 10 nM Hg^{2+} solution increased the conductance of the CNT channel (Fig. 12.4b). Note that 10 nM is the maximum allowable level of Hg^{2+} ions in drinking water

according to an environmental protection agency regulation. From the calibration curve (Fig. 12.4c), we can recognize that the CNT-based sensor responded to Hg^{2+} ions in a wide dynamic range (10 nM^{-1} mM). They fitted the data with the Langmuir isotherm equation and found that K was $\sim 1.4 \times 10^6$ M^{-1} and standard electrode potential E_0 was ~0.67 V, which were consistent with previously reported values.

However, sensors based on bare CNTs often respond to the adsorption of *non-specific* molecules, which limits its selectivity as a sensor. To overcome this drawback, many researchers have developed various biomolecule-immobilized CNT-FETs as a selective receptor. CNTs can be easily combined with various kinds of biomolecules, while maintaining their electrical properties. Also, biomolecules such as antibodies and receptors bind with specific biomolecules such as antigens and ligands. Thus, biomolecule-immobilized CNT-FETs have great advantages in the detection of target molecules with a high selectivity. For an example, Kim et al. [31] reported a highly sensitive biosensor based on antibody fragment-immobilized CNTs for the family-selective detection of antibiotics. The antibody fragment-immobilized CNT-FET biosensors were composed of CNT transducers, linker molecules, and antibody fragments as shown in Fig. 12.5a. When target molecules were bound to antibody fragments, the negatively charged domains of antibody fragments were decreased. Since CNT-FETs exhibited p-type characteristics, the reduced negative charges near the CNT channel resulted in the decrease of a source-drain current in the channel. In the experiments, the authors used two kinds of antibody fragments; A2 and F9. The A2 is the specific receptor of enrofloxacin which is one of antibiotics. The F9 is the general receptor of a fluoroquinolone family including enrofloxacin and norfloxacin. In A2-immobilized CNT sensors, 1 μM norfloxacin had no significant effect on the conductance of the CNT sensors, while a significant decrease in the conductance was detected after the injection of 1 μM enrofloxacin (Fig. 12.5b). This indicates that the A2-immobilized CNT sensors can selectively detect enrofloxacin in real-time. On the other hand, F9-immobilized CNT sensors showed significant changes in the conductance after the injection of the 1 μM solutions of enrofloxacin and norfloxacin (Fig. 12.5c). The F9 recognized both enrofloxacin and norfloxacin which are the same antibiotics family. This result shows that F9-immobilized CNT sensors can be used for the family-selective detection of antibiotics.

CNT-FET sensors using a biomolecule-immobilized electrode also enabled the detection of target molecules with a high sensitivity and a high selectivity. Lee et al. [32] reported an aptamer sandwich-based CNT sensor for the selective and sensitive detection of bisphenol-A (BPA) which is a kind of non-polar species. This sensor contained aptamer molecules which were immobilized on the electrodes of a CNT transistor (Fig. 12.5d). When aptamers on Au electrodes captured target molecules which had negative charges, the work function of the Au electrodes decreased. The work function change induced an increase in the Schottky barrier height between the CNTs and the Au electrodes. The increase of the Schottky barrier height in the CNT-FET sensor resulted in the decrease of a source-drain current. In this study, the authors could not observe significant conductance changes after the injection of BPA solutions up to the concentration of 100 nM (black line in Fig. 12.5e). Since BPA molecules are neutral, they could not affect the conductance of the CNT-FET sensors. For the detection of BPA, they functionalized BPA molecules with negatively

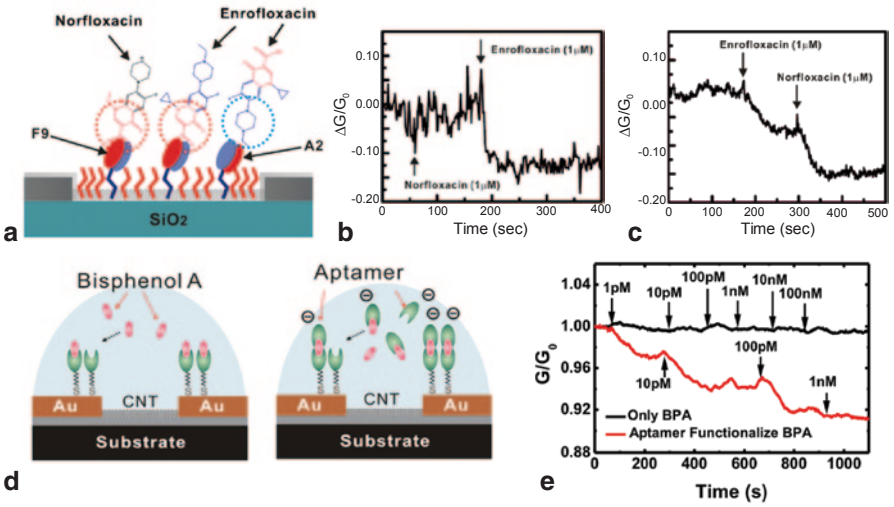

Fig. 12.5 Examples of basic sensors based on biomolecule-immobilized CNTs **a** Schematic diagram depicting the sensing experiment using antibody fragment-immobilized CNT-FET sensors. The antibody fragment A2 specifically recognizes enrofloxacin antibiotics, while the antibody fragment F9 recognizes fluoroquinolone family antibiotics including enrofloxacin and norfloxacin. **b** Real time conductance measurement using an A2-immobilized CNT-FET sensor. A2-immobilized CNT-FET sensors detected enrofloxacin only. **c** Real time conductance measurement using a F9-immobilized CNT-FET sensor. F9-immobilized CNT-FET sensors detected both enrofloxacin and norfloxacin. (Adapted with permission from Kim et al. [31]) **d** Schematic diagram showing the sensing experiment using aptamer-immobilized CNT-FET sensors. The *left* and *right* figures show the sensing experiments of bare bisphenol-A (BPA) and aptamer-functionalized BPA, respectively. **e** Real time conductance measurements using aptamer-immobilized CNT-FET sensors. The aptamer-immobilized CNT-FET sensors showed recognizable response only to the injection of aptamer-functionalized BPA. (Adapted with permission from Lee et al. [32]—Reproduced by permission of The Royal Society of Chemistry)

charged DNA aptamers. After the injection of the functionalized BPA solutions to an aptamer-immobilized CNT-FET sensor, significant changes in the conductance of the CNT-FET sensor were observed even at a concentration as low as ~ 1 pM (red line in Fig. 12.5e). This result indicates that the Schottky barrier modulation can enable the detection of specific target molecules with a high sensitivity and a high selectivity.

12.3 Carbon Nanotube-Based Bioelectronic Nose

12.3.1 Receptor-Based Bioelectronic Nose with a Human-Like Selectivity

Olfactory receptors have unique selectivity to specific odorants, and thus, they could be powerful candidates as the sensing elements for a bioelectronic nose based on CNT-based sensor transducer.

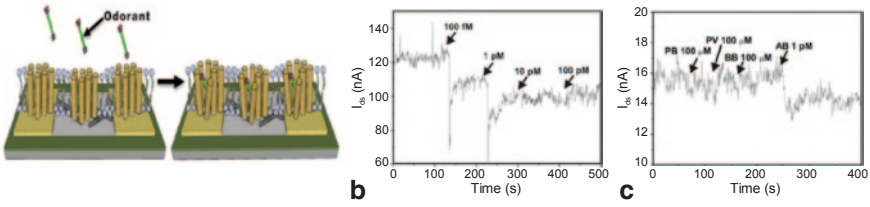

Fig. 12.6 Receptor-based bioelectronic nose mimicking a human nose. **a** Schematic diagram depicting the plausible mechanism of an olfactory receptor-based bioelectronic nose. **b** Real time current measurement using an olfactory receptor-based bioelectronic nose after the injection of amylbutyrate (AB) at various concentrations. **c** Real time current measurement using an olfactory receptor-based bioelectronic nose after the injection of propylbutyrate (PB), pentylvalerate (PV), butylbutyrate (BB), and AB. (Adapted with permission from Kim et al. [33])

Kim et al. [33] reported a bioelectronic nose based on a human olfactory receptor (hOR2AG1)-immobilized CNT-FET for the detection of odorant molecules with a single-carbon-atomic resolution. Figure 12.6a shows the structure of a receptor-based bioelectronic nose and the mechanism of specific odorant detection using the bioelectronic nose. The bioelectronic noses were composed of CNT transducers and immobilized olfactory receptors with a lipid layer. Here, the lipid layer provided cell membrane-like environments to olfactory receptors, which was essential for the receptor to maintain its functionality. When a specific odorant binded to its corresponding receptor, the state of the receptor shifted to an active state with *negative* charges [34, 35]. The negative charges in the receptor resulted in the increase of Schottky barrier heights in CNT-FET sensors. Then, the increase of the Schottky barrier heights induced a conductance decrease in the CNT channels.

Fig. 12.6b shows real-time conductance measurement data obtained from a hOR2AG1-based bioelectronic noseafter the introduction of amylbutyrate (AB), which is one of fruity odorants, with different concentrations. The hOR2AG1-based bioelectronic nosewas first placed in deionized water solution, and then, the AB solutions with different concentrations were introduced. The bioelectronic nose exhibited a significant change in a conductance with the injection of a 100 fM AB solution. This result shows the high sensitivity of a receptor-based bioelectronic nose.

Figure 12.6c shows real-time conductance measurement data obtained from a hOR2AG1-based bioelectronic noseafter the introduction of various odorants. Note that non-target odorants such as propyl butyrate (PB), pentyl valerate (PV), and butyl butyrate (BB) have similar chemical structures to AB. The difference is just the number of carbon atoms. The addition of PB, PV, and BB did not affect the conductance of a hOR2AG1-based bioelectronic nose even at a high concentration (100 μM) whereas the addition of the AB solution at 1 pM resulted in a sharp decrease in the conductance. This result shows that the bioelectronic nose based on hOR2AG1-immobilized CNT-FETs have high selectivity with a single-carbon-atomic resolution.

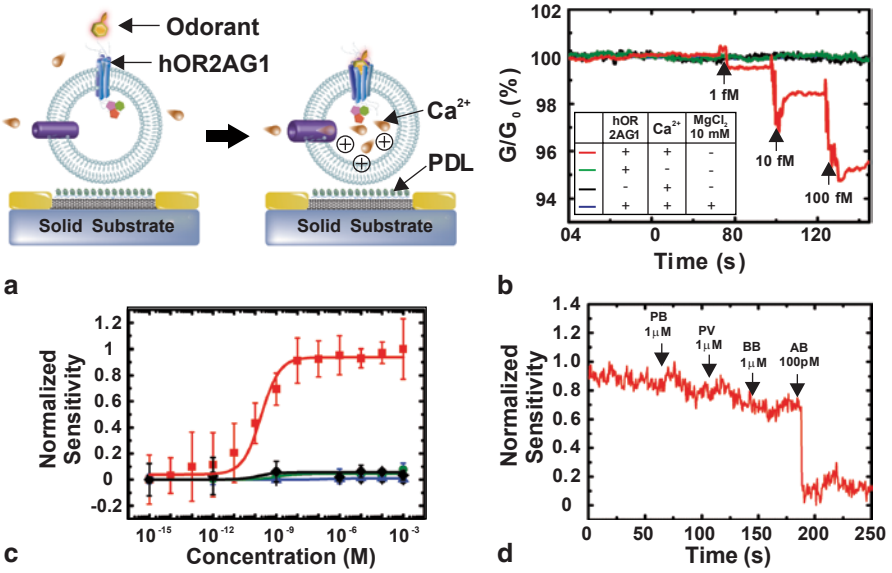

Fig. 12.7 Nanovesicle-based bioelectronic nose mimicking the signal pathways of a human nose **a** Schematic diagram depicting the plausible mechanism of the bioelectronic nose. When a target odorant binds to hOR2AG1 protein, the signal pathway in the nanovesicle is activated. This induces the influx of Ca^{2+} through a calcium ion channel. The increased positive charges in the nanovesicle give a field effect on an underlying CNT channel. Then, the conductance of the CNT channel decreases. **b** Real time conductance measurements. The CNT-FET sensors showed responses to the injection of 1 fM AB solution (*red line*). However, the two control experiments using nanovesicles without hOR2AG1 (*black line*) and PBS without Ca^{2+} (*green line*) showed no significant responses. **c** Graph of the concentration dependent responses to AB solution. **d** Real-time conductance measurement data after the injection of different odorants. The addition of 1 μM PB, PV, and BB solutions had no effect on the conductance of the sensor, while the addition of 100 pM AB solution caused a sharp decrease in the conductance of the sensor. (Adapted with permission from Jin et al. [36])

12.3.2 Nanovesicle-Based Bioelectronic Nose with a Human-Like Selectivity

Cell-derived nanovesicles have been proposed as an artificial cell which can partially mimic cell signal transductions and thus work as a sensing element for bioelectronic noses.

Jin et al. [36] developed a nanovesicle-based bioelectronic nose (NBN) platform which can mimic the signal pathways of human olfactory systems. The structure and the mechanism of nanovesicle-based sensors are depicted in Fig. 12.7a. NBNs were composed of CNT transistor transducers and nanovesicles containing olfactory receptors (hOR2AG1), adenylyl cyclases, and ion channels. When odorant solutions were injected to a NBN, the binding between olfactory receptors and odorant molecules triggered a calcium signal pathway. Then, the successive activation of

olfactory receptors, adenylyl cyclases, and ion channels induced the flux of calcium ions into the nanovesicles. The influx resulted in the accumulation of calcium ions. The accumulated calcium ions gave a positive field effect on the underlying CNT-FET, thus resulting in the decrease of conductance of the CNT-FET.

Based on this mechanism, the NBN detected amylbutyrate (AB), a specific odorant of hOR2AG1, down to 1 fM concentration (Fig. 12.7b). The validity of the mechanism can be supported by the following control experiments. One experiment was conducted using nanovesicles without hOR2AG1, whereas another experiment was performed in calcium-free phosphate buffered saline (PBS). The other experiment was conducted in PBS with $MgCl_2$ which blocks ion channels. In those experiments, there were no changes in the conductance of CNT-FETs. This indicates that olfactory receptors, calcium ions, and ion channels are critical components for the operation of the NBNs. Also, this shows that the NBN platform could mimic the olfactory signal transduction in cells.

Figure 12.7c shows the normalized sensitivity of NBNs after the introduction of odorant molecules with various concentrations. Here, the conductance change of a NBN was measured after the introduction of odorant solutions with different concentrations, and the conductance change was normalized by its maximum to calculate the normalized sensitivity. Note that the conductance change increased as the concentration of AB increased and saturated at a 10 nM concentration, while the others did not show any significant change.

Figure 12.7d shows a real time conductance measurement from an NBN device after the introduction of pentylbutyrate (PB), pentylvalerate (PV), butylbutyrate (BB), and AB. Conductance changes were negligible after injecting 1 μM of non-target odorants such as PB, PV, and BB. On the other hand, after the injection of AB with 100 pM, the significant conductance change was observed. This result indicates the NBNs are highly selective to target molecules with a single-carbon-atomic resolution.

12.3.3 Canine Receptor-Based Bioelectronic Nose

Taking advantages of the high sensitivity and the high selectivity of canine olfactory systems, Park et al. developed a canine receptor-based sensor that mimicked canine nose responses for the sensitive and selective detection of hexanal, an indicator of the oxidation of food [37]. Figure 12.8a shows a scheme depicting the structure of a canine receptor-based sensor. This sensor was composed of a CNT-FET and canine olfactory nanovesicles immobilized on the CNT-FET. In this sensor, the binding of hexanal to canine olfactory receptors (cfOR5269) successively activated G proteins, adenylyl cyclases, and Ca^{2+} channels following the cAMP pathway in the nanovesicle. The activation of Ca^{2+} channels generated the influx of Ca^{2+}, which increased the potential of the nanovesicle in the vicinity of CNTs. Since CNT channels exhibited p-type characteristics under ambient conditions, the increased potential of the nearby nanovesicle resulted in the decrease of the CNT channel conductance. In this bioelectronic nose, the binding of hexanal onto canine

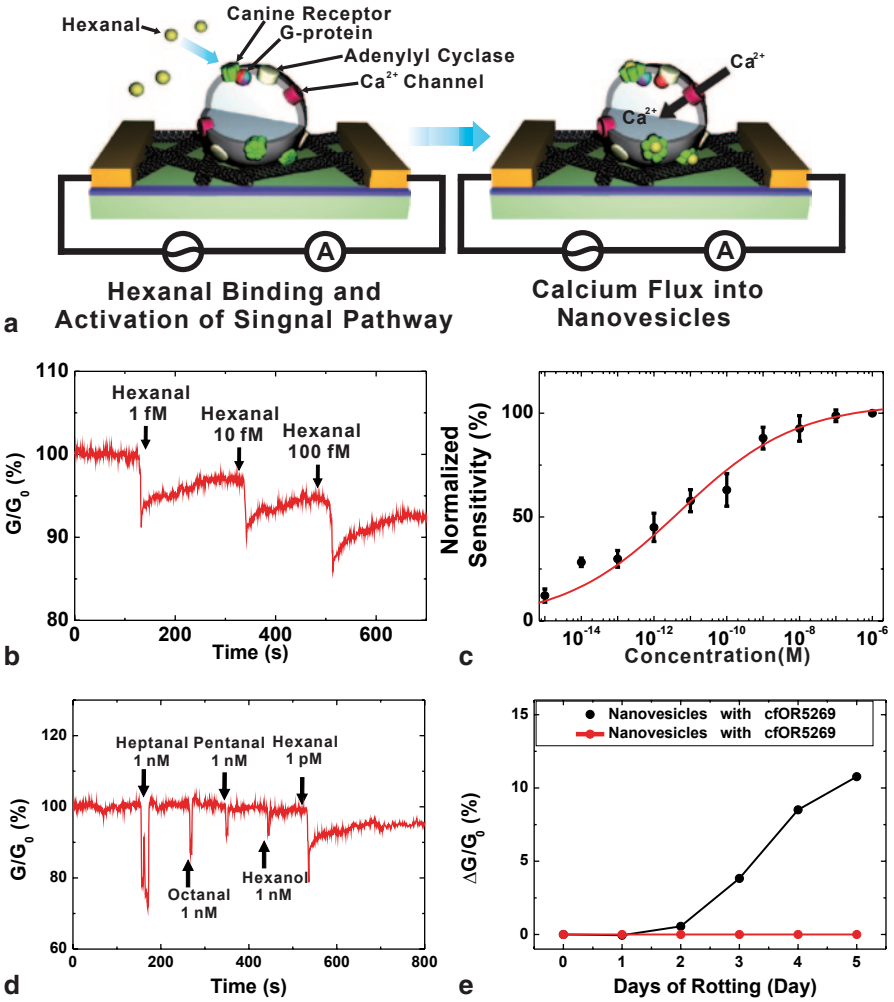

Fig. 12.8 Canine receptor-based bioelectronic nose. **a** Schematic diagram showing the sensing mechanism for the detection of hexanal using a canine receptor-based bioelectronic nose. The binding of hexanal to canine receptors results in a Ca^{2+} influx into the nanovesicles through Ca^{2+} channels. Here, the accumulated Ca^{2+} ions inside the nanovesicles create a positive gate-potential in the vicinity of underlying CNTs, and the increased potential results in the decrease of the conductance in the CNT channel. **b** Real-time conductance measurement data obtained from a canine receptor-based bioelectronic nose after the introduction of hexanal. The conductance decreased after the introduction of a hexanal solution with a femtomolar concentration. **c** Response curve of canine receptor-based bioelectronic nose to hexanal with different concentrations. The responses of the bioelectronic noses were fitted to the Langmuir isotherm curve (*red solid curve*). **d** Real-time conductance measurement data obtained from a canine receptor-based bioelectronic nose after the injection of different odorants. The addition of 1 nM heptanal, octanal, pentanal and hexanol solutions had no effect on the conductance of the sensor, while the addition of 1 pM hexanal solution caused a sharp decrease in the conductance of the sensor. **e** Graph showing the conductance changes in canine receptor-based bioelectronic noses after the introduction of spoiled milk. A canine receptor-based bioelectronic nose showed conductance changes after the introduction of spoiled milk (*black line*). No significant conductance change was observed in the case of a CNT-FET without canine receptors (*red line*). (Adapted with permission from Park et al. [37] —Reproduced by permission of The Royal Society of Chemistry)

olfactory receptors triggered the cAMP signal pathways in the nanovesicles, and the signal was measured by the CNT channels, which enabled the detection of target molecules with a high sensitivity and a high selectivity.

Figure 12.8b shows real-time conductance measurement data obtained from a canine receptor-based sensor after the introduction of hexanal with different concentrations. Here, a canine receptor-based sensor was first placed in a phosphate buffered saline (PBS) solution, and then, the hexanal solutions with different concentrations were introduced. The bioelectronic noseexhibited a significant change in a conductance with the injection of a 1 fM hexanal solution. This result shows the high sensitivity of canine receptor-based sensors.

Figure 12.8c shows the normalized sensitivity of canine receptor-based sensors after the introduction of hexanal with various concentrations. Here, the conductance change of a canine receptor-based sensor was measured after the introduction of hexanal solutions with different concentrations, and the conductance change was normalized by its maximum to calculate the normalized sensitivity. The conductance change increased as the concentration of hexanal increased. Finally, the conductance change was almost saturated at a 1 nM concentration. The data could be fitted using the Langmuir isotherm equation with the estimated equilibrium constant K of 5.0×10^{10} M^{-1}.

Figure 12.8d shows real-time conductance measurement data obtained from a canine receptor-based sensor after the introduction of various odorants. The addition of 1 nM pentanal, heptanal, octanal, and hexanol did not affect the conductance of the canine receptor-based sensor, while the addition of 1 pM hexanal caused a sharp decrease in the conductance. The difference between hexanal and heptanal is just a single carbon atom in their alkane chains. Therefore, this result implicates that canine receptor-based sensors could detect hexanal with a high selectivity.

Figure 12.8e shows the conductance changes of canine receptor-based sensors after the introduction of spoiled milk to the sensors. Since milk contained lots of lipid, hexanal could be produced by a lipid oxidation process. A bioelectronic nosewithout canine receptors did not respond to the addition of the spoiled milk (red line). On the other hand, a canine receptor-based sensor exhibited measurable changes in its conductance after the introduction of the spoiled milk, and the response increased as the days of rotting increased (black line). Presumably, the hexanal in the spoiled milk bound to the canine receptors in nanovesicles and, as a result, caused the conductance change of a CNT channel. This result shows that canine receptor-based sensors can be applied to the fast on-site assessment of food quality.

12.4 Bioelectronic Tongue with a Human-Tongue-Like Selectivity

Human can recognize various tastants such as umami, sweet, and bitter tastants through gustatory receptors in tongues. Thus, the gustatory receptors can be powerful sensing elements for bioelectronic tongues.

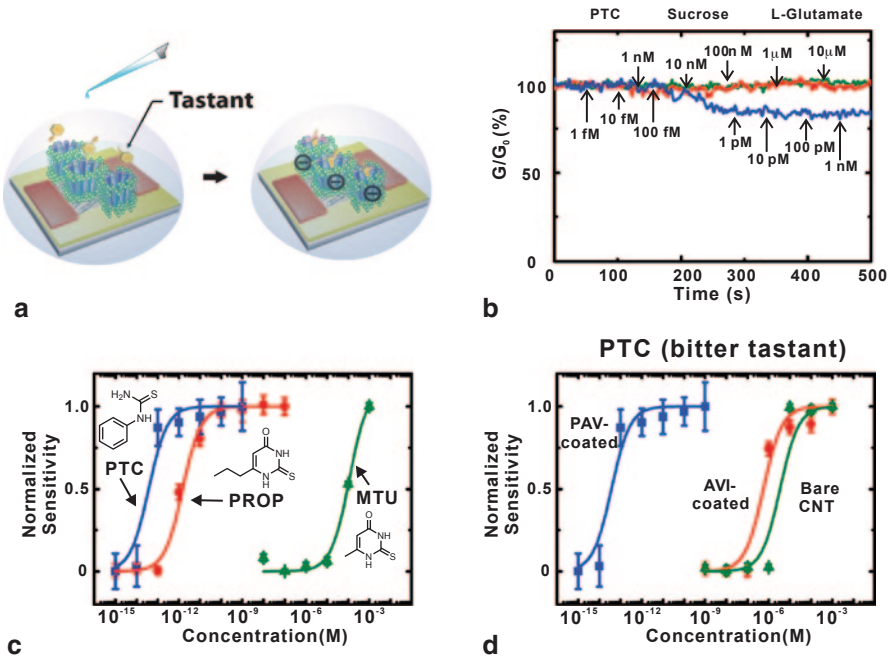

Fig. 12.9 Bioelectronic tongue. **a** Plausible mechanism for the response of a bioelectronic tongue. The binding of bitter tastant molecules with tastant receptors deforms the receptors and induces negative charges, which increases contact resistance between metal electrodes and CNTs. **b** Real-time response of a bioelectronic tongue to PTC (target bitter tastant), L-glutamate (umami tastant), and sucrose (sweet tastant). **c** Response curves of a bioelectronic tongue to PTC, PROP, and MTU. **d** Response curves of bioelectronic tongues with two different gene-type receptors (PAV and AVI) to PTC. (Adapted with permission of Kim et al. [38]—Reproduced by permission of The Royal Society of Chemistry)

Kim et al. [38] reported a bioelectronic tongue based on a human gustatory receptor (hTAS2R38)-functionalized CNT-FET for the detection of *bitter* tastant molecules with a *human-tongue-like* selectivity. The bioelectronic tongues were composed of CNT transistor transducers and immobilized gustatory receptors with a lipid layer. Figure 12.9a shows the structure of hTAS2R38-functionalized bioelectronic tongues and the mechanism of the specific tastant detection using the bioelectronic tongue. G-protein-coupled receptors including taste receptors usually contained ionizable cysteine residues which had active and inactive biophysical states. These states were related to the negatively charged form, and the neutral acid form of cysteine, respectively. The binding of a target molecule to the receptor changed the state of cysteine residues and resulted in negative charges on the receptor [34, 35]. When the hTAS2R38-functionalized CNT-FETs were exposed to specific bitter tastants, the tastant molecules reacted with the hTAS2R38 and induced a conformational change toward the active state with negative charges [34, 35]. This increased the Schottky barrier between the metal electrodes and CNTs, resulting in the reduction in the conductance of CNT channels.

The hTAS2R38-immobilized CNT-FETs showed the detection limit of 100 fM phenylthiocarbamide (PTC) which is a kind of bitter tastants (Fig. 12.9b). On the other hand, the addition of other taste substances such as L-glutamic acid and sucrose which is related to umami and sweet taste, respectively, did not affect the current level even at high concentrations (10 μM). This indicates that the bioelectronic tongue could selectively detect bitter tastants in real-time with a high sensitivity.

Also, the bioelectronic tongue showed a *human-tongue-like selectivity* to various bitter tastants such as PTC, propylthiouracil (PROP) and methylthiouracil (MTU) (Fig. 12.9c). The unique responses of human tongues to taste molecules are originated from the unique binding properties of taste receptors. For example, though PROP and MTU have a very similar chemical structure, only PROP molecules are known to strongly bind to the hTAS2R38 taste receptor protein. On the other hand, the taste receptor protein reacts to the molecular species with quite different chemical structures such as PROP and PTC. Note that even though the chemical structures of PTC and PROP were somewhat different, both tastants produced a sensor response to the bioelectronic tongue. On the other hand, although the MTU had a similar chemical structure to PROP, the bioelectronic tongue responded to MTU only at high-concentrations ($\geq$100 μM). The bioelectronic tongue was sensitive to similar tastes rather than similar chemical structures. This implies that the bioelectronic tongue can be utilized as a taste sensor exactly mimicking the unique selectivity of human taste systems.

Furthermore, the bioelectronic tongue could mimic the response of human tongues with two frequent gene types, PAV- (*taster*) and AVI- (*non-taster*) types (Fig. 12.9d). The bioelectronic tongue functionalized with PAV-type receptors exhibited sensitive sensor responses to PTC. On the other hand, the bioelectronic tongue functionalized with AVI-type receptors showed only non-specific signals caused by the binding of PTC directly to CNT-FETs. These variations involved in taster and non-taster types of hTAS2R38 were exactly same as the human taste system.

Using this strategy, one could differentiate the activities of taster's PAV- and non-taster's AVI-type of hTAS2R38. Also, this strategy enables the detection of bitter tastants with a *human tongue-like selectivity* and a detection limit down to the femtomolar range.

12.5 Chemical Pain Sensor

In mammalian somatosensory systems, receptors play an important role in obtaining hazardous information such as pain. Thus, pain sensory receptors can be utilized as sensing elements for chemical pain sensors.

Jin et al. [39] developed a nanovesicle-based chemical pain sensor platform which mimics the signal pathways of human pain sensory systems. The structure and the mechanism of nanovesicle-based chemical-pain sensors are depicted in Fig. 12.10a. Chemical-pain sensors were composed of CNT-FETs and immobi-

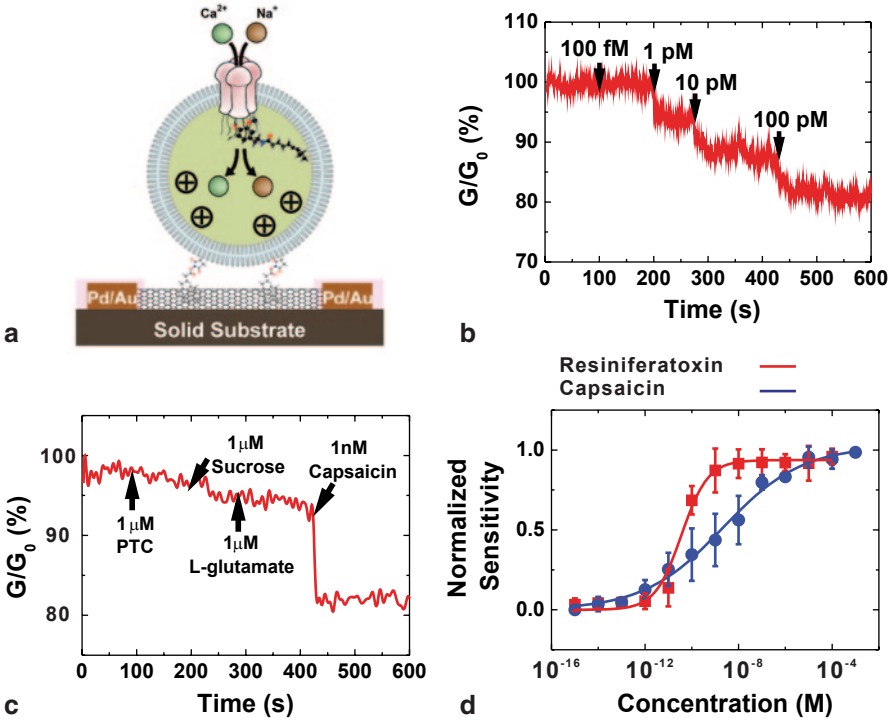

Fig. 12.10 Chemical pain sensor. **a** Plausible mechanism for the response of a chemical-pain sensor. After the injection of chemical stimuli, rTRPV1 protein captured the chemical stimuli molecules and induced the influx of cations, resulting in the conductance decrease of the CNT network channel. **b** Real-time conductance measurement data obtained from chemical pain sensors after the introduction of capsaicin. The conductance decreased after the introduction of capsaicin solution with picomolar concentration. **c** Real-time conductance measurement data obtained from chemical pain sensors after the injection of different chemical stimuli. **d** Dose-dependent responses of chemical pain sensors to resiniferatoxin and capsaicin. (Adapted with permission of Jin et al. [39])

lized chemical pain sensory nanovesicles containing a receptor protein (rTRPV1) for the detection of chemical pain stimuli. When a CNT-FET functionalized with rTRPV1-expressed-nanovesicles was exposed to chemical pain stimuli such as capsaicin and resiniferatoxin, the rTRPV1 on the nanovesicles captures the stimuli molecules, which eventually induced the influx of cations such as Ca^{2+} and Na^{+} into the nanovesicles through the rTRPV1 [40]. The increased concentration of positive ions inside the nanovesicles could give a field effect on the underlying CNT-FET, resulting in the decrease of a channel conductance because CNTs exhibit p-type behaviors under ambient conditions.

The injection of capsaicin solutions with concentrations higher than 1 pM induced a change in the conductance of the CNT channel (Fig. 12.10b). This result indicates the chemical pain sensor can respond to capsaicin in real time with a high sensitivity.

Figure 12.10c shows a real time conductance measurement from chemical pain sensors after the introduction of various chemical stimuli. Note that the conductance changed after injecting 1 μM of non-painful stimuli such as PTC, sucrose, and L-glutamate were minimal. However, after the injection of capsaicin with a rather low concentration (1 nM), a significant conductance change was observed. It indicates that the chemical pain sensors responded selectively to chemical pain stimuli just like an animal pain sensory system.

The response of chemical pain sensors to two different painful stimuli, capsaicin and resiniferatoxin, showed different characteristics, indicating that one could discriminate two different painful stimuli using the chemical pain sensor (Fig. 12.10d). Also, the response curves indicate that resiniferatoxin is a more potent agonist than capsaicin.

12.6 Summary and Vision

The unique one-dimensional structure of CNTs provides an extremely large surface-to-volume ratio, and thus, the electrical properties of CNTs are easily changed by the adsorption of small molecules. Due to this property, CNT-based devices can be ideal sensor transducers for various chemical and biomolecular sensors. Recently, bioelectronic noses based on CNTs have been developed by immobilizing olfactory receptors or nanovesicles on the surface of CNT-FETs. These bioelectronic noses could detect target odorants with a high sensitivity and exhibited highly selective responses to target odorants with a single-carbon-atomic resolution just like human or canine olfactory systems. Also, a CNT-based bioelectronic tongue and a chemical pain sensor showed a human-like selectivity and sensitivity in the detection of tanstants and chemical pain stimuli molecules, respectively. Significantly, the "surface-programmed assembly" method allows one to mass-produce such bioelectronic nose devices with uniform characteristics, which makes CNT-based bioelectronic noses suitable for practical applications.

It also should be mentioned that there are still some hurdles to overcome for real-life applications. For example, one needs a pretreatment process to bring odorant molecules from air into a solution because receptors work only in aqueous solution. Also, we have to develop a method to keep the sensors under ambient condition for a long time period because the receptor proteins may degrade in time. However, considering the development history of other chemical or biological sensors with the similar issues at the beginning of its development, we can envision the current problems of bioelectronic nose devices should be solved in time by engineering efforts.

It is also interesting to imagine what might happen from now on. Let's consider the history of artificial sensory devices for other sensory systems: eyes, ears and touch senses. A while ago, researchers invented artificial sensory devices such as *photosensors, microphones*, and *touch screens* mimicking human *eyes*, *ears* and *touch senses*, respectively. Such inventions allowed one to quantify the stimuli for

the sensory systems based on the signals from the corresponding artificial sensors. For example, *lux* and *decibel* are the units to quantify *lights* and the *sounds, respectively*. Furthermore, such standard signals can be sent over a long distance and utilized to reproduce the corresponding stimuli. For example, one can take a picture using a camera comprised of photosensors, send it through the internet, and reproduce it on display devices, which is one of the key technology in the modern IT and entertainment devices such as smart phones and televisions. Thus, one of the key events which triggered modern IT and entertainment industries can be the development of artificial sensory devices for human eyes, ears and touch senses.

We can envision the development of bioelectronic noses and tongues may trigger the similar progresses in the future. The signals from the *bioelectronic noses* and *tongues* can be utilized to quantify the stimuli for *human noses* and *tongues*, respectively. For example, the standard signals from *perfumes* or *foods* (i.e. wine, coffee etc) measured by *bioelectronic noses* or *tongues* can be sent over a long distance and used to evaluate the *smells* or *tastes* of them, respectively. Eventually, we may be able to develop advanced devices to reproduce such smells or tastes from the standard signals, which may open up the new era of modern entertainment and IT industries. In this sense, we may say that the development of bioelectronic noses is a major breakthrough in modern technology and we are at the dawn of a new technological revolution.

References

1. Reich S, Thomsen C, Maultzsch J (2004) Carbon nanotubes: basic concepts and physical properties. Wiley-VCH Weinheim, Cambridge
2. Deheer WA, Chatelain A, Ugarte D (1995) A carbon nanotube field-emission electron source. Science 270(5239):1179–1180
3. Postma HWC, Teepen T, Yao Z, Grifoni M, Dekker C (2001) Carbon nanotube single-electron transistors at room temperature. Science 293(5527):76–79
4. Kim JR, So HM, Kim JJ, Kim J (2002) Spin-dependent transport properties in a single-walled carbon nanotube with mesoscopic Co contacts. Phys Rev B 66(23):233–401
5. Lee M, Im J, Lee BY, Myung S, Kang J, Huang L, Kwon YK, Hong S (2006) Linker-free directed assembly of high-performance integrated devices based on nanotubes and nanowires. Nat Nanotechnol 1(1):66–71
6. Dai HJ, Hafner JH, Rinzler AG, Colbert DT, Smalley RE (1996) Nanotubes as nanoprobes in scanning probe microscopy. Nature 384(6605):147–150
7. Tans SJ, Devoret MH, Dai HJ, Thess A, Smalley RE, Geerligs LJ, Dekker C (1997) Individual single-wall carbon nanotubes as quantum wires. Nature 386(6624):474–477
8. Bachtold A, Hadley P, Nakanishi T, Dekker C (2001) Logic circuits with carbon nanotube transistors. Science 294(5545):1317–1320
9. Yu WJ, Chae SH, Lee SY, Duong DL, Lee YH (2011) Ultra-transparent, flexible single-walled carbon nanotube non-volatile memory device with an oxygen-decorated graphene electrode. Adv Mater 23(16):1889–1893
10. Lee NS, Chung DS, Han IT, Kang JH, Choi YS, Kim HY, Park SH, Jin YW, Yi WK, Yun MJ, Jung JE, Lee CJ, You JH, Jo SH, Lee CG, Kim JM (2001) Application of carbon nanotubes to field emission displays. Diam Relat Mater 10(2):265–270

11. Wu ZC, Chen ZH, Du X, Logan JM, Sippel J, Nikolou M, Kamaras K, Reynolds JR, Tanner DB, Hebard AF, Rinzler AG (2004) Transparent, conductive carbon nanotube films. Science 305(5688):1273–1276
12. Baughman RH, Cui CX, Zakhidov AA, Iqbal Z, Barisci JN, Spinks GM, Wallace GG, Mazzoldi A, De Rossi D, Rinzler AG, Jaschinski O, Roth S, Kertesz M (1999) Carbon nanotube actuators. Science 284(5418):1340–1344
13. Zhang DH, Ryu K, Liu XL, Polikarpov E, Ly J, Tompson ME, Zhou CW (2006) Transparent, conductive, and flexible carbon nanotube films and their application in organic light-emitting diodes. Nano Lett 6(9):1880–1886
14. Allen BL, Kichambare PD, Star A (2007) Carbon nanotube field-effect-transistor-based biosensors. Adv Mater 19(11):1439–1451
15. Li J, Lu YJ, Ye Q, Cinke M, Han J, Meyyappan M (2003) Carbon nanotube sensors for gas and organic vapor detection. Nano Lett 3(7):929–933
16. Kong J, Soh HT, Cassell AM, Quate CF, Dai HJ (1998) Synthesis of individual single-walled carbon nanotubes on patterned silicon wafers. Nature 395(6705):878–881
17. Huang Y, Duan XF, Wei QQ, Lieber CM (2001) Directed assembly of one-dimensional nanostructures into functional networks. Science 291(5504):630–633
18. Li XL, Zhang L, Wang XR, Shimoyama I, Sun XM, Seo WS, Dai HJ (2007) Langmuir-Blodgett assembly of densely aligned single-walled carbon nanotubes from bulk materials. J Am Chem Soc 129(16):4890–4891
19. Li YL, Kinloch IA, Windle AH (2004) Direct spinning of carbon nanotube fibers from chemical vapor deposition synthesis. Science 304(5668):276–278
20. Yu GH, Cao AY, Lieber CM (2007) Large-area blown bubble films of aligned nanowires and carbon nanotubes. Nat Nanotechnol 2(6):372–377
21. Wang YH, Maspoch D, Zou SL, Schatz GC, Smalley RE, Mirkin CA (2006) Controlling the shape, orientation, and linkage of carbon nanotube features with nano affinity templates. Proc Natl Acad Sci U S A 103(7):2026–2031
22. Martin CA, Sandler JKW, Windle AH, Schwarz MK, Bauhofer W, Schulte K, Shaffer MSP (2005) Electric field-induced aligned multi-wall carbon nanotube networks in epoxy composites. Polymer 46(3):877–886
23. Xia YN, Mrksich M, Kim E, Whitesides GM (1995) Microcontact printing of octadecylsiloxane on the surface of silicon dioxide and its application in microfabrication. J Am Chem Soc 117(37):9576–9577
24. Hong S, Kim TH, Lee J, Byun KE, Koh J, Kim T, Myung S (2007) "Surface-programmed assembly" of nanotube/nanowire-based integrated devices. Nano 2(6):333–350
25. Im J, Huang L, Kang J, Lee M, Lee DJ, Rao SG, Lee NK, Hong S (2006) "Sliding kinetics" of single-walled carbon nanotubes on self-assembled monolayer patterns: beyond random adsorption. J Chem Phys 124(22):224707
26. Lee BY, Sung MG, Lee J, Baik KY, Kwon YK, Lee MS, Hong S (2011) Universal parameters for carbon nanotube network-based sensors: can nanotube sensors be reproducible? ACS Nano 5(6):4373–4379
27. Maeng S, Moon S, Kim S, Lee HY, Park SJ, Kwak JH, Park KH, Park J, Choi Y, Udrea F, Milne WI, Lee BY, Lee M, Hong S (2008) Highly sensitive NO(2) sensor array based on undecorated single-walled carbon nanotube monolayer junctions. Appl Phys Lett 93(11):113111
28. Kong J, Franklin NR, Zhou CW, Chapline MG, Peng S, Cho KJ, Dai HJ (2000) Nanotube molecular wires as chemical sensors. Science 287(5453):622–625
29. Besteman K, Lee JO, Wiertz FGM, Heering HA, Dekker C (2003) Enzyme-coated carbon nanotubes as single-molecule biosensors. Nano Lett 3(6):727–730
30. Kim TH, Lee J, Hong S (2009) Highly selective environmental nanosensors based on anomalous response of carbon nanotube conductance to mercury ions. J Phys Chem C 113(45):19393–19396
31. Kim B, Lim D, Jin HJ, Lee HY, Namgung S, Ko Y, Park SB, Hong S (2012) Family-selective detection of antibiotics using antibody-functionalized carbon nanotube sensors. Sens Actuators B-Chem 166–167:193–199

32. Lee J, Jo M, Kim TH, Ahn JY, Lee DK, Kim S, Hong S (2011) Aptamer sandwich-based carbon nanotube sensors for single-carbon-atomic-resolution detection of non-polar small molecular species. Lab Chip 11(1):52–56
33. Kim TH, Lee SH, Lee J, Song HS, Oh EH, Park TH, Hong S (2009) Single-carbon-atomic-resolution detection of odorant molecules using a human olfactory receptor-based bioelectronic nose. Adv Mater 21(1):91–94
34. Rubenstein LA, Lanzara RG (1998) Activation of G protein-coupled receptors entails cysteine modulation of agonist binding. J Mol Struc (Theochem) 430:57–71
35. Rubenstein LA, Zauhar RJ, Lanzara RG (2006) Molecular dynamics of a biophysical model for beta(2)-adrenergic and G protein-coupled receptor activation. J Mol Graph Model 25(4):396–409
36. Jin HJ, Lee SH, Kim TH, Park J, Song HS, Park TH, Hong S (2012) Nanovesicle-based bioelectronic nose platform mimicking human olfactory signal transduction. Biosens Bioelectron 35(1):335–341
37. Park J, Lim JH, Jin HJ, Namgung S, Lee SH, Park TH, Hong S (2012) A bioelectronic sensor based on canine olfactory nanovesicle-carbon nanotube hybrid structures for the fast assessment of food quality. Analyst 137(14):3249–3254
38. Kim TH, Song HS, Jin HJ, Lee SH, Namgung S, Kim UK, Park TH, Hong S (2011) "Bioelectronic super-taster" device based on taste receptor-carbon nanotube hybrid structures. Lab Chip 11(13):2262–2267
39. Jin HJ, Ahn JM, Park J, Moon SJ, Hong S (2013) "Chemical-pain sensor" based on nanovesicle-carbon nanotube hybrid structures. Biosens Bioelectron 49(15):86–91
40. Chou MZ, Mtui T, Gao YD, Kohler M, Middleton RE (2004) Resiniferatoxin binds to the capsaicin receptor (TRPV1) near the extracellular side of the S4 transmembrane domain. Biochemistry 43(9):2501–2511

Chapter 13
Conducting Polymer Nanomaterial-Based Sensor Platform for Bioelectronic Nose

Oh Seok Kwon and Jyongsik Jang

Abstract Significant efforts in the fabrication of conducting polymer (CP) nanomaterials have enabled various electronic devices such as solar cells, memory devices, batteries, and field-effect transistors (FETs). Specifically, well-designed one-dimensional (1D) CP nanostructures have gained attention in various biosensing applications due to their 1D geometry, which can facilitate efficient charge-transfer behavior and signal amplification. Recently, researchers have demonstrated various nanomaterial-based odorant sensing geometries with sensitivity and selectivity. Although these conventional odorant sensing platforms provide significant and sensitive performance, limitations such as low sensitivity, slow response time, and an unstable platform in the liquid state remain as challenges. Herein, we developed a novel fabrication process for functionalized 1D CP nanomaterials, conjugated with human olfactory receptors (hORs), a so-called "bioelectronic nose" (B-nose), through an immobilization process. The sensing platforms using 1D CP nanomaterials were integrated into a liquid-ion gated FET system, resulting in the development of a high-performance FET-type B-nose. Real-time responses from the B-nose were monitored with ultrasensitive and selective responses at unprecedentedly low concentrations of the target odorant. The B-nose also showed single-atom-resolution for target odorants among similar non-target odorants. Moreover, the 1D CP nanomaterial-based B-nose can discriminate target odorants in the gaseous state, with sensing capability comparable to that of a human expert's nose. The B-nose opens the possibility for efficient methodology for smell mechanism studies. Based on these results, the study of the B-nose using 1D CP nanomaterials opens up challenging research opportunities including these related to the food industry, disease diagnosis, and public safety.

J. Jang (✉) · O. S. Kwon
School of Chemical and Biological Engineering, Seoul National University, Seoul, Republic of Korea
e-mail: jsjang@plaza.snu.ac.kr

T. H. Park (ed.), *Bioelectronic Nose,* DOI 10.1007/978-94-017-8613-3_13,

13.1 Introduction

During the past few decades, there has been enormous interest in the development of preventive safety systems for society [1–4]. Exposure to representative harmful factors, such as toxic molecules, explosive compounds, addictive drugs in food, and environmental hazardous material should be controlled and prevented [5–12]. Based on these demands, many studies have demonstrated sensitive and selective analytical methodologies, including gas chromatography (GC), mass spectrometry (MS), optical spectroscopy, and GC-MS. Owing to advanced electrical technologies using conductive materials, various electrical measurements have been constructed with attractive advantages, such as cost-efficiency, simple design, and real-time monitoring, compared with conventional methods [13–16]. For example, Cynkar et al. introduced a simple, efficient cost effective electronic nose, based on MS, for the wine industry and showed rapid screening of wines. Enormous efforts using electronic devices have created artificial electronic noses to detect specific smell odorants (e.g., usually small, single atoms containing alcohol, ether, ketone, and acids). The artificial electronic nose must have specific selectivity to interact with small single-atomic molecules, which become a driving force for diverse sensing platforms based on conductive or non-conductive materials such as metal oxides and organic semiconductors [17–23]. Although these artificial electronic noses showed significant measurement ability *via* resistance or conductance changes, advancements were needed to improve their low sensitivity and portability.

Artificial noses have generally been constructed with sensing components and platforms. To understand high-performance artificial noses, several critical factors should be considered: (i) chemical functionality for selectivity, (ii) structural ordering for efficient signal transfer, and (iii) the portable sensing platform. Significant achievements in nanotechnology have led to the development of new sensing platforms. Metal or ceramic nanomaterials have been integrated into the electrical substrate; this provides portable and efficient platforms for sensor applications [24, 25]. Li et al. demonstrated field-effect ammonia sensors, based on organic semiconductor films. They fabricated ultrathin, continuous, well-aligned microstripes using dendritic microstripes of organic semiconductros for organic field-effect transistor (OFET)-based sensors and showed high-performance ammonia gas detection. Fernandez et al. also produced FET-type microsensors based on a CY8C29466 microcontroller, which has the advantages of portability, low cost, and integration compatibility. Using these sensors the data were stored for further analysis by coupling the system to a PC serial port. Biosensors using one-dimensional (1D) geometry such as nanotubes (NTs), nanorods (NRs), and nanofibers, which allow efficient charge transport along the long-axis direction at the nanometer scale, have been introduced [26–34]. Due to advanced sensing 1D nanomaterial platforms, attractive biosensing platforms for electronic noses have been demonstrated by combining 1D nanomaterials with bioreceptors, i.e., the so called “bioelectronic nose (B-nose)”. The B-nose provides highly sensitive and selective responses toward specific odorants. Kim et al. reported the detection of odorant molecules with single-carbon-atom resolution using a B-nose created from the human olfactory receptor-(hOR)-adsorbed carbon

nanotube FET (CNT FET) and the G-protein-coupled receptors in cell membranes [35]. Although single-atom-resolution and highly sensitive responses were achieved by B-noses using carbon nanotubes (CNTs), critical limitations, such as complex in functionality and an unstable geometry in the liquid state, still remain as challenges.

Significant advance in conducting polymers (CPs) has prompted the development of devices related to energy and environmental applications [36, 37]. CPs have been developed as alternatives to inorganics and semiconductors, due to their great potential and advantages, such as flexibility, cost-efficiency, and facile processes. With the development of nanotechnology, there is a growing demand for advanced electronics based on functional nanomaterials. Various CP nanomaterials have been investigated from fundamental and practical perspectives, leading to an understanding of their unique chemical and physical characteristics [38–41]. The electrical and optical properties of CP nanomaterials are similar to those of metal or inorganic semiconductors, due to their conjugated π-electron systems [40, 42–45]. From these unique electrical and chemical properties, CP nanomaterials have shown excellent performance in electronic applications [46]. 1D CP geometry has provided outstanding charge-transfer characteristics in analytical methodologies. Specifically, the stable connections between 1D CP geometries and bioreceptors were demonstrated and integrated into an FET system, leading to advanced, reliable sensing platforms for B-nose [34, 35, 47, 48]. B-nose using 1D CP sensing platform shows great sensing performances and reliable sensitivities in liquid or air states.

Considerable progress has been made I in the development of the B-using various sensing platforms with metal or ceramic nanomaterials. However, have several technological challenges such as low sensitivity and slow response times to be improved for general B-nose applications. Herein, we discuss key issues to be considered in the development of the B-nose, using 1D CP nanomaterials. Additionally, we introduce simple fabrication methods and the progression in performance improvement for functionalized 1D CP nanomaterials and their sensing platforms for B-nose applications.

13.2 Fabrication of 1D CP Nanomaterials

CP nanomaterials with enlarged surface areas have received highly attractive attention due to their inherent biocompatibility and facile functionalization, compared with carbon-based nanomaterials, metal-oxides, and ceramic nanomaterials. This has led to various applications, including organic light-emitting diodes, solar cells, memory devices, fuel cells, and sensors [40, 49]. In particular, 1D CP nanomaterials have demonstrated excellent electrical performance, due to their efficient charge transfer along the long-axis direction [36, 37, 50–52]. Thus, numerous processes for fabricating 1D CP nanomaterials have been introduced. Although excellent and unique manufacturing processes have been demonstrated, several technological challenges still remain for tailored and controlled methodologies. Here, we outline the versatile strategies that have been investigated for the fabrication of 1D CP nanomaterials: soft-template, hard-template, and template-free methods.

13.2.1 Hard-Template Methods

The hard-template method, one of the most facile synthesis methods, is advantageous for designing nanomaterials, such as core/shell materials, nanoparticle (NPs), and nano-capsules [53–56]. One-dimensional CP nanomaterials, including nanorods (NRs), nanotubes (NTs), and nanofibers (NFs), can be easily tailored by hard-templates, such as anodic aluminum oxide (AAO) and polycarbonate (PC) membranes. Compared with conventional structured or patterned templates, AAO membranes are widely used in various fields, due to their controllable pore and diameter sizes. For example, polypyrrole (PPy), polyaniline (PANi), polythiophene (PT), and poly (3,4-ethylenedioxythiophene) (PEDOT) NTs have been fabricated using hard templates for electronic devices. Moreover, these 1D CP nanomaterials can be designed not only with fixed diameters and lengths, but also with controlled wall-thicknesses. Park et al. fabricated 1D CP nanomaterials as a transducer in chemical sensor applications (Fig. 13.1a; [57]).

13.2.2 Soft-Template Methods

Recently, various 1D CP nanostructures have been constructed using soft-template methods, such as surfactant, liquid crystalline polymer, cyclodextrin, and functionalized polymer techniques [58–61]. Importantly, surfactants, which imply cationic, anionic, and non-ionic amphiphiles, are mostly used for the formation of micelles as a nanoreactor [40, 62]. The nanoreactors can be formed in micro-emulsions, which are macroscopically homogeneous mixtures of oil, water, and surfactant, leading to a useful medium for polymerization reactions. Thus, this technique allows the preparation of controllable 1D CP nanomaterials with a narrow size distribution, using cylindrical micelle and lamellar phases. We have synthesized various 1D CP nanomaterials, such as PEDOT NTs, PEDOT NRs, and PPy NTs, using soft-template methods. For example, Jang et al. demonstrated 1D PPy NTs using reverse micelle systems and provided their fabrication mechanism (Fig. 13.1b; [34, 63]). It is important to note that the polymerization process in soft-template methods is kinetically and thermodynamically unstable, due to Ostwald ripening, growth by collision between monomer droplets, and monomer consumption during polymerization.

13.2.3 Template-Free Methods

Template-free approaches have been studied extensively for the fabrication of 1D CP nanomaterials, because they are very straightforward, with no specific sacrificial template [64–66]. However, these approaches are limited to particular precursor materials. Compared with the other methods (i.e., soft and hard-templates), these methods can be used to fabricate simple, uniform, and high-quality nanomaterials. We have also demonstrated the fabrication of various shape-controlled

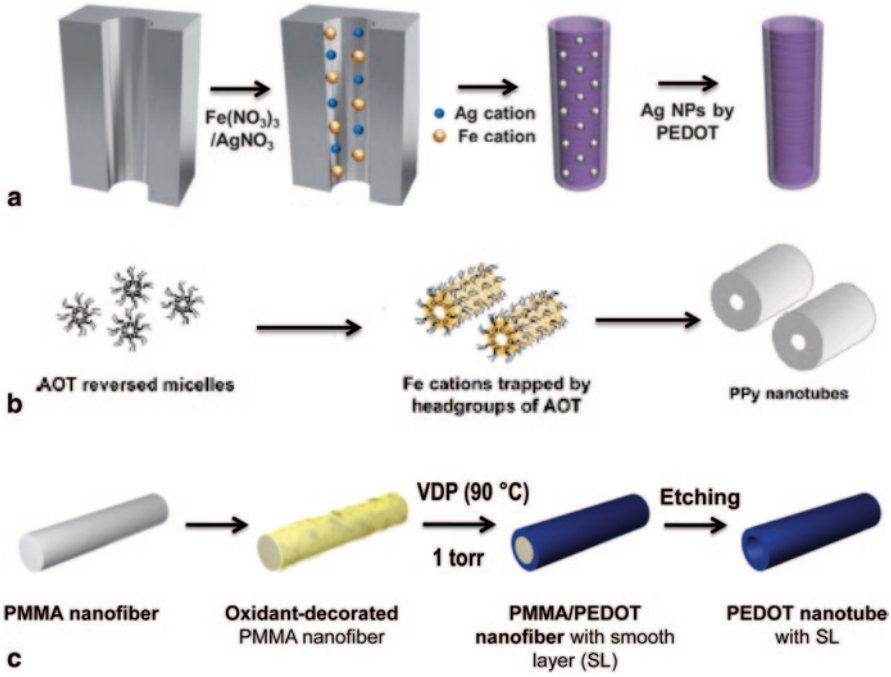

Fig. 13.1 **a** Synthetic route to Ag NPs/PEDOT NTs using hard-template (AAO). Reproduced from ref. 57. with permission of The Royal Society of Chemistry. **b** Fabrication process of polypyrrole NTs using reverse microemulsion polymerization (soft-template method). Reproduced from ref. 63. with permission of The Royal Society of Chemistry. **c** Multidimensional 1D PEDOT NTs using electrospinning and VDP process (template-free method). (Reproduced with permission from ref. 51. Copyright 2012 American Chemical Society)

nanomaterials *via* template-free methods. Electrospinning, one of the template-free methods, is a simple technique used to fabricate continuous 1D CP nanomaterials. One-dimensional multidimensional PEDOT NTs were fabricated by vapor deposition polymerization (VDP) mediated electrospun processes (Fig. 13.1c; [51]).

13.3 Design for B-nose Platform Using Functionalized CP NTs

13.3.1 Fabrication of Carboxylated PPy NTs via Reverse Microemulsion

Attractive methodologies and nanotemplates have been developed for fabricating 1D CP nanomaterials [26, 27–30, 50]. They showed novel physical, chemical, and optical properties, providing opportunities for advanced energy and environmen-

tal applications such as various electronics, energy storages, and sensors. It has a significant difference between tubular nanostructures and other forms (e.g., rods and fibers) due to the enhanced surface-to-volume ratio of the tubular structure. Most approaches for fabricating nanotubular structures, including CNTs, oxide NRs, metal NRs, and CP NFs, focused on the use of hard-templates. Although these methods permit controlled fabrication of the diameter and length, they are limited by high-cost and complicated synthetic steps. Recently, alternative strategies, such as soft-templates, have emerged, which simplify the fabrication process and facilitate large-scale production. Surfactant templates, a type of soft-template, can create various micelles, such as nanoreactors, for synthesizing 1D CP NTs. A reverse micelle, consisting of an aggregate of surfactant molecules containing a nanometer-sized water pool in the oil phase, was introduced using sodium bis(2-ethylhexyl) sulfoccinate (AOT) [40, 67–73]. We demonstrated, for the first time, fabrication of PPy NTs using a reverse micelle system, based on AOT; the PPy NT system was characterized using polarizing optical microscopy (POM) [34]. Moreover, functionalized PPy NTs were developed using a co-polymerization process; the stabilized the electrical properties in the liquid state, providing efficient covalent bonding between the biomolecules and sensing platforms.

Carboxylated polypyrrole nanotubes (CPNTs) were prepared by copolymerizing the pyrrole monomer and pyrrole-3-carboxylic acid (P3CA) in an AOT reverse microemulsion system [32]. An AOT reverse cylindrical micelle phase is formed by combining an apolar solvent (hexane) and $FeCl_3$ solution. Also, appropriate temperature condition was calculated by a ternary phase diagram (Fig. 13.2a; [67]). In the first stage, a reverse cylindrical micelle phase was constructed by cooperative interaction (charge-charge interaction) between Fe cations and AOT molecules to produce a micelle having a diameter on the order of one nanometer. Metal salts in the solution enable the growth of reverse micelles through critical micelle concentration I and II. Second, a PPy and P3CA mixture was added a dropwise to the AOT/hexane mixed solution containing a reverse cylindrical micelle phase. The polymerization progressed rapidly using an oxidizing agent (iron cations) along the surface of the reverse cylindrical micelles. This reaction can be observed with the change of the colors from yellow to black during polymerization. Finally, CPNTs can be obtained by washing process with an ethanol to remove residual reagents and AOT.

13.3.2 Characterization of CPNTs

To confirm the CPTNs, X-ray photoemission spectroscopy (XPS) was observed. Figure 13.2b displays the identification of CPNTs and pristine PPy NTs. The survey scan spectrum showed the presence of the principal C 1s, O 1s, and N 1s core levels. The representative O 1s peak of the CPNTs was characterized by a chemical map of the XPS (Fig. 13. 2c). The amount of O 1s peak was ca. 32% and it is consisted of three components centered at 531, 532.2 and 533.3 eV, corresponding to alcohol, carboxyl, and ether-type oxygens respectively. Field-emission scanning

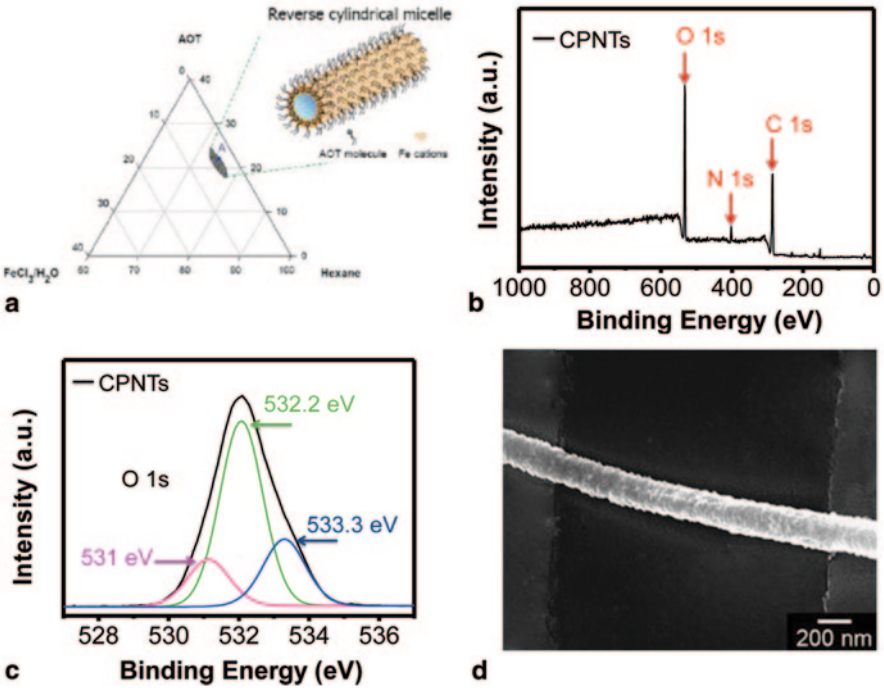

Fig. 13.2 **a** Partial ternary phase diagram for the hexane/AOT/ Fe cations system determinated at 15 °C. Reprinted with permission from ref. 67. Copyright 2005 American Chemical Society. **b** XPS spectra of the CPNTs. **c** XPS O 1s spectrum of the CPNTs. **d** Typical FE-SEM images of CPNTs on the microelectrodes. (Reprinted with permission from ref. 32. Copyright 2012 Elsevier)

electron microscopy (FE-SEM) was used to characteriz morphology of the CPNTs. Figure 13.2d shows the SEM image of the CPTNs on the microelectrodes, which had no impurities and a smooth surface [32].

13.3.3 Preparation of hORs

Two kinds of olfactory receptors as a fusion protein with a glutathione-*S*-transferase (GST) tag at its N terminus were prepared: hOR2AG1 and hOR3A1 were expressed in *Escherichia coli* (*E. coil*). The hOR2AG1 was used for the B-nose in liquid state; the other (hOR3A1) was introduced as a transducer for the B-nose in air. The GST-tag allows the information of olfactory receptor such as successful expression and Western blot analysis. The ORs can be separated from a membrane fraction of *E. coli* cells using Triton X-100, because the impurity proteins are soluble in Triton X-100. These ORs, which belong to a family of G protein-coupled receptors (GPCRs), are used for drug discovery and play a key role in odor discrimination.

13.3.4 Fabrication of OR Conjugated-CPNT Substrate as a B-nose Sensing Platform

An interdigitated microelectrode array (IMA) was patterned on a glass wafer using a photolithographic process and consisted of a pair of gold interdigitated microelectrodes (source and drain) with more than 50 fingers ($W/L = 1000$, $L = 2$ μm channel length). The IMA glass substrate was modified using aminosilane ((3-aminopropyl) triethoxysilane, APS) to introduce amine groups. The CPNTs were attached on the modified surface of IMA *via* the covalent bonding between the carboxylic acid groups of the CPNTs and the amine groups of IMA. To construct stable covalent bonding, an efficient condensing agent, 4-(4,6-dimethoxy-1,3,5-triazin-2-yl)-4-methylmorpholinium chloride (DMT-MM), was added. The DMT-MM facilitates the conjugation reaction at room temperature. The immobilization process of the CPNTs on the IMA stabilizes the electrical properties and induces mild reactions in the liquid state. Consecutively, the ORs were immobilized on the CPNTs *via* similar conjugation reactions. The overall reactions are given as follows (Fig. 13.3):

$$\text{Reaction 1. Hydrolysis}: \mathrm{H_2N(CH_2)_3Si(OCH_3)_3} + 3\mathrm{H_2O} \rightarrow \mathrm{H_2N(CH_2)_3Si(OH)_3} + 3\mathrm{CH_3OH}$$

$$\text{Condensation}: \mathrm{H_2N(CH_2)_3Si(OH)_3} + 3\mathrm{OH} - \text{substrate} \rightarrow \mathrm{H_2N(CH_2)_3Si(O)_3} - \text{substrate}$$

$$\text{Reaction 2. Condensation}: \text{pyrrole} - \mathrm{COOH} + \mathrm{H_2N(CH_2)_3Si(O)_3} - \text{substrate} \rightarrow \text{pyrrole} - \mathrm{CONH(CH_2)_3Si(O)_3} - \text{substrate}$$

$$\text{Reaction 3. Condensation}: \text{pyrrole} - \mathrm{COOH} + \mathrm{H_2N} - \text{lys} - \mathrm{OR} \rightarrow \text{pyrrole} - \mathrm{CONH} - \text{lys} - \mathrm{OR}$$

The FE-SEM image of OR-conjugated CPNTs deposited on the IMA was displayed, as shown Fig. 13.4a. It was clearly observed that the surface of CPNTs had considerably more rugged by the immobilized ORs compared to pristine CPNTs (Fig. 13.2d). Interestingly, no significant evidences of ORs on the surface of IMA, indicating the ORs were selectively immobilized on the surface of the CPNTs through covalent bonding. Compared with conventional physical adsorption, this immobilization process offers several advantages, including mild reaction conditions, stable electrical contact, and successful chemical bonding. Therefore, this sensing platform using immobilization will allow highly selective and sensitive sensing capabilities in B-nose.

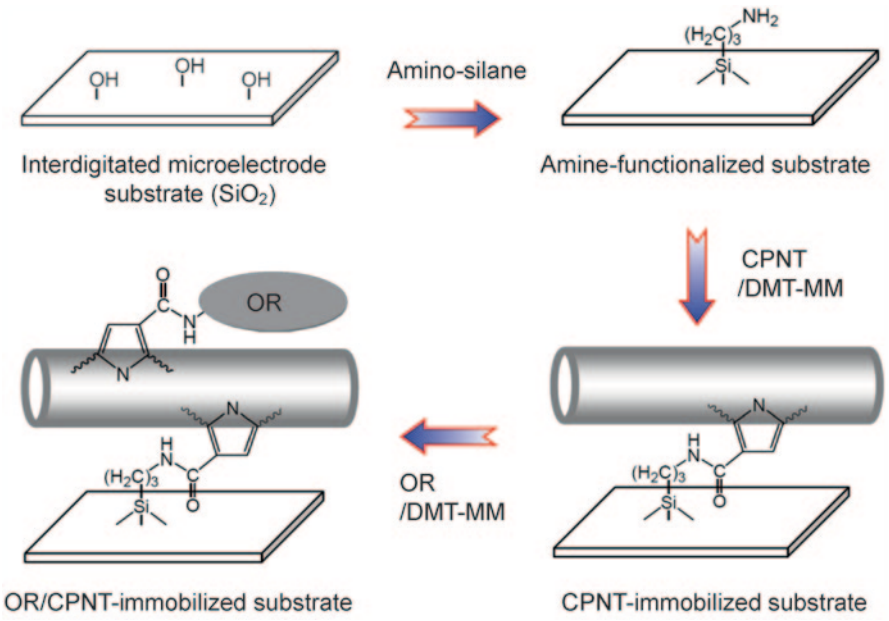

Fig. 13.3 Schematic illustration of fabricating sensing platform of B-nose using CPNT and OR. (Reproduced with permission from ref. [34]. Copyright 2009 Wiley-VHC Verlag GmbH @ Co. KGaA)

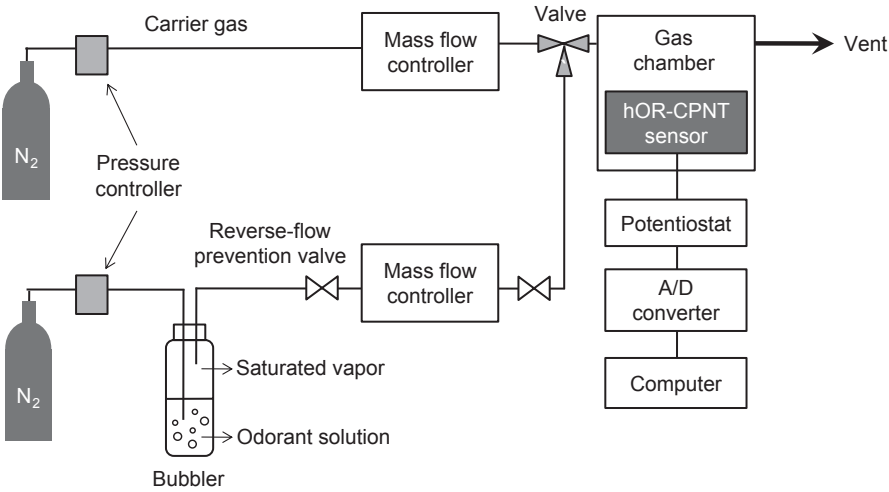

Fig. 13.4 Schematic diagram of standard gas generation system using MFCs and potentiostat. (Reprinted with permission from ref. [32]. Copyright 2012 Elsevier)

13.4 Artificial B-Noses Using OR/CPNT Platform

13.4.1 Chemiresistive B-Nose to Detect Odorant Gases

13.4.1.1 Construction of the Chemiresistive B-Nose

The olfactory system is a highly, precise biological process. The human nose can detect gaseous odorants at low concentrations (sub-part per trillion [ppt] level: 10^{-9}). Thus, it is challenging to mimic the human olfactory system, which can discriminate thousands of odorant molecules [74–79]. Recently, progress in nanotechnology the development of the nanotechnology, B-noses were designed using carbon nanotube (CNT) [35]. However, the B-noses using the CNT platform exhibited limitations such as unstable interaction between receptors and transducers in liquid state and antagonism study. To overcome the critical disadvantages, we attempted to construct a chemiresistive B-nose, based on 1D CP nanomaterials. Chemiresistor-based sensors exhibit several attractive characteristics, such as facile process, label-free detection, and low power consumption. Chemiresistive sensors can be applied to simple resistance change in response to various small molecules, including volatile organic compounds (VOCs) and nerve agents. From their strong points, the B-nose based on a chemiresistive system was created for the APS-treated IMA *via* the immobilization of the human olfactory (hOR3A1) on the CPNT, as shown Fig. 13.3. To assess the chemiresistive sensing platform, a standard gas generation system with a mass flow controller (MFC) was also introduced (Fig. 13.4). The gas generation system consisted of MFCs and measurements sections. The odorant gases that moved through the carrier gas (N_2) were controlled by MFC system, resulting that the odorant gases were reached into the gas chamber.

13.4.1.2 Characterization and Real-Time Responses of the Chemiresistive B-Nose

To confirm the electrical properties of the B-nose, current-voltage (*I-V*) characterizations were carried out. Generally, chemiresistive sensors measure the potential difference across two points, leading to accurate detection *via* simple based on changes in resistance values. Figure 13.5a displays the linear *I-V* values of B-nose based on OR-conjugated CPNTs. The *I-V* values were maintained with continuous linearity after the introduction of the OR on the CPNT. Moreover, a significant change in the *I-V* values was observed, due to the attachment of the ORs. This indicates that excellent electrical contact between the CPNTs and IMAs can be achieved using the immobilization process, which provides reliable electrical resistance properties.

Significant resistance changes from the chemiresistive B-nose can be observed by the introduction of target odorant gas. Figure 13.5b presents the sensing capability of the chemiresistive B-nose upon periodic exposure to helional gas. Rapid

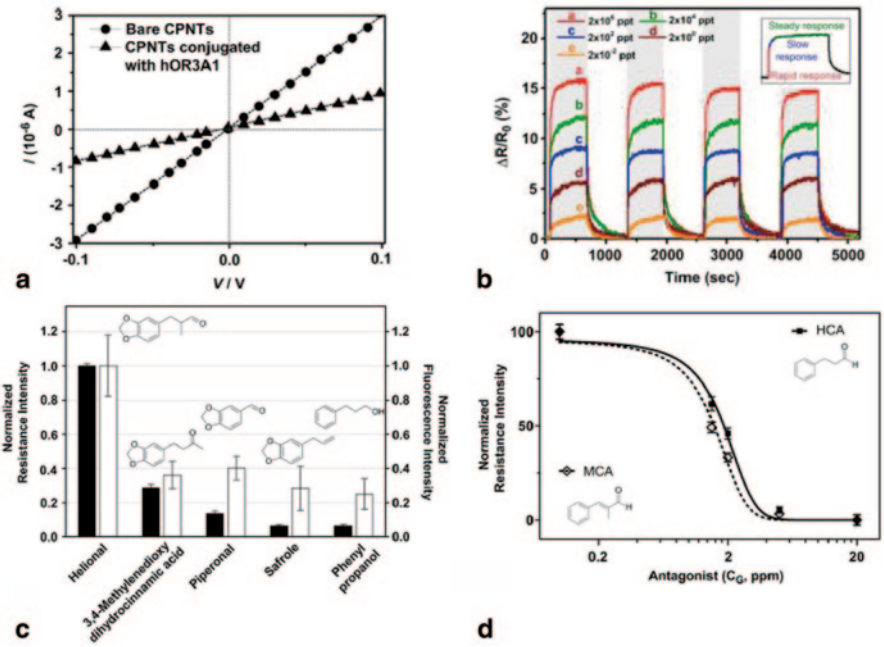

Fig. 13.5 **a** Current–voltage (*I-V*) curves of CPNTs on the IMA. **b** Real-time responses of B-noses. **c** Antagonism of B-nose. **d** Inhibition of odorant-induced B-nose responses by antagonists. (Reprinted with permission from ref. [32]. Copyright 2012 Elsevier)

responses from helional gas were exhibited with increasing resistance and saturation after 50 s; the more odorant concentrations have higher resistance changes. The maximum detectable level (MDL) of the B-nose was *ca*. 0.02 ppt, which means that the B-nose is highly sensitive compared with conventional gas-phase electronic noses (Table 13.1). This can be explained in terms of the interaction between the OR and odorant gases, which controls the p-type CPNT. In this study, the negative charges in ionization status of the OR bound to the odorant gases were transferred into the CPNT backbone. The carrier density (holes) of the p-type CPNT decreased with increasing negative charge, leading to a decrease in the conductance of the CPNT. The MDL value is similar to the noses of human experts. Moreover, the B-nose also showed high reversibility through various helional concentrations and excellent storage ability over long periods of time.

To observe antagonism in the olfactory system, an electronic nose with high sensitivity and selectivity should be constructed because the antagonism of the olfactory is complex. Two kinds of antagonists (methylcinnamaldehyde [MCA] and hydrocinamaldehyde [HCA]) were prepared. The responses from helional and antagonists were monitored with resistance changes. Although some antagonists showed significant responses, the responses from the helional can be clearly identified, due to their high fluorescence intensity (Fig. 13.5c). These results are also in

Table 13.1 Comparison data of conventional electronic noses

Sensing platforms	Analytes	M[a]	R[b]	Ref.
Mass spectrometry	Tempranillo wines	85 %	–	[13]
Mass spectrometry	Fungal growth	98 %	48 h	[14]
Mass spectrometry–gas chromatograhpy	Grain samples	5 μg kg^{-1} (range 0–80)	–	[15]
NIR spectra fluorescence	Foods	–	–	[16]
Silicon cantilever array	1-propanol	500 ppm[c]	–	[17]
Microspheres (sillica/nile) arrays	Toluene	0.84 ppm[c]	–	[19]
Silicon cantilevers	1-butanol, 1-propanol	1 μL	< 100 s	[20]
Cantilever array	Breath sample	30 ppm[c]	20–80	[21]
Fiber-optic chemosensor	Amyl alcohol Butyl alcohol	82 % 91 %	–	[23]
Organic semiconductor	Ammonia	10 ppm[c]	35 s	[25]
CNTs	H_2O/H_2S	–	–	[27]
CNTs	Proteases	0.5 pg/mL	–	[28]
ZnO nanorods	Humidity	< 5 %	–	[29]
CNTs	Amyl butyrate	100 fM	< 1 s	[35]
Graphene	Amyl butyrate	0.04 fM	< 1 s	[67]
1D CP NTs	Helional	0.01 ppt[d]	10 s	[32]
1D CP NTs	Amyl butyrate	10 fM	< 1 s	[34]

[a] Minimum detectable level
[b] Real-time response time (s)
[c] ppm: part-per-million
[d] ppt: part-per-trillion

agreement compared to conventional reports using olfactory neurons. Interestingly, the antagonistic behavior of the B-noses using OR-CPNTs was similar to the human noses (Fig. 13.5d). From these results, the B-noses based on OR-CPNTs were characterized with antagonistic behavior and high-performance sensing capabilities, opening the artificial B-nose similar to human nose.

13.4.2 Liquid-Ion Gated FET-Type B-Nose to Detect Odorants

13.4.2.1 Construction of Liquid-Ion Gated FET-Type B-Nose

Transistor-based biosensors, which combine of a sensing element (transistor) and an amplifier, have shown potential for miniaturization and portable sensing platforms. Various biosensors based on 1D CP nanomaterial transistors have been demonstrated with high-performance sensing capability. In this study, we designed a sensing platform based on 1D CP nanomaterials, which was integrated into the liquid-ion gated FET system for liquid odorant detection. The fabrication process of the liquid-ion gated FET-type B-nose was similar to the sensing platform of the

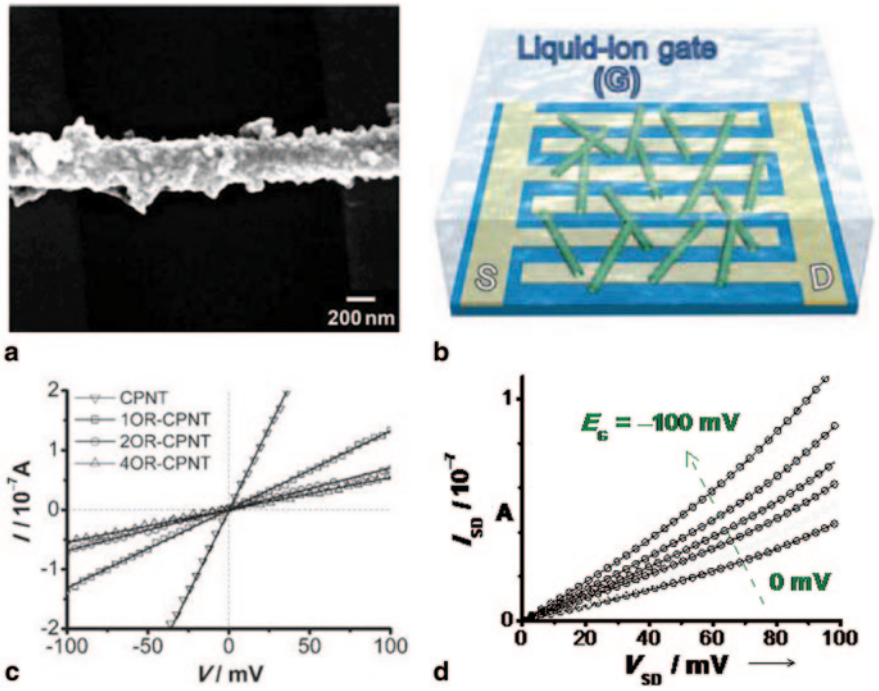

Fig. 13.6 **a** Typical FE-SEM image of a hOR-conjugated CPNT sensing platform. **b** Schematic diagram of a liquid-ion gated FET geometry immobilized hOR-CPNT. **c** Current-voltage curves of CPNTs, 1hOR-CPNT, 2hOR-CPNT, and 4hOR-CPNTs. **d** Out-put characterization of hOR-conjugated CPNT FET. (Reprinted with permission from ref. [34]. Copyright 2009 Wiley-VHC Verlag GmbH @ Co. KGaA)

chemiresistive B-nose previously introduced (Fig. 13.3). First, the IMA was patterned onto a glass substrate by a general lithographic process and engineered with APS to modify the surface properties. The amine-functionalized IMA substrate was combined with carboxylic acid groups of the CPNT *via* a condensation reaction. Compared to conventional lithographic methods, this immobilization approach provides attractive advantages such as a simple introduction process of chemical bonding and stable electrical properties in the liquid state. Continuously, the hOR (hOR2AG1) with terminal amine groups on cysteine (Cys) residues was attached to the CPNT surface through a similar condensation reaction. Figure 13.6a displays a typical FE-SEM image of hOR-conjugated CPNTs immobilized on an IMA substrate. The surface of CPNT was more rugged, and there were no hORs on the IMA substrate. This indicated that the attachment between the CPNTs and hORs was selective. Compared with the non-covalent approach, covalent anchoring allows high-performance analytical sensing in the liquid phase and is capable to design the chemical functionality of the CPNTs to be customized for specific purposes.

The liquid-ion gated FET geometry was constructed on the sensing platform using hOR-conjugated CPNTs (Fig. 13.6b); (i) the liquid-ion gate was consisted of a

phosphate-buffered solution (PBS, pH 7.4). (ii) three electrodes were introduced as source (*S*)/ drain (*D*) electrodes and gating electrodes (*G*). The gating electrodes were applied with the Ag/AgCl reference electrode and platinum counter electrode immersed in the PBS solution, leading to the efficient gating control. This liquid-ion gating can induce effects that enhance efficiency, including intimate contact on the CPNT surface and low-voltage operation, in the liquid state.

13.4.2.2 Characterization of the Liquid-Ion Gated FET-Type B-Nose

Before using the FET-type B-nose for liquid-phase odorant detection, the electrical properties were characterized. Figure 13.6c presents the *I*-*V* curves of hOR-conjugated CPNTs and pristine CPNTs without hOR deposited on the IMA substrate (scan rate = 10 mVs^{-1}). The d*I*/d*V* values of the B-nose sensing platform gradually decreased with increasing concentrations of hOR attachment. Although the gradient of d*I*/d*V* decreased slightly due to hOR attachment, the linearity of the B-nose sensing platform was continuously retained after the coupling reaction and washing process. This result indicates that covalent immobilization of the CNPTs provided stable electrical properties in the liquid state, leading to reliable electrical contact. Moreover, the loading amount of hOR on the CPNT could be controlled by adjusting the feed amount, which allowed to the maximum MDL for the B-nose using the hOR-conjugated CPNT. The observed d*I*/d*V* values from smallest to largest are as follows: hOR-to-CPNT weight ratios 1:4 (1hOR-CPNT) < 1:2 (2hOR-CPNT) < 1:1 (4hOR-CPNT).

To use the hOR-CPNT sensing platform as a signal transducing component of B-noses, we constructed a liquid-ion gated FET system with a PBS solution as the electrolyte. This was possible because the gating remote could be easily controlled. The FET-type sensing geometry was also applied to enhance the sensing performance through signal amplification. Figure 13.6b shows the FET system with three types of electrodes: source, drain, and gate electrodes. The gate potential (V_g) was applied between the reference electrode and the drain electrode through the liquid-ion solution. More than 100 sensing platforms were tested under ambient conditions. Figure 13.6d demonstrates the output curve characterization of the B-nose using an hOR-CPNT sensing platform at room temperature. The source-to-drain current (I_{ds}) negatively increased with negatively increasing gate voltage (V_g), indicating p-type (hole-transporting) behavior. From these experimental results, the binding of odorants to the B-nose was observed by monitoring the current changes *via* the liquid-ion gated FET system.

13.4.2.3 Real-Time Responses of Liquid-Ion Gated FET-Type B-Nose

To investigate the real-time sensing characteristics of the liquid-ion gated hOR-CPNT FET, the I_{sd} was measured at V_{sd} = 50 mV (V_G = 0 mV, a low operating voltage) upon the addition of various odorant concentrations. Generally, odorant amyl

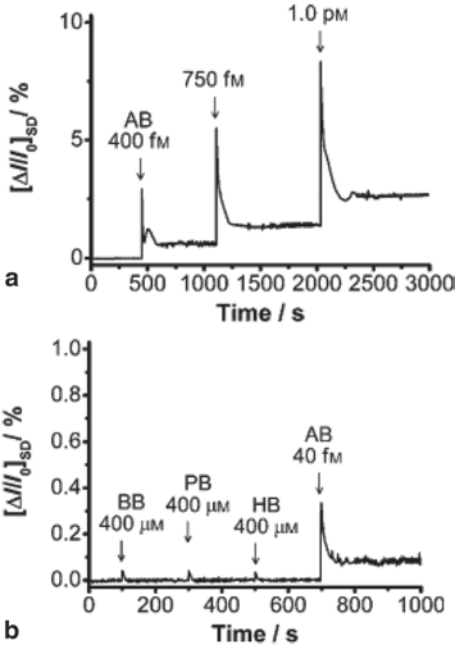

Fig. 13.7 Real-time responses of 1hOR-CPNT FET B-nose measured at V_{sd} = 50 mV: **a** target odorant (AB), **b** non-target (BB, HB, and PB) and target odorant (AB). The sensitivity was recalculated as normalized I_{sd} changes. (Reprinted with permission from ref. [34]. Copyright 2009 Wiley-VHC Verlag GmbH @ Co. KGaA)

butyrate (AB), a common reagent for fruit flavor, is particularly sensitive to the hOR, leading to a rapid response time. Figure 13.7a displays the real-time response of the B-nose to AB. The current values from the B-nose were achieved with a concentration-dependent increase in I_{sd} upon exposure to AB. To avoid electro-chemical oxidation of AB, the applied gate voltage was below the oxidation potential. The highly selective hOR interaction to AB leads to the lowest MDL (*ca*. 400 fM) for the B-nose compared with the conventional B-nose using 1D nanomaterials. The real-time responses of the B-nose were fast (< 1 s) and clearly saturated. Pristine CPNTs were also introduced as an identical experiment: no significant current signals were observed. This was attributed to the ultrasmall olfactory receptor (diameter < 4 nm) being expressed in the insoluble fraction of *E. coli*. It is believed that the sensing mechanism originates from a change in the charge-transport behavior of the CPNTs induced by the binding event of hOR-AB. Specifically, the hOR has both an uncharged (RSH) state and a negatively charged (RS^-) state through the acid-to-base transition of the sulfhydryl group. The structural rearrangement of hORs occurred, due to the interaction of AB, which induced negative point charge formation on the liquid-ion gate dielectric near the CPNTs. Finally, the accumulation of positive charge carriers in the CPNT channel allowed the increasing current to be monitored. Such a molecular gating effect is similar to a p-type doping effect acting indirectly on the liquid-ion gate dielectric, rather than directly affecting the semiconducting layer. Moreover, the B-nose has excellent selectivity with highly specific atomic-level resolution at femto-molar concentrations, as shown Fig. 13.7b. There were no changes in the current from the non-targeted molecules which only differed by the

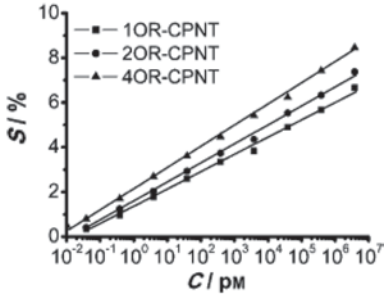

Fig. 13.8 Calibration curves of the FET B-nose using various hOR-CPNT sensing platforms (1hOR-CPNT, 2hOR-CPNT, and 4hOR-CPNT). (Reprinted with permission from ref. [34]. Copyright 2009 Wiley-VHC Verlag GmbH @ Co. KGaA)

number of carbon atoms (butyl butyrate, BB; propyl butyrate, PB; hexyl butyrate, HB); whereas the target molecule (AB) exhibited a significant signal.

To confirm the loading effect of hOR on the CPNT surface, 1hOR-CPNT, 2hOR-CPNT, and 4hOR-CPNT samples were prepared. Figure 13.8 shows the calibration curves of the FET B-nose. The 4hOR-CPNT, which offers the highest degree of functionalization, showed the lowest MDL level (10 fM) as a result of the enhanced hOR-AB interaction. Moreover, the linear curves as normalized changes in I_{ds}, were observed after the addition of various AB concentrations. All of the samples remained stable, as indicated by the linearity of the log-scale *x*-axis. The sensitivity order of the samples over a wide concentration range was as follows: 1hOR-CPNT < 2hOR-CPNT < 4hOR-CPNT. In particular, the sensitivity of the 4hOR-CPNT was approximately twice that of 1hOR-CPNT or 2hOR-CPNT. From these results, a high-performance B-nose can be constructed using hOR-CPNT sensing platform, carefully controlled by the hOR loading amount.

13.5 Conclusion

Owing to attractive advantages, including easy functionality and facile fabrication process, of the 1D CP nanomaterials, we demonstrated the construction of B-nose based on 1D CP nanomaterials. The CPNT geometry, as a sensing platform for the B-nose, can be constructed using an immobilization process on an IMA substrate. His configuration exhibited stable electrical properties and mild reaction conditions in the air or liquid. The B-noses, using the hOR-CPNT geometry, were utilized as two kinds of sensing platforms: (i) as a chemiresistive B-nose using simple changes in resistance, (ii) as a liquid-ion gated FET-type B-nose based on changes in current flow. For discriminating odorant gases, the chemiresistive B-nose showed excellent sensing performance. The FET-type B-nose also exhibited high-performance odorant detection in the liquid state. Considering these results, the hOR-conjugated CPNT sensing platform offers a new direction for mimicking human sensors. Moreover, this methodology can also be utilized for fabricating high-performance biosensors with high sensitivity and selectivity.

References

1. Baş M, Yüksel M, Çavuşoğlu T (2007) Difficulties and barriers for the implementing of HACCP and food safety systems in food businesses in Turkey. Food Control 18(2):124–130
2. Henson S, Caswell J (1999) Food safety regulation: an overview of contemporary issues. Food Policy 24(6):589–603
3. Safety M (2011) Health administration. Approval & Certification Center
4. Yong-hua Y (2009) Observation on law system of food safety in west and its enlightenments to us [J]. Gansu Theory Res 2:030
5. Lill M, Dobler M, Vedani A (2005) In silico prediction of receptor-mediated environmental toxic phenomena-application to endocrine disruption. SAR QSAR Environ Res 16(1–2):149–169
6. Osburn WO, Kensler TW (2008) Nrf2 signaling: an adaptive response pathway for protection against environmental toxic insults. Mutat Res 659(1):31–39
7. Tombelli S, Minunni M, Mascini M (2007) Aptamers-based assays for diagnostics, environmental and food analysis. Biomol Eng 24(2):191–200
8. Tsow F, Forzani E, Rai A, Wang R, Tsui R, Mastroianni S, Knobbe C, Gandolfi AJ, Tao N (2009) A wearable and wireless sensor system for real-time monitoring of toxic environmental volatile organic compounds. IEEE Sens J 9(12):1734–1740
9. Valavanidis A, Vlahogianni T, Dassenakis M, Scoullos M (2006) Molecular biomarkers of oxidative stress in aquatic organisms in relation to toxic environmental pollutants. Ecotoxicol Environ Saf 64(2):178–189
10. He J-L, Yang Y-F, Shen G-L, Yu R-Q (2011) Electrochemical aptameric sensor based on the Klenow fragment polymerase reaction for cocaine detection. Biosens Bioelectron 26(10):4222–4226
11. Liao Y-H, Chou J-C (2008) Drift and hysteresis characteristics of drug sensors based on ruthenium dioxide membrane. Sensors 8(9):5386–5396
12. Yagiuda K, Hemmi A, Ito S, Asano Y, Fushinuki Y, Chen C-Y, Karube I (1996) Development of a conductivity-based immunosensor for sensitive detection of methamphetamine (stimulant drug) in human urine. Biosens Bioelectron 11(8):703–707
13. Cynkar W, Dambergs R, Smith P, Cozzolino D (2010) Classification of Tempranillo wines according to geographic origin: combination of mass spectrometry based electronic nose and chemometrics. Anal Chim Acta 660(1):227–231
14. Vinaixa M, Marín S, Brezmes J, Llobet E, Vilanova X, Correig X, Ramos A, Sanchis V (2004) Early detection of fungal growth in bakery products by use of an electronic nose based on mass spectrometry. J Agric Food Chem 52(20):6068–6074
15. Olsson J, Börjesson T, Lundstedt T, Schnürer J (2002) Detection and quantification of ochratoxin A and deoxynivalenol in barley grains by GC-MS and electronic nose. Int J Food Microbiol 72(3):203–214
16. Farkas J, Dalmadi I (2009) Near infrared and fluorescence spectroscopic methods and electronic nose technology for monitoring foods. Prog Agric Eng Sci 5(1):1–29
17. Baller M, Lang H, Fritz J, Gerber C, Gimzewski J, Drechsler U, Rothuizen H, Despont M, Vettiger P, Battiston F (2000) A cantilever array-based artificial nose. Ultramicroscopy 82(1):1–9
18. Chandiok S, Crawley B, Oppenheim B, Chadwick P, Higgins S, Persaud K (1997) Screening for bacterial vaginosis: a novel application of artificial nose technology. J Clin Pathol 50(9):790–791
19. Dickinson TA, Michael KL, Kauer JS, Walt DR (1999) Convergent, self-encoded bead sensor arrays in the design of an artificial nose. Anal Chem 71(11):2192–2198
20. Lang H, Baller M, Berger R, Gerber C, Gimzewski J, Battiston F, Fornaro P, Ramseyer J, Meyer E, Güntherodt H (1999) An artificial nose based on a micromechanical cantilever array. Anal Chim Acta 393(1):59–65

21. Lang H, Ramseyer J, Grange W, Braun T, Schmid D, Hunziker P, Jung C, Hegner M, Gerber C (2007) An artificial nose based on microcantilever array sensors. J Phys: Conf Ser :663 (IOP Publishing)
22. Persaud K, Pelosi P (1985) An approach to an artificial nose. ASAIO J 31(1):297–300
23. White J, Dickinson TA, Walt DR, Kauer JS (1998) An olfactory neuronal network for vapor recognition in an artificial nose. Biol Cybern 78(4):245–251
24. Fernández DG, Blanco A, Durán A, Jiménez-Jorquera C, Arias-de Fuentes O (2013) Portable measurement system for FET type microsensors based on PSoC microcontroller. J Phys: Conf Series :012015 (IOP Publishing)
25. Li L, Gao P, Baumgarten M, Müllen K, Lu N, Fuchs H, Chi L (2013) High performance field-effect ammonia sensors based on a structured ultrathin organic semiconductor film. Adv Mater 25(25):3419–3425
26. Chang C-T, Huang C-Y, Li Y-R, Cheng H-C (2013) Effect of arrangement of carbon nanotube pillars on its gas ionization characteristics. Sens Actuators A: Phys 195(1):60–63
27. Koleini M, Ciacchi LC (2013) Label-free molecular detection with capped carbon nanotubes. Appl Phys Lett 102:083103
28. Huang Y, Shi M, Hu K, Zhao S, Lu X, Chen Z-F, Chen J, Liang H (2013) Carbon nanotube-based multicolor fluorescent peptide probes for highly sensitive multiplex detection of cancer-related proteases. J Mater Chem B 1:3470–3476
29. Wang K, Qian X, Zhang L, Li Y, Liu H (2013) Inorganic-organic pn heterojunction nanotree arrays for high sensitive diode humidity sensor. ACS Appl Mater Interfaces 5(12):5825–5831
30. Yang L, Wang S, Zeng Q, Zhang Z, Peng LM (2013) Carbon nanotube photoelectronic and photovoltaic devices and their applications in infrared detection. Small 9(8):1225–1236
31. Kwon OS, Park SJ, Lee JS, Park E, Kim T, Park H-W, You SA, Yoon H, Jang J (2012) Multidimensional conducting polymer nanotubes for ultrasensitive chemical nerve agent sensing. Nano Lett 12(6):2797–2802
32. Lee SH, Kwon OS, Song HS, Park SJ, Sung JH, Jang J, Park TH (2012) Mimicking the human smell sensing mechanism with an artificial nose platform. Biomaterials 33(6):1722–1729
33. Song HS, Kwon OS, Lee SH, Park SJ, Kim U-K, Jang J, Park TH (2012) Human taste receptor-functionalized field effect transistor as a human-like nanobioelectronic tongue. Nano Lett 13(1):172–178
34. Yoon H, Lee SH, Kwon OS, Song HS, Oh EH, Park TH, Jang J (2009) Polypyrrole nanotubes conjugated with human olfactory receptors: high-performance transducers for FET-type bioelectronic noses. Angew Chem Int Ed Engl 48(15):2755–2758
35. Kim TH, Lee SH, Lee J, Song HS, Oh EH, Park TH, Hong S (2009) Single-carbon-atomic-resolution detection of odorant molecules using a human olfactory receptor-based bioelectronic nose. Adv Mater 21(1):91–94
36. Huang J, Virji S, Weiller BH, Kaner RB (2003) Polyaniline nanofibers: facile synthesis and chemical sensors. J Am Chem Soc 125(2):314–315
37. Wan M (2008) A template-free method towards conducting polymer nanostructures. Adv Mater 20(15):2926–2932
38. Jang J, Oh JH, Stucky GD (2002) Fabrication of ultrafine conducting polymer and graphite nanoparticles. Angew Chem Int Ed Engl 41(21):4016–4019
39. Kwon OS, Park E, Kweon OY, Park SJ, Jang J (2010) Novel flexible chemical gas sensor based on poly (3, 4-ethylenedioxythiophene) nanotube membrane. Talanta 82(4):1338–1343
40. Jang J (2006) Conducting polymer nanomaterials and their applications. In: Emissive Materials Nanomaterials. ED. Kwang-Sup Lee, Springer, pp 189–260
41. Kwon OS, Ahn SR, Park SJ, Song HS, Lee SH, Lee JS, Hong J-Y, Lee JS, You SA, Yoon H (2012) Ultrasensitive and selective recognition of peptide hormone using close-packed arrays of hPTHR-conjugated polymer nanoparticles. ACS Nano 6(6):5549–5558
42. Leite E, Weber I, Longo E, Varela J (2000) A new method to control particle size and particle size distribution of SnO2 nanoparticles for gas sensor applications. Adv Mater 12(13):965–968

43. Shipway AN, Katz E, Willner I (2000) Nanoparticle arrays on surfaces for electronic, optical, and sensor applications. ChemPhysChem 1(1):18–52
44. Horrillo M, Getino J, Ares L, Robia J, Sayago I, Gutierrez F (1998) Measurements of VOCs with a semiconductor electronic nose. J Electrochem Soc 145(7):2486–2489
45. Vazquez M, Hernando A (1996) A soft magnetic wire for sensor applications. J Phys D: Appl Phys 29(4):939–949
46. Adhikari B, Majumdar S (2004) Polymers in sensor applications. Prog Polym Sci 29(7):699–766
47. Dong Q, Du L, Zhuang L, Li R, Liu Q, Wang P (2013) A novel bioelectronic nose based on brain-machine interface using implanted electrode recording in vivo in olfactory bulb. Biosens Bioelectron 49(15):263–269
48. Kim D, Jin HJ, Lee SH, Kim TH, Park J, Song HS, Park TH, Hong S (2013) Bioelectronic device mimicking human sensory system based on nanovesicle-carbon nanotube hybrid structure. Bull Am Phys Soc, Baltimore, MD, USA,58
49. Liu H, Kameoka J, Czaplewski DA, Craighead H (2004) Polymeric nanowire chemical sensor. Nano Lett 4(4):671–675
50. Dickinson C, Davies R, Davis R (2003) Towards a free-free template for CMB foregrounds. Mon Not Roy Astron Soc 341(2):369–384
51. Kwon OS, Park SJ, Park H-W, Kim T, Kang M, Jang J, Yoon H (2012) Kinetically controlled formation of multidimensional poly (3, 4-ethylenedioxythiophene) nanostructures in vapor-deposition polymerization. Chem Mater 24(21):4088–4092
52. Lu X, Zhang W, Wang C, Wen T-C, Wei Y (2011) One-dimensional conducting polymer nanocomposites: Synthesis, properties and applications. Prog Polym Sci 36(5):671–712
53. Hurst SJ, Payne EK, Qin L, Mirkin CA (2006) Multisegmented one-dimensional nanorods prepared by hard-template synthetic methods. Angew Chem Int Ed Engl 45(17):2672–2692
54. Rossinyol E, Arbiol J, Peiró F, Cornet A, Morante J, Tian B, Bo T, Zhao D (2005) Nanostructured metal oxides synthesized by hard template method for gas sensing applications. Sens Actuators B: Chem 109(1):57–63
55. Zhang X, Zhang J, Song W, Liu Z (2006) Controllable synthesis of conducting polypyrrole nanostructures. J Phys Chem B 110(3):1158–1165
56. Zhang Z, Zuo F, Feng P (2010) Hard template synthesis of crystalline mesoporous anatase TiO2 for photocatalytic hydrogen evolution. J Mater Chem 20(11):2206–2212
57. Park E, seok Kwon O, joo Park S, seop Lee J, You S, Jang J (2012) One-pot synthesis of silver nanoparticles decorated poly (3, 4-ethylenedioxythiophene) nanotubes for chemical sensor application. J Mater Chem 22(4):1521–1526
58. Song Y, Garcia RM, Dorin RM, Wang H, Qiu Y, Coker EN, Steen WA, Miller JE, Shelnutt JA (2007) Synthesis of platinum nanowire networks using a soft template. Nano Lett 7(12):3650–3655
59. Wang C, Chen M, Zhu G, Lin Z (2001) A novel soft-template technique to synthesize metal Ag nanowire. J Colloid Interface Sci 243(2):362–364
60. Wu XJ, Xu D (2010) Soft template synthesis of yolk/silica shell particles. Adv Mater 22(13):1516–1520
61. Yamauchi Y, Kuroda K (2008) Rational design of mesoporous metals and related nanomaterials by a soft-template approach. Chem Asian J 3(4):664–676
62. Kwon OS, Hong T-J, Kim SK, Jeong J-H, Hahn J-S, Jang J (2010) Hsp90-functionalized polypyrrole nanotube FET sensor for anti-cancer agent detection. Biosens Bioelectron 25(6):1307–1312
63. Jang J, Yoon H (2003) Facile fabrication of polypyrrole nanotubes using reverse microcmulsion polymerization. Chem Commun (Camb) 6:720–721
64. Pan H, Feng YP, Lin J, Liu CJ, Wee TS (2007) Catalyst-free template-synthesis of ZnO nanopetals at 60 °C. J Nanosci Nanotechnol 7(2):696–699
65. Wang JC, Sawadogo M, Van Dyke MW (1998) Plasmids for the in vitro analysis of RNA polymerase II-dependent transcription based on a G-free template. Biochim Biophys Acta 1397(2):141–145

66. Zhu C, Chen C, Hao L, Hu Y, Chen Z (2004) Template-free synthesis of $Cu_2Cl(OH)_3$ nanoribbons and use as sacrificial template for CuO nanoribbon. J Crystal Growth 263(1):473–479
67. Jang J, Yoon H (2005) Formation mechanism of conducting polypyrrole nanotubes in reverse micells systems. Langmuir 21(24):11484–11489
68. Park SJ, Kwon OS, Lee SH, Song HS, Park TH, Jang J (2012) Ultrasensitive flexible graphene based field-effect transistor (FET)-type bioelectronic nose. Nano Lett 12(10):5082–5090
69. Yoon H, Jang J (2009) Conducting-polymer nanomaterials for high-performance sensor applications: issues and challenges. Adv Funct Mater 19(10):1567–1576
70. Chen H, He J (2008) Fine control over the morphology and structure of mesoporous silica nanomaterials by a dual-templating approach. Chem Commun (Camb) (37):4422–4424
71. Holmberg K (2004) Surfactant-templated nanomaterials synthesis. J Colloid Interface Sci 274(2):355–364
72. Kumar S, Nann T (2006) Shape control of II-VI semiconductor nanomaterials. Small 2(3):316–329
73. Lopez-Quintela MA (2003) Synthesis of nanomaterials in microemulsions: formation mechanisms and growth control. Curr Opin Colloid Interface Sci 8(2):137–144
74. Bruins M, Bos A, Petit P, Eadie K, Rog A, Bos R, van Ramshorst G, van Belkum A (2009) Device-independent, real-time identification of bacterial pathogens with a metal oxide-based olfactory sensor. Eur J Clin Microbiol Infect Dis 28(7):775–780
75. Lundström I, Erlandsson R, Frykman U, Hedborg E, Spetz A, Sundgren H, Welin S, Winquist F (1991) Artificial 'olfactory' images from a chemical sensor using a light-pulse technique. Nature 352:47–50
76. Miwa H, Umetsu T, Takanishi A, Takanohu H (2001) Human-like robot head that has olfactory sensation and facial color expression. In: Robotics and automation. Proceedings 2001 ICRA. IEEE International Conference on, 2001. IEEE, pp 459–464
77. Sankaran S, Panigrahi S, Mallik S (2011) Olfactory receptor based piezoelectric biosensors for detection of alcohols related to food safety applications. Sens Actuators B: Chem 155(1):8–18
78. Vodyanoy V (1988) Olfactory sensor. In: Engineering in medicine and biology society. Proceedings of the Annual International Conference of the IEEE, pp 997–998
79. Wang P, Liu Q, Xu Y, Cai H, Li Y (2007) Olfactory and taste cell sensor and its applications in biomedicine. Sens Actuators A: Phys 139(1):131–138

Chapter 14
Applications and Perspectives of Bioelectronic Nose

Hwi Jin Ko, Jong Hyun Lim, Eun Hae Oh and Tai Hyun Park

Abstract Detection and discrimination of odorants has great potential for applications in various fields, such as the food industry, fragrance and flavor industry, environmental monitoring, and biomedical diagnosis. For several decades, many efforts have been made to control the process of food production and fragrance and flavor of brands, and to monitor environmental pollutions through the use of comparable technology. There have been several classical methods for these purposes. Conventional methods, such as GC/MS or human sensory panels (olfactometry), have been conventionally used, but they are expensive, labor-intensive, time-consuming and affected by large variations according to the conditions of analysis. These drawbacks increased the requirement for new technique, substituting classical methods, and the electronic nose has been developed over the past couple of decades. However, the electronic nose has also many limitations to be overcome. Recently, the bioelectronic nose, using biological components, has been developed. The bioelectronic nose has a bright prospect as a powerful and effective biosensing system, capable of detecting and discriminating a huge variety of odorant molecules. The most meaningful characteristics of the bioelectronic nose are that it mimics the human olfactory system. The bioelectronic nose is expected to replace the sensory evaluation method. It can be used for standardization of smell, development of code for each smell, and visualization of smell. Consequently, the development of the

T. H. Park (✉) · J. H. Lim
School of Chemical and Biological Engineering, Seoul National University, Seoul, Republic of Korea
e-mail: thpark@snu.ac.kr

E. H. Oh · T. H. Park
Interdisciplinary Program for Bioengineering, Seoul National University, Seoul, Republic of Korea

H. J. Ko · T. H. Park
Bio-MAX Institute, Seoul National University, Seoul, Republic of Korea

T. H. Park (ed.), *Bioelectronic Nose,* DOI 10.1007/978-94-017-8613-3_14,

Table 14.1 Examples of applications of bioelectronic noses

Industry	Application fields	Specific use types
Biomedicine	Pathogen or disease detection	Early diagnosis of sever diseases, patient condition care, metabolic disorders
Food and beverage	Quality control, fermentation process, bacterial contamination	Ingredient confirmation, off-flavor, spoilage, fermentation control
Fragrance and flavor	Consumer's expectation, ripeness, freshness	Cosmetics, perfumes, brand recognition (ex, coffee product)
Environmental monitoring	Air and water pollution monitoring, indoor air monitoring	Fugitive emission, malodor, greenhouse gas emission, toxic gas and spills

bioelectronic nose is expected to open up many new possibilities to improve the quality of our life.

14.1 Applications

The human nose can discriminate among hundreds of thousands of odorant molecules [1, 2]. The olfactory sense in all animals, including human, is used to evaluate food, drink and environmental toxic materials. Recently, many studies on sensing devices mimicking the human olfactory system have been reported, and the possibility for numerous applications has been suggested [3–6]. The bioelectronic nose, described in this book, has a similar function to human olfaction, and a huge variety of possible applications (Table 14.1)

14.1.1 Diagnosis of Disease

Generally, numerous volatile and non-volatile organic compounds, including odorous compounds, are emitted from various parts of human body, such as scalp, feet, oral cavity, axillae, genital, and skin [7]. The emission of volatile compounds is influenced by diet, stress, metabolic diseases, and immune status of the individual. Thus, the change of body odor potentially represents various diseases and even mental health (Table 14.2).

Ancient physicians considered that exhaled breath from human was associated with a certain disease, and might reflect the disorder in physiological and pathophysiological processes [36]. For example, diabetes gives a fruit-like smell of acetone in a patient's breath [16]. Diabetic patients cannot metabolize carbohydrates, including glucose, but catabolize fats into ketone bodies, such as acetone. Urine, sweat, and skin, as well as the exhaled breath are the major paths to emit odorous compounds, and they provide a lot of information about the condition of the human body. Many current researches focus on the analysis of the breath or urine odor to achieve a non-invasive and easy diagnosis.

Table 14.2 Key volatile compounds from patients' breath with diseases

Diseases	Body	Aromatic and volatile compounds	References
Alcohol-induced hepatic injury	Breath	Ethane, pentane (volatile alkanes)	[8]
Asthma	Breath	Hydrogen peroxide, nitrotyrosine, nitric oxide, leukotrienes	[9–11]
Breast cancer	Breath	2-Propanol, heptanal, 2,3-dihydro-1-phenyl-4, 1-phenyl-ethanone	[12]
Cystic fibrosis	Breath	Nitric oxide, leukotriene B(4), 8-isoprostane, interleukin-8	[13–15]
Diabetes mellitus	Breath	Acetone, other ketones	[16]
Liver cancer	Blood	Hexanal, 1-octen-3-ol, octane	[17]
Lung cancer	Breath	Heptanal, nitric oxide	[18, 19]
Pneumonia	Breath	Putrid	[20]
Sickle cell disease	Breath	Carbon monoxide	[21]
Sleep apnea	Breath	8-isoprostane	[22]
Trench mouth	Breath	Halitosis	[23]
Trimethylaminuria	Breath	Trimethylamine	[20]
Uremia and kidney failure	Breath	Dimethylamine, trimethylamine	[24]
Schizophrenia	Alveolar, sweat	Pentane, carbon disulfide, mildy acetic	[25–27]
Rheumatoid arthritis	Alveolar	Pentane	[28]
Hepatic encephalopathy	Blood	3-methylbuthanol	[29]
Congestive heart failure	Heart	Dimethyl sulfide	[30]
Yellow fever	Skin	Butcher's shop	[23, 31]
Tuberculosis lymphadenitis	Skin	Stale beer	[20]
Pseudomonas infection	Skin, sweat	Grape	[20]
Isovaleric acidemia	Skin, sweat	Sweaty feet, cheesy	[20, 23, 32]
Diphtheria	Sweat	Sweet	[20, 23, 31]
Maple syrup urine disease	Sweat	Maple syrup, burnt sugar	[20, 31]
Rubella	Sweat	Freshly plucked feathers	[20]
Hyperhydrosis	Whole body	Unpleasant body odor	[31]
Urinary tract infection	Urine	Isovaleric acid, alkanes	[33]
Metabolic disorders	Urine	Isovaleric acid	[34]
Bladder Infection	Urine	Ammonia	[20]
Tubular necrosis (acute)	Urine	Stale water	[35]

Many studies using conventional sensing techniques have tried to analyze the breath in order to diagnose various diseases, such as a cancer, diabetes, liver failure, bacterial infection, etc. The correlation between the exhaled breath and diseases has been continuously suggested, since the first breath test as a medical assessment was tried in the eighteenth century [37]. Gas chromatography-mass spectroscopy (GC-MS) was developed for the separation and identification of volatile odor compounds in the 1960s, and breath test detecting volatile organic compounds (VOCs) from exhaled breath was used in the 1970s [38]. From the exhaled breath, many

compounds have been identified, from small inorganic molecules, such as nitric oxide and carbon monoxide, to organic compounds, such as acetone, methanol and isoprene [39–42]. However, GC-MS is a labor-intensive and time-consuming technique. In addition, the collection and pre-treatment processes of the breath sample is difficult. Thus, the extensive applications of conventional methods to the disease diagnosis are not practically possible.

Electronic noses for diseases diagnosis were developed to overcome the limitation of GC-MS. The electronic nose consists of several sensor arrays and recognizes specific odors through analyzing the response patterns generated by odor stimulation [43]. Many researches demonstrating the capability of the electronic nose on medical applications have been presented [44]. Electronic noses usually target odors from human exhaled breath or urine, and can be used for the diagnosis of a wide range of diseases, such as lung cancer [45–48], chronic obstructive pulmonary disease [47, 49], and asthma [49, 50]. Recently, a gold nanoparticle-based electronic nose, which can diagnose lung cancer using exhaled breath, has been reported [51]. Peng et al. demonstrated that the sensor can discriminate patients' breath with high accuracy. However, the electronic nose still has limitations in terms of selectivity and sensitivity. Most patients do not have a single disease. For instance, a person who has high blood pressure is also likely to have diabetes or lung cancer. In other words, the combinations of patients' diseases are countless, and the resultant chemical/odor changes are necessarily complex. Thus, high selectivity capable of discriminating specific diseases is required for precise diagnosis. Moreover, the most important point on medical applications is an early diagnosis. Therefore, sufficient sensitivity has to be guaranteed for practical diagnosis.

Bioelectronic noses mimicking human olfaction can achieve an extremely high sensitivity and selectivity. Various biological components, such as living cells, proteins, and even peptides, can be used for the development of bioelectronic noses. Lin et al. constructed a quartz crystal coated with a synthesized peptide which is derived from an olfactory receptor [52]. The peptide-based sensor was able to selectively detect trimethylamine, a biomarker of uremia. This study first showed that the bioelectronic nose was able to be used for the detection of the odorous biomarker.

Recently, Lim et al. developed the bioelectronic nose for the diagnosis of lung cancer [53]. The specific olfactory receptor that binds to heptanal was selected. In the blood from lung cancer patients, the concentration of heptanal is significantly higher than that in the blood from non-patients [54]. By functionalizing the single-walled carbon nanotube field-effect transistors (SWNT-FETs) with nanovesicles containing the selected olfactory receptors, a highly sensitive and selective bioelectronic nose was fabricated. The sensor can detect 100 fM of hetpanal from human blood plasma, even though the plasma sample was not pre-treated (Fig. 14.1).

Most hormone receptors as well as olfactory receptors belong to a GPCR. Therefore, other types of GPCR-based biosensors for the diagnosis of diseases can be developed through a similar fabrication process to that of an OR-based bioelectronic nose. A biosensor which sensitively and selectively detects a human parathyroid hormone (hPTH) has been reported [55]. The sensor was fabricated with human parathyroid hormone receptors (hPTHRs) over-expressed in *E. coli* and conducting

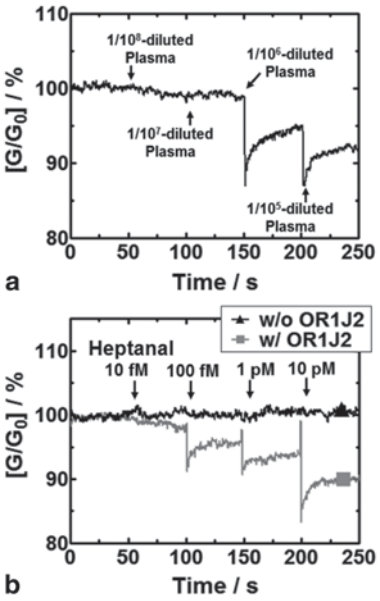

Fig. 14.1 Detection of heptanal from human blood plasma using a nanovesicle-based bioelectronic nose. **a** A real-time measurement for the influence of plasma on the conductance change in the bioelectronics nose. The bioelectronics nose was fabricated using nanovesicles with olfactory receptor, $G\alpha_{olf}$, and receptor-transporting protein 1S (RTP1S). Human blood plasma samples were diluted to different ratios. The $1/10^{-7}$-diluted plasma did not show any effect on the conductance, which means that no pretreatment process is required when $1/10^{-7}$-diluted plasma is used in the experiment. **b** The real-time detection of heptanal from $1/10^{-7}$-diluted plasma using a bioelectronic nose. A bioelectronic nose based on nanovesicles with olfactory receptor (OR), $G\alpha_{olf}$, and RTP1S was able to detect 1×10^{-13} M heptanal (*square*), whereas a bioelectronic nose without ORs was not (*triangle*). (Reprinted from Ref. [53] with permission from John Wiley & Sons Inc.)

polymer nanoparticles. The hPTHRs and conducting polymer nanoparticles play roles in the selective discrimination of hPTHs and in the conversion of bio-signals into the sensitive electrical signals, respectively. The hPTHR-based sensor was able to detect hPTHs from real serum samples with a high sensitivity and selectivity. Human acetylcholine receptor was also used for the development of diagnostic devices [56]. The receptor was over-expressed in *E. coli* and immobilized on the SWNT-FETs. The sensor was able to easily and rapidly detect acetylcholine with high sensitivity and selectivity. These techniques, when applied to the development of biosensors, are expected to offer numerous applications in biomedical fields.

14.1.2 Assessment of Food Quality

Quality and spoilage control of foods are very important to many industries and consumers because a good quality is directly connected to a consumption of products,

consumers' choice of brands and even consumers' health. A consumers' repeat purchase behavior depends on whether the product can consistently satisfy the consumers' expectation of quality. With growing consumer expectation of quality and safety for foods, interest in the effective sensing system for measuring the quality of foods has increased. Various devices have been developed during a couple of decades to satisfy this interest. However, most methods require the destruction of samples and random sampling processes. Therefore, a novel concept of device to assess the quality of foods based on the sense of smell has been suggested.

Off-odor from foods is generated by the oxidation of foods or the contamination by bacteria or fungi [57–59]. Intake of spoiled or contaminated foods can cause severe health problems to human. Thus, it is important to determine the quality of foods before consumption. This is possible by detecting odorous compounds emitted from low-quality foods. In this respect, effective methods to analyze odor from foods have been intensively developed long ago.

In order to detect VOCs generated from foods, GC-MS has been commonly utilized. Especially, through a complementing solid-phase microextraction (SPME) technique, the sensitivity of GC-MS has been remarkably improved [60]. SPME and GC-MS techniques are still used to analyze VOCs from various spoiled or contaminated foods [61–63]. High-performance liquid chromatography (HPLC) and ion-exchange chromatography are also suitable for this purpose, and have been broadly used [64–66]. These techniques can precisely analyze all VOCs generated from foods; however, all kinds of standard molecules have to be procured. In the case of real foods, numerous chemical substrates are decomposed by many factors, such as oxidation, bacterial growth, and thermal degradation. Thus, it is impossible to analyze all VOCs generated in an actual condition rather than a controlled condition. Moreover, large-sized instruments and complicated pretreatment processes make the on-site and real-time analysis difficult.

Many electronic noses that measure the quality of foods have been developed [67–70]. The electronic noses classify food odors through recognizing the response patterns generated from a sensor array. Such devices have many advantages as practical sensors. First of all, their operation can be quite simple. The electronic nose recognizes the odor from foods in a similar manner to the human nose, and subsequent processes can be automated. In addition, the devices can be miniaturized; hence, several portable types of electronic nose have already been commercialized. However, the electronic nose still has limitations. In most cases, various kinds of foods are mixed and even cooked. The quality and combination of ingredients differ at all times. This means that the database of incalculable odor patterns has to be built so as to determine the quality of foods in actual conditions. The electronic nose can differentiate between spoiled and non-spoiled foods in ideal conditions, but cannot selectively recognize the odor from certain spoiled foods when various foods are mixed. Therefore, more advanced concepts of artificial smelling devices are required.

The bioelectronic nose is expected to play this role. Bioelectronic noses have excellent selectivity due to their primary sensing elements, an olfactory receptor [4]. They can recognize only their counterpart ligands, irrespective of mixed degrees or

physical conditions of foods. This is a very important characteristic of the sensing device when the sensor is applied within the food industry. It has been reported that the amount of linear aldehydes, especially hexanal, increases by the oxidation of unsaturated fatty acids [71]. Thus, hexanal is generally considered as an indicator of the degree of decomposition of foods which contain fatty acids. Park et al. developed a bioelectronic nose that can sensitively and selectively detect hexanal [72]. One of the canine olfactory receptors was utilized as a primary sensing element in the form of a nanovesicle. The nanovesicle containing the canine olfactory receptor on its membrane was combined with SWNT-FETs. This bioelectronic nose was able to detect hexanal at a concentration as low as 1 fM with excellent selectivity. Its sensitivity and selectivity facilitated the detection of hexanal from spoiled milk without any pretreatment processes. These results showed that the bioelectronic nose will be an excellent sensing device for the assessment of foods quality.

The remarkable selectivity and sensitivity of the bioelectronic nose resulted in another interesting application. Although many foods are mixed, the degree of decomposition of specific foods can be easily measured. Recently, Lim et al. developed a peptide receptor-based bioelectronics nose (PRBN) by using single walled-carbon nanotube field-effect transistors (SWNT-FETs) functionalized with olfactory receptor-derived peptides (ORPs) [73]. The peptide, which is derived from one of the canine olfactory receptors, specifically binds to trimethylamine, an indicator of seafood decomposition. Even though a small peptide rather than a whole protein was utilized, the selectivity of the olfactory receptor still remained. Thus, the sensor was able to detect trimethylamine from spoiled seafood samples without any pretreatment processes (Fig. 14.2a), and determine the degree of spoilage (Fig. 14.2b, c). Moreover, spoiled seafood was specifically discriminated among other kinds of spoiled foods (milk, tomato, broccoli, and beef) and fresh seafood (Fig. 14.2d). By virtue of its excellent sensitivity and selectivity of the bioelectronic nose, no pretreatment processes of food samples were required. In the near future, the freshness of each food ingredient in a household refrigerator may be automatically measured by the bioelectronic nose.

14.1.3 Determination of Fragrance and Flavor

The sense of smell in human is not considered to be a crucial function for survival, although odor perception plays an important role in the survival of all animals. Nevertheless, the olfactory sense in human is an important motivation factor inducing the development of a fragrance and flavor industry. Many industries are interested in scent, which attracts customers to their products. Depending on the product in question, a customers' propensity to consume products can easily rely on preference to a specific smell. Therefore, the importance of a good scent is emphasized in most products in our daily lives, such as wines, cuisine, cosmetics, perfume, and coffee. This indicates that the control of fragrance and flavor is very important to various industrial fields.

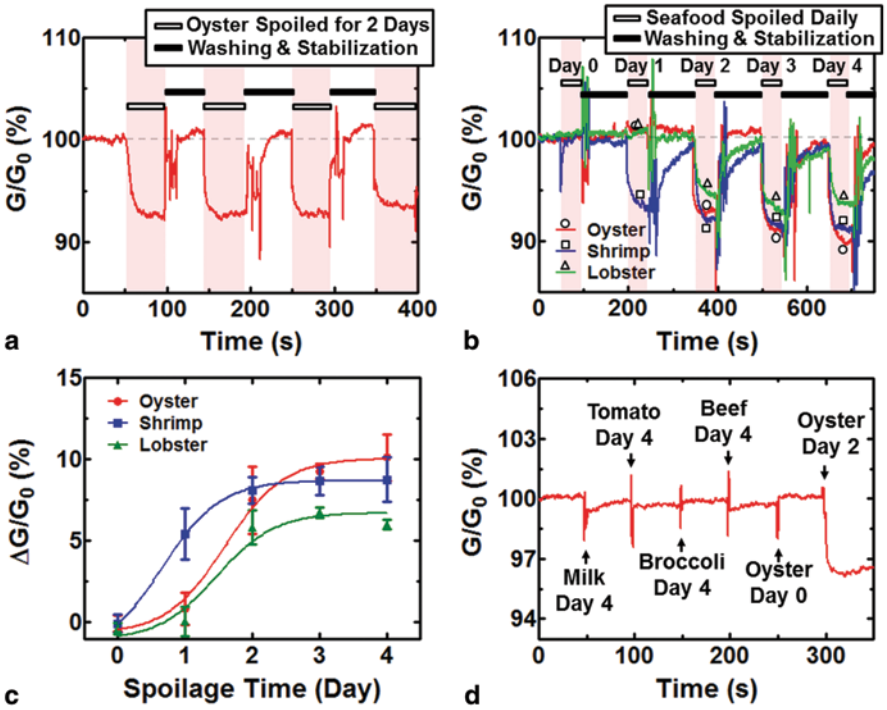

Fig. 14.2 Detection of trimethylamine (TMA) from spoiled seafood using peptide receptor-based bioelectronic noses. **a** A real-time measurement data exhibiting the conductance change generated by repeated treatments with a spoiled oyster sample, which was produced by storing the oyster sample at 25 °C for two days. Consistent and prompt responses were generated by the four treatments. The *gray dotted line* represents the initial base line. **b** Real-time measurements of conductance changes generated by treatments with oyster (*red line*), shrimp (*blue line*), and lobster (*green line*) samples spoiled for different periods of time. Significant decreases in the conductance were observed for the 2 day-spoiled oyster, 1 day-spoiled shrimp, and 2 day-spoiled lobster and the responses increased with an increase in the spoilage time. **c** Response patterns versus the degree of spoilage of the three spoiled seafood samples (oyster, shrimp, and lobster). The generated responses tended to increase with the degree of spoilage. **d** Real-time recognition and distinction of spoiled oyster from other types of spoiled foods (milk, tomato, broccoli, and beef) and fresh oyster. The sample solutions of milk, tomato, broccoli, and beef spoiled for four days and the fresh oyster had no significant effect on the conductance. However, the injection of the oyster sample that had been spoiled for two days caused a sharp decrease in conductance. For interpretation of the references to color in this figure legend, the reader is referred to the web version of this article. (Reprinted from Ref. [73] with permission from Elsevier)

The determination of a good smell largely depends on personal disposition and experience, and can be very subjective. Therefore, to objectively judge the fragrance and flavor, well-trained experts play a role in the development of many products. For instance, a sommelier is a wine connoisseur and a perfumer develops scents for perfumes and cosmetics. However, the method that a person directly smells has many limitations. Many parameters, such as health, fatigue and the specific

conditions of a person can affect the smelling ability; therefore, reproducibility and repeatability cannot be guaranteed through this method. In the case of the fragrance- and flavor-related industries, a vast number of odorous components are used. Also, the actual smell may be extremely changeable depending on the mixing ratio of the used odorants. Thus, it is impossible to determine scent through analytical techniques such as GC-MS. Such techniques can only identify components comprising the smell [74, 75]. This is the most serious drawback of conventional techniques on the applications for the fragrance and flavor industry.

Electronic noses can provide a more objective value of odor. Several groups have reported results showing the capability of electronic noses on applications for the measurement of scent [76, 77]. Electronic noses have successfully discriminated perfumery compounds through a pattern recognition process. However, the patterns generated by the odor stimulation cannot fundamentally represent the real odor that a person perceives, because electronic noses do not use human olfactory receptors. The electronic nose detects volatile compounds including odorants. Thus, various odorless compounds, such as CO_2, CO, and even water vapor, can induce significant responses in the electronic nose. Hence, in the fragrance and flavor industry where the human perception has to be objectively analyzed, the electronic nose has limitations.

Bioelectronic noses utilize olfactory receptors which originally act as a primary sensing element for the recognition of odors. The biological processes for odor perception can be reconstructed *in vitro* using bioelectronic noses. Olfactory receptors of the bioelectronic nose recognize odorants with excellent selectivity. This recognition is identical to that of the human nose [78]. If the sensor is functionalized with all kinds of human olfactory receptors, it can perfectly represent the same response patterns as those which the human nose produces for the perception of odors. In order to apply the sensor to the fragrance and flavor industry, the sensor should objectively analyze the type and intensity of the smell based on the human olfactory sense. This is only possible when human olfactory receptors are incorporated to the sensor system. Eventually, the bioelectronic nose will provide a simple, fast and reliable analysis method to measure scent without the help of the human nose.

14.1.4 Monitoring of Environmental Pollutants

Recently, there has been a growing need to more consistently and specifically monitor environmental pollutants. In a narrow sense, environmental pollution means the emission of greenhouse gases or toxic compounds generated from industrial processes into the atmosphere, soil, or water. This is strictly regulated by law, because pollutants can be seriously harmful to human health. In the broader sense, there are a lot of pollutions that are not officially regulated, but can give rise to unpleasant feelings by malodor. For instance, garbage thrown in the street, spoiled fish in the wastebasket, or smoking in the public area can cause malodor. Thus, it is also a kind

of environmental pollutions although such odor is not restricted. All environmental pollutants, regardless of their regulation, need to be monitored to improve quality of life. For this purpose, the development of further effective methods to monitor various pollutants is required.

GC-MS has been generally used for the detection of environmental pollutants in the atmosphere [79–81]. HPLC is suitable to analyze the composition of water [82–84]. Such techniques can precisely quantify the amount of chemical compounds. Thus, they are effective to monitor restricted pollutants. However, they have disadvantages in terms of portability and immediacy. Because of the large-sized instrument, an on-site measurement is difficult, and sampling processes should be conducted. In addition, real-time measurements are difficult due to the complexity of analysis processes. Furthermore, equipment such as GC and HPLC is too expensive to be used for the broad and continuous detection of less severe pollutants, such as the odor from rotten foods or smoking.

Electronic noses can be effectively and extensively applied to the monitoring of such environmental pollutants. Many electronic noses have been developed for various purposes, such as the monitoring of urban pollution, water pollution, and the quality of indoor air [85–89]. Severe environmental pollutants are mainly toxic gases which are major targets of the electronic noses; thus, electronic noses are appropriate for the monitoring of pollutants. In addition, the sensing processes can be simplified. This is very important to detect hazardous chemicals such as CO, HF, and NO_2. However, the sensitivity of electronic noses is insufficient. The sensor should detect toxic gases before the amount of toxins reaches a dangerous level, and can also selectively recognize the existence of pollutants under any circumstances. However, electronic noses are easily affected by a variety of factors, such as humidity, electromagnetic fields, and temperature.

Bioelectronic noses are being regarded as a better sensor system to monitor a number of environmental pollutants in terms of high sensitivity and selectivity. There is, however, a potential complication as to whether a given biological element is active under dry conditions, because the sensors should be able to detect gas compounds. Wu and Lo addressed this problem by using a synthetic peptide which mimics the binding site of olfactory receptors [90, 91]. The sensor functionalized with peptide receptors was able to selectively detect trimethylamine and ammonia, which are well known as air pollutants due to their pungent odor. Lee et al. demonstrated that whole olfactory receptor proteins were active in the dry condition [78]. They functionalized a conducting polymer nanotube-based sensor with a human olfactory receptor which had been expressed in *E. coli*. This sensor not only detected specific odorants with high sensitivity and selectivity, but also showed human nose-like behaviors such as antagonism. In order to make a better tertiary structure of olfactory receptors, the whole proteins were trapped in a ‘nanodisc’, a self-assembling nano-scale membrane assembly [6]. The nanodiscs containing olfactory receptors were utilized for the functionalization of carbon nanotubes, and the sensor successfully detected gaseous odorants. All things taken together, the bioelectronic nose can fully supplement the weakness of the electronic nose, and will be widely used for the monitoring of a range of environmental pollutants.

14.1.5 Other Applications

There are various other fields where bioelectronic noses can be effectively utilized besides the examples that have been previously discussed. First of all, the bioelectronic nose can be a perfect alternative to direct smelling. To this day, trained dogs play major roles in the detection of narcotics and explosives, such as their use in customs and airports, as well as military institutions. Although dogs have an excellent smelling ability, they have critical limitations such as high costs for training and maintenance. Also, the natural olfactory system is easily and rapidly adapted to the repetitive exposure to odors; thus, the dogs cannot continuously search drugs and explosives [92]. Hence, bioelectronic noses may replace the role of dogs within such industries.

Bioelectronic noses can be utilized for the process monitoring using their excellent sensitivity and selectivity. For instance, they can selectively detect impurities that are contained in food and beverage products during mass production processes. Thus, the quality control of products can be improved. Also, a sensor which detects the smell generated from coffee roasting can accurately determine the degree of roasting. The volatile metabolites generated from bacterial fermentation processes can also be analyzed. Consequently, the progress of such processes can be easily monitored in real-time using the bioelectronic noses. Bioelectronic noses can be effectively applied to not only the examples described above, but also any cases where the process has a resultant smell or chemical release.

14.2 Perspectives

14.2.1 Standardization of Smell

In contrast to the senses of vision and hearing, the sense of smell does not have a method to precisely express the information of smell or flavors, even though it plays an important role in our daily life. It is very difficult to create a database and to standardize the information obtained from the olfactory sense, because it usually responds to complex components consisting of a vast variety of chemical elements. The classification and description of smell depends on quite subjective and abstractive expressions and smell cannot be precisely described or quantified using these kinds of expressions.

In the early classification of smells, they were grouped based on the expertise of scholars, such as a chemist and botanist, and the classification of smells through experiments was begun in the 1900s [93]. The odor prism was proposed by Henning (1916) suggesting verbal odor descriptions using six odor qualities, which are spice, fragrant, resinous, ethereal, foul, and burnt [94]. From the middle of the 1930s, there have been many trials to classify odor quality by connecting the odor perception to its chemical structure [95–99], but it is still not possible to explain odor sensation

and perception. Prior to finding the number of human olfactory receptors, several scientists tried to quantify and classify odors based on the function and type of olfactory receptors [100–103], but this approach has been largely suspended, as it has been identified that the number of human olfactory receptors are at least 320 [104].

Standardization and classification of smell is important not only for the general odor, but also for the malodor. Since standardization of method for measuring malodor was begun by many countries in the 1970s, studies for standardization of malodor have mainly depended on a sensory test using human olfaction. Up to now, malodor is recognized by several detection methods like scentometer and olfactometer, which have been widely used, but these methods do not provide the exact information together with lots of variables, mainly due to dependence on human olfaction. The human-like smell sensing system is useful for these reasons.

Various studies are being currently carried out also for the display of olfaction, for example, the development of a device exuding flavor through the internet, and the development of a method and device for smell transmission. However, these kinds of trials have a limitation, in that the device does not deliver the exact information of a smell because there is no criterion for a variety of smells. Standardization of smell will be an important criterion for digitalization of emotional expression of smell, as well as for various applications of smell and flavor, and therefore, needs to be achieved by mimicking human olfaction as closely as possible.

The bioelectronic nose may be the best device mimicking the human olfactory system, because it utilizes the human olfactory receptors as a sensing element and employs the olfactory signaling processes. It is expected that a method for the standardization of smell can be developed through the qualitative and quantitative measurement by bioelectronic nose, and eventually, that a relationship between data from bioelectronics nose and sensory evaluation data from human olfaction would be established. The established standard of smell can be widely utilized in various industries such as food, beverage, agriculture, flavor and perfume, as well as biomedicine and environmental monitoring.

14.2.2 Multi-channel Bioelectronic Nose

The human olfactory system has an array type recognition system, which consists of about 390 different olfactory neuron cells. Each type of olfactory neuron cell has one kind of its own olfactory receptor on the cell surface. The olfactory system efficiently recognizes even a wide range of odor mixtures, as well as single kind of odor molecule, by employing the array type recognition system. This suggests that multiple odor compounds can be precisely identified using array type sensing system, as in the case of the human olfactory system.

Therefore it is necessary to make an array type of sensor for identifying the profile of a mixture, as well as for enhancing the discriminative ability of the bioelectronic nose. The array type sensor is integrated with several different types of sensors, the number of which depends on the type of samples to be analyzed. The

Fig. 14.3 Multi-channel platform of bioelectronic nose. In each channel, each type of olfactory receptor is combined with a carbon nanotube FET sensor. Signals are generated from the interaction of various olfactory receptors with odor molecules

greater the number of sensor integrated in one platform, the better sensor system is able to identify analytes. In contrast to the conventional electronic nose, using limited number of chemical sensor array, bioelectronic noses, especially those using olfactory receptors as a sensing material, are the best example for developing a multiplexed sensing platform. The bioelectronic nose can utilize lots of biomaterials as a sensing material, for example, 390 different types of human olfactory receptors, which are about 40 % out of approximately 1,000 olfactory receptor genes, are functional, and can be used as sensing materials.

Recently, researchers have tried to integrate a large number of olfactory receptors on a single platform to detect a variety of odor molecules simultaneously, and are developing data processing techniques for the analysis of electrical information produced from a bioelectronic nose consisting of multi-channel sensors (Fig. 14.3). This kind of multi-channel bioelectronic nose can be usefully applied to the analysis of a whole profile of an odorant mixture. For example, various severe diseases, including cancer and diabetes, which produce specific odor molecules as a biomarker, emit not one specific biomarker but many disease-specific biomarkers through the exhaled breath. It is very important to identify multiple biomarkers for the exact diagnosis of these complex diseases. Thus, most target samples to be identified are complex mixtures containing a variety of different odor components. So, many analytical methods have been used to recognize patterns of specific signals obtained from the response of electronic noses to complex mixtures, as well as in order to detect a specific biomarker. Nevertheless, there is a limit to the number of sensor elements which can be integrated in a single platform, and a vast array of potential data to be analyzed. A multi-channel bioelectronic nose would provide a powerful tool for a great advance in various fields of application of these analytical methods.

14.2.3 Visualization of Smell

In order to discriminate among thousands of odors, we do not have any reliable artificial sensing device, but still depend on our human sensory system. However, the information obtained through our natural sensory system does not provide us with the objective information about the odors. Up to now, complex experimental steps, large-scale equipment, well-trained experts, or electronic noses have partially fulfilled the need for the detection or analysis of odors. In addition, it is difficult to collect the data on the odorant response pattern to be used as an objective index. However, if the odor is visualized, the visualized pattern can be used as a code for the odor like a QR code.

Several approaches have been taken to visualize the olfactory signal transduction in the cell-based system. Calcium imaging, cAMP response element (CRE) reporter assay, and bioluminescence resonance energy transfer (BRET) assay are representative methods used for the visualization of odorant response. When the cells expressing ORs are stimulated with specific odorants, the cellular signaling cascade is generated and the ion-channels open. The calcium imaging detects the calcium ion which enters into the cells through the ion-channel, using calcium binding fluorescent dye, and this system is the most widely used odorant detection method [105]. However, its use is limited due to the fact that calcium imaging is time-consuming and labor-intensive, and thus, CRE reporter assay has been developed as an alternative method [106, 107]. In the CRE reporter system, the secondary signal messenger cAMP generated through the odorant stimulation binds to, and activates the signaling molecules, resulting in activation of the CRE promoter to express the luminescence or fluorescence protein as a reporter. For the protein-based visualization of odorant binding response, the BRET assay was carried out by the insertion of sequences encoding a bioluminescent donor and a fluorescent acceptor protein at the C-terminus of olfactory receptor ODR-10 and the third intracellular loop, respectively [108]. The conformational change of the olfactory receptor upon ligand stimulation induced the change of BRET signal. These methods were applied as useful visualization techniques, but have limited use in various olfactory receptors because of the labor-intensive and time-consuming processes involved.

Recently, a simple and low-cost miniaturized odorant screening platform was fabricated by a Micro-Electro-Mechanical system (MEMs) and a reverse transfection technique was used to visualize the odorant response in a high-throughput format [109]. Each different olfactory receptor DNA with transfection reagent was inserted into each PEG microwell, then HEK293 cells containing the CRE report system were spread over the PEG microwell array plate. Using this method, each different olfactory receptor was expressed in each well and the odorant response of each OR was detected using fluorescent CRE reporter protein simultaneously. Since this OR DNA printed-based microwell can be stored stably, a large quantity of the microwell can be fabricated and the odorant response can be visualized easily through seeding the cells containing the CRE reporter system.

Cell-based visualization systems can generate intuitive images of smell. However, a labor-intensive and skilled handling of cells is required to obtain reproducible

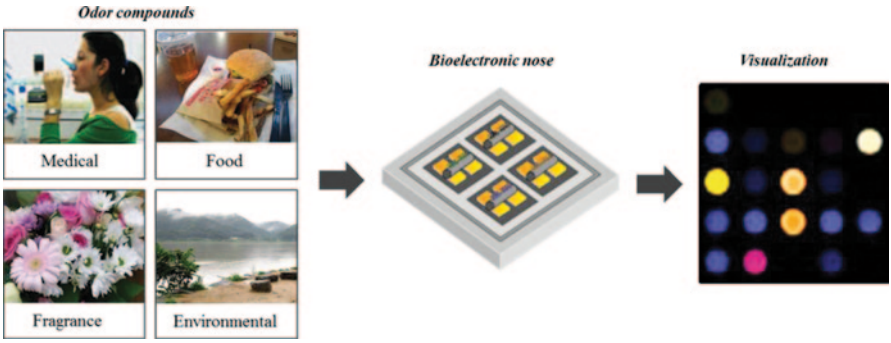

Fig. 14.4 Visualization of odor compounds originating from various sources using a bioelectronic nose. (Reprinted from Ref. [48] with permission from Nature Publishing Group)

and reliable results. Furthermore, the detection of odors in a gas-phase is difficult in the case of the cell-based systems, because a liquid environment is essential for the survival of cells. Bioelectronic noses can offer a perfect solution to these problems if several technologies are combined. First of all, the technique that integrates a lot of independent electronic modules into a single chip with a high density should be applied because all kinds of olfactory receptors have to be used in a multi-channel sensor array. Also, signal processing methods to analyze the parallel signals generated from the multi-channel sensor and to express the results in visual images must be established. In addition, conventional microfluidic systems that constantly supply a small amount of gas samples to the sensor platform can be effectively integrated. A bioelectronic nose that detects gaseous odorants has already been successfully demonstrated [78]. These integrations will facilitate the development of an effective sensor that easily converts smells into a visual representation (Fig. 14.4).

14.3 Conclusion

The bioelectronic nose consists of two major parts, which are primary and secondary transducers. The primary transducer is a biological recognition element, and the secondary transducer is a non-biological signal transducing element. The representative primary transducers are cells, nanovesicles, proteins and peptides. The cell acts as a live sensing material, and may be the best system for mimicking the human nose because it has all the components necessary for signaling induced by analytes. However, it is difficult for cells to be maintained on the sensor platform for a long period. Nanovesicles also can be a good candidate for biosensing material. Although they are not alive, they still have all the components necessary for the olfactory signal transduction like cells. They can be stored in a freezer for several months. Olfactory receptor proteins and peptides are most appropriate for the commercial biosensor, because they are quite stable even at room temperature. The representative secondary transducers are QCM, SPR, EIS, microelectrode, carbon

nanotube, conducting polymer nanotube, conducting polymer nanoparticles, and graphene. The integration of the olfactory biological recognition elements with these nano-devices enables the bioelectronics nose to have extremely high selectivity and sensitivity.

The unique characteristic of the bioelectronic nose is to mimic the human olfactory system in order to detect smell as accurately as a human nose. Eventually, the most ideal bioelectronics nose mimicking the human olfactory system will be developed through the integration of 390 types of human olfactory receptors on a single sensor platform because human olfactory system has 390 different functional olfactory receptors. It will be very meaningful to develop the bioelectronic nose consisting of 390 receptor elements in terms of the artificial realization of the human olfactory sense.

The bioelectronic nose can provide a powerful tool to detect and discriminate among smell compounds, which are emitted from almost everything, and exist everywhere. The change of smell in regard to type and concentration provides us with information on the objects and environments surrounding us. The bioelectronic nose can be applied in various fields, such as in the standardization of smell, development of code for each smell, medical diagnosis, quality assessment of food and beverage, as well as scent-related industries, including perfume, cosmetics, wine and coffee, agricultural application, environmental monitoring, process monitoring, and the detection of explosives, toxicants and drugs. Consequently, the development of a bioelectronic nose system is expected to play an important role in improving the quality of human life.

Acknowledgment This work was supported by the National Research Foundation of Korea (NRF) grant funded by the Ministry of Science, ICT & Future Planning (No. 2013003890, No. 2013K000368) and the Ministry of Education (No. 2013011174).

References

1. Gaillard I, Rouquier S, Giorgi D (2004) Olfactory receptors. Cell Mol Life Sci 61(4):456–469
2. Breer H (2003) Olfactory receptors: molecular basis for recognition and discrimination of odors. Anal Bioanal Chem 377(3):427–433
3. Lee SH, Park TH (2010) Recent advances in the development of bioelectronic nose. Biotechnol Bioproc E 15(1):22–29
4. Kim TH, Lee SH, Lee J, Song HS, Oh EH, Park TH, Hong S (2009) Single-carbon-atomic-resolution detection of odorant molecules using a human olfactory receptor-based bioelectronic nose. Adv Mater 21(1):91–94
5. Yoon H, Lee SH, Kwon OS, Song HS, Oh EH, Park TH, Jang J (2009) Polypyrrole nanotubes conjugated with human olfactory receptors: high-performance transducers for FET-type bioelectronic noses. Angew Chem Int Edit 48(15):2755–2758
6. Goldsmith BR, Mitala JJ, Josue J, Castro A, Lerner MB, Bayburt TH, Khamis SM, Jones RA, Brand JG, Sligar SG, Luetje CW, Gelperin A, Rhodes PA, Discher BM, Johnson ATC (2011) Biomimetic chemical sensors using nanoelectronic readout of olfactory receptor proteins. ACS Nano 5(7):5408–5416

7. Wysocki CJ, Preti G (2000) Human body odors and their perception. Jpn J Taste Smell Res 7(1):12–42
8. Lettéron P, Duchatelle V, Berson A, Fromenty B, Fisch C, Degott C, Benhamou JP, Pessayre D (1993) Increased ethane exhalation, an in vivo index of lipid peroxidation, in alcohol-abusers. Gut 34(3):409–414
9. Hanazawa T, Kharitonov S, Barnes P (2000) Increased nitrotyrosine in exhaled breath condensate of patients with asthma. Am J Respir Crit Care Med 162(4):1273–1276
10. Dohlman AW, Black HR, Royall JA (1993) Expired breath hydrogen peroxide is a marker of acute airway inflammation in pediatric patients with asthma. Am Rev Respir Dis 148(4_pt_1):955–960
11. Montuschi P, Barnes PJ (2002) Exhaled leukotrienes and prostaglandins in asthma. J Allergy Clin Immun 109(4):615–620
12. Phillips M, Cataneo RN, Ditkoff BA, Fisher P, Greenberg J, Gunawardena R, Kwon CS, Rahbari-Oskoui F, Wong C (2003) Volatile markers of breast cancer in the breath. Breast J 9(3):184–191
13. Montuschi P, Kharitonov SA, Ciabattoni G, Corradi M, van Rensen L, Geddes DM, Hodson ME, Barnes PJ (2000) Exhaled 8-isoprostane as a new non-invasive biomarker of oxidative stress in cystic fibrosis. Thorax 55(3):205–209
14. Bodini A, D'Orazio C, Peroni D, Corradi M, Folesani G, Baraldi E, Assael BM, Boner A, Piacentini GL (2005) Biomarkers of neutrophilic inflammation in exhaled air of cystic fibrosis children with bacterial airway infections. Pediatr Pulm 40(6):494–499
15. Lundberg JO, Nordvall SL, Weitzberg E, Kollberg H, Alving K (1996) Exhaled nitric oxide in paediatric asthma and cystic fibrosis. Arch Dis Child 75(4):323–326
16. Nelson N, Lagesson V, Nosratabadi AR, Ludvigsson J, Tagesson C (1998) Exhaled isoprene and acetone in newborn infants and in children with diabetes mellitus. Pediatr Res 44(3):363–367
17. Xue R, Dong L, Zhang S, Deng C, Liu T, Wang J, Shen X (2008) Investigation of volatile biomarkers in liver cancer blood using solid-phase microextraction and gas chromatography/mass spectrometry. Rapid Commun Mass Sp 22(8):1181–1186
18. Gordon SM, Szidon JP, Krotoszynski BK, Gibbons RD, O'Neill HJ (1985) Volatile organic compounds in exhaled air from patients with lung cancer. Clin Chem 31(8):1278–1282
19. Phillips M, Cataneo RN, Cummin ARC, Gagliardi AJ, Gleeson K, Greenberg J, Maxfield RA, Rom WN (2003) Detection of lung cancer with volatile markers in the breath. Chest 123(6):2115–2123
20. Pavlou AK, Turner APF (2000) Sniffing out the truth: clinical diagnosis using the electronic nose. Clin Chem Lab Med 38(2):75–186
21. Sylvester K, Patey R, Rafferty G, Rees D, Thein S, Greenough A (2005) Exhaled carbon monoxide levels in children with sickle cell disease. Eur J Pediatr 164(3):162–165
22. Carpagnano GE, Kharitonov SA, Resta O, Foschino-Barbaro MP, Gramiccioni E, Barnes PJ (2002) Increased 8-isoprostane and interleukin-6 in breath condensate of obstructive sleep apnea patients. Chest 122(4):1162–1167
23. Hayden GF (1980) Olfactory diagnosis in medicine. Postgrad Med 64(4):110–115
24. Simenhoff ML, Burke JF, Saukkonen JJ, Ordinario AT, Doty R, Dunn S (1977) Biochemical profile of uremic breath. N Engl J Med 297(3):132–135
25. Smith K, Sines JO (1960) Demonstration of a peculiar odor in the sweat of schizophrenic patients. AMA Arch Gen Psychiatry 2(2):184–188
26. Smith K, Thompson GF, Koster HD (1969) Sweat in schizophrenic patients: identification of the odorous substance. Science 166(3903):398–399
27. Phillips M, Sabas M, Greenberg J (1993) Increased pentane and carbon disulfide in the breath of patients with schizophrenia. J Clin Pathol 46(9):861–864
28. Humad S, Zarling E, Clapper M, Skosey JL (1988) Breath pentane excretion as a marker of disease activity in rheumatoid arthritis. Free Radical Res 5(2):101–106

29. Goldberg EM, Blendis LM, Sandler S (1981) A gas chromatographic-mass spectrometric study of profiles of volatile metabolites in hepatic encephalopathy. J Chromatogr-Biomed 226(2):291–299
30. Smith M, Simith L, Levinson B (1982) The use of smell in differential diagnosis. The Lancet 2(8313):1452–1453
31. Liddell K (1976) Smell as a diagnostic marker. Postgrad Med J 52(605):136–138
32. Vockley J, Ensenauer R (2006) Isovaleric acidemia: new aspects of genetic and phenotypic heterogeneity. Am J Med Genet C Semin Med Genet 142C(2):95–103
33. Pavlou AK, Magan N, McNulty C, Jones JM, Sharp D, Brown J, Turner APF (2002) Use of an electronic nose system for diagnoses of urinary tract infections. Biosens Bioelectron 17(10):893–899
34. Guernion N, Ratcliffe Norman M, Spencer-Phillips Peter TN, Howe Robin A (2001) Identifying bacteria in human urine: current practice and the potential for rapid, near-patient diagnosis by sensing volatile organic compounds. Clin Chem Lab Med 39(10):893–906
35. Najarian JS (1980) The diagnostic importance of the odor of urine. N Engl J Med 303(19):1128
36. Ma W, Liu X, Pawliszyn J (2006) Analysis of human breath with micro extraction techniques and continuous monitoring of carbon dioxide concentration. Anal Bioanal Chem 385(8):1398–1408
37. Caspary W (1978) Breath tests. Clin Gastroenterol 7(2):351–374
38. Watson JT (1998) A historical perspective and commentary on pioneering developments in gas chromatography/mass spectrometry at MIT. J Mass Spectrom 33(2):103–108
39. Kharitonov S, Barnes P (2001) Exhaled markers of pulmonary disease. Am J Respir Crit Care Med 163(7):1693–1722
40. Studer SM, Orens JB, Rosas I, Krishnan JA, Cope KA, Yang S, Conte JV, Becker PB, Risby TH (2001) Patterns and significance of exhaled-breath biomarkers in lung transplant recipients with acute allograft rejection. J Heart Lung Transpl 20(11):1158–1166
41. Miekisch W, Schubert JK, Noeldge-Schomburg GFE (2004) Diagnostic potential of breath analysis-focus on volatile organic compounds. Clin Chim Acta 347(1–2):25–39
42. Zolotov YA (2005) Breath Analysis. J Anal Chem 60(6):497–497
43. Persaud K, Dodd G (1982) Analysis of discrimination mechanisms in the mammalian olfactory system using a model nose. Nature 299(5881):352–355
44. Thaler ER, Hanson CW (2005) Medical applications of electronic nose technology. Expert Rev Med Devices 2(5):559–566
45. D'Amico A, Pennazza G, Santonico M, Martinelli E, Roscioni C, Galluccio G, Paolesse R, Di Natale C (2010) An investigation on electronic nose diagnosis of lung cancer. Lung Cancer 68(2):170–176
46. Di Natale C, Macagnano A, Martinelli E, Paolesse R, D'Arcangelo G, Roscioni C, Finazzi-Agrò A, D'Amico A (2003) Lung cancer identification by the analysis of breath by means of an array of non-selective gas sensors. Biosens Bioelectron 18(10):1209–1218
47. Dragonieri S, Annema JT, Schot R, van der Schee MPC, Spanevello A, Carratú P, Resta O, Rabe KF, Sterk PJ (2009) An electronic nose in the discrimination of patients with non-small cell lung cancer and COPD. Lung Cancer 64(2):166–170
48. Peng G, Tisch U, Adams O, Kakim M, Shehada N, Broza YY, Billan S, Abdah-Bortnyak R, Kuten A, Haick H (2009) Diagnosing lung cance in exhaled breath using gold nanoparticles. Nat Nanotechnol 4:669–673
49. Fens N, Zwinderman AH, van der Schee MP, de Nijs SB, Dijkers E, Roldaan AC, Cheung D, Bel EH, Sterk PJ (2009) Exhaled breath profiling enables discrimination of chronic obstructive pulmonary disease and asthma. Am J Respir Crit Care Med 180(11):1076–1082
50. Dragonieri S, Schot R, Mertens BJA, Le Cessie S, Gauw SA, Spanevello A, Resta O, Willard NP, Vink TJ, Rabe KF, Bel EH, Sterk PJ (2007) An electronic nose in the discrimination of patients with asthma and controls. J Allergy Clin Immun 120(4):856–862
51. Peng G, Tisch U, Adams O, Hakim M, Shehada N, Broza YY, Billan S, Abdah-Bortnyak R, Kuten A, Haick H (2009) Diagnosing lung cancer in exhaled breath using gold nanoparticles. Nat Nanotechnol 4(10):669–673

52. Lin Y-J, Guo H-R, Chang Y-H, Kao M-T, Wang H-H, Hong R-I (2001) Application of the electronic nose for uremia diagnosis. Sensor Actuat B-Chem 76(1-3):177–180
53. Lim JH, Park J, Oh EH, Ko HJ, Hong S, Park TH (2013) Nanovesicle-based bioelectronic nose for the diagnosis of lung cancer from human blood. Adv Healthc Mater. doi: 10.1002/adhm.201300174
54. Li N, Deng C, Yin X, Yao N, Shen X, Zhang X (2005) Gas chromatography-mass spectrometric analysis of hexanal and heptanal in human blood by headspace single-drop microextraction with droplet derivatization. Anal Biochem 342(2):318–326
55. Kwon OS, Ahn SR, Park SJ, Song HS, Lee SH, Lee JS, Hong J-Y, Lee JS, You SA, Yoon H, Park TH, Jang J (2012) Ultrasensitive and selective recognition of peptide hormone using close-packed arrays of hPTHR-conjugated polymer nanoparticles. ACS Nano 6(6):5549–5558
56. Kim B, Song HS, Jin HJ, Park EJ, Lee SH, Lee BY, Park TH, Hong S (2013) Highly selective and sensitive detection of neurotransmitters using receptor-modified single-walled carbon nanotube sensors. Nanotechnology 24(28):285501
57. Kim YD, Morr CV (1996) Dynamic headspace analysis of light activated flavor in milk. Int Dairy J 6(2):185–193
58. Hu M, McClements DJ, Decker EA (2003) Lipid oxidation in corn oil-in-water emulsions stabilized by casein, whey protein isolate, and soy protein isolate. J Agric Food Chem 51(6):1696–1700
59. Gardner HW (1989) Oxygen radical chemistry of polyunsaturated fatty acids. Free Radical Bio Med 7(1):65–86
60. Prosen H, Zupančič-Kralj L (1999) Solid-phase microextraction. TrAC-Trend Anal Chem 18(4):272–282
61. Heikes DL, Jensen SR, Fleming-Jones ME (1995) Purge and trap extraction with GC-MS determination of volatile organic compounds in table-ready foods. J Agric Food Chem 43(11):2869–2875
62. Xu Y, Cheung W, Winder C, Goodacre R (2010) VOC-based metabolic profiling for food spoilage detection with the application to detecting Salmonella typhimurium-contaminated pork. Anal Bioanal Chem 397(6):2439–2449
63. Bhattacharjee P, Panigrahi S, Lin D, Logue CM, Sherwood JS, Doetkott C, Marchello M (2011) A comparative qualitative study of the profile of volatile organic compounds associated with Salmonella contamination of packaged aged and fresh beef by HS-SPME/GC-MS. J Food Sci Tech 48(1):1–13
64. Lazarus SA, Adamson GE, Hammerstone JF, Schmitz HH (1999) High-performance liquid chromatography/mass spectrometry analysis of proanthocyanidins in foods and beverages. J Agric Food Chem 47(9):3693–3701
65. Merken HM, Beecher GR (2000) Measurement of food flavonoids by high-performance liquid chromatography: a review. J Agric Food Chem 48(3):577–599
66. Hernández-Jover T, Izquierdo-Pulido M, Veciana-Nogués MT, Vidal-Carou MC (1996) Ion-pair high-performance liquid chromatographic determination of biogenic amines in meat and meat products. J Agric Food Chem 44(9):2710–2715
67. Capone S, Epifani M, Quaranta F, Siciliano P, Taurino A, Vasanelli L (2001) Monitoring of rancidity of milk by means of an electronic nose and a dynamic PCA analysis. Sensor Actuat B-Chem 78(1–3):174–179
68. Gardner JW, Shurmer HV, Tan TT (1992) Application of an electronic nose to the discrimination of coffees. Sensor Actuat B-Chem 6(1-3):71–75
69. Schaller E, Bosset JO, Escher F (1998) 'Electronic noses' and their application to food. LWT-Food Sci Technol 31(4):305–316
70. Di Natale C, Macagnano A, Davide F, D'Amico A, Paolesse R, Boschi T, Faccio M, Ferri G (1997) An electronic nose for food analysis. Sensor Actuat B-Chem 44(1–3):521–526
71. Shahidi F, Pegg RB (1994) Hexanal as an indicator of meat flavor deterioration. J Food Lipids 1(3):177–186

72. Park J, Lim JH, Jin HJ, Namgung S, Lee SH, Park TH, Hong S (2012) A bioelectronic sensor based on canine olfactory nanovesicle-carbon nanotube hybrid structures for the fast assessment of food quality. Analyst 137(14):3249–3254
73. Lim JH, Park J, Ahn JH, Jin HJ, Hong S, Park TH (2013) A peptide receptor-based bioelectronic nose for the real-time determination of seafood quality. Biosens Bioelectron 39(1):244–249
74. Mondello L, Casilli A, Tranchida PQ, Dugo G, Dugo P (2005) Comprehensive two-dimensional gas chromatography in combination with rapid scanning quadrupole mass spectrometry in perfume analysis. J Chromatogr A 1067(1–2):235–243
75. Asten AV (2002) The importance of GC and GC-MS in perfume analysis. TrAC-Trend Anal Chem 21(9–10):698–708
76. Carrasco A, Saby C, Bernadet P (1998) Discrimination of Yves Saint Laurent perfumes by an electronic nose. Flavour Frag J 13(5):335–348
77. Branca A, Simonian P, Ferrante M, Novas E, Negri RMn (2003) Electronic nose based discrimination of a perfumery compound in a fragrance. Sensor Actuat B-Chem 92(1–2):222–227
78. Lee SH, Kwon OS, Song HS, Park SJ, Sung JH, Jang J, Park TH (2012) Mimicking the human smell sensing mechanism with an artificial nose platform. Biomaterials 33(6):1722–1729
79. Brown RH, Purnell CJ (1979) Collection and analysis of trace organic vapour pollutants in ambient atmospheres: The performace of a Tenax-GC adsorbent tube. J Chromatogr A 178(1):79–90
80. Albaigés J, Albrecht P (1979) Fingerprinting marine pollutant hydrocarbons by computerized gas chromatography-mass spectrometry. Int J Environ An Ch 6(2):171–190
81. Pellizzari E, Bunch J, Berkley R, McRae J (1976) Determination of trace hazardous organic vapor pollutants in ambient atmospheres by gas chromatography/mass spectrometry/computer. Anal Chem 48(6):803–807
82. Noroozian E, Maris FA, Nielen MWF, Frei RW, de Jong GJ, Brinkman UA Th (1987) Liquid chromatographic trace enrichment with on-line capillary gas chromatography for the determination of organic pollutants in aqueous samples. J High Res Chromatog 10(1):17–24
83. de Almeida Azevedo D, Lacorte S, Vinhas T, Viana P, Barceló D (2000) Monitoring of priority pesticides and other organic pollutants in river water from Portugal by gas chromatography-mass spectrometry and liquid chromatography-atmospheric pressure chemical ionization mass spectrometry. J Chromatogr A 879(1):13–26
84. Rodil R, Quintana JB, López-Mahía P, Muniategui-Lorenzo S, Prada-Rodríguez D (2009) Multi-residue analytical method for the determination of emerging pollutants in water by solid-phase extraction and liquid chromatography-tandem mass spectrometry. J Chromatogr A 1216(14):2958–2969
85. Ryan MA, Shevade AV, Zhou H, Homer ML (2004) Polymer-carbon black composite sensors in an electronic nose for air-quality monitoring. MRS Bull 29(10):714–719
86. Gardner JW, Shin HW, Hines EL, Dow CS (2000) An electronic nose system for monitoring the quality of potable water. Sensor Actuat B-Chem 69(3):336–341
87. Goschnick J, Koronczi I, Frietsch M, Kiselev I (2005) Water pollution recognition with the electronic nose KAMINA. Sensor Actuat B-Chem 106(1):182–186
88. De Vito S, Massera E, Piga M, Martinotto L, Di Francia G (2008) On field calibration of an electronic nose for benzene estimation in an urban pollution monitoring scenario. Sensor Actuat B-Chem 129(2):750–757
89. Zampolli S, Elmi I, Ahmed F, Passini M, Cardinali GC, Nicoletti S, Dori L (2004) An electronic nose based on solid state sensor arrays for low-cost indoor air quality monitoring applications. Sensor Actuat B-Chem 101(1-2):39–46
90. Wu T-Z, Lo Y-R (2000) Synthetic peptide mimicking of binding sites on olfactory receptor protein for use in ‘electronic nose’. J Biotechnol 80(1):63–73
91. Wu T-Z (1999) A piezoelectric biosensor as an olfactory receptor for odour detection: electronic nose. Biosens Bioelectron 14(1):9–18

92. O'Mahony M (1986) Sensory adaptation. J Sens Stud 1(3–4):237–258
93. Kaeppler K, Mueller F (2013) Odor classification: a review of factors influencing perception-based odor arrangements. Chem Senses 38:189–209
94. Henning H (1916) Der Geruch. Verlag von Johann Ambrosius Barth, Leipzig
95. Dyson GM (1938) The scientific basis of odour. J Soc Chem Ind 57:647–651
96. Wright RH, Serenius RSE (1954) Odour and molecular vibration. II. Raman spectra of substances with the nitrobenzene odour. J Appl Chem 4:615–621
97. Schiffman SS (1974) Physicochemical correlates of olfactory quality. Science 185:112–117
98. Amoore JE (1963) Stereochemical theory of olfaction. Nature 199:912–913
99. Brower KR, Schafer R (1975) The recognition of chemical types by odor. The effect of steric hindrance at the functional group. J Chem Educ 52:538–540
100. Amoore JE (1977) Specific anosmia and the concept of primary odors. Chem Senses 2:267–281
101. Cain WS (1970) Odor intensity after self-adaptation and cross-adaptation. Percept Psychophys 7:271–275
102. Todrank J, Wysocki CJ, Beauchamp GK (1991) The effects of adaptation on the perception of similar and dissimilar odors. Chem Senses 16:467–482
103. Pierce JD Jr, Zeng XN, Aronov EV, Preti G, Wysocki CJ (1995) Cross-adaptation of sweaty-smelling 3-methyl-2-hexenoic acid by a structually-similar, pleasant-smelling odorant. Chem Senses 20:401–411
104. Malnic B (2004) The human olfactory receptor gene family. Proc Natl Acad Sci U S A 101:2584–2589
105. Figueroa XA, Cooksey GA, Votaw SV, Horowitz LF, Folch A (2010) Large-scale investigation of the olfactory receptor space using a microfluidic microwell array. Lab Chip 10(9):1120–1127
106. Redmond TM, Ren X, Kubish G, Atkins S, Low S, Uhler MD (2004) Microarray transfection analysis of transcriptional regulation by cAMP-dependent protein kinase. Mole Cell Proteomics 3(8):770–779
107. Saito H, Chi Q, Zhuang H, Matsunami H, Mainland JD (2009) Odor coding by a mammalian receptor repertoire. Sci Signal 2(60):ra9
108. Dacres H, Wang J, Leitch V, Horne I, Anderson AR, Trowell SC (2011) Greatly enhanced detection of a volatile ligand at femtomolar levels using bioluminescence resonance energy transfer (BRET). Biosens Bioelectron 29(1):119–124
109. Oh EH, Lee SH, Lee SH, Ko HJ, Park TH (2014) Cell-based high-throughput odorant screening system through visualization on a microwell array. Biosens Bioelectron 53:18–25

Index

T. H. Park (ed.), *Bioelectronic Nose,* DOI 10.1007/978-94-017-8613-3,